

Lawrence Berkeley National Laboratory

Recent Work

Title

THE REACTION DYNAMICS OF ELECTRONICALLY EXCITED ALKALI ATOMS WITH SIMPLE MOLECULES

Permalink

<https://escholarship.org/uc/item/1x4990gr>

Author

Weiss, P.S.

Publication Date

1986-03-01



Lawrence Berkeley Laboratory

UNIVERSITY OF CALIFORNIA

RECEIVED
LAWRENCE
BERKELEY LABORATORY

Materials & Molecular Research Division

JUN 18 1985

LIBRARY AND
DOCUMENTS SECTION

THE REACTION DYNAMICS OF ELECTRONICALLY EXCITED
ALKALI ATOMS WITH SIMPLE MOLECULES

P.S. Weiss
(Ph.D. Thesis)

March 1986

For Reference
Not to be taken from this room



Prepared for the U.S. Department of Energy under Contract DE-AC03-76SF00098

LBL-21205
e1

DISCLAIMER

This document was prepared as an account of work sponsored by the United States Government. While this document is believed to contain correct information, neither the United States Government nor any agency thereof, nor the Regents of the University of California, nor any of their employees, makes any warranty, express or implied, or assumes any legal responsibility for the accuracy, completeness, or usefulness of any information, apparatus, product, or process disclosed, or represents that its use would not infringe privately owned rights. Reference herein to any specific commercial product, process, or service by its trade name, trademark, manufacturer, or otherwise, does not necessarily constitute or imply its endorsement, recommendation, or favoring by the United States Government or any agency thereof, or the Regents of the University of California. The views and opinions of authors expressed herein do not necessarily state or reflect those of the United States Government or any agency thereof or the Regents of the University of California.

THE REACTION DYNAMICS OF ELECTRONICALLY EXCITED ALKALI ATOMS
WITH SIMPLE MOLECULES

Paul Storch Weiss

Materials and Molecular Research Division
Lawrence Berkeley Laboratory

and
Department of Chemistry
University of California
Berkeley, California 94720

The reactions of electronically excited sodium have been studied using the crossed molecular beams method. The apparatus and optical pumping are described in chapter I.

Chapter II describes the reactions of Na with the hydrogen halides. The reactions of $\text{Na}(3S,3P,4D,5S) + \text{HCl}$ have been studied in detail. A large increase in the reactive cross section with electronic energy is observed. A change in the reaction mechanism leads to very different product scattering distributions for $\text{Na}(3P)$ vs. $\text{Na}(4D,5S)$ scattering. Laser polarization dependences show that this is due to long range electron transfer in $\text{Na}(4D) + \text{HCl}$ that does not occur for $\text{Na}(3P) + \text{HCl}$. No reaction was observed for $\text{Na}(3S,3P,4D) + \text{HF}$ up to collision energies of 13 kcal/mole. $\text{Na}(3S,3P) + \text{HBr}$ behave much like the equivalent HCl reactions, except that the reduced endothermicity leads to more ground state reaction for HBr .

Chapter III describes the reaction of Na with O_2 . No reaction is seen for $Na(3S,3P,4S,4P,5S) + O_2$. Reaction to form $NaO + O$ is observed for $Na(4D) + O_2$ above the threshold translational energy of 15 ± 1 kcal/mole. The reaction cross section is small, $\sigma_R = 0.9 \text{ \AA}^2$ at 18 kcal/mole collision energy. The reaction is direct, does not occur via long range electron transfer, and a near collinear approach geometry is required for reaction. Some information about the transition state symmetry is derived from laser polarization dependences.

The reactions of $Na(3S,3P,4D) + CH_3Br$ are described in chapter IV. As in all previously studied alkali plus alkyl monohalide reactions, the alkali halide product is predominantly back scattered due to steric restrictions. With increasing electronic excitation, a small relaxation of the restriction is observed, leading to NaBr scattered to lower center-of-mass angles than for the ground state reaction.

The reactions of $Na(3S,3P) + Cl_2$ are described in chapter V. At a collision energy of 6 kcal/mole, the reactive cross section increases 60% on electronic excitation, while at a higher collision energy, 19 kcal/mole, there is an increase of only 16%. A stripping mechanism explains the very similar scattering distributions of each state.

Guan T. Lee

ACKNOWLEDGEMENTS

Many people have contributed to the work presented here, both in and out of the laboratory. There is room to mention only a few of them below, but none are forgotten, and I thank them all for their help.

On the experimental team, I have had the good fortune to work with a number of talented and bright individuals. First and foremost among these is Professor Yuan Lee. His proficiency at both molecular beam experiments and their interpretation, and his love for his work are awe-inspiring. Matt Vernon taught me how to use the apparatus, and set up much of what has produced the results described here. He also taught me his sound method of getting things done, which I have occasionally called into service. Dr. James Joseph Anthony Michael O'Brien helped set up the experiment before it came to fruition. The visits of Dr. Hartmut Schmidt and Dr. Jean Michel Mestdagh set the stage for several quantum leaps forward on these studies. Also working on these experiments was Michael "Bud" Covinsky, who was a constant source of entertainment. It has been great fun to work with Barbara Balko, who has shown me unending kindness in the last one and a half years. I have no regrets for keeping her up at lab for 36 hours at a time just for her company. The most recent addition to the A machine is Isabelle Duborg who helped with the final O₂ experiments. I also thank her for her herculean effort in generating a great many of the figures that follow.

Several other members of the Lee group have supported me during these last few difficult months -- Gil Nathanson, Distinguished Miller Fellow, Lisa Yeh, and Babs Balko. I have learned something from everyone in the Lee group, but of particular note, conversations with Gary Robinson, Bob Continetti, Gil Nathanson, Carl Hayden, and Howard Nathel have been helpful in my work and in getting me through the days and nights here. Ann Weightman has gone to much trouble to shield us from many of the harsh realities of bureaucracy, and for this and her help in the preparation of this thesis, I thank her.

A number of the LBL and UC campus support staff have been instrumental in keeping our experiments going. Among these, the ones that saved us time and time again are: Will Lawrence, Charlie Taylor, Tony Moscarelli, Fred Wolfe, and Fred Vogelsberg. I enjoyed my association with Fred Vogelsberg and Jacques Millaud on the multichannel scaler and the Timer-Gater-Scaler projects. A lot of good has come from their skilled and diligent work.

The San Francisco Laser Center, and its director, Dr. Andy Kung have come to the rescue many times when disaster struck or we just wanted to try something new. Steve Bittenson and Tim Ling have been helpful in keeping our lasers running well.

I first got started in chemistry at MIT, and it was Professor Bob Field who provided me with the most stimulating atmosphere I have ever encountered. He was patient, kind, and encouraging, and through his efforts I learned much more than I otherwise could have. All of what I

learned from him and from two of his group members, Rick Gottscho and Ron Marks, has served me well at Berkeley.

This work was supported by the Director, Office of Energy Research, Office of Basic Energy Sciences, Chemical Sciences Division of the U.S. Department of Energy under Contract No. DE-AC03-76SF00098.

Others, outside of science have given me the support I needed to carry out this work, and much more. The O'Connor family, and Harry Pasternack and Liza Cramer helped me through critical times in Berkeley. Kendall's parents, Walter and Judy Munk, and her grandmother, Mrs. Winter Horton have made me feel very special, and this has given me an extra gear to work harder. All my life, my parents have given me their love, confidence, and support, and none of this would have been possible without them.

My wife Kendall and son Walter have waited patiently for me to finish. Kendall has been ever so understanding and encouraging with my odd schedules from the very beginning, and it is to Kendall that this thesis and I are dedicated.

THE REACTION DYNAMICS OF ELECTRONICALLY EXCITED ALKALI ATOMS WITH
SIMPLE MOLECULES

Table of Contents

Abstract	1
Acknowledgements	i
Table of Contents	iv
I. EXPERIMENTAL	
A. The Experimental Apparatus	1
B. Atomic and Molecular Beam Conditions	20
C. Data Acquisition	32
D. Optical Pumping	39
1. Introduction	39
2. The Na D ₂ Transition	43
3. Subsequent Excitation to Na(4 ² D _{5/2})	57
4. Subsequent Excitation to Na(5 ² S _{1/2})	62
E. References	65
II. THE REACTIONS OF GROUND AND EXCITED ALKALI ATOMS WITH HYDROGEN HALIDE MOLECULES	
A. Introduction	68
B. Results	81
1. Na(4D,5S) + HCl	81
2. Na + HF	97
3. Na(3S,3P) + HBr	97

C.	Analysis of Experimental Results	101
D.	Discussion	117
	1. The Mechanism and Distribution of Product Energy in the Na(4D,5S) + HCl Reaction	117
	2. The Lack of Reaction for Na + HF	129
E.	Conclusions	130
F.	References	132
III.	THE STATE SELECTIVE REACTION OF ELECTRONICALLY EXCITED SODIUM ATOMS WITH MOLECULAR OXYGEN	
A.	Introduction	137
B.	Results	144
C.	Analysis of Experimental Results	179
D.	Discussion	194
E.	Conclusions	202
F.	References	204
IV.	THE REACTIONS OF GROUND AND EXCITED STATE ALKALI ATOMS WITH METHYL HALIDE MOLECULES	
A.	Introduction	207
B.	Results	212
C.	Analysis of Experimental Results	218
D.	Discussion	229
	1. Observations on the Experimental Results	229
	2. Other Possible Processes	230
E.	Conclusions	232
F.	References	233

V.	THE REACTIONS OF GROUND AND EXCITED STATE ALKALI ATOMS WITH HALOGEN MOLECULES	
A.	Introduction	237
B.	Results	254
C.	Analysis of Experimental Results	261
D.	Discussion	272
D.	Conclusions	276
E.	References	278
VI.	CONCLUSIONS	
A.	Conclusions on the Reaction Dynamics of Electronically Excited Alkali Atoms	282
VII.	APPENDICES	
A.	Data Acquisition for Angular Distributions, Polarization Dependences, Machine Condition Optimization: The Data Acquisition System and Program SANG	284
1.	Introduction to the Data Acquisition System	284
2.	Introduction to Program SANG	286
3.	Listing of Program SANG	294
B.	Data Acquisition for Time of Flight Measurements: The New Multichannel Scaler and Program TUF	399
1.	The Purpose of the Multichannel Scaler	399
2.	CAMAC Commands for the New Multichannel Scaler	401
3.	Multichannel Scaler Hardware Specifications	406
4.	Multichannel Scaler Circuit Logic and Signal Descriptions	409

5. Introduction to the Program TUF	417
6. Listing of Program TUF	419
C. References	474

To Kendall

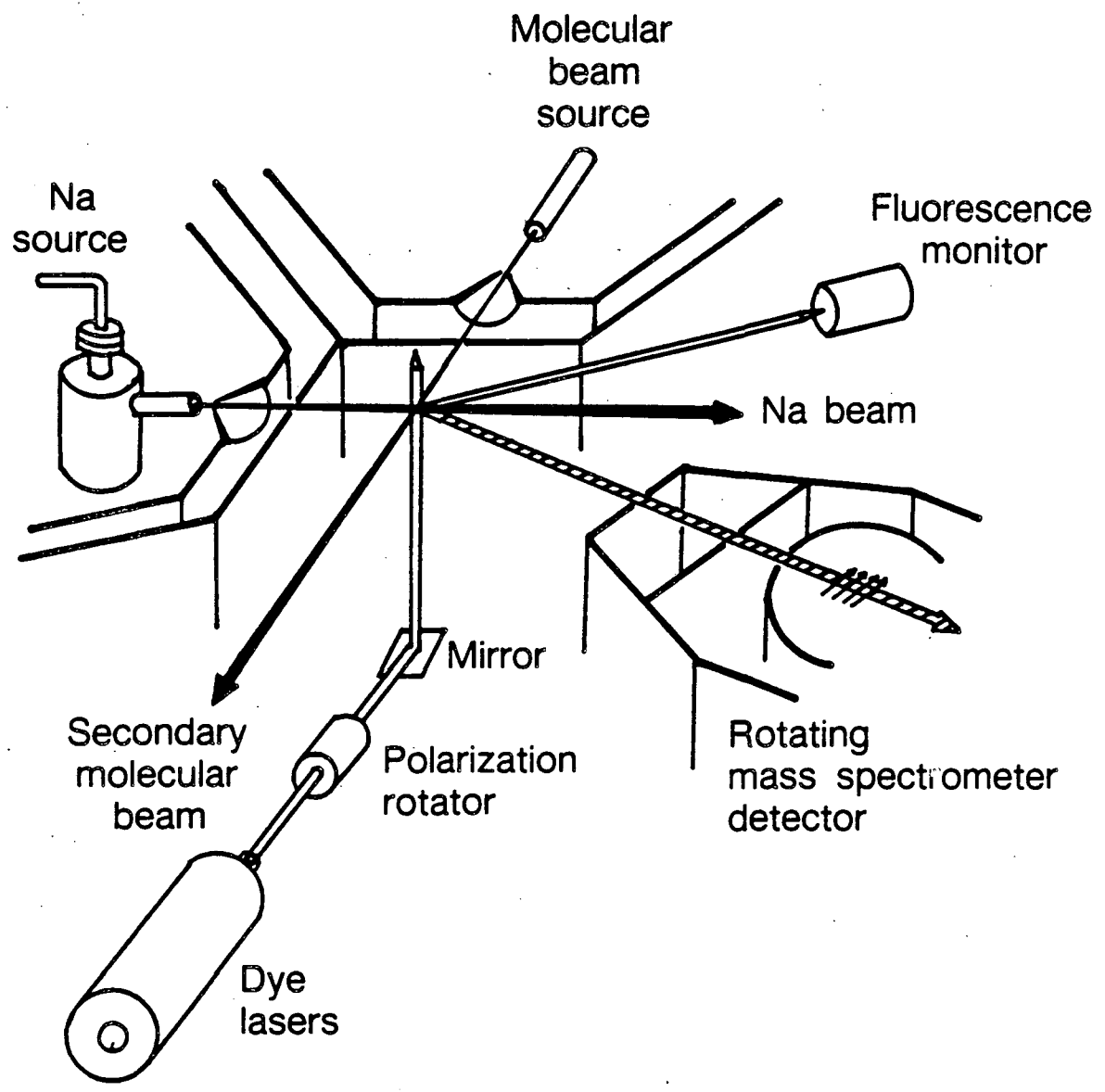
I. EXPERIMENTAL

A. The Experimental Apparatus

The experimental measurements described below were carried out on a crossed molecular beams machine modified to allow laser excitation at the crossing of the atomic and molecular beams. The basic apparatus has been described previously,¹⁻⁵ but will be reviewed here.

An atomic sodium beam, a molecular beam, and one or two dye laser beams cross orthogonally in a vacuum chamber under single collision conditions as shown schematically in figure 1. A mass spectrometric detector rotates about the collision region in the plane defined by the atomic and molecular beams. Three types of experiments are performed: (1) product angular distributions are measured by rotating the detector, (2) product velocities for fixed detector angles are measured by modulating the product directly or the reaction itself by modulating the laser, and (3) the effect of rotating the laser polarization and thus the excited orbital alignment upon the reactive product at a fixed detector angle is measured.

The sodium atomic beam source was designed by Dr. H. Schmidt and is a hybrid of the sodium source design used in the I. V. Hertel group at the Freie Universitaet Berlin, and the lithium source used for earlier measurements of $\text{Li} + \text{HF}$, HCl .³ Figure 2 is a schematic of

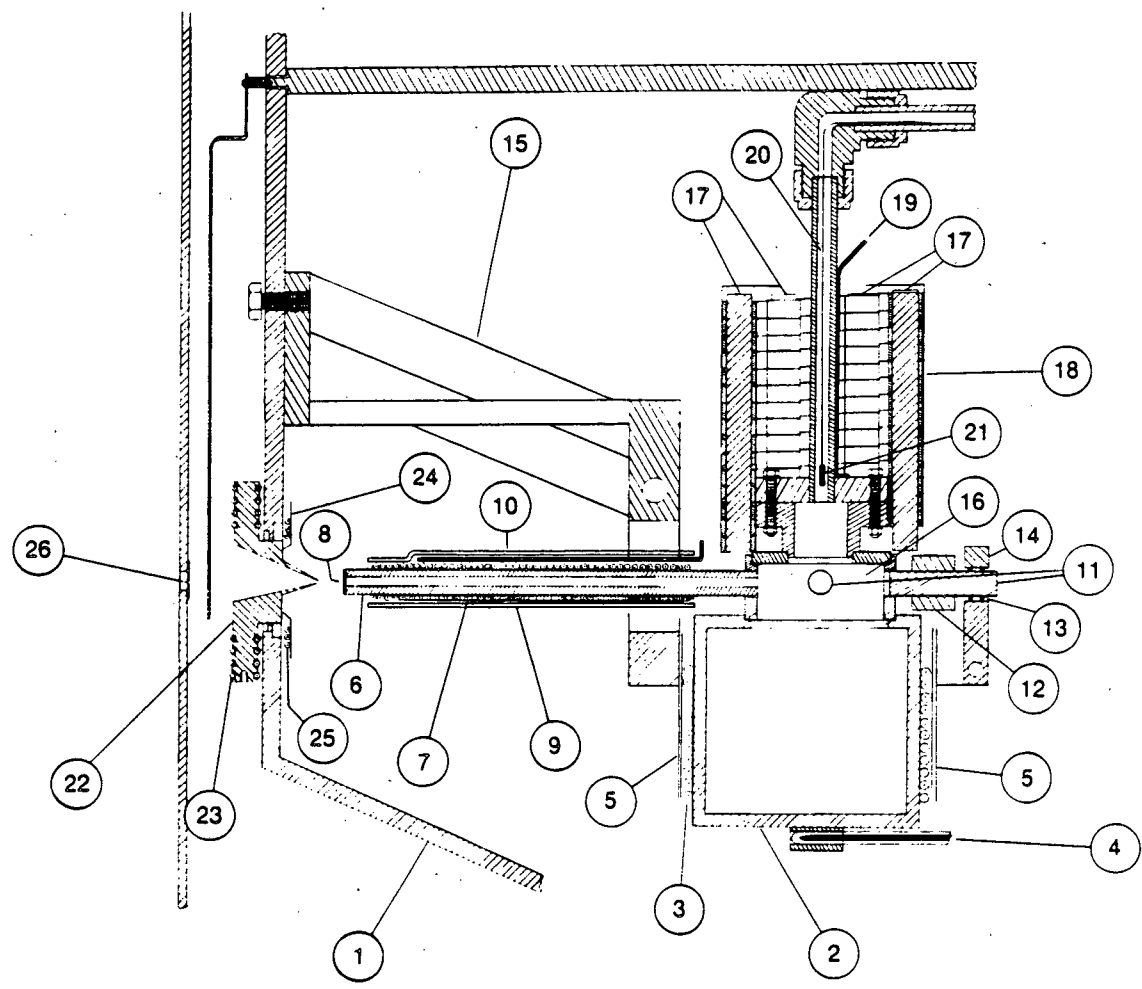


XBL 855-2592 B

Fig. 1. Schematic of the crossed molecular beams apparatus.

Fig. 2. Schematic of the seeded supersonic sodium atomic beam source (adapted from a similar figure in reference 2, with permission):

(1) Primary source chamber, (2) Sodium reservoir, (3) Thermal coaxial heaters for reservoir, (4) Bottom oven thermocouple, (5) Bottom oven radiation shields, (6) Nozzle tube, (7) Thermal coaxial heaters for nozzle, (8) Nozzle disk, (9) Nozzle radiation shields, (10) Nozzle thermocouple, (11) Oven support rods, (12) Insulating ceramic for support rods, (13) Thin wire to thermally insulate support rods from (14) Copper blocks attached to (15) Water-cooled copper structure to hold oven rigidly aligned, (16) Upper reservoir, (17) Radiative heater for upper reservoir, (18) Top oven radiation shields, (19) Upper reservoir thermocouple, (20) Gas inlet tube, (21) Flow constrictor, (22) Heated Skimmer, (23) Thermal coaxial heaters for skimmer, (24) Heated pre-skimmer shield, (25) Thermal coaxial heaters for pre-skimmer, and (26) Rectangular beam-defining aperture.



XBL 834-9475A

Fig. 2

the sodium source chamber (1). The stainless steel oven chamber is divided into three areas. The bottom of the reservoir (2) contains the sodium metal that is heated by thermal coaxial cable brazed to the outside of the chamber (3). The temperature, typically 500°-600°C, of this chamber controls the vapor pressure of the sodium, and is measured by a thermocouple attached to the bottom of the oven (4). Two radiation shields surround the oven (5). This temperature is stabilized to $\pm 0.5^\circ\text{C}$ using a thermocouple comparator circuit to regulate the heater supply. A 3" long, 0.25" diameter tube (6) protrudes from near the top of the bottom reservoir region. This tube is heated separately to 750°C by thermal coaxial cable (7) vacuum brazed to it in order to prevent nozzle clogging, to prevent condensation of the sodium atoms during the supersonic expansion, and to determine the terminal velocity of the atoms. The nozzle temperature is also regulated to $\pm 0.5^\circ\text{C}$ using a thermocouple comparator circuit. A stainless steel disk 0.20" thick is welded to the end of the tube (8). The nozzle diameter in the center of this disk ranges from 100 μ to 250 μ . The nozzle tube is wrapped in three layers of radiation shielding -- thin sheets of stainless steel (9). Underneath the radiation shields approximately 10 mm. from the nozzle, a thermocouple (10) measures the temperature of the tube. The thermocouple is kept this far from the nozzle because by attaching the thermocouple directly to the nozzle enough heat is conducted away from the nozzle to cool and regularly clog the nozzle. When the ovens were heated under identical conditions and the sodium beam had the same velocity and profile, the thermocouple further from

the nozzle measured 120°C lower than the thermocouple at the nozzle. At the same height as the nozzle tube, three $1/4$ " stainless steel rods protrude from the oven (11). A 5 mm. long, loosely fitting ceramic tube (12) is placed on each rod to prevent the top reservoir heater from being in electrical contact with the oven. A thin stainless steel wire (13) is wrapped on the end of these rods to minimize the thermal contact with the water cooled copper blocks (14) that are clamped down on the rods. These blocks are connected to a larger copper structure that attaches rigidly to the front of the source chamber (15) and is used to align the nozzle before placing the source chamber into the molecular beams machine. Since the copper blocks are water cooled and do not change temperature substantially, the oven and nozzle are held in the correct aligned position. The upper reservoir chamber (16) has a conflat-like knife edge seal with a 0.005" nickel gasket. This port is used for loading sodium into the oven. This region is heated radiatively by a tungsten ribbon wrapped around eight alumina posts (17), held in place by slotted beads, and shielded by three layers of radiation shielding -- thin sheets of tantalum (18). A thermocouple (19) is attached to the top of the upper mini-conflat, and the temperature here is kept 25°C hotter than that of the bottom reservoir to prevent any condensation in this region. On the upper mini-conflat a $1/4$ " tube (20) extends up for the introduction of seeding gas into the oven chamber. Inside this tube is a $1/4$ " long molybdenum flow constrictor with a 0.005" clearance from the inside of the tube (21). This flow constrictor is held in place $1/4$ " from the opening of the

inlet tube into the reservoir chamber by a 0.018" wire spot welded several inches back along the gas inlet path. It is essential that this flow constrictor be pulled back from the opening since when it is nearer the opening it frequently clogs the gas inlet line. This flow constrictor prevents back diffusion of the sodium into the gas inlet path by increasing the local velocity of the seed gas around it. Only ultrahigh purity (0.99999) helium, neon, argon, and mixtures of the above are used for seeding the sodium beam.

The beam conditions are optimized for reactive signal and beam quality (high speed ratio). The sodium vapor pressure at 500°-600°C (the bottom reservoir temperature) varies from 3 to 25 torr. The beam velocity distributions for the various seed gases are given in section B below.

The Na rare gas mixture is expanded through the nozzle into a vacuum chamber maintained at $0.5-2 \times 10^{-4}$ torr. 0.25" to 0.30" in front of the nozzle is a stainless steel skimmer (22) with a diameter of 0.045". This skimmer is heated conductively by thermal coaxial cable (23) to 500°-600°C to prevent clogging with condensed sodium. A heated stainless steel shield (24), termed a pre-skimmer, prevents sodium condensation on the inner walls of the water-cooled source chamber, which would otherwise form a bridge to the skimmer, and clog it. The pre-skimmer is made from two disks sandwiching thermal coaxial cable (25), all vacuum brazed together. It is also heated to 500°-600°C.

Beyond the skimmer is a differential pumping region with a typical pressure of $2-10 \times 10^{-6}$ torr. This region is separated from the main chamber in which the scattering takes place by collimating slits. These slits are fashioned from 4 razor blades spot welded together to give a 0.53 mm. by 1.90 mm. rectangular aperture (26). This determines the beam dimensions at the scattering center to be 1.1 mm. high and 3.0 mm. wide.

The collision region is in the main chamber with a liquid nitrogen cold shield, and is typically at $1-2 \times 10^{-7}$ torr. A triply differentially pumped ultrahigh vacuum quadrupole mass spectrometer equipped with an electron bombardment ionizer and a Daly ion detector rotates about the collision region in the horizontal (scattering) plane. Its angular range is -6° to 98.5° (where 0° has the detector pointing into the atomic beam, and 90° has the detector pointing into the molecular beam). For a detailed description of the detector, see reference 5.

The (secondary) molecular beam source is a heated stainless steel tube with a 70μ platinum nozzle on the end as shown in figure 3. This nozzle is an electron microscope aperture held in place with a small copper gasket tightened on by screwing down a stainless steel cap (1) on the threaded end of the tube. Heating tape (2) is wrapped around the tube up to near a keying device (3). Two copper block heaters (4,5) with thermal coaxial cable running through them are clamped on the tube, one in back of the keying device, and one in front, flush with the nozzle tip. There are thermocouples (6) attached to the nozzle's copper block and underneath the heating tape. This source is

Fig. 3. Schematic of the supersonic molecular beam source and the associated chamber (adapted from a similar figure in reference 2, with permission):

- (1) Nozzle cap, (2) Heating tape for the gas inlet tube,
- (3) Keying device, (4) Copper block nozzle heater,
- (5) Nozzle pre-heater, (6) Thermocouple, and (7) Skimmer.

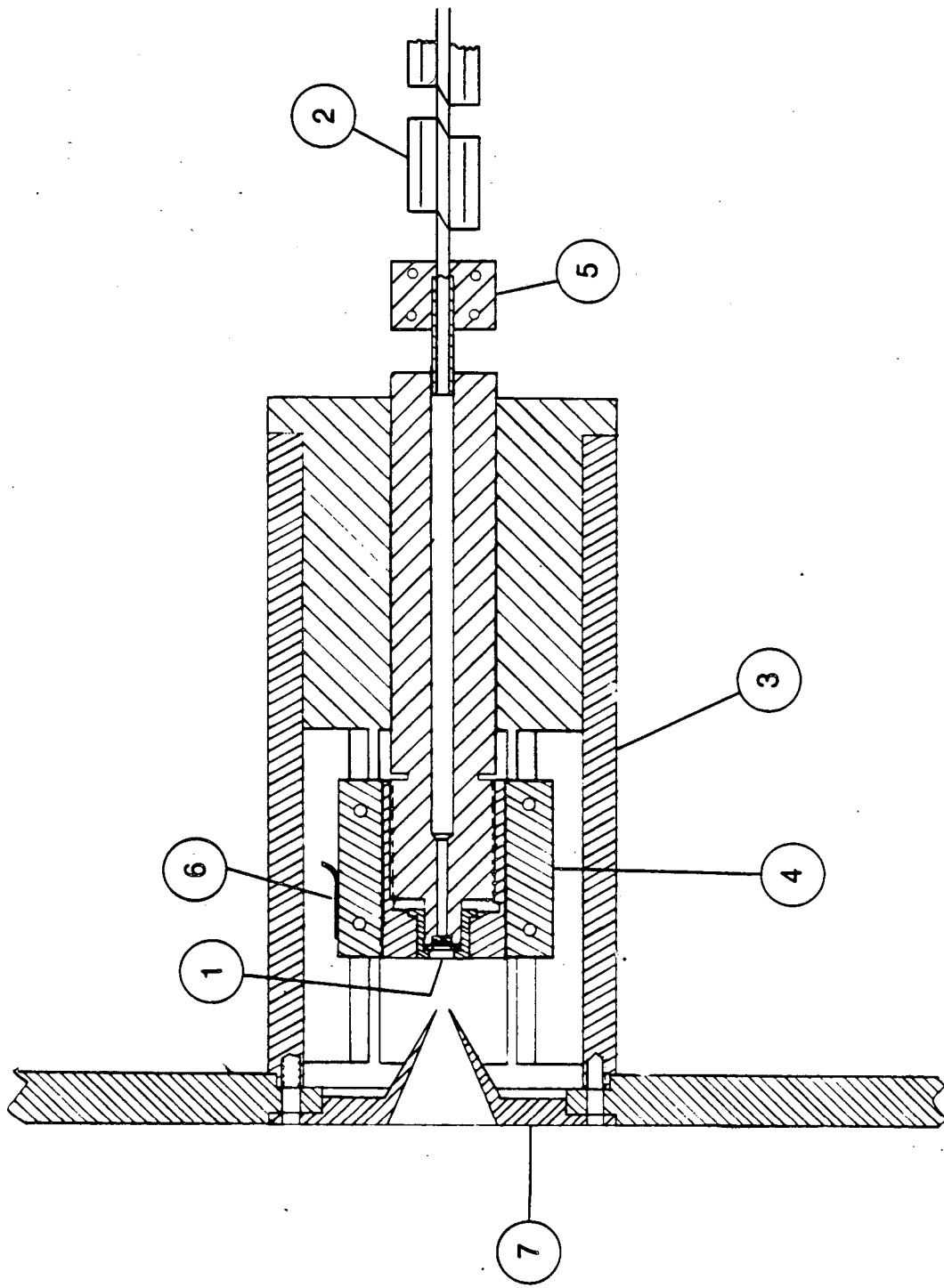


Fig. 3

used for all reactant molecular beams. The temperature of the nozzle's copper block is stabilized to $\pm 0.5^\circ\text{C}$ with a thermocouple comparator circuit referenced to an ice water bath. Neat or seeded supersonic beams are made by passing gas (neat or premixed) or by bubbling a gas through a volatile liquid held in a bubbler. The beam is expanded into a $0.5\text{--}2 \times 10^{-4}$ torr region. The beam is skimmed by a stainless steel skimmer with a diameter of 0.023" (7). Beyond the skimmer is a differential pressure chamber at $1\text{--}5 \times 10^{-6}$ torr which contains a 150 Hz tuning fork chopper (not shown) for modulating the secondary beam. This is mounted on a water cooled copper block mounted on the wall of the source chamber.

A collimating aperture 2.1 mm. high by 1.8 mm. wide similar to the one described above separates the differential region from the main chamber, and defines the secondary beam to be 2.7 mm. high by 2.1 mm. wide at the collision region.

The modifications to the crossed molecular beams machine all have to do with the introduction of the exciting lasers and the monitoring of the atomic fluorescence.

Two optical flats were placed on the main flange of the machine (the main door) facing the secondary molecular beam source -- one directly in the path of the molecular beam, and one 10" below that. One or two dye laser beams enter through the lower window and are reflected up into the crossing region perpendicular to the scattering plane (thus avoiding a Doppler broadening from all but the transverse velocity components of the sodium beam, and also keeping the laser

polarization in the scattering plane). The upper window is used for the collection of atomic fluorescence (particularly when products are predominantly scattered near the sodium beam, and the detector would block the view from the window located on the opposite side of the sodium beam, which is more commonly used). It can also be used for the laser to enter in the scattering plane, but still perpendicular to the sodium beam in order to study the difference between in plane and out of plane atomic orbital alignment.

A large flange in the line of the atomic beam was replaced by one with seven conflat ports. Three of these are equipped with conflat viewports that directly view the collision region. One is directly in the path of the sodium beam, and the image of the sodium beam through the rectangular collimating slits is apparent on it after running for a few hours. Another viewport is in the scattering plane and in line with the detector when the detector is placed at -12.5° . This port is normally used for the fluorescence monitor described below. All the fluorescence measurements shown were recorded with the fluorescence monitor in this position. The detector blocks the view of this port if it is at an angle below 16° .

Two other optical ports are on the machine on the two sides onto which the beam sources are mounted. Each makes a 45° angle with the atomic and molecular beam axes at their crossing point in the scattering plane so as to give a clear line of sight that passes through the crossing region. There is a Brewster window and a set of three sharp blackened apertures at each port to spatially filter the laser

and stray light. The laser is passed through these two ports in order to measure the Doppler profile of the Na D_2 line and thus the velocity profile of the sodium beam. The port near the sodium beam (the laser exit flange for the 45° crossing) is equipped with a simple system to measure two different colors of fluorescence using an interference filter and two photomultipliers.

The optical pumping setup is shown in figure 4. The Na($3^2P_{3/2} \leftarrow 3^2S_{1/2}$) D_2 transition is pumped by a Coherent Radiation Model 599-21 cw single-frequency actively stabilized linear dye laser using Rhodamine 6G, pumped by 2.7 W at 5145\AA using an argon ion laser. This laser outputs 70-100 mW at the 5892\AA (yellow-orange) Na D_2 transition wavelength. A second transition, either the Na($5^2S_{1/2} \leftarrow 3^2P_{3/2}$) transition at 6162\AA (red), or the Na($4^2D_{5/2} \leftarrow 3^2P_{3/2}$) transition at 5690\AA (green), is pumped by a Coherent Radiation Model 699-29 or 699-21 cw single-frequency actively stabilized ring dye laser using Rhodamine 6G pumped with 6.0 W at 5145\AA with an argon ion laser. At the 6162\AA (red) transition it put out 200-500 mW, and at the 5690\AA (green) transition it put out 400-800 mW. In some cases the laser frequencies were dithered $\pm 2-5$ MHz at 510 Hz and 23 Hz, respectively, and locked to the peak of the fluorescence (of the upper transition if two lasers were in use) using lock-in amplifiers. Neutral density filters are inserted into the laser path in order to ensure that saturation effects are not causing a reduction in the fraction of Na atoms optically pumped. This is discussed further in section D.

Fig. 4. Schematic of the optical pumping system used for the sodium atomic excitation. The symbols for optional components are in parentheses. The components are:

(BS) Beam Splitter, (M) Mirror, (GT) Glan-Thompson Prism, ($\lambda/4$) Quarter-Wave Plate, (FP) Fabry-Perot Etalon, (S) Shutter, (F) Filter, (PMT) Photomultiplier and/or Fluorescence Monitor, (Na) Sodium Source, (2°) Secondary Molecular Beam Source, and (MS) Quadrupole Mass Spectrometer.

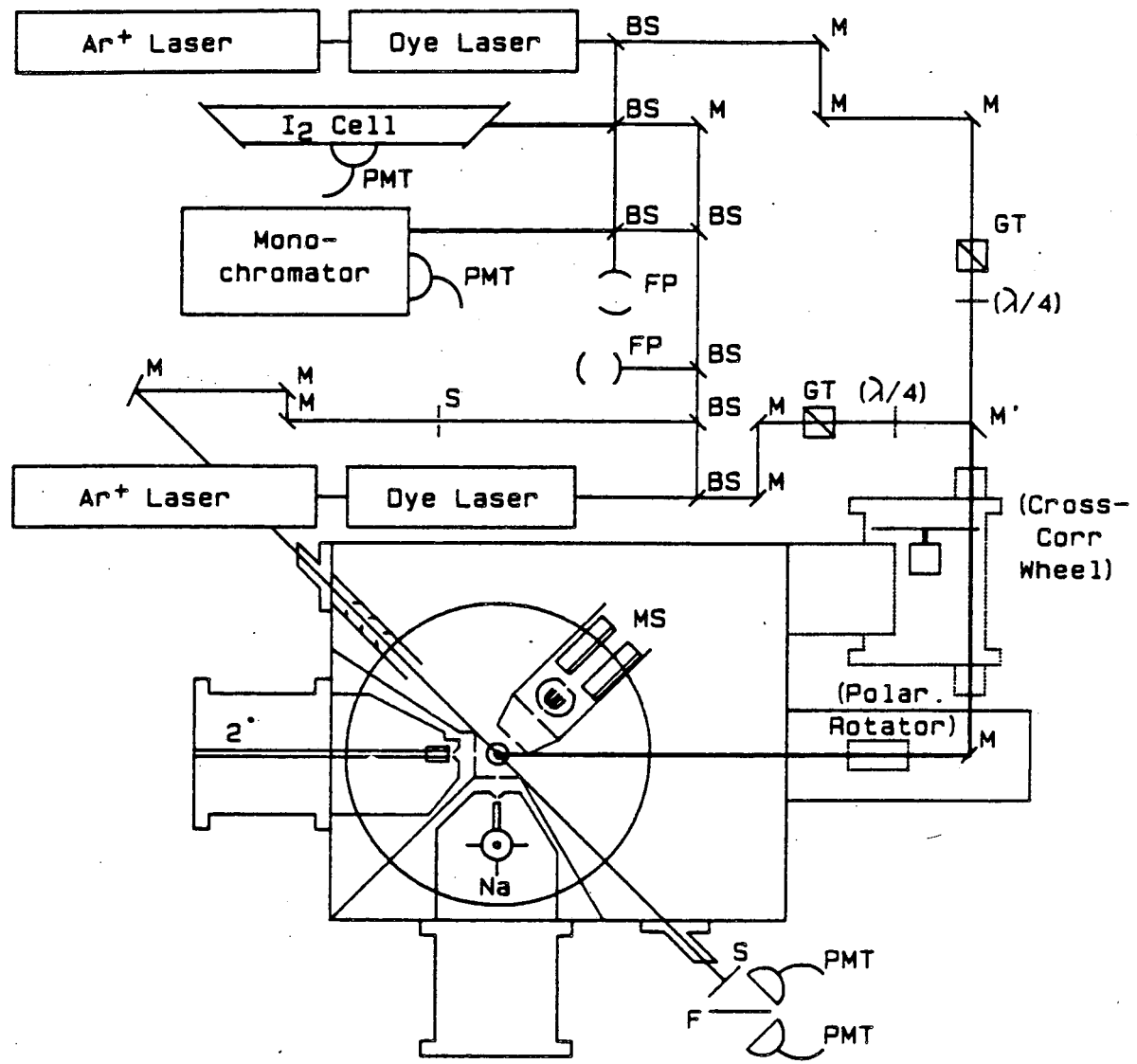
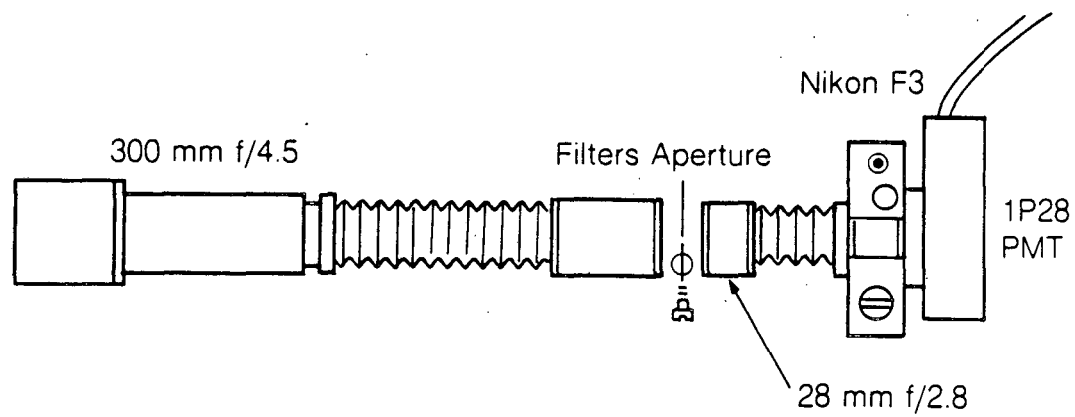


Fig. 4

As shown in figure 4 the two lasers are combined by having one laser beam nearly graze a mirror (M') off the edge of which the other beam is reflected. The two beams are thus very nearly parallel and their overlap is maximized in the collision region (after a path length of greater than 3 m.) by maximizing the laser produced reactive signal. The two laser polarizations are kept parallel at all times. Each laser is monitored with a spectrum analyzer (FP) with a 1.5 GHz free spectral range. An iodine cell is used to determine the frequency of the laser using the iodine atlas of Gerstenkorn and Luc.⁶ Approximately once an hour, a computer controlled shutter (S) sends a fraction of the 5890Å light to the 45° Doppler crossing path in order to measure sodium beam velocity profiles as described above. The lasers can be circularly polarized before being combined using quarter-wave plate ($\lambda/4$) for the 5890Å laser, and another quarter-wave plate or a Soleil-Babinet Compensator for the other laser. After being combined and before entering the main chamber the two lasers can be passed through a cross-correlation time-of-flight wheel. The wheel has a pseudo-random sequence of 255 on/off bits and can be spun up to 400 Hz in a vacuum chamber pumped down to 10^{-2} torr to give a time resolution of 10.0 μ sec.⁷ One or both of the lasers can be modulated at 3 Hz using a stepping motor driven beam flag (not shown) run synchronously with the 150 Hz tuning fork secondary beam chopper. Also the linear laser polarizations can be rotated in tandem using a computer controlled stepping motor driven double fresnel rhomb polarization rotator. As described above, the lasers enter the vacuum

chamber parallel to and below the secondary beam, and are reflected up into the collision region from a mirror on the bottom of the machine. This mirror is mounted on a heated platform to keep diffusion pump oil from condensing on it, and to prevent movement as the liquid nitrogen cold shield is cooled. Above the mirror is an aperture to spatially filter the laser light. This aperture is attached to the rotating detector, but the aperture is located on the detector's rotating axis, and is thus centered vertically below the collision region so that its position does not change as the detector is rotated. A photodiode attached to the differential wall of the machine is directly above the collision region and is used for the rough alignment of the laser position. The fine adjustment of position is done so as to optimize the reactive signal due to the laser excitation as seen by the mass spectrometer.

The machine has three possible positions for fluorescence monitors. The most commonly used positions are in line with the detector positions -12.5° and 90° (relative to the sodium beam). These fluorescence monitors are shown schematically in figure 5. A Nikon 300 mm. $f/4.5$ lens is placed near the machine window and is attached to a Nikon PB-6 bellows. If two lasers are in use, an interference filter or a color filter is placed behind the bellows so that the monitor only views the fluorescence of the upper transition. At the end of another bellows, a focal point is formed by the front lens at which an aperture is placed to spatially filter out stray light. This is followed by a reversed Nikon 28 mm. $f/2.8$ lens which is attached to yet another



XBL 861-10007

Fig. 5. Schematic of the fluorescence monitor used for the magnification and measurement of the sodium atomic fluorescence.

bellows, which is attached to a Nikon F3 35 mm. single lens reflex camera with a hole in its back and a photomultiplier tube (RCA 1P28) attached to it. This set up gives a magnification of 10x, making the 1 mm. x 3 mm. crossing region appear 10 mm. x 30 mm. on the photomultiplier tube. The fluorescence can be viewed visually through a 6X magnifying viewfinder (Nikon DW-4). A fluorescence monitor on the exit of the 45° laser crossing consists of a tilted interference filter which reflects one wavelength and transmits another so that two photomultipliers (RCA 1P28) record each fluorescence wavelength simultaneously. A shutter is closed when a Doppler velocity measurement is being done so as to avoid damaging the photomultipliers, and a different fluorescence monitor is used to record the velocity measurement.

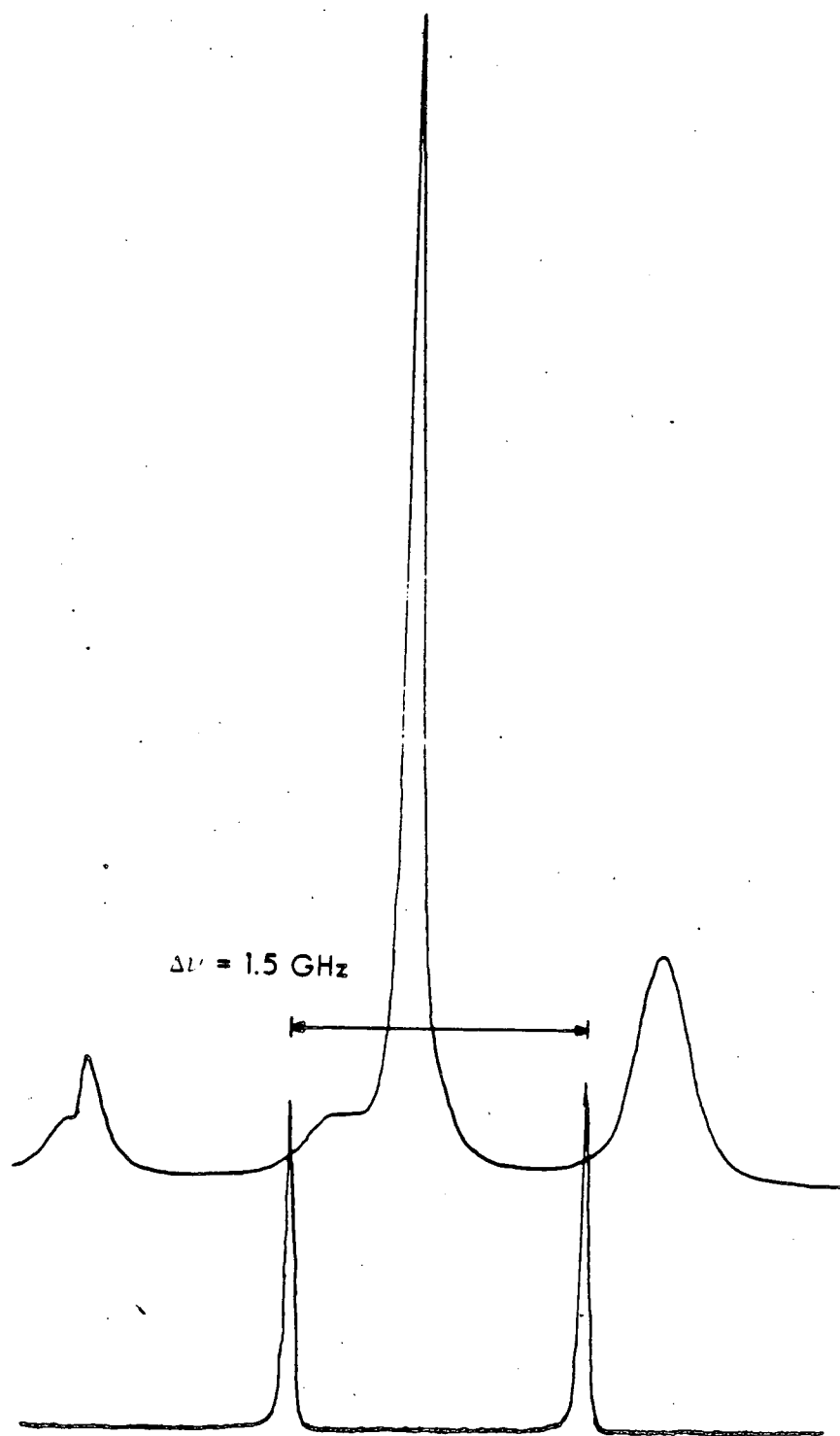
The experiment is controlled by an LSI-11/23 computer. Angular distributions and polarization dependences are recorded, and machine conditions are optimized with a program entitled SANG which is described in Appendix A. Time-of-flight measurements are made with a program named TUF, described in Appendix B. The details of the data acquisition are given in section C, below.

B. Atomic and Molecular Beam Conditions

As discussed above, three sodium atomic beam energies are most commonly used. The rare gas backing pressures used are: 200–1000 torr for helium, 100–400 torr for neon, and 100–400 torr for argon. The large ranges are due predominantly to the various nozzle sizes at which measurements were made. It was found necessary to seed the atomic beam with gases of research grade purity (0.99999, Scientific Gases), as impurities in lower grades of rare gases clogged the sodium beam too quickly for measurements to be made. No additional benefit was found when the backing gases were passed through a liquid nitrogen cold trap. The gas feed line to the reservoir was all metal, and this line must be leak tight.

Figure 6 shows three velocity measurements taken by scanning the dye laser across the $\text{Na}(3^2P_{3/2} \leftarrow 3^2S_{1/2}) D_2$ transition with the laser crossing the Na beam at both 45° and 90° . The recorded fluorescence shows (from right to left -- red to blue) the Doppler broadened and shifted 45° peaks and then the sharp unbroadened, and unshifted 90° peaks. There are two peaks of each type because the two ground state hyperfine levels ($F=1,2$) are separated by 1.77 GHz, and are thus spectrally distinct. Below each fluorescence trace is the simultaneously recorded output of a spectrum analyzer (Fabry-Perot etalon) used as a relative frequency standard. This etalon (Tropel Model 210) has a free spectral range of 1.5 GHz and a finesse of 200. In the cases of sodium

Fig. 6. Velocity measurement of sodium atomic beams produced with three different seed gases: a) Helium, b) Neon, and c) Argon.



XBL 861-85

Fig. 6(a)

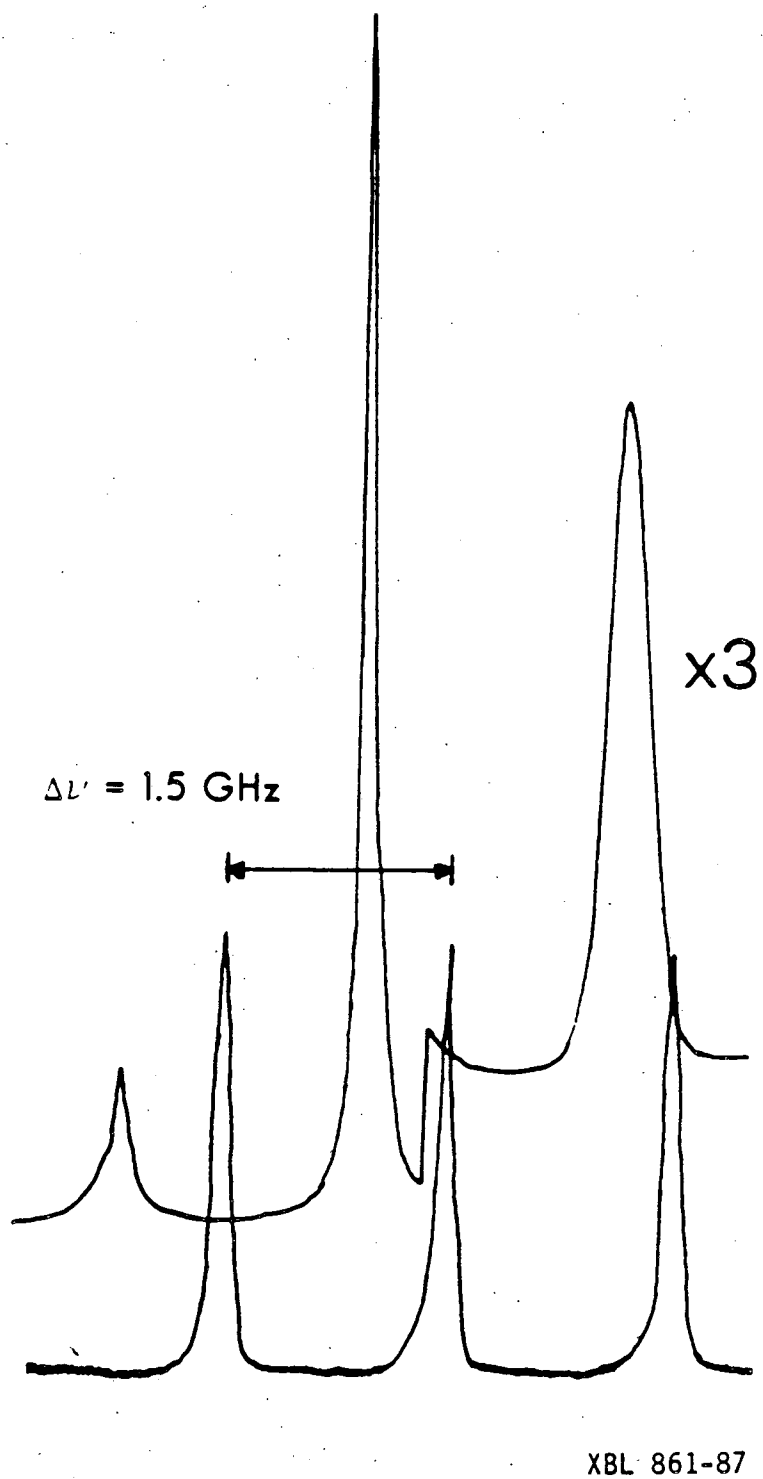
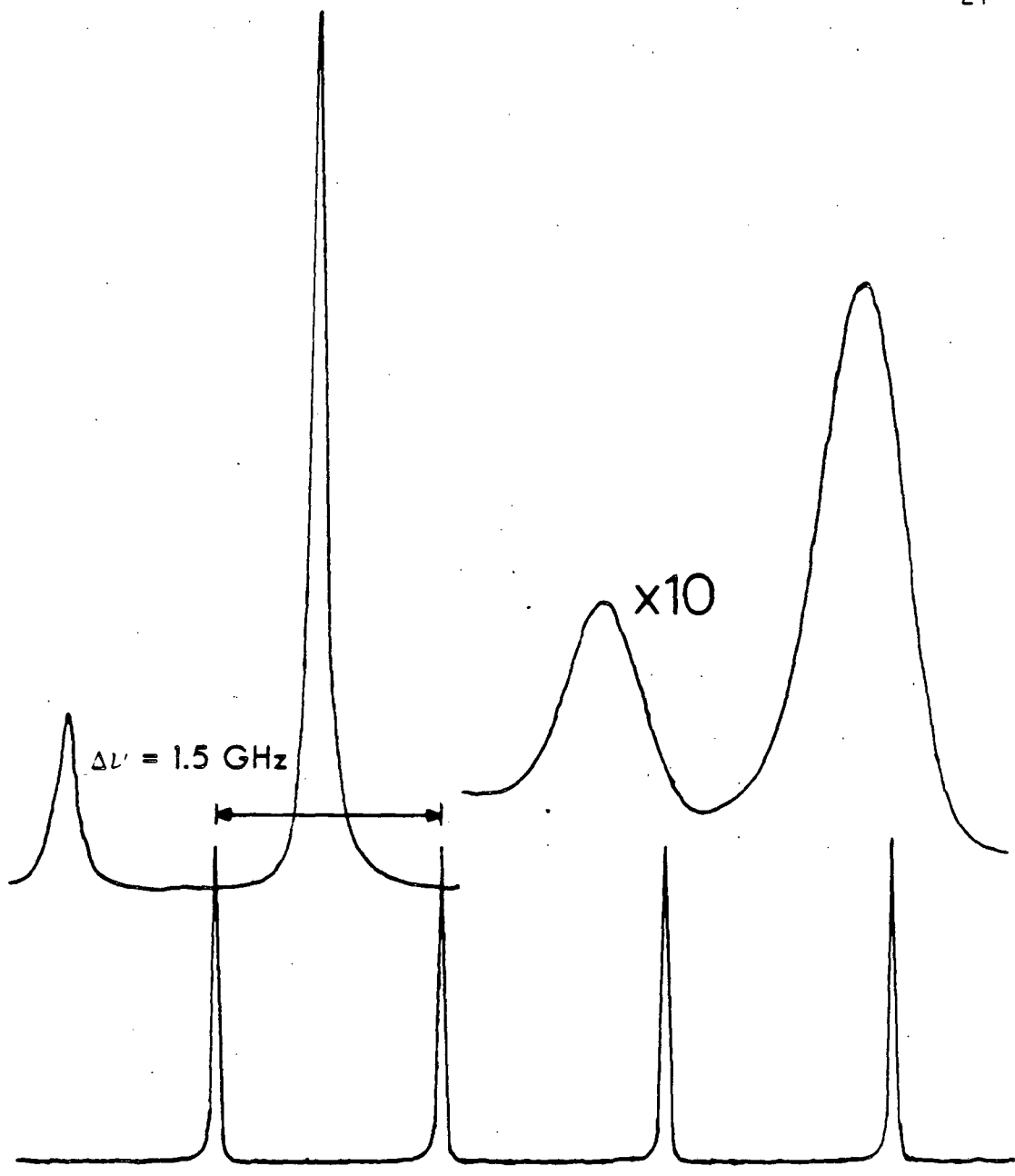


Fig. 6(b)



XBL 861-86

Fig. 6(c)

seeded in neon and argon, the weak (corresponding to $F''=1$) 45° peak is buried under the strong (corresponding to $F''=2$) 90° peak. In each case, to convert the peak separations into velocities the distance between the strong 45° and 90° peaks and between the Fabry-Perot peaks, and the full width half maximum of the strong 45° peak are measured either by hand or if the computer was used to record the Doppler scan, it is also capable of making these measurements automatically. The 90° to 45° peak separation and the 45° width are converted into frequencies and the following Doppler formula is used:

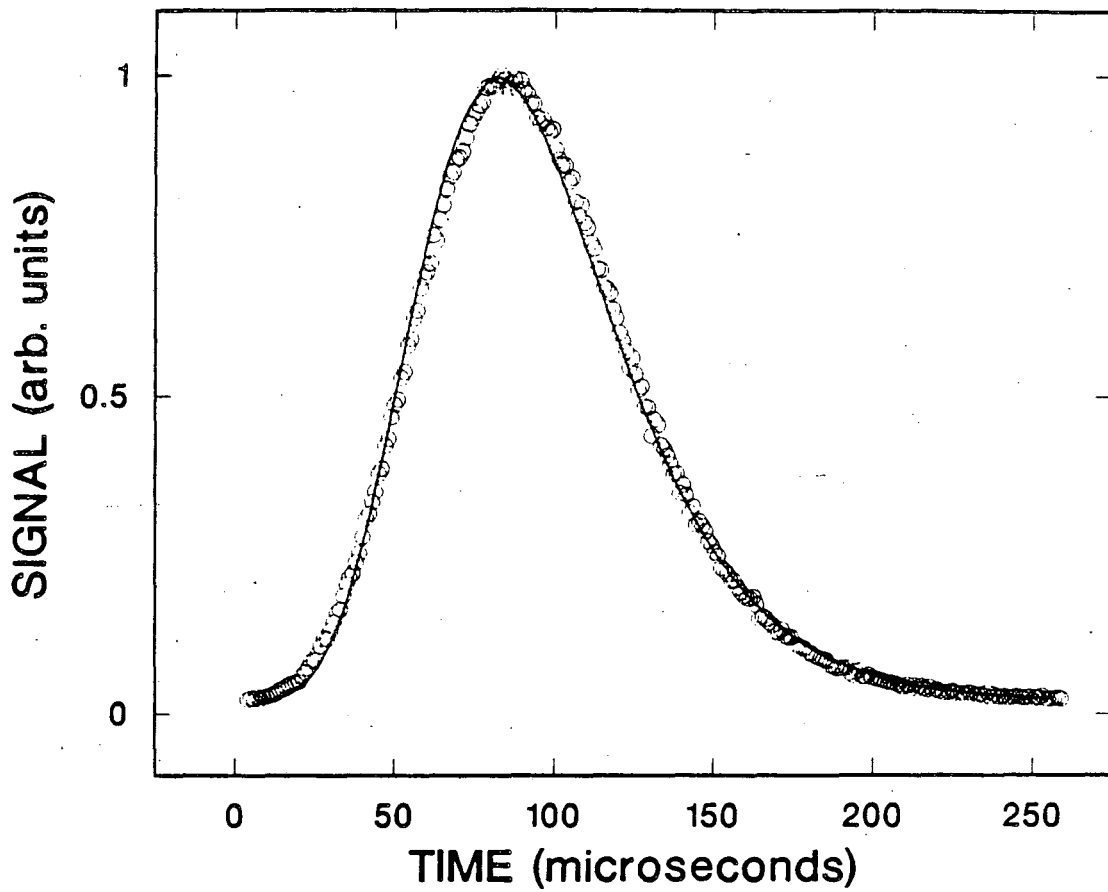
$$v = \frac{c \Delta\nu}{\nu \sin 45^\circ} \quad (1)$$

where v is the velocity being measured in cm/sec, c is the speed of light, in cm/sec, $\Delta\nu$ is the measured frequency difference between the two velocity components of interest in GHz, and ν is the sodium D_2 transition frequency, 5.092×10^5 GHz (16973 cm^{-1}). The speed ratio ($S = v/\Delta\nu$) is just the ratio of the measured 45° to 90° peak separation to the measured width of the 45° peak. The values of the peak velocity and speed ratio for the three backing gases commonly used are shown in table I. Intermediate velocities are obtained by mixing combinations of helium and neon. A Matheson rotameter is used to keep the flow of each gas constant to 5%. In this case, the sodium beam velocity is measured as above.

Table I. Measured sodium beam velocities and speed ratios for the three commonly used seed gases.

Seed Gas	Peak Sodium Velocity (/10 ⁴ cm/sec)	Speed Ratio
Helium	30.0	6
Neon	16.0	5
Argon	10.8	5

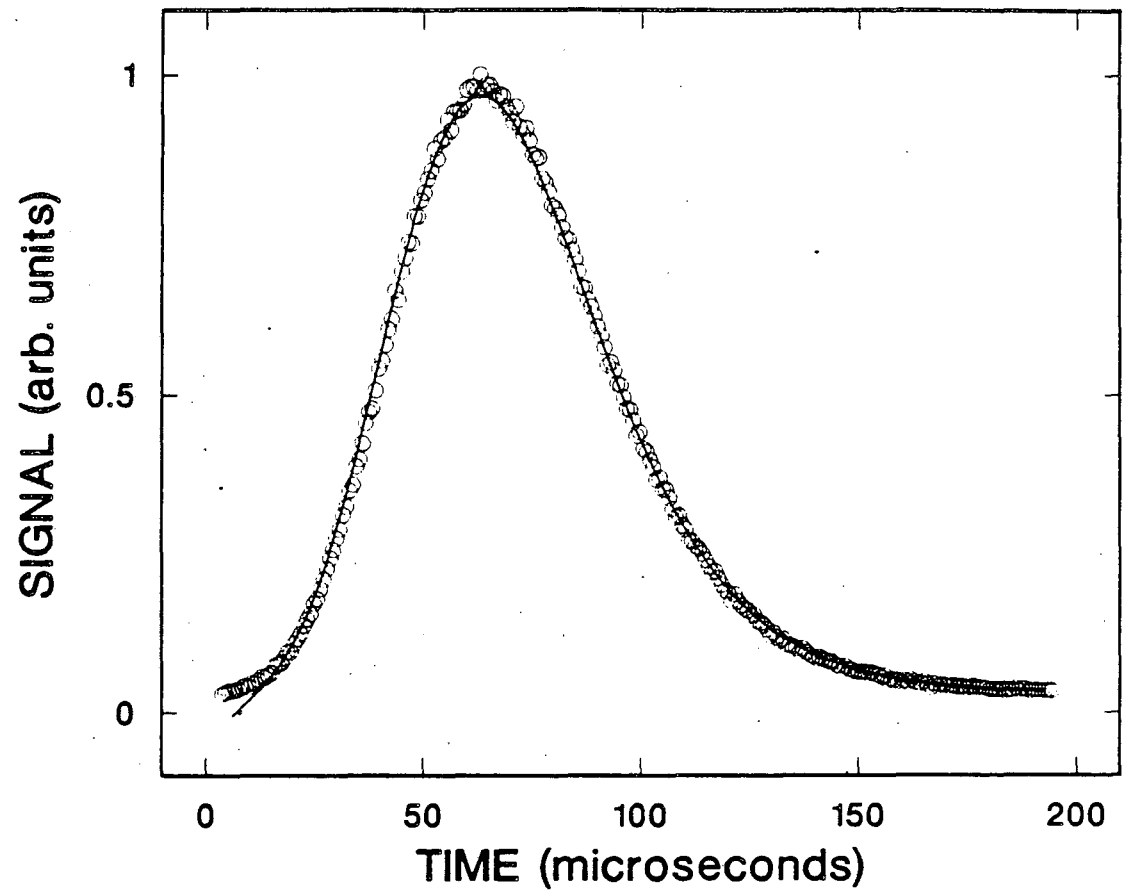
The secondary beams' conditions used for the measurements discussed in the following chapters are shown in table II. When gas mixtures are shown, these are premixed either commercially or in our lab. The beam velocities were measured using the time-of-flight method on another crossed molecular beam machine using flight length and detection delays calibrated with rare gas beams of helium and argon. A 17.8 cm. diameter wheel with eight .75 mm. slots was used to modulate the beam. After modulation, the neutral flight length was approximately 20 cm. The distributions were recorded using the program TUF⁸ with dwell times of 500-1500 nsec per channel. The program KELVIN¹ was modified (to accept the output of TUF) and used to fit the measured distributions to peak velocities and speed ratios. The measured beam time-of-flight distributions are shown for neat beams of HCl and O₂ and O₂ seeded in helium in figures 7, 8a, and 8b, respectively. These measurements were not always made for beams for which quantitative conversions of laboratory data to the center-of-mass frame of reference were not to be



XBL 863-823

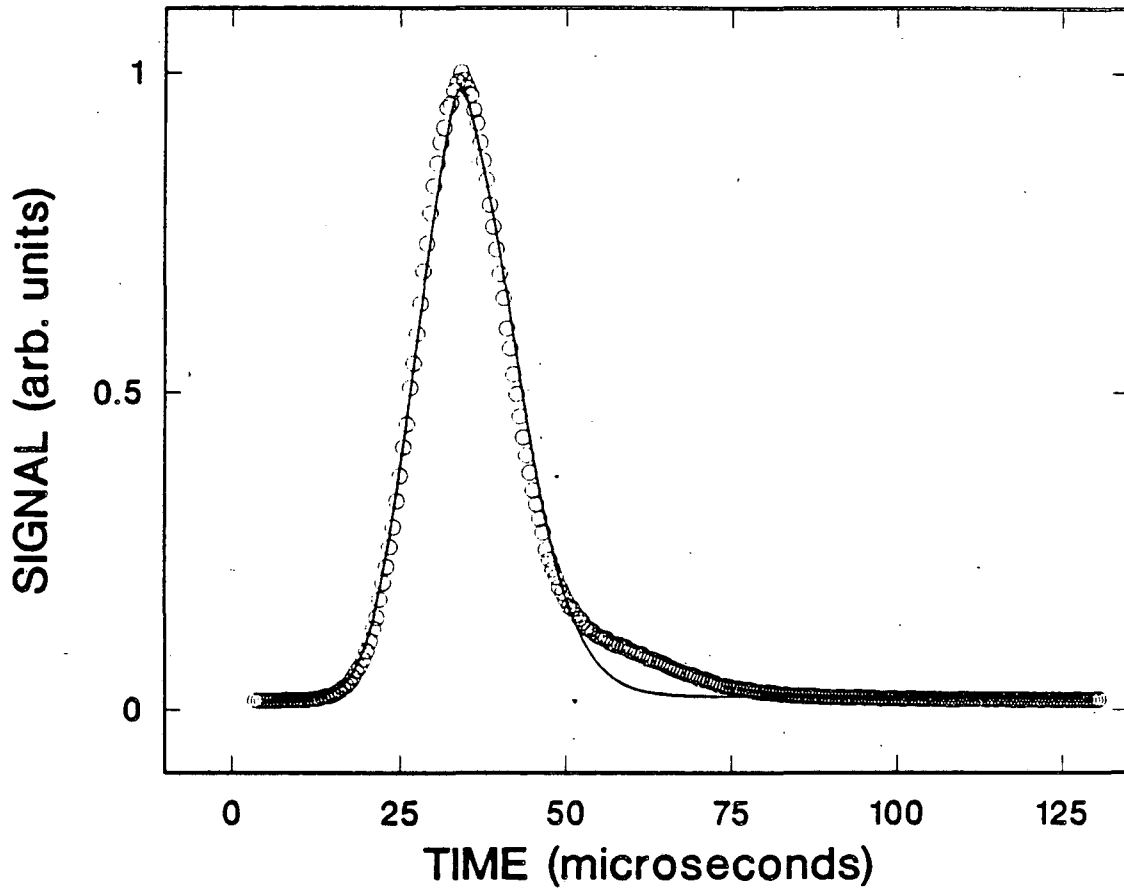
Fig. 7. Measured time-of-flight distribution for a neat HCl molecular beam under the conditions used for the experiments in chapter II. The solid line is the fit to the distribution using program KELVIN.

Fig. 8. Measured time-of-flight distributions for the O_2 molecular beams used for the experiments in chapter III. The solid line is the fit to the distribution using program KELVIN.² The distributions are: a) neat O_2 , and b) O_2 seeded in helium.



XBL 863-824

Fig. 8(a)



XBL 863-825

Fig. 8(b)

made. The velocities of the unmeasured beams were estimated from nozzle temperatures assuming essentially complete rotational relaxation (as in reference 1).

Table II. Velocities and speed ratios for molecular beams used in reactive scattering studies.

Reactant Beam	Seed Gas	Nozzle Temperature (°C)	Beam Velocity ($\times 10^4$ cm/sec)	Speed Ratio	Fig.	Chap.
CH ₃ Br	none	200	5.8	4		4
5% CH ₃ Br	He	200	12.6	4		4
Cl ₂	none	179	6.1	5		5
HBr	none	200	5.8 (Est.)	4		2
HCl	none	179	8.6	4.5	7	2
HF	none	250	12.3 (Est.)	4.6		2
O ₂	none	200	9.8	8	8a	3
5% O ₂	He	200	15.0	12	8b	3

C. Data Acquisition

The data acquisition is automated using a Digital Equipment Corporation LSI-11/23 computer and a CAMAC crate (IEEE Standard 583-1975). The programs used for data acquisition are described in appendices A and B, but their specific usage is described below.

On each new reactive system the first experiment performed is the measurement of one or more product angular distributions. Six channels of data are recorded simultaneously from two sources. These channels are defined in table III. The signal from the quadrupole mass spectrometer (labeled detector in table III) is taken from the Daly detector's photomultiplier (RCA 8850) and put into a quad discriminator (LeCroy 821), the fanout of which is put into the four inputs of a CAMAC 125 MHz quad scaler with external gating (Joerger S1-Ind). The other source of signal is from the fluorescence monitor (labeled fluorescence in table III). This signal is run through a current amplifier (Keithley 427) into a gated integrator (Evans 4130), the overflow of which is converted to NIM pulses and is input into another channel of the quad discriminator for the fanout capabilities, and then is recorded using another (Joerger) quad scaler. The signal is gated using the output of a CAMAC powered Laser Gate Generator (LBL, Lawrence Berkeley Laboratory). This gate generator takes as input the output of a NIM Timer-Gater module (LBL 13X-3050-II) which converts the signal

Table III. The definitions of channels recorded for angular distributions and polarization measurements, and the origins of the various signals.

Channel	Laser(s') Status	Molecular Beam Status	Signal Source
1a	On	On	Detector
1b	On	Off	Detector
2a	Off	On	Detector
2b	Off	Off	Detector
3a	On	Independent	Fluorescence
3b	Off	Independent	Fluorescence

from the 150 Hz tuning fork chopper that modulates the secondary (molecular) beam into gate information. The phase and gate width are variable on this device. The laser gate generator also is used with a CAMAC powered Motor Sync Scaler (LBL 13X-3441-P1-A) which outputs a pulse every 25 periods of the tuning fork chopper in order to change the state of the laser at a frequency of $150/25$, or 6 changes per second, giving a total modulation frequency of 3 Hz. After every 24 periods of the tuning fork chopper, all counting is gated off for 1 period and a stepping motor is used to change the state of the laser beam flag. If only one laser is in use, it is blocked and unblocked. If two lasers are in use, one or both can be blocked and unblocked. In two laser experiments, the reactions of four electronic states are measured. First, the Na(4D) vs. Na(3P) distributions are measured by

having the yellow-orange (Na(3P \leftarrow 3S) transition) laser always on, with the green (Na(4D) \leftarrow Na(3P) transition) laser blocked and unblocked. Then, the Na(5S) vs. Na(3S) distributions are measured by blocking and unblocking the yellow-orange (Na(3P \leftarrow 3S) transition) and the red (Na(5S \leftarrow 3P) transition) lasers with the beam flag.

The scattering signals are derived as shown below. The laser off signal (OFF) is:

$$\text{OFF} = (2a - 2b) / \text{TIME}, \quad (2)$$

where 2a and 2b are the number of counts in scaler channels 2a and 2b, respectively, from table III, and TIME is the actual counting time for each channel. The counting time for a single measurement is:

$$\text{TIME} = \frac{1}{2} \frac{24}{25} 150 (\text{Gate Width}) (\text{Countdown Time}), \quad (3)$$

where the gate width and countdown time are Timer-Gater settings, in seconds. The laser on signal (ON) is:

$$\text{ON} = (1a - 1b) / \text{TIME}. \quad (4)$$

The signal due to the excited state (EXC) can be easily derived from the above:

$$\text{EXC} = \frac{\text{ON} - [(1 - \text{FE})\text{OFF}]}{\text{FE}}, \quad (5)$$

where FE is the fraction excited. Note that the contribution to ON due to the fraction remaining in the lower state (1 - FE) is removed.

"Loop mode" of program SANG (described in appendix A) is used to record the angular distributions. An angular range and an angular interval are chosen for the scan. For example, the range might be 20° to 80° , with data recorded every 2° . Each angle is measured for a set countdown time, typically 60 seconds in real time. An angle is chosen for the normalization of the data (to counteract the effects of long term drifts in machine conditions); this angle is usually chosen to be the peak of the reactive signal. After every ten measurements, this angle is measured two, four, or more times. The time at which each measurement is taken is recorded, and the data is normalized later by taking a linear interpolation in time between successive sets of normalization measurements.

Polarization measurements are recorded with program SANG in "polarization rotation mode" with this same setup, but with the addition of the broadband polarization rotator (Spectra Physics 310A). This polarization rotator is mounted and attached to a stepping motor (Slo-Syn M062-FC09E) driven by a CAMAC pulse generator (Kinetic Systems 3360). The polarization angle resolution (minimum step size) is 0.8° , where 180° is a full cycle. After over 1000 cycles of the polarization rotator no deviation from its expected angular position is observed. Eight steps are typically chosen per cycle, and, as for angular distribution measurements, the measurement is usually made for 60 seconds in real time after which the rotator is automatically advanced to its next position. Note that each polarization rotation measurement is made

with the mass spectrometer held at a fixed angle, and different distributions are seen for different detector angles. For the experiments discussed in subsequent chapters the laser polarization was only rotated in the scattering plane, however by using a different laser entry window, the laser polarization can be rotated out of the scattering plane also. This has been done in recent measurements of Na + HCl.⁹

The favored polarization angle (ϕ) and the amplitude of the polarization dependence ($2A$) are determined by fitting a cosine curve of the form:

$$\text{Normalized Signal} = A\cos(2(\theta - \phi)) + (1 - A) \quad (6)$$

to the reactive signal. The same is done for the fluorescence signal for the signal from a fixed fluorescence monitor in the plane of the scattering. This fluorescence amplitude provides a direct measure of the fraction of atoms aligned as discussed in section D. The fit of equation (6) to the fluorescence data (shown in chapters II and III) gives the amplitudes as $2A=0.35$ for the 3P excitation, and $2A=0.32$ for the 4D excitation.

The time-of-flight measurements reported here are made by modulating the laser with a pseudo-random binary sequence of 255 bits photoetched as slots on a wheel that is spun up to 392 Hz to give a time resolution of 10 μ sec over the 20.8 cm. flight path of the reaction products. As discussed in reference 1, this has the disadvantage of modulating any signal due to ground state in the opposite direction, and this data must be either measured or accurately

synthesized in order to be taken into account in the subsequent data analysis. An auxiliary slot in the cross-correlation wheel is monitored by having a light-emitting diode on one side of the wheel and a photodiode on the other. The brief signal from the wheel is converted into a TTL pulse by triggering a pulse generator (Systron Donner 101) the negative output of which goes to the trigger input of a CAMAC 4096 channel scaler (LBL, described in appendix B). The data is the mass spectrometer signal taken from the fanout of the quad discriminator (described above) which is converted to TTL pulses, then is sent to the data input of the multichannel scaler. Program TUF (described in appendix B) is used to record the time-of-flight data.

The data is transformed from the laboratory frame of reference in which it is recorded to the center-of-mass frame of reference in which it is easily interpretable using a derivative of the program CMLAB¹⁰ entitled GM which runs on the DEC VAX 8600 computers at the Lawrence Berkeley Laboratory computer center. This program assumes separable parameterized center-of-mass angular ($T(\theta)$) and translational energy ($P(E_T)$) distributions, and calculates laboratory angular and velocity distributions taking into account beam velocity spreads, and finite modulation width and ionizer length.^{9,10} The parameters for the center-of-mass distributions are varied iteratively in order to minimize the differences of the measured and calculated laboratory angular and velocity distributions. In this calculation it is assumed that the reactant orientations average to give cylindrically symmetric

product distributions about the relative velocity vector. In the case of laser excited sodium atoms this is, in general, not correct (when the laser polarization is along the relative velocity vector it is correct). The effect of this asymmetry is not more than 15 percent as shown by the polarization dependences in chapters 2 and 3, and thus has been ignored for the analyses done here.

It should be noted that in the version of CMLAB given in reference 10, and the versions used for the last few years, the product translational energy distribution is normalized incorrectly, giving false values of the relative cross sections. As far as can be determined, no such values have been reported. The problem lies in the fact that the laboratory scattering data is synthesized from the center-of-mass information by using a grid of laboratory velocities. As pointed out in reference 10, this is nearly equivalent to using $P(u)$, the probability distribution of product center-of-mass velocities (u), rather than $P(E_T')$, the probability distribution of recoil energies. Thus, since

$$E_T' = \frac{1}{2} \mu_{\text{Prod}} u_{\text{rel}}^2 \quad (7)$$

where μ_{Prod} is the product reduced mass, if $P(u)$ is substituted for $P(E)$ in the transformation Jacobian, there is a further transformation factor:

$$P(u) = P(E) \frac{dE}{du} = P(E) \mu_{\text{Prod}} u_{\text{rel}} \quad (8)$$

The factor u was correctly taken into account in the transformation, but the product reduced mass was not. This made any comparison of branching ratios where product channels have different reduced masses incorrect. Also, calibration of relative cross sections using elastic scattering data was not possible. Furthermore, $P(E)$ was normalized so that all intensity information was carried in the computed scaling factors, and in $T(\theta)$, the center-of-mass product angular distribution. However, since $P(u)$ is used in the transformation, this is what needs to be normalized.

Both the problems of the product reduced mass and the normalization of $P(u)$ have been corrected in all versions of GM dating from the beginning of 1986 onward.

D. Optical Pumping

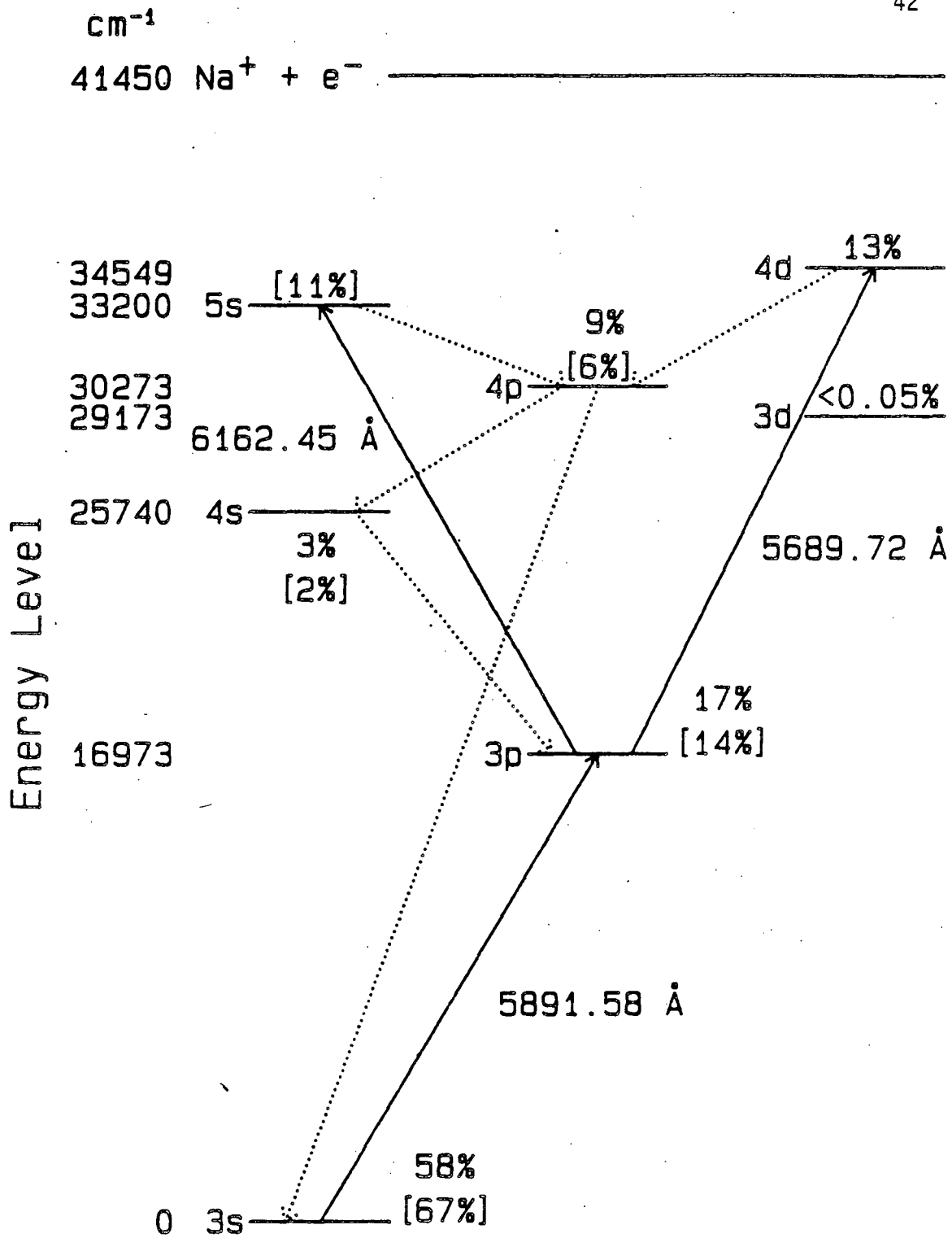
1. Introduction

In determining the reactivity of the excited state atoms it is of fundamental importance to know the fraction of the atoms populating these states. It is difficult in the apparatus described above to make a direct measurement of the optical pumping efficiency. It is certainly possible to optimize the optical pumping (laser frequencies, powers, and positions) on reactive signal due only to the excited state produced, but it remains difficult to know the actual fraction excited.

One possible method of obtaining the fraction excited is to find a system in which the excited state gives no signal under the same circumstances that the ground state does. Then, the fraction of the ground state signal depleted on excitation is exactly equal to the fraction excited. Of course, unless it was certain that the excited state yielded no signal, the excited state fraction obtained in this manner would be only a lower limit. No good example of such a situation was found in the experiments conducted.¹¹

The Na atomic energy levels are shown in figure 9. The fine and hyperfine structure are not shown in this figure. The three upward pointing arrows show the essential transitions optically pumped. The transition moments are quite well known for Na atoms. The Einstein A coefficients have been measured experimentally¹² and calculated¹³ for all the states relevant to the present study. These values are given in table IV. To pump the Na($3^2P_{3/2}$) state a single laser (usually the Coherent 599-21 cw dye laser) is tuned to the $16973.379 \text{ cm}^{-1}$ (yellow-orange) Na($3^2P_{3/2}, F=3 \leftarrow 3^2S_{1/2}, F=2$) transition, part of the Na D₂ line. In order to pump the $5^2S_{1/2}$ state, a second laser (the Coherent 699-21 or 699-29 cw ring dye laser) is tuned to the $16227.317 \text{ cm}^{-1}$ (red) Na($5^2S_{1/2}, F=2 \leftarrow 3^2P_{3/2}, F=3$) transition. To pump the $4^2D_{5/2}$ state, the second laser (the Coherent 699 as for the 5S) is tuned to the $17575.410 \text{ cm}^{-1}$ (green) Na($4^2D_{5/2}, F=4 \leftarrow 3^2P_{3/2}, F=3$) transition. Note that in pumping the $5^2S_{1/2}$ and $4^2D_{5/2}$ states, the 4S and 4P states are radiatively populated. This is discussed further in section D3, below.

Fig. 9. The sodium atomic levels relevant to the optical pumping. The fine and hyperfine structure levels are not shown. The relative populations of the various sodium levels as calculated in reference 22 for optically pumping the $\text{Na}(4^2D_{5/2})$ [$\text{Na}(5^2S_{1/2})$] state.



XBL 861-80

Fig. 9

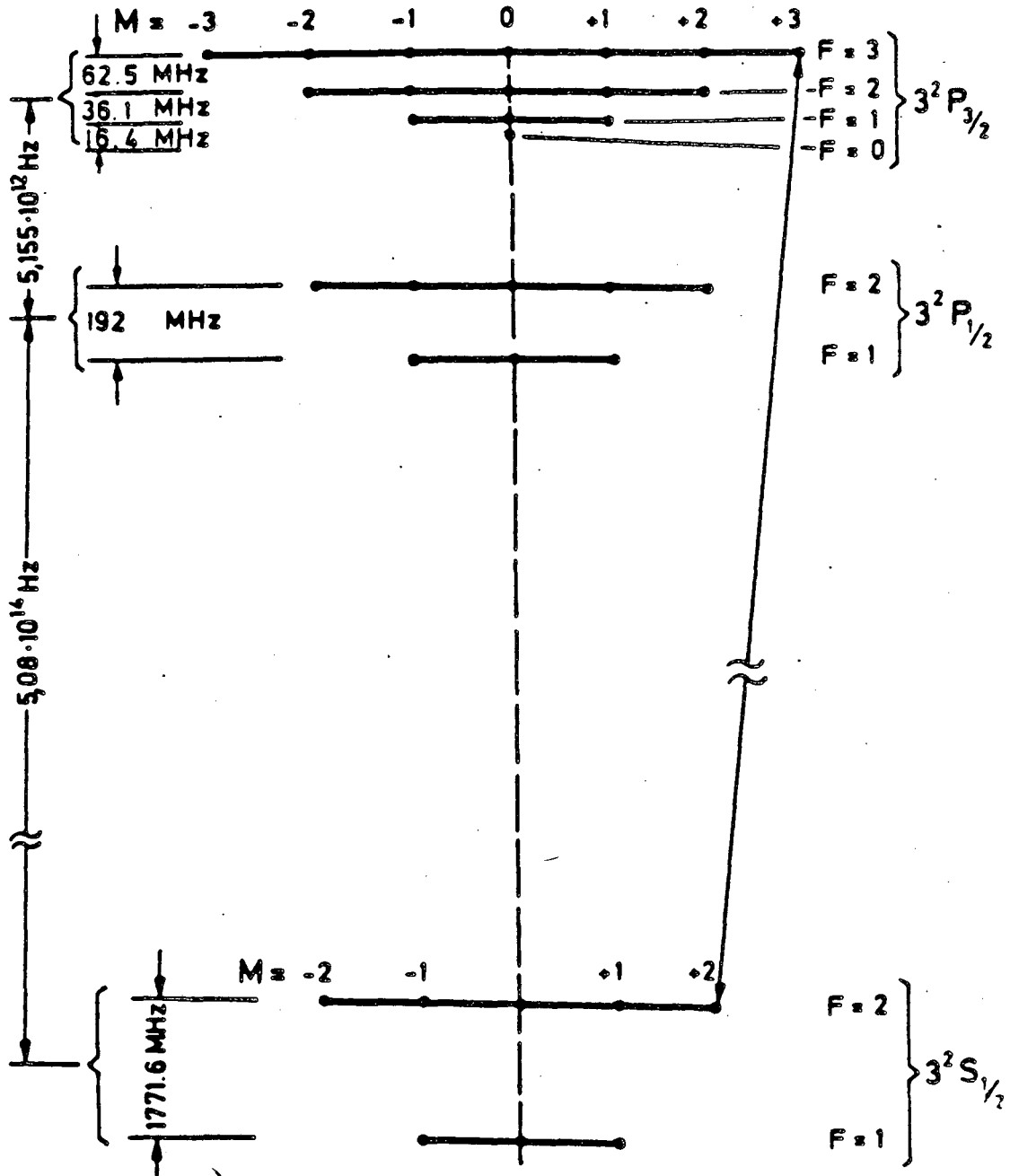
Another important question is what are the population distributions among the various hyperfine levels and sublevels excited? Also, what is the meaning of the hyperfine level and sublevel (F, m_F) populations in terms of the excited electronic orbitals (L, m_L)? If the chemistry of the excited state is to be understood, it would be very useful to have a clear picture of the orbitals produced in the excitation. These pictures can be quantified in terms of the multipole moments of the distributions populated as discussed by Hertel and coworkers,^{14,15} and reviewed below.

2. The Na D_2 Transition

Figure 10 shows the hyperfine levels of the states involved in pumping the Na D_2 line. The quantum numbers $L, S,$ and J have their usual meanings, but since ^{23}Na has a nuclear spin $I=3/2$, the quantum number F , where

$$\underset{\sim}{F} = \underset{\sim}{I} + \underset{\sim}{J} \quad (9)$$

describes the total angular momentum. Fischer and Hertel have discussed the optical pumping of the Na D_2 transition.¹⁴ They came to the conclusion that in steady state 31% of the atoms could be in the excited state.¹⁶ Since the $3P$ lifetime is only 16.9 nsec,¹³ a cycling occurs in the optical pumping in which the atoms are excited and radiatively decay many times while in the laser field. In the experiments described here, the mean number of pumping cycles on the D_2 transition ranges from 60 to 180, depending on the residence time



XBL 863-790

Fig. 10. Hyperfine structure of the $\text{Na}(3^2P_{3/2} \leftarrow 3^2S_{1/2})$ transition. Reproduced for reference 15 with permission.

Table IV. Einstein A coefficients for the transitions important in the optical pumping of the Na(3P,4D,5S) states. The values of A given are in units of 10^6 sec^{-1} .

Lower State	Upper State	Calculated ¹³ A	Experimental ¹² A
$3^2S_{1/2}$	$3^2P_{1/2}$	58.9	61.8
$3^2S_{1/2}$	$3^2P_{3/2}$	59.1	62.2
$3^2S_{1/2}$	$4^2P_{1/2}$	2.85	2.81
$3^2S_{1/2}$	$4^2P_{3/2}$	2.85	2.81
$3^2P_{1/2}$	$4^2S_{1/2}$	8.26	8.9
$3^2P_{1/2}$	$3^2D_{3/2}$	41.3	45.3
$3^2P_{1/2}$	$5^2S_{1/2}$	2.29	2.6
$3^2P_{3/2}$	$3^2D_{3/2}$	8.26	9.0
$3^2P_{3/2}$	$3^2D_{5/2}$	49.5	54.
$3^2P_{3/2}$	$4^2S_{1/2}$	16.4	17.6
$3^2P_{3/2}$	$4^2D_{5/2}$	11.9	12.
$3^2P_{3/2}$	$5^2S_{1/2}$	4.58	5.2
$3^2D_{3/2}$	$4^2P_{1/2}$	0.15	-
$3^2D_{3/2}$	$4^2P_{3/2}$	0.016	-

Table IV, cont.

Lower State	← Upper State	Calculated A ¹³	Experimental A ¹²
$3^2D_{5/2}$	$4^2P_{3/2}$	0.14	-
$4^2S_{1/2}$	$4^2P_{1/2}$	6.44	-
$4^2S_{1/2}$	$4^2P_{3/2}$	6.47	-
$4^2P_{1/2}$	$5^2S_{1/2}$	1.70	-
$4^2P_{3/2}$	$4^2D_{5/2}$	6.84	12.
$4^2P_{3/2}$	$5^2S_{1/2}$	3.38	-

of the Na atoms in the interaction region, and thus upon the Na beam velocity. Subsequent experiments by Hertel and coworkers have shown the optical pumping efficiency to be more on the order of 15-20%.¹⁷ Hertel and Stoll used a rate equation approach to model the excitation process. Cohen-Tannoudji has treated a two level system more rigorously with a "dressed atom" model to take into account more fully the interaction of the atom with the field.¹⁸ Cohen-Tannoudji has shown that for a two level system the rate equation method gives similar results. Hertel and Stoll have extended this to show that rate equations are useful in the case of pumping the Na D₂ transition.

Linearly or circularly polarized light can be used to optically pump this transition. For linearly polarized light, the selection

rules have $\Delta F = \pm 1, 0$, $\Delta m_F = 0$ transitions allowed, except for the forbidden $\Delta F = \Delta m_F = m_F = 0$ transition. For right (left) circularly polarized light only the $\Delta F = \pm 1, 0$, $\Delta m_F = \pm 1$ (-1) transitions are allowed. In fluorescence, the $\Delta F = \pm 1, 0$, $\Delta m_F = \pm 1, 0$ transitions are all allowed except for the forbidden $\Delta F = \Delta m_F = m_F = 0$ transition.

The most stable situation for optically pumping to the 3P level is to pump only the $F'=3 \leftarrow F''=2$ transition, because the selection rule $\Delta F = \pm 1, 0$ forbids radiative decay into the unpumped $F''=1$ level. The ground state levels are spectrally distinct, but care must be taken not to excite into more than one hyperfine level of the excited state, since if the $F'=2$ level is excited, it will fluoresce down to the dark $F''=1$ level.

There are a number of factors contributing to the effective linewidth of the transition pumped. These are the natural linewidth of the transition, the power broadening due to the dynamic Stark effect, and the Doppler width under the conditions used.

Although Hertel and Stoll assumed that the transition was saturated, they made no effort to take power broadening into account. The power broadening can be determined by:¹⁹

$$\Delta\nu_{\text{Power}} = 1.381 \times 10^7 \langle \mu \rangle |S|^{1/2} \quad (10)$$

where $\Delta\nu$ is the half width half maximum (HWHM) of the saturated line width (if $\Delta\nu_{\text{Power}} \gg$ the natural linewidth) in Hz, μ is the transition dipole matrix element in Debye, and S is the Poynting vector (the laser power density in the interaction region) in W/cm^2 . The

Table V. The transverse velocity and resultant Doppler broadening of the Na D₂ transition for the seed gases used. All velocities are in cm/sec.

<u>Seed Gas</u>	<u>Na Beam Velocity</u>	<u>Transverse Velocity</u>	<u>Doppler Broadened Linewidth</u>
Helium	3.0×10^5	3.3×10^4	56 MHz
Neon	1.6×10^5	1.8×10^4	30 MHz
Argon	1.1×10^5	1.2×10^4	20 MHz

dipole transition matrix element can easily be derived from the Einstein A coefficient:²⁰

$$|\mu|^2 = \frac{3hA}{64\pi^4\nu^3}, \quad (11)$$

where μ is the transition dipole matrix element in esu-cm ($=10^{18}$ D), A is the Einstein A factor in sec^{-1} , and ν is the transition frequency in cm^{-1} . From (11), for the D₂ line $\langle\mu\rangle=6.2$ D. For a typical power of 30 mW at the collision region focused to 3 mm. diameter, the power density is .33 W/cm². This yields the power broadened line width of 50 MHz.

Since the transition is optically pumped perpendicular to the motion of the atomic beam only the transverse velocity of the beam is

important in determining the Doppler width. This is sometimes referred to as the second order Doppler effect. To reduce this effect to a minimum the height of the atomic beam at the collision region was reduced to its present value of 1.1 mm. The maximum transverse velocity is related to the beam velocity by a geometric factor, in our case this is just:

$$v_{\perp} = \pm(.011) v_{\text{Na}}. \quad (12)$$

The Doppler width (HWHM) of the transition is then:

$$\Delta\nu_{\text{Doppler}} = \frac{v v_{\perp}}{c}. \quad (13)$$

The values of v_{\perp} and $\Delta\nu$ for the three commonly used Na beam velocities are given in table V. Note that since the transverse velocity is directly proportional to the distance from the center of the atomic beam, and since the laser comes up vertically into the interaction region, the Doppler shift is proportional to the height within the sodium beam. When the total broadening gets too large, it is possible to see (with the naked eye) the top and/or bottom of the sodium beam darken (less excitation results in less fluorescence). This has only been observed with the sodium seeded in helium, which gives the largest Doppler shifts.

The natural linewidth is only 5 MHz. The various contributions to the line width of the transition can be combined approximately as:

$$\Delta\nu_{\text{Total}} \cong [(\Delta\nu_{\text{nat}})^2 + (\Delta\nu_{\text{Power}})^2 + (\Delta\nu_{\text{Doppler}})^2]^{1/2}. \quad (14)$$

This yields values from 54 to 75 MHz for the broadened linewidth.

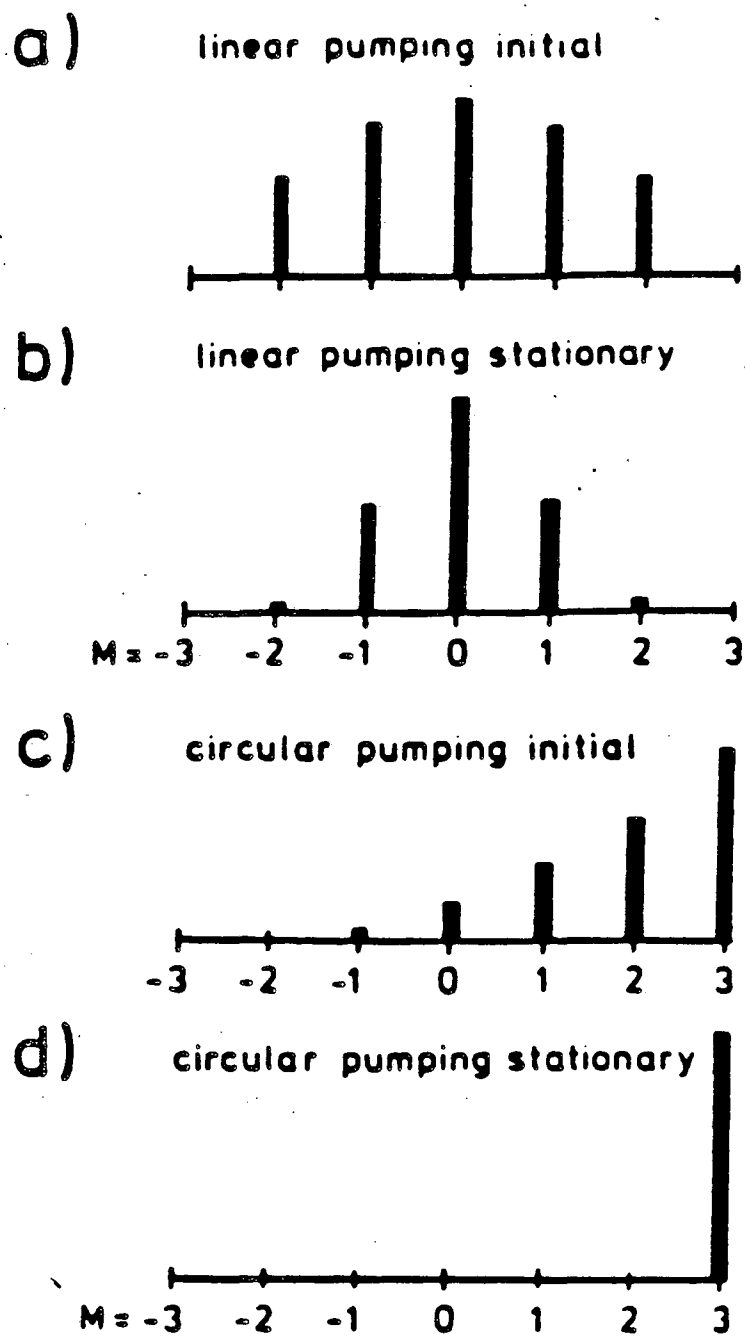
These values compare unfavorably to the separation of the $F'=2$ and $F'=3$

levels shown in figure 10. As Fischer and Hertel have pointed out, the deleterious effects of this broadening are reduced substantially by the selection rule forbidding $\Delta F = \Delta m_F = m_F = 0$ transitions. That is the $F'=2, m_F=0 \leftarrow F''=2, m_F=0$ transition is not allowed whereas the majority of the population in the case of linearly polarized light resides in $m_F=0$ (see below). Also, since the excited state fraction is optimized, and only (nearby) transitions to the red are to be avoided, the optimal laser frequency of the saturated transition would be to the blue (lower wavelength) of the center frequency of the transition, thus reducing the fraction pumped into levels other than $F'=3$.

It has been observed (particularly when the laser is focused) that reducing the power can increase both the fluorescence and the reactive signal due to the excited state. For each experiment the fluorescence and eventually the reactive signal are peaked on the dye laser power using neutral density filters. Under normal operating conditions, however, so long as the laser is not focused, no neutral density filters are required.

Fischer and Hertel have calculated the distribution of populations in the hyperfine sublevels ignoring whatever pumping to levels other than $F'=3$ occurs.¹⁴ In the initial moments of pumping, the distribution reflects only the relative transition moments of the various up transitions. In the quasi-steady state situation the level populations have been redistributed over many pumping-fluorescence cycles. The distributions for linearly and right circularly polarized laser pumping of the transition are shown in figure 11, from reference 14 with

Fig. 11. Estimated relative populations in magnetic sublevels (m_F) of $\text{Na}(^2P_{3/2}, F=3)$ on optical pumping with a) and b) a linearly polarized laser, and c) and d) a circularly polarized laser; a) and c) for initial moment pumping, and b) and d) for steady state pumping. Reproduced from reference 14 with permission.



XBL 863-789

Fig. 11

permission. In the case of right (left) circularly polarized light, with the constant bias of $\Delta m_F = +1$ (-1) with each pumping cycle, all the population ends up in $m_F = (-)F$ for both the ground state level and the excited level pumped (the unpumped ground state level is of course unaffected).

From the hyperfine sublevel populations one can calculate the degree of alignment for linearly polarized light, or the degree of orientation for circularly polarized light. Following the notation of reference 14, the alignment can be quantified as:

$$a_0^{\text{ph}} = \sum_{m=-F}^F [3m^2 - (F(F+1))] \sigma_m / \sum_m \sigma_m, \quad (15)$$

where a_0^{ph} is a measure of the alignment along the z axis in the photon frame of reference (along the electric vector of the laser), m is m_F , and σ_m is the fraction in sublevel m . There is another measure of the alignment along the x axis with respect to the y axis which is 0 everywhere here. The parameter a_0^{ph} for $F=3$ varies between the limits of -12 and 15 , where $a_0^{\text{ph}} = -12$ corresponds to the maximum alignment with all population in $m_F=0$, $a_0^{\text{ph}} = 0$ corresponds to equal population in each m_F level, and $a_0^{\text{ph}} = 15$ corresponds to minimum alignment with all population in $m_F = \pm 3$ (and the maximum orientation if all of the population is in only one of these two levels).

The orientation can be measured by:

$$o_0^{\text{ph}} = \sum_{m=-F}^F m \sigma_m / \sum_m \sigma_m. \quad (16)$$

The limits of parameter o_0^{ph} for $F=3$ are -3 and $+3$ which correspond to all population in $m_F=-3$ and $+3$, respectively, and maximum orientation. The minimum orientation occurs if the sublevel population is symmetric about $m_F=0$, then $o_0^{\text{ph}}=0$. This is the case any time linearly polarized light is used to excite the transition.

The alignment and orientation parameters can be converted into alignment and orientation parameters with respect to the electronic orbital angular momentum L which is a more chemically meaningful representation. The transformation for the alignment parameter is:

$$a_0^{\text{ph}}(L) = a_0^{\text{ph}} V_2(F,L) (2F+1)(2J+1) \left\{ \begin{matrix} F & F & 2 \\ J & J & I \end{matrix} \right\} \left\{ \begin{matrix} J & J & 2 \\ L & L & S \end{matrix} \right\} (-)^{F+2J+L+I+S}, \quad (17)$$

where the bracketed quantities are 6-j coefficients, and

$$V_2(F,L) = (-)^{(2F+2L)} \left[\frac{(2F-2)! (2L+3)!}{(2F+3)! (2L-2)!} \right]^{1/2}. \quad (18)$$

The transformation from F to L for the orientation parameter is:

$$o_0^{\text{ph}}(L) = o_0^{\text{ph}} V_1(F,L) (2F+1)(2J+1) \left\{ \begin{matrix} F & F & 1 \\ J & J & I \end{matrix} \right\} \left\{ \begin{matrix} J & J & 1 \\ L & L & S \end{matrix} \right\} (-)^{F+2J+L+I+S}, \quad (19)$$

where

$$V_1(F,L) = (-)^{(2F+2L)} \left[\frac{(2F-1)! (2L+2)!}{(2F+2)! (2L-1)!} \right]^{1/2} \quad (20)$$

From equation (15) for the $3^2P_{3/2}$, $F=3$ level, the conversion of the alignment parameter is $a_0^{ph}(L) = a_0^{ph}/15$. From equation (19), the conversion of the orientation parameter for this level is $o_0^{ph}(L) = o_0^{ph}/3$.

The fraction of the excited state population in the $3p_z$ orbital (the orbital parallel to the electric vector of the laser) can be related to the $a_0^{ph}(L)$ parameter in the case of linearly polarized laser pumping:

$$P(p_z) = 1/3 - a_0^{ph}(L)/3. \quad (21)$$

If all the excited state population were in $m_F=0$, the fraction in the p_z orbital would be 0.6. The remainder of the excited state population is distributed equally between the p_x and p_y orbitals.

With the magnetic sublevel distributions calculated in reference 14 and shown in figure 11, the initial moment pumping with linearly polarized light gives $a_0^{ph} = -7.2$ and $a_0^{ph}(L) = -0.48$, and steady state values of $a_0^{ph} = -10.$, and $a_0^{ph}(L) = -0.67$.¹⁴ However, the a_0 values can be related to the measured fluorescence dependence $2A$ from equation (6). This relationship is:

$$a_0^{ph} = (2A) / [g^{(2)}(1.5 - 2A)] \quad (22)$$

where $g^{(k)}$ is:

$$g^{(k)} = (-)^{F'-F''} [F'(F'+1)]^{-1} \left\{ \begin{matrix} F' & F' & k \\ 1 & 1 & F'' \end{matrix} \right\} / \left\{ \begin{matrix} F' & F' & k \\ 1 & 1 & F' \end{matrix} \right\}, \quad (23)$$

which for $F''=2$, $F'=3$ gives $g^{(2)}=-1/15$. Fischer and Hertel measured alignments up to $a_0^{\text{ph}}=-9.4$. In the experiments described here, the measured polarization dependence of the fluorescence for the 3S to 3P excitation was typically $2A=0.35$. Assuming that fluorescence from only $F'=3$ is observed, equation (22) yields a value of $a_0^{\text{ph}}=-4.6$, or $a_0^{\text{ph}}=-0.3$. This implies that 0.43 of the excited state population is in the p_z orbital vs. 0.28 in the p_x and p_y orbitals.

Fischer and Hertel show a sharp drop in alignment with increasing Na density above 10^{11} atoms/cc.¹⁴ Above 10^{11} atoms/cc, radiation trapping occurs,¹⁵ that is fluorescence photons are absorbed by other Na atoms, destroying the alignment produced by the laser field. The Na atom densities in the collision region in the experiments described here are in the range of 10^{11} - 10^{12} atoms/cc, and this certainly affects the orbital alignment obtained.

No successful measurements were made of the orientation dependence of any of the reactions described in chapters II-V.²¹ Also, no attempts were made to measure the degree of orientation. Fischer and Hertel predict that in steady state essentially all of the Na(3P) atoms can be pumped to $F=m_F=3$, giving $o_0^{\text{ph}}=3$, and $a_0^{\text{ph}}=15$. Experimentally, they found that the orientation can be as high as $o_0^{\text{ph}}=2.9$, and $a_0^{\text{ph}}=14.7$.¹⁴ Once again radiation trapping becomes significant above 10^{11} atoms/cc, and the orientation drops off sharply above this density.

Thus, the atomic densities that were found necessary to conduct the reactive scattering experiments interfere with but do not preclude

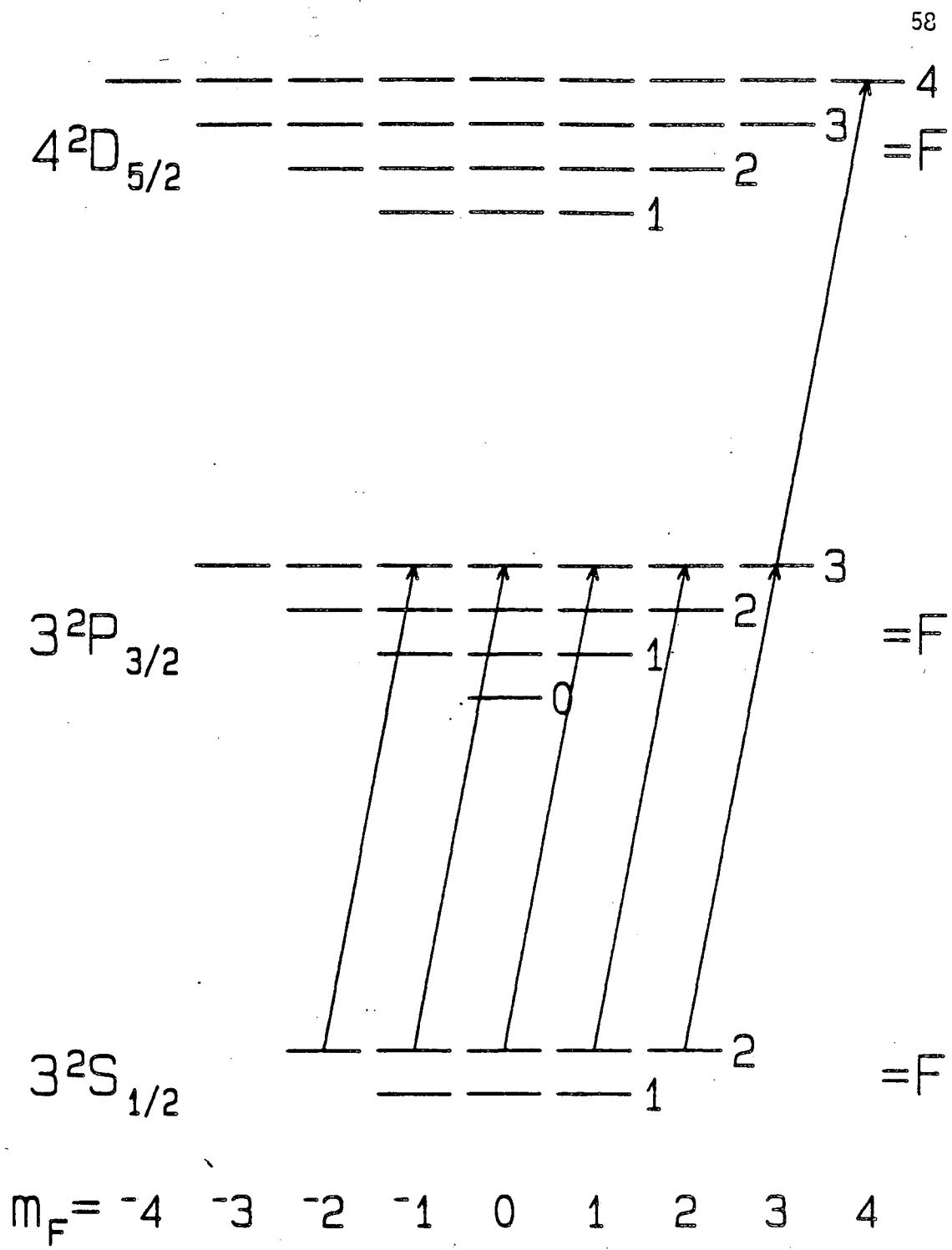
the measurement of alignment and orientation effects upon the reactive differential cross sections of the Na(3P) state.

Since the signal due to the excited state is nearly inversely proportional to the fraction excited (see equation (5)), a larger assumed fraction excited gives a lower estimate of the differential cross section of the excited state. For this reason the fraction excited was assumed to take the value of its upper limit, 20%,¹⁷ for the data analyzed in chapters II-V.

3. Subsequent Excitation to Na($4^2D_{5/2}$)

As discussed above, a second laser can be used to excite the sodium atoms to the $4^2D_{5/2}$ state. In analogy to the pumping of the Na($3^2P_{3/2}$, F=3 \leftarrow $3^2S_{1/2}$, F=2) transition, only the Na($4^2D_{5/2}$, F=4 \leftarrow $3^2P_{3/2}$, F=3) transition is pumped, and the other hyperfine levels are left unpumped. A schematic of the relevant energy levels is shown in figure 12.

Hertel and coworkers have performed quenching experiments with Na(4D,5S) atoms.²² Faced with the same optical pumping problem, they opted for using circularly polarized light to effectively reduce this to a three level case. The three levels are of course $m_F=F$ where F is 2, 3, and 4 for the 3S, 3P, 4D levels, respectively. This automatically isolates the F=4 level of the $4^2D_{5/2}$ state from the lower F levels. However, there is nothing to prevent fluorescence to $\underline{4^2P}_{3/2}$, F=3, instead of $\underline{3^2P}_{3/2}$, F=3 (the branching ratio is 1.7:1 for 3P:4P). When this occurs, there is some scrambling of levels, as the 4P state



XBL 863-784

Fig. 12. Hyperfine structure of the $\text{Na}(4^2D_{5/2} \leftarrow 3^2P_{3/2})$ transition.

decays predominantly to the 4S state (the branching ratio is 2.3:1:0.06 for 4S:3S:3D), which then fluoresces to either $3^2P_{3/2}$ or $3^2P_{1/2}$ (the branching ratio is 2:1) before returning to the ground state (see figure 9). Of course once the $4^2S_{1/2}$ or $3^2P_{1/2}$ levels, or any hyperfine level that can lead to population of the unpumped $3^2S_{1/2}$ level is reached, atoms will become unavailable for pumping. There are additional complications when other hyperfine levels of the $4^2D_{5/2}$ state are pumped. Jamieson et al. have estimated the fraction in each state from the ratios of the Einstein A coefficients of Heavens (reference 13 and table V).²² They assumed pumping with circularly polarized light. Their estimates are shown in figure 9.

Using linearly polarized light, the excited 4d orbital can be aligned much as the 3p orbital was. Using circularly polarized light, the 4d orbital can be oriented, but no orientation effects have been observed in the experiments described.²¹ The interpretation of the alignment experiments is made difficult because in addition to the d_{z^2} orbital the d_{xz} and d_{yz} orbitals contribute to the alignment, and to the alignment parameter a_0^{ph} . No independent measure was made of the population of the d_{xz} and d_{yz} orbitals. There is no problem determining the multipole moments for the excitation as in the previous section. The maximum conceivable alignment occurs for all the excited state population in $F=4$, $m_F=0$. From (15) this gives $a_0^{ph}=-20$. For $F=4$, $L=2$, and $J=5/2$, equation (17) gives $a_0^{ph}(L) = 3a_0^{ph}/14$. For linearly polarized light the orientation is of course still zero; $o_0^{ph}=0$. The other limit of a_0 is for $m_F=\pm F$, which yields $a_0^{ph}=28$. Once again if

all the population is in one or the other outermost m_F level, the maximum orientation is attained, and $a_0^{\text{ph}} = \pm 4$. This is attained with circularly polarized light, both exciting lasers must have the same sense. There is no confusion as to the meaning of the orientation due to the additional orbitals; when $m_F = \pm 4$, $m_L = \pm 4$.

Cycling also occurs for the $3P \rightarrow 4D$ excitation, but the ratio of the lifetimes (derived from table V) shows that the cycling occurs more than three times slower for the upper transition (Rabi flopping via stimulated emission is not included in this since no redistribution of magnetic sublevel population takes place as a result of it). To a good approximation then, the distribution of magnetic sublevels in the $4^2D_{5/2}$, $F=4$ state should reflect those in the $3^2P_{3/2}$, $F=3$ state. Using the values for the steady state populations in the $3P$ state calculated by Hertel and Stoll¹⁵ as the distribution in the $4^2D_{5/2}$, $F=4$ state gives an expected alignment of $a_0^{\text{ph}} = -17.9$, and $a_0^{\text{ph}}(L) = -3.8$. The measured polarization dependence of the fluorescence of the $\text{Na}(4^2D_{5/2})$ state typically gave $2A = 0.32$. Using a narrow band pass filter only the green fluorescence of the $\text{Na}(3^2P_{3/2} \leftarrow 4^2D_{5/2})$ transition was monitored. For $F'=4$, and $F''=3$, from (23), $g^{(2)} = -1/28$, giving $a_0^{\text{ph}} = -7.6$ from (22). This gives $a_0^{\text{ph}}(L) = -1.62$. As discussed above, the fraction in the d_{z^2} orbital cannot be determined from a_0 .

Experiments on reactive scattering have shown that having both lasers circularly polarized in the same sense yields an excited state fraction approximately 15% higher than having both lasers linearly polarized with their electric vectors parallel. If the two lasers are

circularly polarized with the opposite sense, the fraction excited is reduced by more than a factor of 3. Several of the experiments in chapters II-V on the reactive scattering of Na(4D) atoms were performed with both the linear and circular polarization optical pumping schemes, and no fundamental differences were observed between the cases. No polarization dependence of the reactive scattering at a single detector angle of greater than 17° was seen, so this should limit the effect on the angular distributions recorded.

For the reactive scattering experiments of the 4D state, it was not possible to separate the contributions of the radiatively populated 4S and 4P states. Thus, the angular distributions derived for the 4D state in general contain the contributions of these states. No experiments were done to directly excite the Na(4S,4P) states. For the distributions, it was assumed that (1) the excited state fraction in the 3P state remains unchanged when the second laser is added, (2) the ground state contribution to the reactive scattering of the ground state is negligible, and (3) the fraction excited to the 4D state is 80% that to the 3P state. Assumption (1) is based on the experimental observation that the fluorescence from the 3P does not change when the second laser excitation is modulated. Assumption (2) is an empirical observation. Assumption (3) is based on the estimates of Jamieson et al.²² The scattering due to the Na(4D) state was determined as:

$$4D = (ON4D - OFF3P) / 0.8, \quad (24)$$

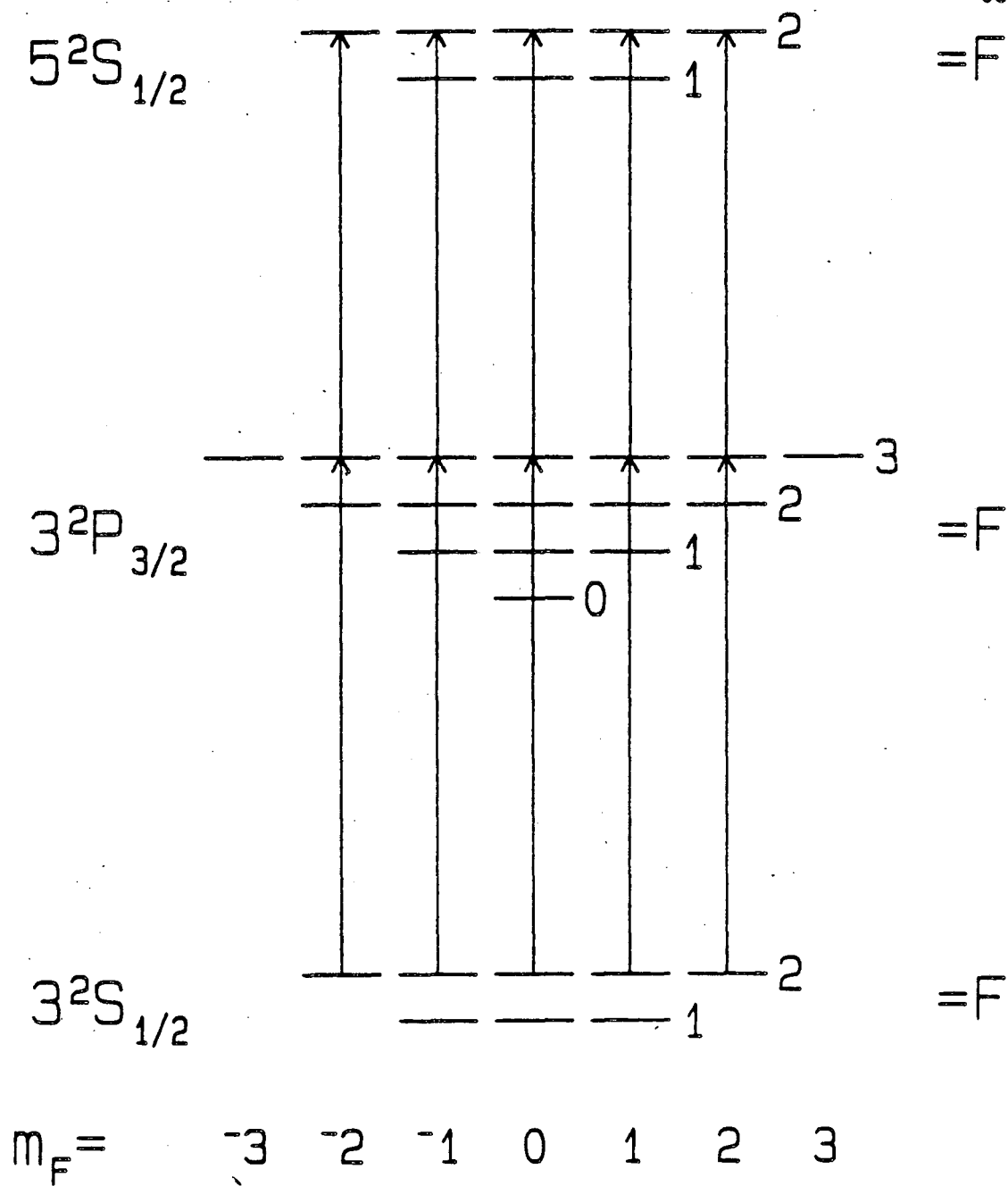
where 4D is the signal due to the Na(4D) state, ON4D is the signal with

both lasers on, OFF3P is the signal with the green laser off and the yellow laser on (so that the 3P level is still excited). Compare this to (5).

4. Subsequent Excitation to $\text{Na}(5^2\text{S}_{1/2})$

As in the 4D case, a second dye laser can be used to excite from the $3^2\text{P}_{3/2}$ level to the $5^2\text{S}_{1/2}$ level. The hyperfine levels involved in the excitation of the $5^2\text{S}_{1/2}$ state are shown in figure 13. The $5^2\text{S}_{1/2}$ level can fluoresce into both the fine structure states of the 3P and 4P states (the branching ratio from table V is 0.5:1:0.4:0.7 for $3^2\text{P}_{1/2}:3^2\text{P}_{3/2}:4^2\text{P}_{1/2}:4^2\text{P}_{3/2}$). There is no simple way to avoid fluorescence into dark levels, but as pointed out by Jamieson et al.,²² and observed here, there does not seem to be a large difference in the pumping efficiency of this level relative to pumping the 4D level.²² Once again, there are no accurate determinations of the fraction excited. Linearly polarized lasers whose electric vectors are parallel are used to pump the transitions. Estimates by Jamieson et al. for the fraction in each state with excitation to the 5S state are shown as the bracketed quantities in figure 9.

As with the 4D state, it was not possible to separate the contributions to the reactive scattering by the radiatively populated 4S and 4P states. Thus, the distributions derived for the 5S state also contain the contributions of these states. The same assumptions regarding the excitation were made as for the excitation of the 4D state (see



XBL 863-785

Fig. 13. Hyperfine structure of the $\text{Na}(5^2S_{1/2} \leftarrow 3^2P_{3/2})$ transition.

above). It was assumed that the fraction excited to the 5S state is 80% that to the 3P state. With the replacement of "5S" for each "4D" equation (24) was used to determine the scattering of the 5S state.

E. References

1. M. F. Vernon, H. Schmidt, P. S. Weiss, M. H. Covinsky, and Y. T. Lee, J. Chem. Phys., to be published.
2. M. F. Vernon, Ph.D. Thesis, University of California, Berkeley (1983).
3. C. H. Becker, P. Casavecchia, P. W. Tiedemann, J. J. Valentini, and Y. T. Lee, J. Chem. Phys. **73**, 2833 (1980).
4. Y. T. Lee, J. D. McDonald, P. R. LeBreton, and D. R. Herschbach, Rev. Sci. Instr. **40**, 1402 (1969).
5. P. E. Siska, J. M. Parson, T. P. Schaefer, and Y. T. Lee, J. Chem. Phys. **55**, 5762 (1971).
6. S. Gerstenkorn and P. Luc, Atlas du Spectre d'Absorption de la Molecule d'Iode, (Editions du CNRS, Paris, 1978).
7. For an explanation of the cross-correlation technique, see: G. Comsa, R. David, and B. J. Schumacher, Rev. Sci. Instrum. **52**, 789 (1981).
8. H. Schmidt, J. M. Mestdagh, M. H. Covinsky, B. A. Balko, and Y. T. Lee, unpublished results (1985).
9. T. T. Warnock and R. B. Bernstein, J. Chem. Phys. **49**, 1878 (1968).
10. R. J. Buss, Ph.D. Thesis, University of California, Berkeley, California (1979).

11. For $\text{Na}(3P,4D) + \text{HCl} \rightarrow \text{NaCl} + \text{H}$ at a collision energy of 3.4 kcal/mole a small decrease is observed in reactive scattering at large laboratory detector angles in going from $3P \rightarrow 4D$, but this is the only case where a decrease has been observed on excitation.
12. W. L. Wiese, M. W. Smith, and B. M. Miles, Atomic Transition Probabilities Volume II: Sodium Through Calcium, Natl. Stand. Ref. Data Ser., Nat. Bur. Stand. (U. S.), Washington, DC (1969).
13. O. S. Heavens, J. Opt. Soc. **51**, 1058 (1961).
14. A. Fischer and I. V. Hertel, Z. Phys. A **304**, 103 (1982).
15. I. V. Hertel and W. Stoll, Adv. At. Mol. Phys. **13**, 113 (1978).
16. This is just one half of the fraction initially in $F=2$ of the ground state ($5/8$); so the excited state fraction would be $5/16$.
17. H. Schmidt and I. V. Hertel, private communication.
18. C. Cohen-Tannoudji, in Atomic Physics 4, 589, G. zu Putlitz, E. W. Weber, and A. Winnacker, eds. (Plenum, New York, 1975).
19. J. C. Hemminger, R. Cavanagh, J. M. Lisy, and W. Klemperer, J. Chem. Phys. **67**, 4952 (1977).
20. G. Herzberg, Molecular Spectra and Molecular Structure I. Spectra of Diatomic Molecules, 20 (Van Nostrand Reinhold Co., New York, 1950).
21. Recent measurements by H. Schmidt, J. M. Mestdagh, B. A. Balko, M. H. Covinsky, and Y. T. Lee on $\text{Na}(4D) + \text{NO}_2$ have shown an orientation dependence.

22. G. Jamieson, W. Reiland, C. P. Schulz, H.-U. Tittes, and I. V. Hertel, J. Chem. Phys. 81, 5805 (1984).

II. THE REACTIONS OF GROUND AND EXCITED STATE ALKALI ATOMS WITH HYDROGEN HALIDE MOLECULES

A. Introduction

The reactions of alkali atoms (M) with hydrogen halide molecules (HX) have been studied in great detail both experimentally¹⁻¹² and theoretically.¹³⁻²² In 1955, Taylor and Datz reported the first angular distribution measured for any reaction in a crossed molecular beams experiment for $K + HBr$.¹ Since then, much more quantitative experiments have been performed in order to determine the dynamics of these reactions as well as the effects of reagent translational,²⁻⁶ vibrational,⁵⁻⁹ and rotational⁸⁻¹⁰ excitation on the reaction. Until recently, the effect of electronic excitation remained unexplored.¹¹

An interesting feature of this family of reactions is that with the appropriate choice of alkali and halogen atoms, the reaction can be made exothermic, thermoneutral, or endothermic to allow tests of the effects of various forms of reagent energy in the threshold region. Of course, this does complicate attempts to make direct comparisons between results measured on different reactions (i.e. on different combinations of reactants). The ΔH_0^0 values for the $M + HX \rightarrow MX + H$ reactions for the various combinations of alkali and halogen atoms,

Table I Heats of reaction (ΔH_0^0) in kcal/mole for $M + HX \rightarrow MX + H$ ($M = Li, Na, K, Rb, Cs$; $X = F, Cl, Br, I$) calculated from the diatomic molecular dissociation constants given in reference 23.

M:	X: F	Cl	Br	I
Li	-1.	-8.8	-12.3	-10.6
Na	13.	4.7	0.4	1.2
K	18.4	2.1	-3.5	-5.9
Rb	20.	3.	-3.3	-5.5
Cs	17.3	-3.4	-9.5	-11.7

calculated from spectroscopic and thermochemical dissociation constants,²³ are given in table I for reference.

At the Conference on Potential Energy Surfaces in Chemistry in 1971, Herschbach proposed that theoreticians calculate an ab initio potential energy surface for studying the dynamics of the prototypical $Li + HF$ system.²⁴ A careful study in crossed molecular beams was performed for the reactions $Li + HX \rightarrow LiX + H$ ($X = F, Cl$) in order to provide a test for theoretical calculations.² Most of the theoretical studies of the reactions of alkali atoms with hydrogen halides have in fact concentrated on $Li + HF$ because of its relative simplicity (i.e. Li, H, and F are all top row elements). The first calculation of the $Li + HF$ system was performed by Lester and Krauss in 1970, who examined some of the features of the entrance channel, and

found a small potential well there.¹⁴ A valence bond calculation by Balint-Kurti and Yardley (BKY) found a small entrance channel well and an exit channel barrier that was lowest for a bent configuration.¹⁵ Included in BKY is a calculation of a few low-lying excited state surfaces including the one corresponding to $\text{Li}(2P) + \text{HF}$. Zeiri and Shapiro calculated semi-empirical potential energy surfaces (ZS), and found a small barrier that was between the entrance and exit channels for a collinear configuration, but moved into the entrance channel with an increasingly bent orientation.¹⁶ They have since extended their calculations to provide potential energy surfaces for 14 of the reactions in the alkali + hydrogen halide family, and in a revised $\text{Li} + \text{HF}$ surface (ZS II) found that the barrier was in the exit channel¹⁷ in agreement with BKY. They found that the barrier was lowest for a bent configuration in the $\text{M} + \text{HF}$ potential energy surfaces, but was lowest for collinear and near collinear geometries in the $\text{M} + \text{HCl}$, HBr , and HI potential energy surfaces. They found a strong orientation dependence with a large barrier (>3 eV) for the collinear $\text{M}-\text{H}-\text{X}$ geometry.¹⁷ Chen and Schaefer have calculated an ab initio potential surface which shows an entrance channel well and an exit channel barrier which is lowest for a bent transition state, much like that of BKY.¹⁸

Shapiro, Zeiri, and Pollack have done classical trajectory calculations on the ZS surface in which they found oscillatory behavior for the reaction probability as a function of collision energy.¹⁹ This was attributed in part to the opening up of inelastic processes

such as HF vibrational excitation with increasing collision energy. NoorBatcha and Sathyamurthy have done quasiclassical trajectory calculations²⁰⁻²² on an analytic function fit to the Chen-Schaefer surface by Carter and Murrell,²⁵ and on the ZS surface. They looked at the effects of vibration, rotation, and orientation on reaction probability. They predicted a large (≈ 1 eV) vibrational threshold to reaction, which was not found in the earlier crossed molecular beam experiments (in which essentially all of the HF and HCl molecules were in $v=0$).² They also predicted an initially decreasing then increasing dependence of reaction probability on rotational energy. This effect, although of a lower magnitude was seen in the experiments of Blackwell, Polanyi, and Sloan¹⁰ described below.

The effect of varying translational energy was studied in the experiments of Becker et al. on $\text{Li} + \text{HF}$, HCl .² At a collision energy of 3 kcal/mole the $\text{Li} + \text{HF}$ forms a long-lived complex (relative to a rotational period of the complex), because the bottom of the potential energy surface is sampled at this energy. At higher collision energies, such as 9 kcal/mole, this complex is not formed, and the reaction proceeds directly to products. The $\text{Li} + \text{HF}$ reaction proceeds with a low cross section, $\sigma_R < 1 \text{ \AA}^2$, at these collision energies, yielding an average opacity of ~ 0.1 . In $\text{Li} + \text{HCl}$, at low collision energy (3 kcal/mole) the LiCl product is scattered backwards relative to the initial Li velocity, whereas at higher collision energy (9 kcal/mole) the LiCl is scattered backwards-sideways. The $\text{Li} + \text{HCl}$

had higher reactive cross sections, $\sigma_R > 25 \text{ \AA}^2$ for the collision energies studied, yielding an average opacity of 1.

Brooks and coworkers have looked at the effect of translational energy on the $\text{K} + \text{HCl}$ reaction.^{4,5} They have found an increase in reaction probability as the collision energy is increased from 3 to 10 kcal/mole, and then a fall-off as the collision energy is further increased to 18 kcal/mole. They have concluded that translational excitation can never be as effective in promoting reaction as the excitation of a single quantum of vibration in HCl.

Heismann and Loesch have looked at the effect of translational energy on the $\text{K} + \text{HX}(v=0,1) \rightarrow \text{KX} + \text{H}$ ($\text{X} = \text{F}, \text{Cl}$).⁶ The drop-off of reaction probability for $\text{K} + \text{HCl}(v=0)$ seen by Geiss et al. was not seen by Heismann and Loesch, who saw reaction probability rise steadily until reaching a constant value for collision energies from 21 kcal/mole up to 48 kcal/mole. This is shown in figure 1 which is adapted from reference 6 with permission. The open circles are the results of Brooks and coworkers, while the squares are the results of Heismann and Loesch. For the substantially endothermic $\text{K} + \text{HF}(v=0) \rightarrow \text{KF} + \text{H}$, the reaction probability rises steadily for collision energies between 18 and 41 kcal/mole.

Lacmann and Herschbach have studied $\text{K} + \text{HCl}$ at collision energies of 1-20 eV, however they only looked for the production of $\text{K}^*(4P)$ and K^+ .³ They only saw K^+ , which was produced only above the threshold for the appearance of both K^+ and Cl^- . Balint-Kurti and Yardley have

Fig. 1. Reaction probability vs. reagent translational energy from the reaction $K + HCl(v=0) \rightarrow KCl + H$ including the data of Brooks and coworkers,^{4,5} as open circles, and that of Heismann and Loesch,⁶ as triangles. This figure is adapted from figure 5 of reference 6, with permission.

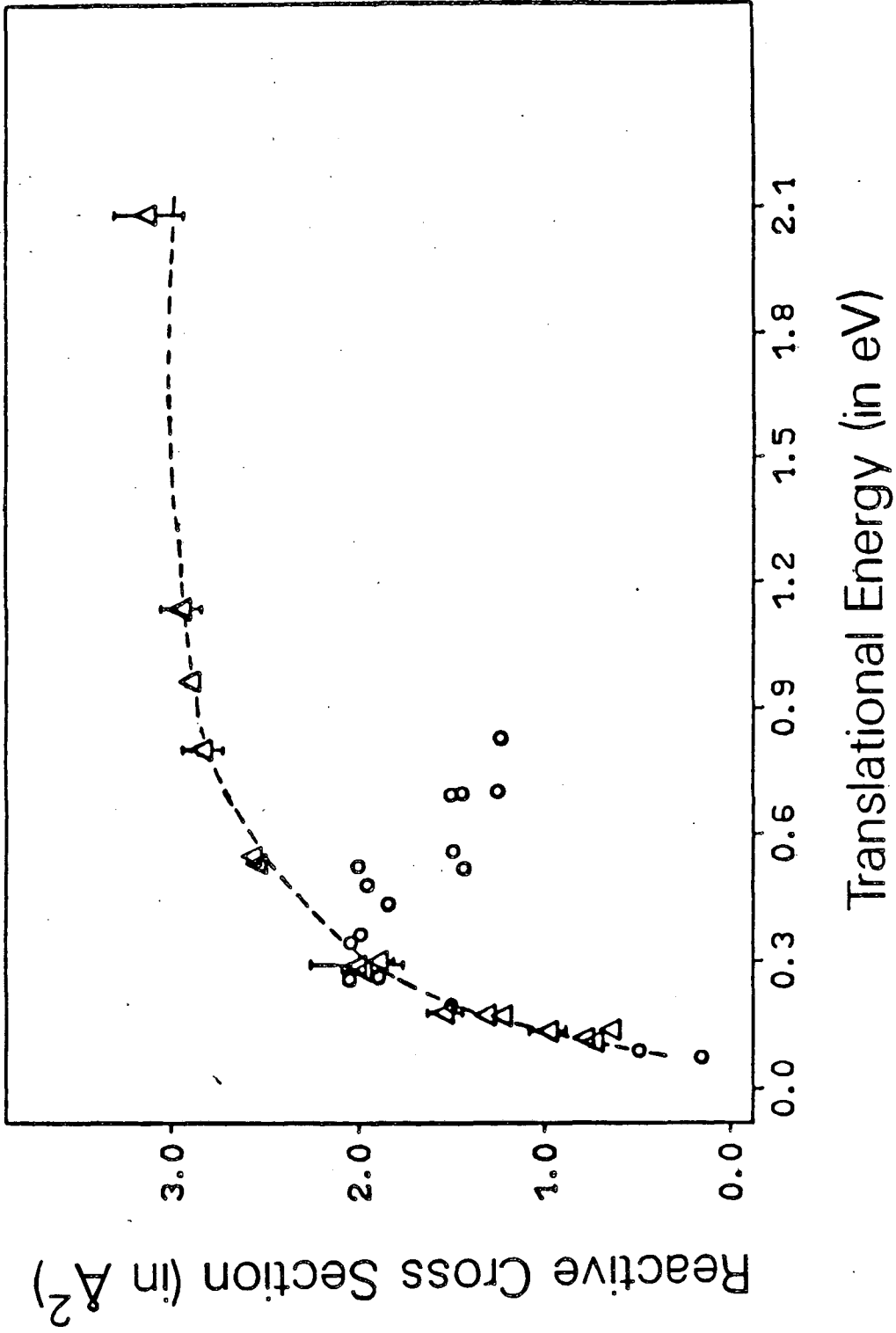


Fig. 1

suggested that this is due to KCl molecules formed in very high vibrational levels which then dissociate to ion pairs.¹⁵

Odiorne, Brooks, and Kasper have studied the effect of reagent vibrational excitation on the reaction $K + HCl(v=0,1) \rightarrow KCl + H$ by exciting the HCl with a cw chemical laser.⁷ They found a rise in the estimated reaction cross section from $\sigma_R(v=0)=0.15 \text{ \AA}^2$ to $\sigma_R(v=1)=20 \text{ \AA}^2$, for a collision energy of 3-4 kcal/mole. This shows that vibrational excitation can effectively lift the $M + HX$ reaction out of the threshold region, and "turn the reaction on."

Heismann and Loesch found similar results for $K + HCl(v=0,1)$ at low collision energies (such as the one studied by Odiorne et al.), but saw a decrease in the vibrational enhancement, measured as:

$$\epsilon = \frac{\sigma_R(v=1)}{\sigma_R(v=0)}, \quad (1)$$

with higher collision energy.⁶ Their vibrational excitation was thermally produced by heating the hydrogen halide molecules in an oven prior to expansion in a molecular beam. Similar behavior was found for the reaction $K + HF(v=0,1) \rightarrow KF + H$, but in this case the much larger endothermicity pushes the threshold of this process out to higher collision energies in the absence of vibrational excitation. It was not possible to reach collision energies at which ϵ fell below 70 (this was reached when $E_{\text{coll}}=48.4 \text{ kcal/mole}$). In both cases, the dropping off of the vibrational enhancement, ϵ , is due more to the increase in

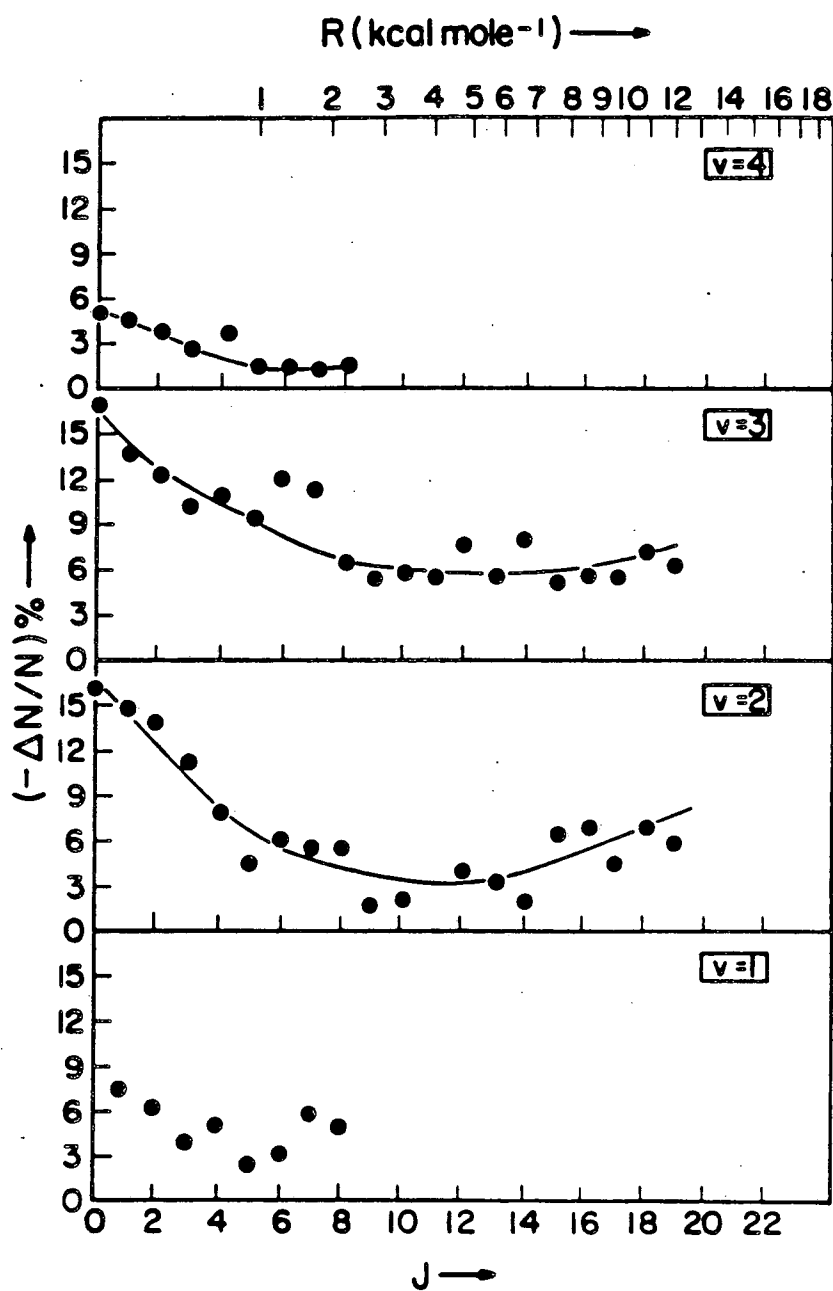
$\sigma_R(v=0)$ with increasing collision energy, than to a large drop in $\sigma_R(v=1)$, although there is a gentle decrease in $\sigma_R(v=1)$ at higher collision energies in the cases of both HCl and HF.

Dispert, Geis, and Brooks have studied the effect of rotation on the $K + HCl(v=1, J) \rightarrow KCl + H$ reaction by exciting specific rotational levels of the HCl($v=1$) level with a cw chemical laser.⁹ They found a factor of 2 decrease in the reactive cross section in going from $J=1$ to $J=4$. This is the anticipated effect, since in going from very low to moderate rotational excitation, the favored orientation for alignment is destroyed.

Along similar lines, Hoffmeister, Potthast, and Loesch have looked at the effect of rotation on the $K + HF(v=1, J) \rightarrow KF + H$ reaction for $J = 5, 6, \text{ and } 7$.⁸ They observed an overall increase in cross section with increasing rotational level. This effect is also as expected; moving from moderate to higher rotational levels there should be a gradual change from the troublesome destruction of favored orientation to a blurring of orientations due to fast rotation. Alternatively, this could be attributed to favorable excitation of bending in the transition state which could help overcome the barrier to reaction. A continued increase in cross section with further rotational excitation (and thus bending excitation) would be expected in an exact analogue to vibrational enhancement of reactivity.

Blackwell, Polanyi, and Sloan looked at the reactions $Na + HX \rightarrow NaX + H$ for $HX = HF(v=1-4, J=0-14)$, and $HX = HCl(v=1-4, J=0-19)$ in a

fascinating series of experiments that monitored the depletion of the infrared chemiluminescence of chemically produced HF and HCl by reaction with Na atoms. Thus, Blackwell et al. were able to compare the reactivities of the various rotational levels within each vibrational level. They saw an initial decrease in reactivity with increasing J , and then a subsequent increase. The minimum $\sigma(J)$ occurred at $J \approx 7$ for HF, and $J \approx 11$ for HCl for each vibrational level studied. Examples of the dependences they observed are shown in figure 2, reproduced with permission from reference 10. The explanation given for this behavior is, as above, a destruction of the proper orientation for reaction with increasing J at first, until after a certain point, the incoming atom sees a spatially averaged potential. The rotational energies achieved in this study are quite high. For HF, $B_e = 20.6 \text{ cm}^{-1}$, so that for $J=14$, the rotational energy is approximately 0.5 eV, or about one-fourth the energy of the first electronic excitation, or about the energy of one vibrational quantum. While there is an effect of rotation, it is certainly not "energy efficient" to try to promote reaction in this way. Also, in general it is very difficult to rotationally excite molecules to such high rotational energy by any method other than this clever chemical production technique, as so many h of angular momentum are needed to reach the requisite J level. It should be noted that for Na + HF, a system discussed in section C2, no depletion, and thus no reaction, was observed for HF($v=1$) which with a collision energy of $>1.7 \text{ kcal/mole}$ is energetically allowed to react to

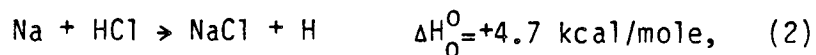


XBL 861-78

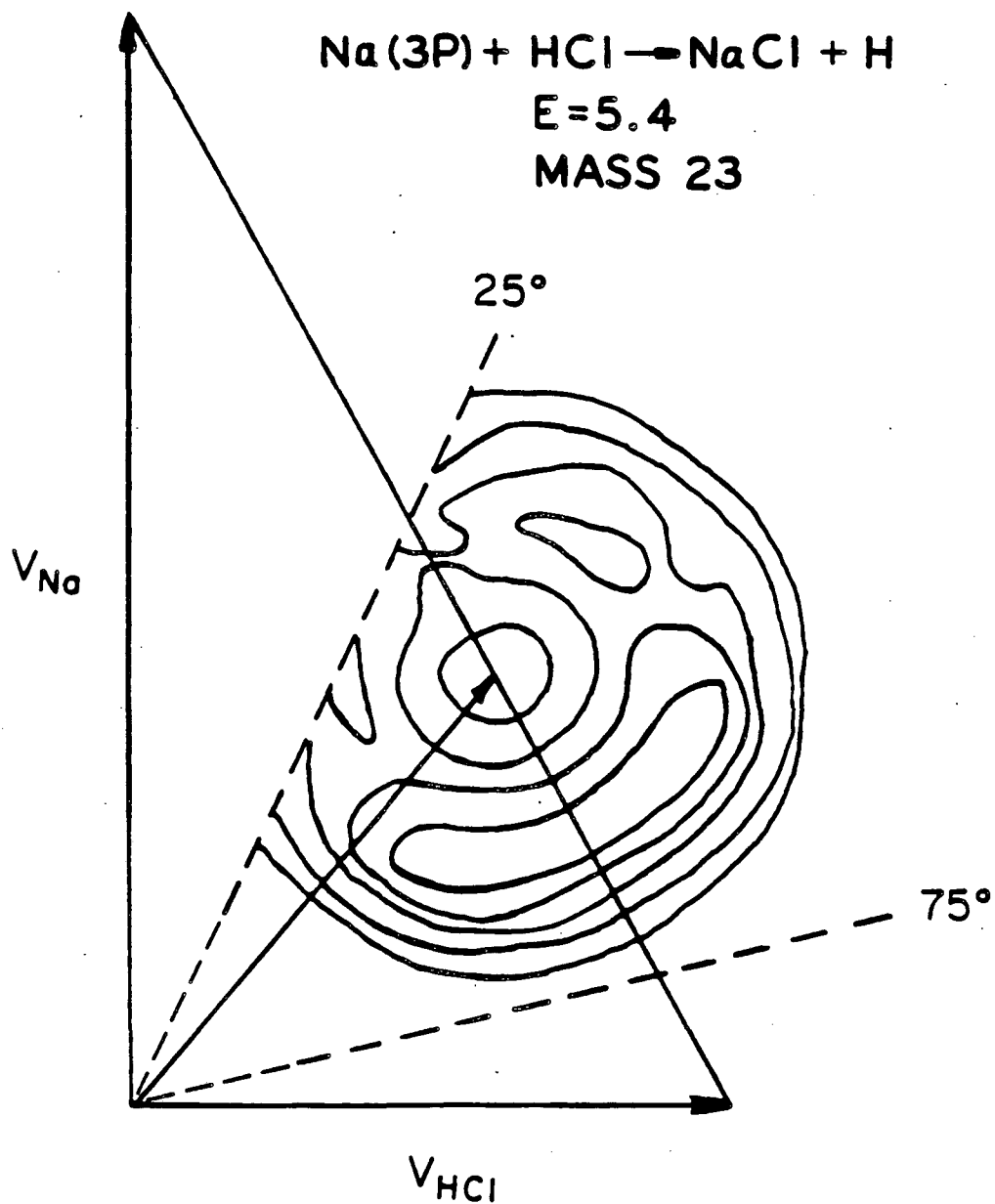
Fig. 2. Reaction probability vs. rotational level for the reaction $\text{Na} + \text{HCl}(v=1-4)$ measured by the chemiluminescence depletion method by Blackwell, Polanyi, and Sloan, and reproduced with permission from reference 10.

NaF + H. This also gives credence to the assumption that depletion of the upper vibrational levels is not due to vibrational relaxation.

The first reaction of electronically excited sodium atoms was studied in our laboratory.¹¹ This was:



for which the reactive scattering of the ground ($3^2S_{1/2}$) and first excited ($3^2P_{3/2}$) states were studied. At a collision energy of 5.4 kcal/mole the ground state barely reacts due to the endothermicity of the process. The reaction of the Na(3P) gives the product NaCl center of mass contour map as shown in figure 3, adapted from reference 11. The product NaCl is predominantly backwards scattered in the center of mass relative to the incoming Na atoms with some forward-sideways peaking. This implies a direct reaction with collinear or near-collinear Na-Cl-H approach geometries required for reaction. The product translational energy distribution was found to be broad and flat, remaining approximately constant from nearly zero translational energy up to all of the available energy going into translation. At high collision energy, 19.4 kcal/mole, there is still an increase in reaction with electronic excitation, but the enhancement is clearly lower. This effect is certainly the same as that seen by Heismann and Loesch for vibrational excitation, where enhancement is largest in (or below) the threshold region.



XBL 861-77

Fig. 3. NaCl center-of-mass contour map from the reaction of Na(3P) + HCl at a collision energy of 5.4 kcal/mole, as determined in reference 11.

The intention in performing the experiments described in section B was to enable a comparison between the effects of reagent electronic excitation on these reactions with the effects of other forms of energy already investigated. Specifically, how do the cross sections vary with electronic energy, and how are the reaction dynamics affected by varying electronic energy and symmetry?

B. Results

Three systems from this family were chosen for a study of the effects of electronic excitation on these reactions. The reactions studied were Na with HF, HCl, and HBr. As discussed in chapter I, the collision energies were varied by changing the seed gases of the sodium beam from argon to neon to helium, and the Na(3P,4D,5S) states were optically pumped with one or two single-frequency cw dye lasers. The experimental apparatus and the treatment of data are described in detail in chapter I.

1. Na(4D,5S) + HCl

When excited to the Na($4^2D_{5/2}, 5^2S_{1/2}$) states and reacted with HCl in crossed molecular beams, the NaCl product angular and velocity distributions change substantially from what was observed for the Na($3^2P_{3/2}$) + HCl reaction. Angular distributions for Na(3S,3P,4D,5S) + HCl \rightarrow NaCl + H were measured at collision energies of 3.4, 5.6, and

16.3 kcal/mole. Newton velocity vector diagrams detailing the kinematics of the system at these three collision energies are shown in figures 4-6. The angular distributions themselves are shown in figures 7-9. The distributions shown are the raw data -- the 4D and 5S curves include the contributions of 3S and 3P as well as the radiatively populated 4S and 4P states.

Two dramatic effects are immediately apparent: the angular distributions have narrowed and the signals have increased in going from Na(3P) to Na(4D,5S). The unexpected narrowing of the NaCl angular distributions with increasing electronic energy is illustrated in figure 10, in which the angular distribution due to Na(3P) is blown up to the same scale as that due to Na(4D) for a collision energy of 5.6 kcal/mole. Time-of-flight measurements for Na(4D) + HCl at collision energies of 3.4 and 5.6 kcal/mole are shown for various detector angles in figures 11 and 12, respectively. Similar time-of-flight measurements for Na(5S) + HCl are shown in figures 13 and 14. The time-of-flight distributions include the contribution of Na(3P) also, as well as the negative contribution due to the depletion of the ground state as discussed in reference 11. These measurements confirm that there is actually less translational energy in the NaCl due to the reaction of Na(4D,5S) than that due to Na(3P).

At a collision energy of 5.6 kcal/mole for Na(4D) + HCl, the dependence of the reactive signal at several detector angles upon the laser polarization was measured as described in chapter I. The derived distributions are shown in figures 15a-e and summarized in table II.

$$E_{\text{coll}} = 3 \text{ kcal/mole}$$

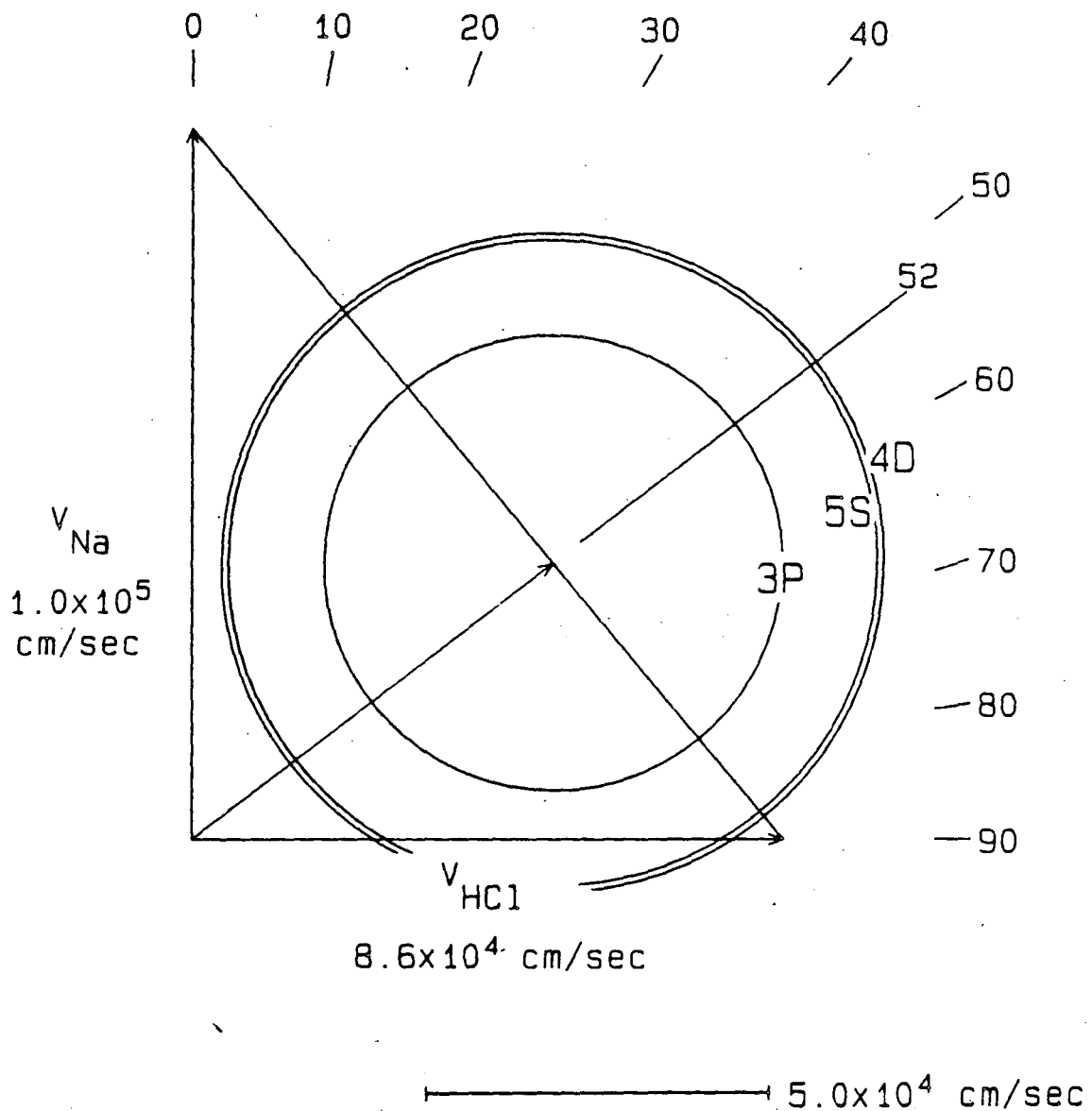


Fig. 4. Newton velocity vector diagram for $\text{Na}(3\text{S}, 3\text{P}, 4\text{D}, 5\text{S}) + \text{HCl} \rightarrow \text{NaCl} + \text{H}$ at a collision energy of 3.4 kcal/mole. The sodium beam is seeded in argon, the HCl beam is neat.

XBL 863-860

$$E_{\text{coll}} = 6 \text{ kcal/mole}$$

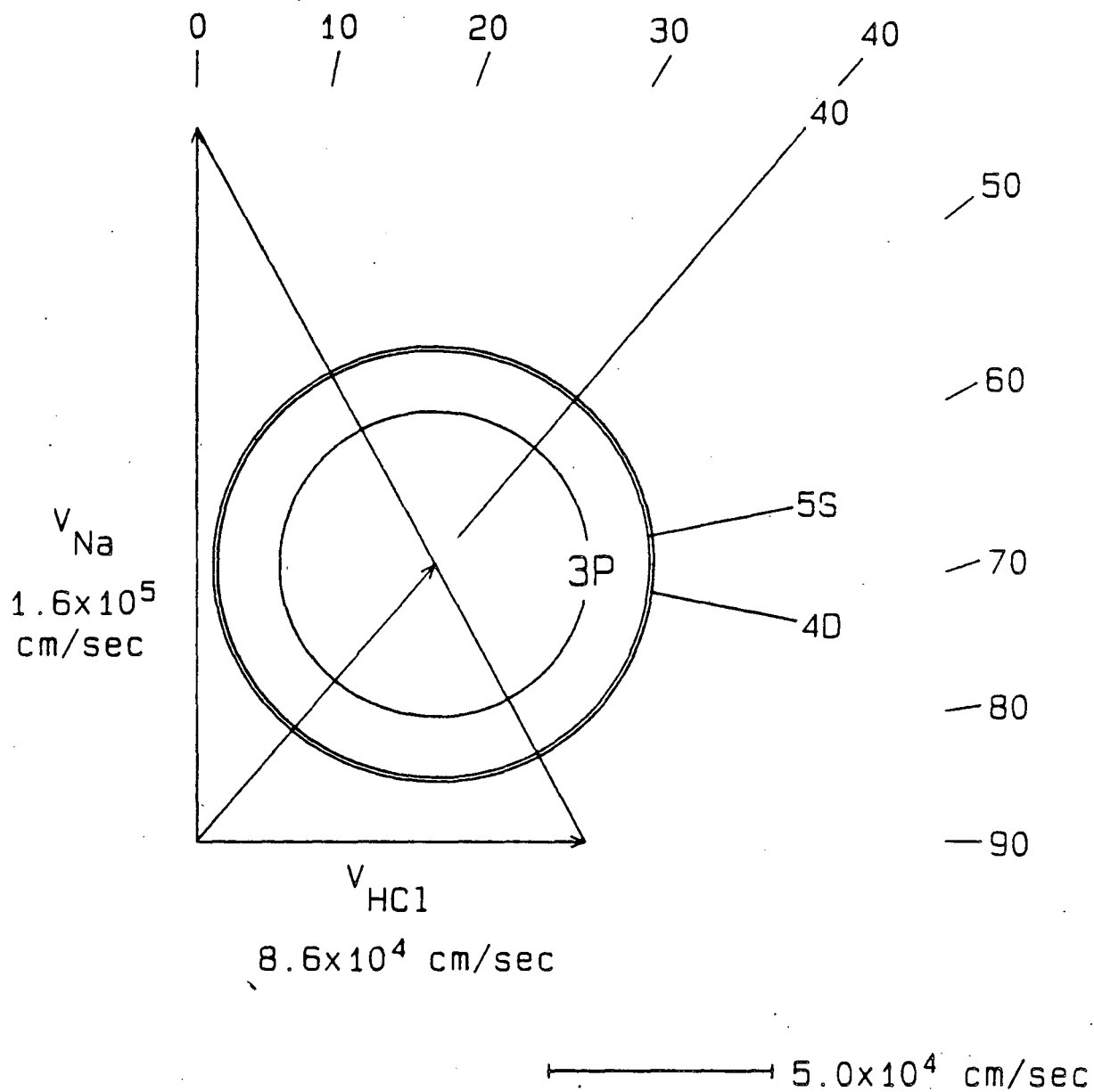
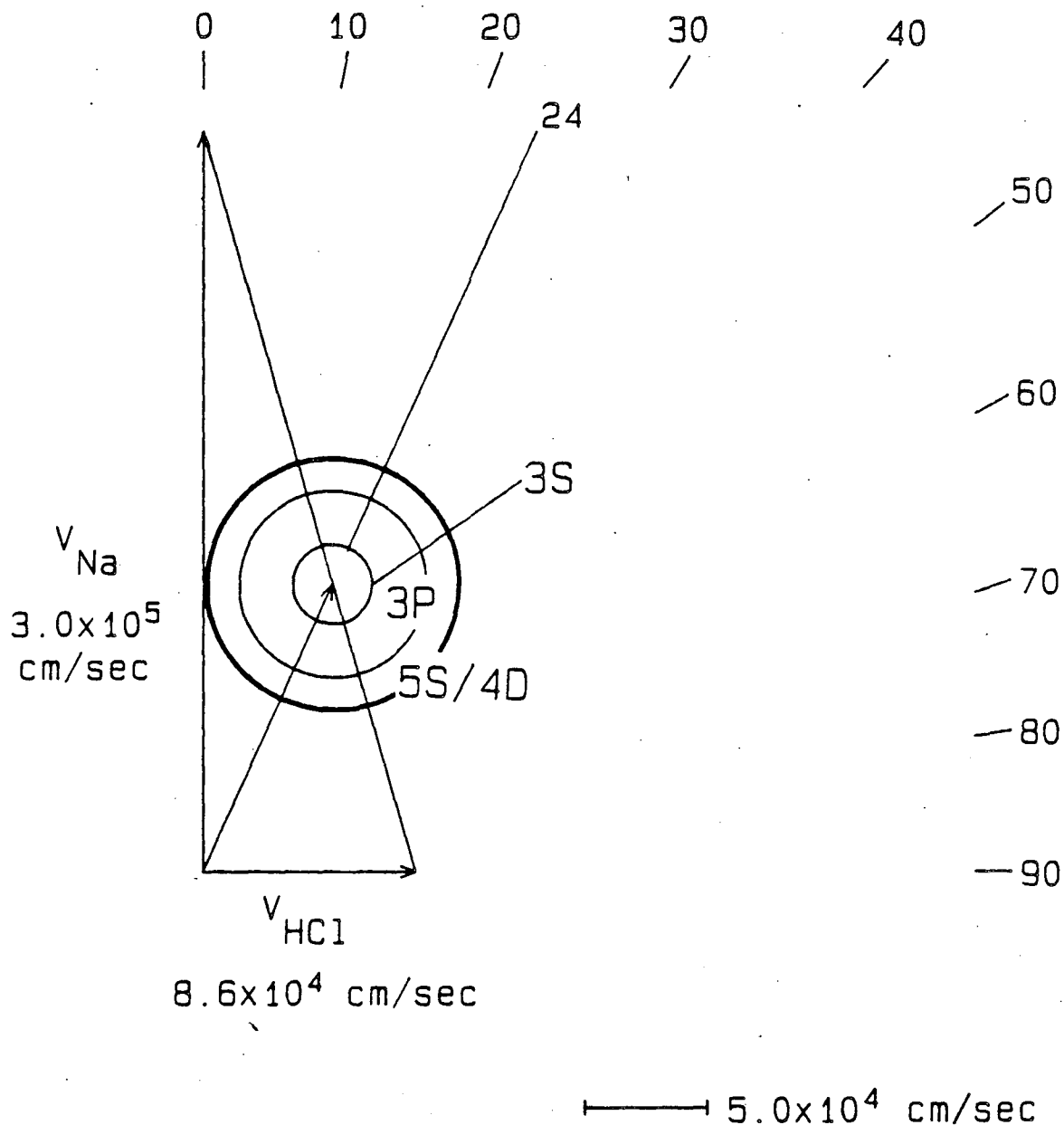


Fig. 5. Newton velocity vector diagram for $\text{Na}(3\text{S}, 3\text{P}, 4\text{D}, 5\text{S}) + \text{HCl} \rightarrow \text{NaCl} + \text{H}$ at a collision energy of 5.6 kcal/mole. The sodium beam is seeded in neon, the HCl beam is neat.

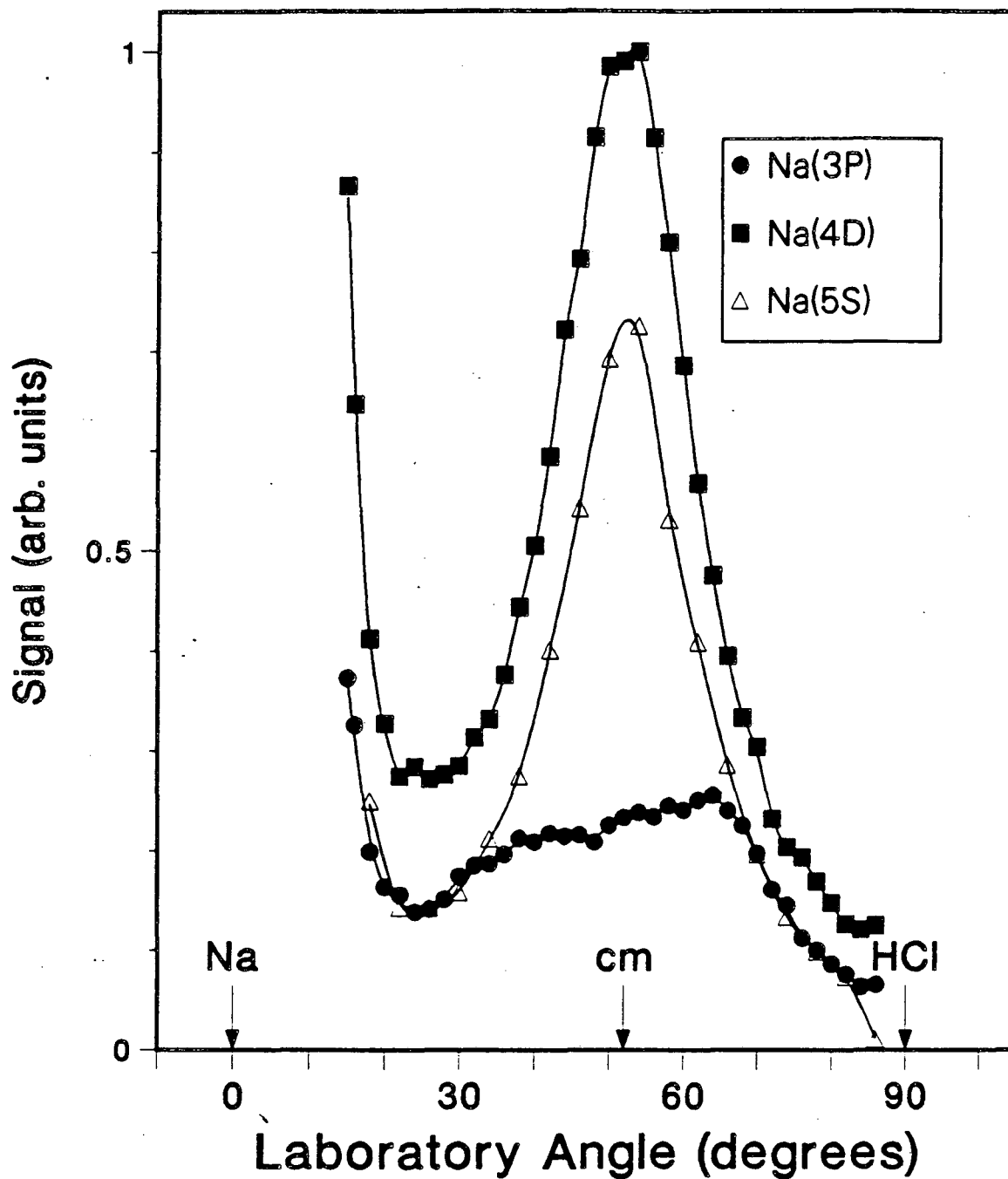
XBL 863-858

$$E_{\text{coll}} = 16 \text{ kcal/mole}$$



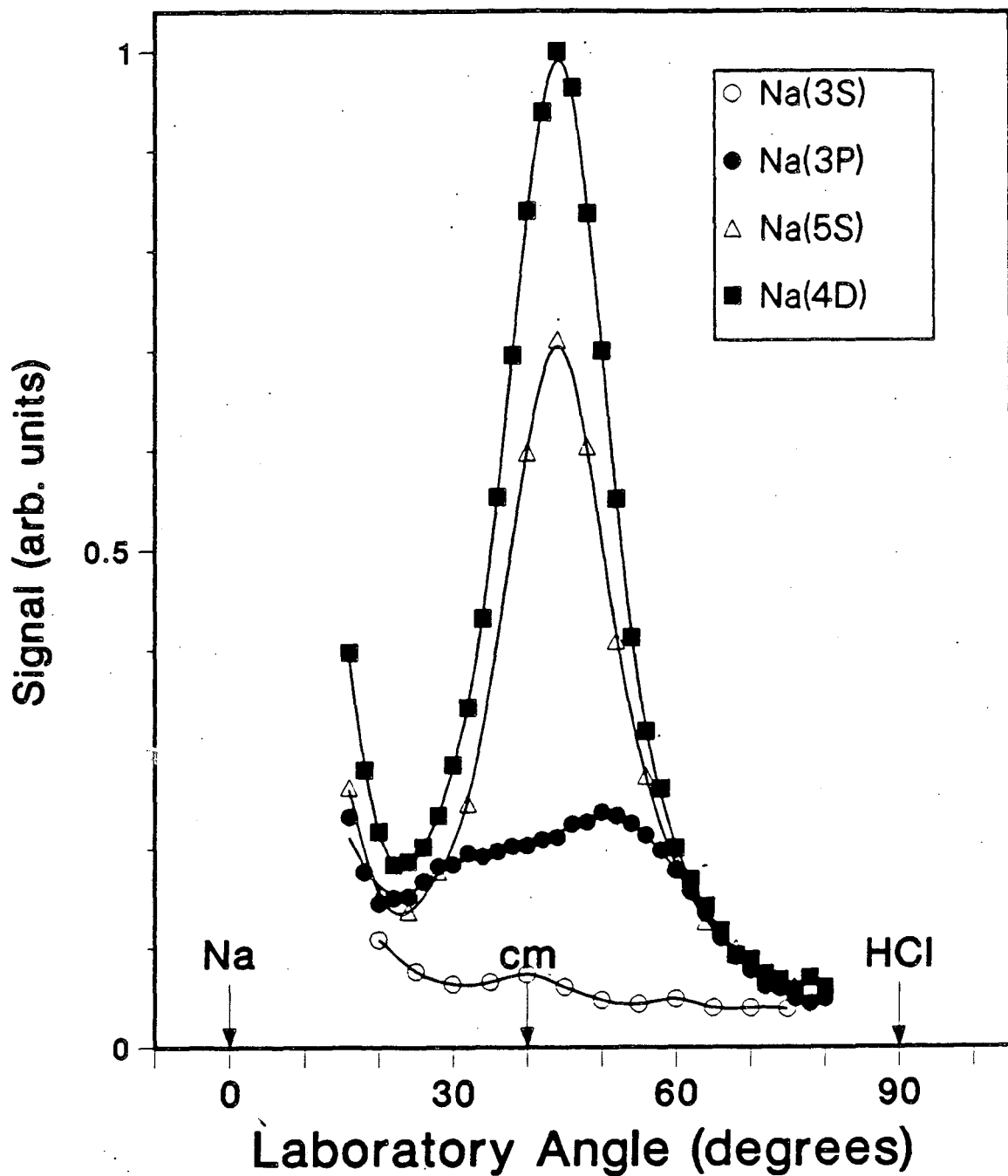
XBL 863-859

Fig. 6. Newton velocity vector diagram for $\text{Na}(3\text{S}, 3\text{P}, 4\text{D}, 5\text{S}) + \text{HCl} \rightarrow \text{NaCl} + \text{H}$ at a collision energy of 16.3 kcal/mole. The sodium beam is seeded in helium, the HCl beam is neat.



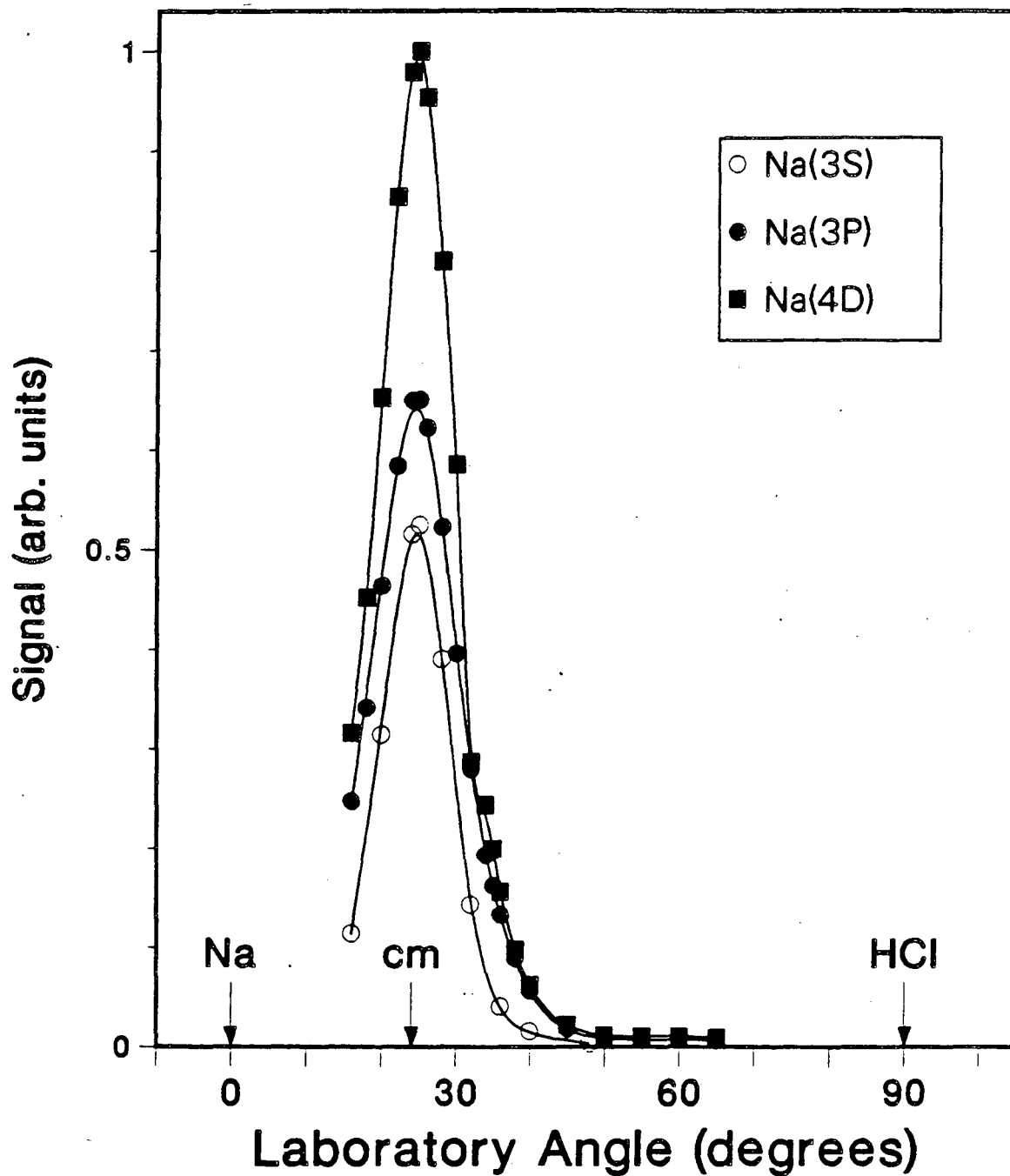
XBL 863-882

Fig. 7. NaCl angular distributions for Na(3S,3P,4D,5S) + HCl at a collision energy of 3.4 kcal/mole.



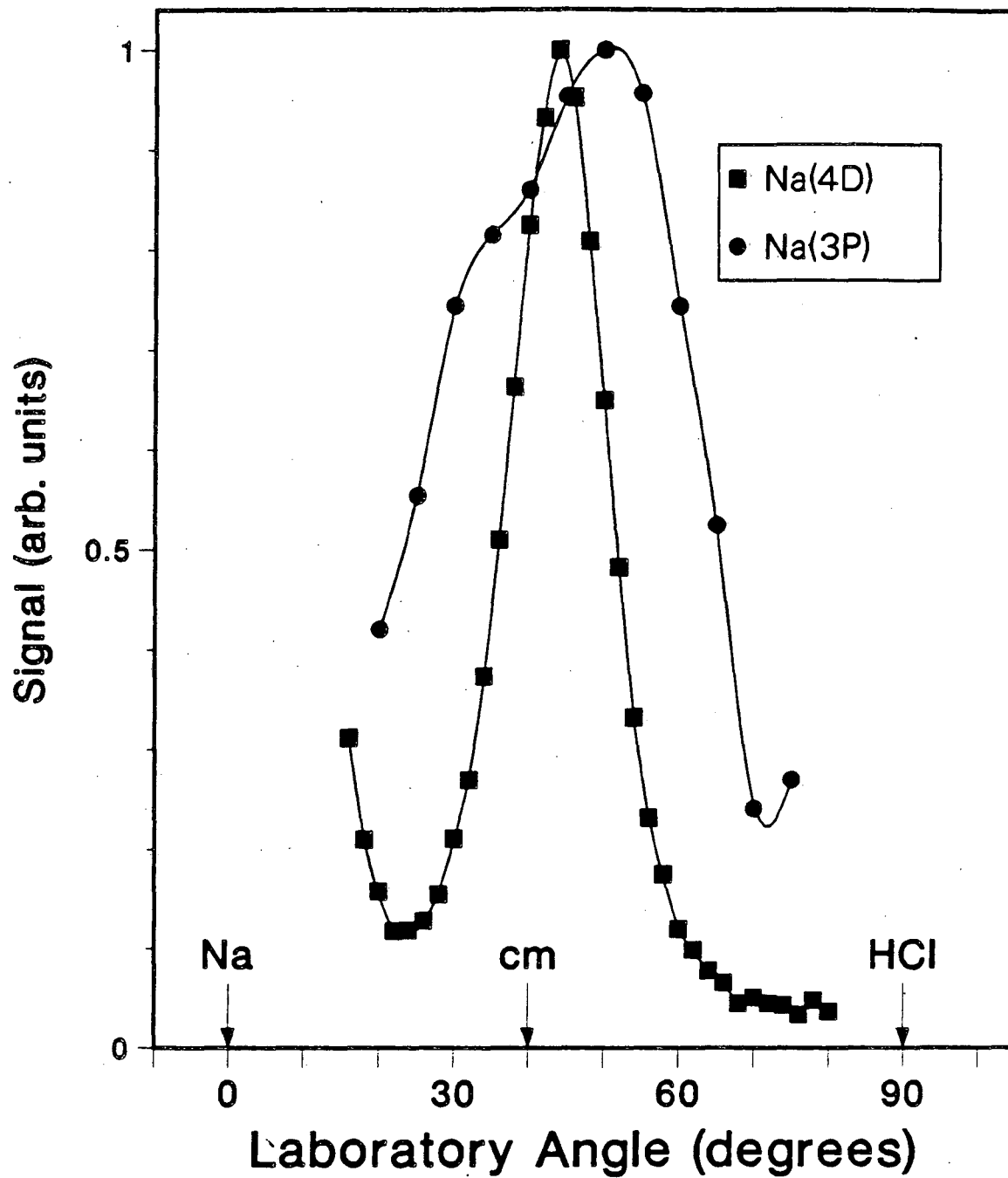
XBL 863-883

Fig. 8. NaCl angular distributions for Na(3S,3P,4D,5S) + HCl at a collision energy of 5.6 kcal/mole.



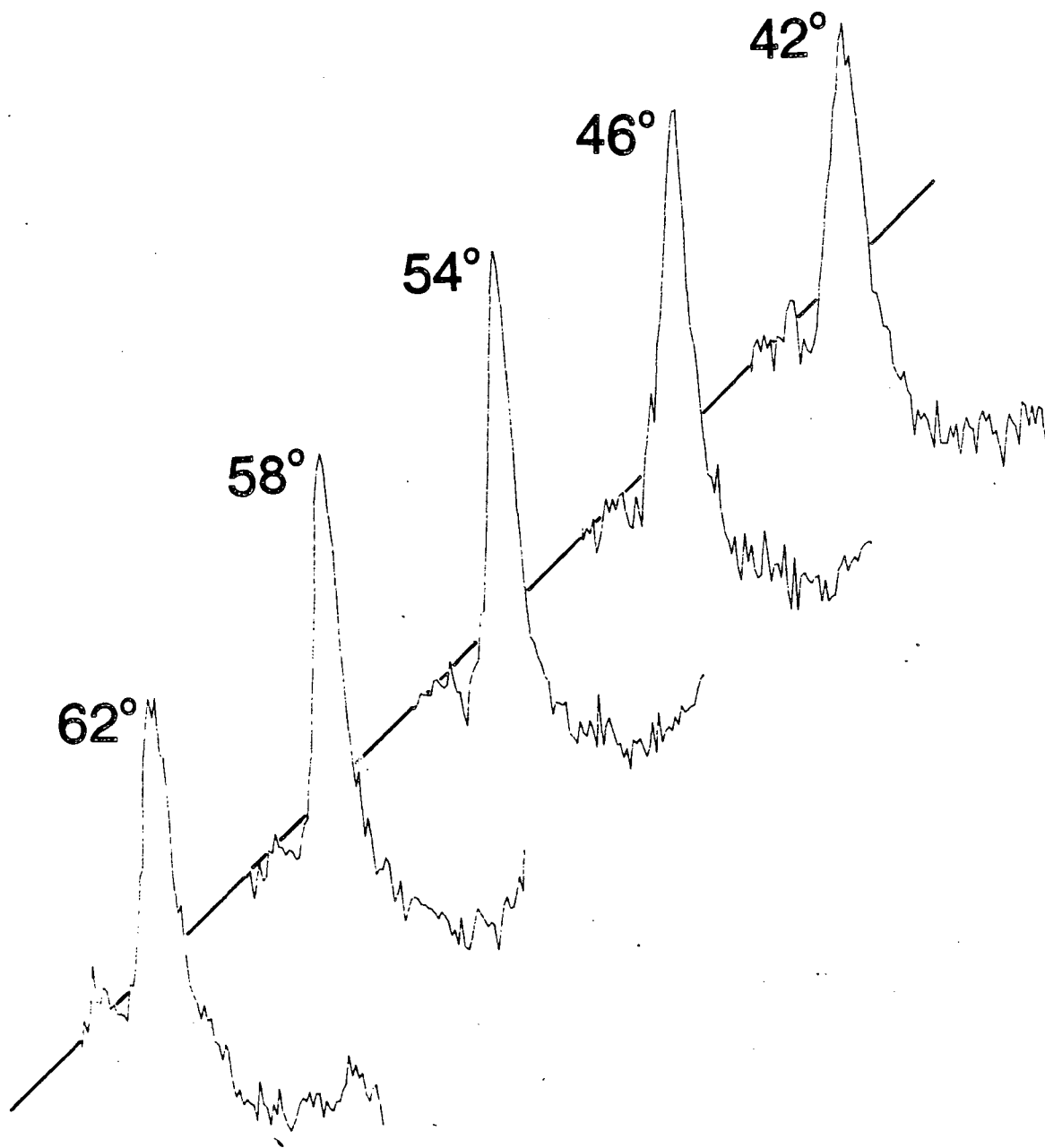
XBL 863-884

Fig. 9. NaCl angular distributions for Na(3S,3P,4D) + HCl at a collision energy of 16.3 kcal/mole.



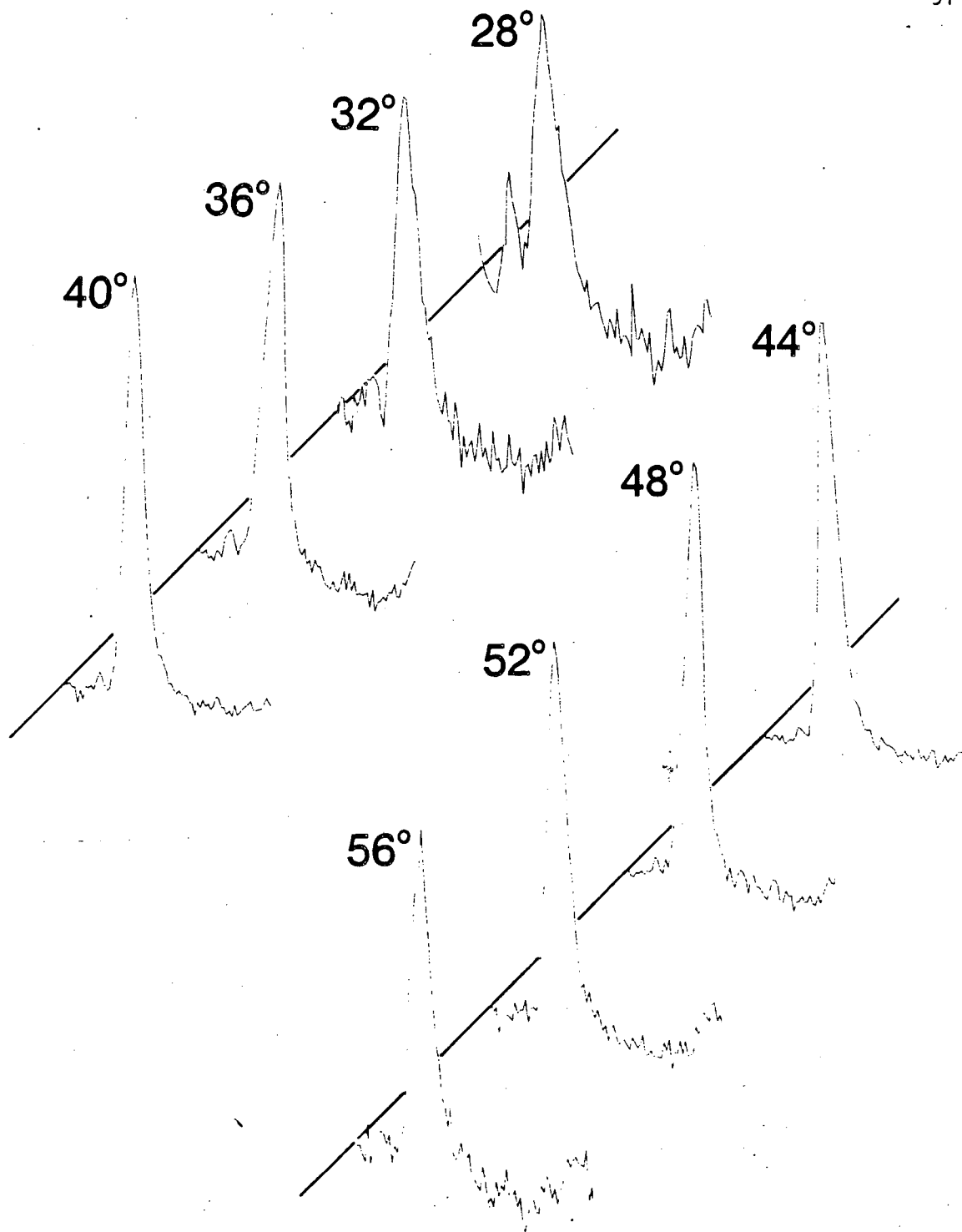
XBL 863-885

Fig. 10. NaCl angular distributions for Na(3P,4D) + HCl at a collision energy of 5.6 kcal/mole from figure 8. The distribution arising from the reaction of Na(3P) is blown up so as to be able to compare the angular widths of the two distributions.



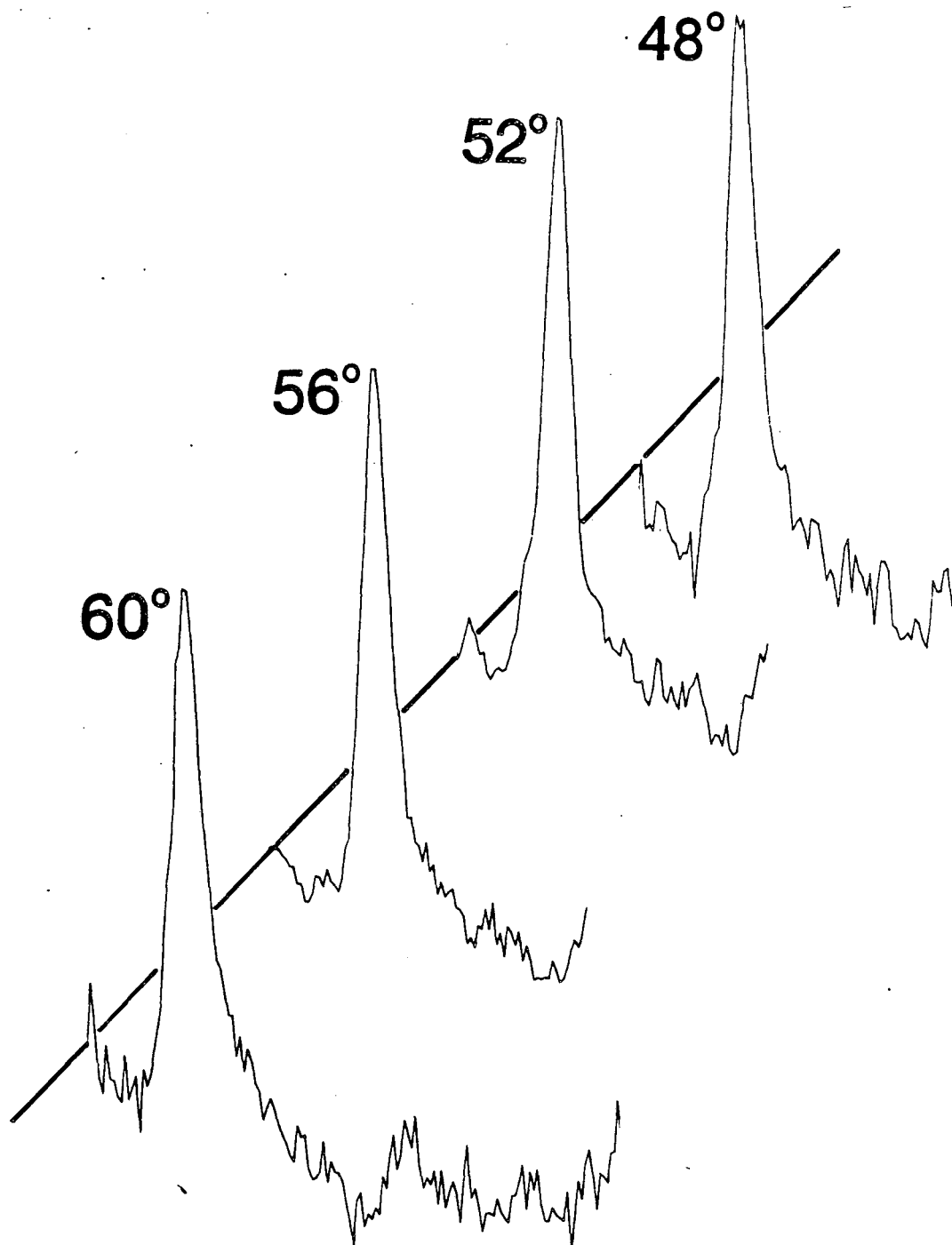
XBL 863-896

Fig. 11. NaCl product time-of-flight measurements for the reaction of Na(4D) + HCl at a collision energy of 3.4 kcal/mole for the laboratory detector angles shown on each frame.



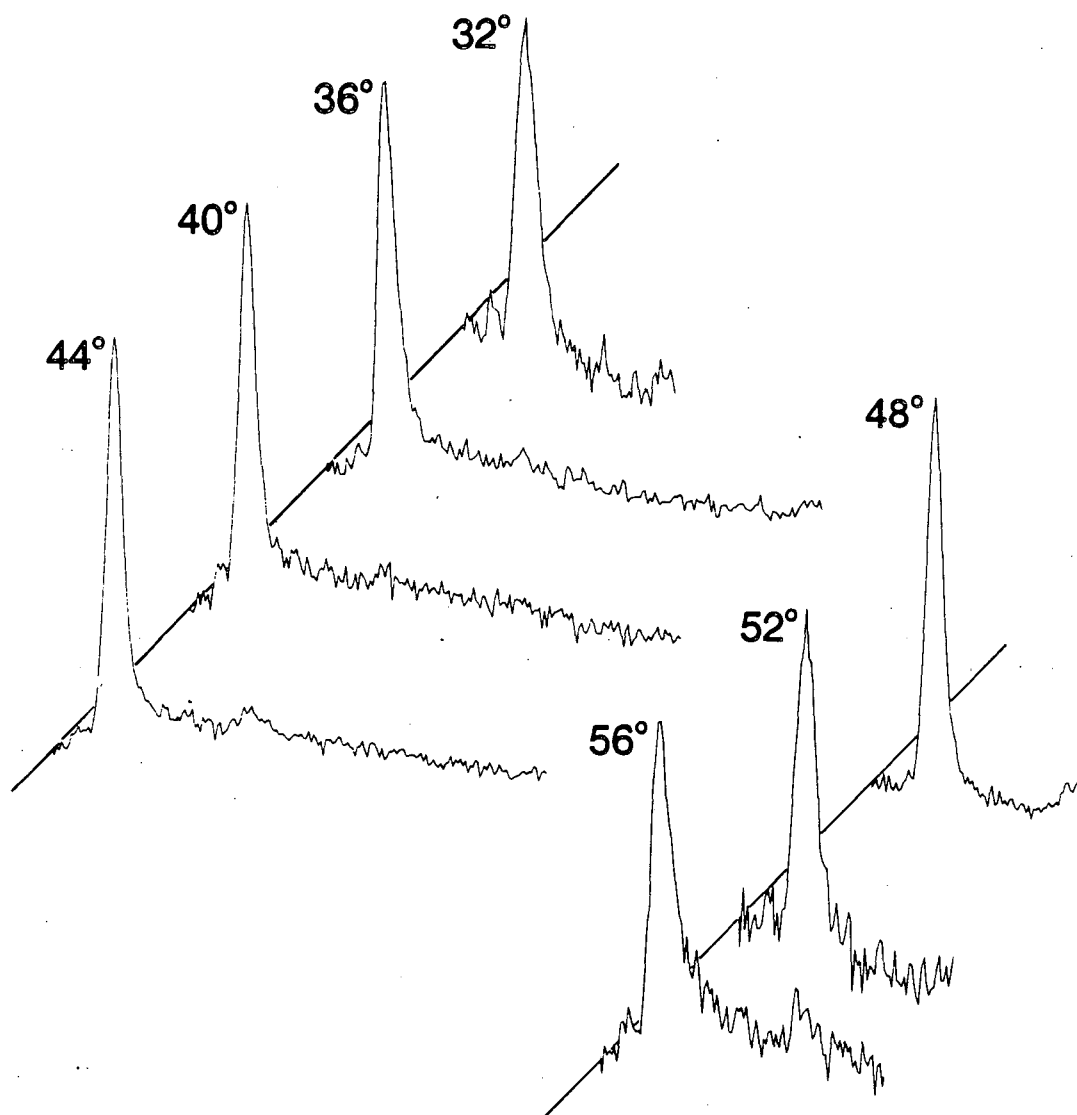
XBL 863-888

Fig. 12. NaCl product time-of-flight measurements for the reaction of Na(4D) + HCl at a collision energy of 5.6 kcal/mole for the laboratory detector angles shown on each frame.



XBL 863-887

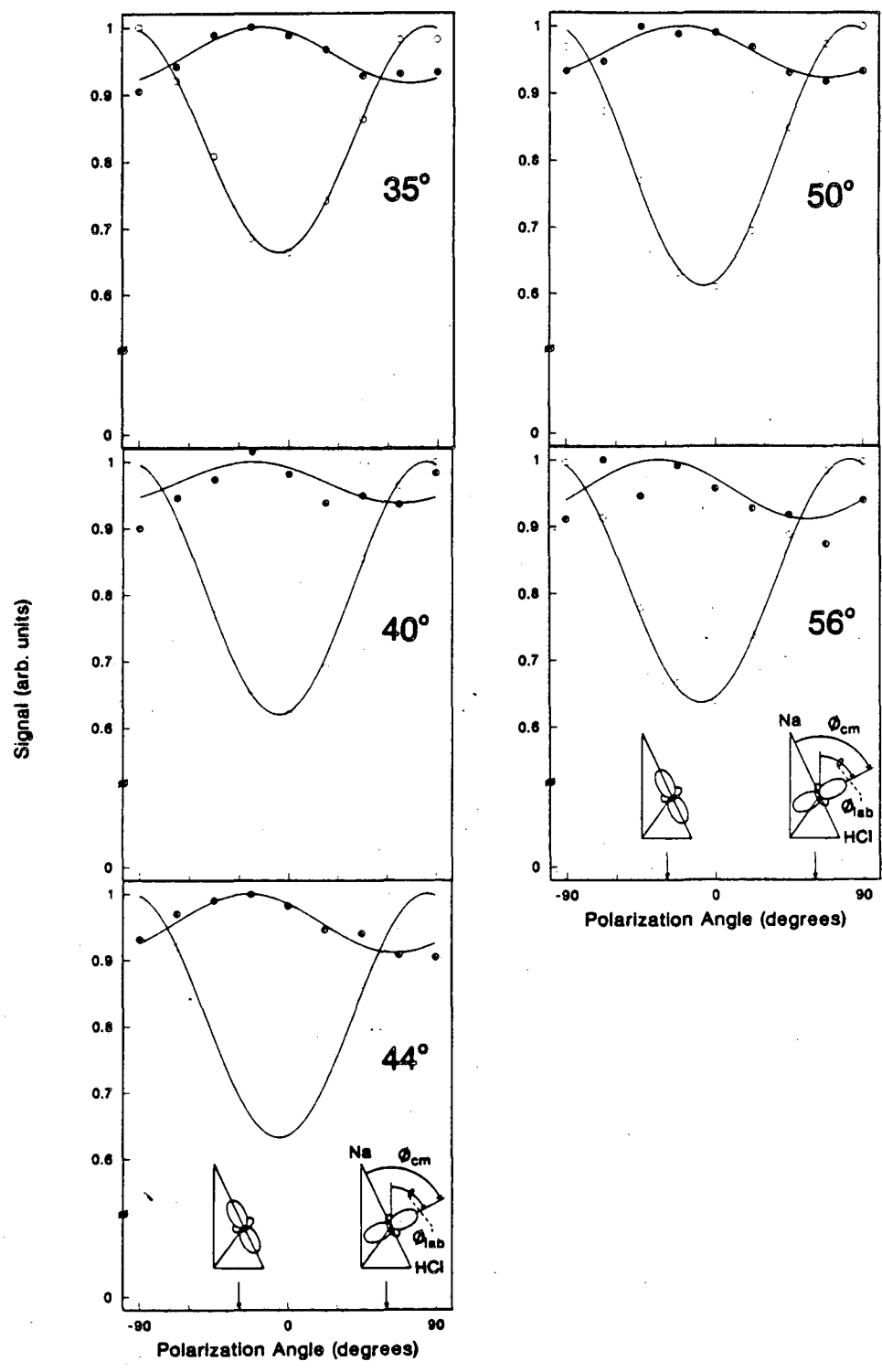
Fig. 13. NaCl product time-of-flight measurements for the reaction of Na(5S) + HCl at a collision energy of 3.4 kcal/mole for the laboratory detector angles shown on each frame.



XBL 863-889

Fig. 14. NaCl product time-of-flight measurements for the reaction of Na(5S) + HCl at a collision energy of 5.6 kcal/mole for the laboratory detector angles shown on each frame.

Fig. 15. Laser polarization dependences of the NaCl reactive signal due to the $\text{Na}(4D) + \text{HCl}$ reaction at a collision energy of 5.6 kcal/mole for the angles shown in each frame. The solid lines are the best fits to the data as discussed in chapter I.



XBL 863-895

Fig. 15

Table II. A summary of polarization dependences found for the reaction $\text{Na}(4D) + \text{HCl} \rightarrow \text{NaCl} + \text{H}$ at a collision energy of 5.6 kcal/mole. These results are tabulated from figures 15a-e.

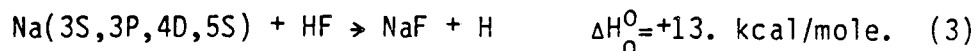
Laboratory Detector Angle	Laboratory Peak of Polarization Dependence (ϕ_{LAB})	Center of Mass Peak of Polarization Dependence (ϕ_{CM})	Amplitude (2A)
35°	-17°	13°	.084
40°	-22°	8°	.062
44°	-25°	5°	.089
50°	-22°	8°	.077
56°	-34°	-4°	.089

As seen in table II, at all detector angles measured the favored polarization angles for reaction are within a few degrees of the relative velocity vector of the system.

Simultaneously recorded polarization dependences for $\text{Na}(3P) + \text{HCl}$ show no polarization dependence except for the farthest backwards scattering (at a laboratory detector angle of 56°) for which a 3% dependence ($2A = 0.03$) is observed favoring reaction when the laser polarization is parallel to the relative velocity vector. In previous measurements, no effect was seen for $\text{Na}(3P) + \text{HCl}$, but the minimum detectable effect for those measurements was 10-15%, so that it is not surprising that nothing was seen.¹¹ The upper limit of any polarization dependences for the other angles (30°-50°) for which none were observed could safely be put at 2%.

2. Na + HF

At collision energies up to 13.4 kcal/mole no reaction was observed for:



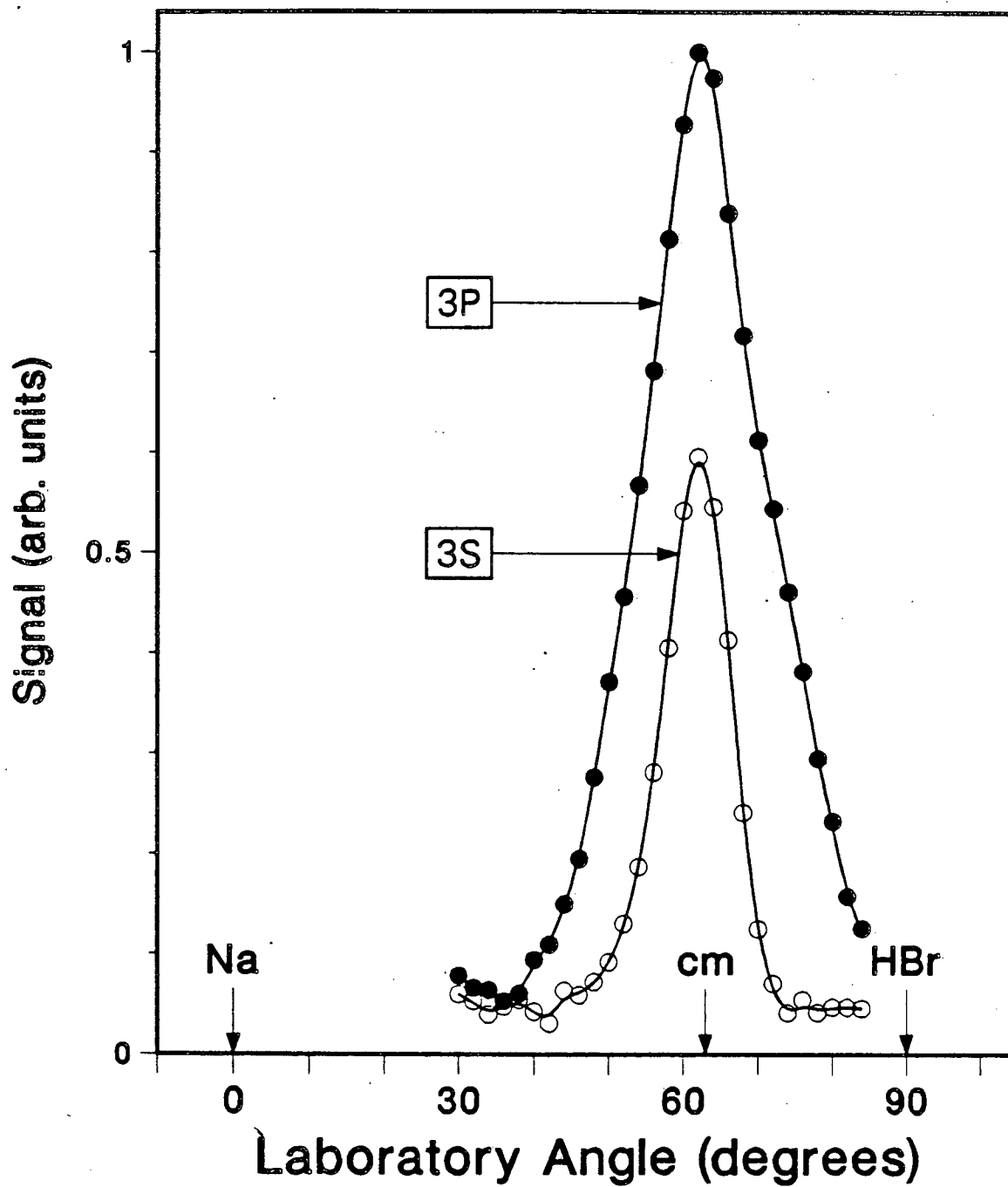
Extensive signal averaging yielded no detectable NaF within the angular limits defined by its kinematics at $m/e=42$ (NaF^+) nor at $m/e=23$ (Na^+). As mentioned above, reaction of ground state sodium atoms with vibrationally excited HF has been observed in chemiluminescence experiments.¹⁰

3. Na(3S,3P) + HBr

Angular distributions have been measured for the reaction:

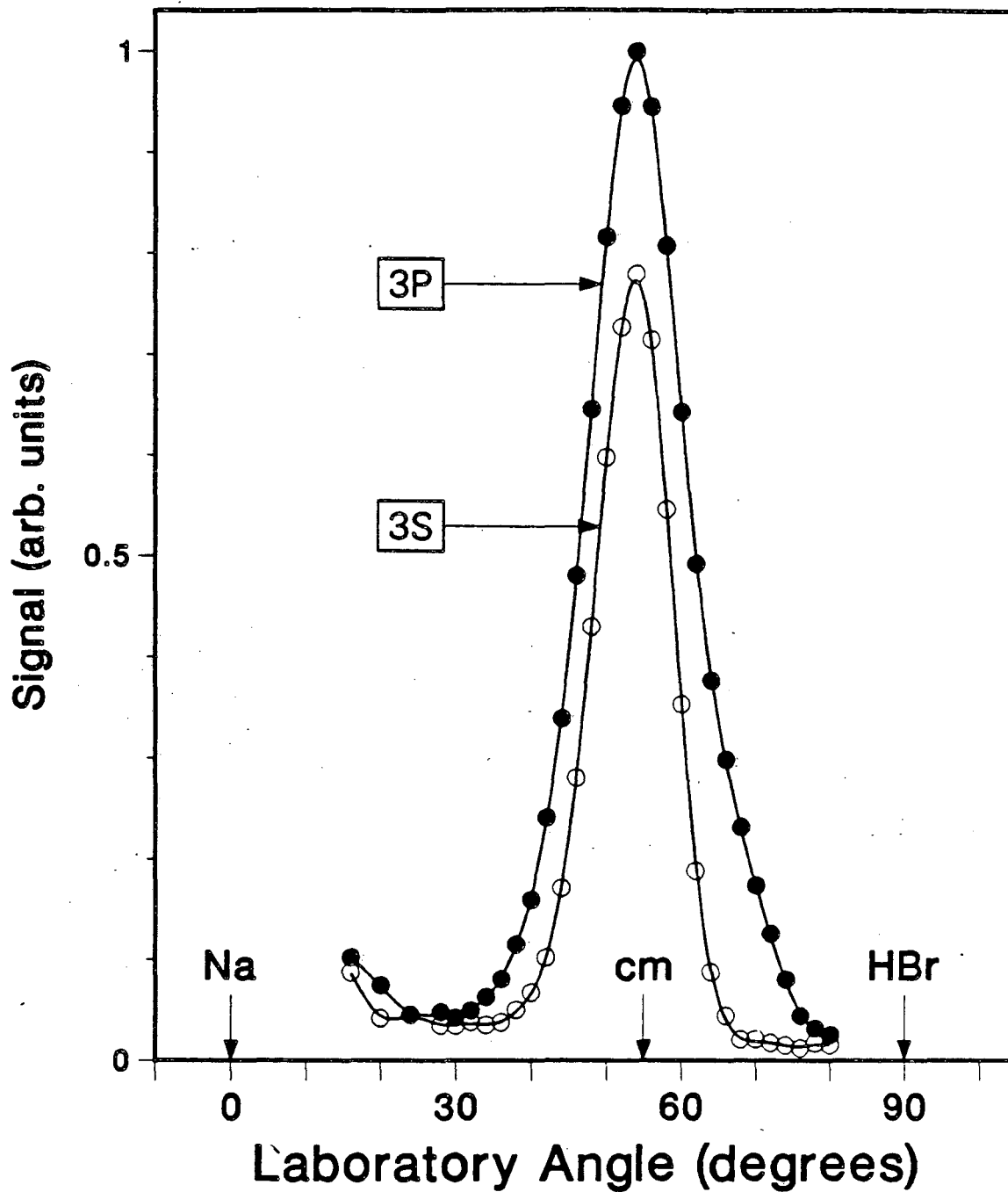


at collision energies of 3.0, 5.3, and 20.0 kcal/mole, as shown in figures 16, 17, and 18, respectively. Being very nearly thermoneutral in the absence of electronic and collision energy, a substantial amount of ground state reaction is observed for each collision energy studied. Still, there is a significant increase in the reactive cross section for the reaction when the Na atoms are excited to the 3P state.



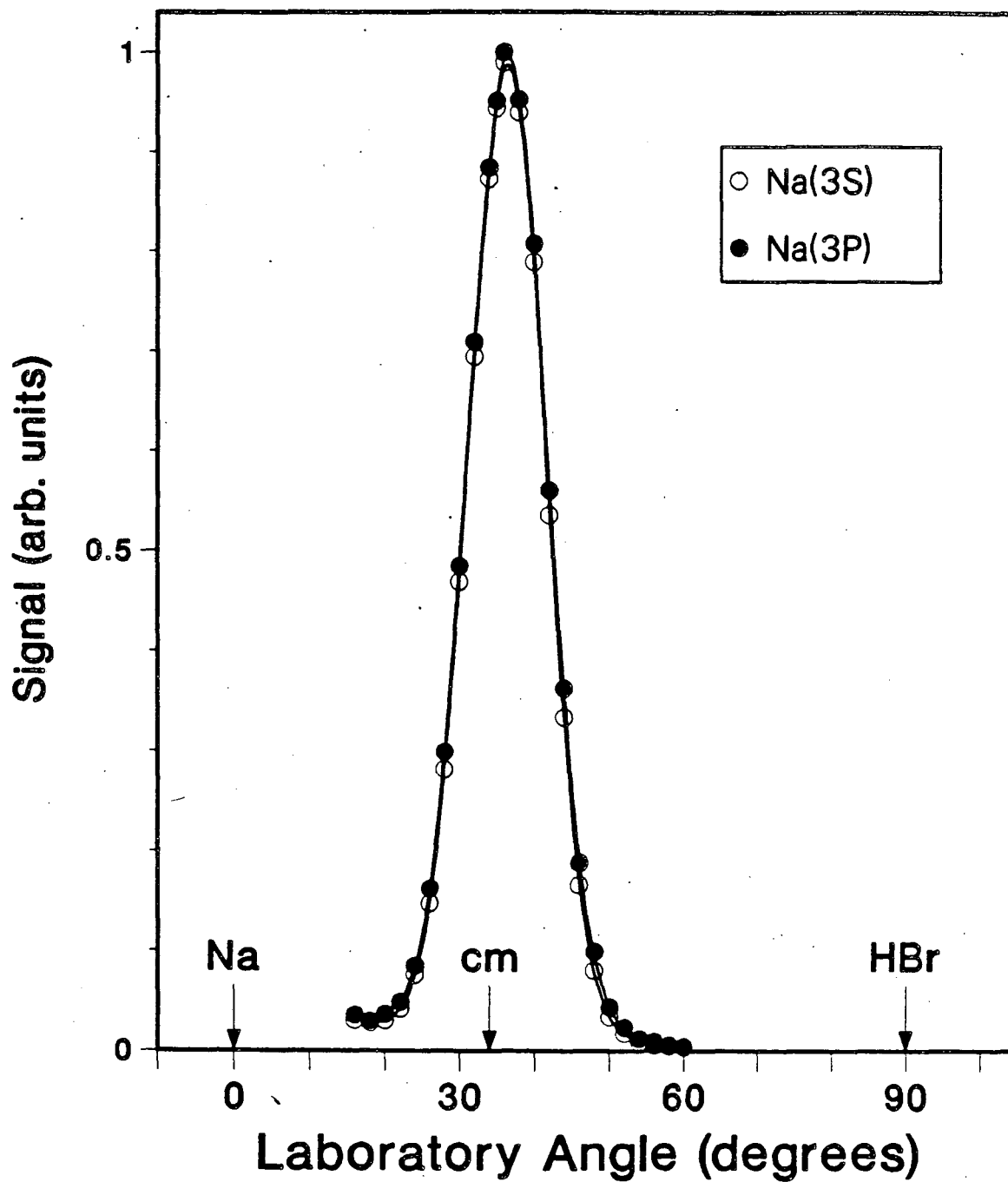
XBL 863-879

Fig. 16. NaBr angular distributions for Na(3S,3P) + HBr at a collision energy of 3.0 kcal/mole.



XBL 863-880

Fig. 17. NaBr angular distributions for Na(3S,3P) + HBr at a collision energy of 5.3 kcal/mole.



XBL 863-881

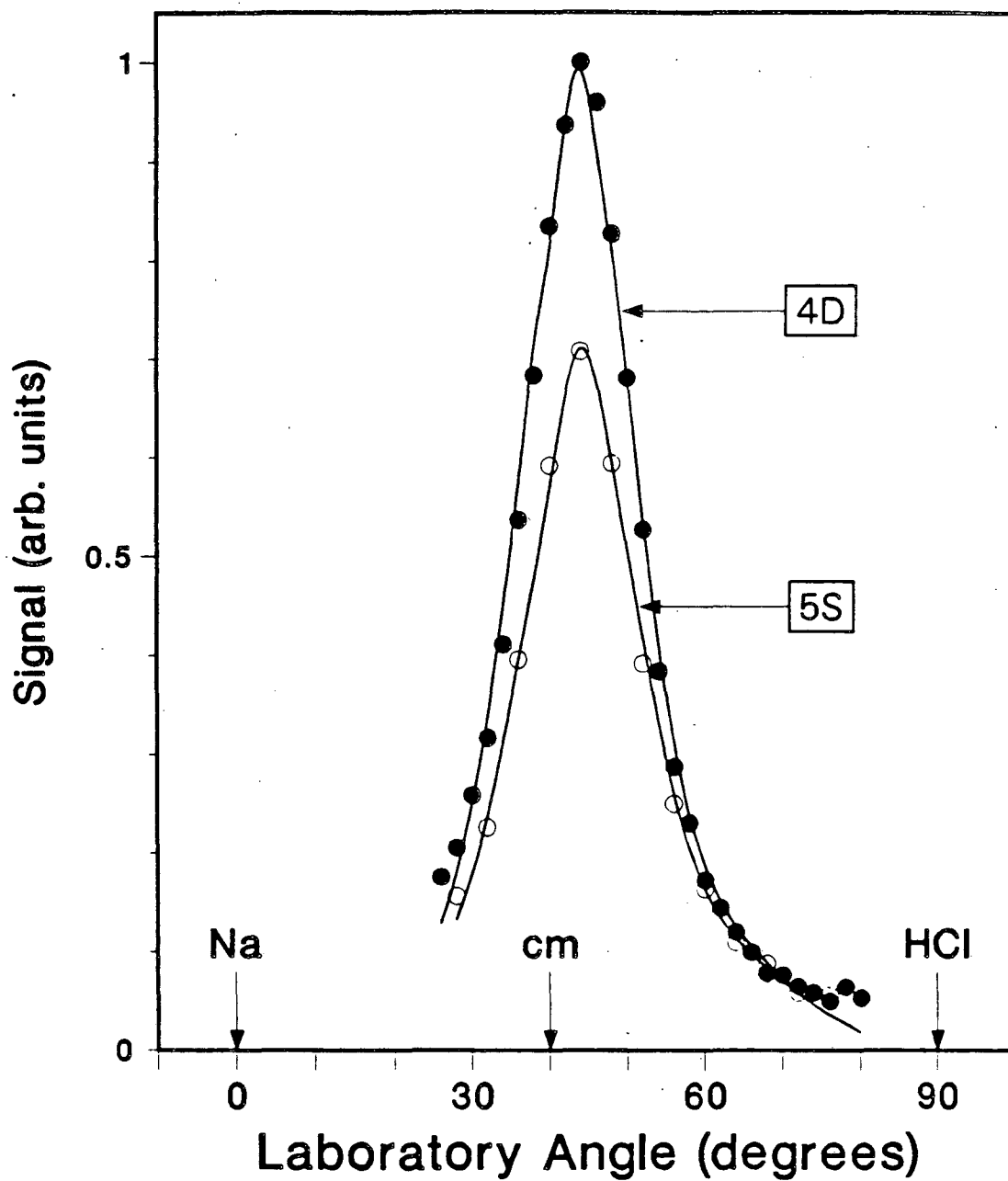
Fig. 18. NaBr angular distributions for Na(3S,3P) + HBr at a collision energy of 20. kcal/mole.

C. Analysis of Experimental Results

As described in chapter I, experimental angular and time-of-flight distributions were fitted using independent center of mass scattering angular and translational energy distributions using the program GM (a derivative of CMLAB). Detailed transformations of Na(4D,5S) + HCl to the center of mass frame were carried out in this way for the 5.6 kcal/mole data. The best fits to the measured angular distributions for Na(4D,5S) + HCl are shown in figure 19. The fits of the same center of mass distributions to the time-of-flight data are shown in figures 20 and 21 for Na(4D) + HCl and Na(5S) + HCl, respectively.

A comparison of the best fit translational energy distributions ($P(E_T)$ distributions) at collision energies of 5.4 kcal/mole for Na(3P) in figure 22, and 5.6 kcal/mole for Na(4D) and Na(5S) in figure 23 points up this large change in the dynamics of the reaction. Note that with increasing electronic energy, the peaks and the mean energies in the $P(E)$ distributions move to lower energy, with $E_T^{\text{peak}} = 16, 7,$ and 4 kcal/mole and $\langle E_T \rangle = 20, 7,$ and 7 kcal/mole for the reactions of the 3P, 5S, and 4D, respectively. The tails of the recoil energy distributions in all cases go out to the maximum possible energy available.

The calculated center of mass angular distributions ($T(\theta)$) shown in figure 24 for the product NaCl due to Na(5S) and Na(4D), at 5.6



XBL 863-761

Fig. 19. Angular distributions for Na(4D,5S) + HCl at a collision energy of 5.6 kcal/mole. The solid lines are the best fit to the data generated from center-of-mass angular and translational energy distributions.

Fig. 20. Time-of-flight distributions for Na(4D) + HCl at a collision energy of 5.6 kcal/mole. The solid lines are the best fit to the data generated from center-of-mass angular and translational energy distributions. The distributions are for the detector angles shown in each frame.

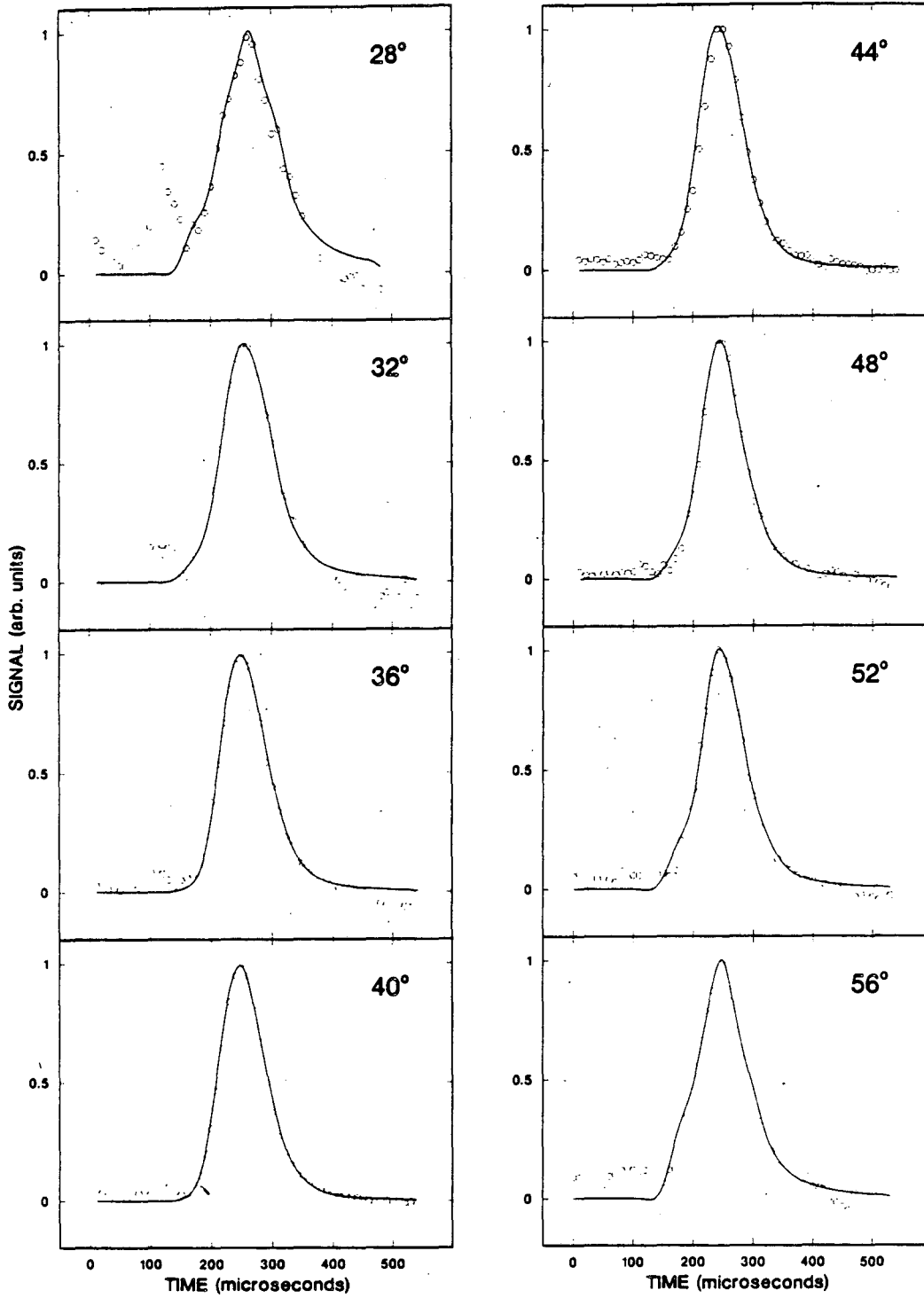
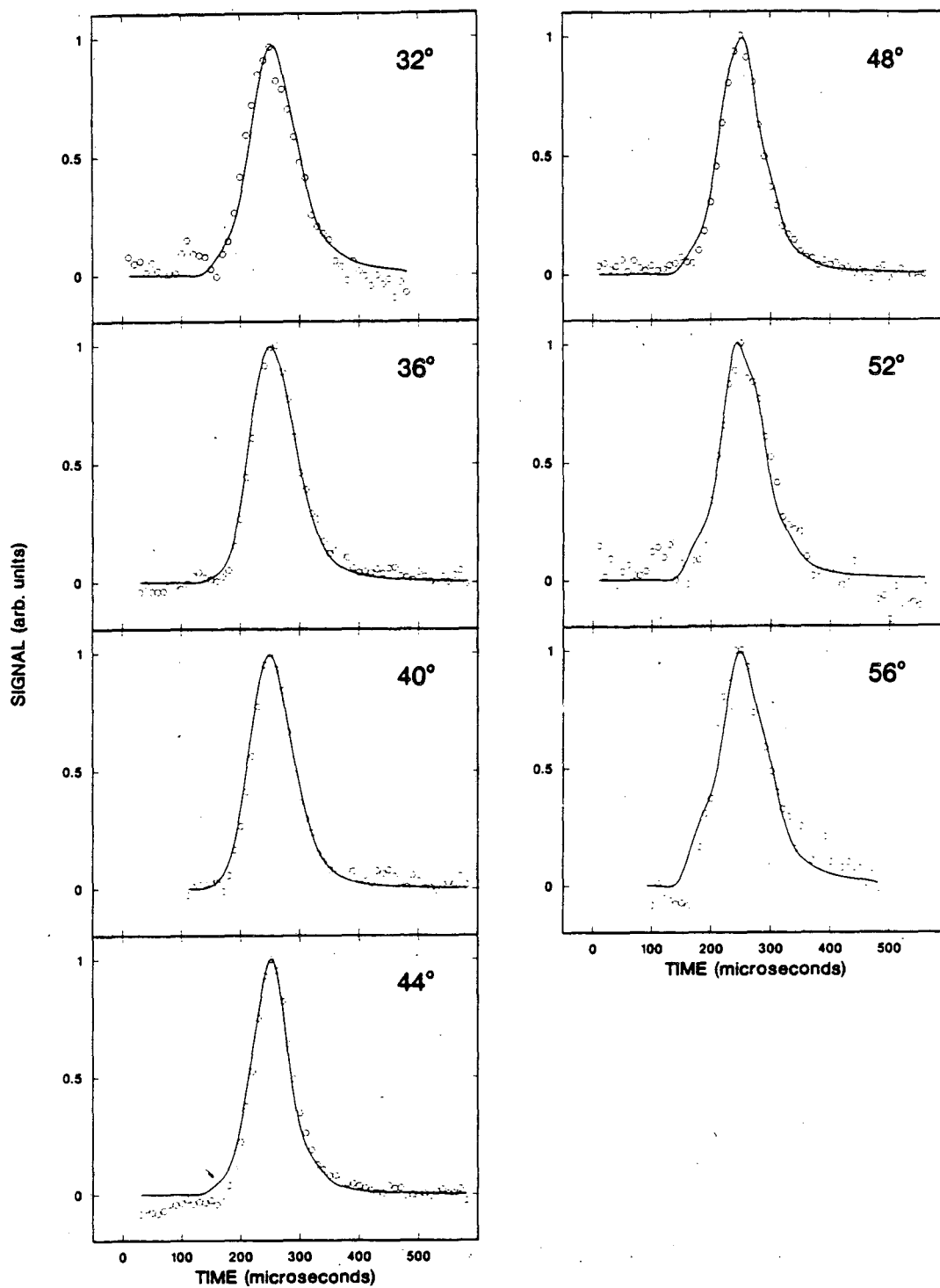


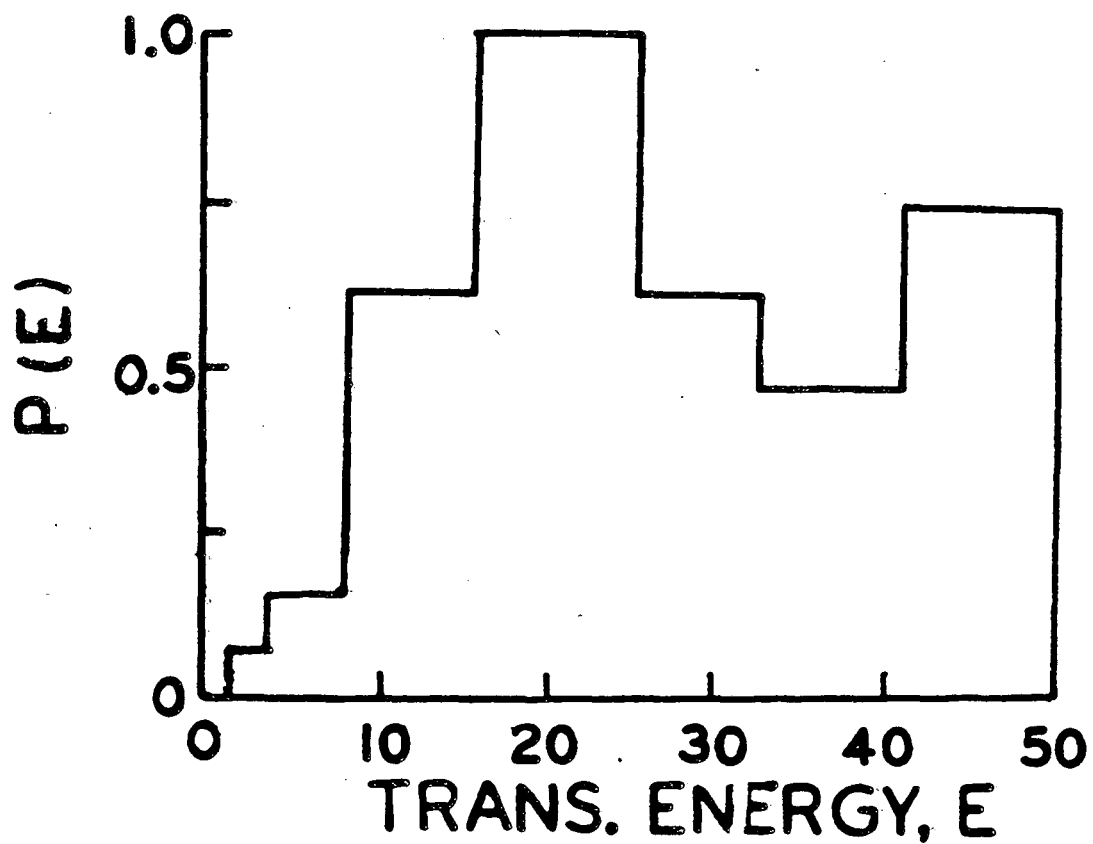
Fig. 20

XBL 863-756



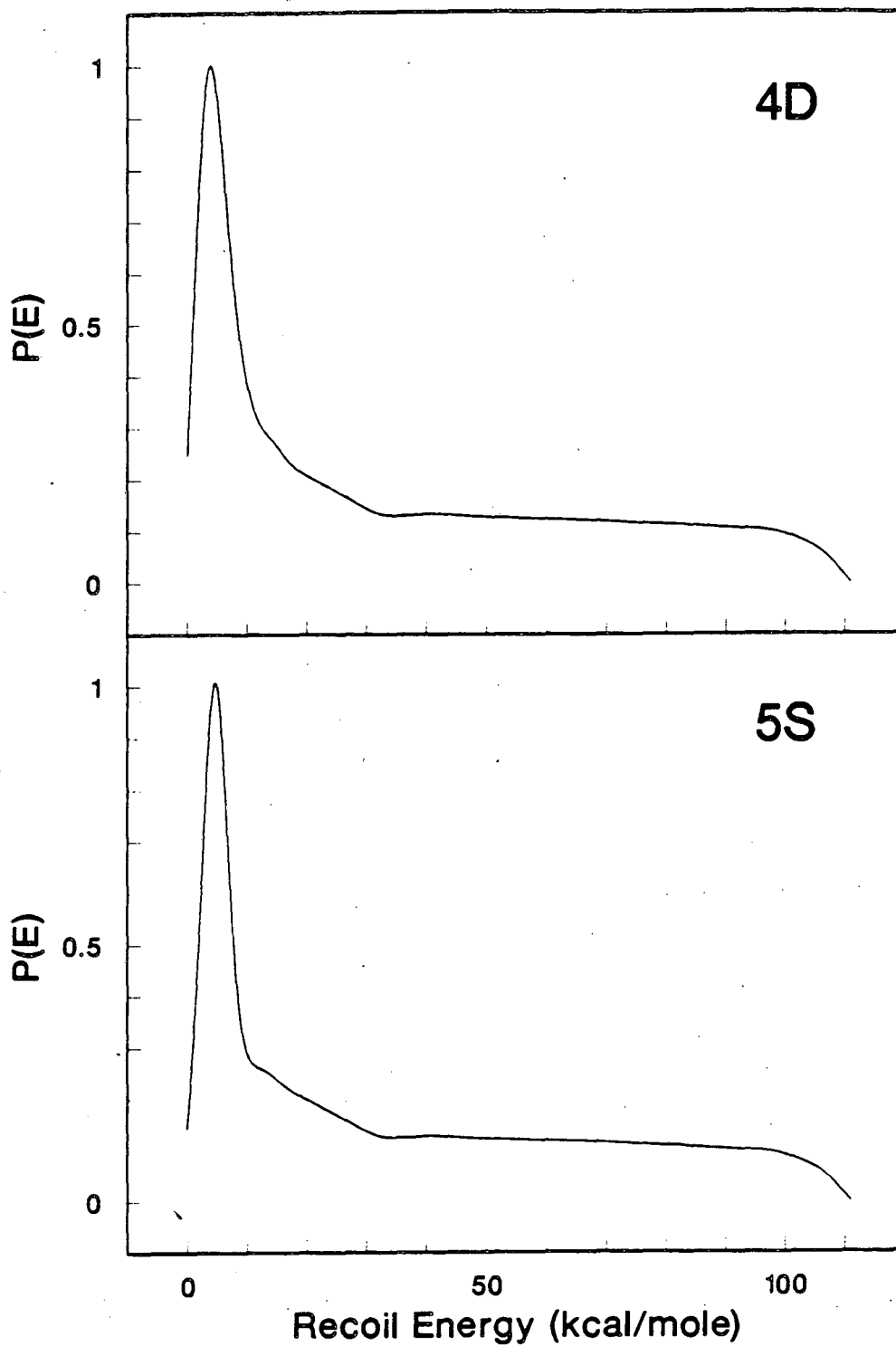
XBL 863-754

Fig. 21. Same as figure 20, but for $\text{Na}(5S) + \text{HCl}$.



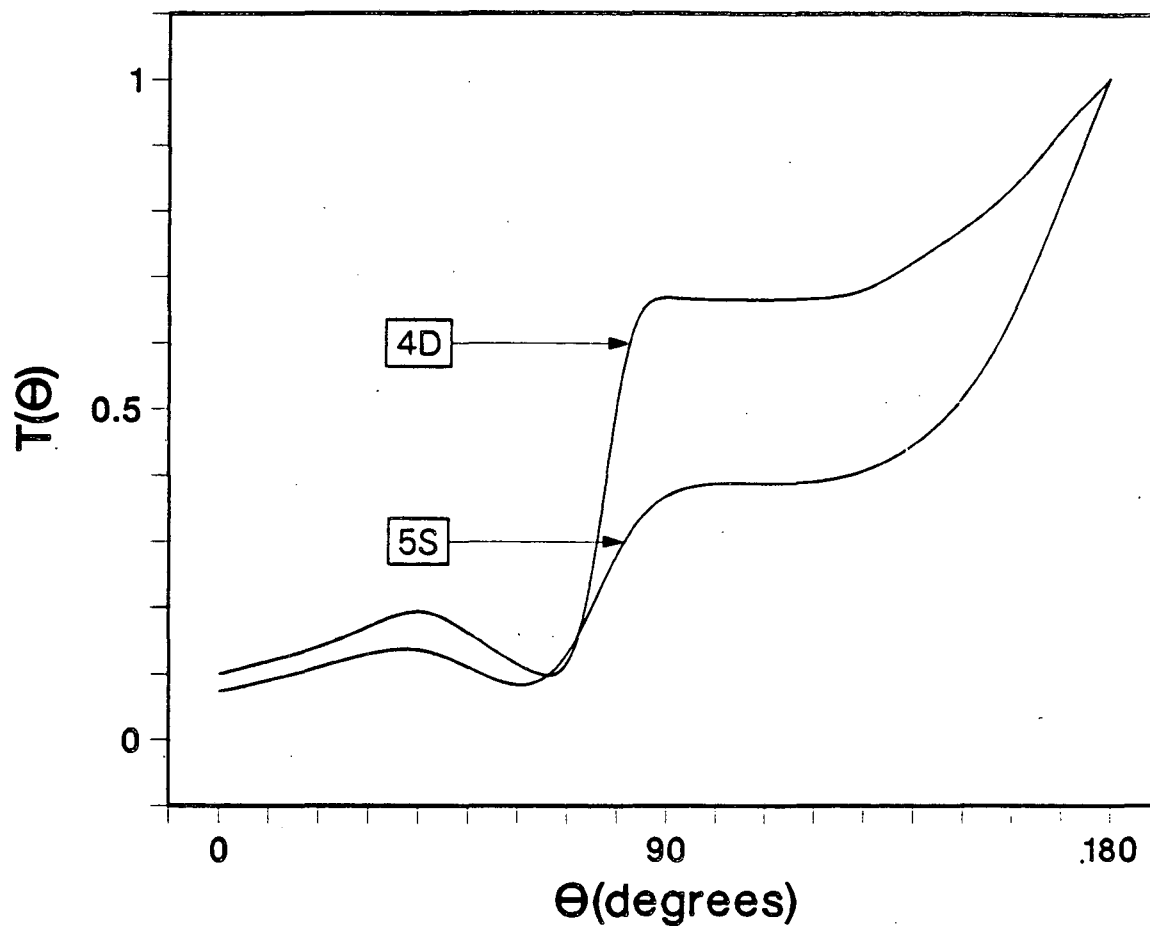
XBL 863-851

Fig. 22. Best fit center-of-mass product translational energy distributions for Na(3P) + HCl at a collision energy of 5.4 kcal/mole, from reference 11.



XBL 863-751

Fig. 23. Best fit center-of-mass product translational energy distributions for $\text{Na}(4\text{D},5\text{S}) + \text{HCl}$, at a collision energy of 5.6 kcal/mole.



XBL 863-762

Fig. 24. Best fit product NaCl center-of-mass scattering angular distributions at a collision energy of 5.6 kcal/mole for Na(4D,5S) + HCl.

kcal/mole show strong backwards peaking with slight forward sideways peaking. This is similar to the $T(\theta)$ found for the reaction of the Na(3P) atoms.¹¹ The features of the two upper state $T(\theta)$ distributions are sharper and exhibit a sharp rise at approximately 90° for each.

The relative integrated cross sections for the reaction at 5.6 kcal/mole substantiate the idea that the cross section increases with increasing electronic energy. The ratios of integrated cross sections for the excited electronic states are:

$$3.5 (4D): 2.4(5S): 1.0 (3P) \quad \text{at 5.6 kcal/mole.} \quad (5)$$

A relative optical pumping efficiency of 0.8 for the upper state (4D or 5S) as compared to the 3P state is assumed. That is, the fraction of atoms in the Na(3P) state is assumed unchanged when the second laser is turned on, and the fraction of atoms in the Na(4D) or Na(5S) state is assumed to be 80% of the fraction in the Na(3P) state as discussed in chapter I.

Assuming 20% efficiency in optically pumping the Na(3P) state from the ground state, the following ratios of reactive cross sections are obtained:

$$90 (3P): 1 (3S) \quad \text{at 5.4 kcal/mole, and} \quad (6)$$

$$6 (3P): 1 (3S) \quad \text{at 16.3 kcal/mole.} \quad (7)$$

The 20% pumping efficiency estimate is quite liberal, particularly in the most difficult to pump case of Na seeded in He (16.3 kcal/mole data) as discussed in chapter I. If the pumping efficiency were lower, it would imply larger enhancements than those reported above. Also, by

lowering the collision energy below the endothermicity of the reaction (turning off the ground state reaction), the enhancement can be made arbitrarily large as long as the Na(3P) still reacts. At 3.4 kcal/mole, this ratio is in fact infinite because of the lack of reaction of Na(3S).

The absolute reactive cross sections can be estimated by comparison with small angle elastic scattering.²⁷ This method eliminates the need to know the reactant beam number densities at the interaction region -- difficult quantities to determine accurately. Also, since both elastically scattered Na and reactively scattered NaCl are observed at $m/e=23$ (as Na^+), only the relative probability of ionization of the two to Na^+ needs to be known, rather than the exact ionization efficiencies and the transmission functions of the quadrupole mass spectrometer at two different masses. In order to make the comparison between elastic and reactive contributions to the $m/e=23$ angular distributions, the absolute differential elastic cross section must be calculated. Then, one or more small angles in the measured ground state angular distribution at which only elastic scattering is observed are used to calibrate the angular distributions for each electronic state at that collision energy and the integrated reactive cross sections derived from them.

If large impact parameter collisions do not lead to chemical reaction, the absolute differential cross section for small angle

elastic scattering can be approximated for a spherically symmetric potential:

$$\left(\frac{d\sigma_{el}}{d\omega}\right)_{abs} = 0.239 \left(\frac{C_6}{E}\right)^{1/3} \theta^{-7/3}, \quad (8)$$

where C_6 is the coefficient for r^{-6} in a van der Waals potential in kcal/mole \AA^6 , E is the collision energy in kcal/mole, and θ is the center of mass scattering angle in radians.²⁸ Equation (8) is the small angle scattering limit of the classical scattering due to a van der Waals interaction $V(r) = C_6 r^{-6}$.²⁸ This approximation is valid where $\sin\theta \approx \theta$. The C_6 parameter is not known for Na-HCl but it can be estimated. The C_6 parameter will have two main contributions -- a dispersion portion and an induction portion -- with

$$C_6 = C_{6,disp} + C_{6,ind}. \quad (9)$$

The dispersive portion can be estimated by the Slater-Kirkwood approximation:^{27,29-30,2}

$$C_{6,disp} = (241.55 \text{ kcal/mole } \text{\AA}^{3/2} / \text{a.u.}) \left(\frac{3 \alpha(\text{Na})\alpha(\text{HCl})}{2 [\alpha(\text{Na})/N(\text{Na})]^{1/2} + [\alpha(\text{HCl})/N(\text{HCl})]^{1/2}} \right) \quad (10)$$

where $C_{6,disp}$ is in kcal/mole \AA^6 , α is the atomic or molecular polarizability in \AA^3 , and N is the effective number of electrons. The polarizability of ground state Na is 24.5\AA^3 .³¹ The polarizability of HCl is 2.63\AA^3 .³² The effective numbers of electrons are: $N(\text{Na})=1$, and $N(\text{HCl})=8$. The value of $C_{6,disp}$ obtained in this way is expected to be

accurate to $\pm 50\%$.³³ Equation (10) yields a value of $C_{6,\text{disp}} = 4230$ kcal/mole \AA^6 . This compares favorably with the C_6 parameter measured for the isoelectronic Na-Ar ground state potential -- $C_6(\text{Na-Ar}) = 5500$ kcal/mole \AA^6 .³⁴ From (10), and the atomic polarizability of Ar $\alpha(\text{Ar}) = 1.6 \text{\AA}^3$,³⁵ the estimated C_6 would be $C_6 = 2630$ kcal/mole \AA^6 , which is off by more than a factor of 2.

The inductive portion of C_6 , the dipole induced dipole contribution, can be estimated from the Debye equation:³⁶

$$C_{6,\text{ind}} = (14.394 \text{\AA}^3 \text{ kcal/mole-D}^2) \alpha(\text{Na}) \mu^2(\text{HCl}), \quad (11)$$

where $\mu(\text{HCl})$ is the permanent dipole moment of HCl, 1.08D,³⁷ and once again α is in \AA^3 . Equation (11) yields a value of $C_{6,\text{ind}} = 411$ kcal/mole \AA^6 .

Thus from equations (9), (10), and (11), $C_6 = 4640$ kcal/mole \AA^6 . The value obtained is expected to be limited by the accuracy of its dominant component $C_{6,\text{disp}}$ to $\pm 50\%$.³³ However, the absolute differential cross section is slowly varying with C_6 (as $C_6^{1/3}$) so that the error induced in $d\sigma_{e1}$ by C_6 is then only 20%.

The lowest laboratory scattering angle measured at a collision energy of 5.6 kcal/mole for (ground state) $\text{Na}(3S) + \text{HCl}$ was 15° . Using the peak beam velocities, the angles and velocities were determined to carry out the center of mass to laboratory frame transformation as described below. Note that a substantial error is introduced by only using one Newton diagram in this manner. The center of mass scattering angle corresponding to $\theta_{\text{lab}} = 15.0^\circ$ is $\theta_{\text{cm}} = 25.1^\circ = 0.438$ radians.

In order to convert from center of mass product flux ($I(\theta_{cm})$) to laboratory frame number density ($N(\theta_{lab})$), the transformation:

$$N(\theta_{lab}, v) = \frac{v}{u^2 |\cos \delta|} I(\theta_{cm}, u) \quad (12)$$

is used.³⁸ The parameters are: the laboratory frame elastically scattered Na velocity $v=1.791$ km/sec, the center of mass frame elastically scattered Na velocity $u=1.108$ km/sec, and the detector viewing angle (the angle between the vectors u and v) $\delta=18.2^\circ$.³⁸ Of course for elastic scattering only one center of mass velocity u is possible for a given collision energy. Thus all elastically scattered Na atoms fall precisely on the Newton sphere, and the laboratory velocity is determined by the scattering angle. Using equation (8) at a center of mass angle of 25.1° , the estimated value of the differential cross section is $15.5 \text{ \AA}^2/\text{steradian}$. Equation (8) is used to calculate the center of mass angular distribution in this manner. Then, a least squares fit to the low angle elastic scattering is carried out to determine the conversion between the relative and absolute differential cross sections.

The same calibration can be made for the elastic scattering of the Na(3P) atoms by HCl. The experimental value for the polarizability of Na($3^2P_{3/2}$) is $\alpha=53.6 \text{ \AA}^3$.^{39,40} From (10), $C_{6,disp} = 6470 \text{ kcal/mole \AA}^6$, and from (11) $C_{6,ind} = 900 \text{ kcal/mole \AA}^6$. This gives a total $C_6 = 7370 \text{ kcal/mole \AA}^6$. All angles and velocities are the same as for the ground state atoms, so that at 15° in the laboratory frame, with the

same assumptions as for the ground state scattering, from (8) the estimated value of the differential scattering is $18.1 \text{ \AA}^2/\text{steradian}$.

It is then necessary to know the relative detection efficiency of Na atoms and NaCl atoms with the mass spectrometer set at $m/e=23$ (Na^+). This is only dependent upon the ionization cross section of Na bombarded by 200 eV electrons, and by the cross section of the fragmentation and ionization of NaCl to Na^+ when bombarded by 200 eV electrons (σ'). The ionization cross section of Na atoms has been measured as 2.1 \AA^2 for 200 eV electrons.⁴¹ The fragmentation ratio of NaCl upon ionization by 200 eV electrons has also been measured as:

$$\frac{[\text{Na}^+]}{[\text{NaCl}^+]} = 1.38, \text{ or } 58\% \text{ fragmentation.}^{42}$$

Note that for much of the

vibrationally excited NaCl^\ddagger produced (from $\text{Na}^* + \text{HCl}$), this ratio is significantly higher.¹¹ However, the ionization cross section of NaCl has not been measured. Following the method described in reference 2, the cross section for ionization of NaCl by 200 eV electrons can be estimated by assuming that the ionization cross section of NaCl varies with electron energy as does that of argon atoms. The ratio of their ionization cross sections at a given electron energy is taken to be equal to the ratio of their polarizabilities. The polarizability of argon is $\alpha(\text{Ar})=1.6 \text{ \AA}^3$.³⁵ The polarizability of NaCl can be estimated from the polarizabilities of Na^+ and Cl^- by:

$$\alpha(\text{NaCl}) = \alpha(\text{Na}^+) + \alpha(\text{Cl}^-).^{36} \quad (13)$$

The polarizabilities of Na^+ and Cl^- within the NaCl molecule at the equilibrium atomic separation have been calculated by Brumer and Karplus to be $\alpha(\text{Na}^+) = 0.239 \text{ \AA}^3$ and $\alpha(\text{Cl}^-) = 2.507 \text{ \AA}^3$.⁴³ Thus from equation (13), the NaCl polarizability is $\alpha(\text{NaCl}) = 2.746 \text{ \AA}^3$. The ionization cross section of argon for 200 eV electrons is 2.46 \AA^2 ,⁴⁴ and the ionization cross section of NaCl is then estimated to be $2.46 \times 2.746 / 1.6 = 4.22 \text{ \AA}^2$. From the fragmentation ratio above, the ionization cross section of NaCl to Na^+ is: $\sigma' = 4.22 \times 0.58 = 2.5 \text{ \AA}^2$. For vibrationally excited NaCl^\ddagger , the fragmentation ratio is assumed to be 90%, and the ionization cross section of NaCl^\ddagger to Na^+ becomes $4.22 \times 0.9 = 3.8 \text{ \AA}^2$.⁴⁵ In any case the values of the ionization cross section of NaCl to Na^+ are probably only good to within a factor of 2, and they limit the accuracy of the value of the total cross sections derived below. The relative detection efficiency (Eff) of NaCl and Na at $m/e=23$ is the ratio of their ionization cross sections to Na^+ , or:

$$\frac{\text{Eff}(\text{NaCl})}{\text{Eff}(\text{Na})} = \frac{\sigma'_{\text{Na}^+}(\text{NaCl})}{\sigma_{\text{Na}^+}(\text{Na})}. \quad (14)$$

For vibrationally cold molecules this is estimated to be 1.2, while for vibrationally hot molecules this is estimated to be 1.8.

The ratio of absolute to relative differential center of mass flux of elastically scattered Na is determined from the elastic signal count rate at small angles, and the transformation Jacobian in equation (12) for both ground state and $\text{Na}(3P)$ scattering. Then by taking into account the relative detection efficiencies of Na and NaCl at $m/e=23$,

Table III. Estimated total reaction cross sections for Na(3S,3P,4D,5S) + HCl at a collision energy of 5.6 kcal/mole from the elastic scattering of Na(3S,3P) atoms and estimates of the absolute cross sections from Van der Waals attraction (VdW, at small angles), and hard sphere collisions (HS, at large angles).

Electronic State	Reactive Cross Sections:		
	from Na(3S) VdW	from Na(3P) VdW	from Na(3S) HS
3S	0.072 Å ²	0.034 Å ²	0.081 Å ²
3P	4.5 Å ²	2.1 Å ²	5.0 Å ²
4D	16 Å ²	7 Å ²	17 Å ²
5S	11 Å ²	5 Å ²	12 Å ²

the factor converting the integrated relative reactive cross sections for each electronic state measured into absolute total reactive cross sections (σ_R) is determined. The cross sections determined have an accuracy of no better than a factor of two. The cross sections for the reaction at a collision energy of 5.6 kcal/mole are given in table III. The ground state cross section is so small that there should be no significant depletion in the elastic scattering measured at small angles. The elastic scattering of the Na(3P) atoms could be depleted by reaction. This would give an underestimate of the reactive cross sections. No calibration could be made at a collision energy of 16.3 kcal/mole, because the kinematics at this collision energy move the reactive scattering to lower angles, and thus even at the lowest angle recorded no elastic scattering is observed. Because there is a

significant increase in background at angles near the sodium beam, it is impossible to measure closer to the beam.

The absolute cross section can also be estimated by comparison with large angle elastic scattering which is attributable to low impact parameter collisions. A hard sphere collision is assumed which will lead to isotropically scattered products if the impact parameter of the collision is smaller than the sum of the spheres' radii. The sum of the radii is equivalent to the classical turning point of the Na-HCl potential curve, which by analogy to $\text{He}^*(2^1\text{S}) + \text{Ar}^{46}$ is estimated to be 3 Å at a collision energy of 5 kcal/mole. This gives a hard sphere cross section of 28 \AA^2 . The values of the absolute reactive cross section obtained in this way are shown in the right hand column of table III, and agree well with the values obtained from the small angle elastic scattering of ground state sodium atoms.

D. Discussion

1. The Mechanism and Distribution of Product Energy in the $\text{Na}(4\text{D}, 5\text{S}) + \text{HCl}$ Reaction

The dominant features of the $\text{Na}^* + \text{HCl}$ scattering are the decreasing product translational energy and the increasing reactive cross section with increasing electronic energy. Most excess energy must necessarily go into NaCl vibration and rotation, since there are no available electronically excited NaCl states and relatively little

was found in product translation. Conservation of energy and angular momentum arguments can be used to determine where the internal energy is deposited.

While an electron jump mechanism has never before adequately explained the dynamics of an alkali-hydrogen halide reaction,¹⁰ the very low ionization potential of the highly excited alkali atoms could increase the effect of such a process. HCl^- is known to be dissociative.⁴⁷ HCl is dissociated by slow electrons, and dissociative electron attachment measurements yield an estimated (negative) vertical electron affinity of -0.815 eV.⁴⁷ Thus if an electron transfers from the sodium atom to the HCl at long range, the HCl^- could quickly dissociate. Since the H atom is so much lighter than the Cl^- ion, the H atom will rapidly depart, and

$$v_{\text{H}} = -35v_{\text{Cl}^-} \quad (15)$$

if the effect of the Na^+ is ignored. The Na^+ and the Cl^- ions are then left at a separation approximately equal to the electron jump radius. The NaCl molecule formed is confined to travel in the direction opposite to the direction of departure of the H atom in the center of mass coordinate, because momentum must be conserved. Also, the velocity of the NaCl is severely restricted by conservation of momentum since the momenta of NaCl and of H must be equal and opposite in the center of mass, giving:

$$v_{\text{H}} = -58v_{\text{NaCl}} \quad (16)$$

This early departure of the H atom is able to explain the low product recoil energy found for the NaCl product.

If an electron jump mechanism is assumed, then the largest impact parameter leading to reaction would be the same as the position of the crossing of the neutral and ionic potential energy curves. By neglecting the long range neutral attractions, this can be estimated by:

$$IP - EA = \frac{e^2}{r_c}, \quad (17)$$

where IP is the ionization potential of the appropriate sodium level, EA is the electron affinity of the HCl molecule, and r_c is the crossing radius of the neutral and ionic curves.⁴⁸ Equation (17) can be rewritten:

$$r_c = \frac{14.35}{IP - EA}, \quad (18)$$

where r_c is in Å, and the ionization potential and electron affinity are in eV. For the calculations below, the electron affinity of HCl is taken to be -0.815 eV.⁴⁷ The well-known Na atomic energies⁴⁹ are used to calculate the ionization potentials of the particular energy levels excited. For the four electronic states of sodium studied, this yields the values of r_c shown in table IV.

As pointed out in reference 11, the electron transfer radii for the Na(3S,3P) states are too small to be able to separate the breakage of the HCl bond (by electron transfer) from the formation of the NaCl bond. By the time the electron transfers from the alkali atom, the H atom is already feeling the repulsion of the closed shell NaCl molecule that is being formed. With the larger electron transfer radii of the

Table IV. Neutral-ionic curve crossing radii for various Na electronic states in the Na + HCl reaction.

<u>Na(nL)</u>	<u>IP[Na(nL)]</u>	<u>r_c</u>	<u>πr_c^2</u>
3S	5.138 eV	2.41 Å	18 Å ²
3P	3.033 eV	3.72 Å	47 Å ²
4D	0.854 eV	8.60 Å	232 Å ²
5S	1.021 eV	7.82 Å	192 Å ²

Na(4D,5S) states, this is no longer the case. The H atom feels only the repulsion of the closed shell Cl⁻ atom.

The electron transfer cross section (σ_e) is expected to be:

$$\sigma_e = \pi r_c^2 . \quad (19)$$

The values of σ_e are given in the right-hand column of table IV.

The center of mass NaCl angular distributions derived for the reactions of Na(4D,5S) with HCl lead to the conclusion that the opacity function (the reaction probability as a function of impact parameter) is not $P(b)=1$ for all $b < r_c$. That is, not all encounters close enough for electron transfer lead to chemical reaction. The strong backwards scattering implies that the necessary configuration for reaction (of Na(4D,5S)) is Na-Cl-H, although the wider center of mass angular range in the backward hemisphere shows that the configuration is less constrained to be nearly collinear than was the reaction configuration of Na(3P) + HCl.

For Na(3P) + HCl the NaCl formed is due to an impulsive interaction which could impart a significant amount of momentum to the departing H atom.¹¹ This puts an upper limit on the impact parameter that leads to reaction which is certainly less than the 3.7 Å predicted by the neutral-ionic curve crossings. Also, the clear dependence of the reaction upon the relative orientation of the three atoms in the reaction of the Na(3P) atoms limits the value of σ_R^{3P} which is in agreement with the values of 2-5 Å² found (see table III). The values of σ_R^{3P} , σ_R^{4D} , and σ_R^{5S} shown in table III are all significantly lower than the electron transfer cross sections given in table IV. Also, from the relative cross sections it is clear that the cross sections do not go up as the square of the crossing radii. This is indicative of what is already known from the center of mass angular distributions — the opacity function $P(b)$ is significantly less than 1 for $b < r_c$.

Evidence that reaction takes place at distances larger than the impact parameter of the reactive collisions comes from the polarization dependences. All favored laboratory polarization angles (ϕ_{LAB}) are near the angle of the relative velocity vector as shown in figure 15 and table II. This is made clear in the ϕ_{CM} values, which are the angles between the favored laboratory polarization angles and the angle of the relative velocity vector of the system in the laboratory frame of reference. This is in sharp contrast to the lack of polarization dependences seen for Na(3P) + HCl. In the case of Na(3P) + HCl at a collision energy of 5.4 kcal/mole the only polarization dependence observed was for the farthest backwards scattered NaCl, corresponding

to the most collinear Na-Cl-H geometries, and this was only a ($2A =$) 3% effect. All smaller laboratory angles had polarization dependences of less than the measurable limit of 2%. In the limiting case of $C_{\infty v}$ (collinear) geometry the required symmetry for reaction to form the ionic NaCl is $^2\Sigma$ since the ion pair derives this symmetry from:



Because of the ground state $\text{HCl}(X^2\Sigma^+)$ symmetry, all the electronic angular momentum of the $\text{Na}(4D)$ must be along the Na-Cl-H axis -- requiring the $4d_{z^2}$ orbital to be along the Na-Cl-H axis. For zero impact parameter collisions, this requires the $4d_{z^2}$ orbital to be aligned along the relative velocity vector of the system.

If this collinear geometry and $^2\Sigma$ symmetry were a strict requirement for reaction, then as the impact parameter was raised the Na-Cl-H orientation (axis) required for reaction would tilt with respect to the relative velocity vector. In the impulsive reaction limit, this would lead to lower center of mass (NaCl) scattering angles and thus lower laboratory scattering angles. Also, this would imply that the favored polarization for reaction would rotate with respect to the relative velocity vector to match the Na-Cl-H axis. Of course, since different impact parameters would lead to different reactive orientations and different scattering angles, the polarization dependence would vary as a function of laboratory scattering angle. This is not observed. Therefore, the assumption of collinearity and/or the impulsive approximation that the scattering angle depends upon the impact parameter are incorrect if larger impact parameters lead to reaction.

From the center of mass angular distributions the relative orientation of the Na-Cl-H was shown to be important. Since the reaction probability depends strongly on the Na-Cl-H angle, similar arguments to those above can be used to show that as the impact parameter is increased, the range of reactive orientations will change with respect to the relative velocity vector, as well as the NaCl scattering angles. By considering the united atom (diatomic-like) approximation in which the HCl molecule shrinks to an Argon ($1S$) atom, the correct symmetry for electron transfer remains 2Σ . Electron transfer from the Na(4D) atom to the HCl requires only that the $4d_z^2$ orbital be aligned toward the (reduced) HCl molecule (i.e. toward the Cl atom which is nearly at the center of mass of the molecule). Once again the polarization dependence would vary as a function of the laboratory scattering angle. Since the variation is not observed, the assumption that larger impact parameter collisions lead to reaction must be false.

If the Na(4D) + HCl reaction only takes place for small impact parameter collisions, two questions remain. First, how small does the impact parameter need to be in order to observe no variation of the polarization dependence with laboratory scattering angle? Secondly, if only small impact parameter collisions lead to reaction, how is the scattering angle determined?

To answer the first question, it is again useful to consider the united atom approximation. Here the center of mass frame favored polarization angle for electron transfer can be described:

$$\phi_{cm} = \sin^{-1} \frac{b}{r_c}, \quad (21)$$

where b is the impact parameter of the collision and r_c is the crossing radius of the neutral and ionic potential curves -- the distance at which electron transfer is expected to occur. To obtain $\phi_{cm} \cong 0^\circ$, it is necessary to have $b \ll r_c$. Therefore this is the restriction on the impact parameters for reactive collisions -- b must be small with respect to the distance at which electron transfer takes place, 8.6 \AA for $\text{Na}(4D) + \text{HCl}$.

To answer the second question, recall that HCl is dissociated by slow electrons. The (dissociative) $\text{HCl}^{(-)}$ orientation at the time of electron transfer is then the dominant determinant of the NaCl product scattering direction (due to conservation of momentum).

Further evidence that only low impact parameters lead to reaction comes from the analysis below. An electron transfer can occur at each crossing point of the neutral and ionic potential curves. While the earliest crossing is at 8.6 \AA for $\text{Na}(4D) + \text{HCl}$, the final crossing is also at 8.6 \AA -- after the Na atom has gone by the molecule. With the opposite orientation of HCl to what normally leads to reaction -- that is initially Na-H-Cl -- after the atom and molecule pass by each other, the orientation becomes Na-Cl-H , perfect for reaction by the arguments above, assuming the excitation has survived to this point. This would lead to forward scattered NaCl as the H atom would be ejected in the backwards direction. This forward scattering is not observed. Therefore one or both of the two underlying assumptions in this argument are

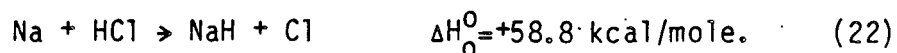
incorrect: the excitation does not survive the collision and/or impact parameters allowing such a "fly by" cannot lead to reaction. Since a large increase in elastic scattering is observed for the increasingly excited electronic states, it seems probable that a significant fraction of the excited atoms survive the collision, and thus the conclusion is that only low impact parameter collisions lead to reaction.

Two features of the reaction imply that it proceeds through long range electron transfer and early H atom departure, even though only in a limited set of orientations and impact parameters. These are the very low product recoil energy, and the polarization dependences for the reaction of Na(4D) versus the lack of a polarization dependence for the reaction of Na(3P). That the reaction occurs through early departure of the H atom, but only for small impact parameter collisions, indicates that a coupling of nuclear and electronic motions is required for reaction. Otherwise, any trajectory for which electron transfer is energetically possible (i.e. any $b < r_c$) would lead to reaction.

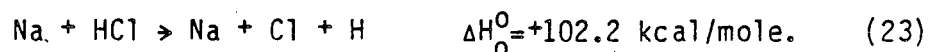
The dynamics of the Na(4D,5S) + HCl systems (the early H atom departure driven by the dissociative HCl⁻) appear to qualify these reactions for the type of calculation carried out by Kuntz, Polanyi, and coworkers, and termed DIPR for "Direct Interaction with Product Repulsion."^{50,51} As pointed out by Harris and Herschbach, the problem with the DIPR model is that it assumes a constant product repulsion, when in fact a distribution of product repulsions would be

more appropriate.^{52,53} The approach of Harris and Herschbach was to assume a distribution of products as in photodissociation (in the DIPR-DIP model), since the negative ionic and electronically excited states of many closed shell systems have very similar dissociative potential energy surfaces.⁵⁴ For HCl^- , an approximate potential has been derived for the dissociative ground state by Bardsley and Wadehra from their dissociative electron attachment experiments.⁴⁷ Since a potential is available for HCl^- , there is no reason to use an excited neutral HCl potential curve, and a new variation on the DIPR theme would be more appropriate, perhaps to be called "Direct Interaction with Product Repulsion -- Distributed as In Electron-induced Dissociation," or "DIPR-DIED." The procedure used in a DIPR-DIED calculation would be exactly the same as for a DIPR-DIP calculation in which a Franck-Condon transition from the ground state potential to the repulsive ionic potential curve using the ground state vibrational wave function is assumed. The only real difference between DIPR-DIED and its previous incarnation (DIPR-DIP) is that DIPR-DIED will be using what is presumably a more accurate potential energy curve. The same limitations apply to the two models, namely that if the incoming alkali atom distorts the molecular reactant bond length, then the vibrational wave function is also distorted, and the product energies calculated will be incorrect. It would be most interesting to examine the geometric dependence of the reaction probability in this way.

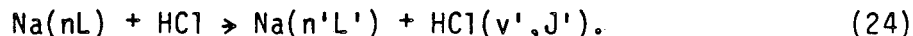
Three other processes are energetically possible under the conditions used in the collisions of electronically excited Na atoms with HCl. It is possible to have the reaction proceed to form NaH:



It is also possible to collisionally dissociate HCl:



The third set of energetically possible processes involves quenching to other electronic states of Na:



The electronic energies available for reaction are 98.8 kcal/mole and 94.9 kcal/mole for the 4D and 5S states of Na, respectively. Both these energies are more than sufficient for the production of NaH (process (22)). However, no evidence for the production of NaH is observed. This is not surprising; if electron transfer occurs at relatively long range, the H atom is quickly ejected, before encountering the alkali atom. Another interpretation has the alkali atom acting as an alkali ion when close to the hydrogen halide. This is helpful in explaining the alkali favoring of the halide end of the HX molecule on approach, as seen in the strong variation of the barrier to (ground state) reaction as a function of M-X-H angle calculated by Shapiro and Zeiri; the barrier rises several eV as the orientation approaches the M-H-X collinear configuration.¹⁷ The long range dispersive forces alone would have the alkali atom favoring the hydrogen end of the molecule.^{11,55}

With collision energies of at least 3.5 kcal/mole and 7.0 kcal/mole, respectively, the 4D and 5S states of Na have enough energy to dissociate HCl (process (23)). This could only occur for the smallest impact parameter collisions, since if a significant amount of energy goes into product NaCl rotation, there will not be enough left to overcome the endothermicity of the dissociation. This is necessary in any case, since the maximum possible impulse would be required to induce dissociation. Another way of looking at collisional dissociation is as reaction to form NaCl, except that NaCl is formed above the dissociation limit. Although $m/e=23$ (Na^+) product is detected, this is not due to collisional dissociation of HCl. Very similar product distributions are seen for collision energies above and below the minimum at which HCl dissociation can occur. The threshold for dissociation to $\text{Na}^+ + \text{Cl}^- + \text{H}$ is at 137.4 kcal/mole, so this process, analogous to that seen by Lacmann and Herschbach,^{3,15} is not yet energetically allowed for the conditions studied.

Quenching (process (24)) certainly occurs, but these measurements are particularly insensitive to it. Therefore, quenching processes will not be discussed. Hertel and coworkers, among others, have performed many experiments on the quenching of excited sodium atoms by various diatomic molecules (although no hydrogen halides have been reported to date), and the quenching cross sections are typically quite large, $\sim 0(10-100 \text{ \AA}^2)$.⁵⁶

$\text{Na}(3\text{S},3\text{P}) + \text{HBr}$

The $\text{Na} + \text{HBr}$ reaction is nearly thermoneutral and there is a substantial cross section for the ground state reaction. However, the reactive cross section still increases upon excitation of the Na atoms to the 3P level. As with $\text{Na} + \text{HCl}$, the ground state cross section increases more with increasing collision energy than does the cross section of the $\text{Na}(3\text{P})$ state. Preliminary analysis of this data has shown it to be very similar in nature to $\text{Na}(3\text{P}) + \text{HCl}$, where product NaX is mostly backwards scattered, but there is some forward sideways peaking, and the product recoil energy distributions are broad and flat, and extend out to the total energy available.

2. The Lack of Reaction for $\text{Na} + \text{HF}$.

No reaction was observed for $\text{Na}(3\text{S},3\text{P},4\text{D},5\text{S}) + \text{HF}$ (3). Apparently, electronic energy was unable to make up for the substantial endothermicity and exit channel barrier (see reference 17) of the reaction of $\text{Na} + \text{HF}$. For comparison, recall that it took two vibrational quanta of HF excitation for Blackwell et al. to observe evidence of reaction to form NaF . There are no close resonances for electronic to vibrational energy transfer of HF that might preclude reaction in the manner predicted by Zeiri et al. for translational to vibrational energy transfer in $\text{Li} + \text{HF}$.¹⁹ The vertical electron affinity of HF is approximately -4 eV and like HCl^- , HF^- is dissociative.²⁶ This puts

the crossing point of the neutral and ionic curves, and thus electron transfer at under 3 Å even for the 4D and 5S states.

In $\text{Li} + \text{HF}$, reaction was observed,² but the energetics were quite a bit different. From table I, the $\text{Li} + \text{HF}$ reaction is slightly exothermic, whereas the $\text{Na} + \text{HF}$ reaction is endothermic by 13 kcal/mole. Also, the barrier to reaction calculated by Zeiri and Shapiro in the ground state surface is 29 kcal/mole (vs. 12 kcal/mole for $\text{Li} + \text{HF}$) not including the effect of the zero point energy which will reduce it by 5 kcal/mole. This says nothing, however, about the electronically excited surfaces on which the reaction was attempted.

E. Conclusions

The electronic excitation of the reagent alkali atom can indeed promote reaction. As seen in $\text{Na}(4\text{D},5\text{S}) + \text{HCl}$, a new mechanism comes to dominate the reaction at high electronic energy, although the reactive cross sections do not reach the limit in which all collisions for which electron transfer is possible lead to reaction. This is due to the restrictive geometric constraints necessary for reaction. Low impact parameter collisions with Na approaching the Cl end of the HCl molecule are almost exclusively responsible for production of NaCl, since a coupling of the electronic and nuclear motion is necessary for reaction.

To some extent electronic excitation is not directly comparable to other forms of energy since the potential energy surface on which the

reaction takes place is different for each electronic state -- with different topography and different possible symmetries. Nevertheless it is certainly interesting to ask how electronic excitation compares to other forms of energy in promoting reaction. Like electronic energy, exciting the first (or second) vibration is capable of turning on the reaction when the collision energy is insufficient to overcome the endothermicity. This was shown for $K + HF$, HCl ⁶ (and for $Na + HF(v=2)$ ¹⁰). As discussed in section B and reference 6, with increasing translational energy the first vibration in $K + HCl$ no longer enhances the reaction cross section, whereas there remains over an order of magnitude enhancement in $K + HF$. Rotational excitation has only been studied in vibrationally excited HCl , $HF + Na$, K , and seems to adversely affect the reaction cross section or have little effect.⁸⁻¹⁰ Translational energy overcomes the threshold to reaction in $K + HCl$, HF and continues to enhance reaction until a saturated value of the reaction cross section is reached.⁶ As shown in the nonreaction of $Na^* + HF$, electronic excitation is not necessarily sufficient for reaction. However, in $Na + HCl$, HBr the initial electronic excitation to $Na(3P)$ enhances the reactivity strongly whether or not there is sufficient collision energy for the ground state reaction. In $Na + HCl$, there is a small further increase (less than a factor of two from $3P \rightarrow 4D, 5S$) with further increased electronic energy.

F. References

1. E. H. Taylor and S. Datz, J. Chem. Phys. 23, 1711 (1955).
2. C. H. Becker, P. Casavecchia, P. W. Tiedemann, J. J. Valentini, and Y. T. Lee, J. Chem. Phys. 73, 2833 (1980).
3. K. Lacmann and D. R. Herschbach, Chem. Phys. Lett. 6, 106 (1970).
4. J. G. Pruett, F. R. Grabiner, and P. R. Brooks, J. Chem. Phys. 63, 1173 (1975).
5. M. W. Geis, H. Dispert, T. L. Budzynski, and P. R. Brooks, in State to State Chemistry, P. R. Brooks and E. F. Hayes, eds., ACS Symposium Series No. 56, 103, (American Chemical Society, Washington, DC, 1977).
6. F. Heismann and H. J. Loesch, Chemical Physics 64, 43 (1982).
7. T. J. Odiorne, P. R. Brooks., and J. V. V. Kasper, J. Chem. Phys. 55, 1980 (1971).
8. M. Hoffmeister, L. Potthast, and H. J. Loesch, Chemical Physics 78, 369 (1983).
9. H. H. Dispert, M. W. Geis, and P. R. Brooks, J. Chem. Phys. 70, 5317 (1979).
10. B. A. Blackwell, J. C. Polanyi, and J. J. Sloan, Chemical Physics 30, 299 (1978).
11. M. F. Vernon, H. Schmidt, P. S. Weiss, M. H. Covinsky, and Y. T. Lee, J. Chem. Phys., to be published.

12. R. R. Herm, in Alkali Halide Vapors: Structure, Spectra, and Reaction Dynamics, 189 (Academic Press, New York, 1979), and references therein.
13. J. L. Kinsey, MTP Int. Rev. Sci., Phys. Chem. Ser. One 9, 173 (1972).
14. W. A. Lester, Jr. and M. Krauss, J. Chem. Phys. 52, 4775 (1970).
15. G. G. Balint-Kurti and R. N. Yardley, Faraday Disc. Chem. Soc. 62, 77 (1977).
16. Y. Zeiri and M. Shapiro, Chem. Phys. 31, 217 (1978).
17. M. Shapiro and Y. Zeiri, J. Chem. Phys. 70, 5264 (1979).
18. M. M. L. Chen and H. F. Schaefer III, J. Chem. Phys. 72, 4376 (1980).
19. Y. Zeiri, M. Shapiro, and E. Pollack, Chem. Phys. 60, 239 (1981).
20. I. NoorBatcha and N. Sathyamurthy, J. Chem. Phys. 76, 6447 (1982).
21. I. NoorBatcha and N. Sathyamurthy, J. Am. Chem. Soc. 104, 1766 (1982).
22. I. NoorBatcha and N. Sathyamurthy, Chem. Phys. Lett. 93, 432 (1982).
23. K. P. Huber and G. Herzberg, Molecular Spectra and Molecular Structure, IV. Constants of Diatomic Molecules (Van Nostrand Reinhold, Co., New York, 1979).
24. D. R. Herschbach, Proceedings of the Conference on Potential Energy Surfaces in Chemistry, 44, W. A. Lester, Jr., ed., IBM Research Laboratory, San Jose, California (1971).
25. S. Carter and J.N. Murell, Mol. Phys. 41, 567 (1980).

26. D. C. Frost and C. A. McDowell, J. Chem. Phys. 29, 503 (1958).
27. J. H. Birely, R. R. Herm, K. R. Wilson, and D. R. Herschbach, J. Chem. Phys. 47, 993 (1967).
28. E. A. Mason, J. T. Vanderslice, and C. J. G. Raw, J. Chem. Phys. 40, 2153 (1964).
29. J. C. Slater and J. G. Kirkwood, Phys. Rev. 37, 682 (1931).
30. K. S. Pitzer, Adv. Chem. Phys. 2, 59 (1959).
31. H.-J. Werner and W. Meyer, Phys. Rev. A 13, 13 (1976).
32. A. A. Maryott and F. Buckley, National Bureau of Standards (U. S.) Circ. 537 (1953).
33. see for example the comparison of C_6 values in ref. 30.
34. G. York, R. Scheps, and A. Gallagher, J. Chem. Phys. 63, 1052 (1975).
35. J. S. Cohen and R. T. Pack, J. Chem. Phys. 61, 2372 (1974).
36. J. O. Hirschfelder, C. F. Curtiss, and R. B. Bird, Molecular Theory of Gases and Liquids (John Wiley and Sons, Inc., New York, 1964).
37. R. D. Nelson, Jr., D. R. Lide, Jr., and A. A. Maryott, National Standard Reference Data Series 10, National Bureau of Standards (U. S.) (1967).
38. For further explanation see R. B. Bernstein, Chemical Dynamics via Molecular Beam and Laser Techniques, pp. 86-7 (Oxford University Press, Oxford, 1982).
39. P. Hannaford, W. R. MacGillivray, and M. C. Standage, J. Phys. B: Atom Molec. Phys. 12, 4033 (1979).

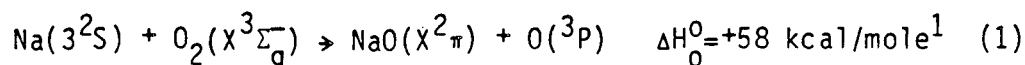
40. H. T. Duong and J.-L. Picque, J. Physique **33**, 513 (1972).
41. R. H. McFarland and J. D. Kinney, Phys. Rev. **137**, A1058 (1965).
42. P. Mohazzabi and A. W. Searcy, Intl. J. Mass Spect. Ion Phys. **24**, 469 (1977).
43. P. Brumer and M. Karplus, J. Chem Phys. **58**, 3903 (1973).
44. S. C. Brown, Basic Data of Plasma Physics, 2nd Ed. (MIT Press, Cambridge, Massachusetts, 1967).
45. The fragmentation ratio of 0.9 is used for the NaCl produced from the reaction of the electronically excited Na atoms.
46. C. H. Chen, H. Haberland, and Y. T. Lee, J. Chem. Phys. **61**, 3095 (1974).
47. J. N. Bardsley and J. M. Wadehra, J. Chem. Phys. **78**, 7227 (1983).
48. J. L. Magee, J. Chem. Phys. **8**, 687 (1940), or R. D. Levine and R. B. Bernstein, Molecular Reaction Dynamics, 86 (Oxford University Press, New York, 1974).
49. W. L. Wiese, M. W. Smith, and B. M. Miles, Atomic Transition Probabilities Volume II: Sodium Through Calcium, Natl. Stand. Ref. Data Ser., Nat. Bur. Stand. (U. S.), Washington, DC (1969).
50. P. J. Kuntz, E. M. Nemeth, and J. C. Polanyi, J. Chem. Phys. **50**, 4607 (1969).
51. P. J. Kuntz, M. H. Mok, and J. C. Polanyi, ibid., 4623 (1969).
52. R. M. Harris, Ph. D. Thesis, Harvard University, Cambridge, Massachusetts (1970).
53. D. R. Herschbach, Faraday Disc. Chem. Soc. **55**, 233 (1973).
54. This is discussed in chapter IV, or see reference 31.

55. H. Schmidt, P. S. Weiss, J. M. Mestdagh, M. H. Covinsky, M. F. Vernon, and Y. T. Lee, in preparation.
56. I. V. Hertel and W. Stoll, Adv. At. Mol. Phys. 13, 113 (1977), and references therein.

III. THE STATE-SELECTIVE REACTION OF ELECTRONICALLY EXCITED SODIUM ATOMS WITH MOLECULAR OXYGEN

A. Introduction

The $\text{Na}^* + \text{O}_2$ reaction has been chosen for study since the energetics preclude reaction in the ground state. The large endothermicity of the reaction:



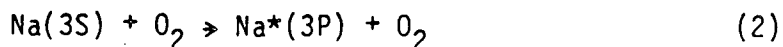
is lower than the electronic energy of Na atoms in the 4S, 4P, 4D, and 5S states.³ With at least 10 kcal/mole of translational energy Na atoms in the 3P state also have more than enough energy to overcome this endothermicity. Another point of interest is that the positive electron affinity of O_2 , $\text{EA} = 0.44 \text{ eV}$,² undoubtedly leads to an ionic intermediate, Na^+O_2^- , which must play an important role in the collision between Na^* and O_2 .

The NaO_2 molecule has been studied both theoretically and spectroscopically.⁴⁻⁷ The theoretically determined lowest energy state of the NaO_2 system, which has C_{2v} symmetry, has the Na atom at the apex of an isocetes triangle, and is 1.6 eV more stable than ground state reactants ($\text{Na}(3^2\text{S}) + \text{O}_2(\text{X}^3\Sigma_g^-)$).⁴ Infrared, Raman, and ESR spectroscopies of NaO_2 trapped in low temperature rare gas matrices have also shown the triatomic to be an isocetes triangle.^{5,6,7}

Calculations on the NaO molecule indicate that it is ionic, Na^+O^- .⁸ The ground state is the $\text{NaO}(X^2\pi)$ state, and there is a very low-lying first excited state at $\sim 1500\text{ cm}^{-1}$, the $\text{NaO}(A^2\Sigma^+)$ state.⁸ Certainly many other states exist for this open shell molecule, but nearly nothing is known of them. The first step to amend this was made by Pfeiffer and Gole, who reported seeing chemiluminescence arising from NaO from $10000\text{--}15000\text{ cm}^{-1}$, but left the observed spectra unassigned.⁹ An attempt is being made to measure and assign the electronic spectra of NaO and other alkali monoxides by the Gole and Schulz groups at Georgia Tech.¹⁰

A compilation of symmetries of important reactant and intermediate states for $\text{Na} + \text{O}_2$ is given in table I for reference in the following discussion.

Kempton and coworkers have studied the excitation of the $\text{Na}(3P)$ level in 1-17 eV collisions with O_2 by monitoring the Na D-line fluorescence.¹¹ In the process:



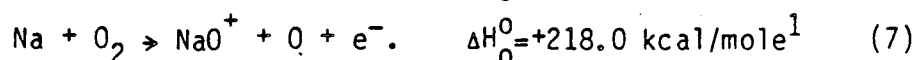
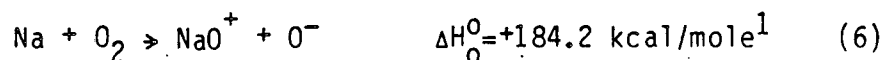
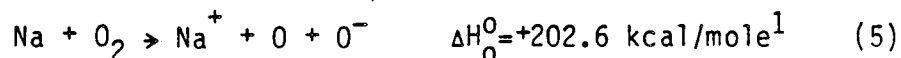
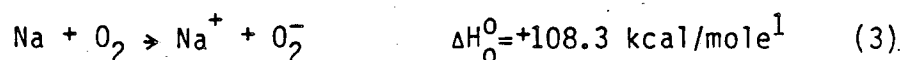
they find the threshold at 2.1 eV, the $\text{Na}(3P)$ excitation energy. At a collision energy of 5 eV, they find the cross section for this process to be 26 \AA^2 , and see a further increase of approximately an order of magnitude at a collision energy of 8 eV. At collision energies of 8 eV and above, 20% of the fluorescence observed appears to be due to states other than $\text{Na}(3P)$, implying higher excitation takes place. The ground and excited states are strongly coupled via the ion-pair state (see table I). Because the difference between the Na ionization potential

Table I. Symmetries of important reactant and intermediate states for Na + O₂ collisions.

<u>System</u>	<u>Symmetry</u>			<u>Multiplicity</u>
	<u>C_{∞v}</u>	<u>C_s</u>	<u>C_{2v}</u>	
Na(ns ² S)+O ₂ (X ³ Σ _g ⁻)	Σ ⁻	A''	B ₁	2,4
Na(np ² P)+O ₂ (X ³ Σ _g ⁻)	Σ ⁻	A''	A ₂	2,4
	π ⁺	A'	A ₁	2,4
	π ⁻	A''	B ₁	2,4
Na(nd ² D)+O ₂ (X ³ Σ _g ⁻)	Σ ⁻	A''	B ₁	2,4
	π ⁺	A'	A ₁	2,4
	π ⁻	A''	A ₂	2,4
	Δ ⁺	A'	B ₂	2,4
	Δ ⁻	A''	B ₁	2,4
NaO ₂ (lowest 2 states)	π ⁻	A''	A ₂	2
	π ⁺	A'	B ₂	2
Na ⁺ (¹ S)+O ₂ ⁻ (X ² π _g)	π ⁺	A'	B ₂	2
	π ⁻	A''	A ₂	2
Na ⁺ (¹ S)+O ₂ ⁻ (a ⁴ Σ _u ⁻)	Σ ⁻	A''	A ₂	4
Na ⁺ (¹ S)+O ₂ ⁻ (² Δ)	Δ ⁺	A'	A ₁	2
	Δ ⁻	A''	B ₁	2

and the electron affinity is larger than the Na(3P) excitation energy, excitation is expected to be more important than collisional ionization.¹²

A merging beams study of Na + O₂ was carried out by Neynaber, Myers and Trujillo at collision energies ranging from 4.7 to 25 eV.¹³ Only processes producing ions were measured, these were:



Ions were observed at collision energies of 6 eV and above, but not at 4.7 eV (the endothermicity of process (3)). The maximum cross section for the production of Na⁺ (the sum of the cross sections of processes (3-5)) was measured to be $\sigma_{\text{Na}} = 0.05 \text{ \AA}^2$. The maximum cross section for the production of NaO⁺ (the sum of the cross sections of processes (6 and 7)) was measured to be $\sigma_{\text{NaO}} = 0.004 \text{ \AA}^2$. The positive ions produced in the charge transfer processes are observed in the forward center-of-mass direction, as expected. There was no attempt to observe neutral products such as NaO or Na*.

Kley, Los, and coworkers have made measurements of charge exchange processes (3, 6, and 7) at collision energies of 4-2000 eV.^{14,15} Cross sections for production of O₂⁻ (process (3)) appear to be as high as 5 Å², while cross sections for production of O⁻ (processes (6 and 7)) are always less than 0.3 Å². The

discrepancy between the cross sections of Neynaber et al.¹³ and those of Kleyn et al.¹³ remains a subject of controversy with conflicting measurements also reported for analogous $M + O_2$ ($M =$ alkali atom) systems by others.^{14,16} In that the calibration of the cross sections in the merging beams apparatus is more difficult, the values of Kleyn et al. are perhaps more dependable. These values are still significantly lower than the excitation cross sections of Kempter et al.,¹¹ bearing out Kempter's predictions as to the relative importance of collisional excitation and ionization.¹² Kleyn et al. have shown that at the high collision energies studied the change of the phase of the $O_2^{(-)}$ vibration during the collision is very important in determining whether ions are produced. This has to do with the relative positions of the neutral and ionic curves after the collision, due to vibrational excitation from the collision; this effect is termed "vibronic excitation." This can only be observed in their studies because the high collision energies lead to very short collision times, $\sim 0(10^{-14}$ sec), which are on the same time scale as the O_2 vibrational period. As such the crossing radius of the neutral and ionic curves, r_c , depends on the phase of the $O_2^{(-)}$ vibration, and formula (18) of chapter II must be rewritten:

$$r_c = \frac{e^2}{IP - EA(r_{O_2})}, \quad (8)$$

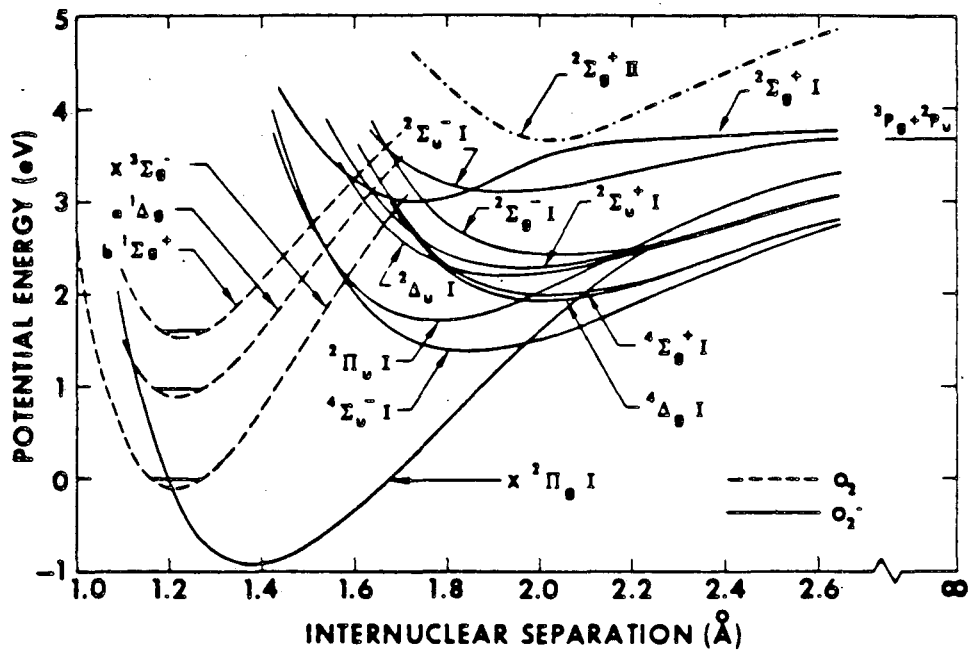
where IP is the ionization potential of the alkali atom, and $EA(r_{O_2})$ is the electron affinity of O_2 , which varies as a function of the O_2

interatomic distance. Some of the known O_2 and O_2^- potential energy curves are shown in figure 1, which is reproduced from reference 17 with permission. Note that the vertical electron affinity of O_2 is approximately zero.

The collisions studied here are at much lower translational energies than those of Kleyn, and the direct effects of vibronic excitation cannot be observed. However, since the collision times are much longer here, it is important to remember that many O_2 vibrations will be taking place, effectively making the energy separation of the neutral and ionic curves oscillate during the collision. Additionally, if the approaching Na atoms allow the O_2 molecule to stretch, then the electron affinity can take on its adiabatic value of 0.44 eV.

Many measurements of charge exchange processes for other alkali atoms with O_2 (analogues to processes (3-7)) have been made.^{14,16} The excitation process is stronger for Na than for heavier alkali atoms¹¹ due in part to its higher ionization potential.

A crude study of the translational energy dependence of all ion-producing processes for $Na(3S,3P) + O_2$ has been performed by Roethe, Mather, and Beck.¹⁸ They have found that there are similar cross sections for ion-producing processes for each state with a lower threshold energy for $Na(3P)$. No values of the threshold, nor of the cross sections were reported. This measurement shows, however, that ionization does not gain appreciable probability when the ionization potential of the alkali is effectively lowered by excitation.



XBL 863-788

Fig. 1. Potential energy curves for O_2 and O_2^- , reproduced from reference 17 with permission.

In the experiments described here, electronic excitation is used in an attempt to overcome the very substantial endothermicity of the neutral reaction (1).

B. Results

The apparatus used to make the measurements reported below is described in chapter I. Laboratory angular distributions of products were measured for each of the three optically pumped Na levels (3P, 4D, 5S) at three center-of-mass collision energies: 8, 16, and 18 kcal/mole. The Newton velocity vector diagrams corresponding to these are shown in figures 2, 3, and 4, while the angular distributions themselves are shown in figures 5, 6, and 7, respectively. Also, angular distributions were recorded for $\text{Na}(3\text{S},4\text{D}) + \text{O}_2$ at mean collision energies of 11, 12, 13, and 22 kcal/mole. The Newton diagrams for these energies are shown in figure 8, for 11-13 kcal/mole, in which the Na velocity was varied by using mixtures of He and Ne as backing gases, and in figure 9 for 22 kcal/mole. The corresponding angular distributions are shown in figures 10a-c, and 11, respectively. At the lowest collision energy (8 kcal/mole) nothing other than elastic scattering was observed for any of the Na levels as shown in the angular distributions in figure 5. At all other collision energies, a peak was observed only when the sodium atoms were optically pumped to the Na(4D) state. Nothing other than elastic scattering was

Fig. 2. Newton velocity vector diagram for $\text{Na}(3P,4D,5S) + \text{O}_2 \rightarrow \underline{\text{NaO}} + \text{O}$ at a collision energy of 8 kcal/mole. The sodium beam is seeded in neon, and the molecular beam is 5% O_2 in helium.

$$E_{\text{coll}} = 8 \text{ kcal/mole}$$

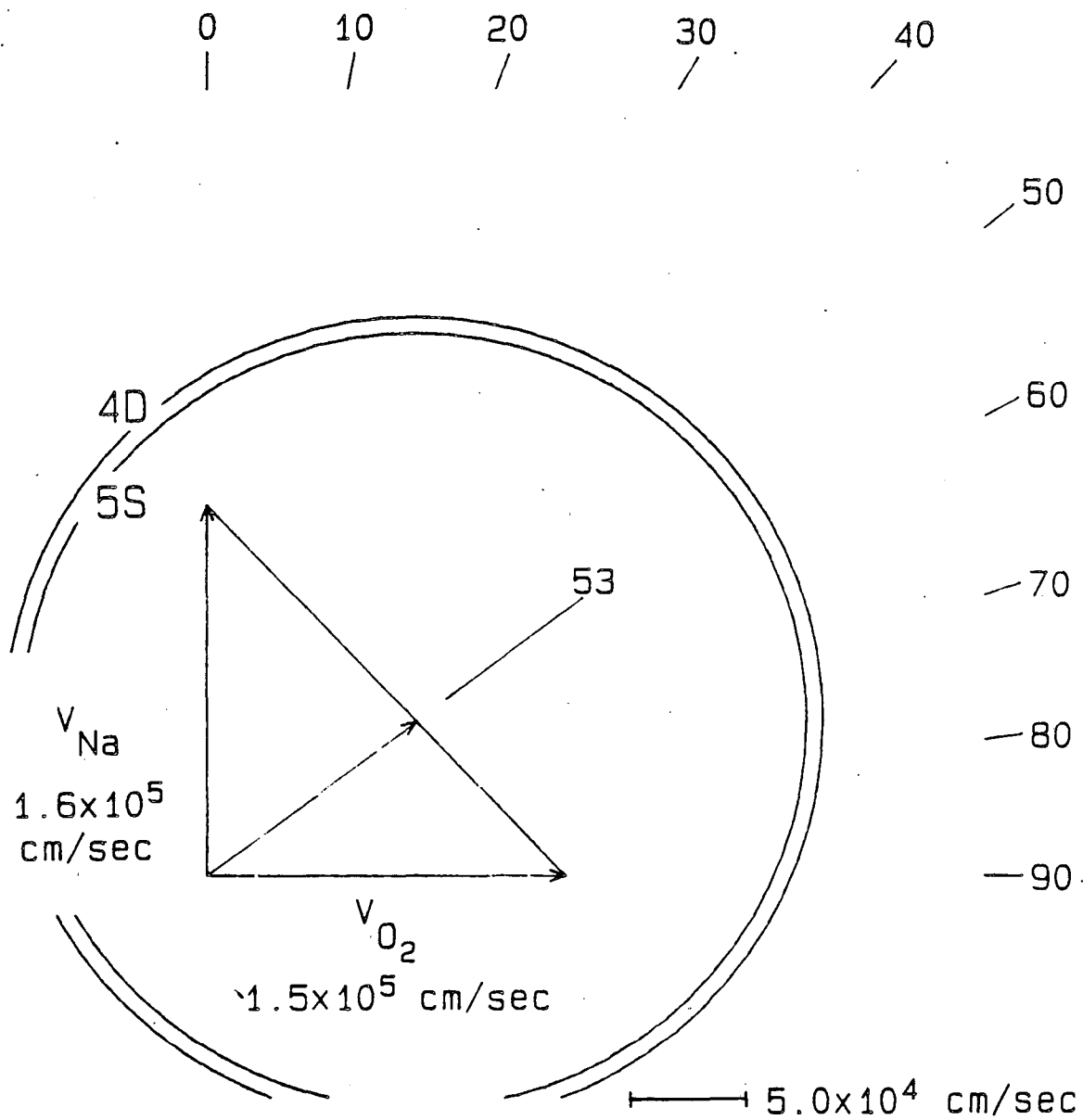


Fig. 2

XBL 863-856

Fig. 3. Newton velocity vector diagram for $\text{Na}(3P,4D,5S) + \text{O}_2 \rightarrow \underline{\text{NaO}} + \text{O}$ at a collision energy of 16 kcal/mole. The sodium beam is seeded in helium, and the molecular beam is neat O_2 .

$$E_{\text{coll}} = 16 \text{ kcal/mole}$$

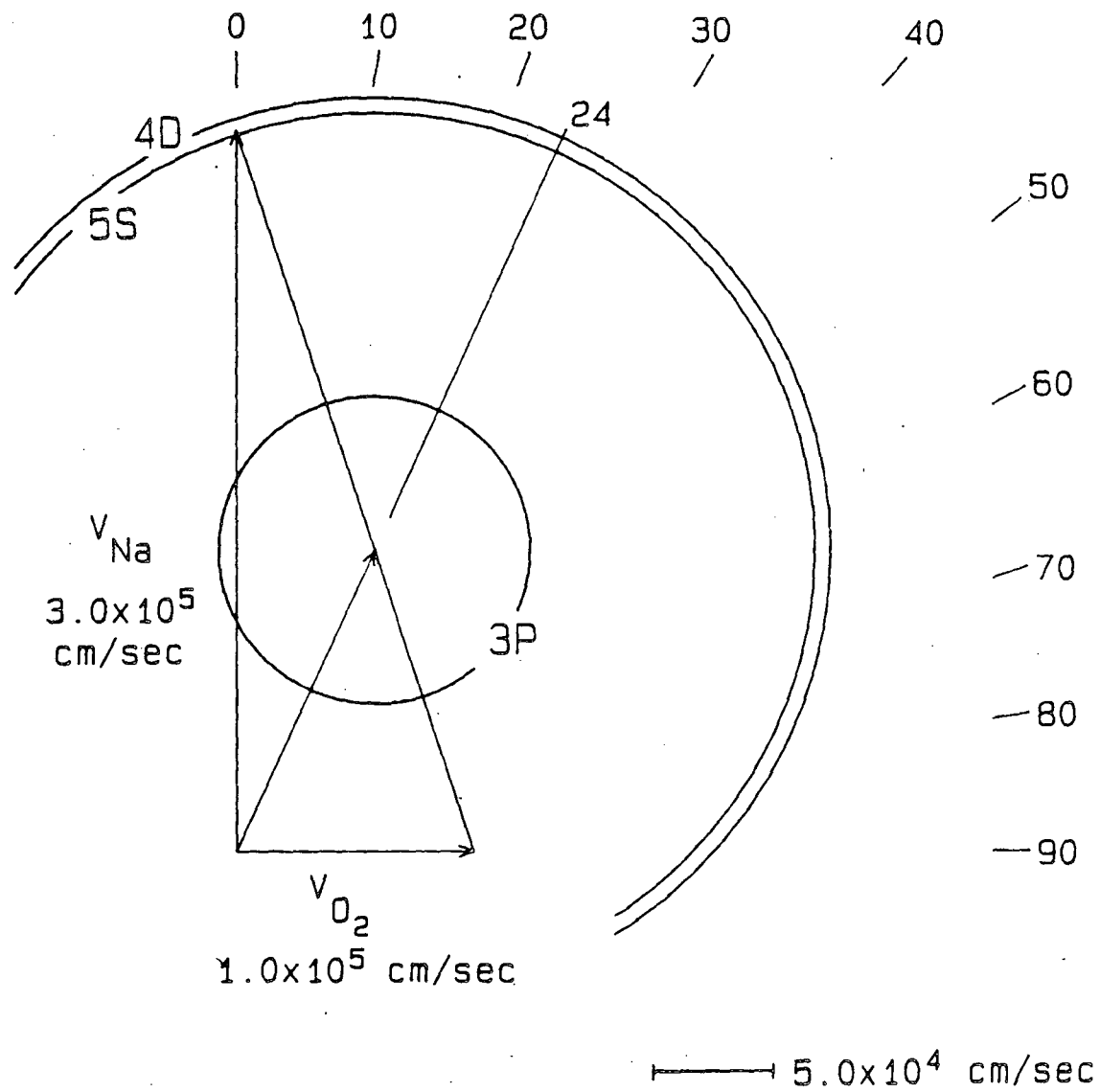


Fig. 3

XBL 863-853

Fig. 4. Newton velocity vector diagram for $\text{Na}(3P,4D,5S) + \text{O}_2 \rightarrow \underline{\text{NaO}} + \text{O}$ at a collision energy of 18 kcal/mole. The sodium beam is seeded in helium, and the molecular beam is 5% O_2 in helium.

$$E_{\text{coll}} = 18 \text{ kcal/mole}$$

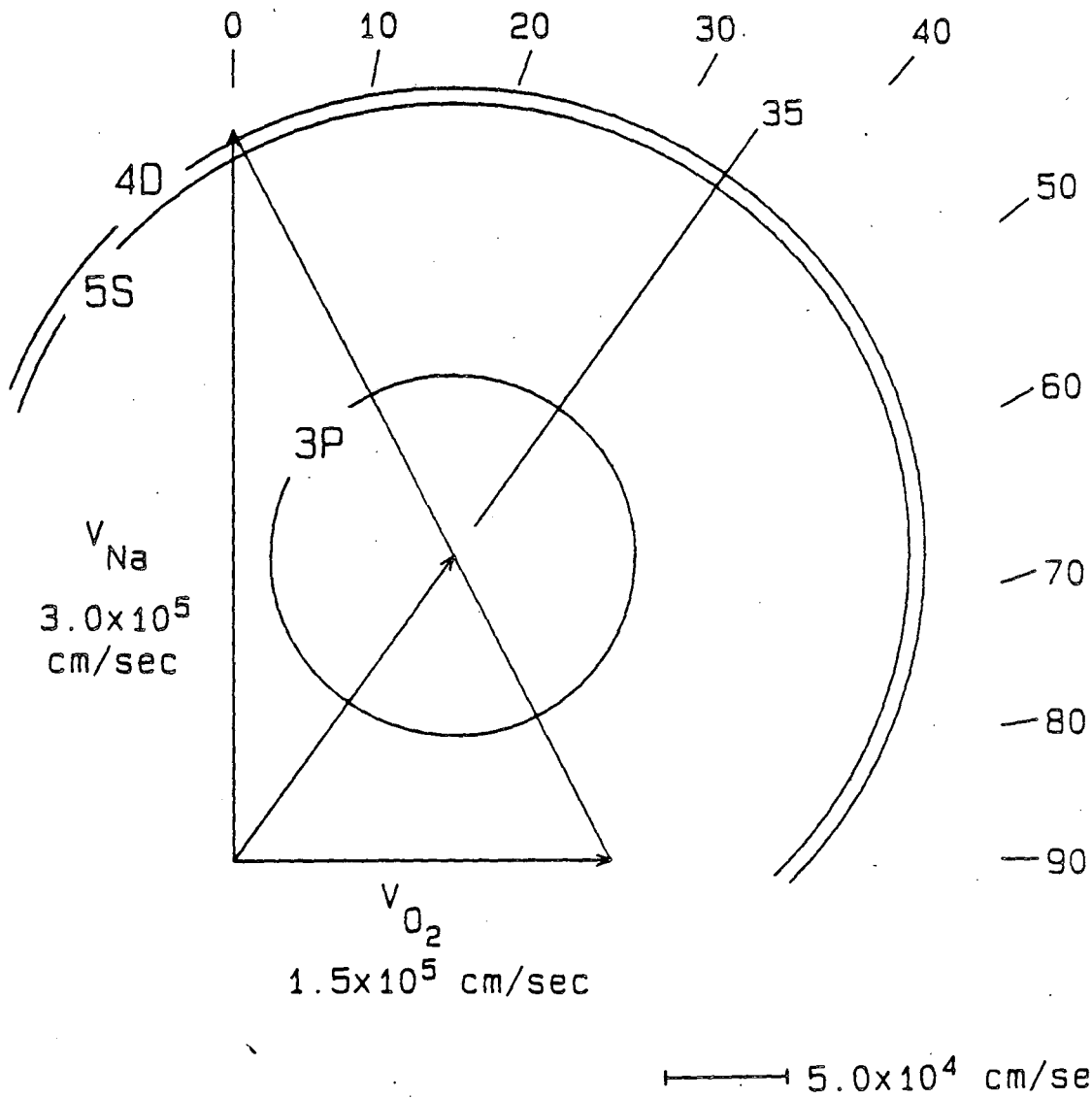


Fig. 4

XBL 863-855

Fig. 5. NaO product angular distribution for Na(3S,4D) + O₂ at a collision energy of 8 kcal/mole. The low angle rise is due to elastically and inelastically scattered Na atoms. Note that no reactive scattering is observed for either state.

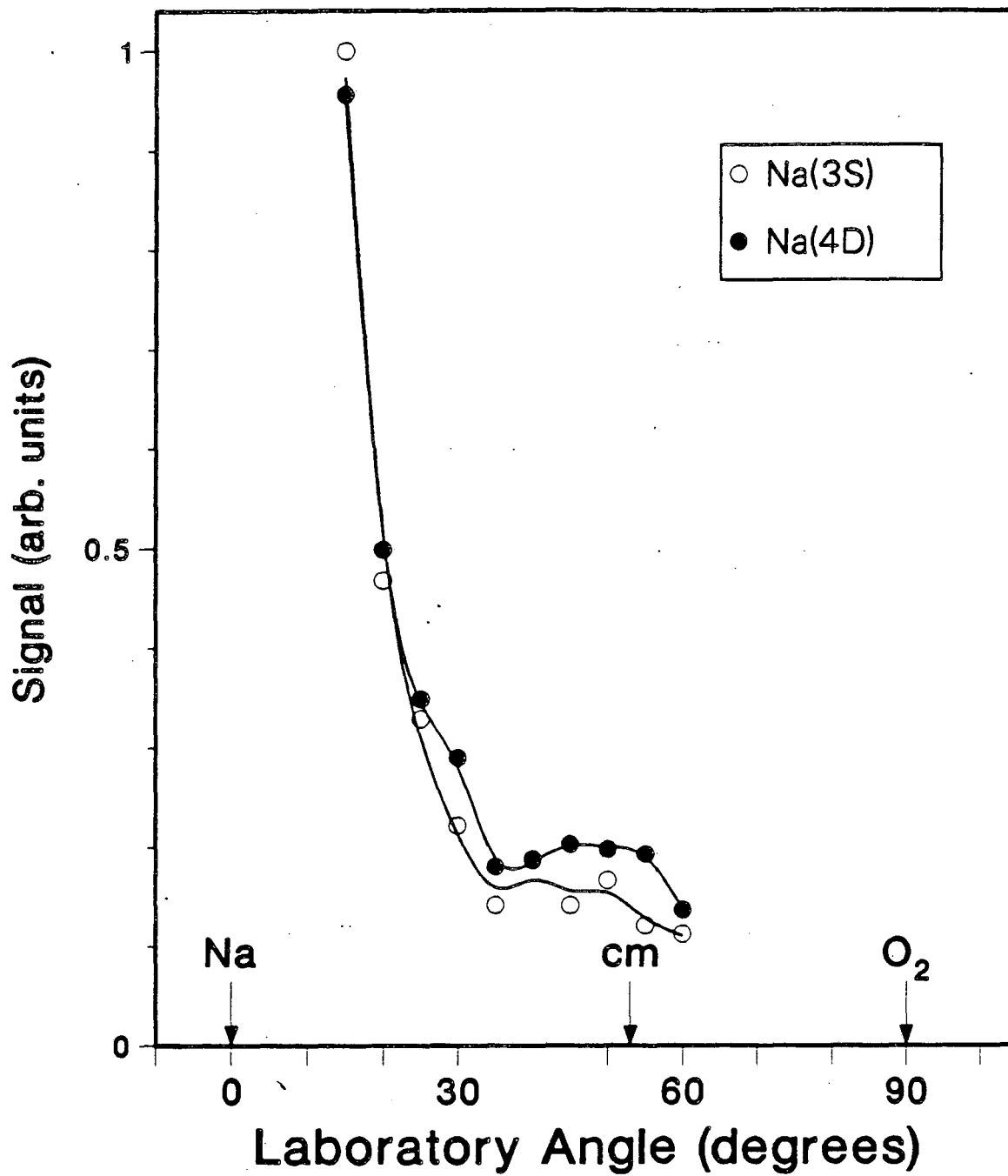
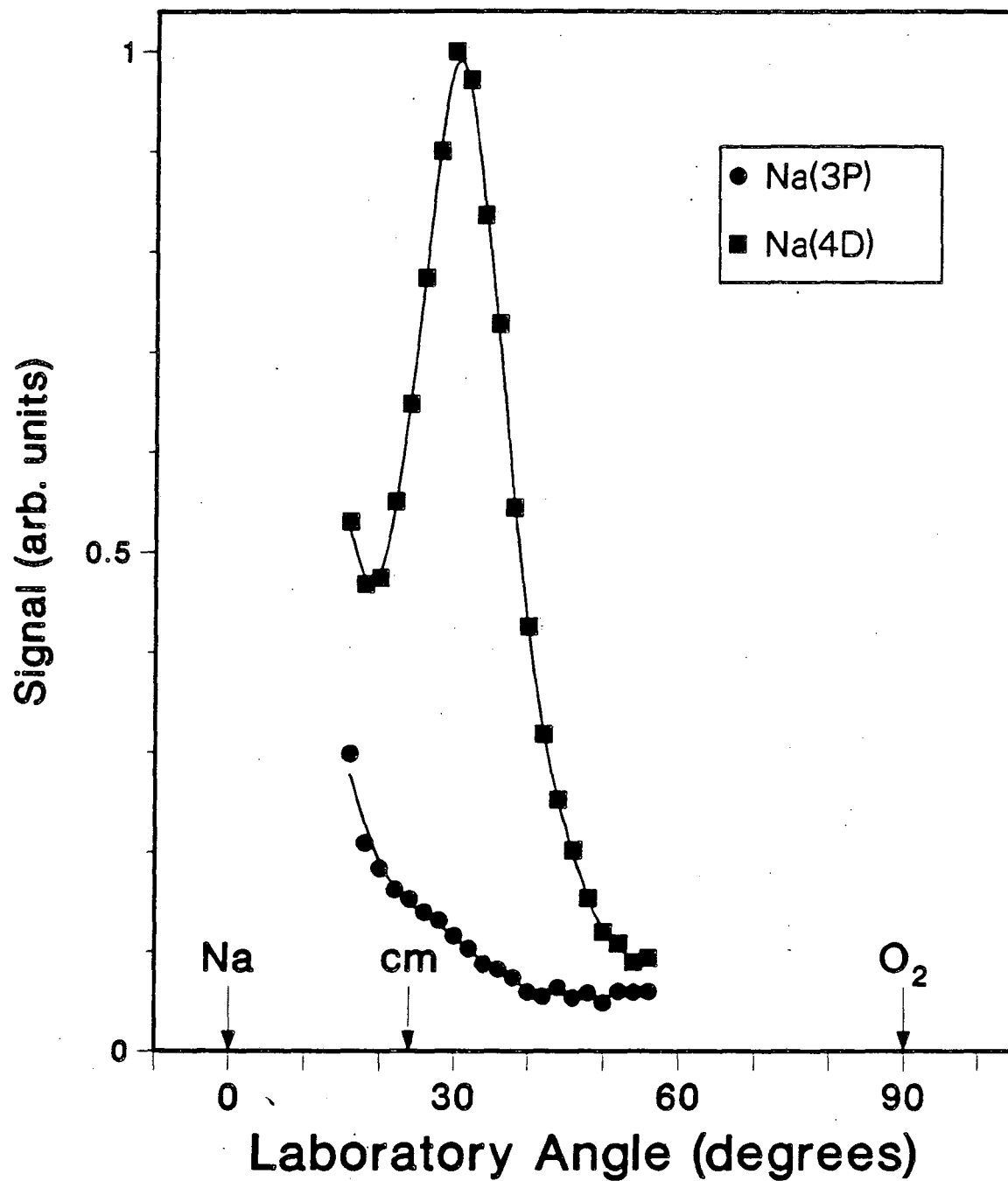


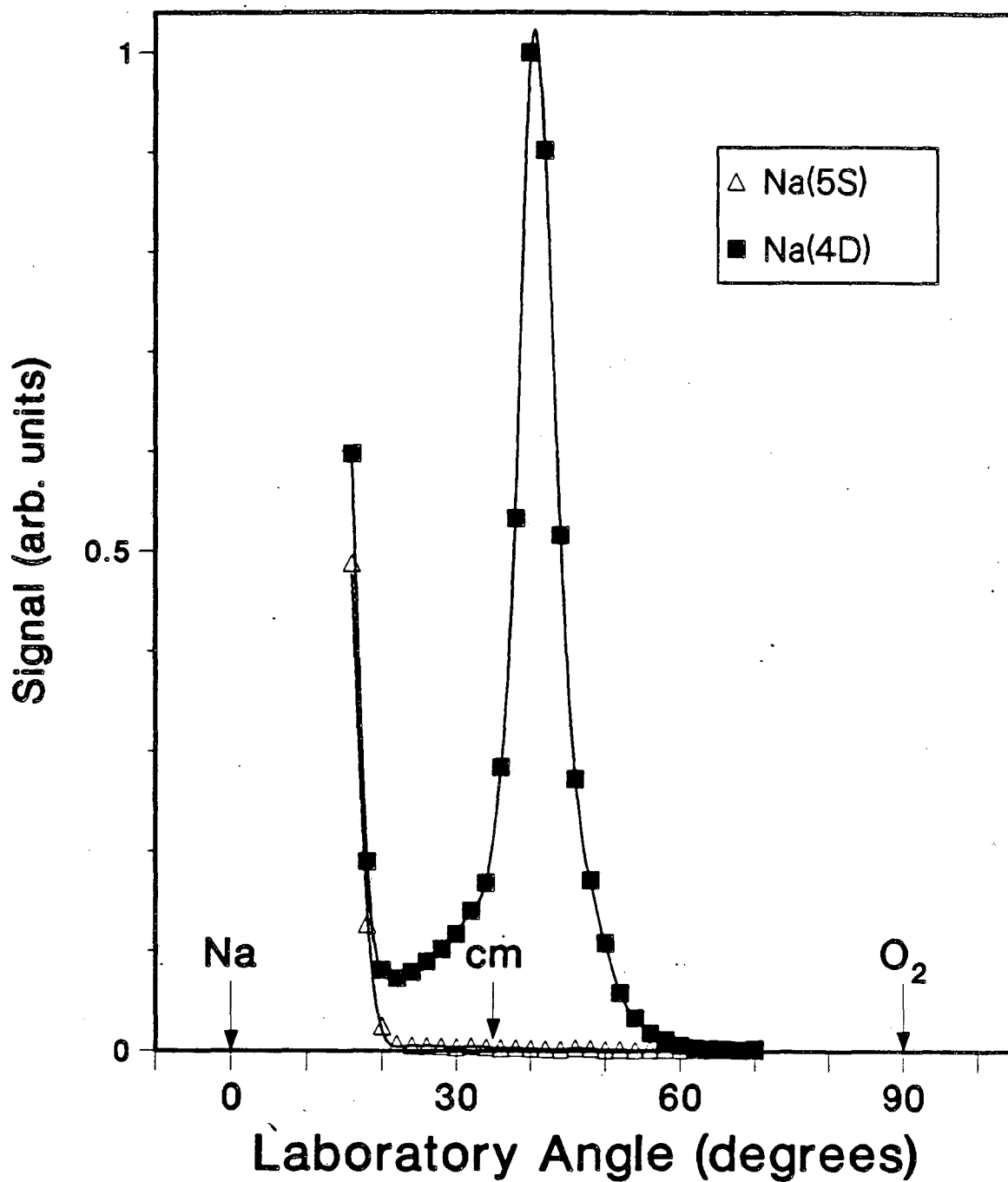
Fig. 5

XBL 863-878



XBL 863-877

Fig. 6. NaO product angular distribution for Na(3P,4D) + O₂ at a collision energy of 16 kcal/mole. The low angle rise is due to elastically and inelastically scattered Na atoms.



XBL 863-867

Fig. 7. NaO product angular distribution for Na(4D,5S) + O₂ at a collision energy of 18 kcal/mole. The low angle rise is due to elastically and inelastically scattered Na atoms.

$$E_{\text{coll}} = \begin{matrix} 13 \\ 12 \text{ kcal/mole} \\ 11 \end{matrix}$$

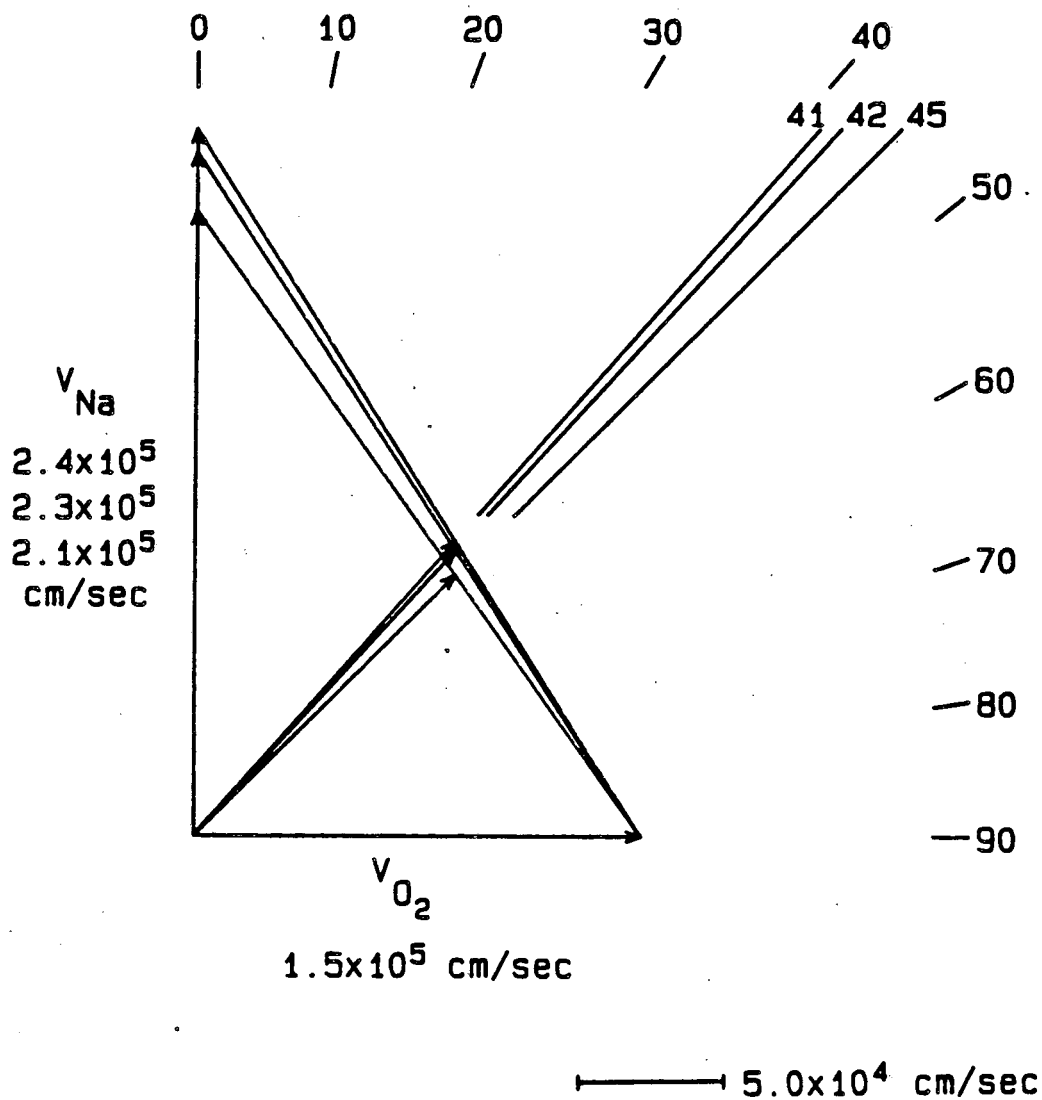
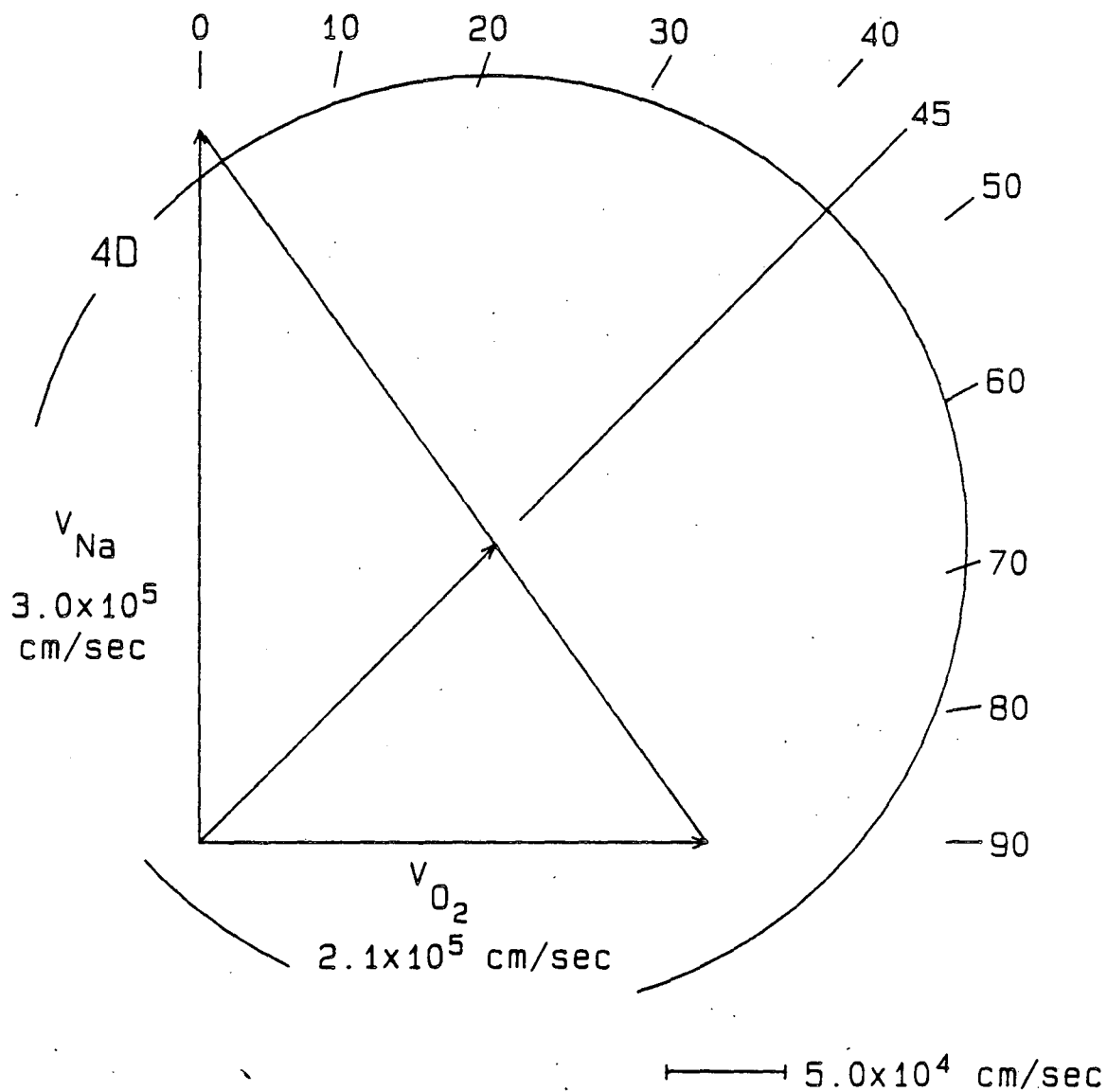


Fig. 8. Newton velocity vector diagram for $\text{Na} + \text{O}_2 \rightarrow \text{NaO} + \text{O}$ at collision energies of 11, 12, and 13 kcal/mole. The sodium beam is seeded in a mixture of helium and neon, and the molecular beam is 5% O_2 in helium. The helium-neon mixture is varied to produce the different Na beam velocities shown.

XBL 863-897

$$E_{\text{coll}} = 22 \text{ kcal/mole}$$



XBL 863-857

Fig. 9. Newton velocity vector diagram for $\text{Na} + \text{O}_2 \rightarrow \text{NaO} + \text{O}$ at a collision energy of 22 kcal/mole. The sodium beam is seeded in helium, and the molecular beam is 5% O_2 in helium.

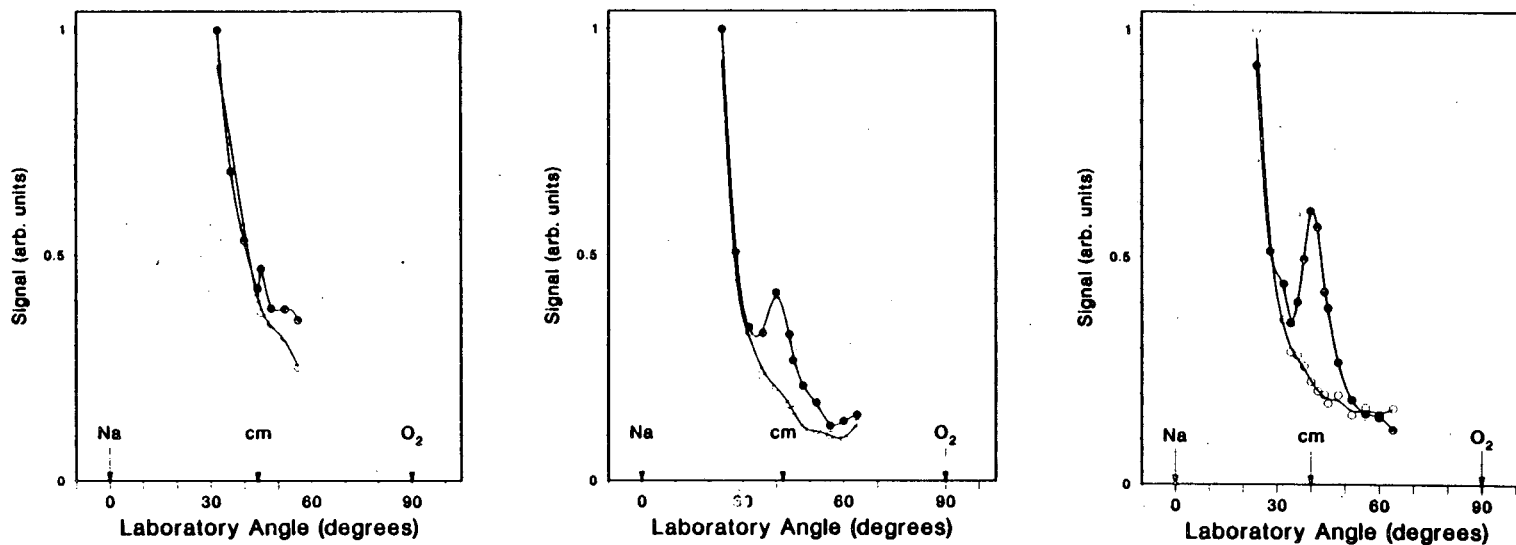
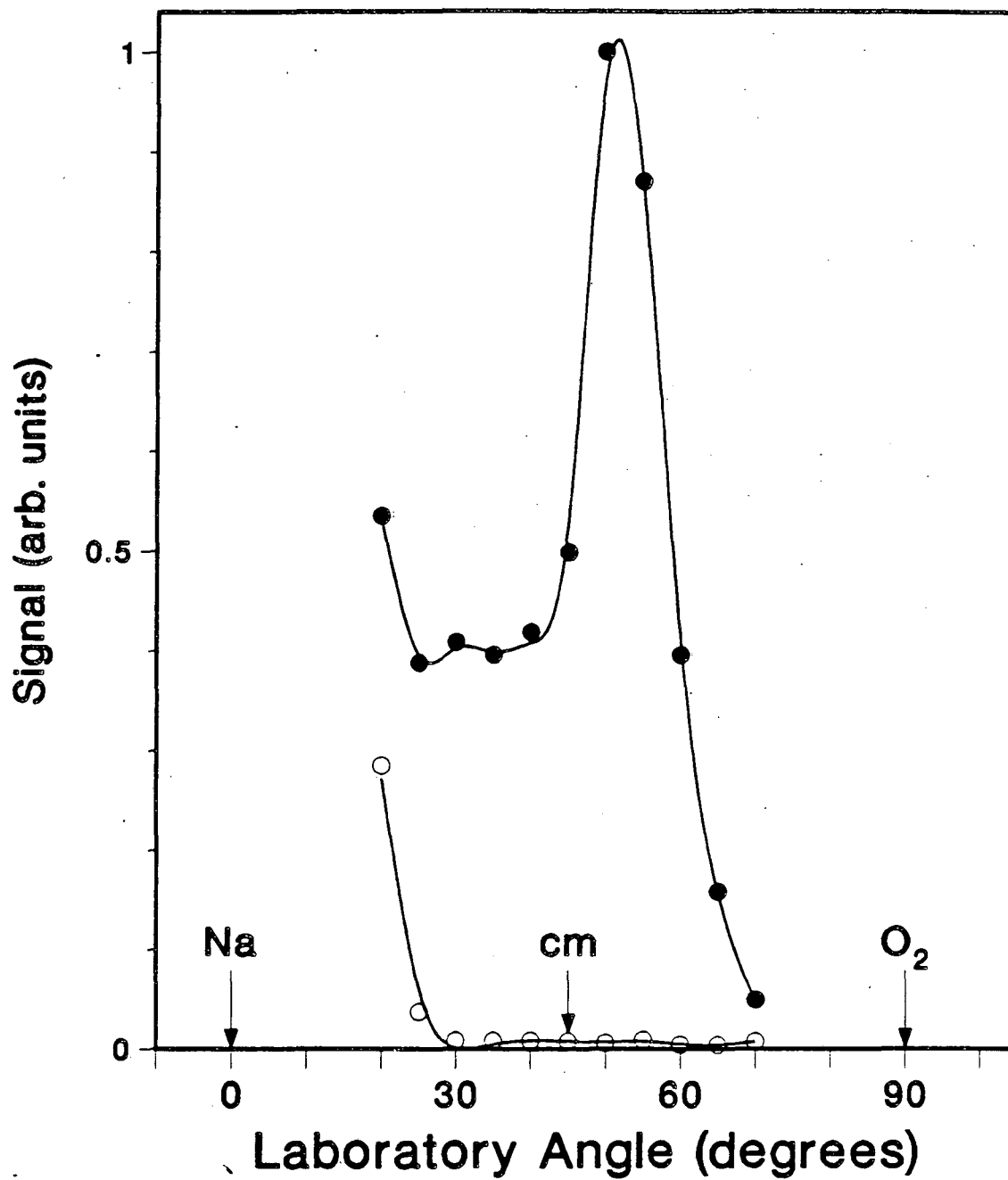


Fig. 10. NaO product angular distributions for Na(3S,4D) + O₂ at collision energies of a) 11 kcal/mole, b) 12 kcal/mole, and c) 13 kcal/mole.

XBL 863-844

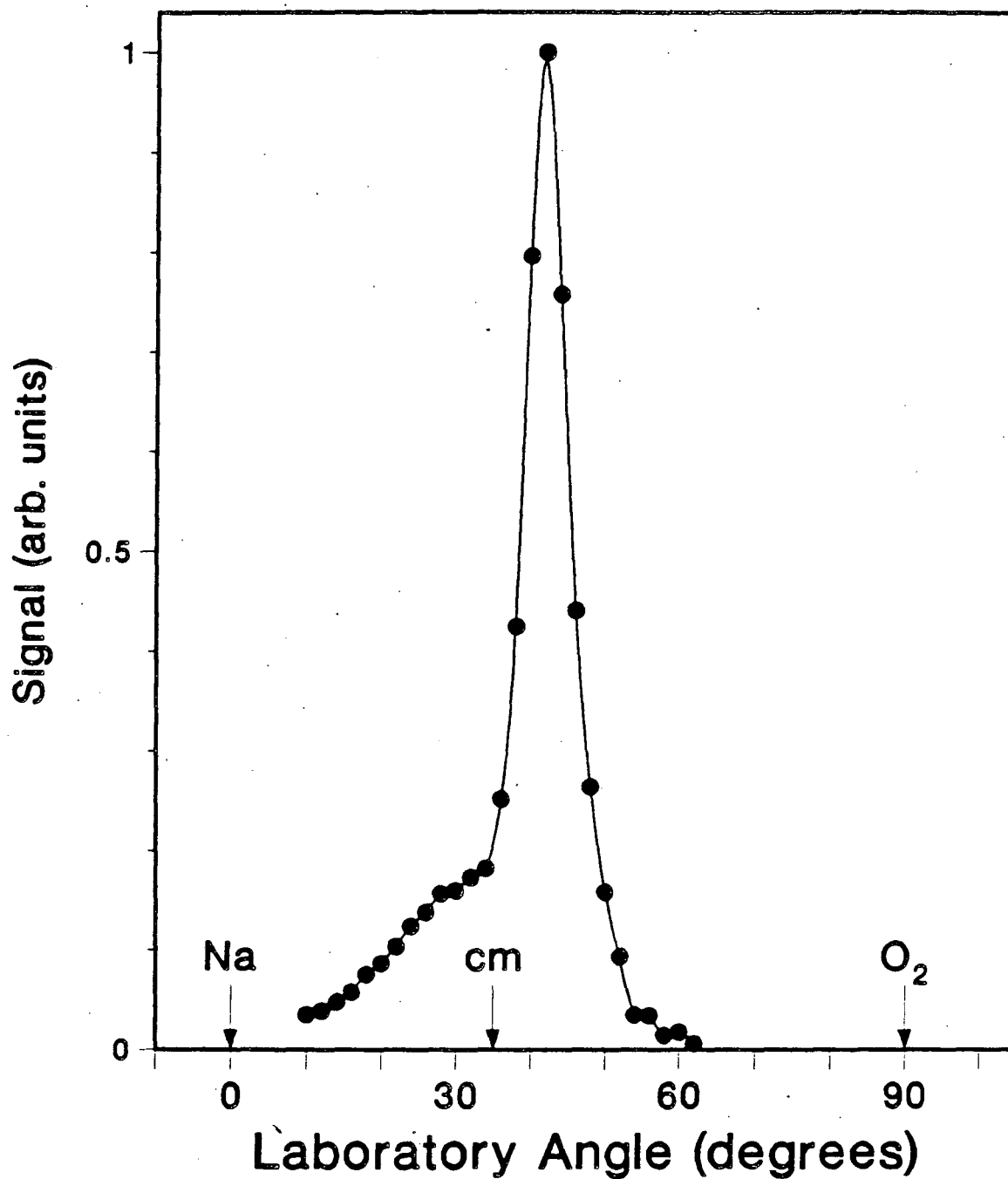


XBL 863-848

Fig. 11. NaO product angular distribution for $\text{Na}(3S,4D) + \text{O}_2$ at a collision energy of 22 kcal/mole. The low angle rise is due to elastically and inelastically scattered Na atoms.

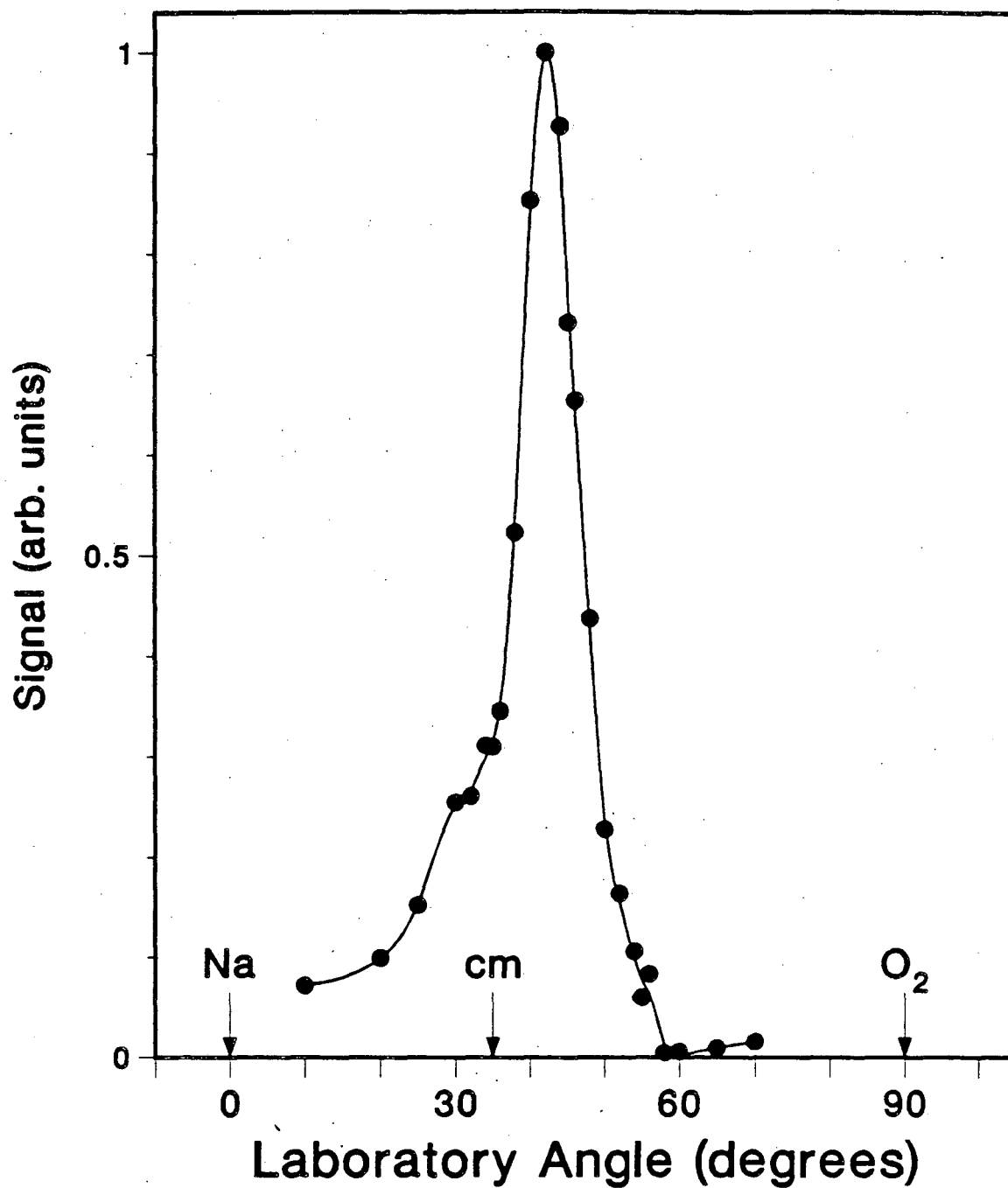
observed for $\text{Na}(5S) + \text{O}_2$. In addition to the distributions shown, an effort was made to see scattering from $\text{Na}(5S)$ at collision energies of 8 and 16 kcal/mole, although only the 18 kcal/mole data is shown. Since the 5S level radiatively populates the 4S and 4P levels, there is no reaction for these levels as well. It is clear that that the signal is indeed due only to the 4D state. All these distributions were measured with the mass spectrometer tuned to a mass to charge ratio (m/q) of 23 (Na^+) because the product NaO would fragment to Na^+ in the electron bombardment ionizer. Angular distributions were also taken for the 18 kcal/mole collision energy with the quadrupole mass spectrometer set to $m/q=16$ (O^+ and O_2^{++}) and $m/q=39$ (NaO^+), and are shown in figures 12 and 13, respectively, however the large background at each of these mass settings frustrated all attempts to observe a true mass-dependent signal. Product velocities were measured by the cross-correlation time-of-flight method at a number of angles for each energy, 16 and 18 kcal/mole, for $m/q=23$ (Na^+), and these are shown in figures 14 and 15, respectively. Time-of-flight distributions were also measured at a collision energy of 18 kcal/mole for $m/q=16$ (O^+ and O_2^{++}) and $m/q=39$ (NaO^+), shown in figures 16 and 17, respectively.

It was discovered while making these measurements that signal could be observed with the detector ionizer and the majority of the ion optics turned off. In fact, only the -30 kV ion target and photo-multiplier need be powered in order to see some signal. Reactive product angular distributions were recorded with the electron



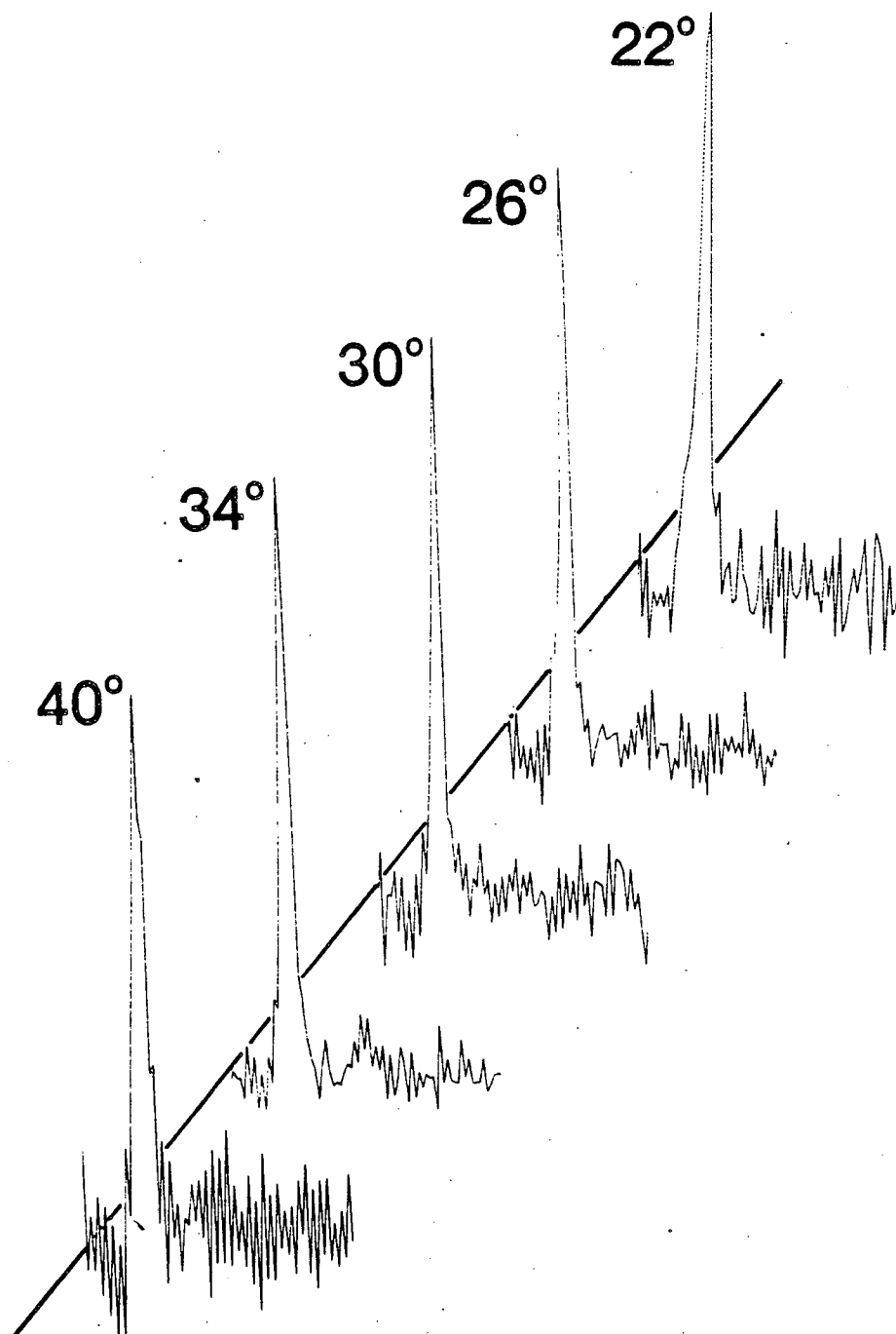
XBL 863-875

Fig. 12. Product angular distribution for $\text{Na}(4D) + \text{O}_2$ at a collision energy of 18 kcal/mole with the detector set to $m/q=16$ (O^+ , O_2^{++}).



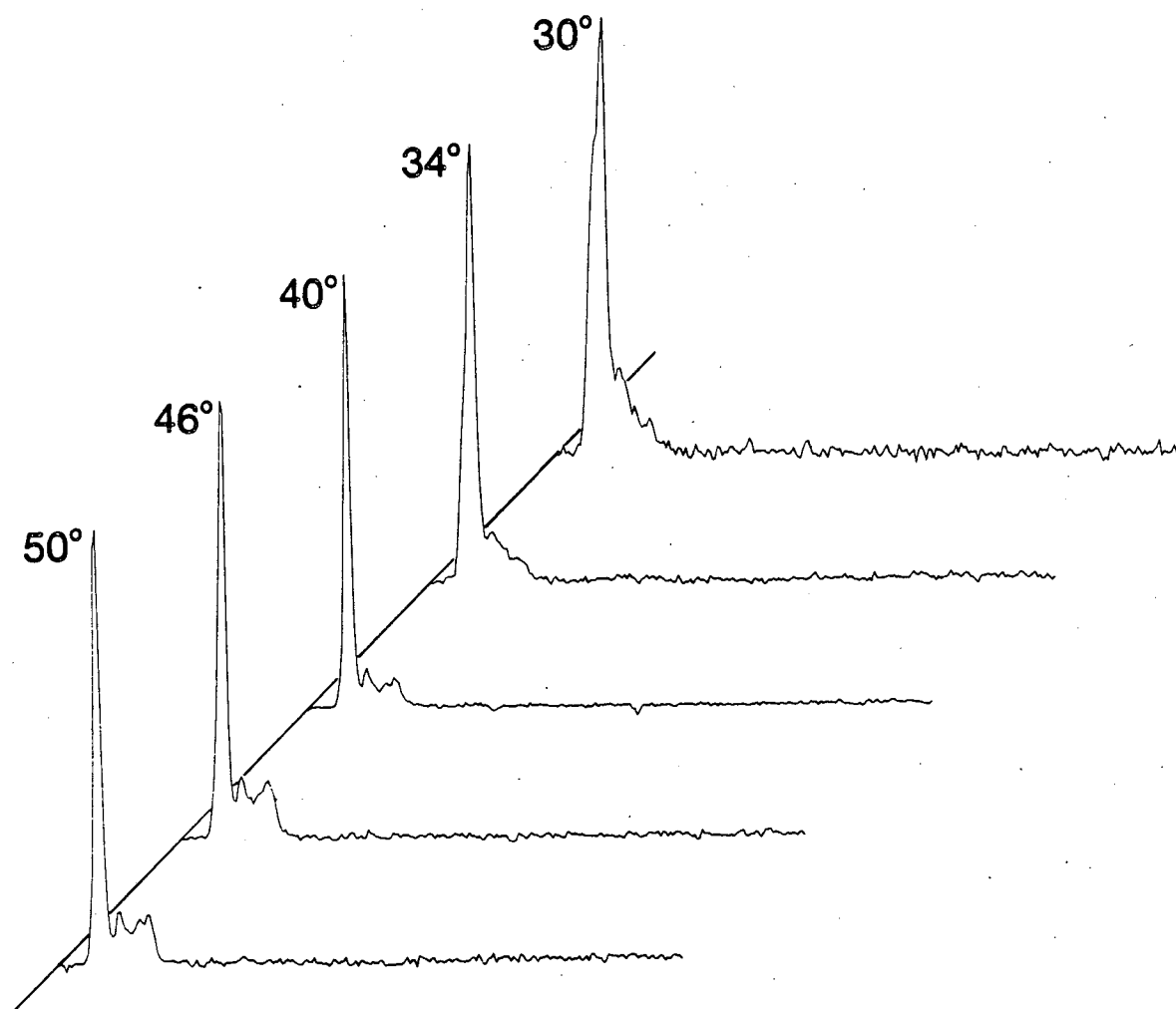
XBL 863-876

Fig. 13. Product angular distribution for $\text{Na}(4D) + \text{O}_2$ at a collision energy of 18 kcal/mole with the detector set to $m/q=39$ (NaO^+).



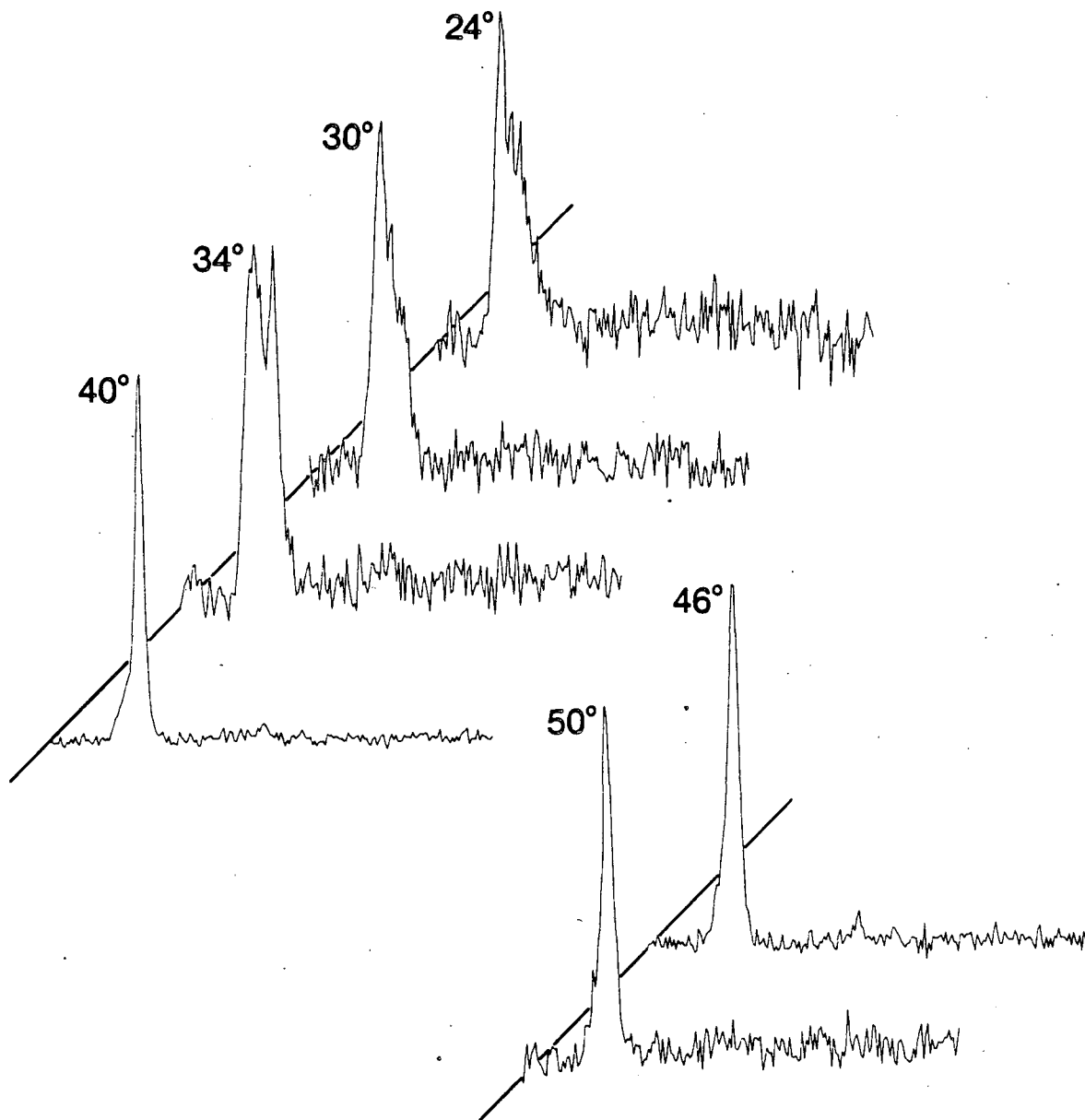
XBL 863-886

Fig. 14. NaO product time-of-flight measurements at various detector angles (shown in each frame) at a collision energy of 16 kcal/mole for $m/q=23$ (Na^+).



XBL 863-890

Fig. 15. NaO product time-of-flight measurements at various detector angles (shown in each frame) at a collision energy of 18 kcal/mole for $m/q=23$ (Na^+).



XBL 863-894

Fig. 16. Product time-of-flight measurements at various detector angles at a collision energy of 18 kcal/mole with the detector set to $m/q=16$ (O^+ , O_2^+).

Fig. 17. Product time-of-flight measurement for 40° at a collision energy of 18 kcal/mole with the detector set to $m/q=39$ (NaO^+).

40°

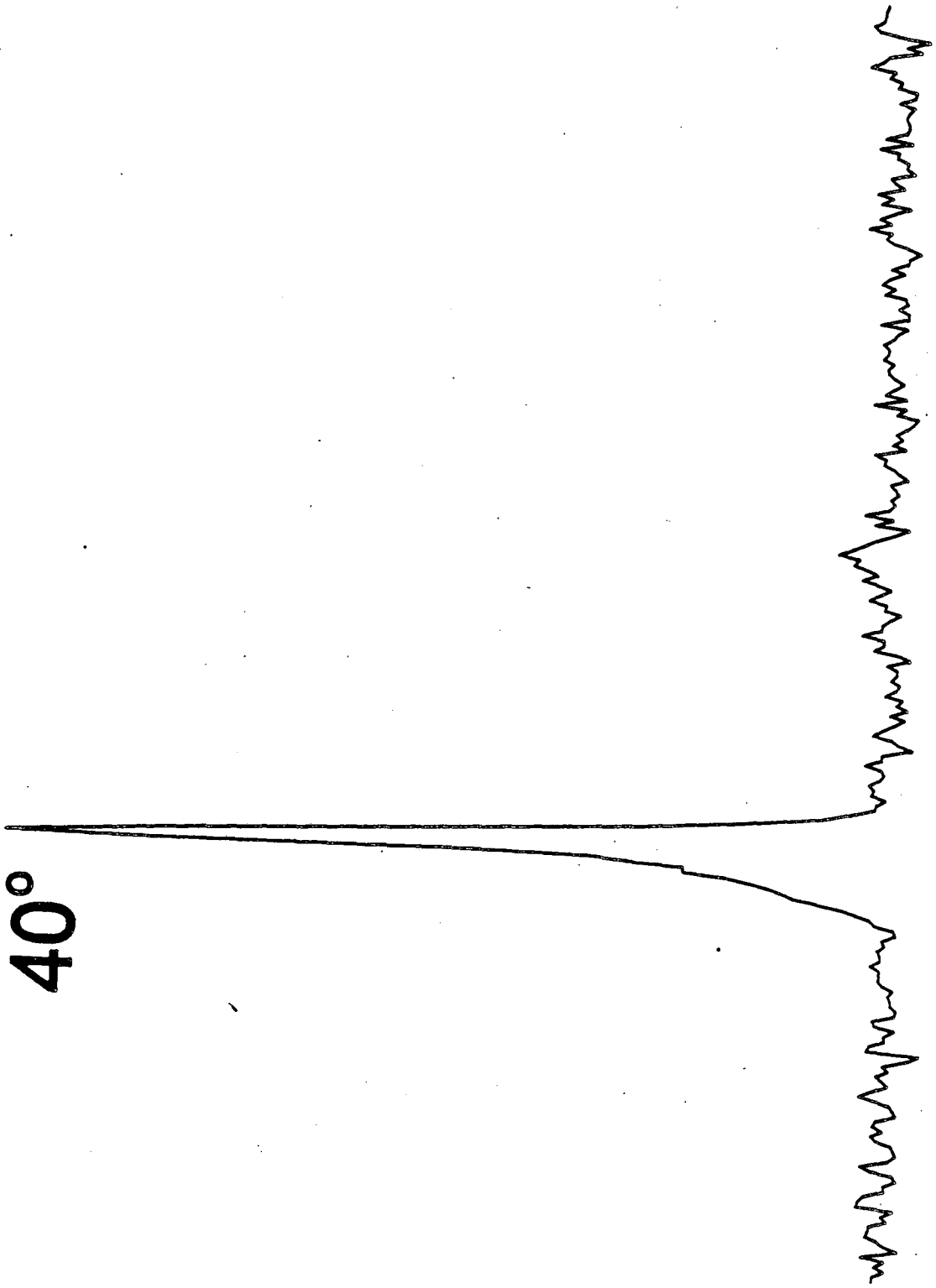


Fig. 17

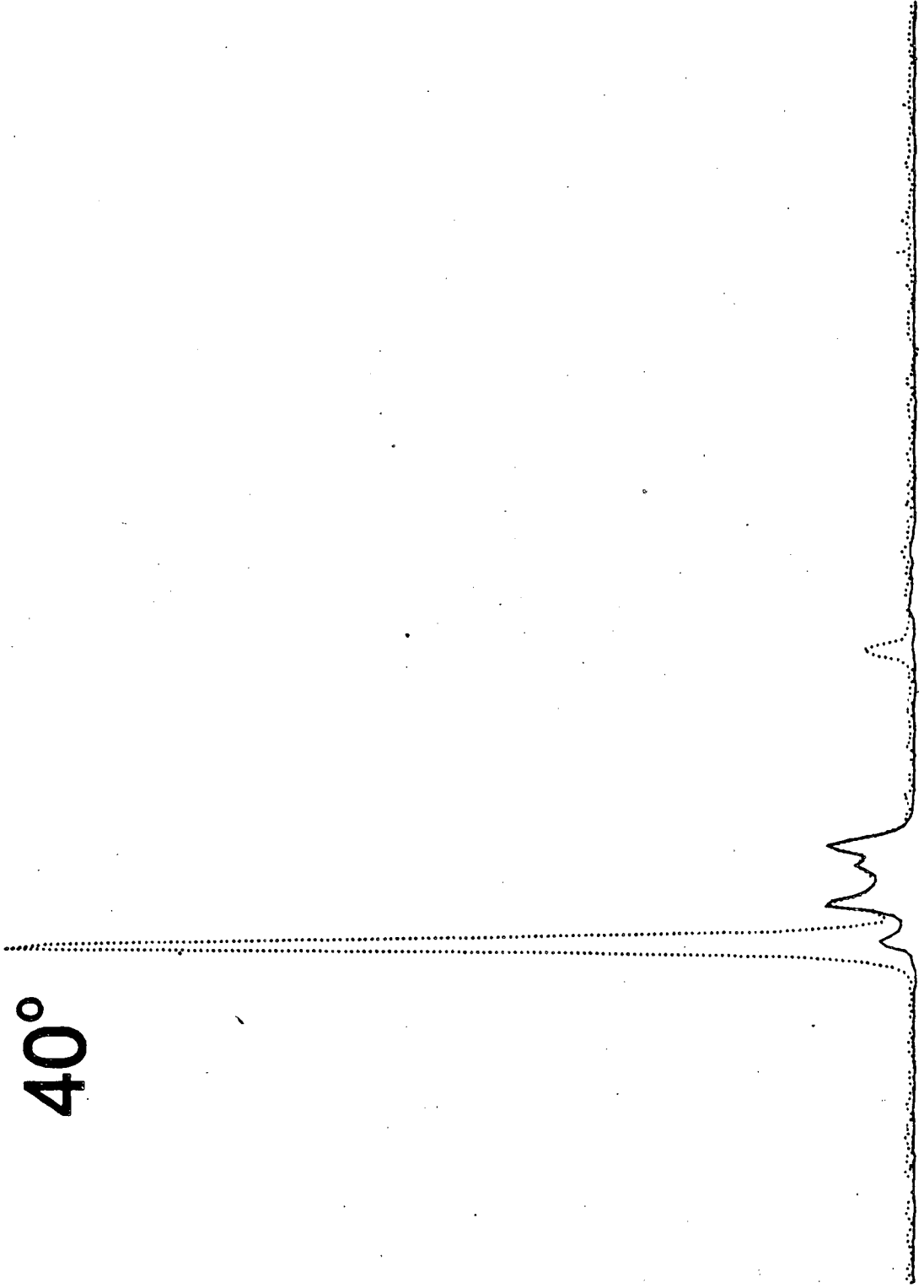
bombardment ionizer filament emission off, but all other conditions the same. This subsequent ionization is what is responsible for the tails on the product velocity distributions in figures 14-17. An example of this effect is shown in the two time-of-flight distributions shown in figure 18. The only difference between the two traces is that for the dotted line the ionizer filament is emitting electrons, and for the solid line, no electrons are emitted. This signal is due to ionization at a number of points in the detector. This has been shown by turning off the detector electronics sequentially and seeing time-of-flight peaks disappear one by one. Of course when this is done the peaks change position since the ion flight time is changed as the various accelerating optics are turned off. Time-of-flight measurements with the ionizer emission off, thus giving no electron bombardment, are shown for the quadrupole spectrometer set to $m/q=16$ (O^+ and O_2^+), $m/q=23$ (Na^+), and $m/q=39$ (NaO^+) for a collision energy of 18 kcal/mole and for a number of detector angles in figures 19, 20, and 21, respectively.

The ratio of the intensity of the first TOF peak, due to electron bombardment ionization, to that of the final peak for which only the doorknob and the photomultiplier need be powered, is 10:1 for the 18 kcal/mole data. This ratio remains constant across the various lab angles measured. This is also seen in that the angular distributions have the same shape with the detector on and off.

Where signal is small, better statistics are found in the emission off distributions. These are shown for collision energies 11, 12, and

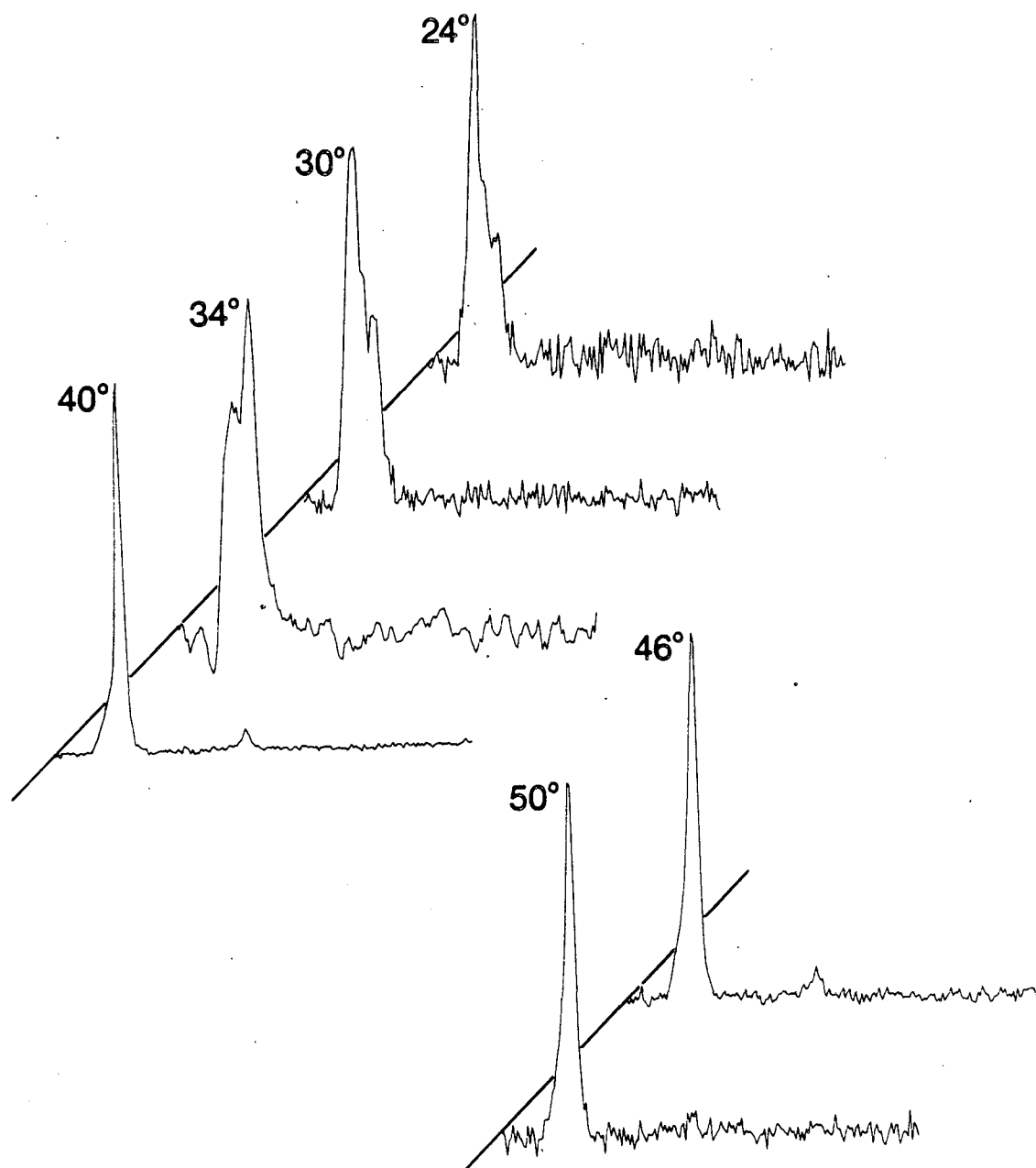
Fig. 18. Time-of-flight distributions for 40° at a collision energy of 18 kcal/mole with the ionizer emission on (dotted line) and off (solid line).

40°



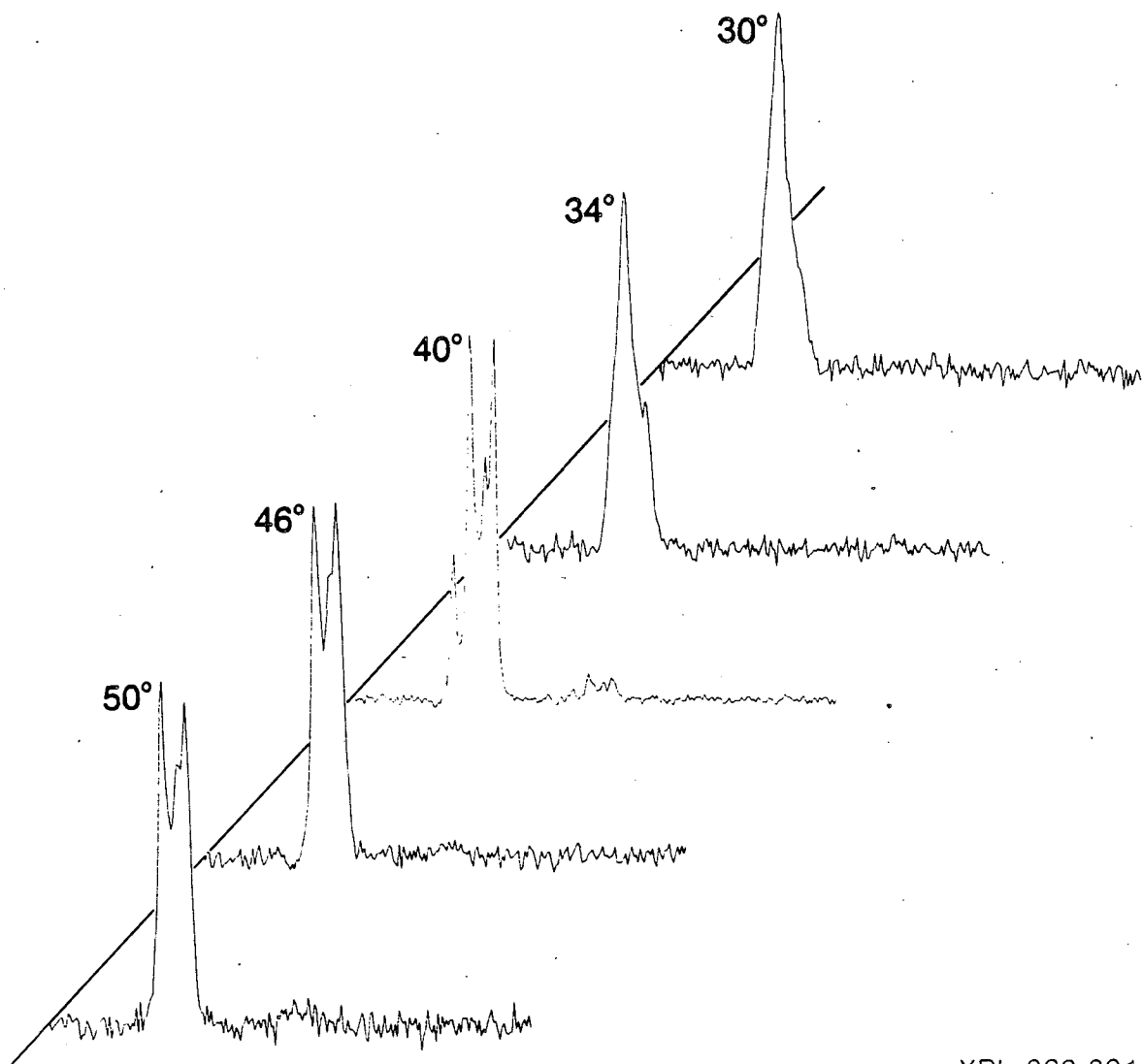
XBL 863-869

Fig. 18



XBL 863-893

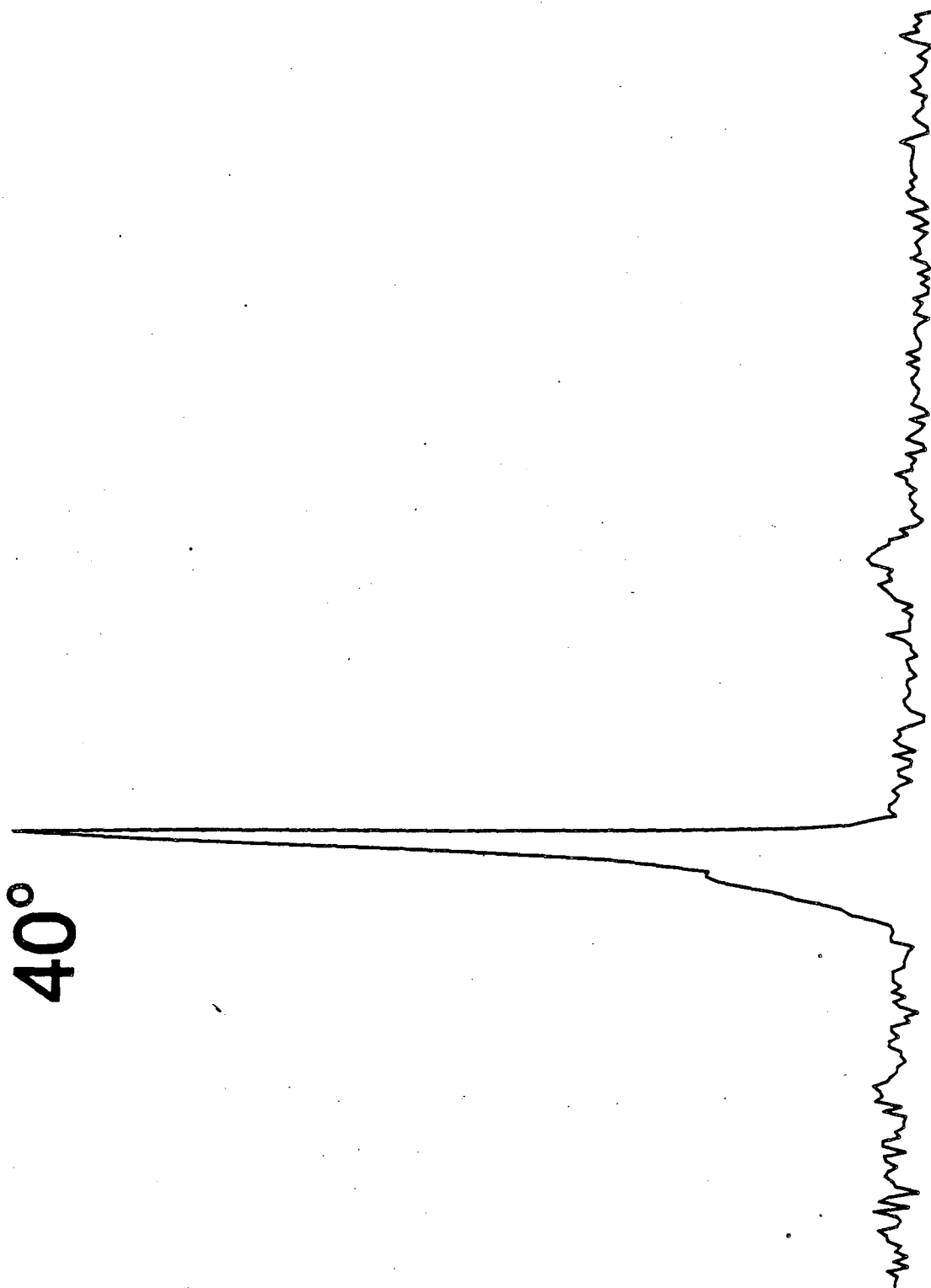
Fig. 19. Time-of-flight distributions for the angles shown with the mass spectrometer set to $m/q=16$ at a collision energy of 18 kcal/mole with the ionizer emission off.



XBL 863-891

Fig. 20. Time-of-flight distributions for the angles shown with the mass spectrometer set to $m/q=23$ at a collision energy of 18 kcal/mole with the ionizer emission off.

Fig. 21. Time-of-flight distribution for 40° at a collision energy of 18 kcal/mole with the mass spectrometer set to $m/q=39$ and with the ionizer emission off.



XBL 863-870

Fig. 21

13 kcal/mole in figures 22a, b, and c, respectively. These low collision energies were studied with a fairly broad Na beam velocity distribution ($S = v/\Delta v < 4$) and the very narrow O_2 beam velocity distribution described in chapter I ($S > 10$). The peak intensity increases strongly for these distributions, but does not change position in the laboratory. Also, a low angle peak seems to come into the distribution with increasing collision energy.

In an effort to understand why the observed process is state-selective, polarization dependences of the differential cross sections were measured in order to try to determine the symmetry of the transition state. These measurements were made as explained in chapter I by rotating the laser polarization in the scattering plane to align the Na excited orbitals, while the signals at fixed detector angles are recorded. These dependences were measured for 5 angles at a collision energy of 18 kcal/mole with the mass spectrometer set to $m/q=23$ (Na^+). The important quantities deduced are the favored polarization angle for reaction at a given detector angle, and the amplitude of this polarization effect. The measured dependences are shown in figures 23a-e, and the best fits to the curves (as determined by the method described in chapter I) are summarized in table II.

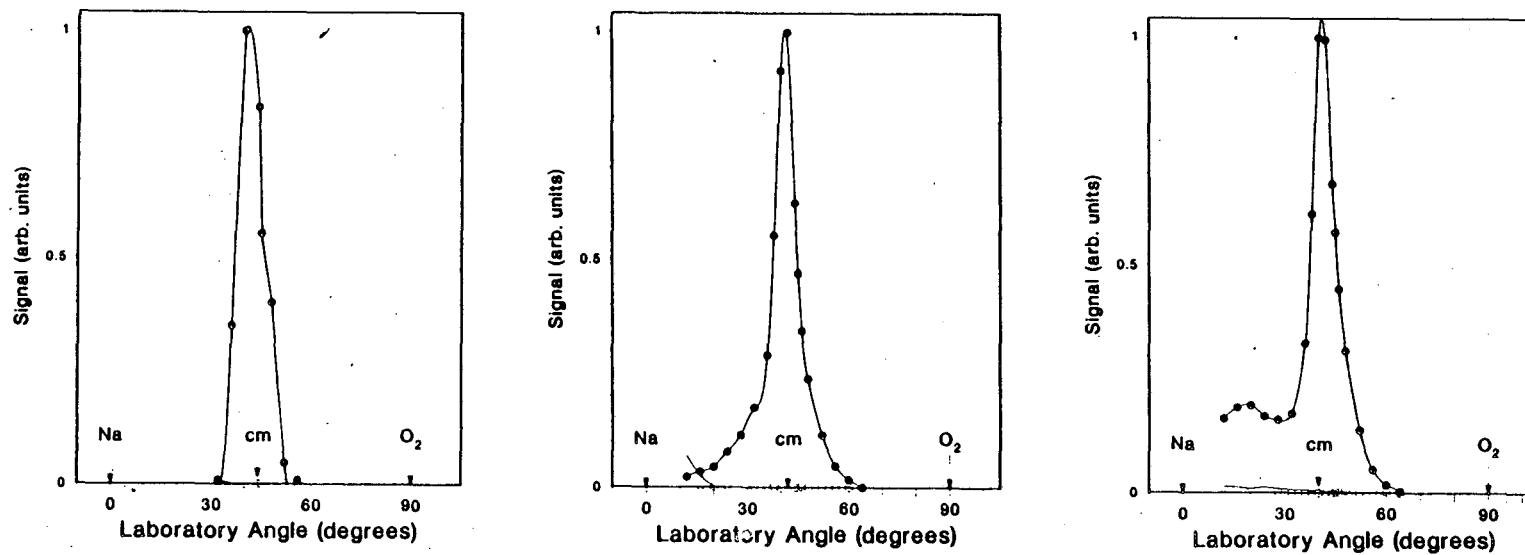
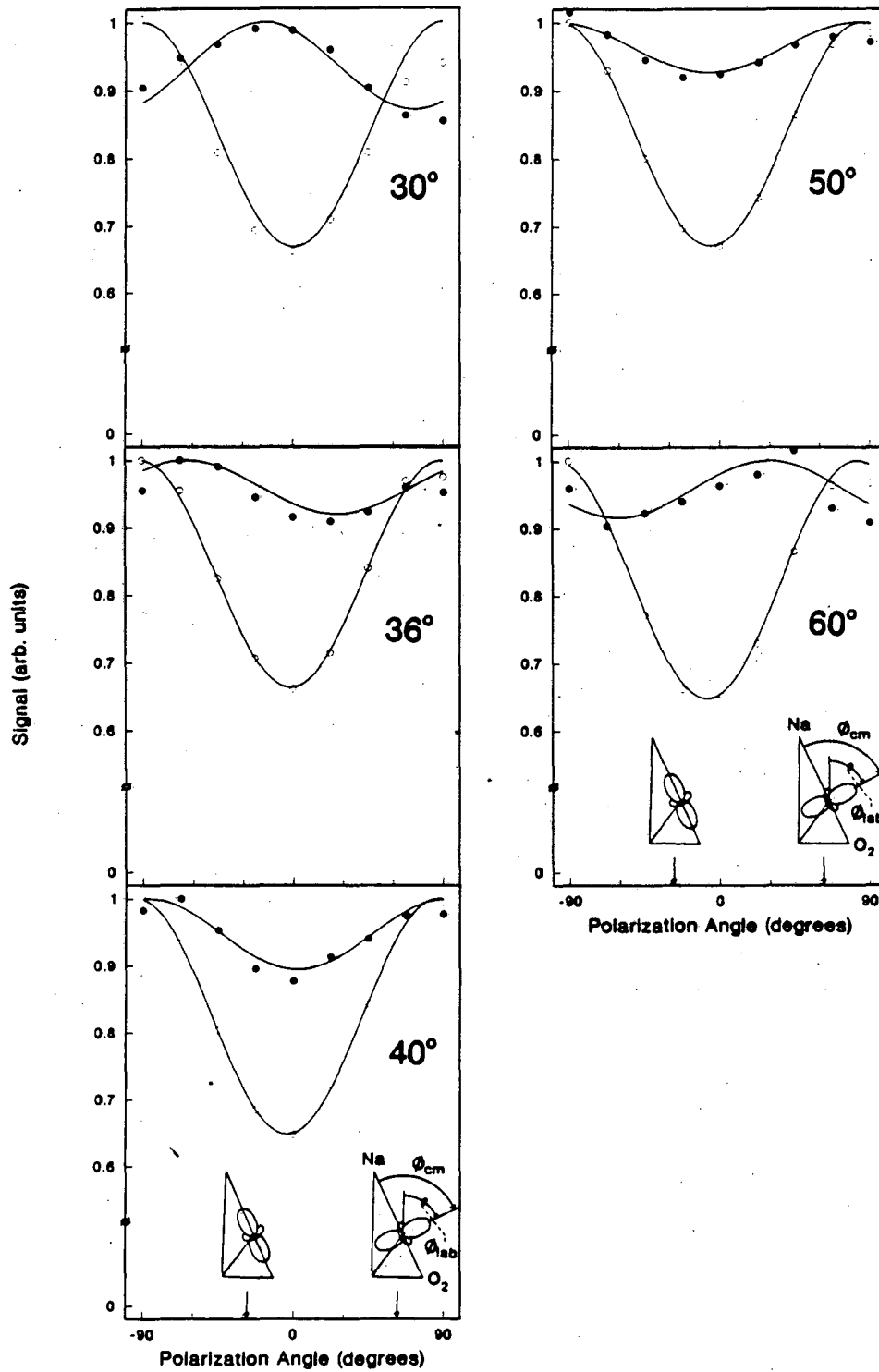


Fig. 22. Product angular distributions recorded with the ionizer emission off for Na(4D) + O₂ at collision energies of a) 11 kcal/mole, b) 12 kcal/mole, and c) 13 kcal/mole.

XBL 863-843

Fig. 23. Laser polarization dependences of the signal due to the $\text{Na}(4D) + \text{O}_2$ reaction at a collision energy of 18 kcal/mole for the detector angles shown in each frame. The solid lines are the best fits to the data as discussed in chapter I.



XBL 863-892

Fig. 23

Table II. The measured polarization dependences for $\text{Na}(4D) + \text{O}_2$ at a collision energy of 18 kcal/mole.

Laboratory Detector Angle	Laboratory Peak of Polarization Dependence (ϕ_{LAB})	Center-of-Mass Peak of Polarization Dependence (ϕ_{CM})	Amplitude (2A)
30°	-18°	9°	.130
36°	-64°	-37°	.080
40°	-88°	-61°	.106
50°	83°	-70°	.074
60°	29°	56°	.084

C. Analysis of Experimental Results

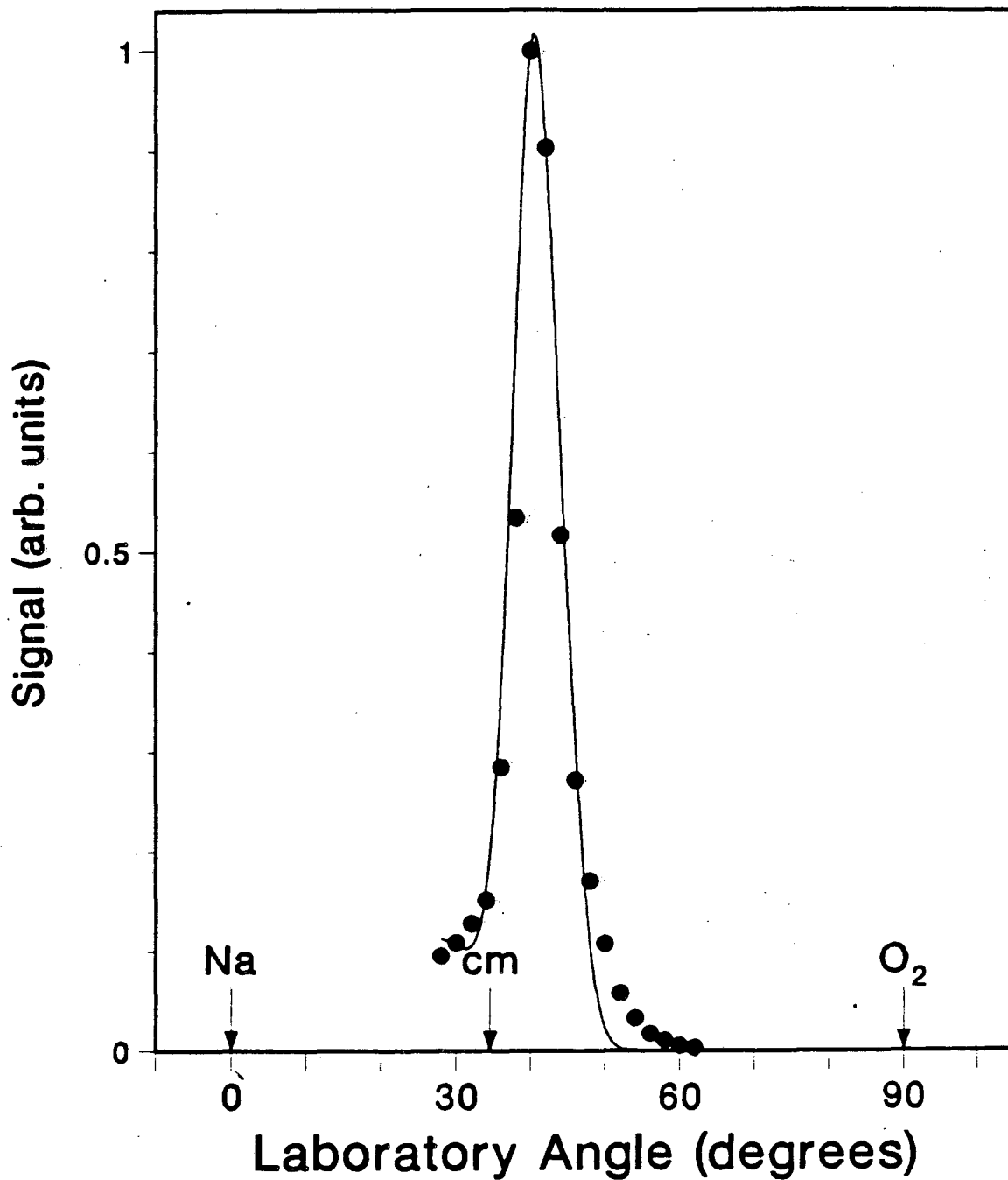
First, it is clear from the data that only the Na(4D) state undergoes whatever process produces the high laboratory angle peak. Since the Na(5S) state radiatively populates the Na(4S,4P) states, the Na(3S,3P,4S,4P,5S) states do not react at a collision energy of 18 kcal/mole.

In transforming the Na(4D) + O₂ data to center-of-mass frame distributions, it is assumed that the reactive process (1), and thus product NaO was responsible for the data at m/q=23 (Na⁺). In fact, since the data is fitted to a center-of-mass angular distribution and a center-of-mass velocity distribution P(u), it does not matter what the product is in fitting the data. The fitted center-of-mass velocity distribution is reported as a function of translational energy, P(E), which is a more meaningful quantity for direct comparison with other experiments, which is dependent on the product masses, however. As shown below, there is a simple scaling factor allowing the inter-conversion of P(E) distributions due to different product masses, but the same center-of-mass velocity distributions. The possibility that other processes are responsible for the signal recorded is also discussed below.

The laboratory angular and velocity data at a collision energy of 18 kcal/mole were transformed to center-of-mass angular and velocity information using program GM as described in chapter I. The best fit

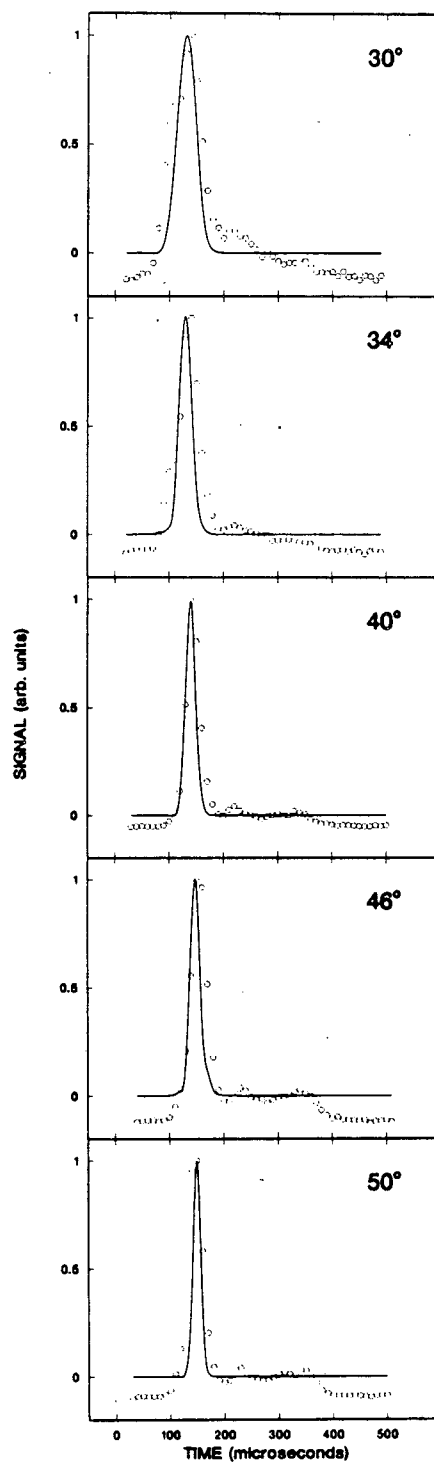
to the angular distribution is shown by the solid line in figure 24, and to the time-of-flight measurements in figure 25. This yielded the translational energy distribution ($P(E_T')$) in figure 26, and the center-of-mass NaO product angular distribution ($T(\theta)$) in figure 27. These remarkable distributions show the extremely limited conditions under which NaO is produced. As expected from examining the laboratory angular distributions, the center-of-mass scattering angular distributions are peaked sharply backwards with respect to the initial Na atom direction. The peak is clearly directly backwards (at $\theta=180^\circ$), with 50% of the NaO product scattering to center-of-mass angles greater than 150° with respect to the incoming Na relative (center-of-mass frame) velocity (this is weighted NaO intensity, i.e. $T(\theta)\sin\theta$). The very low translational energy of the products shows that the products must be very internally excited. The peak of the product recoil energy distribution is at 0.6 kcal/mole, and the mean recoil energy is 0.7 kcal/mole. From conservation of energy considerations, an average of 58 kcal/mole (2.5 eV) must be in the internal excitation of the products.

By weighting the reaction cross section according to collision energy using a step function, the reaction threshold was determined to be 15 ± 1 kcal/mole. It is also evident from the constant peak position in the laboratory angular distributions for 11-13 kcal/mole mean collision energies that the threshold to reaction is dominating the shapes of these distributions. The assumption of a step function is clearly not valid, but is meant to be a zeroth order approximation useful in determining the threshold. Also, an implicit assumption is



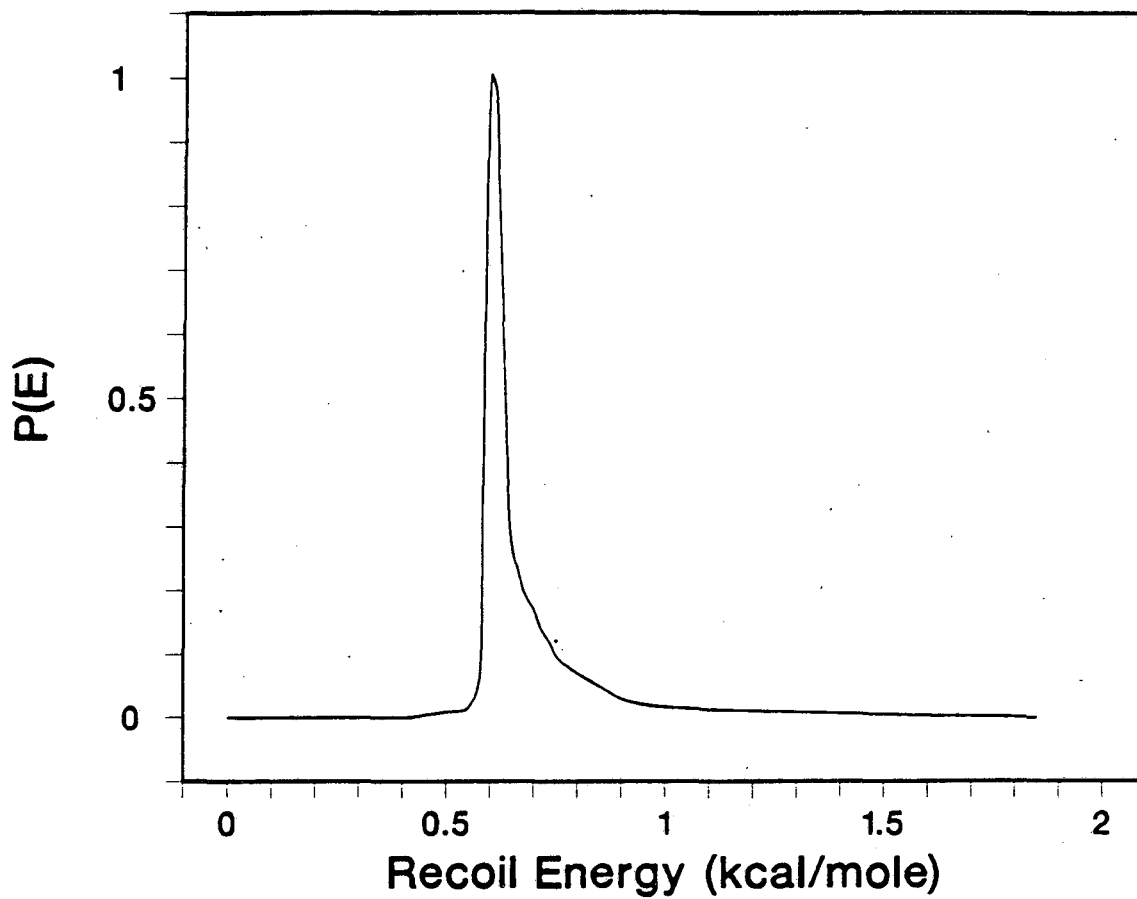
XBL 863-850

Fig. 24. The best fit to the laboratory angular distribution for $\text{Na}(4D) + \text{O}_2 \rightarrow \text{NaO} + \text{O}$ at a collision energy of 18 kcal/mole. The solid line shows the fit to the data.



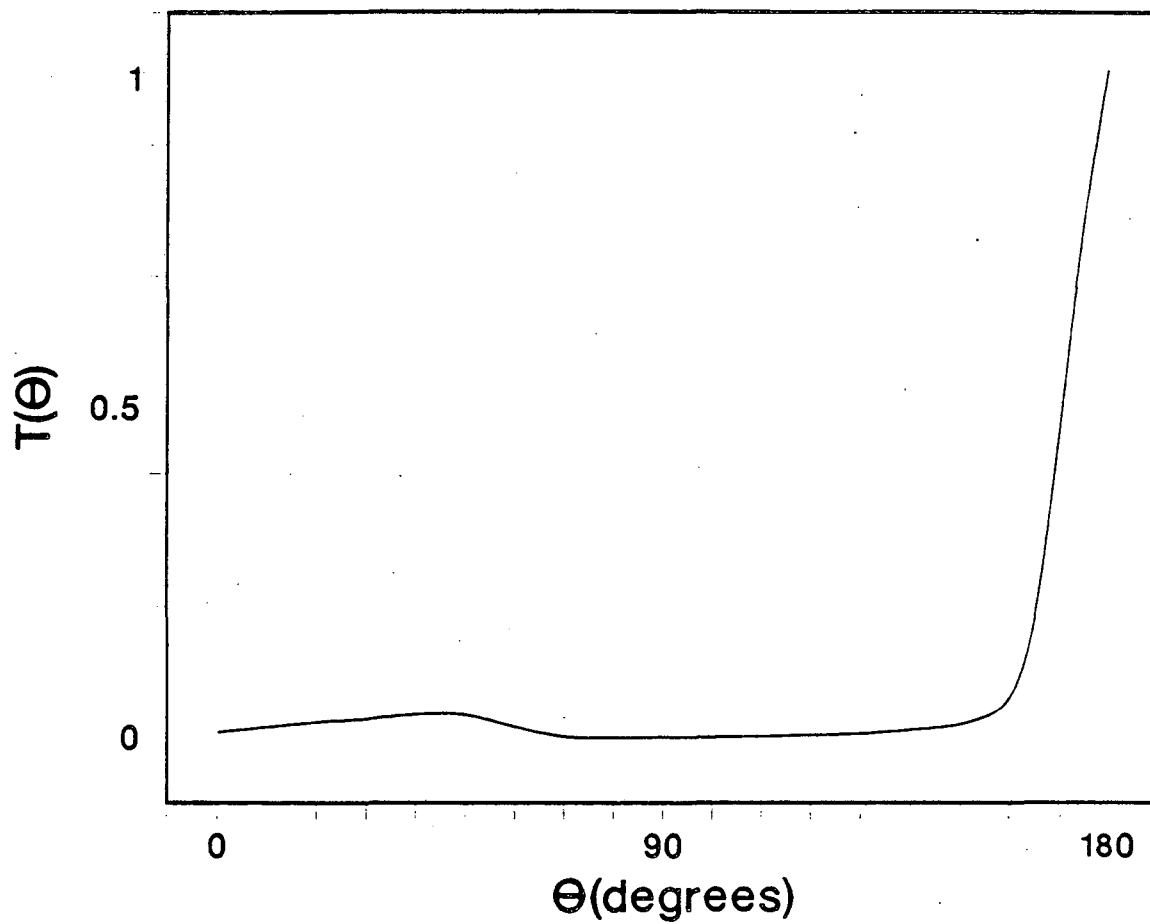
XBL 863-793

Fig. 25. The best fit to the time-of-flight distributions for $\text{Na}(4D) + \text{O}_2 \rightarrow \text{NaO} + \text{O}$ at a collision energy of 18 kcal/mole for the angles shown. The solid lines show the fit to the data.



XBL 863-822

Fig. 26. Center-of-mass product translational energy distribution for $\text{Na}(4D) + \text{O}_2 \rightarrow \text{NaO} + \text{O}$ at a collision energy of 18 kcal/mole.



XBL 863-792

Fig. 27. Center-of-mass scattering angular distribution for $\text{Na}(4D) + \text{O}_2 \rightarrow \text{NaO} + \text{O}$ at a collision energy of 18 kcal/mole.

that the center-of-mass product scattering distributions do not change as a function of collision energy. In the threshold region, these might be expected to change dramatically.

By determining the time at which the subsequent peaks occur in the time-of-flight distributions, it can be deduced at what point in the detector the species is ionized. In fact only the final peak, the one for which only the doorknob (ion target) and photomultiplier need be on, is readily interpretable. The others have unknown ion flight times, whereas the ions responsible for the final peak must be produced in the region of the doorknob, after which their ion flight time should be negligible. By calculating the peak velocities from the main peaks in each of the time-of-flight distributions for the 18 kcal/mole collision energy (figure 14), and from the positions of the final peaks, it is possible to calculate the flight length of the neutral. From the modulation point, the interaction region, to the detection point is a distance of 54 ± 3 cm. This is derived from the peak separations of 19-21 channels of 10 μ sec duration, the peak of the detected product velocities of $1.4-1.7 \times 10^5$ cm/sec, and the ion flight time of (electron bombardment ionization produced) Na^+ , ~ 14 μ sec. This corresponds to the distance from the collision region to the front half of the region between the doorknob and the photomultiplier. Due to the high voltage of the doorknob (-30 kV), the electric field in this region is approximately 10 kV/cm. This would have a minimal effect on the NaO energy, Stark shifting the energy levels less than 2 cm^{-1} .

The back of the detector is approximately 60 cm. from the interaction region, and the ionization does not appear to be occurring there.

Since only signal at $m/q=23$ (Na^+) has been shown to be due to electron bombardment ionization, it is necessary to address the question of whether some species other than NaO could be responsible for the signal observed. Since Na^+ is observed after ionization, the signal-producing species must contain Na. The non-electron bombardment ionization signal does not come from ground state Na atoms, since Na atoms at comparable velocities are produced in these and other experiments, and no similar signal is observed. Na atoms in low-lying excited levels have such short radiative lifetimes (tens of nsec, see chapter I) as to all radiatively decay before reaching the detector. Since the observed products do not occur at the center-of-mass, they are not a NaO_2 complex that lives long enough to make it into the detector. The placement of the products and the intentional destruction of dimers and clusters in the expansions negates the possibility that these could lead to the signal observed. Could metastable Na atoms be responsible for the signal? High Rydberg states of Na do have lifetimes sufficient to survive the transit through the detector to be field ionized. This possibility could be substantiated or eliminated by observing the complementary product O or O_2 , however all attempts to do this were frustrated by the large detector background at these masses ($m/q=16$ and 32), and the fact that the O_2 beam puts a constant load on the detector at these masses.

If the detected product is Na and not NaO, the fit of the center-of-mass angular and velocity distributions described above is still applicable, however the product translational energy distribution must be scaled by a factor related to the product reduced masses. The product translational energy in terms of the velocity of the detected product can be derived as:

$$E_T = \frac{1}{2} m_{\text{det}} u_{\text{det}}^2 \frac{m_{\text{det}} + m_{\text{undet}}}{m_{\text{undet}}}, \quad (9)$$

where m_{det} and m_{undet} are the detected and undetected products, respectively, and u_{det} is the center-of-mass velocity of the detected product. This is derived from conservation of momentum; the momenta of the two products are equal and opposite in the center-of-mass so that not only the masses change, the velocities of the undetected product do also. The ratio of the energies for a given u_{det} is then:

$$\frac{E(\text{det}'=\text{Na})}{E(\text{det}=\text{NaO})} = \frac{m'_{\text{det}} m_{\text{undet}}}{m_{\text{det}} m'_{\text{undet}}}, \quad (10)$$

giving a conversion factor of 0.30 for the E_T distribution fitted for product NaO. Thus, instead of peaking at 0.6 kcal/mole for product NaO, assuming that the product is Na, the $P(E)$ peaks at 0.2 kcal/mole. From conservation of energy, this gives a mean total product internal energy of 116.7 kcal/mole, or 40820 cm^{-1} , for the 18.1 kcal/mole mean collision energy. Including the beam velocity spreads, enough energy exists to remove the Na electron. It should also be noted that all

the collision energies for which product was observed are well above the energy required for electron transfer, process (3).

The signal due to ionization near the doorknob is one-tenth the signal due to electron bombardment ionization (see figures 15 and 18). By the time the atoms reach the detector ionizer, no matter in what state they are produced, the majority of the Na atoms will have radiatively decayed into the ground state. Their detection efficiency can be determined from the filament emission current $I_e = 10 \text{ mA} = 6.2 \times 10^{16} \text{ e}^-/\text{cm}^2\text{-sec}$, and the ionization cross section of Na by 200 eV electrons, $\sigma = 2.46 \text{ \AA}^2$.¹⁹ The ionization rate is then $I_\sigma = 13 \text{ sec}^{-1}$. The atomic velocity is very nearly the velocity of the center-of-mass, $v_{\text{cm}} = 1.5 \times 10^5 \text{ cm/sec}$. The residence time in the 1 cm. long ionizer is $6.7 \times 10^{-4} \text{ sec}$, giving the detection efficiency via electron bombardment as 8.7×10^{-5} . It will be assumed that if metastable Rydberg atoms are the source of this signal, they are detected with unit efficiency via field ionization. Whether a significant fraction of Rydberg atoms can be field ionized depends upon their electronic state. Classically, the field required to ionize a Rydberg atom in state nL is:²²

$$E_c = 1/(16n^4) \text{ a.u.} \quad (11)$$

Thus a field of 10 kV/cm is required to ionize atoms with $n=15$.²² The threshold field strength varies dramatically with n . Since the intensity of the signal at the final peak is one-tenth that due to electron bombardment, the fraction of the metastable atoms that survive in their excited state to the region of the doorknob must be 9×10^{-6} .

This means that $-\ln(9 \times 10^{-6}) = 11.6$ or fewer lifetimes of the metastable have passed during the transit from the collision region to the back of the detector. The measured flight times to the final peaks were typically 340 μsec . The lifetime is then at least $340 \mu\text{sec} / 11.6 = 29 \mu\text{sec}$. The assumption of unit detection efficiency is not correct. The detector geometry is optimized to detect ions that have been accelerated through the quadrupole mass spectrometer, and designed to hit the center of the ion target. If an atom is field ionized it will not necessarily go to the center of the doorknob, and the secondary electrons will not necessarily go to the relatively small sensitive area of the scintillator/photomultiplier. It is not possible to estimate the detection efficiency. This requires that the lifetime be longer than the estimate given above.

If essentially all the available product internal energy goes into excitation of the sodium atoms, the first three levels listed in table III are accessible at the mean collision energy. Of these, only the nP states have lifetimes close to those predicted by the above arguments. Whatever fraction of the atoms might be produced in states other than nP (at this energy) will not be detected by field ionization, since they would not survive the transit to the detector, and this will lower the observed fraction of signal that could be due to field ionization. However, all states up to the ionization limit are accessible to the high velocity components of the beams. Since the Rydberg state lifetimes vary as n^3 ,²² nS, nD, and nF Rydberg levels have lifetimes sufficient to survive the transit to the doorknob for $n \sim 22$

Table III. Relevant Na atomic energy levels²⁰ of Na and their lifetimes.²¹

<u>State</u>	<u>Energy (cm⁻¹)</u>	<u>Lifetime (μsec)</u>
14 ² S	40769.5	2.8
14 ² P	40814.5	22, 27 (J=1/2, 3/2)
13 ² D	40798.8	2.1
15 ² S	-40870	3.5
15 ² P	40901.1	28, 34 (J=1/2, 3/2)
14 ² D	40890.0	2.6

Table IV. Relevant Na atomic energy levels²⁰ and their lifetimes.²¹

<u>State</u>	<u>Energy (cm⁻¹)</u>	<u>Lifetime (μsec)</u>
10 ² S	39983.0	0.88
9 ² P	39795.	5.1
9 ² D	40091.	0.68
9 ² F	40093.	0.77

and above. Additionally, peaks are observed in the TOF spectra too early for field ionization in the doorknob region, and are unrelated to the electron bombardment. The strongest field before the doorknob is that of the quadrupole mass spectrometer, where the electric field is at most 2 kV/cm for standard operating conditions. This also requires that higher Na levels are produced if they are to explain the detector off signal. For field ionization by 2 kV/cm, n must be greater than about 22 (see (11)). All these levels are possible to excite, but require higher beam velocities.

A number of observations contradict the possibility that the observed signal is due to Rydberg atoms. First, the threshold is inconsistent with Rydberg atom formation, since the detector off signal occurs even at threshold collision energies. At 16 kcal/mole collision energy, the highest excitable Rydberg levels are those shown in table IV. With a 5.1 μ sec lifetime, the Na(9^2P) states could not possibly survive the transit to the detector, not to mention to the back of the detector. With a shorter than expected flight time to the ionizer of 130 μ sec, $130/5.1=25$ lifetimes would pass, and only $e^{-25}=10^{-11}$ of the Rydberg atoms produced would retain their excitation, an undetectably small fraction. Secondly, a detector off signal due to Rydberg atoms would be extremely sensitive to product flight time, and thus to laboratory velocity. The detector on and off distributions would be very different with a strong weighting for observing high laboratory velocities. This is not seen. Thirdly, at a collision energy of 18 kcal/mole, it is necessary to assume that all the internal energy goes

into the Na atoms. If this were true at a collision energy of 22 kcal/mole, the Na atoms would be ionized, whereas similar center-of-mass distributions are observed. It is then necessary to invoke an increasing O_2 internal excitation to exactly compensate for the increasing collision energy.

Thus, while the detector off signal cannot be adequately explained, Rydberg atom production is not consistent with the experimental observations. One possible process that could give such a signal is surface ionization of the very internally excited NaO. It is possible that each surface on which the NaO impinges gives some ion counts. There is no surface 54 cm. from the modulation position, however, for which the final peak is observed. This peak is thus left unexplained. The back of the detector which presumably would also lead to surface ionization is 60 cm. away from the modulation point.

As discussed in chapter II, the absolute reactive cross section can be determined by calibrating the reactive scattering with the small angle elastic scattering. This is done by estimating the absolute differential elastic cross sections due to the van der Waals attraction, and estimating the relative detection efficiencies of the reactively scattered molecules and the elastically scattered atoms.

The Slater-Kirkwood approximation can be used to estimate the van der Waals attraction,²³ as shown in chapter II. The polarizability of O_2 in the gas phase has been calculated to be $\alpha(O_2)=1.57 \text{ \AA}^3$.²⁴ The effective number of electrons of O_2 is $N(O_2)=12$. All the

values for Na remain the same as those used in chapter II. Using the Slater-Kirkwood approximation -- equation (10) of chapter II -- yields $C_{6,disp} = 2620 \text{ kcal/mole } \text{\AA}^6$. Since O_2 is a homonuclear diatomic molecule, its electric dipole moment is zero, and there is no inductive contribution to the C_6 constant. Equation (8) of chapter II gives the approximate classical small angle elastic scattering of a van der Waals potential. This is used to calculate the absolute differential cross sections for small angle elastic scattering for comparison with the small laboratory angle signal due to the elastic scattering shown in figure 8. As in chapter II, the center-of-mass angular distribution is determined for only the peak of the beam velocities while distributions of beam velocities are used in the transformation from the center-of-mass frame to the laboratory frame distributions and for the elastic recoil energy.

The ionization cross section of Na atoms by 200 eV electrons is known, $\sigma_{ion}(Na) = 2.46 \text{ \AA}^2$.¹⁹ The ionization cross section of NaO can be estimated from the ionization cross section of O_2 , and the ratio of the polarizabilities of O_2 and NaO.²⁵ The molecular polarizability of O_2 is $\alpha(O_2) = 1.57 \text{ \AA}^3$.²⁴ The molecular polarizability of NaO is approximately the sum of the polarizabilities of Na^+ and O^- .^{4,26} These are $\alpha(Na^+) = 0.155 \text{ \AA}^3$, and $\alpha(O^-) = 2.85 \text{ \AA}^3$,²⁷ giving the polarizability of NaO as $\alpha(NaO) = 3.0 \text{ \AA}^3$. Since the ionization cross section of O_2 by 200 eV electrons is 2.7 \AA^2 ,²⁸ the ionization cross section of NaO should be approximately $\sigma_{ion}(NaO) = 5.2 \text{ \AA}^2$. Since no signal was observed at $m/q=39$ (NaO^+), it is assumed that all

NaO ionized fragments to $\text{Na}^+ + \text{O} + \text{e}^-$, and thus that the ionization cross section of NaO is the same as the ionization cross section of NaO to Na^+ . Neglecting those molecules not ionized by electron bombardment (which were found to contribute only a small fraction of the signal provided the detector was on), the relative detection efficiency (see equation (14) of chapter II) of NaO/Na is 2.1. Using the small angle elastic scattering, and assuming that the product is indeed NaO, gives the total reactive scattering cross section as $\sigma_R = 0.9 \text{ \AA}^2$ at a collision energy of 18 kcal/mole. If Rydberg atoms are formed, doing the same calibration as discussed earlier in this section gives the total cross section for their production as $\sigma = 2.2 \text{ \AA}^2$.

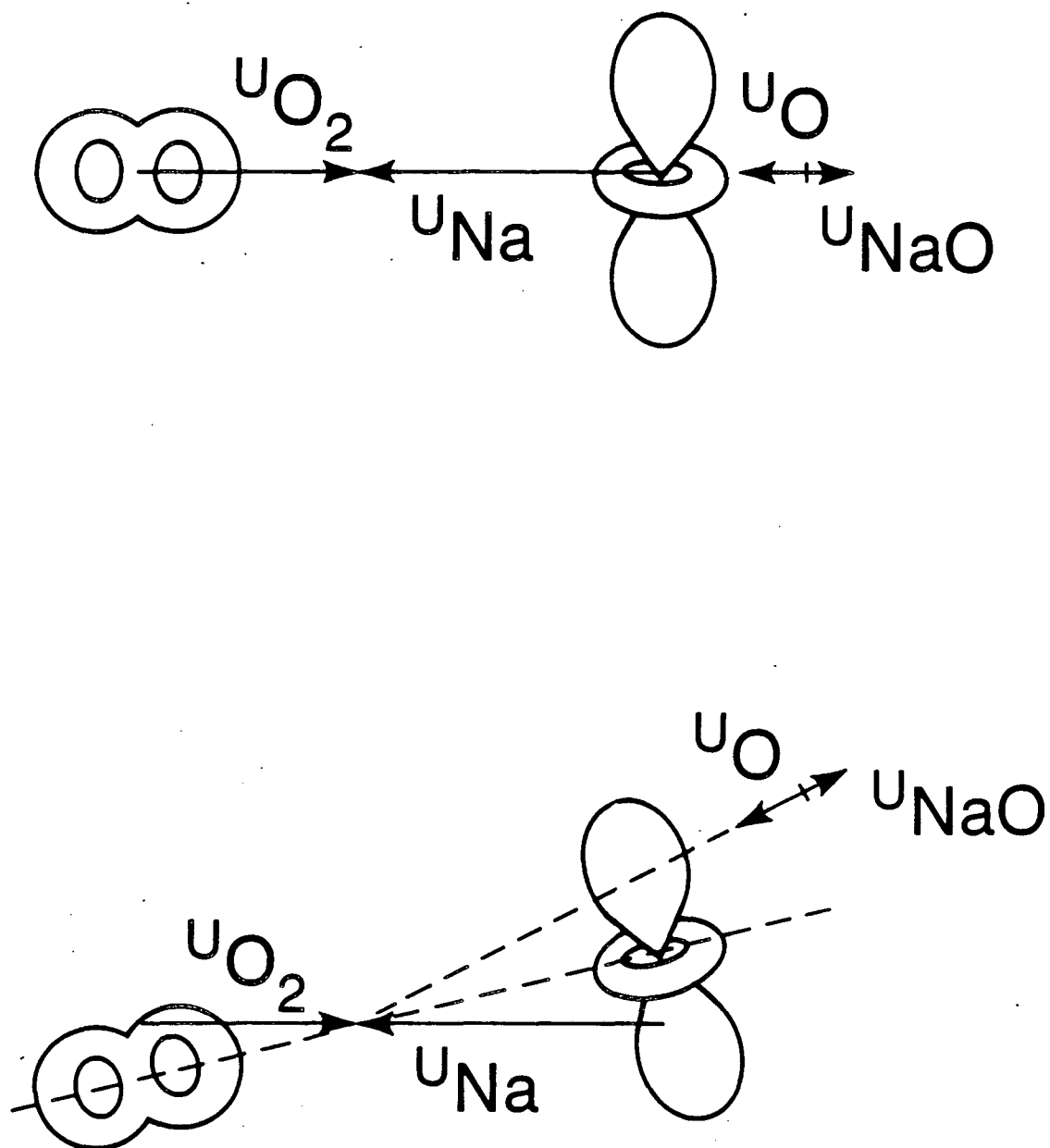
D. Discussion

Of course, the most spectacular feature of these measurements is the state-selectivity observed for the production of NaO + O. Because only the Na(4^2D) state reacts, and the Na(5^2S) state does not, and since both states are known to radiatively populate the Na($3\text{S}, 3\text{P}, 4\text{S}, 4\text{P}$) states,²⁹ it is clear that these states also do not react to produce NaO.

The strong back scattering of the NaO product with respect to the incoming Na atoms is evidence of a direct (i.e. no long-lived collision complex is formed), collinear reaction. The especially narrow NaO center-of-mass angular range points up the exceptionally restrictive

constraints on the impact parameter and relative orientation required for reaction to proceed. This requirement of very small impact parameters leading to reactive products puts an upper limit of a few \AA^2 on the reactive cross section, which is borne out in the estimated reactive cross section.

The polarization dependences show that the reaction mechanism is completely different than that observed for $\text{Na}(4D) + \text{HCl}$ in chapter II. The favored polarization for reaction (ϕ_{CM}) decreases with increasing laboratory detector angle. Since the reaction product is so strongly backwards peaked, the reaction must proceed directly, so that there is a correspondence between laboratory and center-of-mass scattering angles. The smaller the laboratory scattering angle, the smaller the average center-of-mass scattering angle. The favored polarization for reaction appears to stay nearly perpendicular to the Na-O-O axis as shown in figure 28. This could have one or both of the following origins. First, the symmetry chosen by this favored orbital alignment is the least favorable for long range electron transfer (i.e. the opposite of that observed in chapter II). Secondly, this could be the required transition state symmetry for reaction. An interaction between the $\text{Na}(4d)$ orbital and the half empty π^* antibonding orbitals could lead to a collinear ($C_{\infty v}$) transition state of Δ symmetry which would be inaccessible to $\text{Na}(nS, nP)$ states (see table I), and would be capable of producing a NaO molecule with π or Δ symmetry.



XBL 8511-11568

Fig. 28. Higher impact parameters lead to scattering to smaller center-of-mass angles. The required geometry for reaction has the Na-O-O collinear, so that with increasing impact parameter, the Na-O-O axis must be tilted with respect to the relative velocity vector. The Na($4d_{z^2}$) orbital remains perpendicular to the Na-O-O axis as shown.

The back scattering also shows that the reaction does not proceed via long range electron transfer. The outermost neutral-ionic potential energy curve crossing, using values of 0.854 eV for the ionization potential of the Na(4D) level (this is just the difference between the ionization potential of sodium, 5.138 eV, and the excitation energy of the Na(4D) level, 4.284 eV), and 0.44 eV for the adiabatic electron affinity of O_2 , occurs at $r_c = 35 \text{ \AA}$. This is too far out for any significant interaction of the potential curves, and no electron transfer is expected at this long range. A second reason that this mechanism is not responsible for reaction is that in long range electron transfer there would be no discrimination between excited sodium levels of different symmetries (see table I). Thus, the Na(5S) level would have nearly the same cross section as the Na(4D) level. This is clearly not the case. A third reason is that long range electron transfer would likely lead to formation of a long-lived collision complex which is not observed for the reactively scattered NaO. It is not surprising that a long-lived complex does not lead to NaO formation, since a complex would statistically be most likely to decay to low energy products, in this case quenched Na atoms.

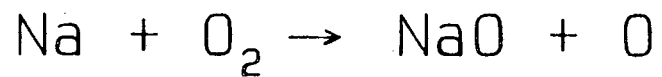
The very narrow product translational energy distribution in figure 26 shows that very little of the excess energy of this reaction goes into translation. How then is the energy distributed among the various forms of internal energy of the products? Since low impact parameter collisions lead to reaction directly, it is unlikely that a significant amount of energy is carried away in rotation. This leaves

electronic excitation of NaO and/or O, and vibrational excitation of the NaO molecule. Figure 29 is a diabatic correlation diagram which shows the relative energies of the reactants and products in the outermost columns. The only accessible electronically excited O atom level is $O(^1D)$, 1.98 eV above the ground state. Only the $NaO(X^2\Pi, A^2\Sigma^+)$ levels are shown since these are the only known levels, although many other levels must exist in the first 3 eV above the ground state. Thus, reaction to electronically and/or vibrationally excited NaO is likely to be responsible for the signal observed, but not enough of the spectroscopy is known to determine what state is produced. It is unlikely that very specific, very high vibrational levels of NaO could be produced to give rise to such a narrow $P(E)$, so that one might expect that a large fraction of the internal energy is in the electronic excitation of the NaO molecule.

The lack of reaction at low collision energy implies a barrier in the entrance channel, which the translational energy is required to surmount.³⁰ The height of the barrier must be at least 15 ± 1 kcal/mole, as this was the observed threshold for reaction. That a barrier occurs on the particular surface leading to reaction is not terribly surprising considering the myriad of crossing potential surfaces in this region.

In fact, this lack of reaction at low collision energy also gives further evidence that long range electron transfer does not lead to reaction, as there would be no barrier for this process. An alternative explanation for the lack of reaction at low collision energy

Fig. 29. Diabatic correlation diagram for $\text{Na} + \text{O}_2$ in a collinear approach geometry for states of spin multiplicity 2. No attempt has been made to accurately portray the energies of any of the transition states with the exception of the lowest energy NaO_2 state calculated by M. Alexander in reference 4.



C_{∞v}

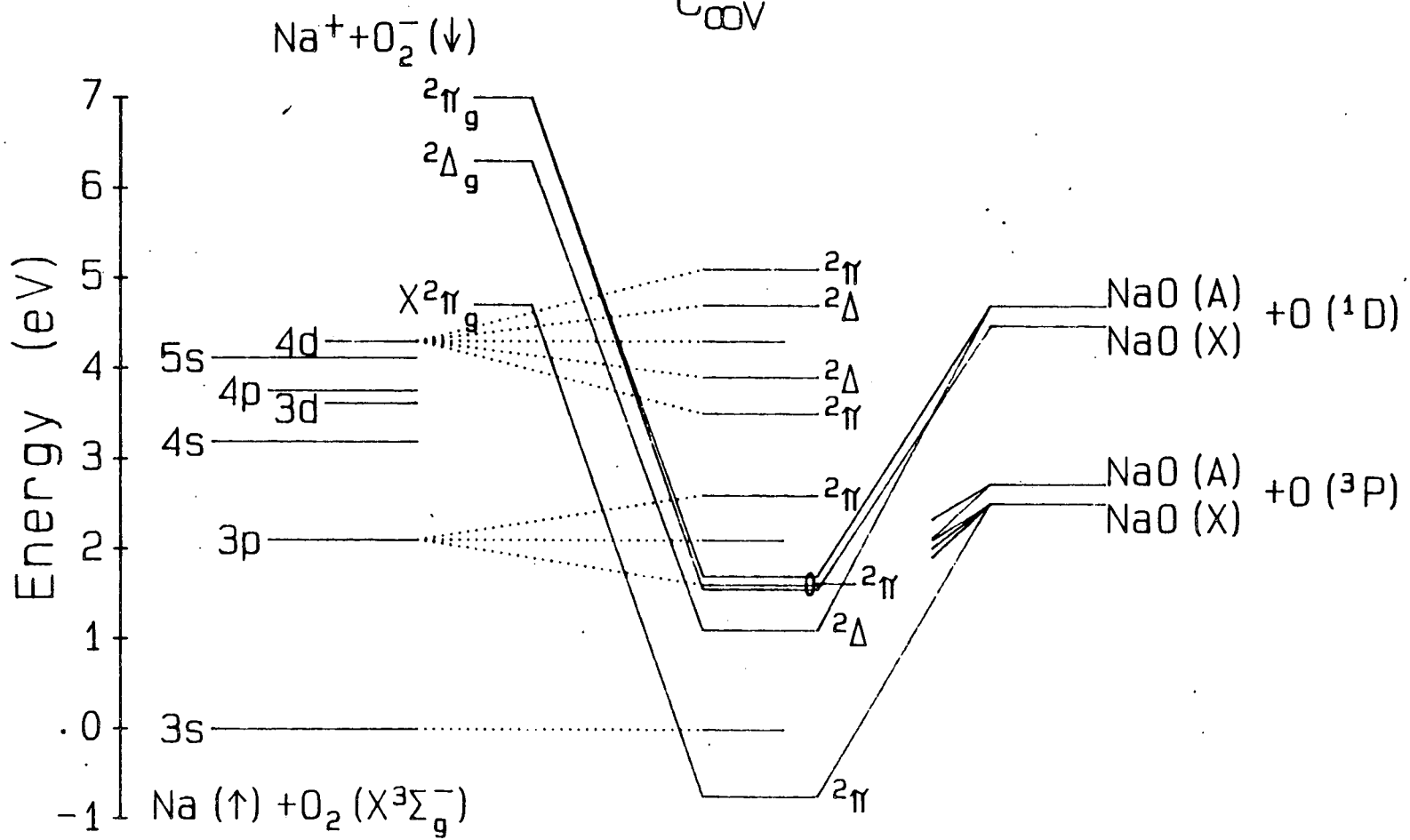


Fig. 29

XBL 863-826

would be that the slower the excited atom and the molecule come together, the more likely they are to proceed adiabatically, along the lowest potential energy surface. This would imply long range electron transfer occurs with higher efficiency at lower collision energy, and this does not lead to reaction. At higher collision energy, however, the system is more likely to proceed through the crossing region remaining on the same diabatic (covalent) surface.

Looking once again at the alternative explanation, it is conceivable that Rydberg atom formation takes place. If electron transfer has taken place, and the $\text{Na}^+ + \text{O}_2^-$ are separating after the collision, at large separation the electron on the O_2^- is in approximately the correct position for the Rydberg atom. That is, there is some overlap of the Rydberg orbital with the O_2^- orbitals. There are many crossings of the potential surfaces at these large separations, and it is conceivable that these could lead to some electron transfer back to the Na Rydberg levels. The very slow recoil (known from the $P(E)$) would help the Na- O_2 system follow adiabatic potentials back to neutral products. If this should occur with the cross section measured to be over 2 \AA^2 , it would be highly unusual to say the least.

E. Conclusions

There is strong circumstantial evidence pointing to the production of NaO, however no direct measurement was successful in definitively establishing this. The NaO is very internally excited, most likely to an excited electronic state. The production of NaO leaves some observations unexplained. An alternative explanation is that if Rydberg atoms are produced by the collisions, they are produced in very specific levels corresponding to a crossing far out in the exit channel. The level requirement comes from the need for a fraction of the excitation to survive to the back of the detector and to be field ionized by 2-10 kV/cm electric fields.

The $\text{Na} + \text{O}_2$ reaction most likely produces NaO when the Na(4D) level is excited, but not when the Na(3S,3P,4S,4P,5S) levels are. The translational threshold to reaction is 15 ± 1 kcal/mole, implying an entrance channel barrier of at least this magnitude. The reaction does not proceed via long range electron transfer, nor via complex formation, despite the favorable energetics of each. The NaO produced is very internally excited with less than 2% of the total available energy going into relative product translation. The neutral chemical reaction is only a minor product channel, with a reactive cross section at a collision energy of 18 kcal/mole of $\sigma_R = 0.9 \text{ \AA}^2$.

Clearly, further experiments are required to sort out the products of this reaction. Of particular interest would be to spectroscopically determine the neutral products and product states. It would also be interesting, and relatively simple, to see what the ionic products of the collisions are.

F. References

1. Calculated from D_0^0 values in reference 2.
2. K. P. Huber and G. Herzberg, Molecular Spectra and Molecular Structure, IV. Constants of Diatomic Molecules (Van Nostrand Reinhold, Co., New York, 1979).
3. see figure 9 of chapter I.
4. M. H. Alexander, J. Chem. Phys. 69, 3502 (1978).
5. L. Andrews, J. Phys. Chem. 73, 3922 (1969).
6. R. R. Smardzewski and L. Andrews, J. Chem. Phys. 57, 1327, (1972).
7. F. J. Adrian, E. L. Cochran, and V. A. Bowers, J. Chem. Phys. 59, 56 (1973).
8. P. A. G. O'Hare and A. C. Wahl, J. Chem. Phys. 56, 4516 (1972).
9. J. Pfeiffer and J. L. Gole, J. Chem. Phys. 80, 565 (1980).
10. J. L. Gole and P. A. Schulz, private communication (1985).
11. V. Kempter, W. Mecklenbrauck, M. Menzinger, Ch. Schlier, Chem. Phys. Lett. 11, 353 (1971).
12. V. Kempter, Adv. Chem. Phys. 30, 417 (1975).
13. R. H. Neynaber, B. F. Myers, and S. M. Trujillo, Phys. Rev. 180, 139 (1969).
14. A. W. Kleyn, Ph.D. Thesis, Stichting voor Fundamenteel Onderzoek der Materie, Amsterdam, The Netherlands (1982).
15. A. W. Kleyn, M. M. Hubers, and J. Los, Chem. Phys. 34, 55 (1978).

16. A. P. M. Baede, Adv. Chem. Phys. 30, 463 (1975), and references therein.
17. G. J. Schulz, Rev. Mod. Phys. 45, 423 (1973), and H. H. Michels and F. E. Harris, in Seventh International Conference on the Physics of Electronic and Atomic Collisions: Abstracts of Papers, Volume II, 1170 (North-Holland, Amsterdam, 1971).
18. E. W. Rothe, B. P. Mather, and G. P. Reck, Chem. Phys. Lett. 51, 71 (1977).
19. R. H. McFarland and J. D. Kinney, Phys. Rev. 137, A1058 (1965).
20. C. E. Moore, National Bureau of Standards (U. S.) Circ. 467 (1949).
21. C. E. Theodosiou, Phys. Rev. A 30, 2881 (1984).
22. S. A. Edelstein and T. F. Gallagher, Adv. At. Mol. Phys. 14, 365 (1978).
23. J. H. Birely, R. R. Herm, K. R. Wilson, and D. R. Herschbach, J. Chem. Phys. 47, 993 (1967).
24. S. Nir, S. Adams, and R. Rein, J. Chem. Phys. 59, 3341 (1973).
25. C. H. Becker, P. Casavecchia, P. W. Tiedemann, J. J. Valentini, and Y. T. Lee, J. Chem. Phys. 73, 2833 (1980).
26. J. O. Hirschfelder, C. F. Curtiss, and R. B. Bird, Molecular Theory of Gases and Liquids (John Wiley and Sons, Inc., New York, 1964).
27. J. Thorhallsson, C. Fisk, and S. Fraga, Theoret. Chim. Acta (Berl.) 10, 388 (1968).
28. S. C. Brown, Basic Data of Plasma Physics, 2nd Ed. (MIT Press, Cambridge, Massachusetts, 1967).

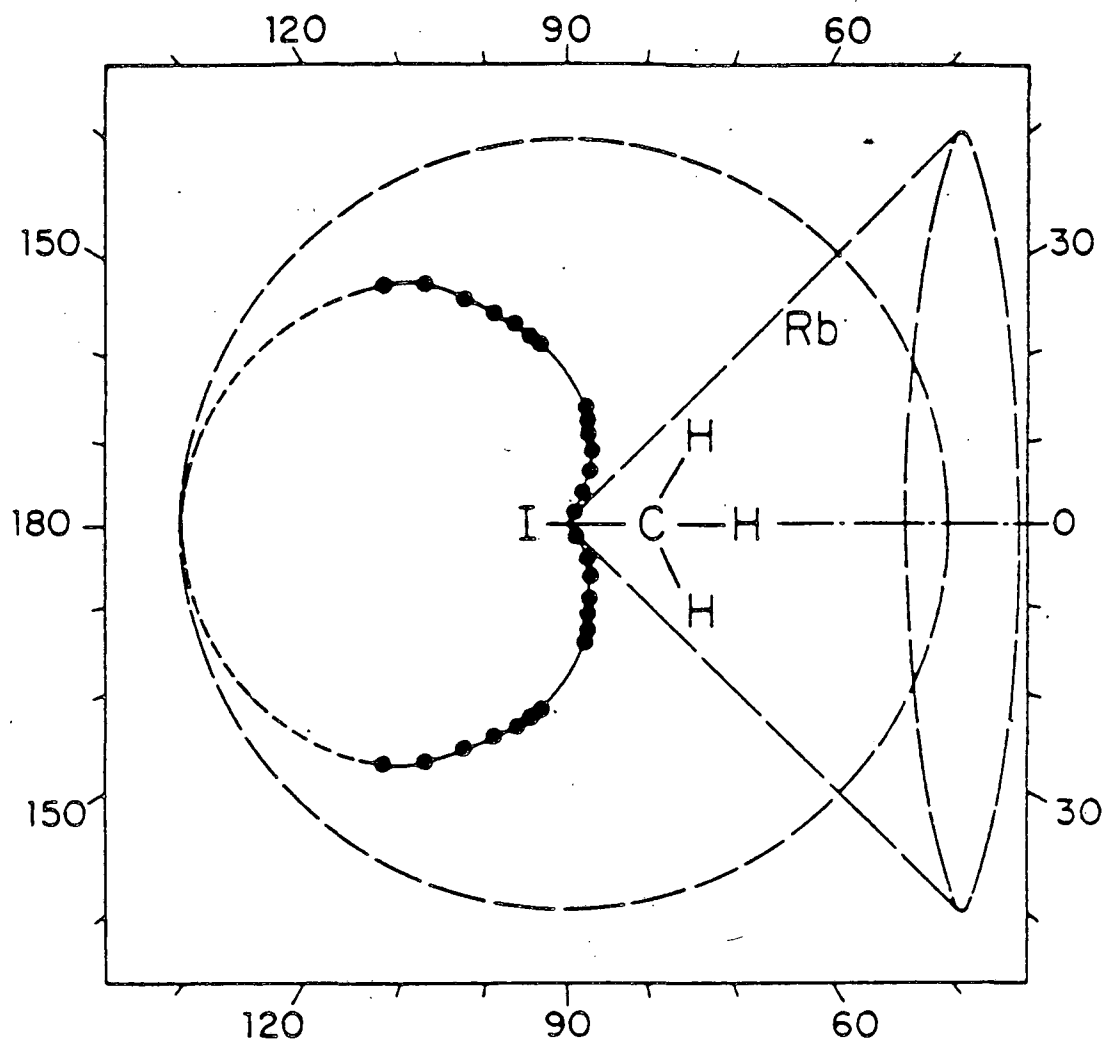
29. see Chapter I of this thesis, or G. Jamieson, W. Reiland, C. P. Schulz, H.-U. Tittes, and I. V. Hertel, J. Chem. Phys. 81, 5805 (1984).
30. A. M. G. Ding, L. J. Kirsch, D. S. Perry, and J. C. Polanyi, Faraday Disc. Chem. Soc. 55, 252 (1973).

IV. THE REACTIONS OF GROUND AND EXCITED STATE ALKALI ATOMS WITH METHYL HALIDE MOLECULES

A. Introduction

The reactions of alkali atoms (M) with methyl halide molecules (CH_3X) have been extensively studied for more than 50 years.¹⁻¹² The first crossed molecular beam experiment on $\text{K} + \text{CH}_3\text{I}$ revealed the rebound mechanism found in all subsequent experiments.² The elegant work of Bernstein and coworkers,⁴ and Brooks and coworkers⁵ in orienting methyl halide molecules in a molecular beam prior to reaction confirmed the steric effect earlier ascribed to the reaction. That is, for small impact parameter collisions if the alkali atom comes in at the halogen end of the molecule, then the reaction probability is unity, but if the alkali atom comes in at the methyl end of the molecule, then the reaction probability is zero.² Bernstein and coworkers have correlated this steric effect with a cardioid dependence of reaction probability on molecular orientation, as shown for $\text{Rb} + \text{CH}_3\text{I}$ in the polar plot in figure 1 (reproduced with permission from reference 4).

The result of this steric effect is a backwards peaked angular distribution (with respect to the incoming alkali atoms' direction). The farthest backwards scattered MX product (highest laboratory angle) corresponds to the most collinear C-X-M geometry. Lower C-X-M approach



XBL 852-1140

Fig. 1. The dependence of reaction probability on methyl iodide orientation in the reaction $\text{Rb} + \text{CH}_3\text{I}$ as measured by Parker et al. Reproduced with permission from reference 4.

angles (α) correspond to smaller center-of-mass scattering angles, and thus smaller laboratory scattering angles.

The mechanism for this reaction has an electron transferring from the alkali atom to the methyl halide molecule. This electron goes into the lowest unoccupied molecular orbital which is an antibonding orbital of the C-X bond (σ^* in diatomic terms) which causes the rupture of this bond. It was for the reaction of alkali atoms with halogen and alkali halide molecules that Kuntz, Mok, and Polanyi originally proposed the "Direct Interaction with Product Repulsion" (DIPR) model.¹³ In this model only two interactions are taken into account; these are: $[\text{CH}_3\text{-X}]^-$, and $\text{M}^+\text{-X}^-$. Furthermore, the DIPR model uses a fixed repulsive energy release R_0 to determine the translational energy release in the reaction.

The ideas in this model were extended by Harris and Herschbach to explain the dynamics of these alkali + methyl halide reactions more quantitatively.^{3,14} Their work assumes a distribution of product energies as in photodissociation of the halogen containing molecule, thus the acronym DIPR-DIP -- "Direct Interaction with Product Repulsion - Distributed as In Photodissociation." This assumption is based on the fact that the molecular orbital configuration of CH_3X in the united atom (diatomic-like) approximation is:

$$\dots (\sigma_g)^2 (\pi_u)^4 (\pi_g^*)^4 (\sigma_u^*)^0. \quad (1)$$

The π_g^* orbital is weakly antibonding, and the σ_u^* orbital is strongly antibonding with a node between the C and X atoms. The first

excited molecular orbital configuration, and the one that leads to photodissociation is then:

$$\dots (\sigma_g)^2 (\pi_u)^4 (\pi_g^*)^3 (\sigma_u^*)^1. \quad (2)$$

This is very similar to the ground state CH_3X^- molecular orbital configuration:

$$\dots (\sigma_g)^2 (\pi_u)^4 (\pi_g^*)^4 (\sigma_u^*)^1, \quad (3)$$

the only difference being the extra electron in the π_g^* orbital which makes little contribution to $\text{CH}_3\text{-X}$ potential. Harris and Herschbach have concluded that the potential curves for CH_3X^* and CH_3X^- have very similar shapes and in particular similar slopes on their repulsive walls.

The DIPR-DIP model predicts very little variation of product angular and momentum distributions with changing mass combinations and alkali ionization potential. This was borne out in the crossed molecular beams experimental data on the reactions of various alkali atoms with a number of alkyl monoiodides.^{3,12} A relatively large change in product angular distributions is predicted with varying geometric reaction probability. That is, as different collision geometries lead to reaction, the product angular distributions change substantially. This is expected from such an impulsive model.

Of the methyl monohalides, only the reactions of alkali atoms with CH_3I and CH_3Br have been studied in crossed molecular beams.¹² The reactions of all of the alkalis with CH_3I have been studied.¹² Many reactions of alkali atoms with alkyl polyhalides have also been

studied in crossed beams, but these follow stripping mechanisms of the type described in the following chapter, and will not be discussed here. All the reactions of alkali atoms with alkyl monohalides studied follow the rebound mechanism described above.^{3,12}

Bernstein and coworkers have measured the dependence of the reactive cross sections (σ_R) of:



as a function of collision energy.^{6,8} They estimate that their values of the absolute cross sections are good to within a factor of two, but their relative values are good to 15%.^{6,8} The cross section of process (4) peaks at $\sigma_R = 35 \text{ \AA}^2$ at 4 kcal/mole and drops to 1/3 of its peak value by 20 kcal/mole collision energy.⁶ The cross section of process (5) drops steadily from $\sigma_R = 23 \text{ \AA}^2$ at 3 kcal/mole, falling to 40% of its low energy value at 20 kcal/mole collision energy.⁸

Goldbaum and Martin have measured the reactive cross section for:



to be $\sigma_R = 3 \text{ \AA}^2$ by comparing it to the 35 \AA^2 cross section for process (4).¹⁰

In process (5), with increasing collision energy, the RbI product is scattered less backwards (relative to the motion of the incoming alkali atom) in the center-of-mass frame, and actually peaks at angles lower than 180° for collision energies of 22 and 36 kcal/mole.⁹ The product recoil energies increases approximately linearly with collision energy.⁹ This behavior of the product recoil energy is also observed

for $K + CH_3I$.^{7,11} The increased product translational energy with increasing reactant translational energy is explained in terms of being able to run up higher on the repulsive walls of a potential surface, acquiring more potential energy than possible for lower collision energies, and then having a release of this energy into product translation.¹⁵ This can also explain the center-of-mass angular distributions to some extent. The release of the more repulsive geometries accessible only to the higher collision energies allows scattering to wider angles than those seen at lower collision energies.

Polanyi's diffusion flame studies showed that for $Na + CH_3X$ the reaction cross sections increase by several orders of magnitude as X is changed through the sequence F, Cl, Br, I .¹ Recent measurements of thermal energy rate constants for $Na + CH_3F, CH_3Cl, CH_3Br$ concur with this strong trend in the reactivity.¹⁶

B. Results

The reaction:



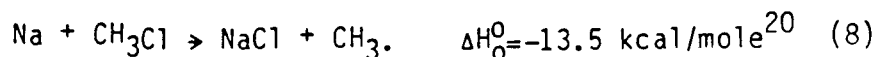
was studied at a collision energy of 21 kcal/mole in the apparatus described in chapter I. This corresponds to seeding the sodium atoms in helium, and running a neat supersonic molecular beam of $\dot{C}H_3Br$. A Newton velocity vector diagram for these conditions is shown in figure

2. The angular distributions recorded for $\text{Na}(3\text{S},3\text{P},4\text{D}) + \text{CH}_3\text{Br}$ are shown in figure 3. The statistics for this data are very poor, but these distributions took 72 hours to record, so that a brute force attempt to improve their quality would not be fruitful. The data shows qualitatively similar angular distributions for the reactions of each of the three Na levels. The only difference between the distributions due to the $\text{Na}(3\text{S})$ and $\text{Na}(3\text{P})$ states appears to be on the low angle side of the reactive peak. This difference is more pronounced for the reactive scattering of the $\text{Na}(4\text{D})$ atoms.

Before the second laser became available, this region of the angular distribution for $\text{Na}(3\text{S},3\text{P}) + \text{CH}_3\text{Br}$ was expanded over the useful angular range of the detector by seeding the CH_3Br in helium, as shown in the Newton diagram in figure 4 (note that the collision energy is increased to 25 kcal/mole). The NaBr product angular distribution (or more accurately -- partial angular distribution) obtained is shown in figure 5. The same behavior is exhibited in that the distribution of the $\text{Na}(3\text{P}) + \text{CH}_3\text{Br}$ remains higher than the distribution for $\text{Na}(3\text{S}) + \text{CH}_3\text{Br}$ in this region.

The statistics were too poor for this experiment to allow the measurement of time-of-flight or polarization dependences. These would certainly be of interest.

Against unfavorable kinematics and the reduced reaction probability,^{1,10,16} an attempt was made to measure the differential cross section of:



$$E_{\text{coll}} = 21 \text{ kcal/mole}$$

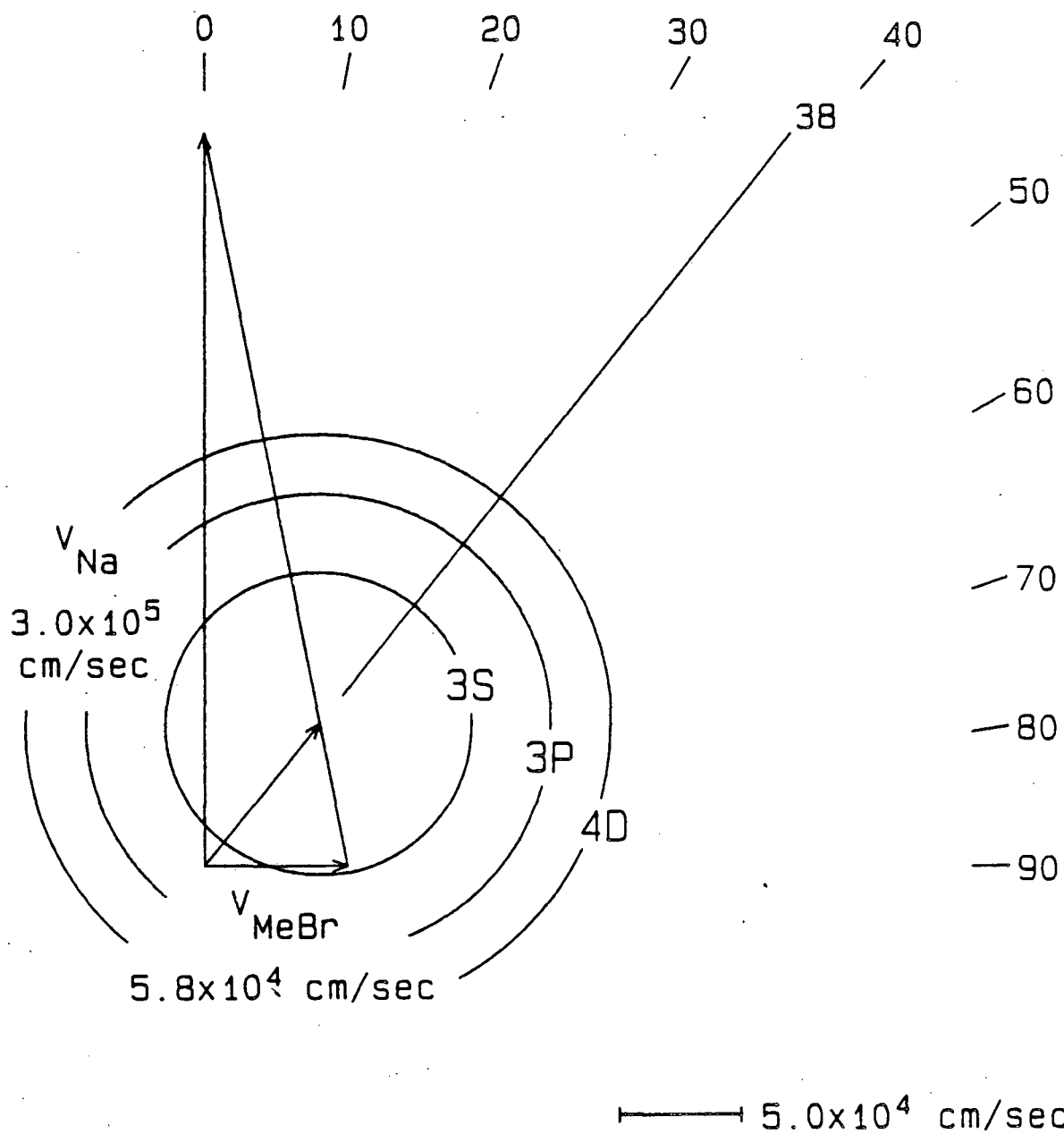
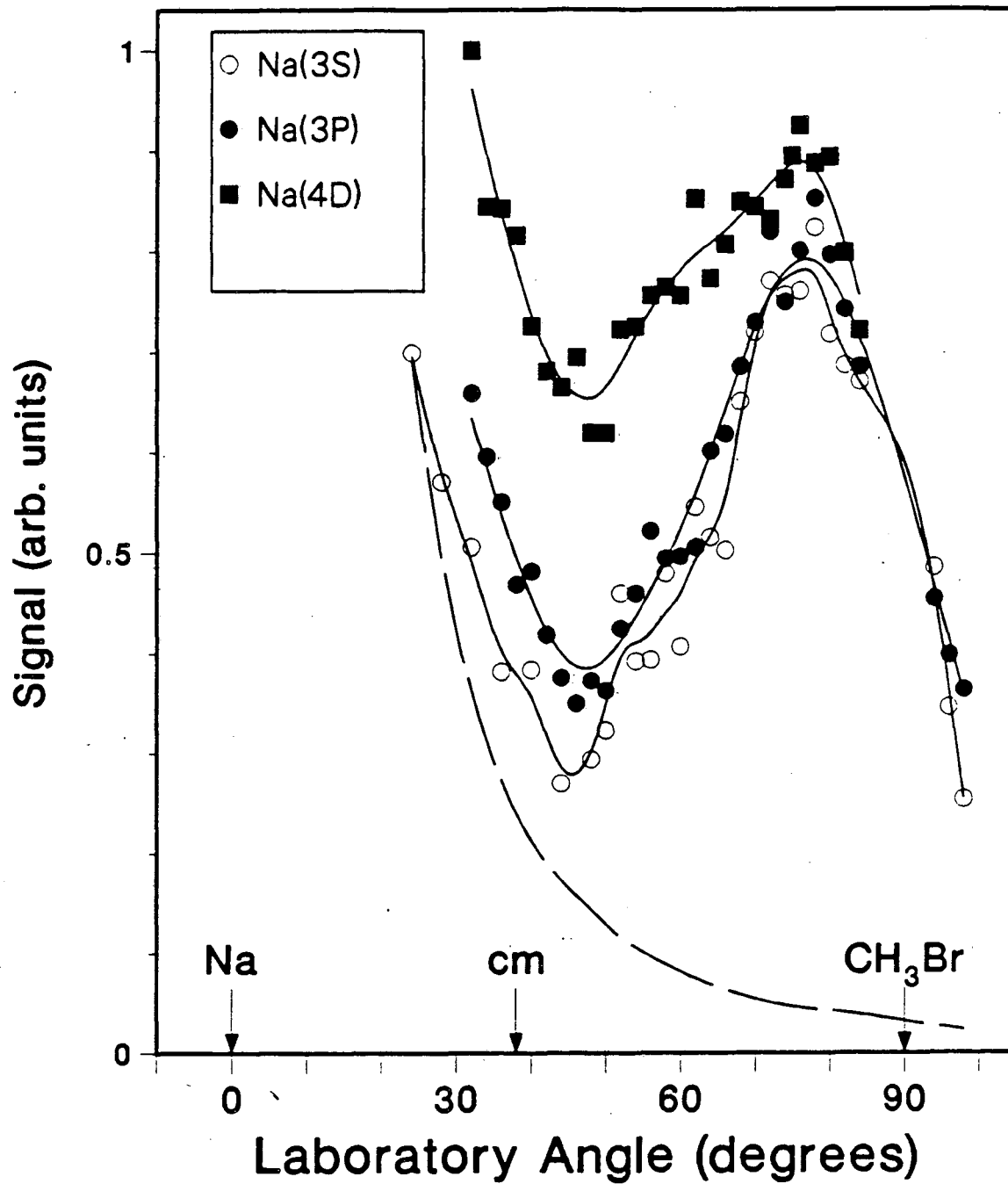


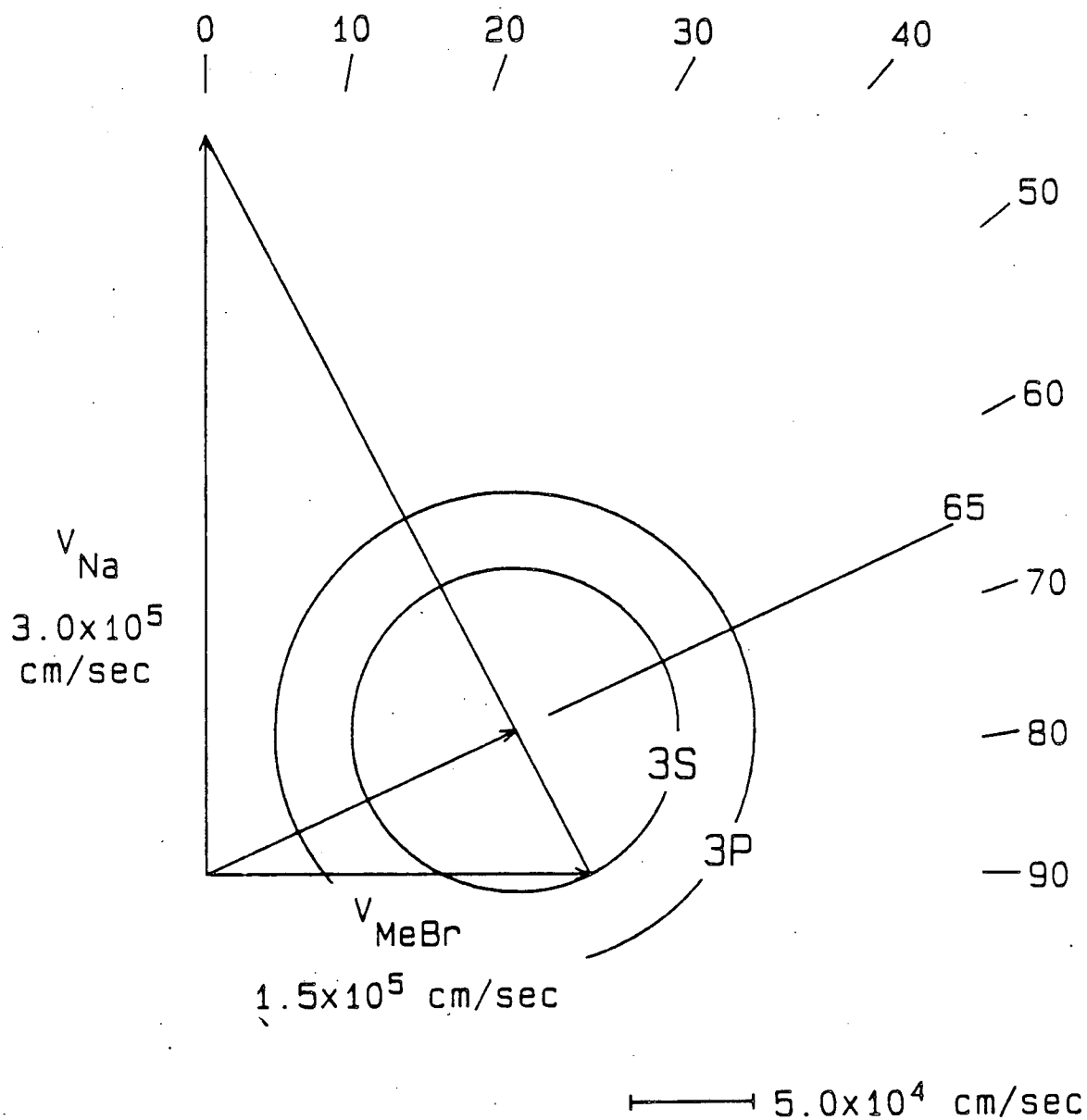
Fig. 2. Newton velocity vector diagram for $\text{Na}(3\text{S}, 3\text{P}, 4\text{D}) + \text{CH}_3\text{Br} \rightarrow \text{NaBr} + \text{CH}_3$ at a collision energy of 21 kcal/mole.

XBL 863-852



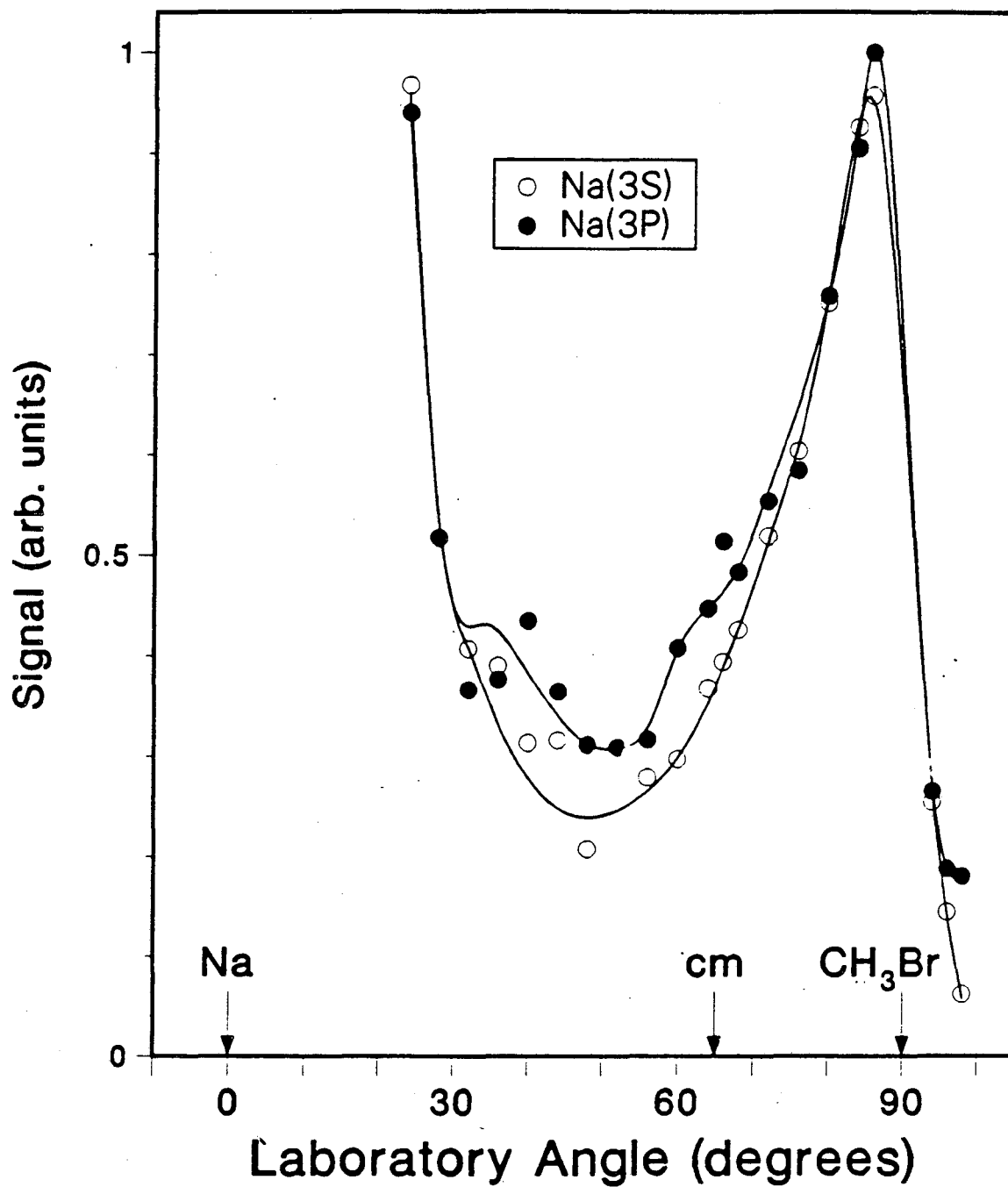
XBL 863-874

Fig. 3. NaBr product angular distributions for Na(3S,3P,4D) + CH₃Br at a collision energy of 21 kcal/mole.

$E_{\text{coll}} = 25 \text{ kcal/mole}$ 

XBL 863-854

Fig. 4. Newton velocity vector diagram for $\text{Na}(3\text{S}, 3\text{P}) + \text{CH}_3\text{Br} \rightarrow \text{NaBr} + \text{CH}_3$ at a collision energy of 25 kcal/mole.



XBL 863-873

Fig. 5. NaBr product angular distributions for Na(3S,3P) + CH₃Br at a collision energy of 25 kcal/mole.

Although some reactive scattering signal was observed, it was not possible to measure a laboratory angular distribution. A further complication was that the signal at $m/q=23$ (Na^+) appeared to be contaminated by elastically scattered CH_3Cl and modulated background at $m/q=23.5-25$ ($\text{CH}_0\text{-}_3\text{Cl}^{++}$) due to fragmentation of CH_3Cl in the electron bombardment ionizer. The $m/q=58$ (NaCl^+) signal was too small to measure.

C. Analysis of Experimental Results

As in the previous chapters the data was fitted using the program GM, a derivative of CMLAB,²² as described in chapter I. Independent product center-of-mass angular and recoil energy distributions were assumed, and a laboratory angular distribution was calculated. Ordinarily this would be extremely difficult to do in the absence of product velocity (e.g. time-of-flight) measurements, however due to sharp back scattering the transformation from the center-of-mass frame to the laboratory frame is nearly one-to-one.

Due to the poor statistics in the angular distributions, and to the similarities between the angular distributions for the different states, rather than try to subtract the already noisy distributions, the raw data shown in figure 3 was used to represent the data for each level excited. This has the effect of underestimating the differences in the scattering of the different states, but should still be able to

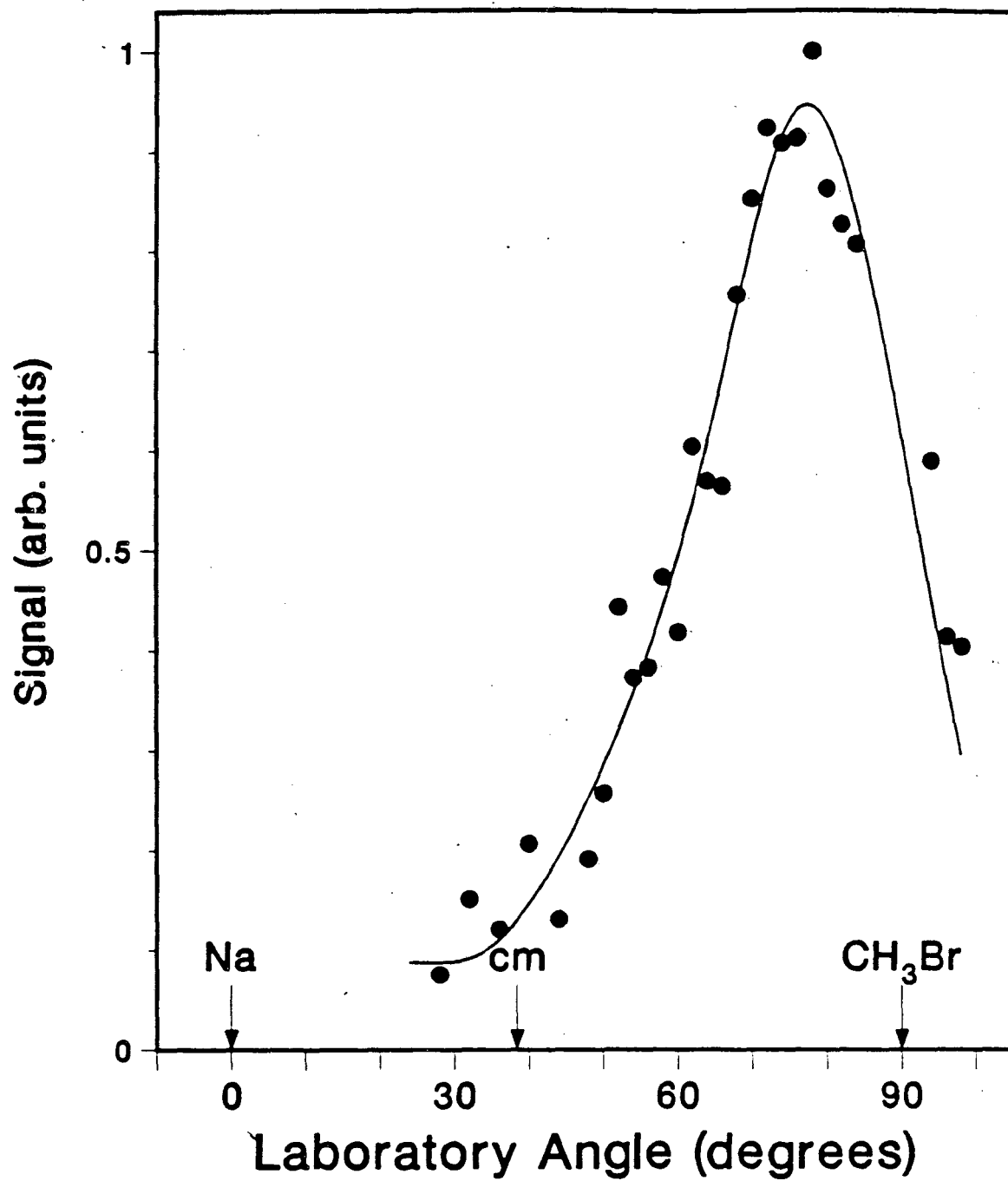
Table I. A summary of features of the center-of-mass distributions fitted to the laboratory angular distributions for Na + CH₃Br at a collision energy of 21 kcal/mole.

<u>Na Level</u>	<u>FWHM of T(θ)</u>	<u>% Backward Scattered</u>	<u>Peak Recoil Energy</u>	<u>$\sigma(nL)/\sigma(3S)$</u>
3S	73°	84%	33 kcal/mole	1
3P	74°	84%	33 kcal/mole	1.6
4D	83°	79%	33 kcal/mole	2.8

point out the trends in the reactivity. Elastic scattering was estimated using the small angle elastic scattering formula given in chapter II, and the C_6 constants estimated below. The signal subtracted away is shown as the dashed lines in figure 3.

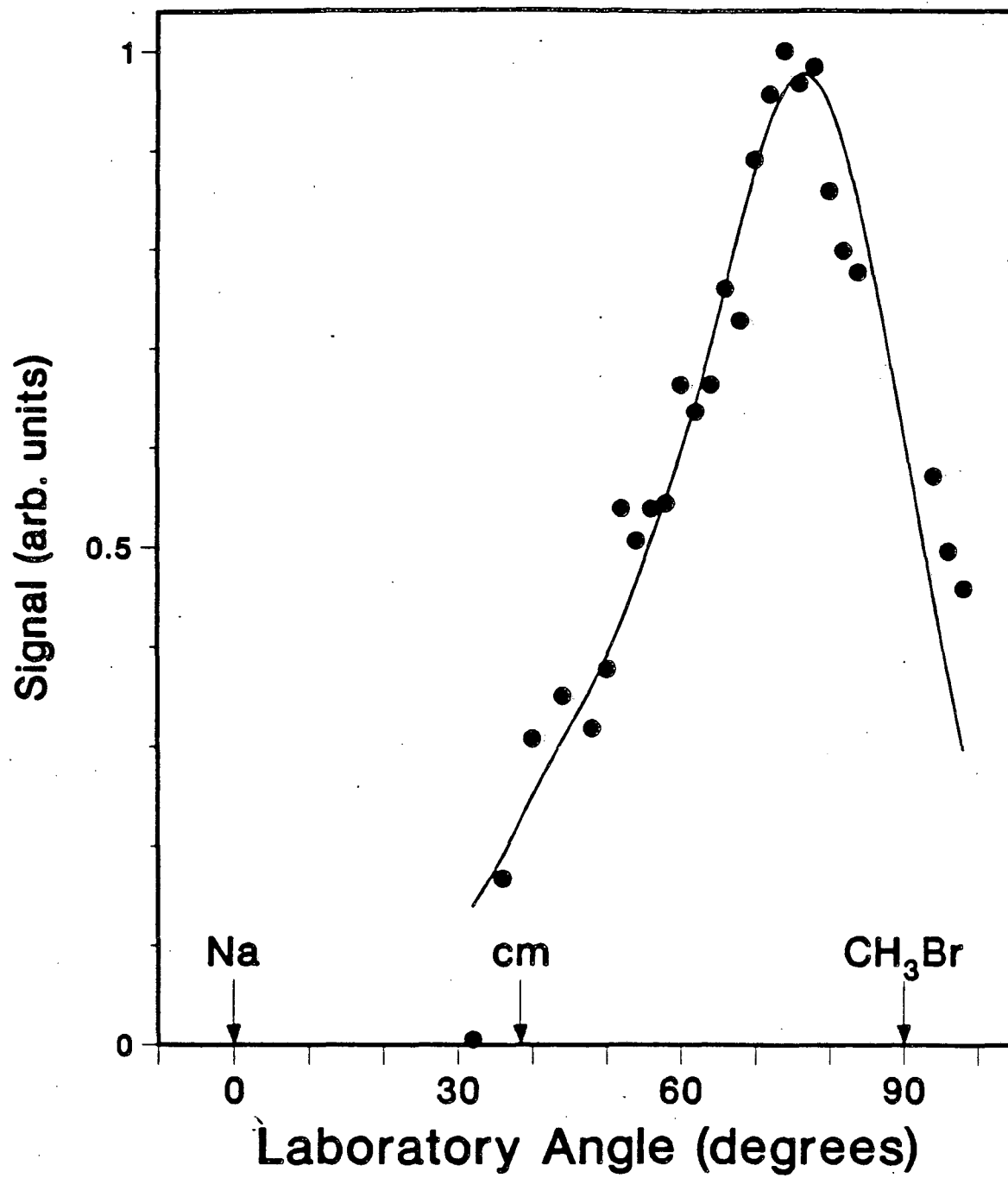
The best fits to the angular distributions are shown as the solid curves in figures 6a, b, and c. The center-of-mass angular distributions used are shown in figure 7, and the recoil energy distributions used are shown in figure 8 for Na(3S,3P,4D) scattering, respectively. Some features of the fits are shown in table I. The relative cross sections (right hand column) have been corrected for the excitation fractions given in chapter I. It is assumed that 20% of the Na atoms are in the Na(3P) state when the D₂ transition is excited. It is also assumed that this does not change on subsequent excitation for which it is assumed that 16% of the atoms are in the Na(4D) state.

Fig. 6. Best fits to the laboratory angular distributions for Na + CH₃Br at a collision energy of 21 kcal/mole for a) Na(3S), b) Na(3P), and c) Na(4D). The solid lines are the fit to the data.



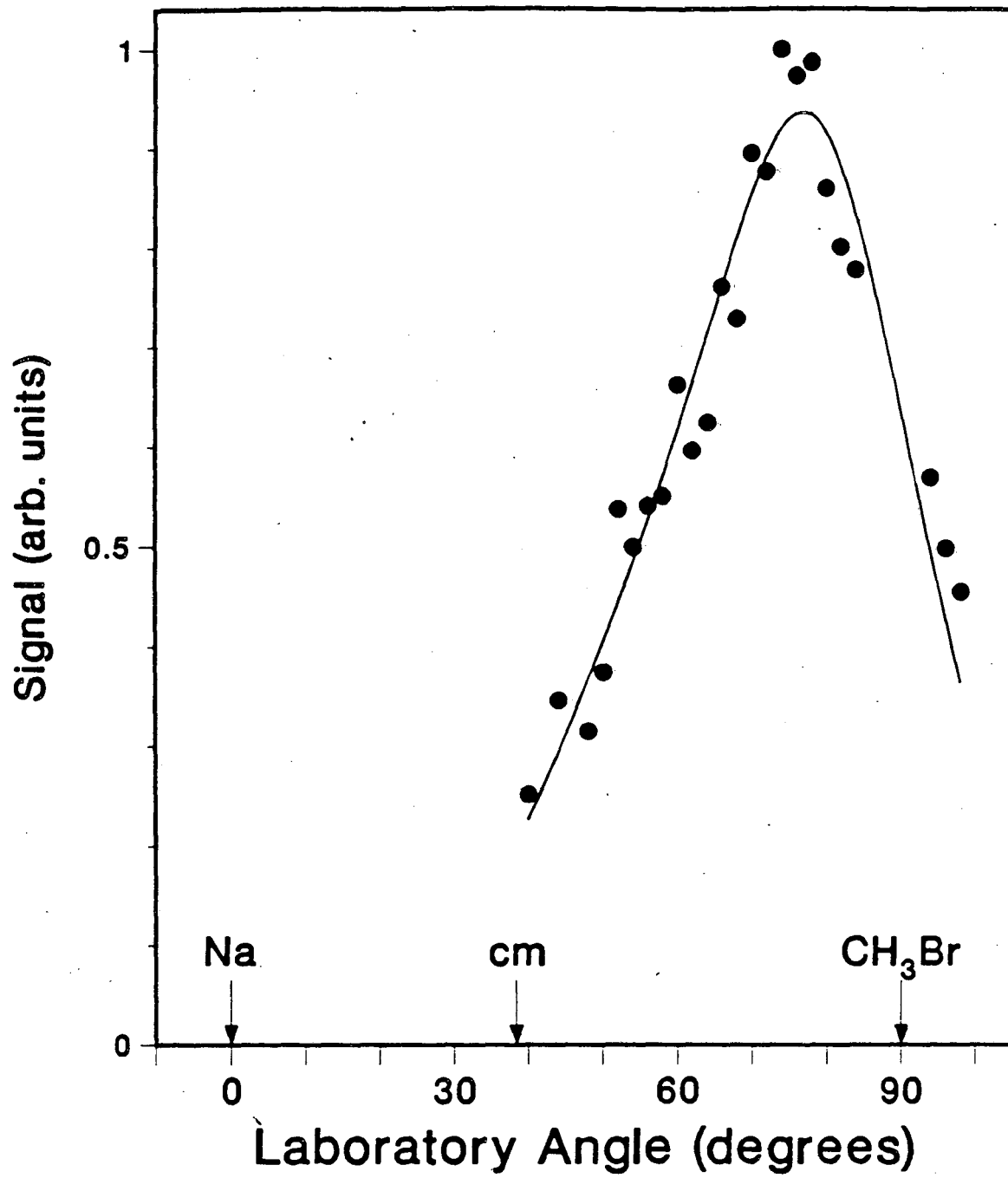
XBL 862-664

Fig. 6(a)



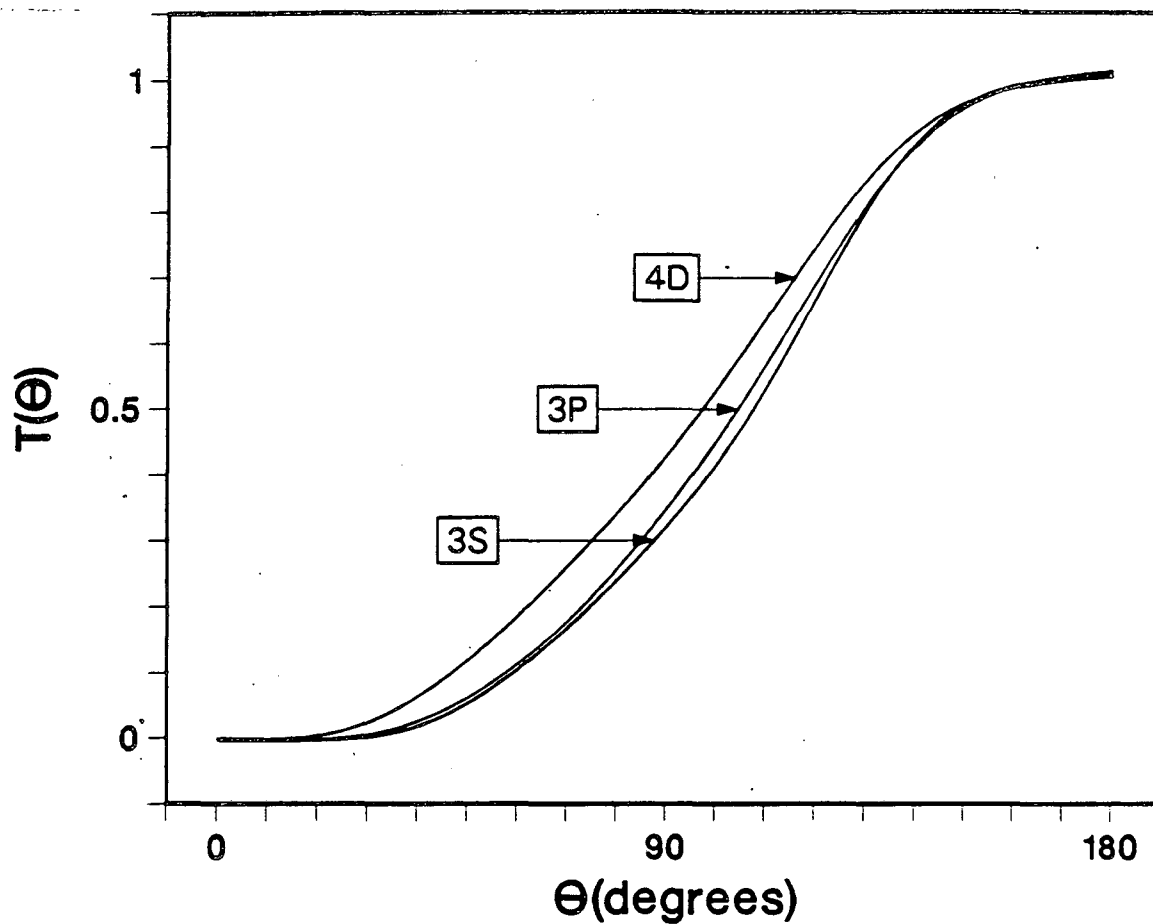
XBL 862-665

Fig. 6(b)



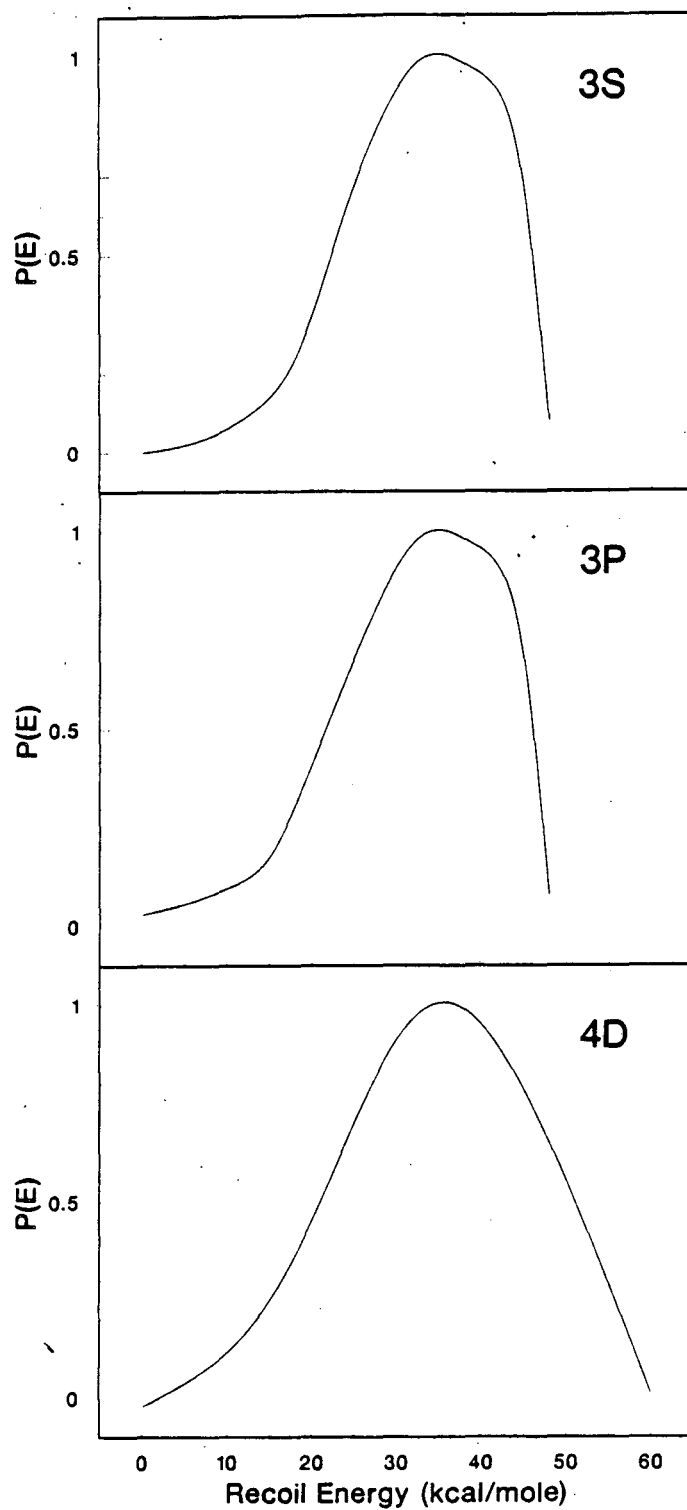
XBL 862-666

Fig. 6(c)



XBL 862-663

Fig. 7. Center-of-mass angular distributions used for the fits shown in figure 6 of $\text{Na} + \text{CH}_3\text{Br} \rightarrow \text{NaBr} + \text{CH}_3$ at a collision energy of 21 kcal/mole for $\text{Na}(3\text{S}, 3\text{P}, 4\text{D})$.



XBL 863-755

Fig. 8. Product recoil energy distributions for the fits shown in figure 6 of Na + CH₃Br at a collision energy of 21 kcal/mole for Na(3S,3P,4D).

As in chapter II, the reactive cross sections can be calibrated using the low angle elastic scattering.^{23,24} Briefly, the low angle elastic scattering is estimated from the small angle approximation to the classical scattering due to a van der Waals potential,^{24,25} formula (8) of chapter II. This scattering depends upon the collision energy and the C_6 constant of the van der Waals potential. The C_6 constant is estimated using the Slater-Kirkwood formula for the dispersive portion,^{26,27} formula (10) of chapter II, and the Debye formula for the dipole-induced-dipole portion,^{28,29} formula (11) of chapter II. The two contributions are then added to get the C_6 constant,^{23,29} as in formula (9) of chapter II.

The Slater-Kirkwood formula estimates the dispersive portion of the van der Waals potential from the polarizabilities (α) and effective number of electrons (N) of the collision partners. For Na, these are $\alpha(\text{Na}(3S))=24.5 \text{ \AA}^3$,³⁰ $\alpha(\text{Na}(3P))=53.6 \text{ \AA}^3$,³¹ and $N(\text{Na})=1$. The polarizability of CH_3Br can be estimated from the sum of the polarizabilities of its bonds:²⁸

$$\alpha(\text{CH}_3\text{Br}) = \sum_{\text{all bonds}} \alpha_{\text{bond}} = \sum_{\text{all bonds}} \frac{1}{3} (\alpha_{//} + 2\alpha_{\perp}), \quad (9)$$

where $\alpha_{//}$ and α_{\perp} are the bond polarizabilities parallel and perpendicular to the bond axis. The bond polarizabilities are $\alpha_{//}(\text{C-Br})=5.04 \text{ \AA}^3$, $\alpha_{\perp}(\text{C-Br})=2.88 \text{ \AA}^3$, $\alpha_{//}(\text{C-H})=0.79 \text{ \AA}^3$, and $\alpha(\text{C-H})=0.58 \text{ \AA}^3$.²⁸ From (8), the polarizability of methyl bromide is $\alpha(\text{CH}_3\text{Br})=5.55 \text{ \AA}^3$. The effective number of electrons is

$N(\text{CH}_3\text{Br})=14$. This gives the dispersive portion of the C_6 constant for Na(3S) scattering to be $C_{6,\text{disp}}=8830 \text{ kcal/mole } \text{\AA}^6$. For Na(3P) scattering, $C_{6,\text{disp}}=13560 \text{ kcal/mole } \text{\AA}^6$.

The dipole-induced-dipole contribution is determined from the Na atomic polarizability and the electric dipole moment of CH_3Br , using the Debye formula.^{28,29} The electric dipole moment of methyl bromide is $\mu(\text{CH}_3\text{Br})=1.81 \text{ D}$.³² This gives the inductive portion of the C_6 constant for ground state scattering as $C_{6,\text{ind}}=1160 \text{ kcal/mole } \text{\AA}^6$, and the total ground state C_6 constant as $9990 \text{ kcal/mole } \text{\AA}^6$. For Na(3P) scattering, $C_{6,\text{ind}}=2530 \text{ kcal/mole } \text{\AA}^6$, and the total $C_6=16090 \text{ kcal/mole } \text{\AA}^6$.

The absolute differential elastic scattering cross sections are then estimated as described in chapter II, and compared to the low laboratory angle scattering intensity. A least squares fit is made to the lowest laboratory angles measured, and a scaling factor is determined between the absolute differential cross sections and the relative numbers measured in the scattering experiment. In order to convert the reactive cross sections into absolute cross sections, the relative detection efficiency of reactively and elastically scattered products must be known. The relative detection efficiency in this case is the ratio of the ionization cross sections for Na and NaBr to Na^+ . The ionization cross section of Na by 200 eV electrons has been measured as $\sigma(\text{Na})=2.1 \text{ \AA}^2$.³³ The ionization cross section of NaBr can be estimated by comparing its polarizability to that of a species for which the ionization cross section is known.^{23,34} The

Table II. Reactive cross sections of $\text{Na}(nL) + \text{CH}_3\text{Br} \rightarrow \text{NaBr} + \text{CH}_3$.

<u>Na Level</u>	<u>From 3S Data</u>	<u>From 3P Data</u>	<u>Average</u>
3S	5.6 Å ²	5.8 Å ²	5.7 Å ²
3P	8.7 Å ²	9.0 Å ²	8.9 Å ²
4D	15.7 Å ²	16.2 Å ²	16.0 Å ²

polarizability of NaBr is approximately the sum of the polarizabilities of Na^+ and Br^- .²³ These are $\alpha(\text{Na}^+) = 0.227 \text{ Å}^3$, and $\alpha(\text{Br}^-) = 3.585 \text{ Å}^3$ in the NaBr molecule,³⁵ giving $\alpha(\text{NaBr}) = 3.812 \text{ Å}^3$. By comparing this to the polarizability of isoelectronic Kr, $\alpha(\text{Kr}) = 2.86 \text{ Å}^3$,³⁶ for which the cross section for ionization by 200 eV electrons is $\sigma(\text{Kr}) = 2.8 \text{ Å}^2$,³⁷ a total ionization cross section of $\sigma(\text{NaBr}) = 3.7 \text{ Å}^2$ is derived. If it is assumed as for vibrationally excited NaCl that 90% fragmentation to Na^+ occurs, then the cross section for ionization to Na^+ is $\sigma'(\text{NaBr}) = 3.3 \text{ Å}^2$. This gives a relative detection efficiency of $\text{Eff}(\text{NaBr})/\text{Eff}(\text{Na}) = 1.6$.

The cross sections derived for the reactions of $\text{Na}(3S, 3P, 4D)$ atoms are shown in table II. As pointed out in chapter II, the absolute cross sections are probably only good to within a factor of 2, and are strongly dependent on the excitation fraction assumed. Since the reactive geometries are exactly those that would lead to large angle

elastic scattering, and reactive signal appears at the highest laboratory angles studied, the hard sphere approximation cannot be used to estimate the reactive cross sections.

D. Discussion

1. Observations on the Experimental Results

The only differences with increasing electronic energy appear to be the increasing reactive cross sections and the slowly widening center-of-mass angular distributions. The rebound mechanism is seen for the reactions of the excited states as well as the ground state of Na with CH_3Br .

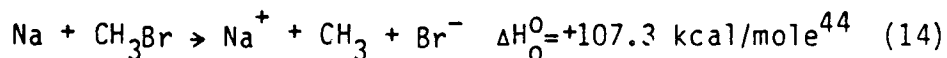
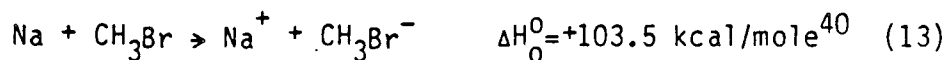
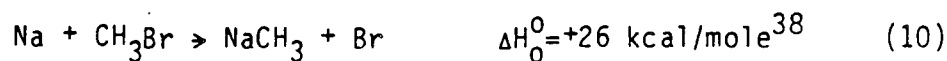
The slightly widening center-of-mass angular distributions (see figure 7 and table I) support the idea that an opening of the steric angle for reaction occurs with increasing electronic energy and thus sodium orbital size. The less strict geometrical requirements on the approach geometry lead to the broader center-of-mass angular distributions. This is visible in the raw data (figure 3) as the increase in signal on the low side of the reactive peak.

The fact that the recoil energy distributions do not shift with changing electronic energy implies that the idea of ions released at a distance and coming together to form a vibrationally excited ionic molecule as brought forth in the DIPR-DIP model appears to be correct. That is that as the electron jump distance moves further out for

successively higher electronic states of sodium (with successively lower ionization potentials) the distance at which the M^+-X^- attraction takes over becomes larger, and the resultant M^+X^- molecule is produced in successively higher vibrational levels. A nearly vertical $CH_3Br \rightarrow CH_3Br^-$ transition takes place so that the translational energy released is essentially the same for each electronic state.

2. Other Possible Processes

Gersh and Bernstein have discussed energetically possible products in high energy (>1 eV) collisions of $K + CH_3I$, and several of these processes, mutatis mutandis, are energetically possible here:



All these processes (10-14) are substantially endothermic, but with the electronic excitation to $Na(4D)$, 98.8 kcal/mole, and the collision energy of over 20 kcal/mole, all are energetically possible.

It is unlikely that methyl sodium is formed via process (10) because this would require Na to approach the methyl end of the molecule. As shown for $K + CH_3I$, there is a substantial repulsion for the alkali approaching the methyl end of the methyl halide⁴⁵ in

the ground state potential, and this is certain to hold true for the excited state potentials as well.

Formation of NaH (process (11)) is also unlikely because it involves approach via a repulsive geometry and the breakage of the strong H-CH₂Br bond. No evidence is seen for NaH, although it is also expected to be observed at $m/q=23$ (Na⁺).

It is possible that at high collision energy the Na could dissociate the CH₃Br as in process (12). This is most likely to happen where effectively NaBr is produced above its dissociation limit to atoms -- a neutral equivalent to the observations of Lacmann and Herschbach for K + HCl,⁴⁶ discussed further below.

The present experiments are not sensitive to the production of ions such as in processes (13-14). Furthermore, CH₃Br⁻ has such a small potential well (3.8 kcal/mole), offset significantly from the equilibrium geometry of the neutral,⁴² that it is extremely unlikely that it could be produced. However, it is quite possible that the Na⁺ + Br⁻ ion pair could be produced via process (14). This is equivalent to the process seen by Lacmann and Herschbach for K + HCl.⁴⁶ As interpreted by Balint-Kurti and Yardley highly vibrationally excited KCl is produced above the dissociation limit to ions.⁴⁷ An experiment such as Mariella's described in chapter III would be able to observe such a process and measure its cross section.⁴⁸

E. Conclusions

The most striking feature of the reactions of the various states is their similarity. The rebound mechanism describes the reaction of the ground and excited Na states with CH_3Br . Besides the increasing cross sections, the main difference in the reaction dynamics appears to be that the steric angle of acceptance opens somewhat for higher electronic states, and thus for larger electronic orbitals. Of course the lack of a change in the product translational energy with increasing electronic energy implies that the product internal energy increases substantially.

Further study, perhaps of the more reactive methyl iodide system, could provide insight into the symmetry aspects of the reactions of the excited states.

F. References

1. M. Polanyi, Atomic Reactions (Williams and Northgate, London, 1932).
2. D. R. Herschbach, G. H. Kwei, J. A. Norris, J. Chem. Phys. 34, 1842 (1961).
3. D. R. Herschbach, Faraday Disc. Chem. Soc. 55, 233 (1973).
4. D. H. Parker, K. K. Chakravorty, and R. B. Bernstein, J. Phys. Chem. 85, 466 (1981).
5. G. Marcelin and P. R. Brooks, J. Am. Chem. Soc. 97, 1710 (1975).
6. M. E. Gersch and R. B. Bernstein, J. Chem. Phys. 56, 6131 (1972).
7. A. M. Rulis and R. B. Bernstein, J. Chem. Phys. 57, 5497 (1972).
8. H. E. Litvak, A. Gonzalez Urena, and R. B. Bernstein, J. Chem. Phys. 61, 4091 (1974).
9. A. Gonzalez Urena and R. B. Bernstein, ibid., 4101 (1974).
10. R. H. Goldbaum and L. Robbin Martin, J. Chem. Phys. 62, 1181 (1975).
11. G. Rotzoll, R. Viard, and K. Schuegerl, Chem. Phys. Lett. 35, 353 (1975).
12. R. R. Herm, in Alkali Halide Vapors: Structure, Spectra, and Reaction Dynamics, 189 (Academic Press, New York, 1979), and references therein.
13. P. J. Kuntz, M. H. Mok, and J. C. Polanyi, J. Chem. Phys. 50, 4623 (1969).

14. R. M. Harris, Ph.D. Thesis, Harvard University, Cambridge, Massachusetts (1970).
15. A. M. G. Ding, L. J. Kirsch, D. S. Perry, and J. C. Polanyi, Faraday Disc. Chem. Soc. **55**, 252 (1973).
16. D. Husain and P. Marshall, Int. J. Chem. Kin. **18**, 83 (1986).
17. Calculated from the $\text{H}_3\text{C}-\text{Br}$ dissociation energy (66.2 kcal/mole) in reference 18, and the D_0^0 value for NaBr (86.9 kcal/mole) given in reference 19.
18. G. N. A. van Veen, Ph. D. Thesis, Rijksuniversiteit te Utrecht, Utrecht, The Netherlands (1984).
19. K. P. Huber and G. Herzberg, Molecular Spectra and Molecular Structure, IV. Constants of Diatomic Molecules (Van Nostrand Reinhold, Co., New York, 1979).
20. Calculated from the $\text{H}_3\text{C}-\text{Cl}$ bond strength (84.0 kcal/mole) in reference 21, and the D_0^0 value for NaCl (97.5 kcal/mole) given in reference 19.
21. "CRC Handbook of Chemistry and Physics," 65th Ed., R. C. Weast, ed., (CRC Press, Boca Raton, Florida, 1984).
22. R. J. Buss, Ph.D. Thesis, University of California, Berkeley, California (1979).
23. See chapter II of this thesis.
24. J. H. Birely, R. R. Herm, K. R. Wilson, and D. R. Herschbach, J. Chem. Phys. **47**, 993 (1967).
25. E. A. Mason, J. T. Vanderslice, and C. J. G. Raw, J. Chem. Phys. **40**, 2153 (1964).

26. J. C. Slater and J. G. Kirkwood, Phys. Rev. **37**, 682 (1931).
27. K. S. Pitzer, Adv. Chem. Phys. **2**, 59 (1959).
28. J. O. Hirschfelder, C. F. Curtiss, and R. B. Bird, Molecular Theory of Gases and Liquids (John Wiley and Sons, Inc., New York, 1964).
29. H.-J. Werner and W. Meyer, Phys. Rev. A **13**, 13 (1976).
30. P. Hannaford, W. R. MacGillivray, and M. C. Standage, J. Phys. B: Atom Molec. Phys. **12**, 4033 (1979).
31. H. T. Duong and J.-L. Picque, J. Physique **33**, 513 (1972).
32. R. D. Nelson, Jr., D. R. Lide, Jr., and A. A. Maryott, National Standard Reference Data Series 10, National Bureau of Standards (U. S.) (1967).
33. R. H. McFarland and J. D. Kinney, Phys. Rev. **137**, A1058 (1965).
34. C. H. Becker, P. Casavecchia, P. W. Tiedemann, J. J. Valentini, and Y. T. Lee, J. Chem. Phys. **73**, 2833 (1980).
35. P. Brumer and M. Karplus, J. Chem. Phys. **58**, 3903 (1973).
36. J. Thorhallsson, C. Fisk, and S. Fraga, Theoret. Chim. Acta (Berl.) **10**, 388 (1968).
37. S. C. Brown, Basic Data of Plasma Physics, 2nd Ed. (MIT Press, Cambridge, Massachusetts, 1967).
38. Calculated from the H₃C-Br dissociation energy (66.2 kcal/mole) in reference 18, and an estimated Na-CH₃ bond strength of 40 kcal/mole.

39. Calculated from the $\text{H-CH}_2\text{Br}$ dissociation energy (102 kcal/mole) in reference 21, and the D_0^0 value for NaH (43 kcal/mole) given in reference 19.
40. Calculated from the ionization potential of Na (118.5 kcal/mole),⁴¹ and the $\text{H}_3\text{C-Br}^-$ bond strength of 3.8 kcal/mole from reference 42, and the electron affinity of Br (77.4 kcal/mole) from reference 43.
41. W. L. Wiese, M. W. Smith, and B. M. Miles, Atomic Transition Probabilities Volume II: Sodium Through Calcium, Natl. Stand. Ref. Data Ser., Nat. Bur. Stand. (U. S.), Washington, DC (1969).
42. W. E. Wentworth, R. George, and H. Keith, J. Chem. Phys. 51, 1791 (1969).
43. R. S. Berry and C. W. Riemann, J. Chem. Phys. 38, 1540 (1963).
44. Calculated from the $\text{H}_3\text{C-Br}$ dissociation energy (66.2 kcal/mole) in reference 18, the ionization potential of Na (118.5 kcal/mole),⁴¹ and the electron affinity of Br (77.4 kcal/mole) from reference 42.
45. L. M. Raff and M. Karplus, J. Chem. Phys. 44, 1212 (1966), and references therein.
46. K. Lacmann and D. R. Herschbach, Chem. Phys. Lett. 6, 106 (1970).
47. G. G. Balint-Kurti and R. N. Yardley, Faraday Disc. Chem. Soc. 62, 77 (1977).
48. R. P. Mariella, Jr., J. Chem. Phys. 76, 2965 (1981).

V. THE REACTIONS OF GROUND AND EXCITED STATE ALKALI ATOMS WITH HALOGEN MOLECULES

A. Introduction

The reactions of alkali atoms (M) with diatomic halogen molecules (X_2) were shown to have exceptionally large cross sections in Michael Polanyi's classic diffusion flame experiments in the early 1930's.¹ These reactions have been studied in detail in crossed molecular beams for over 20 years.²⁻¹⁶ The alkali halide product is in all cases found to be: sharply peaked forwards, produced with large cross section, and with little translational energy. In analogy to nuclear stripping reactions, these reactions have been regarded as "spectator stripping reactions," in which the alkali atom and one halogen atom interact but leave the other halogen atom (the spectator) essentially unperturbed.^{2,3} It was for these reactions that the "harpoon" mechanism was put forth.^{1,17} The basic reaction mechanism has an electron transferring to (harpooning) the halogen molecule at long range. The alkali ion then "reels in" the halide ion. This leads to larger than gas kinetic cross sections as Polanyi originally observed.¹

The spectator stripping features of these reactions can be quantified.¹⁸ Since the spectator halogen atom is expected to continue undisturbed by the reaction, the product alkali halide molecule must remain confined to the center-of-mass angle and velocity

defined by the alkali atom and the halogen atom involved in the reaction. As illustrated in figure 1, this means that the alkali halide product must appear at the laboratory angle

$$\theta_s = \tan^{-1}(m_X v_{X_2} / m_M v_M), \quad (1)$$

where m_M and m_X are the masses of the alkali and halogen atoms, respectively, and v_M and v_{X_2} are the incident laboratory frame velocities of the alkali atom and the halogen molecule, respectively.⁵ Furthermore, since the final velocity of the spectator halogen atom must be the same as the initial velocity of the halogen molecule in both the laboratory (v) and the center-of-mass (u) frames ($v_X' = v_{X_2}$, and $u_X' = u_{X_2}$), the product recoil energy (E_{recoil}) is related to the collision energy ($E_{\text{collision}}$), and is simply derived to be:

$$E_{\text{recoil}} = \frac{m_M}{2m_{MX}} E_{\text{collision}} \quad (2)$$

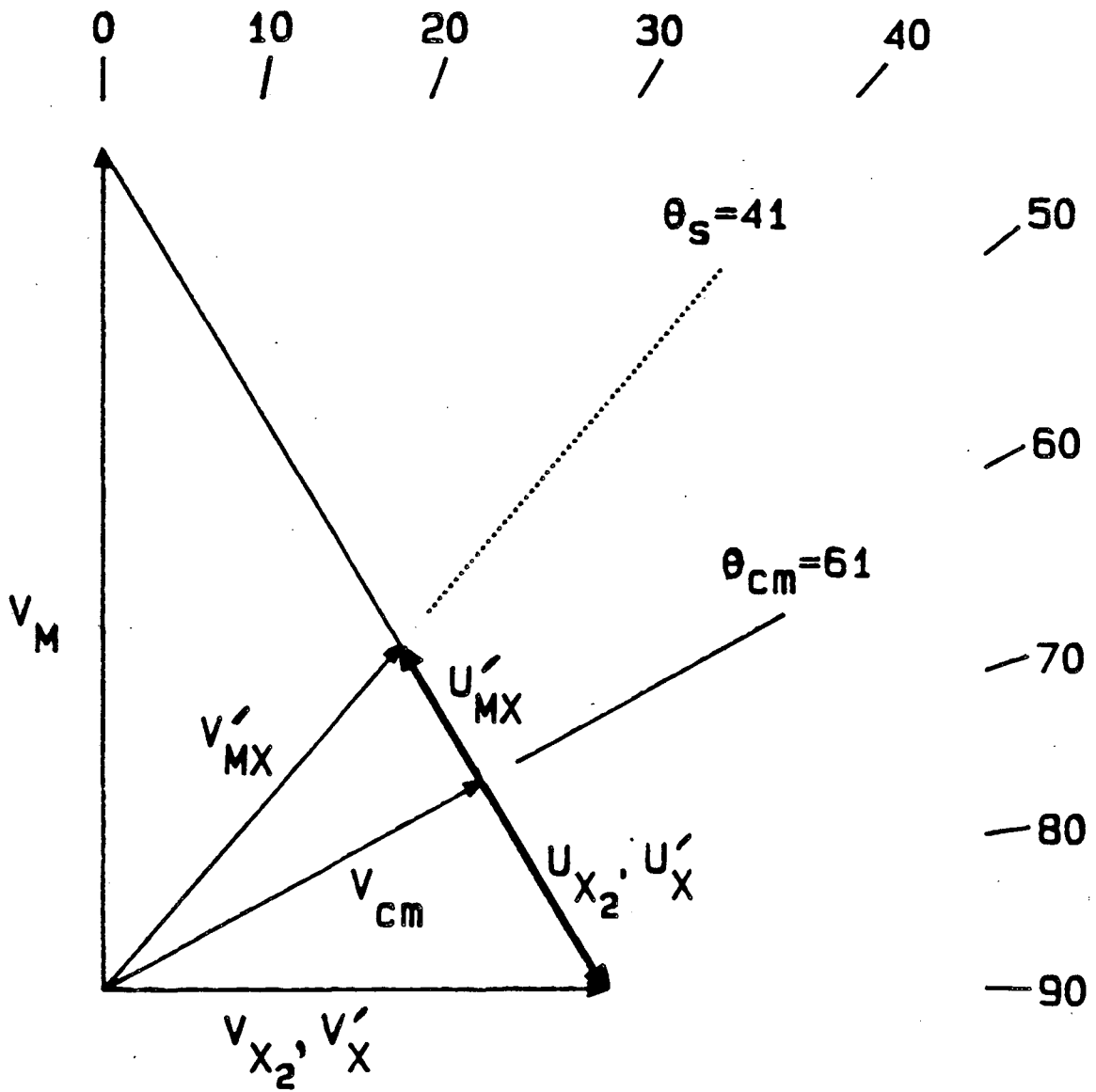
in the absence of reactant internal energy.¹¹ If the reactant halogen molecules' internal energy (E_{internal}) is included, an additional term is added, and the recoil energy becomes:

$$E_{\text{recoil}} = \frac{m_M}{2m_{MX}} E_{\text{collision}} + \frac{m_M + m_{X_2}}{2m_{MX}} E_{\text{internal}} \quad (3)$$

and the product MX is scattered to laboratory angles smaller than those given by (1).

Clearly, in describing nearly collinear, small impact parameter collisions the spectator stripping model is physically unrealistic, because due to geometric constraints alone, the alkali halide molecule

Fig. 1. Newton velocity vector diagram for $M + X_2 \rightarrow MX + X$ showing the spectator stripping angle θ_s , and the product scattering velocity vectors in the spectator stripping limit. The masses are taken to be those of Na (for M) and Cl_2 (for X_2). This figure is adapted from figure 1 of Botscwina, Meyer, Hertel, and Reiland, J. Chem. Phys. 75, 5438 (1981) with permission.



XBL 863-898

Fig. 1

must be backwards scattered. However, the electron transfer cross sections are expected to be so large that the fraction of collisions leading to backwards scattering in this way is small.

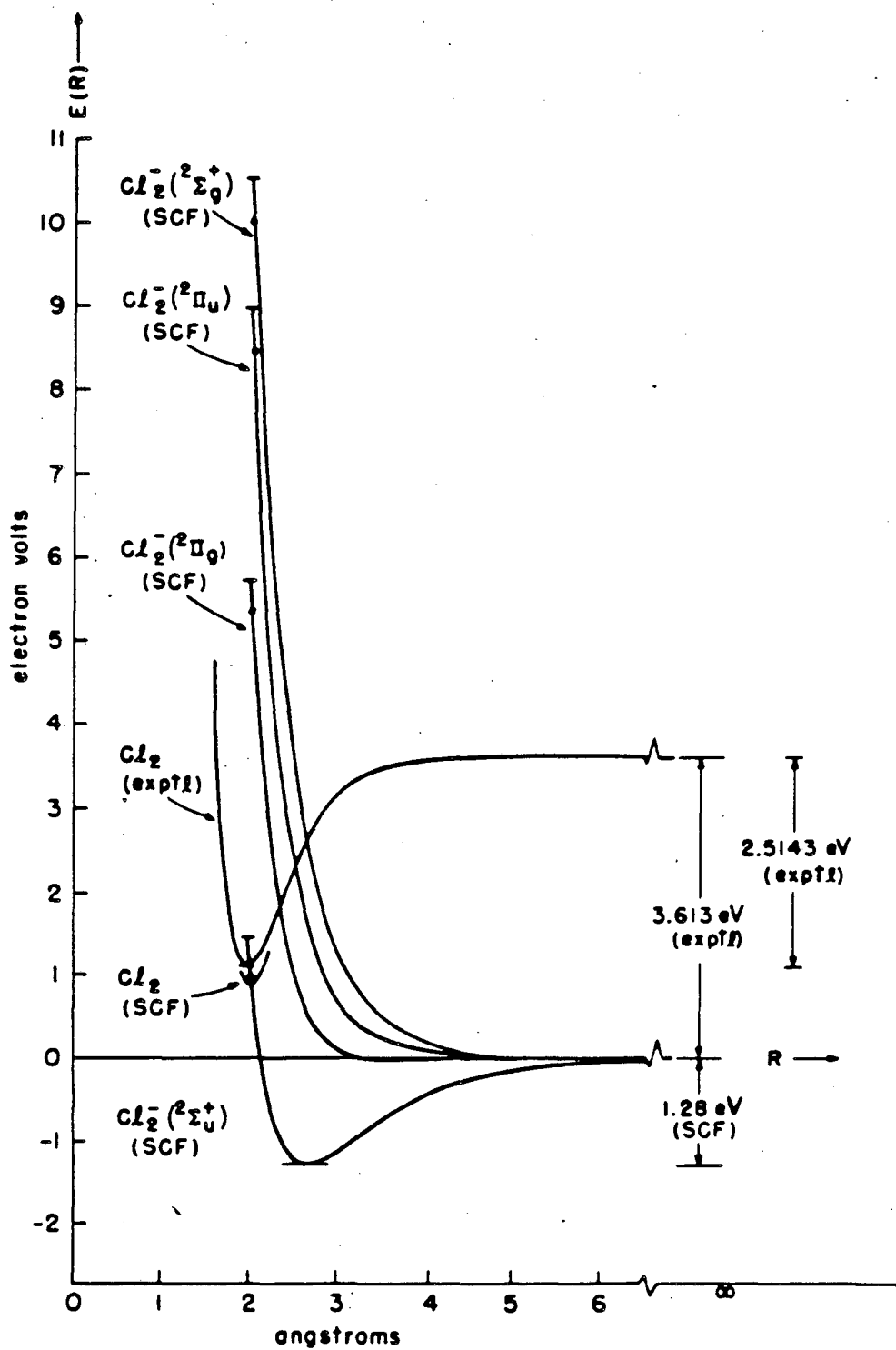
As shown in several experiments, the "spectator" aspect of these reactions must be regarded only as a limit, and the more general, phenomenological term "stripping mechanism" is sometimes adopted for a reaction in which scattering is predominantly forwards, but cannot be quantitatively described as in (1-3) above.^{19,20}

As discussed in the previous chapter, it was for these reactions, as well as the reactions of alkali atoms with alkyl halide molecules, that the DIPR (Direct Interaction with Product Repulsion) model was developed.^{20,21} The difference in the treatment of these two reactive systems is that for halogen molecules charge is allowed to migrate from one atom to the other, whereas for alkyl halides this is obviously not possible. Also, the repulsions for the negative ions of the diatomic halogen molecules are much lower than those for the (dissociative) negative ions of the alkyl halide molecules. Birely, Herschbach, and coworkers have pointed out that the electric field of the alkali ion is strong enough to dissociate the diatomic halogen ion in less than one vibrational period.^{6,7} The electric field at 10 Å separation is approximately 10^7 V/cm,^{7,22} and diatomic ions such as vibrationally excited H_2^+ have been shown to be dissociated by externally applied electric fields of 10^6 V/cm.^{6,23} Additionally, if a vertical transition is assumed, the Cl_2^- is formed on the repulsive wall, above its dissociation limit as shown in the Cl_2 and

Cl_2^- potential energy curves in figure 2, adapted from reference 24 with permission.

The charge migration and lower repulsion lead to some possible problems in the use of the DIPR model. Up to 1/3 of the trajectories for some mass combinations and neutral-ionic crossing points have "secondary collisions" in which the alkali atom interacts with the departing halogen atom.²¹ As pointed out in reference 21, this clearly violates two of the conditions of the model -- first, that there be no interaction between the alkali atom and the departing halogen atom, and secondly, that the repulsive potential for the departing halogen atom be monotonically decreasing. In the calculations of Kuntz, Mok, and Polanyi (KMP), the effect that these secondary collisions have on the product distributions is that there is a large increase in forward scattering.²¹ In fact, KMP dispute the conclusion that spectator stripping is the source of the forward scattering. Their calculations suggest that the predominance of forward scattering is due only to secondary encounters. However, the DIPR model reduces to spectator stripping in the limit when the collision energy greatly exceeds the strength of the halogen-halogen interatomic interaction.²¹

In the reactions of excited alkali atoms, where due to the decreased effective alkali ionization potential the crossing point of the neutral and ionic curves has moved out to larger distances, these problems should be less important because the halogen atom has more time to depart, and there should thus be fewer secondary encounters.



XBL 863-791

Fig. 2. Potential energy curves for Cl_2 and Cl_2^- adapted from reference 24, with permission.

A naive view would predict very similar recoil distributions of product since the X_2^- repulsion remains the same. The only differences would be in the larger cross sections and product internal energies with increasing electronic energy. The product internal energies would be expected to increase simply because the coulombic M^+X^- attraction begins at larger distance, giving more vibrational and rotational energy to the MX molecule (much like the reaction of $Na(4D,5S) + HCl^{25}$). According to the conclusions of KMP, however, electronic excitation should lead to less forward scattering and more backwards scattering, because of the smaller number of secondary encounters.

Anderson has discussed the effect of increasing the distance at which the neutral-ionic curves cross, r_c .²⁷ The interaction of the ground state neutral and ionic curves is strongest for a collinear $C_{\infty v}$ (M-X-X) geometry in which both the neutral $M-X_2$ (covalent) and the ionic $M^+X_2^-$ have $^2\Sigma^+$ symmetry. The interaction has the effect of reducing the energy of the covalent potential energy. In the C_{2v} geometry (an isosceles triangle with the alkali atom at the apex), the covalent $M-X_2$ has 2A_1 symmetry, but the ionic $M^+X_2^-$ has 2B_1 symmetry. Thus in C_{2v} geometry the interaction between the neutral and ionic curves is small (zero in the Born-Oppenheimer approximation), and the cross section for electron transfer remains small. In the intermediate case, C_s symmetry, both the neutral and ionic symmetries are $^2A'$, and there is an interaction which will smoothly vary as a function of the $M-X_2$ orientation between the $C_{\infty v}$ and C_{2v} limits. The anisotropic potential valid outside the crossing radius ($r > r_c$) can be approximated:

$$V(r, \beta) = -V_{\text{disp}}(r) - Ae^{-\alpha r} \cos^2 \beta \quad (4)$$

where r is the $M-X_2$ separation, β is the angle between the X_2 molecular axis and the $M-X_2$ axis (the line connecting the M atom with the X_2 center-of-mass), and A and α are parameters derivable from the properties of the separated atom and molecule.^{28,29} The more collinear the configuration, the more attractive it is, and the more probable electron transfer is. Low energy collisions will allow some reorientation into these configurations -- this is termed "tracking"²⁷ -- that are more favorable for electron transfer. The higher energy the collision, the smaller the effects of tracking, and the more likely are noncollinear collisions to proceed diabatically, without electron transfer or reaction. If the crossing radius is increased, the interaction of the covalent and ionic curves is decreased, and not only is electron transfer at large r less likely for this reason, but also because of the reduced anisotropy. Excessive rotation of the halogen (at the flywheel limit) will reduce the effects of this anisotropy by averaging over it, however in a supersonic expansion the molecular rotation is efficiently cooled.

Another consequence of the mixing of the potential curves is that the harpoon can be thought of as slow. This helps to explain why the harpoon cross sections calculated from the vertical electron affinities of the halogens are often too low.^{30,31} The longer interaction time allows some pre-stretching of the halogen bond, thus lowering the effective electron affinity. This has been shown by the measurements of Los and coworkers which show a decrease in electron transfer cross

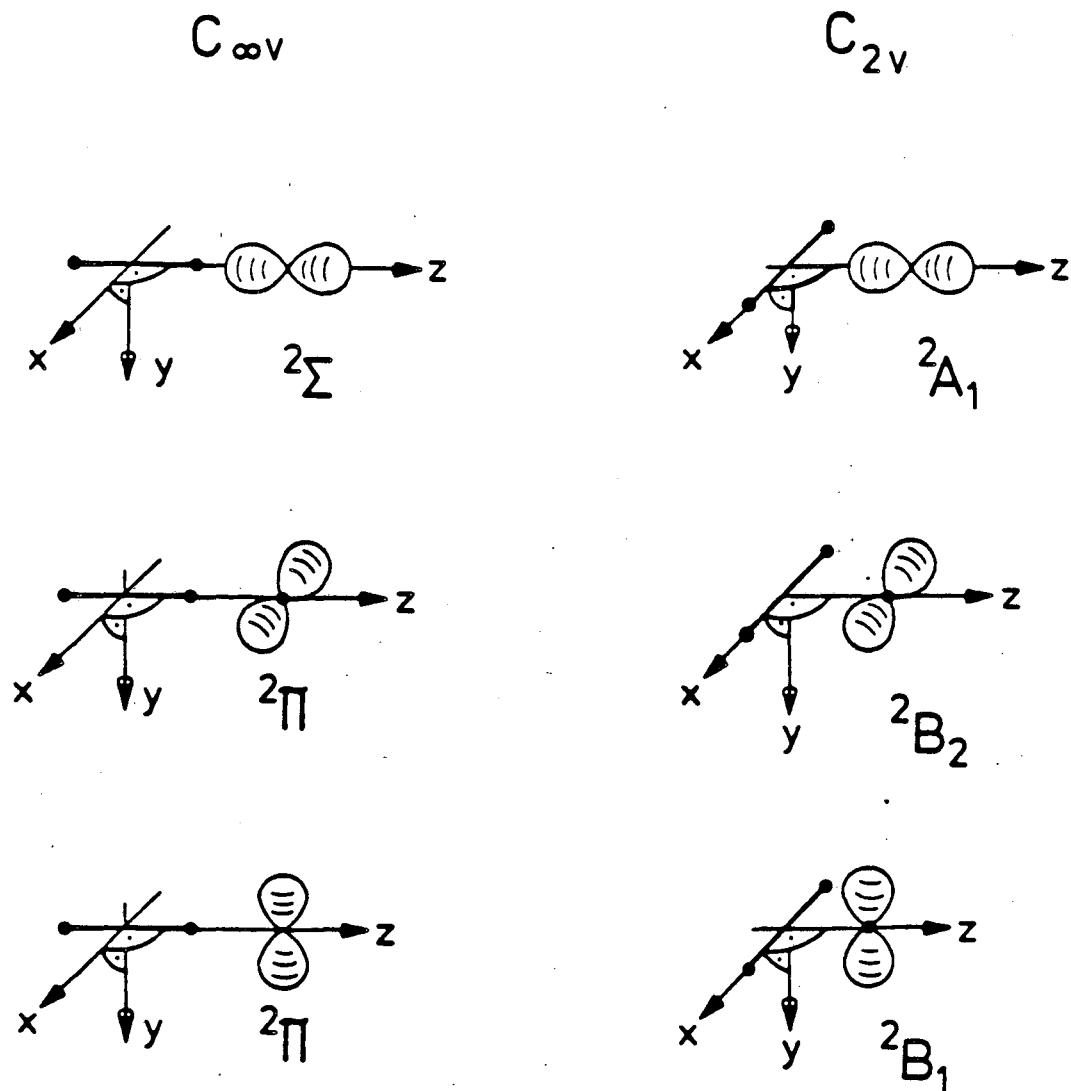
sections with increasing collision energies (up to 120 eV) in alkali-halogen collisions.^{32,33} This implies that the electron transfer cross section goes down as the collision is shortened so as not to allow this pre-stretching.

In what is called the orbiting model, the maximum distance at which the reaction can occur, r_0 , is larger than r_c because it is determined only by the position of the centrifugal barrier on the potential given in (4) above, any collision energies above the centrifugal barrier are captured in the attractive potential, lead to electron transfer, and subsequently to reaction. The centrifugal energy is given by:

$$E_{\text{centrifugal}} = + \frac{b^2}{r_0^2} E_{\text{collision}} \quad (5)$$

where b is the impact parameter of the collision and r_0 is the maximum in the potential, the sum of (4) and (5).²⁷ At low collision energies this leads to an increase in the cross section above that predicted by the harpoon mechanism. The orbiting model predicts a decreasing reactive cross section with increasing collision energy since the centrifugal barrier increases. It makes no predictions, however, as to the shape of the reactive product angular distributions.

The symmetry considerations discussed above apply to the scattering of the ground state. This discussion can be extended to the excited state, and the relevant symmetries for ground and excited state scattering are given in table I. Figures 3a-c show the three possible



XBL 862-630

Fig. 3. $M(np)$ orbital alignments for the three symmetries of the $M-X_2$ system in C_v and C_{2v} geometries.

Table I. Symmetries of important states in the process $M(nS, nP) + X_2 \rightarrow M^+ + X_2^-$.

Separated	$C_{\infty V}$	C_{2V}	C_S	Figure
$M(n^2S) + X_2(X^1\Sigma_g^+)$	$2\Sigma^+$	$2A_1$	$2A'$	
$M(n^2P) + X_2(X^1\Sigma_g^+)$	$2\Sigma^+$	$2A_1$	$2A'$	3a
$M(n^2P) + X_2(X^1\Sigma_g^+)$	$2\pi^+$	$2B_2$	$2A'$	3b
$M(n^2P) + X_2(X^1\Sigma_g^+)$	$2\pi^-$	$2B_1$	$2A''$	3c
$M^+(1S) + X_2^-(X^2\Sigma_u^+)$	$2\Sigma^+$	$2B_1$	$2A'$	

alignments of the alkali np orbital with respect to the $M-X_2$ axis for $C_{\infty V}$ and C_{2V} geometries. It can be seen from table I that with these three alignments of the np orbital, different interactions take place. For the p orbital aligned along the $M-X_2$ axis, as in figure 3a, the symmetries and interactions will be the same as for the ground state alkali atom (s orbital). For the p orbital in the MX_2 plane, but perpendicular to the $M-X_2$ axis, as in figure 3b, the interaction is weak for the C_S symmetry, and essentially zero for both the $C_{\infty V}$ and C_{2V} geometries. Finally, for the p orbital perpendicular to the MX_2 plane, as in figure 3c, the situation is the reverse of the ground state case. The symmetries of the covalent and ionic curves match for C_{2V} geometry, and mismatch for $C_{\infty V}$ geometry. Therefore,

the maximum attraction and electron transfer probability will occur for C_{2v} geometry, and at low collision energies the $M-X_2$ system will be drawn toward this configuration. Because of the nature of the reaction mechanism, the reaction geometry would likely have little effect on the product scattering distributions, and it would be difficult to verify these predictions experimentally.

Several previous experimental measurements of ground state scattering have been performed with well defined collision energies -- using velocity-selected effusive^{4-6,10,13} or sputtered,¹³ or supersonic^{11,12} alkali atomic beams. Except for the K sputtering source of van der Meulen et al.,¹³ this has given collision energies of up to only 5.5 kcal/mole. With relatively intense seeded supersonic beams, and a judicious choice of collision partners, it is possible to reach collision energies over 200 kcal/mole, and to vary the collision energy.

It has been shown that at low collision energies (0.5-1.3 kcal/mole) the center-of-mass angular distributions are essentially identical for any alkali atom with a particular halogen molecule.^{6,7} Grice and Emedocles found a single center-of-mass angular scattering distribution that adequately describes the product scattering for the reactions:



at collision energies under 1 kcal/mole, where $M = K, Rb,$ and Cs .⁷

The first study of the effect of collision energy on these reactions appears to be that of Gillen, Rulis, and Bernstein who used a velocity-selected effusive K atom source.¹⁰ They studied the reaction $K + I_2$ at collision energies ranging from 1.9 to 3.6 kcal/mole and saw relatively small changes in reactive cross sections, and center-of-mass angular and recoil energy distributions. Work on this and other systems was continued by Grice and coworkers using a neat supersonic K atom source.^{11,12} For $K + I_2$ at a collision energy of 5.5 kcal/mole they saw an increase in forward scattering as well as a decrease in the reactive cross section when the collision energy was increased from the thermal energies of reference 10.¹² Similar behavior was observed for the reaction $K + Br_2$ at a collision energy of ~5 kcal/mole¹¹ when compared to thermal collision energy data.⁷

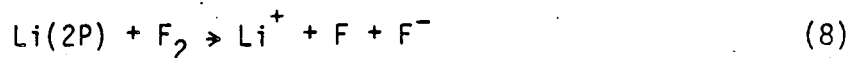
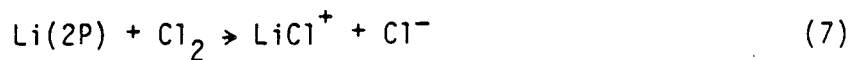
Van der Meulen, Rulis, and de Vries have studied the reaction $K + Br_2$ as a function of translational energy for collision energies up to 58 kcal/mole using velocity-selected effusive and sputtered K atomic beam sources.¹³ They find that the reactive cross section decreases with increasing collision energy. The reaction cross section drops to 70% of its thermal energy value (measured for 1.3 kcal/mole²⁶) at a collision energy of 19.4 kcal/mole, to 50% at 39 kcal/mole, and to a value too small for the authors to measure ($<10 \text{ \AA}^2$) at 58 kcal/mole. These values correspond well to what is expected from the orbiting model of Grice, Anderson, Herschbach, and coworkers,^{27,28} except at 58 kcal/mole, and not at all well to what is expected for spectator stripping. They see the product recoil energy increase from 27% of the

total available energy at 1.3 kcal/mole, to 81% at 19.4 kcal/mole, to 95% at 39 kcal/mole. These values are somewhat suspect as they do not correspond to other experiments on the alkali-halogen systems at low collision energy in which the recoil energies are typically less than 10% of the total available energies of 40 kcal/mole or more. It is possible that this discrepancy is due to the difficulty of accurately extracting the reactive product angular distributions from the sharply skewed Newton diagrams that result from the very fast K atom beam. Nevertheless, the authors show that this behavior correlates better with a simple harmonic model of Kuntz, Polanyi, and coworkers²⁰ than with spectator stripping. The center-of-mass angular distributions change somewhat, but show no smooth variation with collision energy. All the center-of-mass angular distributions have full widths at half maxima between 13° and 18°, and all except the highest collision energy for which product KBr was detected (39 kcal/mole) peak at 0°.

Although the reaction dynamics of excited alkali atoms with halogens have not previously been studied in crossed molecular beams, the quenching cross sections of such collision partners have been measured.³⁴ These measurements have been made by dissociating alkali halide vapors in a gas cell using ultraviolet light, and then measuring the decay of the fluorescing excited alkali atomic state produced. The alkali state and velocity can be varied by changing the wavelength of the UV light source. The quenching of Li(2P), Na(3P,4P), and K(4P,5P) by I₂, and of Na(3P) by Br₂ have been studied in this way.³⁴⁻³⁸ For both Na and K the total quenching cross sections, which include all

processes that remove the excited state alkali atom (i.e. reaction and deexcitation), for the first excited state are larger than the ground state reactive cross sections, but then decrease on further excitation to the next nP state.^{36,37} This is most dramatic for $K(4P,5P)$ in which the quenching cross section decreases by a factor of 5 for $K(5P)$ as compared to $K(4P)$.³⁷ This decrease was attributed to the neutral M^*-X_2 potential energy curve being at all $(M-X_2)$ distances higher than the ionic curve. This is not strictly true, because at various halogen interatomic distances the vertical electron affinity can be higher or lower than the equilibrium vertical electron affinity, as discussed above. The first excited states of Na and K have cross sections substantially larger than (approximately twice) the ground state reactive cross sections. All the first excited state quenching cross sections measured decrease with increasing collision energy, typically 30-40% from thermal energies to 10-15 kcal/mole. Once again this can be attributed to the surmounting of a centrifugal barrier as described by Anderson.²⁷

Mariella has studied the chemiionization of excited Li by Cl_2 and F_2 .³⁹ He has measured the cross sections of the processes:

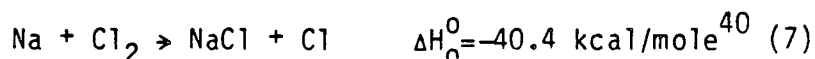


The cross section of process (7) was measured to be $\sigma=0.2 \text{ \AA}^2$. The cross section of process (8) was measured to be $\sigma=2 \text{ \AA}^2$. No other ionic channels were detected in either case.

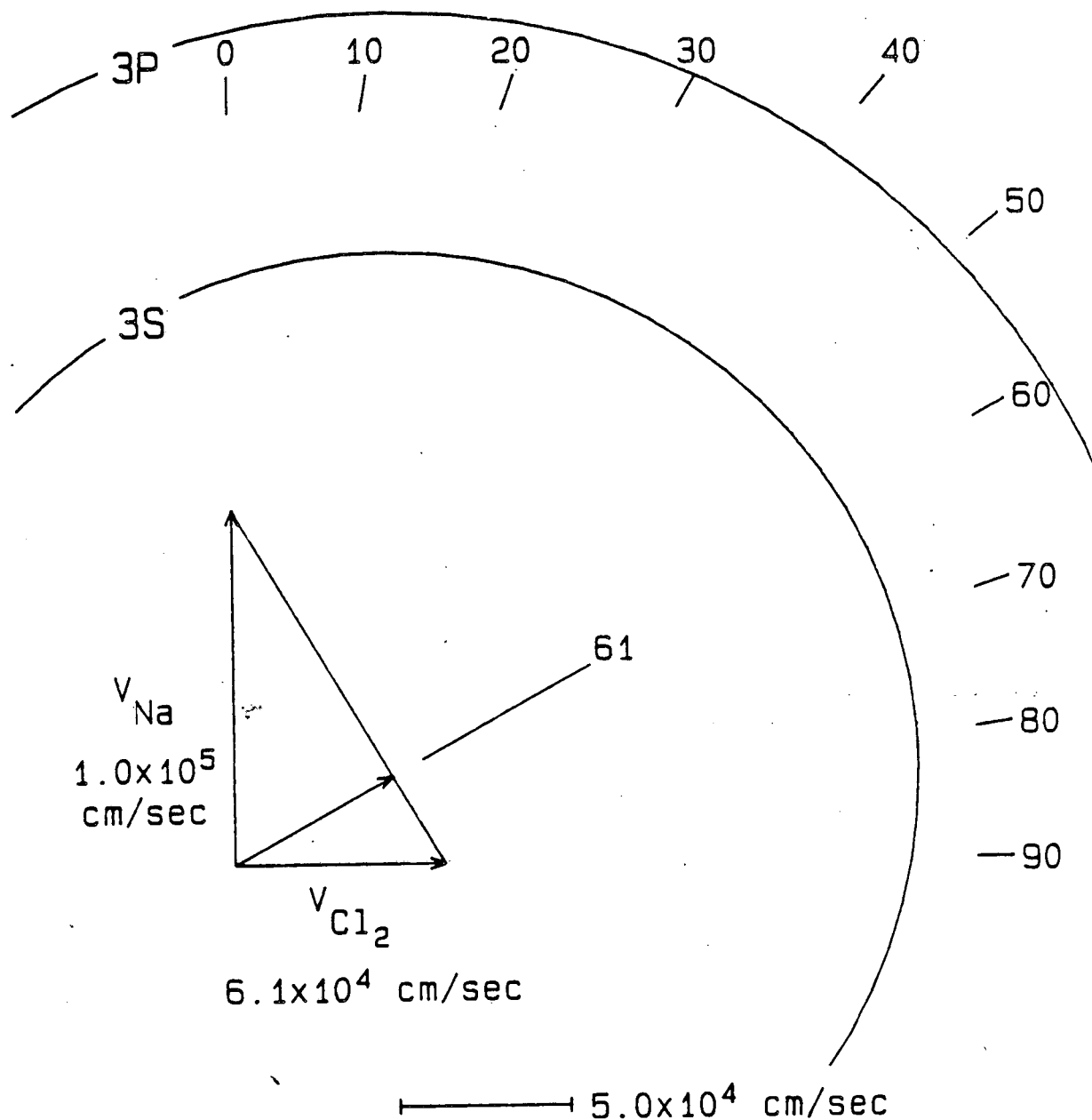
Since it has previously been possible to change only reactant combinations, and thus change mass ratios and ionization potential and/or electron affinities simultaneously, no direct experimental determination has been made to show that one or another set of factors is responsible for the variations seen or predicted for these reactions. Experiments on the reactions of excited state atoms should be able to isolate the effects due to the position of the neutral-ionic potential energy curve crossing as the excitation process to first order changes only the ionization potential of the alkali atom. Such experiments should also determine whether the large quenching cross sections observed for halogens with excited alkali atoms are due to reaction or deexcitation processes.

B. Results

Angular distributions of the NaCl product for the exothermic reaction

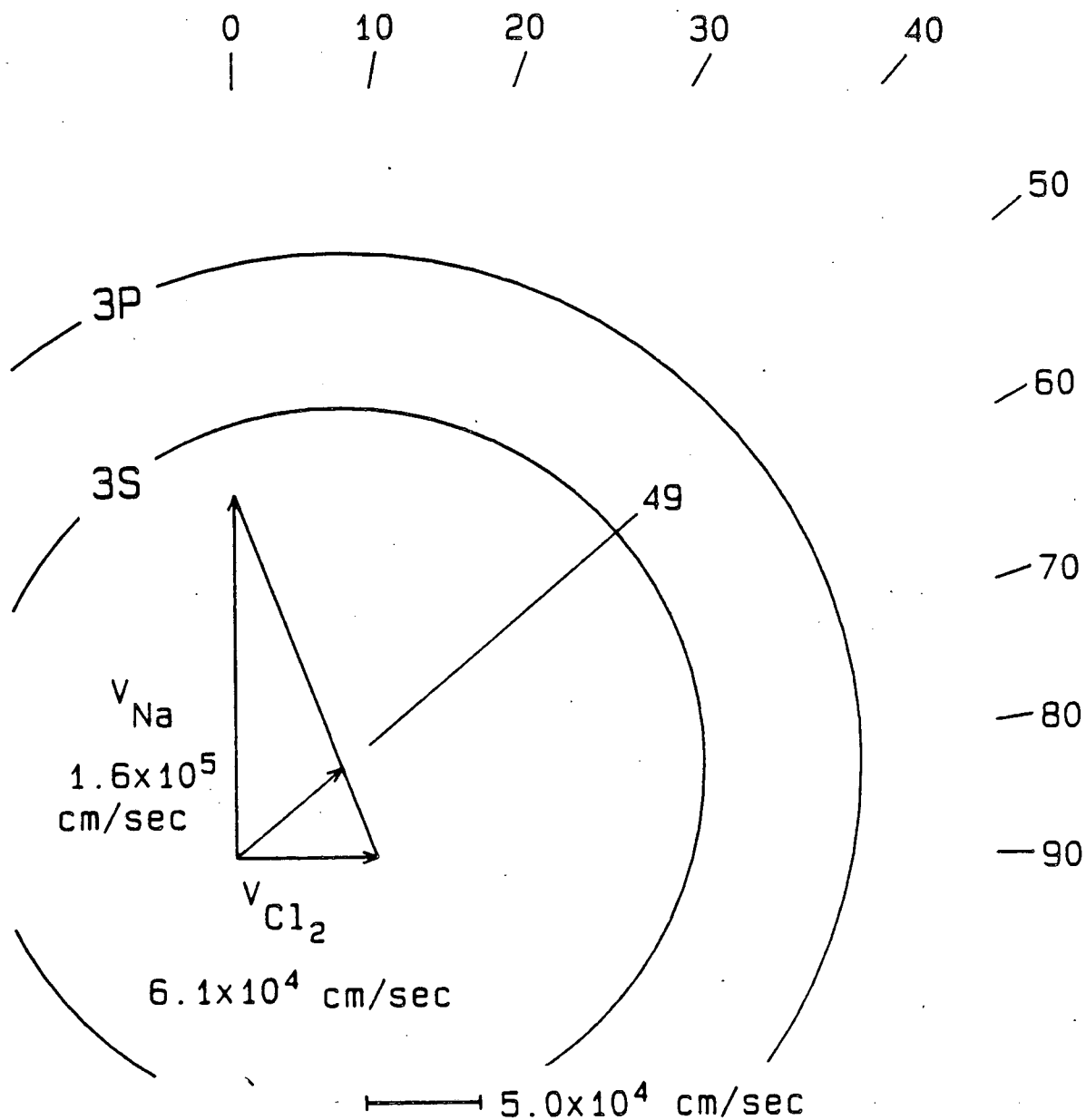


were recorded as described in chapter I for three collision energies: 3, 6, and 19 kcal/mole. The Newton velocity vector diagrams for these collision energies are shown in figures 4-6. The measured angular distributions for the reactions of the Na(3S,3P) states are shown in figures 7-9. All the angular distributions are very narrow compared to the possible product NaCl angular ranges shown in the Newton diagrams as has been observed in all previous alkali-halogen reactions. The shapes of the distributions change very little in going to higher electronic energy, although as will be shown below, the peaks of the angular distributions move to lower laboratory angles for the scattering due to Na(3P) versus that due to Na(3S). All these angular distributions were recorded with the quadrupole mass spectrometer set to a mass to charge ratio (m/q) of 23 (Na⁺) as it is expected that the vibrationally excited NaCl produced will fragment under electron bombardment predominantly to Na⁺.²⁵ The rising signal at low laboratory angles is due to elastically scattered Na which also is detected at m/q=23. Thus the effect of varying ionization efficiencies will be smallest in the data recorded at m/q=23.^{25,42} An angular distribution was recorded for Na(3S,3P) + Cl₂ at m/q=58 (NaCl⁺) at



XBL 863-845

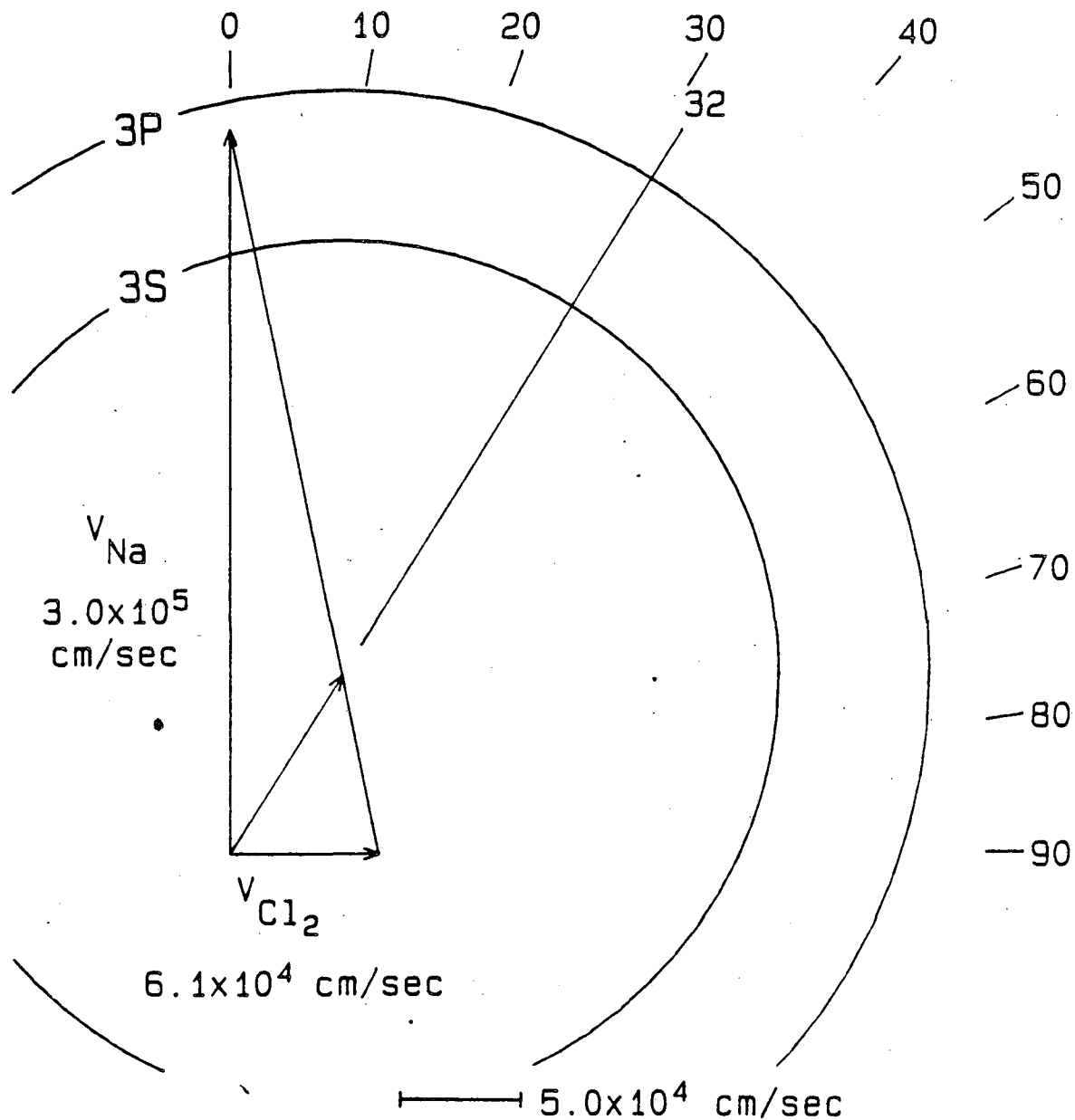
Fig. 4. Newton velocity vector diagram for $\text{Na}(3\text{S},3\text{P}) + \text{Cl}_2 \rightarrow \text{NaCl} + \text{Cl}$ at a collision energy of 3 kcal/mole. The sodium beam is seeded in argon, and the chlorine beam is neat.

$E_{\text{coll}} = 6 \text{ kcal/mole}$


XBL 863-847

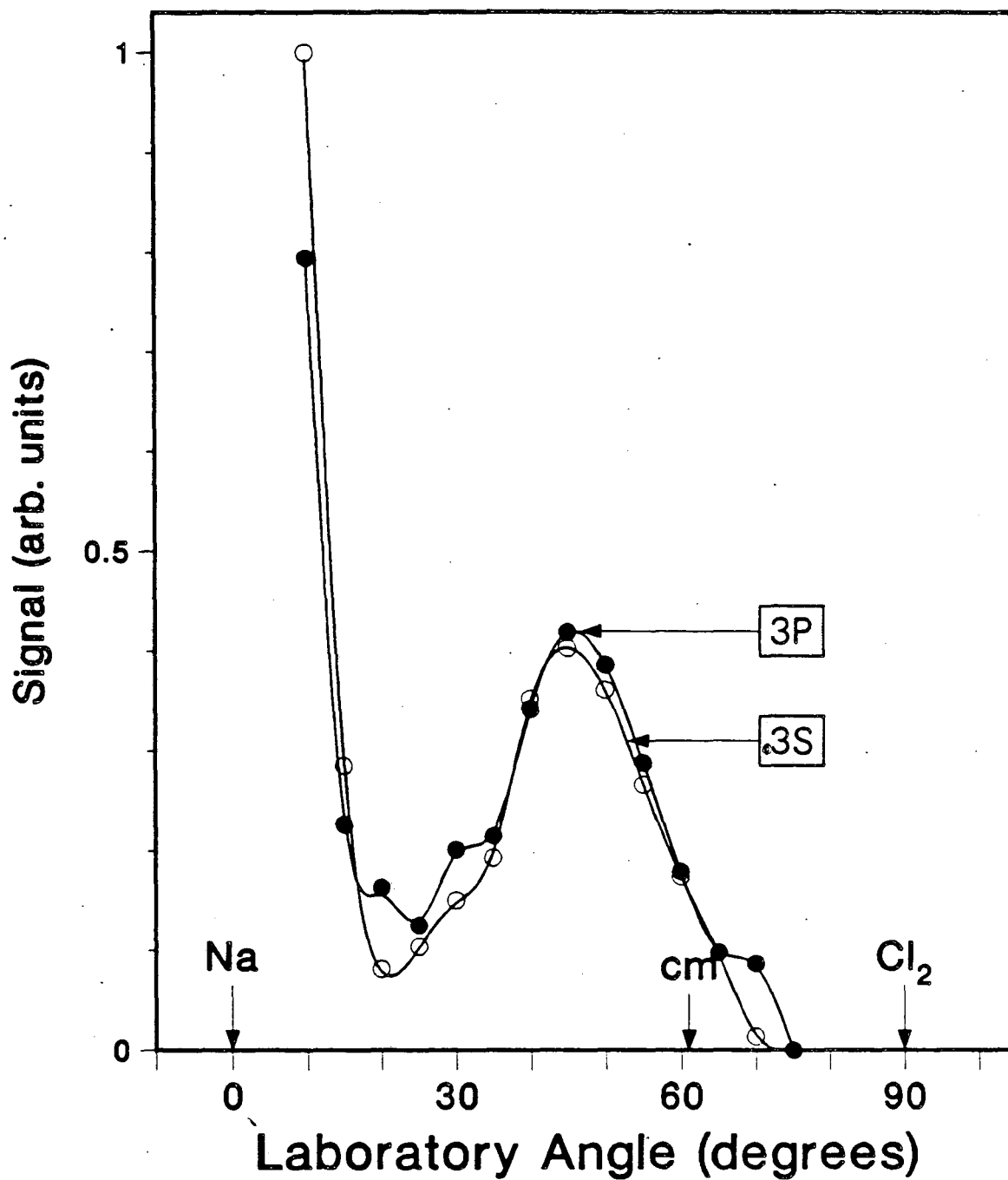
Fig. 5. Newton velocity vector diagram for $\text{Na}(3\text{S},3\text{P}) + \text{Cl}_2 \rightarrow \text{NaCl} + \text{Cl}$ at a collision energy of 6 kcal/mole. The sodium beam is seeded in neon, and the chlorine beam is neat.

$$E_{\text{coll}} = 19 \text{ kcal/mole}$$



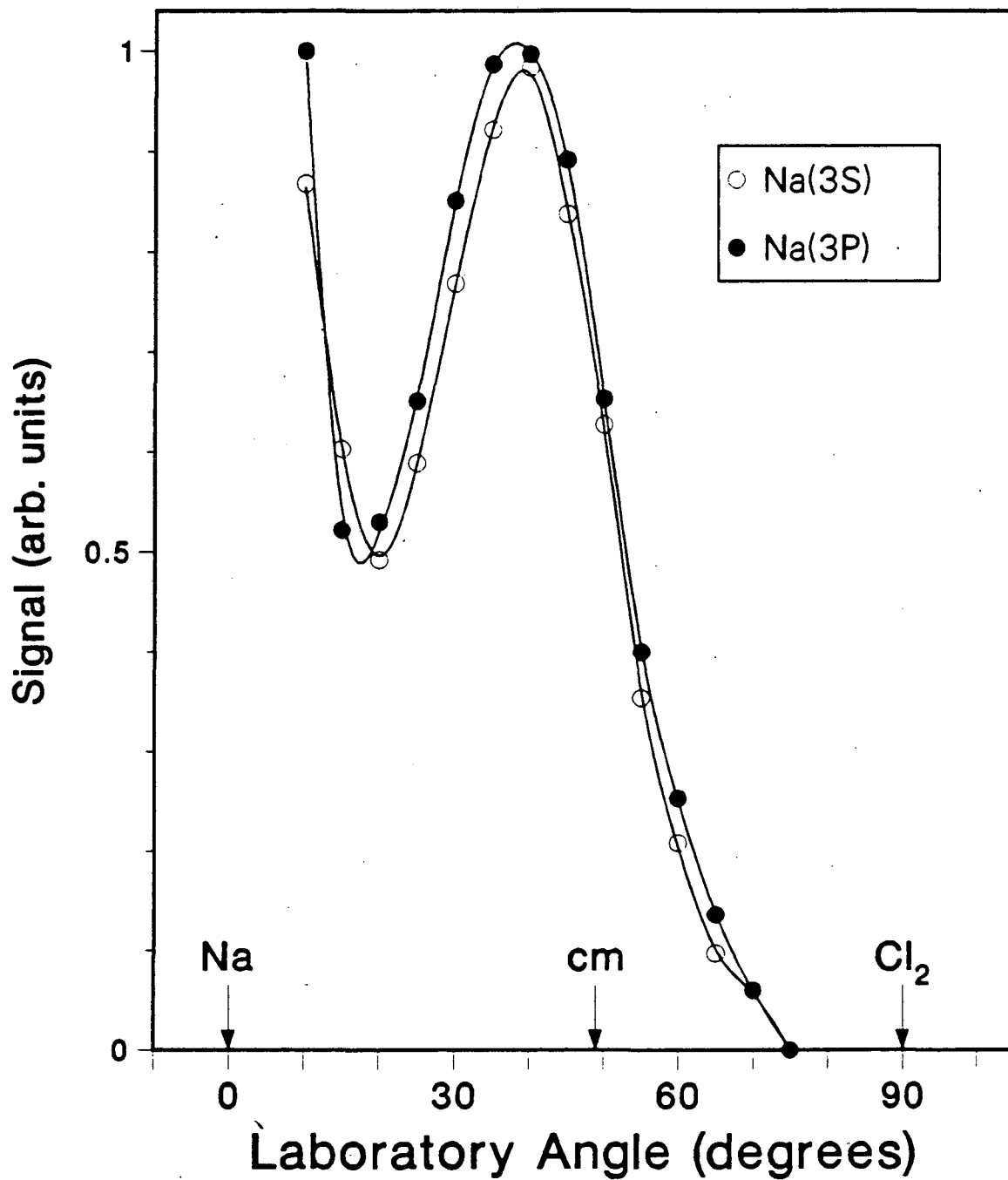
XBL 863-846

Fig. 6. Newton velocity vector diagram for $\text{Na}(3\text{S}, 3\text{P}) + \text{Cl}_2 \rightarrow \text{NaCl} + \text{Cl}$ at a collision energy of 19 kcal/mole. The sodium beam is seeded in helium, and the chlorine beam is neat.



XBL 863-866

Fig. 7. NaCl product angular distributions for Na(3S,3P) + Cl₂ at a collision energy of 3 kcal/mole. The sodium beam is seeded in argon, and the chlorine beam is neat. These distributions were recorded at $m/q=23$ (Na⁺).



XBL 863-865

Fig. 8. NaCl product angular distributions for Na(3S,3P) + Cl₂ at a collision energy of 6 kcal/mole. The sodium beam is seeded in neon, and the chlorine beam is neat. These distributions were recorded at $m/q=23$ (Na⁺).

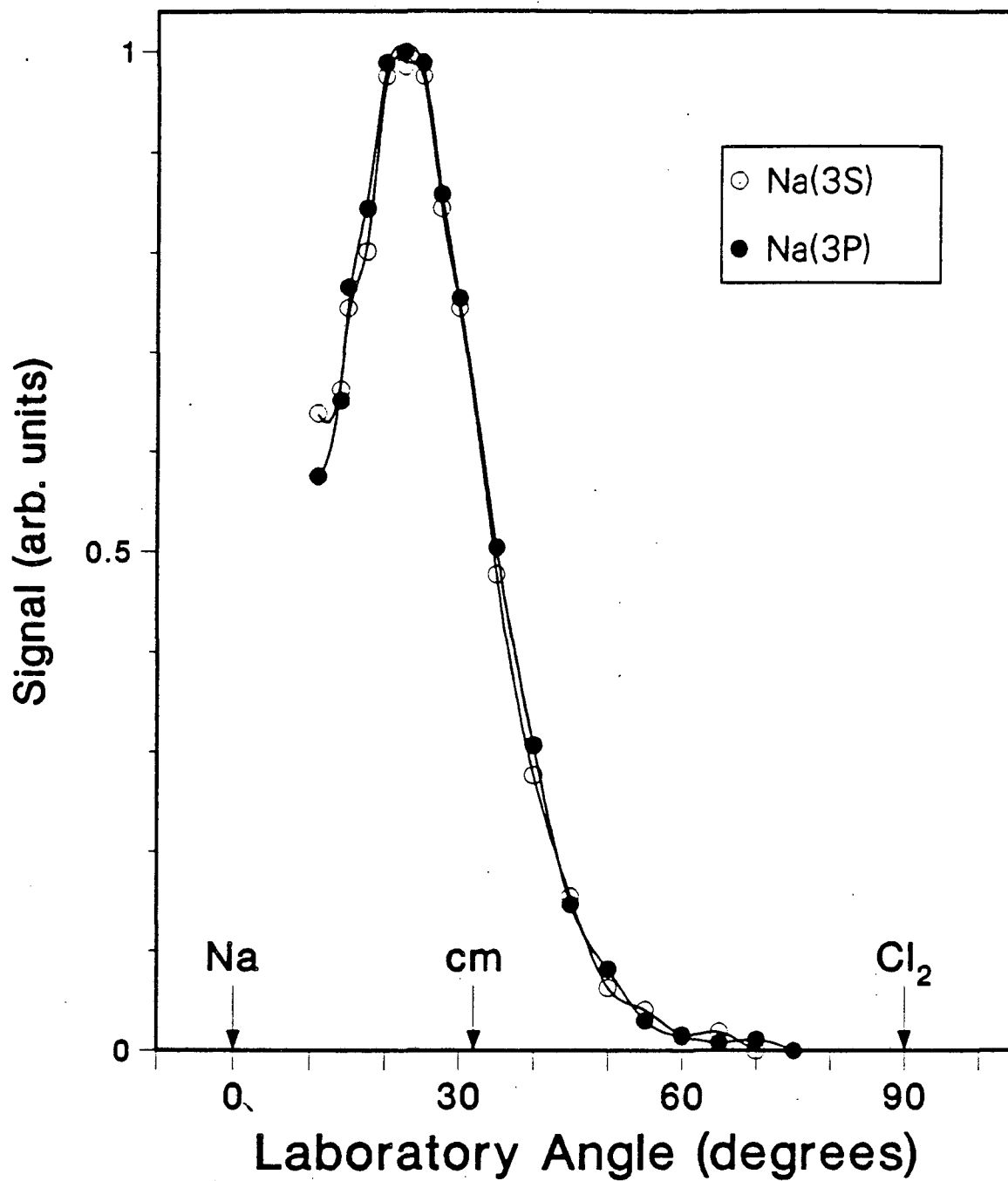


Fig. 9. NaCl product angular distributions for Na(3S,3P) + Cl₂ at a collision energy of 19 kcal/mole. The sodium beam is seeded in helium, and the chlorine beam is neat. These distributions were recorded at $m/q=23$ (Na⁺). XBL 863-868

a collision energy of 6 kcal/mole, and is shown in figure 10. Within the rather large error bars of this measurement, the distribution is superimposable on the distribution recorded at $m/q=23$ (Na^+).

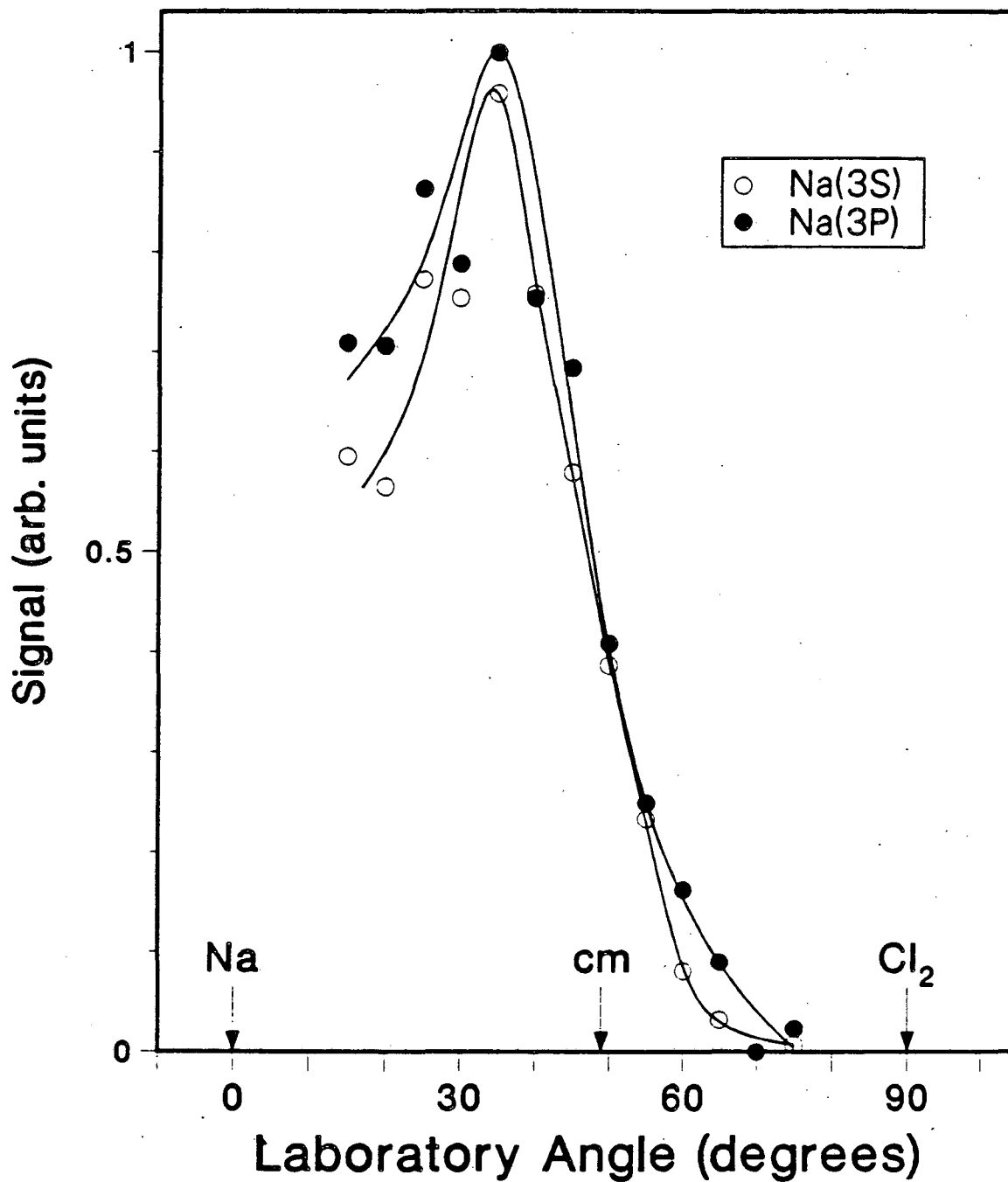
Due to the small difference in the angular distributions between ground and excited state, no time-of-flight product velocity measurements, nor any polarization dependences were measured.

C. Analysis of Experimental Results

As in the previous chapters, the laboratory data was fitted using the program GM which calculates a laboratory scattering distribution from independent assumed center-of-mass angular and recoil energy distributions. Although no laboratory velocity data was recorded, the predominance of forward scattering and the narrow recoil energy distributions give nearly single-valued laboratory to center-of-mass frame transformations such as those which allowed the early studies of these reactions to derive center-of-mass distributions from their relatively primitive laboratory angular distributions.⁴⁻⁹

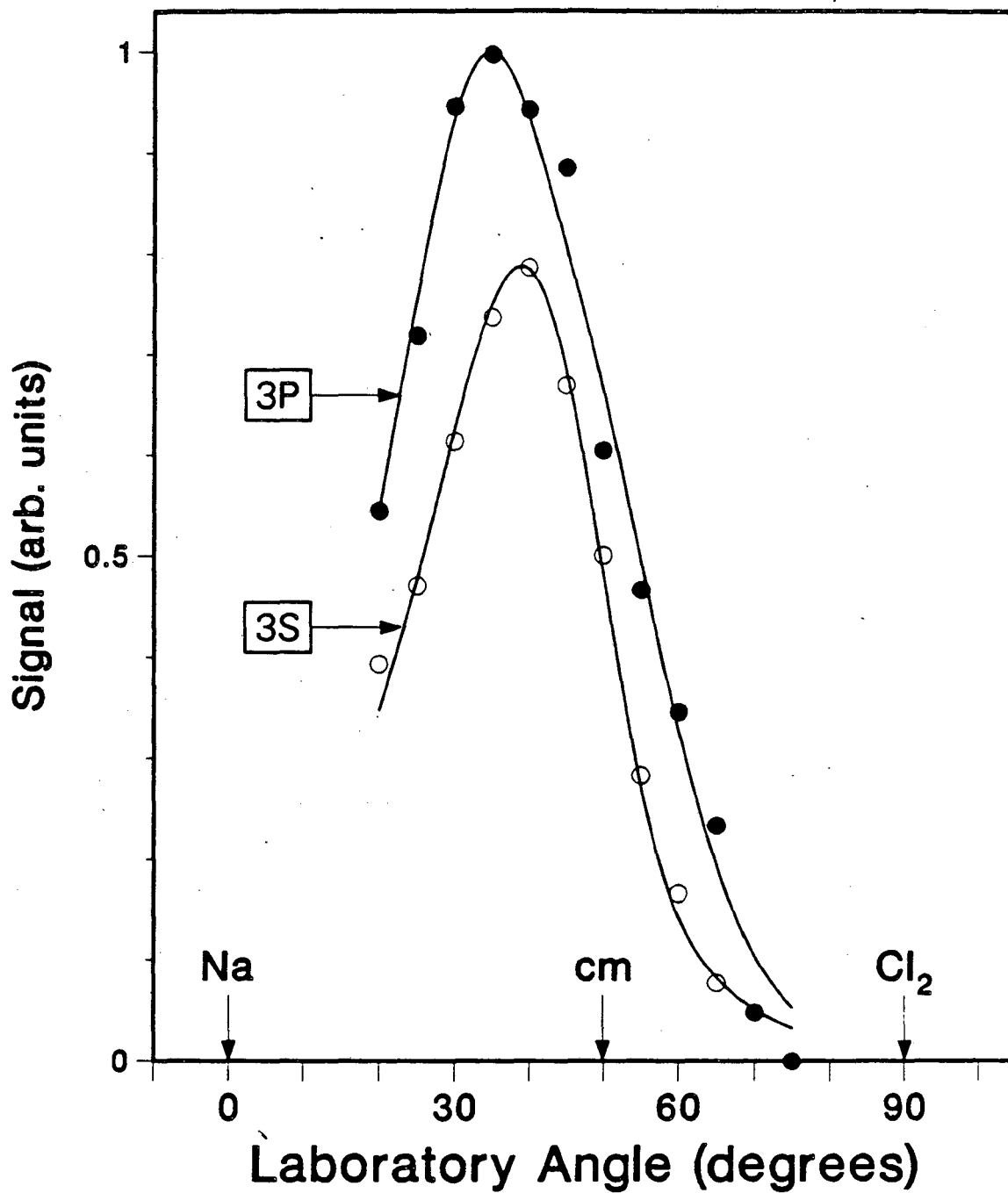
The single center-of-mass angular distribution derived by Grice and Emedocles for $\text{K,Rb,Cs} + \text{Cl}_2$ at collision energies under 1 kcal/mole was unable to fit the measured angular distributions for $\text{Na} + \text{Cl}_2$.

The best fits to the laboratory angular distributions for $\text{Na}(3S,3P) + \text{Cl}_2$ at a collision energy of 6 kcal/mole are shown in figure 11. The center-of-mass angular distributions ($T(\theta)$) derived



XBL 863-872

Fig. 10. NaCl product angular distributions recorded at $m/q=58$ (NaCl^+) for $\text{Na}(3\text{S},3\text{P}) + \text{Cl}_2$ at a collision energy of 19 kcal/mole. The sodium beam is seeded in helium, and the chlorine beam is neat.



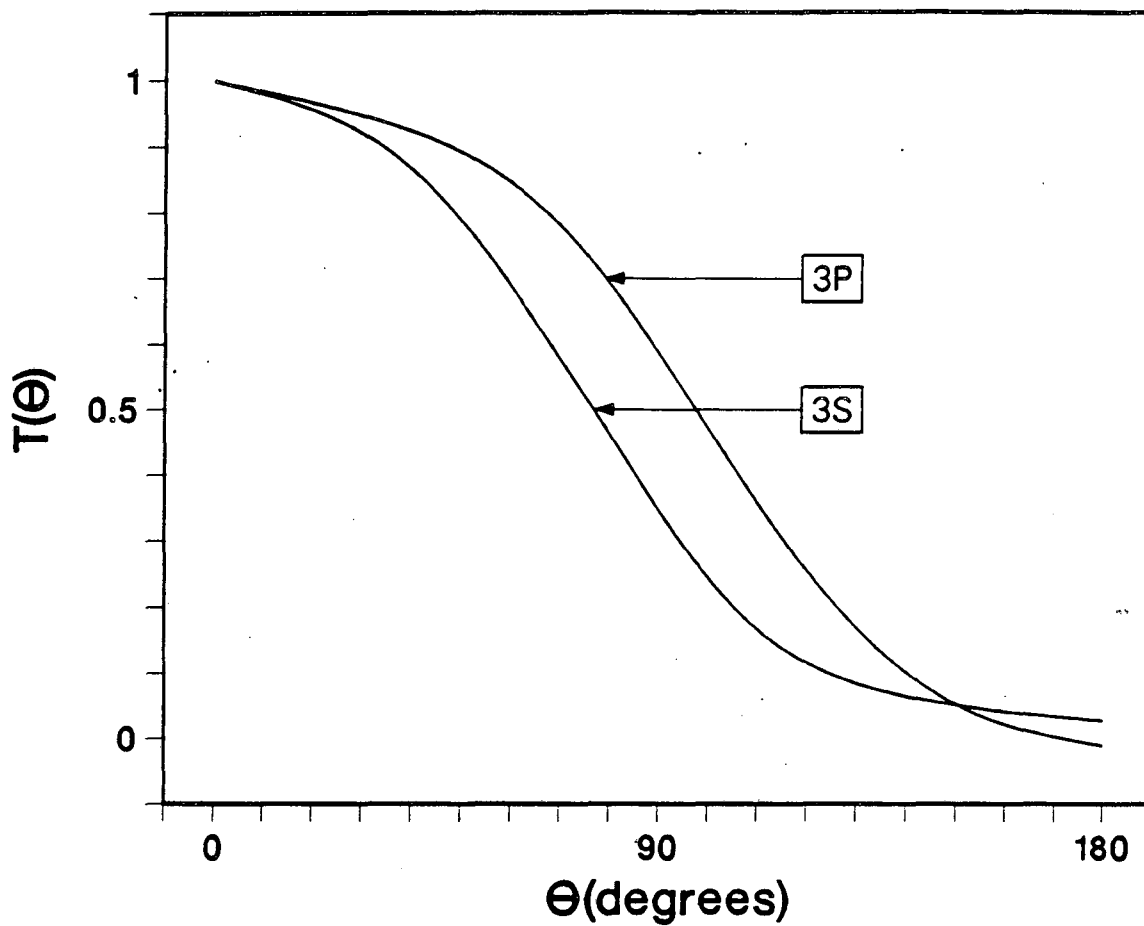
XBL 862-559

Fig. 11. Best fits to the laboratory angular distributions for $\text{Na}(3\text{S},3\text{P}) + \text{Cl}_2$ at a collision energy of 6 kcal/mole. The solid lines are the fit to the data.

for these fits are shown in figure 12. Significantly different recoil energy distributions ($P(E)$) were required to fit each, and these are shown in figures 13a and b for $\text{Na}(3\text{S},3\text{P}) + \text{Cl}_2$, respectively. With increasing electronic energy the peak recoil energy moves out to higher energy. The peak recoil energies are 0.6 and 1.2 kcal/mole for $\text{Na}(3\text{S},3\text{P}) + \text{Cl}_2$, respectively, at this collision energy. The total cross section for the reaction of the $\text{Na}(3\text{P})$ atoms is 58% higher than that for $\text{Na}(3\text{S})$ at a collision energy of 6 kcal/mole.

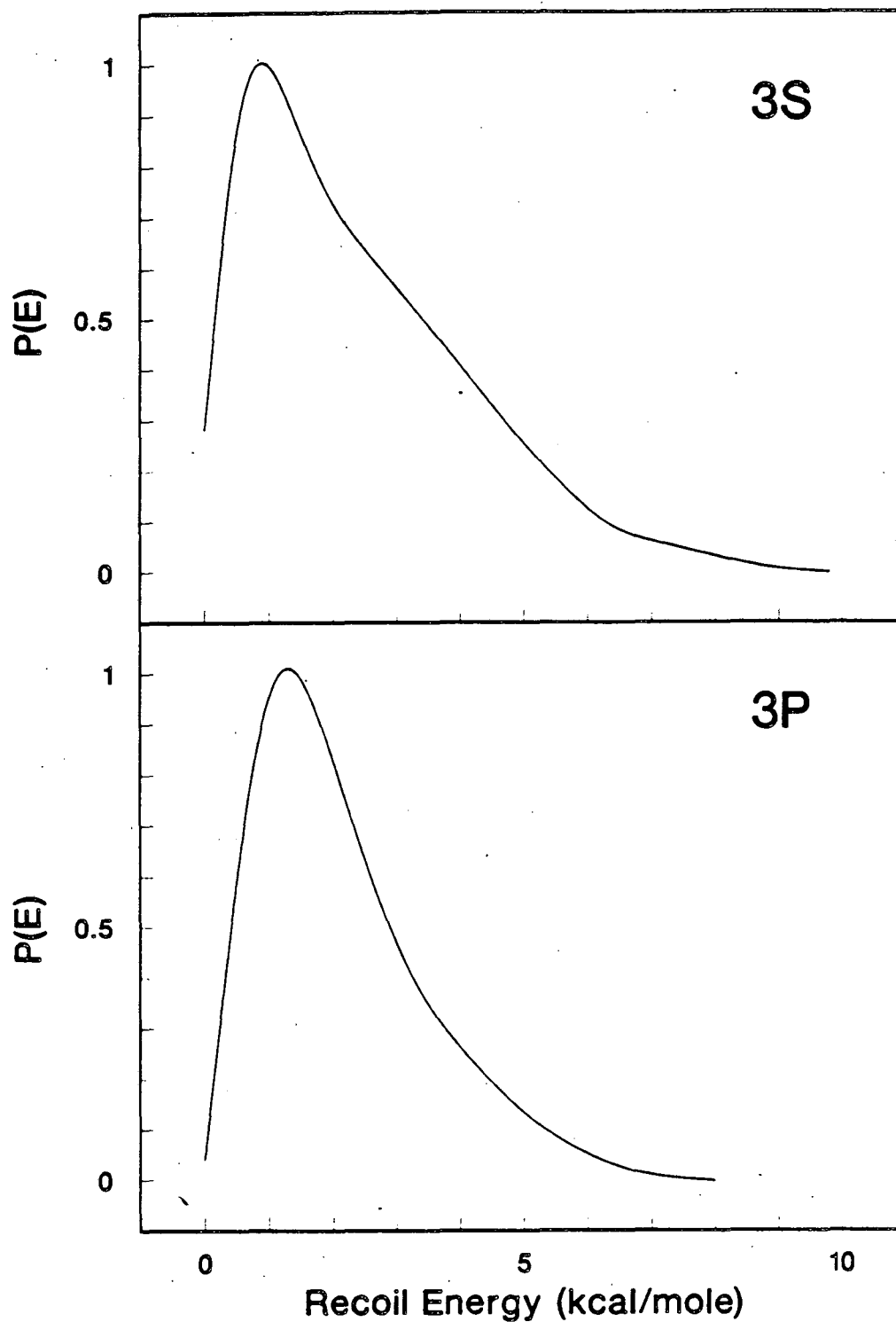
The best fits to the laboratory angular distributions for $\text{Na}(3\text{S},3\text{P}) + \text{Cl}_2$ at a collision energy of 19 kcal/mole are shown in figure 14. The center-of-mass angular distributions are shown in figure 15. The recoil energy distributions are shown in figures 16a and b for $\text{Na}(3\text{S},3\text{P}) + \text{Cl}_2$, respectively. With increasing electronic energy, the peak recoil energy once again moves out to higher energy, from 0.8 and 1.0 kcal/mole for $\text{Na}(3\text{S},3\text{P}) + \text{Cl}_2$, respectively. The relative total reaction cross section for $\text{Na}(3\text{P})$ is 16% higher than for $\text{Na}(3\text{S})$ at this collision energy.

A summary of some of the features of the four fits is given in table II. It can be seen that the center-of-mass angular distributions are somewhat wider for the reaction of $\text{Na}(3\text{P})$ than those for $\text{Na}(3\text{S})$. Also, as mentioned above, the peak recoil energies increase in going from $\text{Na}(3\text{S})$ to $\text{Na}(3\text{P})$. It should be noted that the column labeled "Percent Forward Scattered" gives the fraction of the weighted intensity, $T(\theta)\sin\theta$, that is in the forward hemisphere.



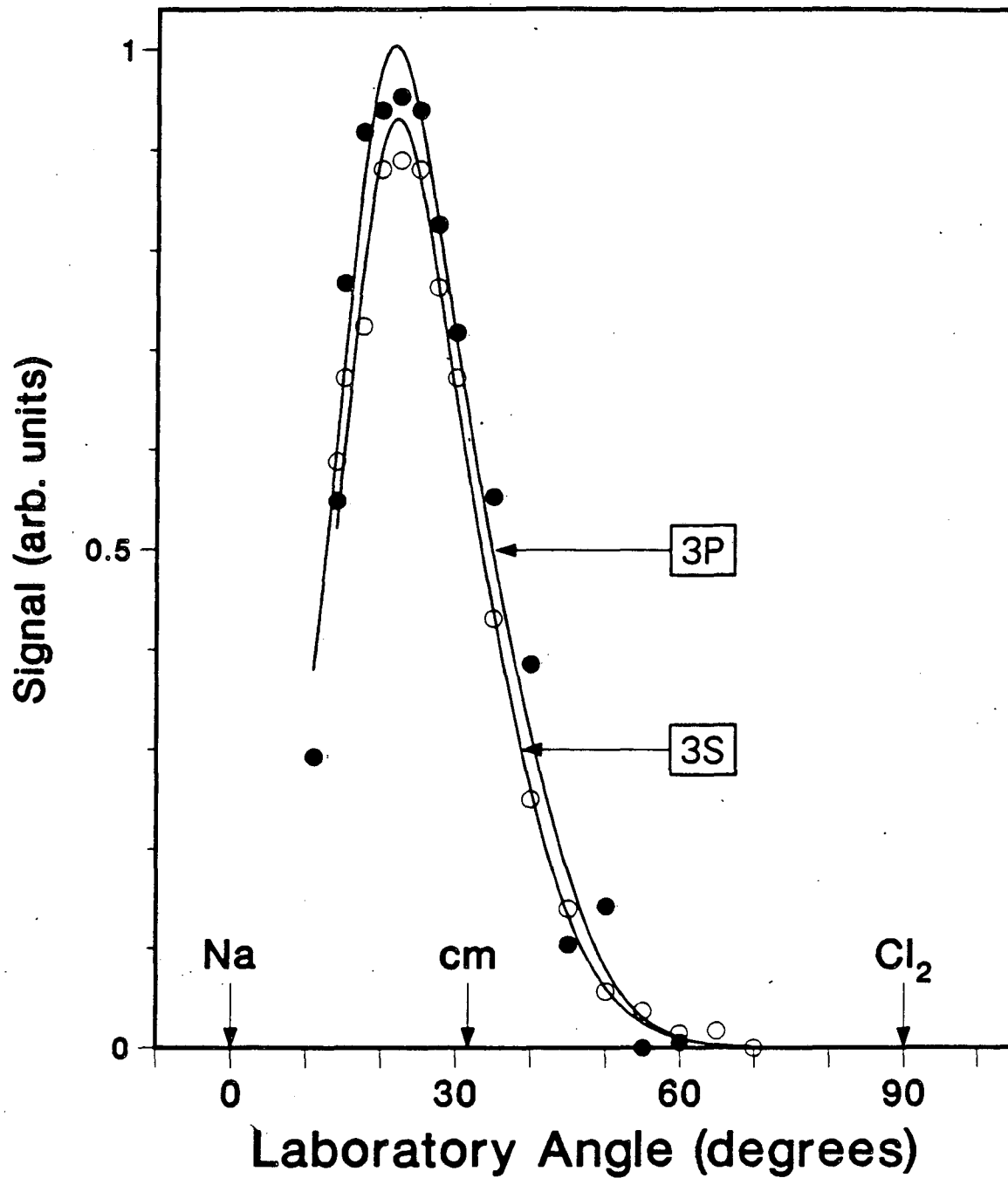
XBL 862-662

Fig. 12. Center-of-mass angular distributions used for the fits in figure 11 of $\text{Na}(3\text{S},3\text{P}) + \text{Cl}_2 \rightarrow \text{NaCl} + \text{Cl}$ at a collision energy of 6 kcal/mole.



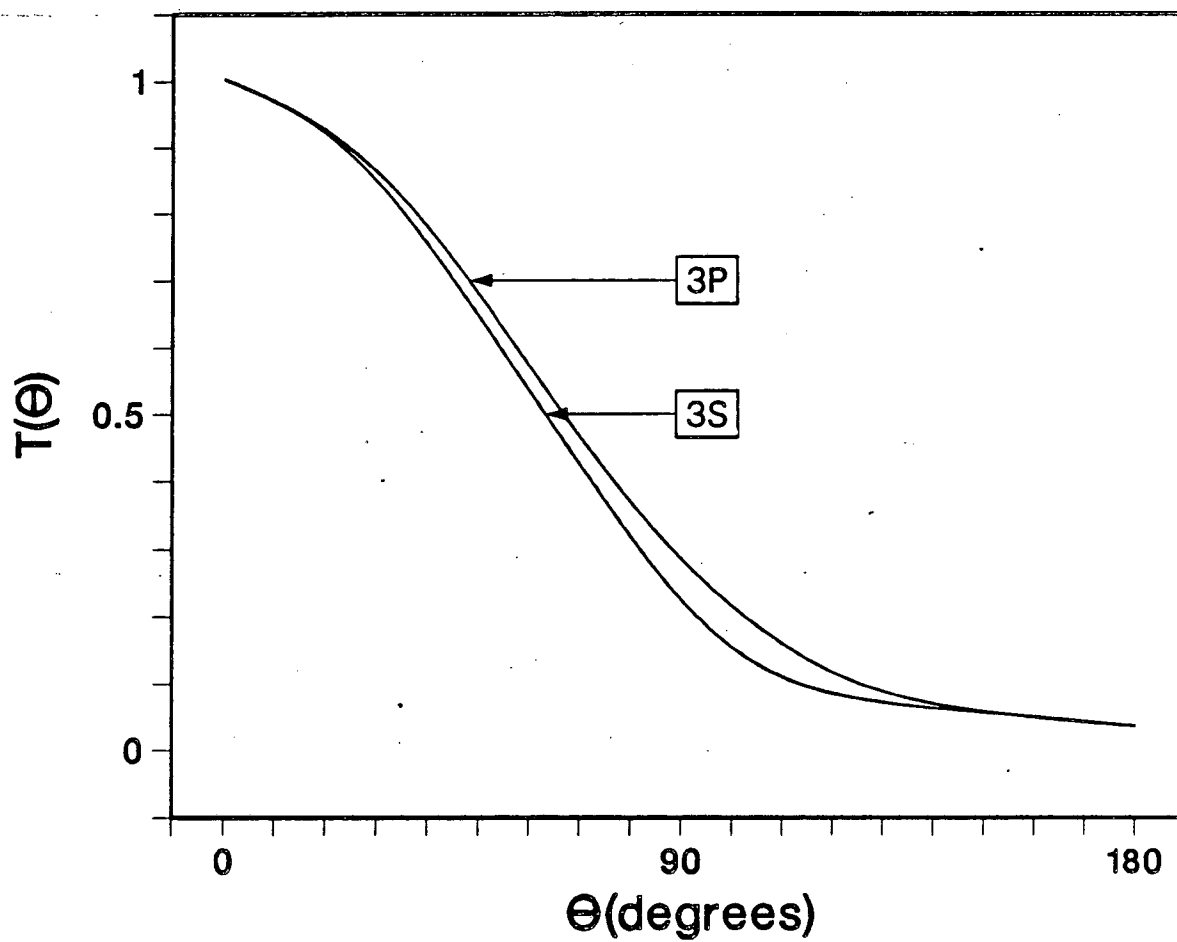
XBL 863-753

Fig. 13. Product recoil energy distributions for the fits in figure 11 of Na(3S,3P) + Cl₂ at a collision energy of 6 kcal/mole.



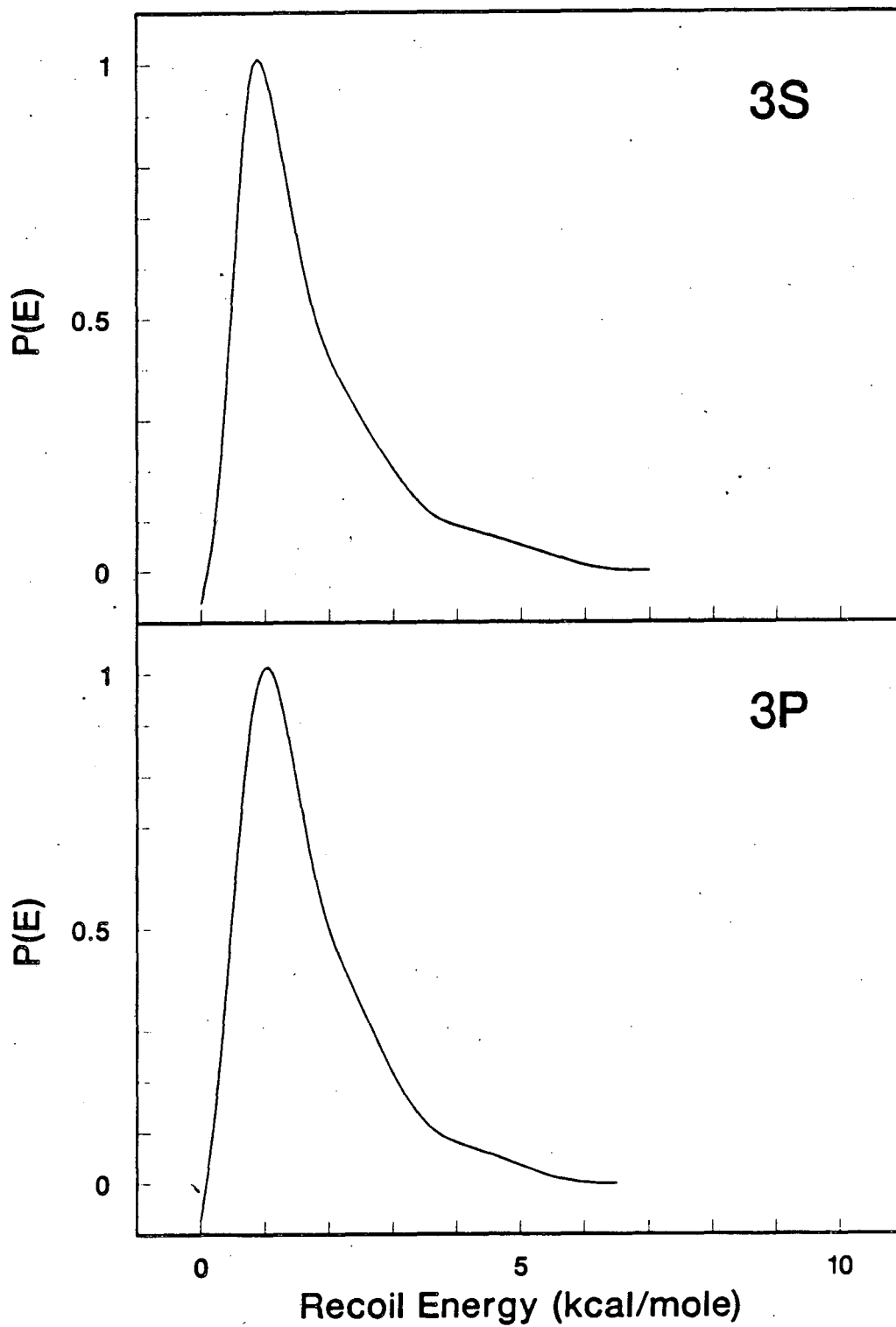
XBL 862-667

Fig. 14. Best fits to the laboratory angular distributions for $\text{Na}(3\text{S},3\text{P}) + \text{Cl}_2$ at a collision energy of 19 kcal/mole. The solid lines are the fit to the data.



XBL 862-668

Fig. 15. Center-of-mass angular distributions used for the fits in figure 14 of $\text{Na}(3\text{S},3\text{P}) + \text{Cl}_2 \rightarrow \text{NaCl} + \text{Cl}$ at a collision energy of 19 kcal/mole.



XBL 863-752

Fig. 16. Product recoil energy distributions for the fits in figure 14 of Na(3S,3P) + Cl₂ at a collision energy of 19 kcal/mole.

Table II. A summary of features of the center-of-mass distributions fitted to the laboratory angular distributions for Na(3S,3P) + Cl₂. All energies are in kcal/mole.

<u>Na Level</u>	<u>E_{coll}</u>	<u>FWHM of T(θ)</u>	<u>% Forward Scattered</u>	<u>Peak Recoil Energy</u>	<u>σ(3P)/σ(3S)</u>
3S	6.	76°	83	0.6	1.58
3P	6.	97°	76	1.2	
3S	19.	64°	85	0.8	1.16
3P	19.	68°	82	1.0	

As in chapter II, the total reactive cross section can be determined by calibrating the reactive scattering to the small angle elastic scattering. This is done using the small angle approximation to the classical scattering from a van der Waals r^{-6} potential,^{6,43} equation (8) of chapter II. As in chapter II, the van der Waals C_6 constant can be estimated using the Slater-Kirkwood formula,^{44,45} equation (10) of chapter II. The polarizability of Cl₂ is $\alpha=4.61 \text{ \AA}^3$,⁴⁶ and its number of valence electrons is $N(\text{Cl}_2)=14$. This yields a C_6 constant for ground state Na(3S) of 7410 kcal/mole \AA^6 , using the polarizability of ground state Na $\alpha(\text{Na})=24.5 \text{ \AA}^3$ as given in chapter II.⁴⁷ This agrees well with the theoretical value derived by Anderson and Herschbach for Na-Cl₂, $C_6=7460 \text{ kcal/mole \AA}^6$.⁴⁸ The C_6 constant determined for elastic scattering of the Na($3^2P_{3/2}$) atoms by Cl₂ is 11340 kcal/mole \AA^6 as derived from the polarizability of the excited atom $\alpha(\text{Na}(3^2P_{3/2}))=53.6 \text{ \AA}^3$.^{49,50} The ionization cross section of Na by 200 eV electrons is 2.1 \AA^2 .⁵¹ It was assumed that all NaCl

Table III. Total reactive cross sections for $\text{Na}(nL) + \text{Cl}_2 \rightarrow \text{NaCl} + \text{Cl}$ at a collision energy of 6 kcal/mole.

<u>Sodium Level</u>	<u>Using 3S Scaling Factor</u>	<u>Using 3P Scaling Factor</u>	<u>Average of Two Values</u>
3S	79 Å ²	64 Å ²	72 Å ²
3P	124 Å ²	101 Å ²	113 Å ²

produced was vibrationally excited, so that the ionization cross section of the NaCl to Na^+ ($m/q=23$) was $\sigma'=3.8 \text{ \AA}^2$ as in chapter II.⁵² This gives a relative detection efficiency of 1.8 for $\text{Eff}(\text{NaCl}^+)/\text{Eff}(\text{Na})$. The low angle elastic scattering is then fit and scaled to the distribution given by formula (8) of chapter II. The scaling factors derived are used to determine the total reactive cross sections given in table III. As described in chapter I, it was assumed that 20% of the Na atoms are excited to the 3P level. Note that it is not possible to use the hard sphere elastic scattering approximation to calculate the reactive cross section as the large angle elastic scattering is depleted by reaction.

D. Discussion

All the laboratory angular distributions peak at angles higher than the spectator stripping angles. From (1), using the most probable beam velocities at each energy, the spectator stripping angles, θ_s , are 41° , 31° , and 17° for collision energies of 3, 6, and 19 kcal/mole, respectively. As discussed in section A, if the finite vibrational temperature of Cl_2 is considered, these angles shift to still lower values. Since the neutral-ionic curve crossing moves to larger distances for electronically excited Na, it would be expected that the NaCl product would be scattered more in the forward direction. While the recoil energy distribution does increase, moving the peak in the angular distribution closer to the spectator stripping angle, the center-of-mass angular distributions are actually wider for the reaction of the Na(3P) atoms. This is consistent with the idea that if the transfer takes place at longer range, there is less interaction of the Na and the Cl_2 before the transfer. Then there is a greater energy release due to the dissociation of the Cl_2^- higher up on the repulsive wall of its potential surface. This is inconsistent with the DIPR model calculation's prediction that without secondary interactions (MX-X) no preference for forward scattering will be observed.

The shift of the center-of-mass angular distributions to more forward scattering with increasing collision energy was observed, corroborating the results of Grice and coworkers.^{11,12} The

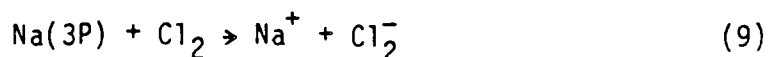
Table IV. The calculated crossing radii and electron transfer cross sections for the Na(3S,3P) + Cl₂ interaction. The adiabatic (Adia) electron affinity of Cl₂ is 2.39 eV,⁴¹ and the vertical (Vert) electron affinity of Cl₂ is taken to be 0.7 eV.²⁴

<u>Sodium Level</u>	<u>Ionization Potential</u>	<u>Crossing Radius</u> r_c		<u>Estimated Electron Transfer Cross Section</u>	
		<u>Adia</u>	<u>Vert</u>	<u>Adia</u>	<u>Vert</u>
3S	5.138 eV	5.22 Å	3.2 Å	86 Å ²	32 Å ²
3P	3.033 eV	22.3 Å	6.2 Å	1560 Å ²	121 Å ²

center-of-mass angular distributions are all wider than the distribution derived by Grice and Emedocles for K, Rb, Cs + Cl₂.⁸ It is possible that at low collision energies this distribution is also inadequate for Na + Cl₂, but that was not determined here.

The reaction cross section does increase with electronic excitation at low collision energy, but not as much as the estimates of the crossing of the neutral and ionic potential curves would predict. The crossing radii (r_c) and estimated reactive cross sections (σ_R), calculated as discussed in chapter II, are given in table IV. The adiabatic electron affinity of Cl₂ was taken to be 2.39 eV.⁴¹ The vertical electron affinity of Cl₂ from reference 24 is approximately 0.7 eV. In a study of the cross sections of the reactions of alkali

atoms with halogen molecules, Maya and Davidovitz found that the measured effective (reactive) electron affinity of Cl_2 was 1.6 eV,²⁶ however, as they point out, this is certainly an overestimate because the Cl_2 in their experiments was at 1015°K, allowing the thermal population of several vibrational levels. Excited vibrational levels will have significantly greater electron affinities than $v=0$ due to the steep slope of the Cl_2^- repulsive wall in this region, as seen in figure 2. This smaller than expected increase in reactivity is due to the small electron transfer probability at long range ($r_c > 10 \text{ \AA}$). Recall from chapter III that many Cl_2 vibrations occur during a collision at these energies, so that the electron affinity of the Cl_2 is effectively modulated, giving the possibility of electron transfer each time the covalent and ionic potential energies become comparable. At very long range the interaction of the states is so small that electron transfer does not occur. On closer approach, the effective electron affinity has decreased, and the interaction of the states is smaller, so that if electron transfer occurs, it reaches higher on the repulsive wall of the Cl_2^- potential curve, giving higher recoil energies. These higher recoil energies are observed, but are a relatively small effect. A further explanation for the cross section not rising up to the harpoon limit for the $\text{Na}(3P)$ reaction is that other processes involving electron transfer, such as quenching via electron transfer back to the Na atom, could be taking place. More likely is that electron transfer is taking place, that is



which becomes energetically accessible at a collision energy of 15 kcal/mole. Also, as discussed in section A, one third of the atoms have a symmetry for which there is little or no interaction with the ionic state necessary for electron transfer. The effects of tracking may be important in the smaller increase in the cross section at the higher collision energy. Additionally, since the relative velocities are higher, the collision times are shorter, and there are then fewer crossings of the "oscillating" potential curves (see above). There is also less time for the "prestretching" of the Cl_2 bond, which has the effect of increasing the Cl_2 electron affinity, and thus increasing the reactive cross section.

Maya and Davidovitz have performed careful measurements of the cross sections of the reactions of alkali atoms with halogen molecules at thermal energies in a gas cell.^{26,30} The value that they derive for $\text{Na} + \text{Cl}_2$ at a mean collision energy of 1.6 kcal/mole is $\sigma_R = 124 \text{ \AA}^2$, with a reported absolute accuracy of $\pm 15\%$.³⁰ By comparison, the value obtained here for the ground state, 72 \AA^2 , is qualitatively consistent with the drop-off of cross section observed by van der Meulen et al.¹³ The limited accuracy of this measurement precludes quantitative comparisons, but at a collision energy of 6 kcal/mole, van der Meulen et al. saw a 20% decrease in the cross section of $\text{K} + \text{Br}_2$ from the thermal energy value.

The low collision energy increase in cross section is in line with the quenching cross section expected for $\text{Na}(3P)$ from the experiments of Bersohn, Herm, and coworkers described in section A. The small increase

in cross section at higher collision energy implies that some other mechanism, such as charge transfer (9), is responsible for the quenching of the Na(3P) excitation.

The fact that the recoil energy distributions change little upon excitation to Na(3P) implies that only a small fraction of the available energy goes into product translational energy with increasing electronic energy. This is consistent with the naive expectations of the dynamics. That is, after electron transfer, the molecular halogen ion (X_2^-) immediately begins to dissociate and the alkali ion (M^+) and the halide ion (X^-) are drawn together. If the electron transfer occurs at longer range, the M^+ and X^- ions start out further apart, and thus more energy goes into the vibrational and rotational energy of the MX molecule. The small differences in the distributions could possibly be attributed to more Cl_2^- repulsion due to electron transfer inside the first crossing of the covalent and ionic curves, and thus higher up on the Cl_2^- repulsive wall.

E. Conclusions

The cross section of the $Na + Cl_2$ reaction does not increase as much as the simple harpoon mechanism transfer predicts upon excitation of the Na atom. A larger increase of the cross section for Na(3P) reaction is observed for the reaction at 6 kcal/mole, than at 19 kcal/mole

collision energy. This relates to the small interaction of the covalent and ionic states at long range.

The product recoil energy distributions change little with reagent Na electronic energy, and nearly all electronic energy must be converted into the internal energy of the product NaCl. The release of the alkali and halide ions at larger separation leads to the deposition of nearly all the electronic energy into the rotational and vibrational energy of the product alkali halide molecule. The small broadening of the center-of-mass angular distributions and increase of the product recoil energy with electronic excitation observed are attributable to slightly more repulsive energy release in the Cl_2^- dissociation.

Finally, while these reactions studied do not reach the spectator stripping limit, their general behavior is well described by the more general stripping mechanism.

F. References

1. M. Polanyi, Atomic Reactions (Williams and Northgate, London, 1932).
2. S. Datz and R. E. Minturn, J. Chem. Phys. **41**, 1153 (1964).
3. K. R. Wilson, G. H. Kwei, J. A. Norris, R. R. Herm, J. H. Birely, and D. R. Herschbach, ibid., 1154 (1964).
4. A. E. Grosser and R. B. Bernstein, J. Chem. Phys. **43**, 1140 (1965).
5. R. E. Minturn, S. Datz, and R. L. Becker, J. Chem. Phys. **44**, 1149 (1966).
6. J. H. Birely and D. R. Herschbach, ibid., 1690 (1966).
7. J. H. Birely, R. R. Herm, K. R. Wilson, and D. R. Herschbach, J. Chem. Phys. **47**, 993 (1967).
8. R. Grice and P. Empedocles, J. Chem. Phys. **48**, 5352 (1968).
9. D. D. Parrish and R. R. Herm, J. Chem. Phys. **51**, 5467 (1969).
10. K. T. Gillen, A. M. Rulis, and R. B. Bernstein, J. Chem. Phys. **54**, 2831 (1971).
11. J. C. Whitehead, D. R. Hardin, and R. Grice, Mol. Phys. **23**, 787 (1972).
12. S.-M. Lin, D. J. Mascord, and R. Grice, Mol. Phys. **28**, 975 (1974).
13. A. van der Meulen, A. M. Rulis, and A. E. deVries, Chem. Phys. **7**, 1 (1975).
14. C. M. Scholeen, L. A. Gundel, and R. R. Herm, J. Chem. Phys. **65**, 3223 (1976).

15. R. R. Herm, in Alkali Halide Vapors: Structure, Spectra, and Reaction Dynamics, 189 (Academic Press, New York, 1979), and references therein.
16. J. L. Kinsey, MTP Int. Rev. Sci., Phys. Chem. Ser. One 9, 173 (1972), and references therein.
17. J. L. Magee, J. Chem. Phys. 8, 687 (1940).
18. D. R. Herschbach, Appl. Opt. Suppl. 2, 128 (1965).
19. J. C. Polanyi, Disc. Faraday Soc. 44, 293 (1967).
20. P. J. Kuntz, E. M. Nemeth, and J. C. Polanyi, J. Chem. Phys. 50, 4607 (1969).
21. P. J. Kuntz, M. H. Mok, and J. C. Polanyi, ibid., 4623 (1969).
22. The strength of the electric field at 7 Å was incorrectly reported as 3×10^9 V/cm in reference 6, but was corrected to 3×10^7 V/cm in reference 7.
23. A. C. Riviere, D. R. Sweetman, Phys. Rev. Lett. 5, 560 (1960).
24. T. L. Gilbert and A. C. Wahl, J. Chem. Phys. 55, 5247 (1971).
25. See Chapter II of this thesis.
26. J. Maya and P. Davidovitz, J. Chem. Phys. 59, 3143 (1973).
27. R. W. Anderson, Ph. D. Thesis, Harvard University, Cambridge, Massachusetts (1968).
28. R. Grice, Ph. D. Thesis, Harvard University, Cambridge, Massachusetts (1967).
29. R. Grice and D. R. Herschbach, Mol. Phys. 27, 159 (1974).
30. J. Maya and P. Davidovitz, J. Chem. Phys. 61, 1082 (1974).

31. P. Davidovits, in Alkali Halide Vapors: Structure, Spectra, and Reaction Dynamics, 331 (Academic Press, New York, 1979).
32. J. A. Aten and J. Los, Chem. Phys. 25, 47 (1977).
33. J. Los and A. W. Kleyn, in Alkali Halide Vapors: Structure, Spectra, and Reaction Dynamics, 275 (Academic Press, New York, 1979).
34. R. Bersohn, ibid., 345.
35. L. E. Brus, J. Chem. Phys. 52, 1716 (1970).
36. R. Bersohn and H. Horwitz, J. Chem. Phys. 63, 48 (1975).
37. B. L. Earl and R. R. Herm, J. Chem. Phys. 60, 4568 (1974).
38. S.-M. Lim and R. E. Weston, J. Chem. Phys. 65, 1443 (1976).
39. R. P. Mariella, Jr., J. Chem. Phys. 76, 2965 (1982).
40. Calculated from diatomic molecular dissociation constants (D_0^0) given in reference 41.
41. F. P. Huber and G. Herzberg, Molecular Spectra and Molecular Structure, IV. Constants of Diatomic Molecules, Van Nostrand Reinhold, Co., New York, New York (1979).
42. M. F. Vernon, H. Schmidt, P. S. Weiss, M. H. Covinsky, and Y. T. Lee, J. Chem. Phys., to be published, and M. F. Vernon, Ph. D. Thesis, University of California, Berkeley, Berkeley, California (1983).
43. E. A. Mason, J. T. Vanderslice, and C. J. G. Raw, J. Chem. Phys. 40, 2153 (1964).
44. J. C. Slater and J. G. Kirkwood, Phys. Rev. 37, 682 (1931).
45. K. S. Pitzer, Adv. Chem. Phys. 2, 59 (1959).

46. J. O. Hirschfelder, C. F. Curtiss, and R. B. Bird, Molecular Theory of Gases and Liquids (John Wiley and Sons, Inc., New York, 1964).
47. H.-J. Werner and W. Meyer, Phys. Rev. A **13**, 13 (1976).
48. R. W. Anderson and D. R. Herschbach, J. Chem. Phys. **62**, 2666 (1975).
49. P. Hannaford, W. R. MacGillivray, and M. C. Standage, J. Phys. B: Atom Molec. Phys. **12**, 4033 (1979).
50. H. T. Duong and J.-L. Picque, J. Physique **33**, 513 (1972).
51. R. H. McFarland and J. D. Kinney, Phys. Rev. **137**, A1058 (1965).
52. This is derived by assuming 90% fragmentation of NaCl to Na⁺ in the electron bombardment ionizer, and by estimating the ionization cross section of NaCl from that of Ar using their relative polarizabilities.

VI. CONCLUSIONS

A. Conclusions on the Reaction Dynamics of Electronically Excited Alkali Atoms

Representatives of four families of excited alkali atom reactions have been studied in crossed molecular beams. In the cases where electrons can effectively dissociate the molecular reaction partner, as in alkali atoms with methyl halide and halogen molecules, the simple ideas of the product repulsion qualitatively describe the reactions well. The very small changes in the reactivity and mechanism in these cases were surprising, but can be understood in terms of two competing effects. The lowered ionization potential of the excited states of Na has the tendency to make the upper states "super-reactive," but the shift of the crossing of the potential curves to larger separation reduces the interaction of the neutral and ionic states, and makes the excited states less reactive than they would otherwise be. This can be seen clearly in the case of $\text{Na}(3P,4D,5S) + \text{HCl}$. The first excited state does not proceed via long range electron transfer, because the crossing point of the neutral and ionic curves is small enough that the NaCl molecule is formed before the HCl^- repulsion can play a role, and it is the NaCl-H repulsion that dominates the product scattering. When the ionization potential of the Na atoms is lowered further by subsequent excitation to $\text{Na}(4D,5S)$, the reaction becomes more like the

electron transfer reactions, and the HCl^- repulsion dominates the scattering. While these states are not "super-reactive," they are more reactive than the ground and first excited states.

On the other hand, in $\text{Na} + \text{O}_2$ the importance of orbital symmetry on the reaction dynamics is clearly apparent. Here the neutral chemical pathway is certainly a minor process. Nonetheless, it exhibits very unusual behavior, having a threshold to reaction, very small product recoil energies, and very specific angular scattering. As pointed out in chapter 3, measurements of the other processes taking place should certainly be performed, as well as further measurements of what was observed. Of particular interest would be a spectroscopic study of the products, first to prove their identity, and second to identify where the large amount of internal energy has been deposited. Also of interest would be the measurement of the ionic products, and the transition state symmetry required for those processes.

Future investigations should elucidate more of the important features of the transition states in these excited state reactions that are so complicated by the large number of potential energy surfaces involved.

VII. APPENDICES

A. Data Acquisition for Angular Distributions, Polarization Dependences, and Machine Condition Optimization: The Data Acquisition System and Program SANG

1. Introduction to the Data Acquisition System

The data acquisition system is comprised of four types of electronics: NIM standard modules,¹ CAMAC standard modules,² and Q-Bus standard boards,³ as well as some stand alone devices. As discussed in chapter I, data signals are received from two or three photomultipliers -- one photomultiplier tube (RCA 8850⁴) that monitors the signal from the mass spectrometer, and one or two photomultipliers (RCA 1P28⁴) on the fluorescence monitors. A further description of exactly what these measure can be found in chapter I. The gating and timing for the various electronics are derived from the 150 Hz tuning fork chopper used to modulate the secondary molecular beam.

A map of the electronics can be found in figure 1. The tuning fork chopper signal is input to a Timer-Gater module (LBL 13X-3050 II). This uses a variable phase and a variable gate width to output two gate pulses "A" and "B," which correspond to the secondary beam on and off, respectively. The Timer-Gater module can be started and reset using a parallel line unit (DEC DRV-11⁵) on the Q-Bus of the controlling minicomputer (DEC LSI-11/23⁵). The gate width is set by matching

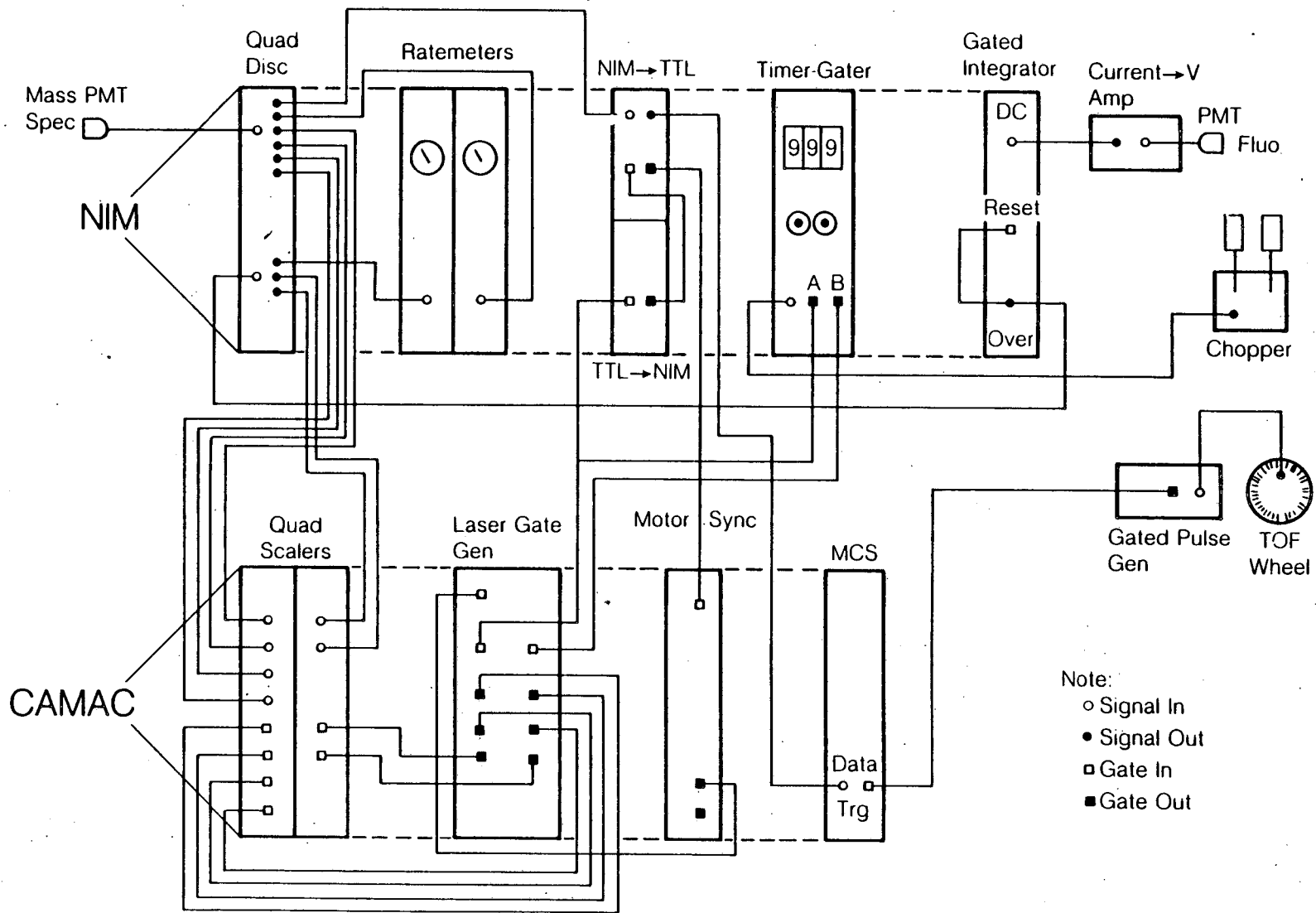


Fig. 1. Schematic of the data acquisition electronics.

XBL 861-10008

the width of the A and B pulses to the minimum of the measured beam on and off times. This measurement is made with the mass spectrometer and the time-of-flight program described in appendix B. The phase is coarsely set so as to maximize the mass spectrometer signal to noise ratio for beam on vs. beam off when looking directly into the secondary beam. The phase is later fine tuned on the reactive signal. Both of these optimizations are done using Test mode of program SANG, described below.

The A and B outputs go to a CAMAC powered Laser Gate Generator (Lawrence Berkeley Laboratory), built by Matt Vernon, Jim O'Brien, and Fred Vogelsberg. The A output is also sent to a CAMAC powered Motor Sync Scaler (LBL 13X3441-P1-A), which just divides down the A pulses by 25 giving pulses at 6 Hz. The Motor Sync Scaler output pulse goes to the Laser Gate Generator which has outputs to a stepper motor controller which changes the state of the laser beam flag, as described in chapter I. The Laser Gate Generator also outputs six gate levels corresponding to the detector signals described in chapter I. These go to two CAMAC Quad Scalers (Joerger S1-Ind⁶) which are read by the computer via the CAMAC dataway.

2. Introduction to Program SANG

Program SANG is designed to be used for machine condition optimization, and for recording angular distributions and polarization dependences. Because of this, there are several modes of data acquisition in which program SANG operates. These are designed to be

flexible enough to allow for any circumstances that could take place during an experiment, without the necessity of exiting and restarting the program. Along these lines, comments and machine conditions can be written directly to the data file and hard copy printer output, laboratory notebook style, data files can be closed, and new files begun. One function that does not exist is the deletion of data already recorded. Subsequent comments should be sufficient to mark bad points for later editing. The program has the facility (although not included in the listing below) of measuring the Doppler profile of the $\text{Na}(D_2)$ transition at 45° and 90° laser crossings (as described in chapter I) automatically, and thus directly recording the velocity and speed ratio of the sodium beam.

The program is designed to be nearly independent of the hardware described in section 1 so that only minor changes would be needed to the MACRO subroutines in the file SANGLE.MAC to accommodate hardware changes. Everything else such as the number and definitions of data channels recorded can be modified while running SANG (using command DC). All of the gating of the data channels is done in hardware and SANG in no way depends upon this.

Commands are read from the console using "special screen mode" which is accessed by setting bit 12 in the job status word (see MACRO subroutines ENSPEC and EXSPEC).⁷ All commands are one or two letters. There are help screens describing each set of commands. As the various functions of the program are described below, the commands relating to those functions are listed. Refer to the program listing

or the help screens for more complete discussions of the commands described.

Data Acquisition Modes

The various modes of data acquisition are described below. Of course there is a great deal of overlap between each of the modes. The only real differences between modes are in the outermost shells of control in which the data acquired at different points are linked together, and the points at which data are recorded are chosen according to the loop specific to that mode. A flag word (IFLAG in subroutines SDONE and SWRITE) is written to the data file on disk to specify under which mode each data point was recorded. The definition of this word is given in subroutine SDONE.

Single Point Data Acquisition:

The simplest mode of data acquisition is the recording of a single point, with the user deciding where to proceed after each point. This is available through the commands CA, CI, and RD, which choose the angle to be measured, and the countdown interval, and start the countdown, respectively.

Normalization Mode:

After a certain number of points are recorded (often 10), data is recorded at a certain angle multiple times (often two or four) in order to allow for a correction for long term drifts in machine conditions.

This is usually done in single point mode above, as well as loop mode, described below. The angle and interval at which data are recorded for normalization purposes are chosen with the commands NA and NI, respectively, as well as with NP and CN. The command NR determines how many times the data is acquired at the normalization point. After the requisite number of Timer-Gater countdowns, the user is queried as to whether the whole series of normalization countdowns should be repeated. This is especially useful where some optimization is done; a second set of normalization points provides a new starting point for normalizing data, and a direct comparison of data from before and after optimization.

Loop Mode:

It is often useful to record data over an angular range, with a certain angular interval. The mass spectrometer is moved back and forth across the range, and the data recorded is normalized to a single value (see normalization mode above). All of the angular distributions reported in chapters II-V were recorded in this way using loop mode. The loop mode parameters can be set with the commands LA, LB, LD, LE, LI, LN, LP and CL. The loop can be started and continued with the commands LS and LC, respectively. Note that normalization mode can be called from within loop mode, and is automatically called at the beginning of a loop. The parameters can be changed during the loop to expand or contract the loop, etc.

Rotate Polarization Mode:

When lasers are used to optically prepare an excited state for reaction, as shown in chapters II and III it can be interesting to measure the polarization dependence of the various signals recorded at fixed detector angles. Rotate polarization mode can be used to measure the differences produced by left and right circularly polarized light or the dependences as the electric vector of linearly polarized light is rotated. The command RA changes the laboratory detector angle at which the polarization scan is recorded while the command RM changes the step size for the polarization rotator; the command RP changes both. The command RS starts a polarization scan. The data is stored in such a way that the detector and laser polarization angles can be easily determined. The angle written to disk is:

$$\text{Angle} = \theta_{\text{LAB}} + \frac{\phi_{\text{POLAR}}}{10000}, \quad (1)$$

where θ_{LAB} is the laboratory detector angle and ϕ_{POLAR} is the laboratory polarization angle as described above. Thus if the detector is at 45° and the laser polarization angle is 90° (the electric vector of the laser/lasers is 90° from vertical in the laboratory), the angle written to disk would be 45.0090° . Left and right circularly polarized light have values of 0° , 90° , and 180° . The polarization is rotated by a stepping motor (Superior Electric Co. Slo-Syn Synchronous Stepping Motor M062-FC09E⁸) that rotates a double fresnel rhomb polarization rotator (Spectra-Physics 310A⁹) as described in chapter I. The stepping motor is sent pulses by a CAMAC Pulse Generator (Kinetic Systems

3360¹⁰). All of the polarization dependences reported in chapters II and III were recorded with rotate polarization mode. Like loop mode, the polarization is rotated back and forth from 0° to 180°. The motor is only driven in one direction however and is accurate to better than 1° after over 100 full rotations. A separate display mode is available for viewing polarization data, and recording the data (using the small angular offset related to the laser polarization) as discussed above facilitates setting up this special display window.

Test Mode:

Machine optimization is accomplished by repeating the same measurement many times and optimizing the signal and/or the signal to noise ratio of a channel. To this end, test mode also has a special display window. In the same manner as the rotate polarization mode the data is recorded with a slight offset added to the detector angle. The data recorded in test mode is labeled sequentially and the angle recorded is then the detector angle plus an offset related to the number of the point recorded. This gives the test mode data point's angle as:

$$\text{Angle} = \theta_{\text{LAB}} + \frac{\text{Test Number}}{100000}, \quad (2)$$

in the data file. Typically various machine parameters are varied while the reactive signal is monitored and optimized at a particular detector angle at which signal is expected or known to occur. The

display is used to histogram the effect of the variation of each machine parameter. When the optimization is complete, the test mode data is zeroed (this can only be done in the accumulated data arrays, not in the data already written to disk) and/or a new data file is opened and the full data acquisition is begun. The commands TA, TI, and TN change the detector angle, the countdown interval, and the number of measurements for test mode, respectively. The commands TS and TC start and continue test mode data acquisition, respectively, while the command TE terminates test mode after the current countdown is completed.

Other Functions of Program SANG

The machine conditions -- detector settings, pressures, temperatures, etc. -- are recorded by the user and can be output to various devices. The conditions recorded are meant to serve as a laboratory notebook, which is otherwise difficult information to integrate with data files stored on disk. The commands: MA, MB, MD, MF, MI, MM, MR, MS, and MT change these conditions. These conditions are purely cosmetic and have no bearing on the data or its acquisition. Whenever information is written to disk it is also written to the printer to serve as an easily available record of the experiment. The definitions and number of thermocouples and pressure regions can be changed with the commands DP and DT. The readings held by the computer can be written to console, the printer, or the disk data file with the commands: PM, PS, SM, SS, WM, and WS.

The primary data acquisition parameters such as the countdown interval and the gate widths can be changed with the commands: CA, CC, CE, CG, CI, CN, and CP. The current data acquisition configuration including all the parameters of the data acquisition mode in use can be written to the console, the printer, and the disk data file with the commands SC, PC, and WC, respectively. In addition, the parameters of the data acquisition modes not in use can be written to these three devices with similar commands. The parameters for the various data acquisition modes can be changed with the commands discussed briefly above. Laboratory notebook style comments can be written to the disk data file and the printer or just to the printer with the commands WI and PI, respectively.

All of the settings for data acquisition, the definitions of pressure regions and thermocouples, as well as the actual pressures, temperatures, and detector settings have default values when SANG is begun. These are set in subroutine SINIT and are meant to approximately reproduce typical running conditions.

The size of program SANG far exceeds the memory limits of the LSI-11 computers. As such, many subroutines are "overlaid" -- moved in and out of memory as needed. This must be done explicitly in RT-11, and the LINKer command file lists the 65 segments in the three overlay regions. The size is still close enough to the upper limit that two other special steps are required. First, the FORTRAN files are all compiled with the /NOLINENUMBERS option as shown in the compilation

file CNSANG.COM. This has the effect that if a run time error should occur, the subroutine in which, but not the line at which the error occurred is displayed on the console. Secondly, the program is linked with the library file \$SHORT included in the LINKer command file LTUF.COM. This eliminates the text of the FORTRAN error messages, but not the error number, so that the text can be looked up in the DEC manuals.

All data files must be edited to remove the comments (and usually all bad data points) before further processing. The original unedited data file is of course archived for future reference. A number of routines are available on the LBL VAXes for the compilation and normalization of angular distributions and polarization data. Most frequently used is the program ANGBAB, which can do much of the data manipulation automatically.

3. Listing of Program SANG

A listing of program SANG follows. The order of the files is that done by backup/update/printout command file CPSANG.COM, which is also included.

PROGRAM SANG

File SANG.FOR begins on the previous line.

Version Date: November 11, 1985

Paul S. Weiss

Program SANG takes angular scan data on up to 16 scalers channels. Machine optimization is done and laser polarization measurements can be recorded at a number of angles. Control is maintained through subroutine SCOMM. All computer controlled hardware is driven through the MACRO routines found in SANGLE.MAC.

SANG must be linked with all the files found in LINKer file LSANG.COM.

INTEGER*4 JDATA

```
COMMON /CUR/ ANGLE,INTERV,NUMANG,MANGLE,IRNFLG
COMMON /DATA/ DATA(256,20),WORK1(256),WORK2(256)
COMMON /FNAME/ INAME(7),ISTORE
COMMON /DISP/ IDSP(1064),MODSPT,MODSPB,DSPB,DSTEP,NDSP,INDEP
COMMON /DSPCHA/ MDSPT,NDSP,MDSPT,MDSPT,MDSPT,MDSPT
COMMON /DSPZER/ ITYZER,IBYZER
COMMON /DSCR/ DSCR(20)
COMMON /SCR/ SCR(20)
COMMON /TGSMAX/ DWLMAX,MAXCHN
COMMON /SETS/ GATE(16),TIM(16),EXCFRC(2),CLOCK,INTACQ,NCHAN
COMMON /LASSET/ LASDWL,FRQLAS,LASSTP,FSRLAS,LASCHA
COMMON /LOPSET/ ANLPBE,ANLPFN,ANLPIN,LPNRFQ,ANLPCU,LPFLAG
COMMON /NRMSET/ ANGNRM,INTNRM,NRMRPT,NRMFLG
COMMON /POLSET/ ANGPOL,POLSTP,POSIT,IPOSIT,IPLFLG
COMMON /TSTSET/ TSTANG,NUMTST,TSTCUR,TSTFLG
COMMON /VELO/ DELF,HALFH,DELPPI,VELB,SPDRIO
COMMON /SDONE/ ISWFLG,JDATA(20)
COMMON /CHADEF/ CHADEF(20,10)
COMMON /PRES/ PRM(8),IPRE(8),PFORE(8),IDG(8),IPEM(8)
1,PBACK(2),PION(3)
COMMON /TPRIM/ THMCPL(8)
COMMON /MACDEF/ TCDEF(8,4),NTC,PRDEF(8,6),NPR,BACK(4,2)
COMMON /DET/ AGRD,AFIL,VEB,VIE,VEXT
1,VEN,QPST,QPR,MAS,VEX,VDK,VPMT
```

DEFINITION OF /COMMON/ VARIABLES AND ARRAYS

C COMMON Block /CUR/ Contains the current data acquisition parameters:

C
 C ANGLE The detector angle.
 C INTERV The countdown interval on the TGS.
 C NUMANG The number of detector angles that have been recorded.
 C MANGLE The position of the current angle out of all the angles
 C that have been recorded (Data is stored in order
 C of increasing angle).
 C IRNFLG The TGS running flag. If IRNFLG > 0, the TGS is running.
 C
 C COMMON Block /DATA/ Contains the accumulated data, and two work arrays:
 C
 C DATA(I,J) The accumulated data, stored in order of increasing
 C angle. Different detector angles are different
 C subscript I's. The J's are:
 C J=1 Detector Angle
 C J=2 Time Recorded
 C J=2*n+1 Channel n Signal } n=1,8
 C J=2*n+2 Channel n Background } n=1,8
 C WORK1(I) Work Buffer for upper display. Subscript I is the
 C detector angle subscript, as in DATA(I,J).
 C WORK2(I) The same as WORK1(I), but for the lower display channel.
 C
 C COMMON Block /FNAME/ Contains the filename, and the number of data points
 C stored in it.
 C
 C INAME(I) The ASCII name of the data file, for example:
 C DLO:ANG123.ANG
 C ISTORE The number of data points stored in the data file.
 C
 C COMMON Block /DISP/ Contains the display array and modes.
 C
 C IDISP(I) The array for display by the Data Translation DT2771
 C Direct Memory Access Display Driver.
 C MODSPT The Display Mode of the upper (Top) display channel.
 C MODSPB The Display Mode of the lower (Bottom) display channel.
 C For the values of MODSPT/B, see Subroutines SCHDSP and SDCHOS.
 C DSPB The initial detector angle for display.
 C DSTEP The angular step for the display (i.e. the display
 C resolution).
 C NDSP The number of detector angles to be displayed. Up to 256.
 C INDEP Flag to determine whether or not to scale display channels
 C independently. If INDEP > 0, display channels
 C independently.
 C
 C COMMON Block /DSPCHA/ Contains the data channels to be displayed.
 C

C MDSPT,NDSPT The data channels to be used for the upper (Top)
 C display channel.
 C MDSPB,NDSPB The data channels to be used for the lower (Bottom)
 C display channel.
 C
 C COMMON Block /DSPZER/ Contains the zero levels for the two display
 C channels.
 C
 C ITYZER The zero level for the top display channel.
 C IBYZER The zero level for the bottom display channel.
 C
 C COMMON Block /DSCR/ Contains the scratch values of the current data
 C for the display loader Subroutine SDVAL.
 C
 C DSCR(I) The scratch data for the display loader. I has the same
 C meaning as the J subscript in DATA(I,J) above.
 C
 C COMMON Block /SCR/ Contains the scratch values of the data.
 C
 C SCR(I) The scratch data, kept here while determining if it is
 C to be saved or not. I has the same meaning as
 C the J subscript in DATA(I,J) above.
 C
 C COMMON Block /TGSMAX/ Contains the maximum values associated with the
 C Timer-Gater-Scaler system in use. These are set
 C in Subroutine SINIT, for easy manipulation.
 C
 C DWLMAX No Meaning.
 C MAXCHN The maximum number of data channels allowed.
 C
 C COMMON Block /SETS/ Contains the TGS Settings.
 C
 C GATE(I) The gating times of each of up to 16 scalers.
 C TIM(I) The time each of up to 16 scalers are recorded.
 C EXCFRC(I) The excited state fractions for each excited state.
 C CLOCK The TGS Clock Frequency.
 C INTACQ The standard TGS countdown interval.
 C NCHAN The number of data channels eing recorded.
 C
 C COMMON Block /LASSET/ Contains the Velocity measurement settings.
 C
 C LASDWL The dwell time for each point of a computer-driven
 C laser scan. Not currently used.
 C
 C FRQLAS The laser frequency in cm-1.

C LASSTP The D/A step size for a computer-driven laser scan.
 C Not currently used.
 C FSRLAS The Free Spectral Range of the Frequency Standard
 C (i.e. Fabrey-Perot Etalon) in GHz.
 C LASCHA The data channel on which the laser fluorescence
 C and Frequency Standard signal come.
 C
 C COMMON Block /LOPSET/ Contains the Loop mode settings.
 C
 C ANLPBE The beginning angle of the Loop.
 C ANLPFN The ending (finishing) angle of the Loop.
 C ANLPIN The angular interval (step size) of the Loop.
 C LPNRFQ The frequency with which normalizations are to be
 C recorded for the Loop (after LPNRFQ angles
 C are recorded, a normalization measurement is
 C made).
 C ANLPCU The current angle in the Loop.
 C LPFLAG The flag to show that SANG is in Loop Mode. If
 C LPFLAG < 0, Loop mode has just begun, and
 C a normalization is to be done. If LPFLAG > 0,
 C LPFLAG = the number of angles since the
 C last normalization.
 C
 C COMMON Block /NRMSET/ Contains the Normalization Settings.
 C
 C ANGNRM The normalization detector angle.
 C INTNRM The countdown interval for normalization measurements.
 C NRMRPT The number of times the normalization measurement is
 C repeated.
 C NRMFLG The Normalization Flag. If NRMFLG > 0, NRMFLG counts
 C the number of times that the TGS has counted
 C down (until NRMFLG = NRMRPT).
 C
 C COMMON Block /POLSET/ Contains the Rotation of Polarization Settings.
 C
 C ANGPOL The detector angle at which rotation of polarization
 C measurements are to be made.
 C POLSTP The step size of the polarization rotator in degrees.
 C POSIT The ideal position of the rotator in steps if step
 C resolution were infinite.
 C IPOSIT The actual position of the rotator (0-125).
 C IPLFLG The rotation of polarization flag. If IPLFLG > 0,
 C SANG is acquiring polarization rotation
 C information.
 C
 C COMMON Block /TSTSET/ Contains the Test Mode Settings.

C
 C TSTANG The detector angle for Test Mode Measurements.
 C NUMTST The number of TGS countdowns to do in Test Mode.
 C TSTCUR The current angular offset to use for storing a data
 C point. Each test mode point is stored in a
 C different
 C
 C COMMON Block /VELO/ Contains the measured beam velocity.
 C
 C DELF The measured distance between the 45 and 90 degree laser
 C crossing in arbitrary units.
 C HALFH The measured Full Width Half Maximum for the 45 degree
 C peak in the units of DELF.
 C DELPIP The measured distance between Frequency Standard peaks
 C in the units of DELF.
 C VELB The beam velocity in cm/sec.
 C SPDRIO The beam speed ratio.
 C
 C COMMON Block /SDONE/ Contains the flag to show that the TGS has counted
 C down, and the raw data in I*4.
 C
 C ISWFLG The flag to show that the TGS has counted down. If
 C ISWFLG > 0, the TGS has counted down, and has
 C been serviced and read by an interrupt service
 C routine, and needs to have Subroutine SDONE,
 C capture the data for display and saving. If
 C ISWFLG = 0, accumulation has begun, and the
 C display needs to be updated by Subroutine SDISP,
 C via Subroutine SDONE. In both cases, ISWFLG is
 C cleared by Subroutine SDONE.
 C JDATA(I) The raw data in an INTEGER*4 array, as read from the
 C scalers through the CAMAC crate. The subscript
 C I corresponds to the scaler read:
 C I=2*n-1 Channel n Signal
 C I=2*n Channel n Background
 C
 C COMMON Block /CHADEF/ Contains the definitions of the data channels.
 C
 C CHADEF(I,J) The definition of channel J, up to 80 ASCII characters,
 C stored in I=1,20
 C
 C COMMON Block /PRES/ Contains the measured machine pressures. Note that
 C the pressure regions can be defined by the user.
 C
 C PRM(I) The mantissa of the ionization gauge reading in pressure
 C region I.

C IPRE(I) The exponent of the ionization gauge reading in pressure
 C region I.
 C PFORE(I) The foreline pressure in region I.
 C IDG(I) The flag for whether the Degas is on in pressure region I.
 C If IDG=1, the Ion Gauge is on; if IDG=2, the Ion
 C Gauge is off.
 C IPEM(I) The emission current of the ionization gauge reading in
 C pressure region I.
 C PBACK(I) The backing pressure of the sources. I=1 for the
 C Primary Source; I=2 for the Secondary Source.
 C PION(I) The ion pump currents in detector region I.
 C
 C COMMON Block /TPRIM/ Contains the measured thermocouple voltages.
 C
 C TPRIM(I) The measured thermocouple voltages on thermocouple I.
 C
 C COMMON Block /MACDEF/ Contains the definitions and numbers of thermocouples
 C pressure regions, and backing gases.
 C
 C TCDEF(I,J) The definition of thermocouple I, in up to 16 ASCII
 C characters, in J=1-4.
 C NTC The number of thermocouples defined.
 C PRDEF(I,J) The definition of pressure region I, in up to 24 ASCII
 C characters, in J=1-6.
 C NPR The number of pressure regions defined.
 C BACK(I,J) The definition backing gas J, in up to 16 ASCII
 C characters, in I=1-4.
 C
 C COMMON Block /DET/ Contains the Detector settings.
 C
 C AGRD The grid (emission) current, in mA.
 C AFIL The filament current, in A.
 C VEB The electron beam energy, in V.
 C VIE The ion energy, in V.
 C VEXT The ion extractor voltage, in V.
 C VEN The entrance lens voltage, in V.
 C QPST The Quadrupole Mass Spectrometer Mass Potentiometer Setting.
 C QPRS The Quadrupole Mass Spectrometer Resolution Potentiometer
 C Setting.
 C MAS The mass measured, in amu.
 C VEX The exit lens voltage, in V.
 C VDK The doorknob voltage, in kV.
 C VPMT The photomultiplier tube supply voltage, in V.
 C
 C
 C

C*****

C
C
C
C
C
C
C
C
C
C
C

INITIALIZE ALL COMMON BLOCK DATA AND FLAGS

CALL SINIT

OPEN A DATA FILE FOR OUTPUT

CALL SFILE(1)

TRANSFER CONTROL TO SCOMM FOR USER COMMANDS AND CONTROL

CALL SCOMM

END

SUBROUTINE SCOMM

Second routine in file SANG.FOR.

Version Date: August 15, 1985

Paul S. Weiss

Subroutine SCOMM maintains control of operations for the program.

It accepts 1 or 2 character commands from the user, then calls the appropriate subroutines.

C
C
C
C
C
C
C
C
C
C
C

INTEGER COM1, COM2, COMT

INTEGER*4 JDATA

COMMON /CUR/ ANGLE, INTERV, NUMANG, MANGLE, IRNFLG

COMMON /DATA/ DATA(256, 20), WORK1(256), WORK2(256)

COMMON /FNAME/ INAME(7), ISTORE

COMMON /DISP/ IDSP(1064), MODSPT, MODSPB, DSPB, DSTEP, NDSP, INDEP

COMMON /DSPCHA/ MDSPT, NDSPT, MDSPB, NDSPB

COMMON /DSPZER/ ITYZER, IBYZER

COMMON /DSCR/ DSCR(20)

COMMON /SCR/ SCR(20)

COMMON /TGSMAX/ DWLMAX, MAXCHN

COMMON /SETS/ GATE(16), TIM(16), EXCFRC(2), CLOCK, INTACQ, NCHAN

COMMON /LASSET/ LASDWL, FRQLAS, LASSTP, FSRLAS, LASCHA

COMMON /LOPSET/ ANLPBE, ANLPFN, ANLPIN, LPNRFQ, ANLPCU, LPFLAG

COMMON /NRMSET/ ANGNRM, INTNRM, NRMRPT, NRMFLG

COMMON /POLSET/ ANGPOL, POLSTP, POSIT, IPOSIT, IPLFLG

COMMON /TSTSET/ TSTANG, NUMTST, TSTCUR, TSTFLG

COMMON /VELO/ DELF, HALFH, DELPIP, VELB, SPDRIO

COMMON /SDONE/ ISWFLG, JDATA(20)

COMMON /CHAEDEF/ CHAEDEF(20, 10)

COMMON /PRES/ PRM(8), IPRE(8), PFORE(8), IDG(8), IPEM(8)

1, PBACK(2), PION(3)

COMMON /TPRIM/ THMCPL(8)

```
COMMON /MACDEF/ TCDEF(8,4),NTC,PRDEF(8,6),NPR,BACK(4,2)
COMMON /DET/ AGRD,AFIL,VEB,VIE,VEXT
1, VEN, QPST, QPR, MAS, VEX, VDK, VPMT
```

C
C
C

THE FOLLOWING IS A TABLE OF THE ASCII CHARACTERS USED AS COMMANDS

```
DATA IA,IB,IC,ID,IE /65,66,67,68,69/
DATA IF,IG,IH,II,IL,IM,IN /70,71,72,73,76,77,78/
DATA IO,IP,IR,IS,IT /79,80,82,83,84/
DATA IU,IV,IW,IX,IZ /85,86,87,88,90/
TYPE 2100
```

1
95

```
TYPE 95
FORMAT(' Command?',/)
```

C
C
C

RECORD COMMAND ENTRY USING SPECIAL SCREEN MODE

200

```
CALL ENSPEC
IF(ISWFLG.GE.0) CALL SDONE
COM1 = ITTINR(1)
IF(COM1.LT.0) GO TO 200
IGNORE CARRIAGE RETURNS AND LINE FEEDS
IF((COM1.EQ.13).OR.(COM1.EQ.10)) GO TO 200
COM2 = 32
```

C
C
C

ECHO CHARACTERS

250
255
300

```
TYPE 255,COM1,COM2
FORMAT('+',2A1,25X)
IF(ISWFLG.LT.0) GO TO 320
CALL SDONE
GO TO 250
```

320

```
COMT = ITTINR(1)
IF(COMT.LT.0) GO TO 300
IF(COMT.EQ.13) GO TO 500
```

380
390
400

```
COM2 = COMT
TYPE 255,COM1,COM2
IF(ISWFLG.LT.0) GO TO 420
CALL SDONE
GO TO 390
```

C
C
C

LOOK FOR CARRIAGE RETURN, OR ANOTHER CHARACTER

420

```
COMT = ITTINR(1)
IF(COMT.LT.0) GO TO 400
IF(COMT.EQ.13) GO TO 500
```

C
C
C

IF MORE THAN TWO CHARACTERS ARE TYPED IN, SHIFT COM2 TO COM1

```
COM1 = COM2
GO TO 380
```

```

C
C
C
500  READ SECOND HALF OF CARRIAGE RETURN (LINE FEED)
      COMT = ITTINR(1)
      IF(COMT.LT.0) GO TO 500
      TYPE 510,COM1,COM2
510  FORMAT('+',2A1,25X,/)
      CALL EXSPEC
C
C
C
      EXIT SPECIAL SCREEN MODE BEFORE CHECKING COMMAND LIST
C
C
      GO TO 1300

```

```

C
C
C
      MATCH UP COMMANDS AND EXECUTE DESIRED FUNCTION
C
C
      THE BASIC COMMANDS ARE:

```

```

C*   Change Commands
D*   Define and Display Commands
EX   Exit
G*   Graph Commands
H    Help
L*   Loop Commands
M*   Machine Condition Commands
N*   Normalization Commands
P*   Print Commands
R*   Record Commands
S*   Show Commands
T*   Test Commands
V*   Velocity Measurement Commands
W*   Write Commands
Z*   Zero Commands

```

```

C*

```

```

      The Change Commands are:

```

```

      CA   Change Angle
      CC   Change Clock Frequency
      CE   Change Excited State Fractions
      CF   Change File
      CG   Change Gate Widths
      CH   C Help
      CI   Change Interval for Acquisition Countdown
      CL   Change Loop Parameters
      CN   Change Normalization Parameters
      CP   Change Data Acquisition Parameters
      CU   Change Number of Channels in Use
      CV   Change Velocity Measurement Parameters

```

```

C
1300 IF(COM1.NE.IC) GO TO 1401
      IF(COM2.NE.IA) GO TO 1311
      CALL SCANG
      GO TO 1
1311 IF(COM2.NE.IC) GO TO 1321
      CALL SCHPAR(2)
      GO TO 1
1321 IF(COM2.NE.IE) GO TO 1326
      CALL SCHPAR(5)
      GO TO 1
1326 IF(COM2.NE.IF) GO TO 1331
      CALL SFILE(0)
      GO TO 1
1331 IF(COM2.NE.IG) GO TO 1336
      CALL SCHPAR(4)
      GO TO 1
1336 IF(COM2.NE.II) GO TO 1341
      CALL SCHPAR(3)
      GO TO 1
1341 IF(COM2.NE.IL) GO TO 1351
      CALL SCHLOP(0)
      GO TO 1
1351 IF(COM2.NE.IN) GO TO 1356
      CALL SCHNRM(0)
      GO TO 1
1356 IF(COM2.NE.IP) GO TO 1376
      CALL SCHPAR(0)
      GO TO 1
1376 IF(COM2.NE.IU) GO TO 1381
      CALL SCHPAR(1)
      GO TO 1
1381 IF(COM2.NE.IV) GO TO 1399
      CALL SCHVEL(0)
      GO TO 1
1399 IF(COM2.NE.IH) TYPE 9100
      CALL SCOMLC
      GO TO 1

```

```

C
C
C D*
C The definition and display commands are:
C      DA      Display: Change All
C      DB      Define Beams
C      DC      Define Channels
C      DH      D Help
C      DI      Display: Scale Channels Independently
C      DL      Display: Change Lower Channel
C      DP      Define Pressure Regions
C      DR      Display: Refresh
C      DS      Display: Scale Channels to the Same Value

```

```

C          DT      Define Thermocouples
C          DU      Display: Change Upper Channel
C          DW      Display: Change Window
C
1401      IF(COM1.NE.ID) GO TO 1501
          IF(COM2.NE.IA) GO TO 1406
          CALL SCHDSP(0)
          GO TO 1
1406      IF(COM2.NE.IB) GO TO 1411
          CALL SCHDEF(4)
          GO TO 1
1411      IF(COM2.NE.IC) GO TO 1436
          CALL SCHDEF(1)
          GO TO 1
1436      IF(COM2.NE.II) GO TO 1441
          INDEP = 1
          GO TO 1
1441      IF(COM2.NE.IL) GO TO 1456
          CALL SCHDSP(2)
          GO TO 1
1456      IF(COM2.NE.IP) GO TO 1461
          CALL SCHDEF(3)
          GO TO 1
1461      IF(COM2.NE.IR) GO TO 1471
          CALL SDISP
          GO TO 1
1471      IF(COM2.NE.IS) GO TO 1473
          INDEP = 0
          GO TO 1
1473      IF(COM2.NE.IT) GO TO 1476
          CALL SCHDEF(2)
          GO TO 1
1476      IF(COM2.NE.IU) GO TO 1481
          CALL SCHDSP(1)
          GO TO 1
1481      IF(COM2.NE.IW) GO TO 1499
          CALL SCHDWN(0)
          GO TO 1
1499      IF(COM2.NE.IH) TYPE 9100
          CALL SCOMLD
          GO TO 1
C
C          E
C          Exit
C
1501      IF(COM1.NE.IE) GO TO 1701
          CALL SLEAVE
          GO TO 1
C
C

```

```

C
C
C      G*
C      The graph commands are:
C          GB      Graph Both Displays
C          GH      G Help
C          GL      Graph Lower Display
C          GU      Graph Upper Display
C
1701  IF(COM1.NE.IG) GO TO 1801
      IF(COM2.NE.IB) GO TO 1741
      CALL SGRAPH(0)
      GO TO 1
1741  IF(COM2.NE.IL) GO TO 1776
      CALL SGRAPH(-1)
      GO TO 1
1776  IF(COM2.NE.IU) GO TO 1799
      CALL SGRAPH(1)
      GO TO 1
1799  IF(COM2.NE.IH) TYPE 9100
      CALL SCOMLG
      GO TO 1

C
C      H
C      Help -- Print out command list.
C
1801  IF(COM1.NE.IH) GO TO 2201
      CALL SCMLST
      GO TO 1

C
C      L*
C      The loop commands are:
C          LA      Loop: Change Current Angle
C          LB      Loop: Change Beginning Angle
C          LC      Loop: Continue
C          LD      Loop: Change Direction
C          LE      Loop: Change Ending Angle
C          LH      L Help
C          LI      Loop: Change Angular Interval
C          LN      Loop: Change Normalization Frequency
C          LP      Change All Loop Parameters
C          LS      Loop: Start
C
2201  IF(COM1.NE.IL) GO TO 2301
      IF(COM2.NE.IA) GO TO 2206
      CALL SCHLOP(6)
      GO TO 1
2206  IF(COM2.NE.IB) GO TO 2211
      CALL SCHLOP(1)
      GO TO 1
2211  IF(COM2.NE.IC) GO TO 2216

```

```

CALL SLOOP(0)
GO TO 1
2216 IF(COM2.NE.ID) GO TO 2221
CALL SCHLOP(5)
GO TO 1
2221 IF(COM2.NE.IE) GO TO 2236
CALL SCHLOP(2)
GO TO 1
2236 IF(COM2.NE.II) GO TO 2251
CALL SCHLOP(3)
GO TO 1
2251 IF(COM2.NE.IN) GO TO 2256
CALL SCHLOP(4)
GO TO 1
2256 IF(COM2.NE.IP) GO TO 2266
CALL SCHLOP(0)
GO TO 1
2266 IF(COM2.NE.IS) GO TO 2299
CALL SLOOP(1)
GO TO 1
2299 IF(COM2.NE.IH) TYPE 9100
CALL SCOMLL
GO TO 1

```

```

C
C
C
C
C
C
C
C
C
C
C
C
C
C
C
C
C
C
C
C
C
C
C
C
C
C
C
C
C
C

```

M*

The Machine Condition commands are:

MA	Machine Conditions:	Change All Detector Settings
MB	Machine Conditions:	Change Backing Pressures
MD	Machine Conditions:	Change Daly Detector (post-QPMS)
MF	Machine Conditions:	Change Filament and Ionizer Settings
MH	Machine Conditions:	Help
MI	Machine Conditions:	Change Ion Lens Settings
MM	Machine Conditions:	Change Quadrupole Mass Spectrometer Settings
MR	Machine Conditions:	Change Regional Pressures
MS	Machine Conditions:	Change Source Conditions
MT	Machine Conditions:	Change Thermocouple Readings

```

2301 IF(COM1.NE.IM) GO TO 2401
IF(COM2.NE.IA) GO TO 2306
CALL SCHMAD(5)
GO TO 1
2306 IF(COM2.NE.IB) GO TO 2316
CALL SCHMAP(1)
GO TO 1
2316 IF(COM2.NE.ID) GO TO 2326
CALL SCHMAD(4)
GO TO 1
2326 IF(COM2.NE.IF) GO TO 2336

```



```

CALL SCHMAD(1)
GO TO 1
2336 IF(COM2.NE.II) GO TO 2346
CALL SCHMAD(2)
GO TO 1
2346 IF(COM2.NE.IM) GO TO 2361
CALL SCHMAD(3)
GO TO 1
2361 IF(COM2.NE.IR) GO TO 2366
CALL SCHMAP(3)
GO TO 1
2366 IF(COM2.NE.IS) GO TO 2371
CALL SCHMAP(4)
GO TO 1
2371 IF(COM2.NE.IT) GO TO 2399
CALL SCHMAP(2)
GO TO 1
2399 IF(COM2.NE.IH) TYPE 9100
CALL SCOMLM
GO TO 1

```

C
C
C
C
C
C
C
C
C
C
C
C

N*

The available Normalization Commands are:

C	NA	Change Normalization Angle
C	NH	N Help
C	NI	Change Normalization Countdown Interval
C	NP	Change All Normalization Parameters
C	NR	Change Normalization Repetitions
C	NS	Normalization: Start

```

2401 IF(COM1.NE.IN) GO TO 2601
IF(COM2.NE.IA) GO TO 2436
CALL SCHNRM(1)
GO TO 1
2436 IF(COM2.NE.II) GO TO 2456
CALL SCHNRM(2)
GO TO 1
2456 IF(COM2.NE.IP) GO TO 2461
CALL SCHNRM(0)
GO TO 1
2461 IF(COM2.NE.IR) GO TO 2466
CALL SCHNRM(3)
GO TO 1
2466 IF(COM2.NE.IS) GO TO 2499
CALL SNORM
GO TO 1
2499 IF(COM2.NE.IH) TYPE 9100
CALL SCOMLN
GO TO 1

```

C
C
C
C P*
C The P*, S*, and W* commands are sorted out in subroutine SNUCH
C The Print Commands are as follows:
C PA Print Accumulated Data
C PC Print Current Configuration
C PD Print Data Channel Definition
C PG Print Current Graphics Display
C PH P Help
C PI Print Information
C PL Print Loop Mode Parameters
C PM Print Machine Condition
C PN Print Normalization Parameters
C PS Print Detector Settings
C PT Print Test Mode Parameters
C

2601 IF(COM1.NE.IP) GO TO 2801
NU = 6
CALL SNUCH(NU,COM2)
IF(NU.NE.0) GO TO 1
2699 IF(COM2.NE.IH) TYPE 9100
CALL SCOMLP
GO TO 1

C
C R
C The available Record Data and Rotation of Polarization Commands are:
C RA Rotation of Polarization: Change Detector Angle
C RD Record Data
C RH R Help
C RI Reinitialize TGS System
C RM Rotation of Polarization: Change Motor Step Size
C RP Rotation of Polarization: Change All Parameters
C RS Rotation of Polarization: Start
C

2801 IF(COM1.NE.IR) GO TO 2901
IF(COM2.NE.IA) GO TO 2816
CALL SCHPOL(1)
GO TO 1
2816 IF(COM2.NE.ID) GO TO 2836
CALL SSTART(1)
GO TO 1
2836 IF(COM2.NE.II) GO TO 2846
CALL INIT(ISWFLG,JDATA)
GO TO 1
2846 IF(COM2.NE.IM) GO TO 2856
CALL SCHPOL(2)
GO TO 1
2856 IF(COM2.NE.IP) GO TO 2866
CALL SCHPOL(0)

```

GO TO 1
2866 IF(COM2.NE.IS) GO TO 2899
CALL SPOLAR
GO TO 1
2899 IF(COM2.NE.IH) TYPE 9100
CALL SCOMLR
GO TO 1

```

```

C
C
C S*
C The P*, S*, and W* commands are sorted out in subroutine SNUCH
C The available show commands are:
C SA Show Accumulated Data
C SC Show Current Configuration
C SD Show Data Channel Definition
C SG Show Curent Graphics Display
C SH S Help
C SI Show Time Information
C SL Show Loop Mode Parameters
C SM Show Machine Condition
C SN Show Normalization Parameters
C SS Show Detector Settings
C ST Show Test Mode Parameters
C

```

```

2901 IF(COM1.NE.IS) GO TO 3001
NU = 7
CALL SNUCH(NU,COM2)
IF(NU.NE.0) GO TO 1
2999 IF(COM2.NE.IH) TYPE 9100
CALL SCOMLS
GO TO 1

```

```

C
C
C T*
C The Test Commands are as follows:
C TA Change Test Angle
C TC Test Mode: Continue
C TE Test Mode: Exit
C TH T Help
C TN Test Mode: Change Number of Countdowns
C TP Change All Test Mode Parameters
C TS Test Mode: Start
C

```

```

3001 IF(COM1.NE.IT) GO TO 3201
IF(COM2.NE.IA) GO TO 3011
CALL SCHKST(1)
GO TO 1
3011 IF(COM2.NE.IC) GO TO 3021
CALL STEST(1)
GO TO 1
3021 IF(COM2.NE.IE) GO TO 3051

```

```

TSTFLG = - TSTFLG
GO TO 1
3051 IF(COM2.NE.IN) GO TO 3056
      CALL SCHKST(2)
      GO TO 1
3056 IF(COM2.NE.IP) GO TO 3066
      CALL SCHKST(0)
      GO TO 1
3066 IF(COM2.NE.IS) GO TO 3099
      CALL SCHKST(0)
      GO TO 1
3099 IF(COM2.NE.IH) TYPE 9100
      CALL SCOMLT
      GO TO 1

```

C
C
C
C
C
C
C
C
C
C
C
C

V*

The Velocity Measurement Commands are as follows:

C	VA	Change Velocity Measurement Accumulation Time
C	VF	Change Velocity Measurement Frequency Standard
C	VH	V Help
C	VL	Change Velocity Measurement Laser Frequency
C	VM	Measure Velocity
C	VP	Change All Velocity Measurement Parameters
C	VS	Change Velocity Measurement Step Size

```

3201 IF(COM1.NE.IV) GO TO 3301
      IF(COM2.NE.IA) GO TO 3226
      CALL SCHVEL(4)
      GO TO 1
3226 IF(COM2.NE.IF) GO TO 3241
      CALL SCHVEL(2)
      GO TO 1
3241 IF(COM2.NE.IL) GO TO 3246
      CALL SCHVEL(1)
      GO TO 1
3246 IF(COM2.NE.IM) GO TO 3256
      CALL SVELO
      GO TO 1
3256 IF(COM2.NE.IP) GO TO 3266
      CALL SCHVEL(0)
      GO TO 1
3266 IF(COM2.NE.IS) GO TO 3299
      CALL SCHVEL(3)
      GO TO 1
3299 IF(COM2.NE.IH) TYPE 9100
      CALL SCOMLV
      GO TO 1

```

C
C
C

W*

The P*, S*, and W* commands are sorted out in subroutine SNUCH

C The Write Commands are as follows:
 C WA Write Accumulated Data
 C WC Write Current Configuration
 C WD Write Data Channel Definition
 C WG Write Current Graphics Display
 C WH W Help
 C WI Write Information
 C WL Write Loop Mode Parameters
 C WM Write Machine Condition
 C WN Write Normalization Parameters
 C WS Write Detector Settings
 C WT Write Test Mode Parameters
 C

3301 IF(COM1.NE.IW) GO TO 3601
 NU = 9
 CALL SNUCH(NU,COM2)
 IF(NU.NE.0) GO TO 1
 3399 IF(COM2.NE.IH) TYPE 9100
 CALL SCOMLW
 GO TO 1

C
 C Z*
 C The Zero Commands are as follows:
 C ZA Zero Arrays
 C ZH Z Help
 C ZS Zero Angular Segment
 C ZT Zero Test Mode Data
 C

3601 IF(COM1.NE.IZ) GO TO 3700
 IF(COM2.NE.IA) GO TO 3666
 CALL SZERO(1)
 GO TO 1
 3666 IF(COM2.NE.IS) GO TO 3671
 CALL SZERO(2)
 GO TO 1
 3671 IF(COM2.NE.IT) GO TO 3699
 CALL SZERO(3)
 GO TO 1
 3699 IF(COM2.NE.IH) TYPE 9100
 CALL SCOMLZ
 GO TO 1

C
 C TYPE OUT THE FOLLOWING IF AN UNRECOGNIZED COMMAND WAS ISSUED
 C
 3700 TYPE 9100
 TYPE 2100
 2100 FORMAT(' For a list of commands, type H')
 GO TO 1
 9100 FORMAT(/,' This is not a command.')

RETURN

END

SUBROUTINE SACCUM(NU)

File SACCUM.FOR begins on the previous line.

Version Date: July 5, 1984
Paul S. Weiss

Subroutine SACCUM accumulates the data and outputs it to unit NU.

COMMON /CUR/ ANGLE,INTERV,NUMANG,MANGLE,IRNFLG
COMMON /DATA/ DATA(256,20),WORK1(256),WORK2(256)
COMMON /SETS/ GATE(16),TIM(16),EXCFRC(2),CLOCK,INTACQ,NCHAN

RETURN IF TGS IS RUNNING

IF(IRNFLG.EQ.0) GO TO 50
TYPE *, 'Abort Data Accumulation -- TGS is running!'
GO TO 9000

50 IF(NUMANG.GT.0) GO TO 100
TYPE *, 'No data has been accumulated!'
GO TO 9000

100 WRITE(NU,110) 12,NUMANG
110 FORMAT(1X,A1, ' ACCUMULATED DATA',/,1X,I3, ' angles')
DO 900 IN=1,NUMANG

300 WRITE(NU,300) DATA(IN,1),DATA(IN,2)
FORMAT(/, ' Angle: ',F9.5, ' degrees, measured for: ',F8.3
1, ' sec.',/, ' Channel',3X,'A',10X,'B',11X,'Signal'
2,9X,'Error',6X,'Signal/Noise')
DO 700 J=1,NCHAN

IS = (2*J) + 1
IB = IS + 1
SIG = (DATA(IN,IS) - DATA(IN,IB))/DATA(IN,2)
ERR = (SQRT(DATA(IN,IS) + DATA(IN,IB)))/DATA(IN,2)
SGTON = 0.

IF(ERR.NE.0.) SGTON = SIG/ERR
WRITE(NU,500) J,DATA(IN,IS),DATA(IN,IB),SIG,ERR,SGTON
500 FORMAT(1X,I1,2X,F9.0,2X,F9.0,5X,F11.2, ' +/- ',F9.2,5X,F9.1)
700 CONTINUE
900 CONTINUE

WRITE(NU,1100) 12
1100 FORMAT(1X,A1, ' RAW DATA',/)
9000 RETURN
END

SUBROUTINE SCANG

File SCANG.FOR begins on the previous line.

C
C
C
C
C
C
C

Version Date: June 28, 1984
Paul S. Weiss

Subroutine SCANG changes the detector angle.

```
COMMON /CUR/ ANGLE,INTERV,NUMANG,MANGLE,IRNFLG
TYPE *,'What is the new detector angle?'
ACCEPT *,ANGLE
RETURN
END
```

SUBROUTINE SCHDEF(IOPT)

File SCHDEF.FOR begins on the previous line.

C
C
C
C
C
C
C
C
C
C
C
C
C

Version Date: July 18, 1984
Paul S. Weiss

Subroutine SCHDEF changes the definitions of the: data channels, the thermocouples, the pressure regions, and the backing gases.

The argument of SCHDEF determines the definitions to change, as follows:

```
IOPT=1 Change Data Channel Definitions
IOPT=2 Change Thermocouple Definitions
IOPT=3 Change Pressure Region Definitions
IOPT=4 Change Backing Gas Definitions
```

```
COMMON /TGSMAX/ DWLMAX,MAXCHN
COMMON /SETS/ GATE(16),TIM(16),EXCFRC(2),CLOCK,INTACQ,NCHAN
COMMON /CHADEF/ CHADEF(20,10)
COMMON /MACDEF/ TCDEF(8,4),NTC,PRDEF(8,6),NPR,BACK(4,2)
GO TO(1100,2100,3100,4100),IOPT
```

C
C
C
C
C
C
C
C
C
C
C
C
C

CHANGE DATA CHANNEL DEFINITIONS

```
1100 DO 1400 I=1,NCHAN
TYPE 1210,I,(CHADEF(J,I),J=1,20)
1210 FORMAT(' Change the definition of Channel #'
1,I1,'? The current definition is:','/,1X,20A4)
ACCEPT 1000,ANS
1000 FORMAT(A1)
IF(ANS.NE.'Y') GO TO 1400
TYPE 1310
1310 FORMAT(' Enter the new definition.')
ENABLE LOWER CASE INPUT
```

```

C
    CALL LCASE
    ACCEPT 1350, (CHADEF(J,I), J=1,20)
1350  FORMAT(20A4)
C
C    DISABLE LOWER CASE INPUT
C
    CALL UCASE
1400  CONTINUE
    GO TO 9000
C
C    CHANGE THE NUMBER AND DEFINITIONS OF THERMOCOUPLES
C
2100  TYPE 2110,NTC
2110  FORMAT(' There are currently ',I1,' thermocouples in use.'
1,' Has this changed?')
    ACCEPT 1000,ANS
    IF(ANS.NE.'Y') GO TO 2300
2200  TYPE *,'How many thermocouples are being used?'
    ACCEPT *,NTC
    MAXTC = 8
    IF((NTC.LE.0).OR.(NTC.GT.MAXTC)) GO TO 2200
2300  DO 2500 I=1,NTC
    TYPE 2410,I,(TCDEF(I,J),J=1,4)
2410  FORMAT(' Thermocouple #',I1,' is currently: ',4A4
1,/, ' Has this changed?')
    ACCEPT 1000,ANS
    IF(ANS.NE.'Y') GO TO 2500
    TYPE 1310
C
C    ENABLE LOWER CASE INPUT
C
    CALL LCASE
    ACCEPT 1350, (TCDEF(I,J), J=1,4)
C
C    DISABLE LOWER CASE INPUT
C
    CALL UCASE
2500  CONTINUE
    GO TO 9000
C
C    CHANGE THE NUMBER AND DEFINITIONS OF THE PRESSURE REGIONS
C
3100  TYPE 3110,NPR
3110  FORMAT(' There are ',I1,' pressure regions '
1,'measured with ion gauges. Has this changed?')
    ACCEPT 1000,ANS
    IF(ANS.NE.'Y') GO TO 3300
3200  TYPE *,'How many pressure regions are being measured?'
    ACCEPT *,NPR

```



```

MAXPR = 8
IF((NPR.LE.0).OR.(NPR.GT.MAXPR)) GO TO 3200
3300 DO 3500 I=1,NPR
      TYPE 3410,I,(PRDEF(I,J),J=1,6)
3410 FORMAT(' Change the definition of Pressure Region #'
1,I1,'?',/,', The current definition is: ',6A4)
ACCEPT 1000,ANS
IF(ANS.NE.'Y') GO TO 3500
TYPE 1310

C
C   ENABLE LOWER CASE INPUT
C

CALL LCASE
ACCEPT 1350,(PRDEF(I,J),J=1,6)

C
C   DISABLE LOWER CASE INPUT
C

CALL UCASE
3500 CONTINUE
GO TO 9000

C
C   CHANGE BACKING GAS DEFINITIONS
C
4100 TYPE 4210,(BACK(J,1),J=1,4)
4210 FORMAT(' The Primary backing gas is ',4A4
1,' Has this changed?')
ACCEPT 1000,ANS
IF(ANS.NE.'Y') GO TO 4400
TYPE 1310

C
C   ENABLE LOWER CASE INPUT
C

CALL LCASE
ACCEPT 1350,(BACK(J,1),J=1,4)

C
C   DISABLE LOWER CASE INPUT
C

CALL UCASE
4400 TYPE 4410,(BACK(J,2),J=1,4)
4410 FORMAT(' The Secondary backing gas is ',4A4
1,' Has this changed?')
ACCEPT 1000,ANS
IF(ANS.NE.'Y') GO TO 9000
TYPE 1310

C
C   ENABLE LOWER CASE INPUT
C

CALL LCASE
ACCEPT 1350,(BACK(J,2),J=1,4)
C

```

```

C      DISABLE LOWER CASE INPUT
C
C      CALL UCASE
9000   RETURN
      END

      SUBROUTINE SCHDSP(IUPLow)
C                                     File SCHDSP.FOR begins on the previous line.
C
C      Version Date:  July 5, 1984
C      Paul S. Weiss
C
C      Subroutine SCHDSP changes one or both of the display channels.
C
C      The argument IUPLow specifies which display channel will be changed,
C      as follows:
C          IUPLow=0      Change both channels
C          IUPLow=1      Change Top channel
C          IUPLow=2      Change Bottom Channel
C
C
COMMON /DISP/ IDSP(1064),MODSPT,MODSPB,DSPB,DSTEP,NDSP,INDEP
COMMON /DSPCHA/ MDSPT,NDSP,MDSPB,NDSPB
COMMON /SETS/ GATE(16),TIM(16),EXCFRC(2),CLOCK,INTACQ,NCHAN
C
      IF(IUPLow.EQ.2) GO TO 2100
50     TYPE 100,NCHAN,'upper'
100    FORMAT(/,' The available diplay modes are (m,n=1-',I1,'):'
      1,/, ' Cn      Channel n Signal'
      2,/, ' Dmn     Difference of 2 Channels (m-n)'
      3,/, ' Emn     Excited State Signal'
      4,/, ' Fmn     Signal/Noise of the Difference of'
      4, ' Channels (m-n)'
      5,/, ' Sn      Signal/Noise of Channel n'
      6,/, ' Tn      Time an Angle has been measured on Channel n',
      7,/, ' Please enter your choice for the ',A5,' display.')
```

CALL SDCHOS(MODSPT,MDSPT,NDSP)

```

      IF(MODSPT.EQ.0) GO TO 50
      IF(IUPLow.EQ.1) GO TO 8000
2100   TYPE 100,NCHAN,'lower'
      CALL SDCHOS(MODSPB,MDSPB,NDSPB)
      IF(MODSPB.EQ.0) GO TO 2100
8000   TYPE *, 'Scale the channels independently?'
      INDEP = 1
      ACCEPT 1000,ANS
1000   FORMAT(A1)
      IF(ANS.NE.'Y') INDEP = 0
      RETURN

```

END

SUBROUTINE SDCHOS(MD,M,N)

Second routine of file SCHDSP.FOR.

Version Date: June 25, 1984

Paul S. Weiss

Subroutine SDCHOS Sets the mode number for the various display modes.

COMMON /SETS/ GATE(16),TIM(16),EXCFRC(2),CLOCK,INTACQ,NCHAN
DATA NANS /0/

M = 0

N = 0

ACCEPT 2000,NANS,M,N

2000 FORMAT(A1,2I1)

MD = 0

IF(NANS.EQ.'C') MD = 1

IF(NANS.EQ.'D') MD = 2

IF(NANS.EQ.'E') MD = 3

IF(NANS.EQ.'F') MD = 4

IF(NANS.EQ.'S') MD = 5

IF(NANS.EQ.'T') MD = 6

BE SURE THAT THERE IS A CHANNEL TO PLOT

IF((M.EQ.0).OR.(M.GT.NCHAN)) MD = 0

IF TWO CHANNELS ARE REQUIRED, MAKE SURE BOTH ARE OK

IF((MD.GT.1).AND.(MD.LT.5).AND.((N.EQ.0).OR.(N.GT.NCHAN)
1.OR.(M.EQ.N))) MD = 0

IF(MD.EQ.0) TYPE 3100,7,7

3100 FORMAT(/,' Invalid Option!!',2A1)

RETURN

END

SUBROUTINE SCHDWN(IOPT)

File SCHDWN.FOR begins on the previous line.

Version Date: September 27, 1984

Paul S. Weiss

Subroutine SCHDWN changes the display window.

The argument of SCHDWN is as follows:

```

C      IOPT=0  Ask user to choose display window.
C      IOPT=1  Set window for test mode.
C      IOPT=2  Set window for polarization rotation mode.
C
COMMON /DISP/  IDSP(1064),MODSPT,MODSPB,DSPB,DSTEP,NDSP,INDEP
COMMON /POLSET/ ANGPOL,POLSTP,POSIT,IPOSIT,IPLFLG
COMMON /TSTSET/ TSTANG,NUMTST,TSTCUR,TSTFLG
IF(IOPT.EQ.0) GO TO 1
GO TO (3200,2200),IOPT
1      TYPE 100
100     FORMAT(/,' The display window choices are:'
1,/,,' D      Default setting (-10 to 100 degrees)'
2,/,,' P      Polarization Rotation setting (single angle)'
2,/,,' T      Test Mode setting (single angle)'
3,/,,' W      Window setting (User set)'
4,/,,' Please enter choice')
ACCEPT 1000,ANS
1000    FORMAT(A1)
IF(ANS.NE.'D') GO TO 2100
DSPB = -10.
DSTEP = .5
NDSP = 221
GO TO 5000
2100    IF(ANS.NE.'P') GO TO 3100
2200    DSPB = ANGPOL
DSTEP = 1.E-4
NDSP = 181
GO TO 5000
3100    IF(ANS.NE.'T') GO TO 4100
3200    DSPB = TSTANG
DSTEP = 1.E-5
NDSP = 256
GO TO 5000
4100    IF(ANS.NE.'W') GO TO 9100
TYPE *,'Enter beginning angle of display window'
ACCEPT *,DSPB
TYPE *,'Enter angular step for display'
ACCEPT *,DSTEP
5000    IF(IOPT.NE.0) GO TO 9000
TYPE 5010,DSPB,(DSPB + ((NDSP-1)*DSTEP)),DSTEP
5010    FORMAT(/,' The display will be from ',F9.5,' to ',F9.5,
1,' degrees',',/,', in ',F7.5,' degree steps.'
2,/,,' Is this correct?')
ACCEPT 1000,ANS
IF(ANS.NE.'Y') GO TO 1
9000    RETURN
9100    TYPE *,'This is not an option'
GO TO 1
END

```

SUBROUTINE SCHLOP(IOPT)

File SCHLOP.FOR begins on the previous line.

Version Date: July 19, 1984

Paul S. Weiss

Subroutine SCHLOP changes one or all of the Loop Mode parameters in SANG.

The argument IOPT specifies which parameters are to be changed as follows:

IOPT=0 Change all Parameters
 IOPT=1 Change Beginning Angle (ANLPBE)
 IOPT=2 Change Ending Angle (ANLPFN)
 IOPT=3 Change Angular Interval (ANLPIN)
 IOPT=4 Change Normalization Frequency (LPNRFQ)

Other changes:

IOPT=5 Change Direction (Sign of ANLPIN)
 IOPT=6 Change Current angle of Loop

```

COMMON /SETS/ GATE(16),TIM(16),EXCFRC(2),CLOCK,INTACQ,NCHAN
COMMON /LOPSET/ ANLPBE,ANLPFN,ANLPIN,LPNRFQ,ANLPKU,LPFLAG
IF(IOPT.GT.0) GO TO (1100,2100,3100,4100,5100,6100),IOPT
1100 TYPE 1110,ANLPBE
1110 FORMAT(' The beginning angle of the Loop is ',F5.1
1,' degrees. Change this?')
ACCEPT 1000,ANS
1000 FORMAT(A1)
IF(ANS.NE.'Y') GO TO 2000
TYPE *,'Enter beginning angle of Loop'
ACCEPT *,ANLPBE
2000 IF(IOPT.NE.0) GO TO 9000
2100 TYPE 2110,ANLPFN
2110 FORMAT(' The ending angle of the Loop is ',F5.1
1,' degrees. Change this?')
ACCEPT 1000,ANS
IF(ANS.NE.'Y') GO TO 3000
TYPE *,'Enter ending angle of Loop'
ACCEPT *,ANLPFN
3000 IF(IOPT.NE.0) GO TO 9000
3100 TYPE 3110,ANLPIN
3110 FORMAT(' The angular interval of the Loop is ',F5.1
1,' degrees. Change this?')
ACCEPT 1000,ANS
IF(ANS.NE.'Y') GO TO 4000
TYPE *,'Enter angular interval of Loop'
ACCEPT *,ANLPIN
C
C MAKE SURE THAT SIGN OF INTERVAL IS CORRECT

```

```

C
IF(((ANLPFN-ANLPBE)*ANLPIN).LT.0.) ANLPIN = -ANLPIN
4000 IF(IOPT.NE.0) GO TO 9000
C
C CHANGE NORMALIZATION FREQUENCY
C
4100 TYPE 4110,LPNRFQ
4110 FORMAT(' The data is Normalized every ',I5
1,' measurements. Change this?')
ACCEPT 1000,ANS
IF(ANS.NE.'Y') GO TO 9000
4300 TYPE *,'Normalize after how many measurements?'
ACCEPT *,LPNRFQ
IF(LPNRFQ.LE.0) GO TO 4300
GO TO 9000
C
C CHANGE DIRECTION OF LOOP
C
5100 A = ANLPBE
ANLPBE = ANLPFN
ANLPFN = A
ANLPIN = - ANLPIN
GO TO 9000
C
C CHANGE CURRENT ANGLE
C
6100 TYPE 6110,ANLPCU
6110 FORMAT(' The current angle is ',F5.1,' degrees. Change this?')
ACCEPT 1000,ANS
IF(ANS.NE.'Y') GO TO 9000
TYPE *,'Enter angle to measure next in Loop'
ACCEPT *,ANLPCU
9000 RETURN
END

```

```

SUBROUTINE SCHMAD(IOPT)

```

```

File SCHMAD.FOR begins on the previous line.

```

```

Version Date: July 18, 1984
Paul S. Weiss

```

```

Subroutine SCHMAD changes the detector settings.

```

```

Argument IOPT determines which settings are to be changed,
as follows:

```

```

IOPT=1 Change Filament Settings

```

```

C          IOPT=2  Change Ion Lenses' Settings
C          IOPT=3  Change Quadrupole Mass Spectrometer Settings
C          IOPT=4  Change Daly Detector Settings
C          IOPT=5  Change All of the Above
C
COMMON /DET/ AGRD,AFIL,VEB,VIE,VEXT
1,VEN,QPST,QPR,MAS,VEX,VDK,VPMT
GO TO (1100,2100,3100,4100,1100),IOPT
1100      TYPE 1110,AGRD
1110      FORMAT(' The Grid Current is ',F4.1,' mA.')
          TYPE 1120
1120      FORMAT(' Has this changed?')
          ACCEPT 1000,ANS
1000      FORMAT(A1)
          IF(ANS.NE.'Y') GO TO 1200
          TYPE *,'Enter Grid Current (in mA).'
          ACCEPT *,AGRD
1200      TYPE 1210,AFIL
1210      FORMAT(' The Filament Current is ',F4.2,' A.')
          TYPE 1120
          ACCEPT 1000,ANS
          IF(ANS.NE.'Y') GO TO 1300
          TYPE *,'Enter Filament Current (in A).'
          ACCEPT *,AFIL
1300      TYPE 1310,VEB
1310      FORMAT(' The Electron Beam Energy is ',F5.0,' V.')
          TYPE 1120
          ACCEPT 1000,ANS
          IF(ANS.NE.'Y') GO TO 1400
          TYPE *,'Enter Electron Beam Energy (in V).'
          ACCEPT *,VEB
1400      TYPE 1410,VIE
1410      FORMAT(' The Ion Energy is ',F7.2,' V.')
          TYPE 1120
          ACCEPT 1000,ANS
          IF(ANS.NE.'Y') GO TO 2000
          TYPE *,'Enter Ion Energy (in V).'
          ACCEPT *,VIE
2000      IF(IOPT.NE.5) GO TO 9000
2100      TYPE 2110,VEXT
2110      FORMAT(' The Ion Extraction Voltage is ',F5.0,' V.')
          TYPE 1120
          ACCEPT 1000,ANS
          IF(ANS.NE.'Y') GO TO 2200
          TYPE *,'Enter Ion Extraction Voltage (in V).'
          ACCEPT *,VEXT
2200      TYPE 2210,VEN
2210      FORMAT(' The Entrance Lens Voltage is ',F5.0,' V.')
          TYPE 1120
          ACCEPT 1000,ANS

```

```
IF(ANS.NE.'Y') GO TO 3000
TYPE *, 'Enter Entrance Lens Voltage (in V).'
ACCEPT *, VEN
3000 IF(IOPT.NE.5) GO TO 9000
3100 TYPE 3110, QPST
3110 FORMAT(' The Quadrupole Mass Setting is ', F5.2)
TYPE 1120
ACCEPT 1000, ANS
IF(ANS.NE.'Y') GO TO 3200
TYPE *, 'Enter the Mass Setting.'
ACCEPT *, QPST
3200 TYPE 3210, QPR
3210 FORMAT(' The Quadrupole Resolution is ', F5.2)
TYPE 1120
ACCEPT 1000, ANS
IF(ANS.NE.'Y') GO TO 3300
TYPE *, 'Enter Quadrupole Resolution.'
ACCEPT *, QPR
3300 TYPE 3310, MAS
3310 FORMAT(' The Mass is ', I5)
TYPE 1120
ACCEPT 1000, ANS
IF(ANS.NE.'Y') GO TO 4000
TYPE *, 'Enter mass.'
ACCEPT *, MAS
4000 IF(IOPT.NE.5) GO TO 9000
4100 TYPE 4110, VEX
4110 FORMAT(' The Exit Lens Voltage is ', F6.0, ' V.')
TYPE 1120
ACCEPT 1000, ANS
IF(ANS.NE.'Y') GO TO 4200
TYPE *, 'Enter Exit Lens Voltage (in V).'
ACCEPT *, VEX
4200 TYPE 4210, VDK
4210 FORMAT(' The Doorknob Voltage is ', F5.1, ' kV.')
TYPE 1120
ACCEPT 1000, ANS
IF(ANS.NE.'Y') GO TO 4300
TYPE *, 'Enter the Doorknob Voltage (in kV).'
ACCEPT *, VDK
4300 TYPE 4310, VPMT
4310 FORMAT(' The Photomultiplier Voltage is ', F6.0, ' V.')
TYPE 1120
ACCEPT 1000, ANS
IF(ANS.NE.'Y') GO TO 9000
TYPE *, 'Enter Photomultiplier Voltage (in V).'
ACCEPT *, VPMT
9000 RETURN
END
```


SUBROUTINE SCHMAP(IOPT)

File SCHMAP.FOR begins on the previous line.

Version Date: September 4, 1984
Paul S. Weiss

Subroutine SCHMAP changes the Machine pressures and temperatures.

```

DIMENSION NONOFF(2)
COMMON /PRES/ PRM(8),IPRE(8),PFORE(8),IDG(8),IPEM(8)
1,PBACK(2),PION(3)
COMMON /TPRIM/ THMCPL(8)
COMMON /MACDEF/ TCDEF(8,4),NTC,PRDEF(8,6),NPR,BACK(4,2)
DATA NONOFF /'n ','ff'/

```

```

C
GO TO (1100,2100,3100,1100) IOPT
1100 TYPE 1110,PBACK(1),(BACK(J,1),J=1,4)
1110 FORMAT(/,' The Primary Source backing pressure is',F8.1
1,' torr with ',4A4,/,,' Has this changed?')
ACCEPT 1000,ANS
1000 FORMAT(A1)
IF(ANS.NE.'Y') GO TO 1300
TYPE 1210,(BACK(J,1),J=1,4)
1210 FORMAT(' What is the pressure of ',4A4,?'')
ACCEPT *,PBACK(1)
1300 TYPE 1310,PBACK(2),(BACK(J,2),J=1,4)
1310 FORMAT(/,' The Secondary Source backing pressure is',F8.1
1,' torr with ',4A4,/,,' Has this changed?')
ACCEPT 1000,ANS
IF(ANS.NE.'Y') GO TO 1900
TYPE 1210,(BACK(J,2),J=1,4)
ACCEPT *,PBACK(2)
1900 IF(IOPT.NE.4) GO TO 9000
C
CHANGE THE MEASURED THERMOCOUPLE VOLTAGES
C
2100 DO 2700 I=1,NTC
TYPE 2210,(TCDEF(I,J),J=1,4),THMCPL(I)
2210 FORMAT(' The ',4A4,' thermocouple voltage is ',F5.2
1,' mV.',/,,' Has this changed?')
ACCEPT 1000,ANS
IF(ANS.NE.'Y') GO TO 2700
TYPE 2310,(TCDEF(I,J),J=1,4)
2310 FORMAT(' What is the ',4A4,' thermocouple voltage '
1,' (in mV)?')
ACCEPT *,THMCPL(I)
2700 CONTINUE

```

```

GO TO 9000
C
C CHANGE REGIONAL PRESSURES
C
3100 DO 3500 I=1,NPR
      TYPE 3210,(PRDEF(I,J),J=1,6),PRM(I),IPRE(I),PFORE(I)
      1,NONOFF(IDG(I)),IPEM(I)
3210 FORMAT(' The ',6A4,' Pressures are: '
      1,/,1X,F5.2,'x10',I3,' torr, foreline: ',F4.0
      2,' u, Degas 0',A2,',',I2,' mA',/, ' Have these changed?')
      ACCEPT 1000,ANS
      IF(ANS.NE.'Y') GO TO 3500
      TYPE *, 'Has the ion gauge reading changed?'
      ACCEPT 1000,ANS
      IF(ANS.NE.'Y') GO TO 3300
      TYPE *, 'Enter the ion gauge mantissa.'
      ACCEPT *,PRM(I)
      TYPE *, 'Enter the ion gauge exponent.'
      ACCEPT *,IPRE(I)
3300 TYPE *, 'Has the foreline pressure changed?'
      ACCEPT 1000,ANS
      IF(ANS.NE.'Y') GO TO 3350
      TYPE *, 'Enter the foreline pressure in mtorr (u).'
      ACCEPT *,PFORE(I)
3350 TYPE 3360,NONOFF(3-IDG(I))
3360 FORMAT(' Has the degas been turned o',A2,'?')
      ACCEPT 1000,ANS
      IF(ANS.EQ.'Y') IDG(I) = 3 - IDG(I)
      TYPE *, 'Has the emission current changed?'
      ACCEPT 1000,ANS
      IF(ANS.NE.'Y') GO TO 3500
      TYPE *, 'Enter the emission current in mA.'
      ACCEPT *,IPEM(I)
3500 CONTINUE
C
C CHECK ION PUMP CURRENTS
C
      DO 3700 I=1,3
      TYPE 3610,I,PION(I)
3610 FORMAT(' The Region ',I1,' Ion Pump Current is ',F6.1
      1,' uA.',/, ' Has this changed?')
      ACCEPT 1000,ANS
      IF(ANS.NE.'Y') GO TO 3700
      TYPE 3660,I
3660 FORMAT(' What is the Region ',I1,' Ion Pump Current (in uA)?')
      ACCEPT *,PION(I)
3700 CONTINUE
9000 RETURN
      END

```

SUBROUTINE SCHNRM(IOPT)

File SCHNRM.FOR begins on the previous line.

Version Date: July 19, 1984

Paul S. Weiss

Subroutine SCHNRM changes one or all of the Normalization parameters in SANG.

The argument IOPT specifies which parameters are to be changed as follows:

IOPT=0 Change all Parameters

IOPT=1 Change Normalization Angle (ANGNRM)

IOPT=2 Change Normalization Countdown Interval (INTNRM)

IOPT=3 Change Normalization Repetitions (NRMRPT)

COMMON /SETS/ GATE(16),TIM(16),EXCFRC(2),CLOCK,INTACQ,NCHAN
COMMON /NRMSET/ ANGNRM,INTNRM,NRMRPT,NRMFLG

IF(IOPT.GT.0) GO TO (1100,2100,3100),IOPT

1100 TYPE 1110,ANGNRM

1110 FORMAT(' The Normalization angle is ',F5.1,' degrees.'
1,' Change this?')

ACCEPT 1000,ANS

1000 FORMAT(A1)

IF(ANS.NE.'Y') GO TO 2000

TYPE *,'Enter Normalization angle'

ACCEPT *,ANGNRM

2000 IF(IOPT.NE.0) GO TO 9000

2100 TYPE 2110,INTNRM

2110 FORMAT(' The Normalization countdown interval is ',I5
1,' Change this?')

ACCEPT 1000,ANS

IF(ANS.NE.'Y') GO TO 3000

2300 TYPE *,'Enter countdown interval for Normalization'

ACCEPT *,INTNRM

IF(INTNRM.LE.0) GO TO 2300

3000 IF(IOPT.NE.0) GO TO 9000

3100 TYPE 3110,NRMRPT

3110 FORMAT(' The Normalization measurement is repeated ',I5
1,' times. Change this?')

ACCEPT 1000,ANS

IF(ANS.NE.'Y') GO TO 9000

3300 TYPE *,'Enter number of repetitions at each Normalization'

ACCEPT *,NRMRPT

IF(NRMRPT.LE.0) GO TO 3300

9000 RETURN

END

```

SUBROUTINE SCHPAR(IOPT)
C                                     File SCHPAR.FOR begins on the previous line.
C
C
C   Version Date:  July 19, 1984
C   Paul S. Weiss
C
C   Subroutine SCHPAR changes one or all of the data acquisition
C   parameters in SANG.
C
C   The argument IOPT specifies which parameters are to be changed
C   as follows:
C       IOPT=0  Change all Parameters
C       IOPT=1  Change the Number of Channels in Use (NCHAN)
C       IOPT=2  Change Clock Frequency (CLOCK)
C       IOPT=3  Change Interval for Data Acquisition (INTACQ)
C       IOPT=4  Change Gate Widths (GATE)
C       IOPT=5  Change Excited State Fractions (EXCFRC)
C
COMMON /TGSMAX/ DWLMAX,MAXCHN
COMMON /SETS/  GATE(16),TIM(16),EXCFRC(2),CLOCK,INTACQ,NCHAN
COMMON /CHAEF/ CHAEF(20,10)
C
IF(IOPT.GT.0) GO TO (1100,2100,3100,4100,5100),IOPT
C
CHANGE THE NUMBER OF DATA CHANNELS IN USE
C
1100  TYPE 1110,NCHAN
1110  FORMAT(1X,I1,' Data Channels are in use.  Change this?')
      ACCEPT 1000,ANS
1000  FORMAT(A1)
      IF(ANS.NE.'Y') GO TO 2000
1200  TYPE 1210
1210  FORMAT(' How many Data Channels are to be used'
1, ' (A channel consists of 2 scalers)?')
      ACCEPT *,NCHAN
      IF((NCHAN.LE.0).OR.(NCHAN.GT.MAXCHN)) GO TO 1200
2000  IF(IOPT.NE.0) GO TO 9000
C
CHANGE CLOCK FREQUENCY
C
2100  TYPE 2110,CLOCK
2110  FORMAT(' The clock frequency is ',F3.1,' Hz.  Change this?')
      ACCEPT 1000,ANS
      IF(ANS.NE.'Y') GO TO 3000
2300  TYPE *,'Enter clock frequency'
      ACCEPT *,CLOCK
      IF((CLOCK.NE.1.0).AND.(CLOCK.NE.1.5)) GO TO 2300
3000  IF(IOPT.NE.0) GO TO 9000
C

```

```

C      CHANGE ACQUISITION INTERVAL
C
3100  TYPE 3110,INTACQ
3110  FORMAT(' The countdown interval is ',I5,' Change this?')
      ACCEPT 1000,ANS
      IF(ANS.NE.'Y') GO TO 4000
3300  TYPE *,'Enter countdown interval for data acquisition'
      ACCEPT *,INTACQ
      IF(INTACQ.LE.0) GO TO 3300
4000  IF(IOPT.NE.0) GO TO 9000
C
C      CHANGE GATE WIDTHS
C
4100  TYPE 4110,GATE(1)
4110  FORMAT(' The gate widths are set at ',F5.2
      1,' msec. Change this?')
      ACCEPT 1000,ANS
      IF(ANS.NE.'Y') GO TO 5000
      TYPE *,'Enter the Gate Width for the A and B Channels'
      ACCEPT *,GATE(1)
5000  IF(IOPT.NE.0) GO TO 9000
C
C      CHANGE EXCITED STATE FRACTIONS
C
5100  DO 5400 I=1,2
      TYPE 5210,I,EXCFRC(I)
5210  FORMAT(' The fraction in Excited State #',I1,' is ',F6.4
      1,' Change this?')
      ACCEPT 1000,ANS
      IF(ANS.NE.'Y') GO TO 5400
5300  TYPE 5310,I
5310  FORMAT(' Enter Excited State fraction #',I1)
      ACCEPT *,EXCFRC(I)
      IF((EXCFRC(I).LT.0.).OR.(EXCFRC(I).GT.1.)) GO TO 5300
5400  CONTINUE
9000  RETURN
      END

```

SUBROUTINE SCHPOL(IOPT)

File SCHPOL.FOR begins on the previous line.

```

C
C      Version Date:  September 5, 1984
C      Paul S. Weiss
C
C      Subroutine SCHPOL changes one or all of the Polarization
C      Rotation Mode parameters in SANG.
C
C      The argument IOPT specifies which parameters are to be changed

```

```

C      as follows:
C          IOPT=0  Change all Parameters
C          IOPT=1  Change Polarization Rotation Detector Angle (ANGPOL)
C          IOPT=2  Change Polarization Rotation Motor Step Size (POLSTP)
C
COMMON /POLSET/ ANGPOL,POLSTP,POSIT,IPOSIT,IPLFLG
C
C
C      IF(IOPT.GT.0) GO TO (1100,2100),IOPT
1100   TYPE 1110,ANGPOL
1110   FORMAT(' The detector angle for the Polarization Rotation '
1      1,'Loop is ',F5.1,' degrees.'
2      2,/, ' Change this?')
ACCEPT 1000,ANS
1000   FORMAT(A1)
IF(ANS.NE.'Y') GO TO 2000
TYPE *, 'Enter detector angle.'
ACCEPT *,ANGPOL
2000   IF(IOPT.NE.0) GO TO 9000
2100   TYPE 2110,POLSTP,INT((180./POLSTP) + 0.5)
2110   FORMAT(' The motor step size is ',F6.3,' degrees.'
1      1,/, ' Rotating 180 degrees in ',I3,' steps.'
2      2,/, ' Change this?')
ACCEPT 1000,ANS
IF(ANS.NE.'Y') GO TO 9000
2200   TYPE 2210
2210   FORMAT(' Enter the number of steps in which to rotate the'
1      1,' polarization 180 degrees.')
ACCEPT *,NSTEP
IF((NSTEP.LT.2).OR.(NSTEP.GT.200)) GO TO 2200
POLSTP = 180. / (1. * NSTEP )
9000   RETURN
      END

SUBROUTINE SHTST(IOPT)
C
C          File SHTST.FOR begins on the previous line.
C
C      Version Date:  June 28, 1984
C      Paul S. Weiss
C
C      Subroutine SHTST changes one or all of the Test Mode
C      parameters in SANG.
C
C      The argument IOPT specifies which parameters are to be changed
C      as follows:
C          IOPT=0  Change all Parameters
C          IOPT=1  Change Angle (TSTANG)

```

```

C          IOPT=2 Change Number of Countdowns (NUMTST)
C
COMMON /TGSMAX/ DWLMAX,MAXCHN
COMMON /SETS/ GATE(16),TIM(16),EXCFRC(2),CLOCK,INTACQ,NCHAN
COMMON /TSTSET/ TSTANG,NUMTST,TSTCUR,TSTFLG
C
IF(IOPT.GT.0) GO TO (1100,2100),IOPT
1100 TYPE *, 'Enter angle for Test'
ACCEPT *,TSTANG
IF(IOPT.NE.0) GO TO 9000
2100 TYPE *, 'Enter number of countdowns for Test'
ACCEPT *,NUMTST
9000 RETURN
END

SUBROUTINE SCHVEL(IOPT)
C          File SCHVEL.FOR begins on the previous line.
C
C          Version Date: July 19, 1984
C          Paul S. Weiss
C
C          Subroutine SCHVEL changes one or all of the Velocity Measurement
C          parameters in SANG.
C
C          The argument IOPT specifies which parameters are to be changed
C          as follows:
C          IOPT=0 Change all Parameters
C          IOPT=1 Change Laser Frequency (FRQLAS)
C          IOPT=2 Change Relative Frequency Standard (FSRLAS)
C          IOPT=3 Change Velocity Measurement Step Size (LASSTP)
C          IOPT=4 Change Velocity Measurement Accumulation Time (LASDWL)
C
COMMON /TGSMAX/ DWLMAX,MAXCHN
COMMON /SETS/ GATE(16),TIM(16),EXCFRC(2),CLOCK,INTACQ,NCHAN
COMMON /LASSET/ LASDWL,FRQLAS,LASSTP,FSRLAS,LASCHA
C
IF(IOPT.GT.0) GO TO (1100,2100,3100,4100),IOPT
1100 TYPE 1110,FRQLAS
1110 FORMAT(' The laser frequency is ',F11.4
1,' cm-1. Has this changed?')
ACCEPT 1000,ANS
1000 FORMAT(A1)
IF(ANS.NE.'Y') GO TO 2000
1300 TYPE *, 'Enter Laser Frequency (in cm-1).'
ACCEPT *,FRQLAS
IF(FRQLAS.LE.0.) GO TO 1300
2000 IF(IOPT.NE.0) GO TO 9000
2100 TYPE 2110,FSRLAS
2110 FORMAT(' The Fabrey-Perot Free Spectral Range is ',F5.2
1,' GHz. Has this changed?')

```

```

ACCEPT 1000,ANS
IF(ANS.NE.'Y') GO TO 3000
2300 TYPE 2310
2310 FORMAT(' Enter the Relative Frequency Standard '
1,'(FSR of the Fabrey-Perot etalon, in GHz).')
ACCEPT *,FSRLAS
IF(FSRLAS.LE.0.) GO TO 2300
3000 GO TO 9000
3100 TYPE *,'Enter Velocity Measurement Step Size (1-4096)'
ACCEPT *,LASSTP
IF(LASSTP.LE.0) GO TO 3100
4000 IF(IOPT.NE.0) GO TO 9000
4100 TYPE *,'Enter Velocity Measurement Accumulation Time (1-30000)'
ACCEPT *,LASDWL
IF(LASDWL.LE.0) GO TO 4100
9000 RETURN
END

```

SUBROUTINE SCMLST

File SCMLST.FOR begins on the previous line.

C
C
C
C
C
C
C
C
C

Version Date: August 15, 1985
Paul S. Weiss

Subroutine SCMLST lists the command groups for SANG. It provides
the general help screen for SANG.

```

TYPE 100
100 FORMAT(//,' The available commands are as follows:'
1,/, ' C* Change Commands'
2,/, ' D* Define and Display Commands'
3,/, ' EX Exit'
4,/, ' G* Graph Commands'
5,/, ' H Help'
6,/, ' L* Loop Commands'
7,/, ' M* Machine Condition Commands'
7,/, ' N* Normalization Commands')
TYPE 200 \
200 FORMAT(' P* Print Commands'
1,/, ' R* Record Data, and Rotate Polarization Commands'
2,/, ' S* Show Commands'
3,/, ' T* Test Commands'
4,/, ' V* Velocity Measurement Commands'
5,/, ' W* Write Commands'
6,/, ' Z* Zero Commands')
TYPE 300
300 FORMAT(/,' To get a listing of the various options of'
1,' a starred command, ',/, ' enter an "H" in place of the "*" '
2,' (i.e. "PH" for a list of the Print commands).')
RETURN

```


END

SUBROUTINE SCOMLC

File SCOMLC.FOR begins on the previous line.

Version Date: July 7, 1984

Paul S. Weiss

Subroutine SCOMLC lists all the C* commands relating to changing the fundamental parameters of the data acquisition.

TYPE 100

100 FORMAT(/, ' The available Change Commands are as follows:'

1,/, ' CA	Change Angle'
2,/, ' CC	Change Clock Frequency'
3,/, ' CD	Change Definitions of Channels'
4,/, ' CE	Change Excited State Fractions'
5,/, ' CF	Change File'
6,/, ' CG	Change Gate Widths')

TYPE 200

200 FORMAT(' CH C Help'

1,/, ' CI	Change Interval for Acquisition Countdown'
2,/, ' CL	Change Loop Parameters'
3,/, ' CN	Change Normalization Parameters'
4,/, ' CP	Change Data Acquisition Parameters'
5,/, ' CU	Change Number of Channels Used'
6,/, ' CV	Change Velocity Measurement Parameters')

RETURN

END

SUBROUTINE SCOMLD

File SCOMLD.FOR begins on the previous line.

Version Date: July 18, 1984

Paul S. Weiss

Subroutine SCOMLD lists all the D* commands relating to display and the cosmetic definitions of channels and machine hardware.

TYPE 100

100 FORMAT(/, ' The available Definition and '

1, 'Display	Commands are as follows:'
1,/, ' DA	Display: Change All'
2,/, ' DB	Define Beams'
3,/, ' DC	Define Channels'
4,/, ' DH	D Help'

```

200 5,, ' DI      Display: Scale Channels Independently'
    6,, ' DL      Display: Change Lower Channel'
    7,, ' DP      Define Pressure Regions')
    TYPE 200
    FORMAT(' DR      Display: Refresh'
    9,, ' DS      Display: Scale Channels to the Same Value'
    1,, ' DT      Define Thermocouples'
    2,, ' DU      Display: Change Upper Channel'
    3,, ' DW      Display: Change Window')
    RETURN
    END

```

SUBROUTINE SCOMLG

File SCOMLG.FOR begins on the previous line.

C
C
C
C
C
C
C

```

Version Date: September 17, 1984
Paul S. Weiss

```

Subroutine SCOMLG lists all the G* commands relating to plotting.

```

100 TYPE 100
    FORMAT(/, ' The available Graph Commands are as follows:'
    1,, ' GE      Graph Both Displays'
    2,, ' GH      G Help'
    3,, ' GL      Graph Lower Display'
    4,, ' GP      Graph Upper Display')
    RETURN
    END

```

SUBROUTINE SCOMLL

File SCOMLL.FOR begins on the previous line.

C
C
C
C
C
C
C

```

Version Date: June 23, 1984
Paul S. Weiss

```

Subroutine SCOMLL lists all the L* commands relating to loop mode.

```

100 TYPE 100
    FORMAT(/, ' The available Loop Commands are as follows:'
    1,, ' LA      Loop: Change Current Angle'
    2,, ' LB      Loop: Change Beginning Angle'
    3,, ' LC      Loop: Continue'
    4,, ' LD      Loop: Change Direction'
    5,, ' LE      Loop: Change Ending Angle')
    TYPE 200
    FORMAT(' LH      L Help'
    1,, ' LI      Loop: Change Angular Interval'
    2,, ' LN      Loop: Change Normalization Frequency'

```

```

3,/, ' LP      Change All Loop Parameters'
4,/, ' LS      Loop: Start')
RETURN
END

```

SUBROUTINE SCOMLM

File SCOMLM.FOR begins on the previous line.

```

Version Date: July 18, 1984
Paul S. Weiss

```

```

Subroutine SCOMLM lists all the M* commands having to do with
the current machine conditions.

```

TYPE 100

100 FORMAT(/, ' The available Machine Condition'

1, ' Commands are as follows:'

1,/, ' MA Machine Conditions: '

1, 'Change All Detector Settings'

2,/, ' MB Machine Conditions: '

2, 'Change Backing Pressures'

3,/, ' MD Machine Conditions: '

3, 'Change Daly Detector (post-QPMS)')

TYPE 200

200 FORMAT(' MF Machine Conditions: '

3, 'Change Filament/Ionizer Settings'

4,/, ' MH Machine Conditions: Help'

5,/, ' MI Machine Conditions: Change Ion Lens Settings'

6,/, ' MM Machine Conditions: '

6, 'Change Mass Spectrometer Settings'

7,/, ' MR Machine Conditions: Change Regional Pressures'

8,/, ' MS Machine Conditions: '

9, 'Change Source Conditions'

1,/, ' MT Machine Conditions: '

1, 'Change Thermocouple Readings')

RETURN

END

SUBROUTINE SCOMLN

File SCOMLN.FOR begins on the previous line.

```

Version Date: June 23, 1984
Paul S. Weiss

```

```

Subroutine SCOMLN lists all the N* commands relating to normalization
mode of SANG.

```

```

TYPE 100
100 FORMAT(/, ' The available Normalization Commands are as follows:')
1,/, ' NA      Change Normalization Angle'
2,/, ' NH      N Help'
3,/, ' NI      Change Normalization Countdown Interval'
4,/, ' NP      Change All Normalization Parameters'
5,/, ' NR      Change Normalization Repetitions'
6,/, ' NS      Normalization: Start')
RETURN
END

```

SUBROUTINE SCOMLP

File SCOMLP.FOR begins on the previous line.

C
C
C
C
C
C
C
C

Version Date: July 24, 1984
Paul S. Weiss

Subroutine SCOMLP lists all the P* commands relating to printing information on the line printer.

```

TYPE 100
100 FORMAT(/, ' The available Print Commands are as follows:')
1,/, ' PA      Print Accumulated Data'
2,/, ' PC      Print Current Configuration'
3,/, ' PD      Print Data Channel Definitions'
5,/, ' PG      Print Current Graphics Display'
6,/, ' PH      P Help'
7,/, ' PI      Print Information on the Line Printer')
TYPE 200
200 FORMAT('          PL      Print Loop Parameters'
9,/, ' PM      Print Machine Conditions'
1,/, ' PN      Print Normalization Parameters'
2,/, ' PR      Print Rotation of Polarization Parameters'
3,/, ' PS      Print Detector Settings'
4,/, ' PT      Print Test Mode Parameters'
5,/, ' PV      Print Velocity Parameters and Measurement.')
RETURN
END

```

SUBROUTINE SCOMLR

File SCOMLR.FOR begins on the previous line.

C
C
C
C
C
C
C
C

Version Date: July 24, 1984
Paul S. Weiss

Subroutine SCOMLR lists all the R* commands relating to polarization rotation mode of SANG, recording data, and hardware reset.

```

TYPE 100
100  FORMAT(/, ' The available Record Data and Rotation of'
      1, ' Polarization Commands are as follows:'
      1,/, ' RA      Rotation of Polarization:  Change Angle'
      2,/, ' RD      Record Data'
      3,/, ' RH      R Help'
      4,/, ' RI      Reinitialize TGS System'
      5,/, ' RM      Rotation of Polarization:  Change Motor'
      5, ' Step Size'
      5,/, ' RP      Rotation of Polarization:  Change All '
      5, 'Parameters'
      6,/, ' RS      Rotation of Polarization:  Start')
RETURN
END

```

SUBROUTINE SCOMLS

File SCOMLS begins on the previous line.

C
C
C
C
C
C
C
C

Version Date: July 24, 1984
Paul S. Weiss

Subroutine SCOMLS lists all the S* commands relating to typing information on the console terminal.

```

TYPE 100
100  FORMAT(/, ' The available Show Commands are as follows:'
      1,/, ' SA      Show Accumulated Data'
      2,/, ' SC      Show Current Configuration'
      3,/, ' SD      Show Data Channel Definitions'
      5,/, ' SG      Show Current Graphics Display')
TYPE 200
200  FORMAT(' SH      S Help'
      1,/, ' SI      Show Time Information'
      2,/, ' SL      Show Loop Mode Parameters'
      9,/, ' SM      Show Machine Conditions'
      3,/, ' SN      Show Normalization Parameters'
      4,/, ' SR      Show Rotation of Polarization Parameters'
      3,/, ' SS      Show Detector Settings'
      5,/, ' ST      Show Test Mode Parameters'
      6,/, ' SV      Show Velocity Parameters and Measurement')
RETURN
END

```

SUBROUTINE SCOMLT

File SCOMLT.FOR begins on the previous line.

C
C
C
C

Version Date: June 23, 1984
Paul S. Weiss

C
C Subroutine SCOMLT lists all the T* commands relating to test mode
C of SANG.
C

```

TYPE 100
100 FORMAT(/, ' The available Test Mode Commands are as follows: '
1,/, ' TA Change Test Angle '
2,/, ' TC Test Mode: Continue '
3,/, ' TE Test Mode: Exit '
4,/, ' TH T Help '
5,/, ' TN Test Mode: Change Number of Countdowns '
6,/, ' TP Change All Test Mode Parameters '
7,/, ' TS Test Mode: Start ')
RETURN
END

```

SUBROUTINE SCOMLV

File SCOMLV.FOR begins on the previous line.

C
C
C Version Date: June 23, 1984
C Paul S. Weiss
C

C Subroutine SCOMLV lists all the V* commands relating to the
C measurement of a beam velocity by measuring the Doppler shift
C of a transition.
C

```

TYPE 100
100 FORMAT(/, ' The available Velocity Measurement Commands '
1, ' are as follows: '
2,/, ' VA Change Velocity Measurement Accumulation Time '
3,/, ' VF Change Velocity Measurement Frequency Standard '
4,/, ' VH V Help '
5,/, ' VL Change Velocity Measurement Laser Frequency '
6,/, ' VM Measure Velocity '
7,/, ' VP Change All Velocity Measurement Parameters '
8,/, ' VS Change Velocity Measurement Step Size ')
RETURN
END

```

SUBROUTINE SCOMLW

File SCOMLW.FOR begins on the previous line.

C
C
C Version Date: September 3, 1984
C Paul S. Weiss
C

C Subroutine SCOMLW lists all the W* commands relating to writing
C information to the data file.
C

```

C
100 TYPE 100
    FORMAT(/, ' The available Write to Disk Commands'
1, ' are as follows:')
1,/, ' WA      Write Accumulated Data'
2,/, ' WC      Write Current Configuration'
3,/, ' WD      Write Data Channel Definitions'
5,/, ' WG      Write Current Graphics Display'
6,/, ' WH      W Help'
7,/, ' WI      Write and Print Information')
TYPE 200
200 FORMAT('      WL      Write Loop Mode Parameters'
9,/, ' WM      Write Machine Conditions'
1,/, ' WN      Write Normalization Parameters'
2,/, ' WR      Write Rotation of Polarization Parameters'
3,/, ' WS      Write Detector Settings'
4,/, ' WT      Write Test Mode Parameters'
5,/, ' WV      Write Velocity Parameters and Measurement.')
RETURN
END

```

SUBROUTINE SCOMLZ

File SCOMLZ.FOR begins on the previous line.

```

C
C
C Version Date: June 23, 1984
C Paul S. Weiss
C

```

Subroutine SCOMLZ lists all the Z* commands relating to zeroing all or part of the accumulated data.

```

C
100 TYPE 100
    FORMAT(/, ' The available Zero Commands are as follows:')
1,/, ' ZA      Zero Arrays'
2,/, ' ZH      Z Help'
3,/, ' ZS      Zero Angular Segment'
4,/, ' ZT      Zero Test Mode Data')
RETURN
END

```

SUBROUTINE SDISP

File SDISP.FOR begins on the previous line.

```

C
C
C Version Date: September 25, 1984
C Paul S. Weiss
C

```

Subroutine SDISP loads the display array for the DT2771 DMA display driver. The current point is brightened by

```

C      a factor of 10X.
C
C      WARNING: Subroutines SDISP and SDVAL make up the largest
C                segment of overlay region 1. Enlarging either of them
C                will directly increase the total size of SANG.
C
COMMON /DATA/ DATA(256,20),WORK1(256),WORK2(256)
COMMON /DISP/ IDSP(1064),MODSPT,MODSPB,DSPB,DSTEP,NDSP,INDEP
COMMON /DSPCHA/ MDSPT,NDSPT,MDSPB,NDSPB
COMMON /DSPZER/ ITYZER,IBYZER
COMMON /SCR/ SCR(20)
COMMON /DSCR/ DSCR(20)
COMMON /CUR/ ANGLE,INTERV,NUMANG,MANGLE,IRNFLG
C
C      FIRST STOP DISPLAY
C
      CALL STOPD
      NWRITE = 0
      DO 100 I=1,NDSP
      IT = 2*I - 1
      IB = (2*NDSP) + IT
      IDSP(IB) = 16*I - 8
      IDSP(IT) = 16*I - 8
      IDSP(IB + 1) = 0
      IDSP(IT + 1) = 2040
100    CONTINUE
      DO 200 I=1,256
      WORK1(I) = 0.
      WORK2(I) = 0.
200    CONTINUE
C
C      FIRST DETERMINE THE FIRST ANGLE TO BE DISPLAYED
C
      DO 1300 IBE=1,NUMANG
      IF(DATA(IBE,1).GE.DSPB) GO TO 1500
1300   CONTINUE
C
C      INITIALIZE MAXIMA AND MINIMA
C
1500   TMAX = 0.
      TMIN = 0.
      BMAX = 0.
      BMIN = 0.
C
C      LOAD NEW DATA INTO SCRATCH ARRAY FOR DISPLAY LOADING
C
      DO 1600 I=2,20
      DSCR(I) = SCR(I)
1600   CONTINUE
C

```



```

C      DETERMINE VALUES OF NEW DATA
C
      CALL SDVAL(MODSPT,MDSPT,NDSPT,TVAL,TMAX,TMIN)
      CALL SDVAL(MODSPB,MDSPB,NDSPB,BVAL,BMAX,BMIN)
C
C      INITIALIZE THE MINIMUM AND MAXIMUM OF DISPLAY Y VALUES TO THE
C      NEW DATA VALUES
C
C      THE SUBROUTINE SDVAL WILL CONTINUE TO CHECK FOR MINIMA AND
C      MAXIMA AS IT LOADS THE VALUES OF EACH DATA POINT
C
C      DETERMINE WHICH ANGLES ARE DISPLAYED WHERE, NOTE THAT IF MORE
C      THAN ONE DATA POINT WOULD BE DISPLAYED AT A DISPLAY POINT,
C      THESE ARE COMBINED, AS IF TAKEN AT EXACTLY THE SAME ANGLE.
C
C      THE DISPLAY RESOLUTION IS DETERMINED BY THE VARIABLE DSTEP
C
      DO 2500 I=1,NDSP
      IF(IBE-NUMANG.GT.0) GO TO 3000
      NDANG = 0
      DO 2000 J=IBE,NUMANG
      IF(DATA(J,1).GT.(DSPB+(I*DSTEP))) GO TO 2100
      NDANG = NDANG + 1
2000   CONTINUE
C
C      IF THERE IS NO DATA FOR THIS DISPLAY POINT, GO ON TO NEXT
C
2100   IF(NDANG.EQ.0) GO TO 2500
C
C      LOAD TOTAL DATA FOR THIS DISPLAY POINT INTO DSCR
C
      DO 2300 K=2,20
      DSCR(K) = 0.
      DO 2200 J=1,NDANG
      DSCR(K) = DSCR(K) + DATA(IBE+J-1,K)
2200   CONTINUE
2300   CONTINUE
C
C      SDVAL DETERMINES THE VALUE OF THE DISPLAY POINT
C
      CALL SDVAL(MODSPT,MDSPT,NDSPT,WORK1(I),TMAX,TMIN)
      CALL SDVAL(MODSPB,MDSPB,NDSPB,WORK2(I),BMAX,BMIN)
C
C      ADVANCE THE POINT AT WHICH THE DATA IS FIRST
C      CHECKED TO SEE IF A POINT IS TO BE DISPLAYED
C
      IBE = IBE + NDANG
2500   CONTINUE
C
C      IF CHANNELS ARE TO SCALED TO THE SAME VALUE, FIND MAXIMUM AND MINIMUM

```

```

C
3000  IF(INDEP.NE.0) GO TO 3500
      TMAX = AMAX1(TMAX,BMAX)
      TMIN = AMIN1(TMIN,BMIN)
      BMAX = TMAX
      BMIN = TMIN

C
C      DETERMINE THE Y RANGE OF THE UPPER AND LOWER DISPLAYS
C
3500  TRANGE = (TMAX - TMIN) / 2000.
      BRANGE = (BMAX - BMIN) / 2000.

C
C      CONVERT TO 12 BIT INTEGERS FOR DISPLAY
C
      DO 5000 I=1,NDSP
      IF(TRANGE.LE.0.) GO TO 5000
      IDSP(2*I) = INT((WORK1(I) - TMIN) / TRANGE) + 2040
      IF(BRANGE.LE.0.) GO TO 5000
      IDSP(2*(I+NDSP)) = INT((WORK2(I) - BMIN) / BRANGE)
5000  CONTINUE

C
C      LOAD BRIGHTENED POINT
C
      ITYSCR = 2040
      IBYSCR = 0
      XSCR = (SCR(1) - DSPB)/DSTEP

C
C      SEE IF THE CURRENT DATA FITS ON THE DISPLAY WINDOW
C      IF IT DOES NOT, ONLY DISPLAY ARRAYS (I.E. LEAVE NBRITE = 0)
C
      IF((XSCR.LT.0.) .OR. (XSCR.GT.256.)) GO TO 8500
      NBRITE = 20
      IXSCR = INT(16.*XSCR) - 8
      IF(TRANGE.GT.0.) ITYSCR = INT((TVAL - TMIN)/TRANGE) + 2040
      IF(BRANGE.GT.0.) IBYSCR = INT((BVAL - BMIN)/BRANGE)
      DO 6000 I=1,10
      NDY = (4*NDSP) + (2 * I)
      IDSP(NDY-1) = IXSCR
      IDSP(NDY) = ITYSCR
      IDSP(NDY + 19) = IXSCR
      IDSP(NDY + 20) = IBYSCR
6000  CONTINUE

C
C      CALL MACRO TO DO DISPLAY
C
8500  CALL DISPL(IDSP,((2*NDSP)+NBRITE))

C
C      FIND ZERO LEVELS FOR TOP AND BOTTOM IN ORDER TO PLOT DISPLAYS
C      IF CALLED FOR
C

```

```

ITYZER = 2040
IBYZER = 0
IF (TRANGE.GT.0.) ITYZER = INT( - TMIN / TRANGE) + 2040
IF (BRANGE.GT.0.) IBYZER = INT( - BMIN / BRANGE)
9000 RETURN
END

```

```

SUBROUTINE SDVAL(MODD,MDS,NDS,VAL,VMAX,VMIN)
C                                     Second routine in file SDISP.FOR.
C

```

```

C   Version Date:  July 27, 1984
C   Paul S. Weiss
C

```

```

C   Subroutine SDVAL determines the correct display value
C   for the cuurent point given the display.  It then determines
C   the new minimum and maximum.
C

```

```

COMMON /SETS/ GATE(16),TIM(16),EXCFRC(2),CLOCK,INTACQ,NCHAN
COMMON /DSCR/ DSCR(20)
MS = (2*MDS) + 1
MB = MS + 1
NS = (2*NDS) + 1
NB = NS + 1
VAL = 0.
IF (DSCR(2).LT.1.E-5) GO TO 2000
1100 GO TO (1100,1200,1300,1400,1500,1600),MODD
VAL = (DSCR(MS) - DSCR(MB)) / DSCR(2)
GO TO 2000
1200 VAL = (DSCR(MS) - DSCR(MB) - DSCR(NS) + DSCR(NB)) / DSCR(2)
GO TO 2000
1300 X = 1.
IF (EXCFRC(1).NE.0.) X = EXCFRC(1)
VAL = (DSCR(MS) - DSCR(MB) - ((1. - X)
1 * (DSCR(NS) - DSCR(NB)))) / (DSCR(2) * X)
GO TO 2000
1400 VD = SQRT( DSCR(MS) + DSCR(MB) + DSCR(NS) + DSCR(NB) )
IF (VD.EQ.0.) GO TO 2000
VAL = (DSCR(MS) - DSCR(MB) - DSCR(NS) + DSCR(NB)) / VD
GO TO 2000
1500 VD = SQRT( DSCR(MS) + DSCR(MB) )
IF (VD.EQ.0.) GO TO 2000
VAL = (DSCR(MS) - DSCR(MB)) / VD
GO TO 2000
1600 VAL = DSCR(2)
2000 IF (VAL.GT.VMAX) VMAX = VAL
IF (VAL.LT.VMIN) VMIN = VAL
RETURN

```

END

SUBROUTINE SDLONO(ISTART)

File SDLONO.FOR begins on the previous line.

Version Date: September 27, 1984

Paul S. Weiss

Subroutine SDLONO is called during Loop mode after a normalization.

COMMON /CUR/ ANGLE,INTERV,NUMANG,MANGLE,IRNFLG

COMMON /SCR/ SCR(20)

COMMON /SETS/ GATE(16),TIM(16),EXCFRC(2),CLOCK,INTACQ,NCHAN

COMMON /LOPSET/ ANLPBE,ANLPFN,ANLPIN,LPNRFQ,ANLPCU,LPFLAG

COMMON /NRMSET/ ANGNRM,INTNRM,NRMRPT,NRMFLG

IF(NRMFLG.NE.0) GO TO 9000

ISTART = 1

GO TO (1100,2100),-LPFLAG

CONTINUE LOOP

1100 TYPE *, 'End data taking loop?'

ACCEPT 1000,ANS

1000 FORMAT(A1)

IF(ANS.EQ.'Y') GO TO 8900

ANLPCU = ANLPCU + ANLPIN

HAS THE END OF A SCAN BEEN REACHED?

IF((ANLPCU.GT.AMAX1(ANLPBE,ANLPFN)).OR.(ANLPCU

1.LT.AMIN1(ANLPBE,ANLPFN))) GO TO 7000

GO TO 6500

IF LOOP HAS JUST BEGUN, START AT BEGINNING OF LOOP
(AFTER NORMALIZATION)

2100 ANLPCU = ANLPBE

SET UP ANGLE FOR ACQUISITION

6500 LPFLAG = 1

ANGLE = ANLPCU

INTERV = INTACQ

GO TO 9000

REVERSE DIRECTION IF THE END OF A SCAN HAS BEEN REACHED

```

C
7000  A = ANLPFN
      ANLPFN = ANLPBE
      ANLPBE = A
      ANLPIN = - ANLPIN
      ANLPCU = ANLPBE
      TYPE 7010
7010  FORMAT(/, ' The angular scan has been completed.'
1,/, ' Rescan in the opposite direction from ',F5.1,' to '
2,F5.1,' degrees, ',/, ' in ',F5.1,' degree steps?')
ACCEPT 1000,ANS
IF(ANS.EQ.'Y') GO TO 6500

C
C      DO NOT RESTART IF LOOP IS NOT TO BE CONTINUED
C
8900  ISTART = 0
      LPFLAG = 0
9000  RETURN
      END

```

```

SUBROUTINE SDLOP(NKEEP,ISTART)

```

```

File SDLOP.FOR begins on the previous line.

```

```

C
C      Version Date:  September 27, 1984
C      Paul S. Weiss

```

```

C
C      Subroutine SDLOP decides whether or not to keep a data point,
C      and continue the data taking loop.
C
C

```

```

COMMON /CUR/  ANGLE,INTERV,NUMANG,MANGLE,IRNFLG
COMMON /SCR/  SCR(20)
COMMON /SETS/ GATE(16),TIM(16),EXCFRC(2),CLOCK,INTACQ,NCHAN
COMMON /LOPSET/ ANLPBE,ANLPFN,ANLPIN,LPNRFQ,ANLPCU,LPFLAG
COMMON /NRMSET/ ANGNRM,INTNRM,NRMRPT,NRMFLG

```

```

C
      NKEEP = 1
      ISTART = 1
100   TYPE 110, ' ', 'a'
110   FORMAT(' Save this point',A1,:
1,A1,'nd continue data taking loop?')
ACCEPT 1000,ANS
1000  FORMAT(A1)
      IF(ANS.EQ.'Y') GO TO 5000
      TYPE 110, '?'
ACCEPT 1000,ANS
      IF(ANS.EQ.'Y') GO TO 3000
      NKEEP = 0

```

```

TYPE *, 'Repeat this point?'
ACCEPT 1000, ANS
IF (ANS.EQ.'Y') GO TO 9000
TYPE *, 'Change detector angle?'
ACCEPT 1000, ANS
IF (ANS.NE.'Y') GO TO 3000
TYPE *, 'Enter correct angle.'
ACCEPT *, SCR(1)
NKEEP = 1
3000 TYPE *, 'End data taking loop?'
ACCEPT 1000, ANS
IF (ANS.NE.'Y') GO TO 100
GO TO 8900

C
C CONTINUE LOOP
C
C IS IT TIME FOR A NORMALIZATION?
C IF SO, SET DETECTOR AND INTERVAL ACCORDINGLY
C
5000 IF (LPFLAG.LT.LPNRFQ) GO TO 6000
NRMFLG = 1
ANGLE = ANGNRM
INTERV = INTNRM
LPFLAG = -1.
TYPE 5210
5210 FORMAT(/, ' Normalization!', /)
GO TO 9000

C
C INCREMENT COUNTER AND ANGLE FOR NEXT ANGLE IN LOOP
C
6000 LPFLAG = LPFLAG + 1
ANLPCU = ANLPCU + ANLPIN

C
C HAS THE END OF A SCAN BEEN REACHED?
C
IF ((ANLPCU.GT.AMAX1(ANLPBE, ANLPFN)) .OR. (ANLPCU
1.LT.AMIN1(ANLPBE, ANLPFN))) GO TO 7000

C
C SET UP NEXT ANGLE
C
6500 ANGLE = ANLPCU
INTERV = INTACQ
GO TO 9000

C
C REVERSE DIRECTION IF THE END OF A SCAN HAS BEEN REACHED
C
7000 A = ANLPFN
ANLPFN = ANLPBE
ANLPBE = A
ANLPIN = - ANLPIN

```

```

ANLPCU = ANLPBE
TYPE 7010,ANLPBE,ANLPFN,ANLPIN,7,7,7,7,7
7010  FORMAT(/,' The angular scan has been completed.'
      1,' Rescan in the opposite direction',/, ' from ',F5.1,' to '
      2,F5.1,' degrees, in ',F5.1,' degree steps?',5A1)
ACCEPT 1000,ANS
IF(ANS.EQ.'Y') GO TO 6500

C
C  DO NOT RESTART IF LOOP IS NOT TO BE CONTINUED
C
8900  ISTART = 0
      LPFLAG = 0
9000  RETURN
      END

```

```

SUBROUTINE SDNRM(NKEEP,ISTART)
C                                     File SDNRM.FOR begins on the previous line.
C
C  Version Date:  July 19, 1984
C  Paul S. Weiss
C
C  Subroutine SDNRM decides whether or not to keep a data point.
C  It is called during a normalization.
C
C
COMMON /CUR/ ANGLE,INTERV,NUMANG,MANGLE,IRNFLG
COMMON /NRMSET/ ANGNRM,INTNRM,NRMRPT,NRMFLG
C
      ISTART = -1
      NKEEP = 1
      TYPE *, 'Save this normalization point?'
ACCEPT 1000,ANS
1000  FORMAT(A1)
      IF(ANS.EQ.'Y') GO TO 2000
      NKEEP = 0
      TYPE 1210
1210  FORMAT(/,' Abort this normalization point.'
      1,/, ' Measure it again?')
ACCEPT 1000,ANS
C
C  IF POINT NEEDS TO BE RETAKEN, DO NOT INCREMENT NORMALIZATION
C  FLAG, AND QUERY THAT DETECTOR IS READY
C
      IF(ANS.NE.'Y') GO TO 2000
      ISTART = 1
      GO TO 9000
C
C  TO CONTINUE NORMALIZATION, INCREMENT REPETITION COUNTER, AND

```

```

C      SEE IF THE CORRECT NUMBER OF REPETITIONS HAVE BEEN DONE.
C
2000  IF(NRMFLG.GE.NRMRPT) GO TO 7000
      NRMFLG = NRMFLG + 1
      GO TO 9000

C
C      IF THE NUMBER OF REPETITIONS REQUESTED HAVE BEEN COMPLETED,
C      STOP NORMALIZING, AND SEE IF ANOTHER NORMALIZATION IS DESIRED
C
7000  NRMFLG = 0
      ISTART = 0
8000  TYPE *, 'End of Normalization.  Normalize again?'
      ACCEPT 1000,ANS
      IF(ANS.NE.'Y') GO TO 9000
      ISTART = 1
      NRMFLG = 1
9000  RETURN
      END

```

SUBROUTINE SDONE

File SDONE.FOR begins on the previous line.

```

C
C      Version Date:  October 30, 1984
C      Paul S. Weiss

```

```

C
C      Subroutine SDONE outputs the scratch data from the scalars
C      (using SOUT), displays the data (using SDISP), and calls the
C      appropriate routines depending upon how the data was taken
C      (SDLOP for Loop Mode, SDNRM for Normalization, SDPOL for Rotation
C      of Polarization, SDTST for Test Mode, and SDSIN for single
C      angle acquisition).
C
C

```

```

C
C      INTEGER*4 JDATA
COMMON /CUR/  ANGLE, INTERV, NUMANG, MANGLE, IRNFLG
COMMON /DATA/ DATA(256,20), WORK1(256), WORK2(256)
COMMON /SCR/  SCR(20)
COMMON /SETS/ GATE(16), TIM(16), EXCFRC(2), CLOCK, INTACQ, NCHAN
COMMON /LASSET/ LASDWL, FRQLAS, LASSTP, FSRLAS, LASCHA
COMMON /LOPSET/ ANLPBE, ANLPFN, ANLPIN, LPNRFQ, ANLPCU, LPFLAG
COMMON /NRMSET/ ANGNRM, INTNRM, NRMRPT, NRMFLG
COMMON /POLSET/ ANGPOL, POLSTP, POSIT, IPOSIT, IPLFLG
COMMON /TSTSET/ TSTANG, NUMTST, TSTCUR, TSTFLG
COMMON /SDONE/ ISWFLG, JDATA(20)

```

```

C
C      LEAVE SPECIAL SCREEN MODE
C

```

```

C      CALL EXSPEC

```



```
C
C   IF AN OVERFLOW HAS OCCURRED, HANDLE IT IN ROUTINE SOVER
C
C   IF(ISWFLG.LT.2) GO TO 200
C   CALL SOVER(ISTART)
C   GO TO 8000
C
C   IF THERE IS NEW DATA, GET IT
C
C   200 IF(ISWFLG.EQ.1) CALL SGTSCR
C
C   DISPLAY NEW DATA
C
C   CALL SDISP
C
C   RESET CALLING FLAG, AND RETURN IF ONLY CALLED FOR DISPLAY PURPOSES
C
C   I = ISWFLG
C   ISWFLG = -1
C   IF(I.EQ.0) GO TO 8900
C
C   OUTPUT NEW DATA ON TERMINAL
C
C   CALL SOUT(7)
C
C   DETERMINE WHAT MODE THE DATA WAS TAKEN IN AND CALL THE APPROPRIATE
C   ROUTINES
C
C   NKEEP = 0
C   ISTART = 0
C
C   ACCUMULATE FLAGS' STATUS SO THAT THIS CAN BE WRITTEN TO DISK AS ONE
C   WORD, IFLAG
C
C   IFLAG = 0
C   IF(NRMFLG.NE.0) IFLAG = 1
C   IF(LPFLAG.NE.0) IFLAG = IFLAG + 10
C   IF(IPLFLG.NE.0) IFLAG = IFLAG + 100
C   IF(TSTFLG.NE.0) IFLAG = IFLAG + 1000
C
C   TEST MODE?
C
C   IF(TSTFLG.EQ.0) GO TO 2100
C   CALL SDTST(NKEEP, ISTART)
C   GO TO 7000
C
C   NORMALIZING?
C
C   2100 IF(NRMFLG.EQ.0) GO TO 3100
C   CALL SDNRM(NKEEP, ISTART)
```

```

C
C   IF NORMALIZATION IS IN LOOP, ALSO CALL SDLONO
C
C   IF(LPFLAG.NE.0) CALL SDLONO(ISTART)
C   GO TO 7000
C
C   LOOP MODE, BUT NOT CURRENTLY NORMALIZING?
C
C   3100 IF(LPFLAG.EQ.0) GO TO 4100
C        CALL SDLOP(NKEEP,ISTART)
C        GO TO 7000
C
C   ROTATION OF POLARIZATION?
C
C   4100 IF(IPLFLG.EQ.0) GO TO 5100
C        CALL SDPOL(NKEEP,ISTART)
C        GO TO 7000
C
C   SINGLE POINT ACQUISITION?
C
C   5100 CALL SDSIN(NKEEP)
C   7000 IF(NKEEP.EQ.0) GO TO 8000
C
C   IF DATA IS SATISFACTORY, WRITE TO LINE PRINTER AND DATA FILE
C
C   CALL SSAVE
C   CALL SOUT(6)
C   CALL SWRITE(IFLAG)
C   8000 IF(ISTART.NE.0) CALL SSTART(ISTART)
C        TYPE 8010
C   8010 FORMAT(' Command?',/)
C
C   REENTER SPECIAL SCREEN MODE
C
C   8900 CALL ENSPEC
C        RETURN
C        END

```

```

SUBROUTINE SDPOL(NKEEP,ISTART)

```

```

File SDPOL.FOR begins on the previous line.

```

```

Version Date: September 25, 1984

```

```

Paul S. Weiss

```

```

Subroutine SDPOL decides whether or not to keep a data point,
and continue the polarization rotation data taking loop.

```

```

COMMON /CUR/ ANGLE, INTERV, NUMANG, MANGLE, IRNFLG
COMMON /SETS/ GATE(16), TIM(16), EXCFRC(2), CLOCK, INTACQ, NCHAN
COMMON /POLSET/ ANGPOL, POLSTP, POSIT, IPOSIT, IPLFLG

C
POLCUR = POSIT*180./200.
NKEEP = 1
ISTART = 1
INTERV = INTACQ
100 TYPE 110, ' ', 'a'
110 FORMAT(' Save this point', A1, :
1, A1, 'nd continue polarization rotation loop?')
ACCEPT 1000, ANS
1000 FORMAT(A1)
IF(ANS.EQ.'Y') GO TO 6000
TYPE 110, '?'
ACCEPT 1000, ANS
IF(ANS.EQ.'Y') GO TO 3000
NKEEP = 0
TYPE *, 'Repeat this point?'
ACCEPT 1000, ANS
IF(ANS.EQ.'Y') GO TO 8900
3000 TYPE *, 'End polarization rotation loop?'
ACCEPT 1000, ANS
IF(ANS.EQ.'Y') GO TO 8800
GO TO 100

C
C CONTINUE POLARIZATION ROTATION LOOP
C
C INCREMENT COUNTER FOR NEXT POLARIZATION IN LOOP
C
6000 STEP = POLSTP * 200. / 180.
POSIT = POSIT + STEP

C
C HAS THE END OF A SCAN BEEN REACHED?
C
IF(POSIT.LT.0.) GO TO 7000

C
C HAS 180 DEGREES BEEN REACHED?
C
IF(POSIT.GT.200.) GO TO 8000

C
C IF IN THE MIDDLE OF A SCAN, MOVE ROTATOR, AND INCREMENT/DECREMENT
C POLARIZATION ANGLE
C
MOVE = INT(POSIT + 0.5) - IPOSIT
IF(MOVE.LT.0) MOVE = MOVE + 800
IPOSIT = INT(POSIT + 0.5)

C
C MACRO MOT MOVES THE POLARIZATION ROTATOR
C

```

```

CALL MOT(-MOVE)
ANGLE = ANGLE + (POLSTP * 1.E-4)
GO TO 8900

C
C   IF THE SCAN HAS REACHED 0 DEGREES, QUERY USER AS TO WHETHER OR NOT
C   TO CONTINUE
C
7000  POSIT = 0.
      IPOSIT = 0
      ANGLE = ANGPOL
      IF(POLSTP.LT.0.) POLSTP = - POLSTP
      TYPE 7110,7,7,7,7,7
7110  FORMAT(/,' The polarization rotation scan has been completed.'
      1,/, ' Rescan from 0 to 180 degrees and back?',5A1)
      ACCEPT 1000,ANS

C
C   DO NOT RESTART IF LOOP IS NOT TO BE CONTINUED
C
      IF(ANS.NE.'Y') GO TO 8800
      GO TO 8900

C
C   IF THE SCAN HAS REACHED 180 DEGREES, REPEAT 180, BUT REVERSE STEP
C   DIRECTION
C
8000  POSIT = 200.
      IPOSIT = 200
      POLSTP = - POLSTP
      GO TO 8900

C
C   IF THE LOOP IS TO BE CANCELLED, SET POL FLAG OFF,
C   AND RESTART FLAG OFF
C
8800  TYPE *, 'Abort further Rotation of Polarization Measurements'
C
      MOVE ROTATOR BACK TO VERTICAL
C
      CALL MOT(IPOSIT-800)
      POSIT = 0.
      IPOSIT = 0
      IPLFLG = 0
      ISTART = 0
8900  IF(ISTART.NE.0) TYPE 8910, (POSIT*180./200.)
8910  FORMAT(' The laser polarization is ',F7.3
      1,' degrees from vertical.'):
      RETURN
      END

SUBROUTINE SDSIN(NKEEP)
C
C   File SDSIN.FOR begins on the previous line.

```

C
C
C
C
C
C
C
C
C

Version Date: July 1, 1984
Paul S. Weiss

Subroutine SDSIN decides whether or not to keep a data point.
It is called when in single point acquisition mode.

COMMON /CUR/ ANGLE,INTERV,NUMANG,MANGLE,IRNFLG
COMMON /DATA/ DATA(256,20),WORK1(256),WORK2(256)
COMMON /SCR/ SCR(20)
COMMON /SETS/ GATE(16),TIM(16),EXCFRC(2),CLOCK,INTACQ,NCHAN
COMMON /LASSET/ LASDWL,FRQLAS,LASSTP,FSRLAS,LASCHA
COMMON /LOPSET/ ANLPBE,ANLPFN,ANLPIN,LPNRFQ,ANLPCU,LPFLAG
COMMON /NRMSET/ ANGNRM,INTNRM,NRMRPT,NRMFLG
COMMON /TSTSET/ TSTANG,NUMTST,TSTCUR,TSTFLG

C

1000

NKEEP = 1
TYPE *, 'Save this data?'
ACCEPT 1000,ANS
FORMAT(A1)
IF(ANS.NE.'Y') NKEEP = 0
RETURN
END

SUBROUTINE SDTST(NKEEP,ISTART)
File SDTST.FOR begins on the previous line.

C
C
C
C
C
C
C
C
C

Version Date: July 24, 1984
Paul S. Weiss

Subroutine SDTST continues test mode unless TSTFLG has been
made 0.

COMMON /CUR/ ANGLE,INTERV,NUMANG,MANGLE,IRNFLG
COMMON /DATA/ DATA(256,20),WORK1(256),WORK2(256)
COMMON /SCR/ SCR(20)
COMMON /SETS/ GATE(16),TIM(16),EXCFRC(2),CLOCK,INTACQ,NCHAN
COMMON /LASSET/ LASDWL,FRQLAS,LASSTP,FSRLAS,LASCHA
COMMON /LOPSET/ ANLPBE,ANLPFN,ANLPIN,LPNRFQ,ANLPCU,LPFLAG
COMMON /NRMSET/ ANGNRM,INTNRM,NRMRPT,NRMFLG
COMMON /TSTSET/ TSTANG,NUMTST,TSTCUR,TSTFLG

C

C

ISTART = -1
NKEEP = 1
IRNFLG = 0
INTERV = INTACQ

```

C      CONTINUE TEST MODE?
C
C      IF(TSTFLG.LE.0.) GO TO 2000
C
C      DONE WITH CYCLES?
C
C      IF(TSTFLG.LT.NUMTST) GO TO 4000
2000   TSTFLG = 0.
       ISTART = 0
       TYPE 2010,7,7,7,7,7
2010   FORMAT(/,' End of Test',5A1)
       GO TO 9000
C
C      ADD .00001 TO ANGLE AND CONTINUE TEST
C
C
4000   TSTFLG = TSTFLG + 1.
       TSTCUR = TSTCUR + .00001
       ANGLE = TSTANG + TSTCUR
9000   RETURN
       END

SUBROUTINE SFILE(IOPT)
C
C      File SFILE.FOR begins on the previous line.
C
C      Version Date:  July 7, 1984
C      Paul S. Weiss
C
C      Subroutine SFILE opens a data file on unit 9 for output of data
C      in ASCII form.
C
C
C
C
C      LOGICAL*1 BNAME(14)
C      COMMON /FNAME/ INAME(7),ISTORE
C      EQUIVALENCE (BNAME(1),INAME(1))
C      DATA INAME /'DL','O:','AN','GD','AT','A','NG'/
C
C      IF(IOPT.EQ.0) CLOSE(UNIT=9,DISPOSE='SAVE')
C
C      RESET THE NUMBER OF DATA POINTS STORED
C
C
C      ISTORE = 0
100    TYPE 110
110    FORMAT(' Enter the six letter data file name:')
       ACCEPT 500,(INAME(I),I=3,5)
500    FORMAT(3A2)
       INAME(6) = 'A'
       INAME(7) = 'NG'

```

```

C
C   IF THE FIRST LETTER IS A SPACE, OR ANY CHARACTER OTHER THAN A LETTER
C   GO BACK AND GET THE CORRECT FILENAME
C
C   IF(BNAME(5) .LT.64) GO TO 100
C
C   IF THERE ARE FEWER THAN SIX LETTERS, SHIFT THE EXTENSION DOWN
C
C   LNAME = 14
C   DO 600 I=1,6
C   B = BNAME(11-I)
C
C   IF THE CHARACTER IN QUESTION IS A LETTER OR NUMBER, SAVE IT
C   OTHERWISE ELIMINATE
C
C   IF((B.GT.64) .OR. ((B.GT.47) .AND. (B.LT.58))) GO TO 700
C
C   KEEP TRACK OF NAME LENGTH
C
C   LNAME = 14 - I
C   DO 550 J=11-I,14-I
C   BNAME(J) = BNAME(J+1)
550  CONTINUE
C   BNAME(15-I) = 0
600  CONTINUE
C
C   CHECK AND SEE IF FILE ALREADY EXISTS
C
C   OPEN(UNIT=9,ERR=2000,NAME=BNAME,TYPE='OLD')
700  OPEN(UNIT=9,ERR=2000,NAME=BNAME,TYPE='OLD')
C
C   IF IT EXISTS SEE IF IT SHOULD BE WRITTEN OVER
C
C   CLOSE(UNIT=9,DISPOSE='SAVE')
C
C   FILL IN NULLS IN DATA FILE NAME WITH BLANKS FOR OUTPUT
C
C   IF(LNAME.EQ.14) GO TO 800
C   DO 750 I=LNAME+1,14
C   BNAME(I) = 32
750  CONTINUE
C   TYPE 810, (BNAME(I), I=1, LNAME), 7,7,7,7,7,0
800  TYPE 810, (BNAME(I), I=1, LNAME), 7,7,7,7,7,0
810  FORMAT(1X,14A1, ' already exists! '
C   1, 'Would you like to write over it?', 6A1)
C   ACCEPT 1000,ANS
1000 FORMAT(A1)
C   IF(ANS.NE.'Y') GO TO 100
2000 CALL ASSIGN(9, INAME, LNAME, 'NEW', 'CC')
C
C   FILL IN NULLS IN DATA FILE NAME WITH BLANKS FOR OUTPUT

```

```

C
IF(LNAME.EQ.14) GO TO 2200
DO 2150 I=LNAME+1,14
BNAME(I) = 32
2150 CONTINUE
2200 TYPE 2210, (BNAME(I), I=1, LNAME), 7, 7, 7, 7, 7, 7, 7, 7, 7, 7, 0
2210 FORMAT(' The data file: ', 14A1
1, ' has been opened successfully!', 11A1)
RETURN
END

```

```

SUBROUTINE SGRAPH(IOPT)

```

```

File SGRAPH.FOR begins on the previous line.

```

```

Version Date: November 11, 1985
Paul S. Weiss

```

```

Subroutine SGRAPH plots the angular distribution on the
HP 7470A or HP 7475A plotter which is defined to be on unit 8.

```

```

The argument is:

```

```

IOPT=-1 Plot lower display.
IOPT=0 Plot both displays.
IOPT=1 Plot upper display.

```

```

COMMON /DISP/ IDSP(1064), MODSPT, MODSPB, DSPB, DSTEP, NDSP, INDEP
COMMON /DSPZER/ ITYZER, IBYZER
DATA NESC /27/

```

```

IOP = IOPT

```

```

SET UP THE HP 7470A (7475A) PLOTTER

```

```

WRITE(8,10) NESC, ' .I11;;;17:', NESC, ' .N;19:'
10 FORMAT('$', A1, A9, A1, A6)

```

```

C XON AND XOFF HAVE NOW BEEN ESTABLISHED, ESC I11;;;17 SETS THE XON
C THRESHOLD TO 11 REMAINING BYTES AND XON CHARACTER TO DC1, ESC .N;19:
C SETS THE XOF CHARACTER TO DC3.

```

```

INITIALIZE THE PLOTTER.

```

```

WRITE(8,*) 'IN;SC 0,4095,0,2048;'

```



```

C      GIVE RANGE OF PLOT
C
C      WRITE(8,*) 'IP 500,600,9500,7000;'
C
C      GET OFFSET OF ARRAY ARGUMENT FOR POINTS TO BE PLOTTED IF LOWER
C      DISPLAY IS TO BE PLOTTED
C
C      IAROFF = 0
C      IF(IOP.LE.0) IAROFF = 2 * NDSP
C
C      SET ZERO OFFSET OF DISPLAY TO BE PLOTTED TO ONLY PLOT NON-ZERO POINTS
C
C      IYOFF = IBYZER
C      IF(IOP.GT.0) IYOFF = ITYZER
C
C      SEND SYMBOL FOR PLOT (* FOR UPPER, 0 FOR LOWER)
C      CHOOSE PEN FOR PLOT (LEFT FOR UPPER, RIGHT FOR LOWER)
C
C      IPEN = 1
C      SYMBOL = '*'
C      IF(IOP.GT.0) GO TO 1400
C      SYMBOL = '0'
C      IPEN = 2
C
1400   WRITE(8,1410) SYMBOL,IPEN
1410   FORMAT(' SM',A1,',','SP',I1,',')
C
C      PLOT ALL NON-ZERO POINTS
C
C      DO 2000 I=1,NDSP
C      IARG = (2*I) + IAROFF
C      IF(IDSP(IARG).NE.IYOFF) WRITE(8,*) 'PU;PA '
C      1,IDSP(IARG-1),',',(IDSP(IARG)-IYOFF),',';PD;'
2000   CONTINUE
C      WRITE(8,*) 'SP;PU;PA 4000,2000;'
C      IF(IOP.NE.0) GO TO 9000
C
C      IF BOTH ARE TO BE PLOTTED, GO BACK AND DO UPPER
C
C      IOP = IOP + 1
C      GO TO 100
9000   REWIND 8
C      RETURN
C      END

```

```

SUBROUTINE SGTSCR

```

```

File SGTSCR.FOR begins on the previous line.

```

```

C      Version Date: September 25, 1984
C      Paul S. Weiss
C
C      Subroutine SGTSCR converts scaler contents, currently stored in
C      JDATA, into real numbers stored in SCR, and resets the run flag.
C
C      INTEGER*4 JDATA
C      COMMON /CUR/ ANGLE, INTERV, NUMANG, MANGLE, IRNFLG
C      COMMON /SCR/ SCR(20)
C      COMMON /SETS/ GATE(16), TIM(16), EXCFRC(2), CLOCK, INTACQ, NCHAN
C      COMMON /SDONE/ ISWFLG, JDATA(20)
C
C      IRNFLG = 0
C      SCR(1) = ANGLE
C
C      DETERMINE THE TIME COUNTED
C
C      SCR(2) = .150 * GATE(1) * INTERV / (CLOCK * 2.)
C      DO 100 I=1, ((2*NCHAN) - 2)
C      SCR(I+2) = AJFLT(JDATA(I))
100    CONTINUE
C
C      IN LAST CHANNEL, SHOW THE DIFFERENCE OF THE FIRST TWO CHANNELS
C      WITH THE CORRECT SIGNAL TO NOISE BY:
C      nA = 1A + 2B
C      nB = 1B + 2A
C
C      SCR((2*NCHAN) + 1) = SCR(3) + SCR(6)
C      SCR((2*NCHAN) + 2) = SCR(4) + SCR(5)
C
C      MAKE THE REMAINDER OF THE CHANNELS 0
C
C      IF(NCHAN.GE.9) GO TO 9000
C      DO 200 I=(2*NCHAN)+3,20
C      SCR(I) = 0.
200    CONTINUE
9000   RETURN
      END

```

```

SUBROUTINE SINIT

```

File SINIT.FOR begins on the previous line.

```

C      Version Date: November 11, 1985
C      Paul S. Weiss
C
C
C
C
C
C
C

```

```

Subroutine SINIT initializes the parameters of angular
scan program SANG to the default values given below.

```

```

INTEGER*4 JDATA
COMMON /CUR/ ANGLE, INTERV, NUMANG, MANGLE, IRNFLG
COMMON /DATA/ DATA(256,20), WORK1(256), WORK2(256)
COMMON /DISP/ IDSP(1064), MODSPT, MODSPB, DSPB, DSTEP, NDSP, INDEP
COMMON /DSPCHA/ MDSPT, NDSPT, MDSPB, NDSPB
COMMON /TGSMAX/ DWLMAX, MAXCHN
COMMON /SETS/ GATE(16), TIM(16), EXCFRC(2), CLOCK, INTACQ, NCHAN
COMMON /LASSET/ LASDWL, FRQLAS, LASSTP, FSRLAS, LASCHA
COMMON /LOPSET/ ANLPBE, ANLPFN, ANLPIN, LPNRFQ, ANLPCU, LPFLAG
COMMON /NRMSET/ ANGNRM, INTNRM, NRMRPT, NRMFLG
COMMON /POLSET/ ANGPOL, POLSTP, POSIT, IPOSIT, IPLFLG
COMMON /TSTSET/ TSTANG, NUMTST, TSTCUR, TSTFLG
COMMON /VELO/ DELF, HALFH, DELPIP, VELB, SPDRIO
COMMON /SDONE/ ISWFLG, JDATA
COMMON /CHAEDEF/ CHAEDEF(20,10)
COMMON /PRES/ PRM(8), IPRE(8), PFORE(8), IDG(8), IPEM(8)
1, PBACK(2), PION(3)
COMMON /TPRIM/ THMCPL(8)
COMMON /MACDEF/ TCDEF(8,4), NTC, PRDEF(8,6), NPR, BACK(4,2)
COMMON /DET/ AGRD, AFIL, VEB, VIE, VEXT
1, VEN, QPST, QPR, MAS, VEX, VDK, VPMT

```

```

C
DATA CHAEDEF /'Lase', 'r On', ' Det', 'ecto', 'r Si', 'gnal', 14* ' '
1, 'Lase', 'r Of', 'f De', 'tect', 'or S', 'igna', 'l ' , 13* ' '
2, 'Lase', 'r FI', 'uore', 'scen', 'ce ' , 15* ' '
3, 'Lase', 'r On', ' - L', 'aser', ' Off', ' Det', 'ecto', 'r Si'
3, 'gnal', 11* ' '
4, 120* ' '/

```

```

C
DATA TCDEF /'Na T', 'Na B', 'Na N', 'Na p', 'Na S', 'Cold', 'Seco'
1, 'None', 'op 0', 'otto', 'ozzl', 're-S', 'kimm', ' Shi', 'ndar', ' '
2, 'ven ' , 'm Ov', 'e ' , 'kimm', 'er ' , 'eld ' , 'y No', 2* ' '
3, 'en ' , ' ' , 'er ' , 2* ' ' , 'zzle', ' ' /

```

```

C
DATA PRDEF /2*'Prim', 'Main', 2*'Seco', 'Regi', 'Betw', 'None'
1, 2*'ary ' , ' Cha', 2*'ndar', 'on 3', 'een ' , ' '
2, 'Sour', 'Diff', 'mber', 'y So', 'y Di', ' ' , 'Turb', ' '
4, 'ce ' , 'eren', ' ' , 'urce', 'ffer', ' ' , 'os', ' '
5, ' ' , 'tial', 2* ' ' , 'enti', 7* ' ' , 'al ' , 3* ' '/

```

```

C
DATA BACK /'Heli', 'um ' , 2* ' ' , 'HCI ' , 3* ' '/

```

```

C
C
C
C
RELAY ADDRESSES TO MACROS

```

```

CALL INIT(ISWFLG, JDATA)

```

```

C
TYPE 1

```

```

1
FORMAT(/, ' Angular Scan Program'
1, /, ' Version Date: November 11, 1985', /)

```

C
C
C

SET DATA ACQUISITION PARAMETER DEFAULTS

MAXCHN = 8
ISWFLG = 0
CLOCK = 1.5
INTACQ = 90
NCHAN = 4
EXCFRC(1) = .3
EXCFRC(2) = 0.
DO 2200 I=1,16
GATE(I) = 3.2
CONTINUE

2200

C
C
C

SET CURRENT ACQUISITION DEFAULTS

ANGLE = 40.
INTERV = 90
NUMANG = 0
MANGLE = 1
IRNFLG = 0

C
C
C

SET NORMALIZATION DEFAULTS

ANGNRM = 40.
INTNRM = 90
NRM RPT = 2
NRMFLG = 0

C
C
C

SET DISPLAY DEFAULTS

MDSPT = 1
MDSPB = 2
NDSPT = 1
NDSPB = 2
DSPB = -10.
NDSP = 221
DSTEP = .5
MODSPT = 1
MODSPB = 1
INDEP = 0

C
C
C

SET LOOP MODE DEFAULTS

ANLPBE = 25.
ANLPFN = 75.
ANLPIN = 5.
ANLPCU = 25.
LPFLAG = 0
LPNRFQ = 10

C
C
C
SET ROTATION OF POLARIZATION DEFAULTS

ANGPOL = 45.
POLSTP = 22.5
POSIT = 0.
IPOSIT = 0
IPLFLG = 0

C
C
C
SET TEST MODE DEFAULTS

TSTANG = 0.
NUMTST = 200
TSTCUR = 0.
TSTFLG = 0.

C
C
C
C
SET MACHINE CONDITION DEFAULTS
FIRST THERMOCOUPLE DEFAULTS

NTC = 7
THMCPL(1) = 23.
THMCPL(2) = 21.3
THMCPL(3) = 25.
THMCPL(4) = 19.
THMCPL(5) = 17.5
THMCPL(6) = -6.2
THMCPL(7) = 7.33
THMCPL(8) = 0.

C
C
C
SET PRESSURE DEFAULTS

NPR = 7
DO 2500 I=1,8
PRM(I) = 1.0
IPRE(I) = -4
PFORE(I) = 10.
IDG(I) = .1
IPEM(I) = 1
2500 CONTINUE
IPRE(2) = -5
IPRE(3) = -7
IPRE(5) = -5
IPRE(6) = -10
IPRE(7) = -7
IPEM(3) = 10
IPEM(6) = 10
IPEM(7) = 10
PFORE(6) = 0.
PFORE(7) = 0.
PION(1) = 35.

PION(2) = 6.
 PION(3) = 0.
 PBACK(1) = 500.
 PBACK(2) = 500.
 IDG(6) = 2
 IDG(7) = 2

C
 C
 C

SET DETECTOR SETTING DEFAULTS

AGRD = 10.
 AFIL = 5.5
 VEB = 200.
 VIE = -75.
 VEXT = -150.
 VEN = -250.
 QPST = 4.68
 QPR = 3.75
 MAS = 23
 VEX = -600.
 VDK = -30.
 VPMT = -2350.

C
 C
 C

SET VELOCITY MEASUREMENT DEFAULTS

FRQLAS = 16973.
 FSRLAS = 1.5
 LASDWL = 100
 LASSTP = 1
 LASCHA = 4
 VELB = 0.
 SPDRIO = -1.

C
 C
 C

SET CHANNEL DEFINITION DEFAULTS

DO 3200 I=5,10
 CHADEF(1,I) = 'None'
 CONTINUE \

3200

C
 C
 C

ZERO DATA FILES

DO 4200 I=1,256
 DATA(I,1) = -100.
 DO 4100 J=2,20
 DATA(I,J) = 0.
 CONTINUE
 CONTINUE
 RETURN
 END

4100
 4200

SUBROUTINE SLEAVE

File SLEAVE.FOR begins on the previous line.

Version Date: July 4, 1984
 Paul S. Weiss

Subroutine SLEAVE is the termination routine for SANG, the
 angular scan program.

```
COMMON /FNAME/ INAME(7),ISTORE
TYPE *,'Exit? Are you sure?'
ACCEPT 1000, ANS
1000  FORMAT(A1)
      IF(ANS.NE.'Y') RETURN
```

TURN OFF INTERRUPTS AND DISPLAY WITH MACRO SUBROUTINE SEXIT

```
CALL SEXIT
CLOSE(UNIT=9,DISPOSE='SAVE',ERR=9100)
9000  STOP
9100  TYPE 9110,(INAME(I),I=1,7),7,7,7,7
9110  FORMAT(/,' Error closing file ',7A2,4A1)
      GO TO 9000
      END
```

SUBROUTINE SLOOP(IOPT)

File SLOOP.FOR begins on the previous line.

Version Date: July 4, 1984
 Paul S. Weiss

Subroutine SLOOP starts or continues the data taking loop.
 It is called from SCOMM.

Its argument IOPT is used as follows:

```
IOPT=0 Continue
IOPT=1 Start Loop
```

```
COMMON /CUR/ ANGLE,INTERV,NUMANG,MANGLE,IRNFLG
COMMON /SETS/ GATE(16),TIM(16),EXCFRC(2),CLOCK,INTACQ,NCHAN
COMMON /LOPSET/ ANLPBE,ANLPFN,ANLPIN,LPNRFQ,ANLPCU,LPFLAG
COMMON /NRMSET/ ANGNRM,INTNRM,NRMRPT,NRMFLG
COMMON /SDONE/ ISWFLG,JDATA(20)
```

IF(IRNFLG.NE.0) GO TO 8900

```

IF(IOPT.NE.0) GO TO 2100
C
C CONTINUE LOOP FROM WHERE IT LEFT OFF
C
LPFLAG = 1
ANGLE = ANLPCU
INTERV = INTACQ
GO TO 8000
C
C IF STARTING A LOOP, SET ANGLE FOR A NORMALIZATION
C
2100 TYPE *, 'Start Loop with a Normalization!'
      ANGLE = ANGNRM
      INTERV = INTNRM
      LPFLAG = -2
      NRMFLG = 1
C
C SET FLAG FOR LOOP MODE
C
8000 CALL SSTART(1)
      GO TO 9000
8900 TYPE *, 'Abort Acquisition -- TGS is Running!'
9000 RETURN
      END

SUBROUTINE SNORM
C
C File SNORM.FOR begins on the previous line.
C
C Version Date: July 2, 1984
C Paul S. Weiss
C
C Subroutine SNORM starts the Normalization.
C
C
C COMMON /CUR/ ANGLE, INTERV, NUMANG, MANGLE, IRNFLG
COMMON /SETS/ GATE(16), TIM(16), EXCFRC(2), CLOCK, INTACQ, NCHAN
COMMON /NRMSET/ ANGNRM, INTNRM, NRMRPT, NRMFLG
COMMON /SDONE/ ISWFLG, JDATA(20)
C
C
1000 TYPE *, 'Normalization? Are you sure?'
      ACCEPT 1000, ANS
      FORMAT(A1)
      IF(ANS.NE.'Y') GO TO 9000
      NRMFLG = 1
      ANGLE = ANGNRM
      INTERV = INTNRM
      CALL SSTART(1)
9000 RETURN

```


END

SUBROUTINE SNUCH(NU,ICOM)

File SNUCH.FOR begins on the previous line.

Version Date: July 24, 1984

Paul S. Weiss

Subroutine SNUCH chooses which subroutine to call for the P*, S*, and W* commands. It was created to streamline the program by removing some of the command burden from subroutine SCOMM.

The arguments of SNUCH are as follows:

NU Logical Unit for output.
ICOM Letter of command typed in.

COMMON /LOPSET/ ANLPBE,ANLPFN,ANLPIN,LPNRFQ,ANLPCU,LPFLAG

COMMON /NRMSET/ ANGNRM,INTNRM,NRMRPT,NRMFLG

COMMON /TSTSET/ TSTANG,NUMTST,TSTCUR,TSTFLG

COMMON /POLSET/ ANGPOL,POLSTP,POSIT,IPOSIT,IPLFLG

DATA IA,IC,ID,IG /65,67,68,71/

DATA II,IL,IM,IN,IR,IS,IT,IV /73,76,77,78,82,83,84,86/

The commands are:

*A Write Accumulated Data
*C Write Current Configuration
*D Write Data Channel Definition
*G Write Current Graphics Display
*I Write Information
*L Write Loop Mode Parameters
*M Write Machine Condition
*N Write Normalization Parameters
*R Write Rotation of Polarization Parameters
*S Write Detector Settings
*T Write Test Mode Parameters
*V Write Velocity Measurement and Parameters

IF(ICOM.NE.IA) GO TO 11

CALL SACCUM(NU)

GO TO 100

11 IF(ICOM.NE.IC) GO TO 16

CALL SSHCUR(NU)

IF LOOP MODE, TEST MODE, OR NORMALIZATION IS ACTIVE, ALSO
SHOW THOSE SETTINGS

IF(LPFLAG.NE.0) CALL SSHLOP(NU)

```

IF(TSTFLG.NE.O.) CALL SSHTST(NU)
IF(NRMFLG.NE.O) CALL SSHNRM(NU)
IF(IPLFLG.NE.O) CALL SSHPOL(NU)
GO TO 100
16  IF(ICOM.NE.ID) GO TO 31
    CALL SSHDEF(NU)
    GO TO 100
31  IF(ICOM.NE.IG) GO TO 36
    CALL SSHDSP(NU)
    GO TO 100
36  IF(ICOM.NE.II) GO TO 41
    CALL SPRII(NU)
    GO TO 100
41  IF(ICOM.NE.IL) GO TO 46
    CALL SSHLOP(NU)
    GO TO 100
46  IF(ICOM.NE.IM) GO TO 51
    CALL SSHMP(NU)
    GO TO 100
51  IF(ICOM.NE.IN) GO TO 61
    CALL SSHNRM(NU)
    GO TO 100
61  IF(ICOM.NE.IR) GO TO 66
    CALL SSHPOL(NU)
    GO TO 100
66  IF(ICOM.NE.IS) GO TO 71
    CALL SSHMD(NU)
    GO TO 100
71  IF(ICOM.NE.IT) GO TO 81
    CALL SSHTST(NU)
    GO TO 100
81  IF(ICOM.NE.IV) GO TO 99
    CALL SSHVEL(NU)
    GO TO 100
99  NU = 0
100 RETURN
    END

```

SUBROUTINE SOUT(NU)

File SOUT.FOR begins on the previous line.

Version Date: September 5, 1984
Paul S. Weiss

Subroutine SOUT outputs the current data to logical unit
NU.

COMMON /SETS/ GATE(16),TIM(16),EXCFRC(2),CLOCK,INTACQ,NCHAN
COMMON /CUR/ ANGLE,INTERV,NUMANG,MANGLE,IRNFLG

C
C
C
C
C
C
C
C
C

```

COMMON /POLSET/ ANGPOL,POLSTP,POSIT,IPOSIT,IPLFLG
COMMON /SCR/ SCR(20)
C
LOGICAL*1 ITIME(8)
CALL TIME(ITIME)
WRITE(NU,100) SCR(1),SCR(2),(ITIME(I),I=1,8),7
100  FORMAT(/,' Angle: ',F5.1,' degrees, measured for: ',F8.3,' sec.'
1,6X,'Time: ',9A1)
C
IS THIS A POLARIZATION ROTATION SCAN? IF SO, PRINT POLARIZATION
C ANGLE
C
IF(IPLFLG.NE.0) WRITE(NU,120) (10000.*(SCR(1)-(INT(SCR(1))))))
120  FORMAT(' The laser polarization is ',F5.1
1,' degrees from vertical.')
WRITE (NU,140)
140  FORMAT(' Channel',3X,'A',10X,'B',11X,'Signal'
3,9X,'Error',6X,'Signal/Noise')
DO 250 I=1,NCHAN
IS = (2*I) + 1
IB = IS + 1
SIG = (SCR(IS) - SCR(IB))/SCR(2)
ERR = SCR(IS) + SCR(IB)
ERR = SQRT(ERR)/SCR(2)
SGTON = 0.
IF(ERR.NE.0.) SGTON = SIG/ERR
WRITE(NU,200) I,SCR(IS),SCR(IB),SIG,ERR,SGTON
200  FORMAT(1X,I1,2X,F9.0,2X,F9.0,5X,F11.2,' +/- ',F9.2,5X,F9.1)
250  CONTINUE
RETURN
END

```

```

SUBROUTINE SOVER(ISTART)
C File SOVER.FOR begins on the previous line.
C
C Version Date: October 30, 1984
C Paul S. Weiss
C
C Subroutine SOVER "handles" overflows. It tells the user of the
C condition, and asks whether or not to restart the acquisition.
C
TYPE 100,7,7,7,7,7,7,7,7,7,7
100  FORMAT(' *****'
1,/, ' An overflow has occurred!'
2,/, ' *****',10A1
3,///, ' Try retaking this point?')
ISTART = 0
ACCEPT 1000,ANS

```

```

1000  FORMAT(A1)
      IF(ANS.NE.'Y') GO TO 9000
      ISTART = 1
      TYPE *, 'Be sure to lower the gain in some way before restarting!'
9000  RETURN
      END

```

SUBROUTINE SPOLAR

File SPOLAR.FOR begins on the previous line.

Version Date: September 27, 1984
Paul S. Weiss

Subroutine SPOLAR starts the polarization rotation data taking loop.
It is called from SCOMM.

```

COMMON /CUR/ ANGLE,INTERV,NUMANG,MANGLE,IRNFLG
COMMON /SETS/ GATE(16),TIM(16),EXCFRC(2),CLOCK,INTACQ,NCHAN
COMMON /POLSET/ ANGPOL,POLSTP,POSIT,IPOSIT,IPLFLG

```

```

      IF(IRNFLG.NE.0) GO TO 8800
      TYPE *, 'Polarization Rotation Loop? Are you sure?'
      ACCEPT 1000,ANS
1000  FORMAT(A1)
      IF(ANS.NE.'Y') GO TO 8900
      TYPE *, 'Change display window for polarization rotation scan?'
      ACCEPT 1000,ANS
      IF(ANS.EQ.'Y') CALL SCHDWN(2)

```

START A LOOP, SET ANGLE FOR POLARIZATION

ANGLE = ANGPOL

SET COUNTDOWN INTERVAL

INTERV = INTACQ

SET FLAG FOR POLARIZATION ROTATION LOOP MODE

IPLFLG = 1

SET STEP INDICATORS, AND OTHER PARAMETERS OF MEASUREMENT

POSIT = 0.

IPOSIT = 0

IF(POLSTP.LT.0.) POLSTP = - POLSTP

TYPE *, 'Set the laser polarization vertical at the Main Door.'

```

8000  CALL SSTART(1)
      GO TO 9000
8800  TYPE *, 'TGS is Running!'
8900  TYPE *, 'Abort Acquisition'
9000  RETURN
      END

```

```

SUBROUTINE SPRII(NU)

```

```

File SPRII.FOR begins on the previous line.

```

```

C
C
C   Version Date:  September 3, 1984
C   Paul S. Weiss
C

```

```

C   Subroutine SPRII prints information on the line printer or
C   into a disk file to be associated with a data file.
C

```

```

C   The arguments of SPRII are as follows:

```

```

C       NU      Unit number to which information is to be written.
C               Note that if information is written to disk, the
C               same information is also written to the printer.
C
C

```

```

C
C   LOGICAL*1 CHAR(80), ITIME(8)
C   INTEGER JDATE(3)
C   IF(NU.EQ.7) GO TO 150
C   TYPE 110
110  FORMAT(/, ' Include date and time?')
      ACCEPT 1000,ANS
1000 FORMAT(A1)
      IF(ANS.NE.'Y') GO TO 1100
150  CALL IDATE(JDATE(1), JDATE(2), JDATE(3))
      CALL TIME(ITIME)
      WRITE(NU,200) JDATE(1), JDATE(2), (JDATE(3)+1900), (ITIME(I), I=1,8)
200  FORMAT(/, ' Date:  ',2(I2,'/'),I4,/, ' Time:  ',8A1,/)
      IF(NU.EQ.9) WRITE(6,200) JDATE(1), JDATE(2)
      1, (JDATE(3)+1900), (ITIME(I), I=1,8)
C
C   IF ONLY WRITING TO THE TERMINAL, EXIT
C
C   IF(NU.EQ.7) GO TO 9000
C
C   ENABLE LOWER CASE INPUT
C
C   CALL LCASE
1100  TYPE 1110
1110  FORMAT(/, ' Type information in. To stop, begin a line with'
1, ' a =',/)
1200  DO 1205 I=1,80
      CHAR(I) = 0

```

```

1205 CONTINUE
ACCEPT 1210, (CHAR(I), I=1, 80)
1210 FORMAT(80A1)
IF (CHAR(1) .EQ. 61) GO TO 8000
WRITE (NU, 1310) (CHAR(I), I=1, 80)
1310 FORMAT(1X, 80A1)
C
C IF WRITING TO DISK, ALSO WRITE TO THE PRINTER
C
IF (NU .EQ. 9) WRITE (6, 1310) (CHAR(I), I=1, 80)
GO TO 1200
C
C DISABLE LOWER CASE INPUT
C
8000 CALL UCASE
9000 RETURN
END

SUBROUTINE SSAVE
C
C File SSAVE.FOR begins on the previous line.
C
C Version Date: July 4, 1984
C Paul S. Weiss
C
C Subroutine SSAVE puts new data in the accumulated data
C array DATA, and adjusts the order of the array so that
C there is room for the new data.
C
C
C
C
COMMON /CUR/ ANGLE, INTERV, NUMANG, MANGLE, IRNFLG
COMMON /DATA/ DATA(256, 20), WORK1(256), WORK2(256)
COMMON /SCR/ SCR(20)
COMMON /SETS/ GATE(16), TIM(16), EXCFRC(2), CLOCK, INTACQ, NCHAN
C
IF (NUMANG .EQ. 0) GO TO 1200
DO 100 I=1, NUMANG
IF (SCR(1) - DATA(I, 1)) 2000, 5000, 100
100 CONTINUE
C
IF THE DO LOOP HAS RUN OUT, THEN INCREASE NUMANG, AND
C PUT NEW DATA AT THE LAST POINT
C
IF (NUMANG .LT. 256) GO TO 1200
TYPE 1110, 7, 7
1110 FORMAT(/, ' Accumulated data array full!', 2A1
1, /, ' Abort Storage!')
GO TO 9000
1200 NUMANG = NUMANG + 1
MANGLE = NUMANG

```

```

GO TO 3000
C
C   IF THE NEW DATA ANGLE FALLS IN THE MIDDLE OF THE ARRAY DATA
C   (ORGANIZED BY ANGLE), THEN MOVE ALL SUBSEQUENT DATA UP BY ONE
C   AND PUT THE NEW DATA IN THE CORRECT PLACE
C
2000  IF(NUMANG.LT.256) GO TO 2200
      TYPE 1110,7,7
      GO TO 9000
2200  NUMANG = NUMANG + 1
      MANGLE = I
C
C   SHIFT OLD DATA TO MAKE ROOM FOR NEW DATA
C
      DO 2400 I=1,NUMANG-MANGLE
      IOLD = NUMANG - I
      INEW = IOLD + 1
      DO 2300 J=1,20
      DATA(INEW,J) = DATA(IOLD,J)
2300  CONTINUE
2400  CONTINUE
C
C   INSERT NEW DATA
C
3000  DO 3200 J=1,20
      DATA(MANGLE,J) = SCR(J)
3200  CONTINUE
      IF(NUMANG.EQ.256) TYPE 3310,7,7,7
3310  FORMAT(/,' Warning -- Accumulated data array is now full!'
1,/, ' Do not take data at any new angles! ',3A1)
      GO TO 9000
5000  MANGLE = I
      DO 5200 J=2,20
      DATA(MANGLE,J) = DATA(MANGLE,J) + SCR(J)
5200  CONTINUE
9000  RETURN
      END

```

```

SUBROUTINE SSHCUR(NU)

```

```

File SSHCUR.FOR begins on the previous line.

```

```

C
C
C
C
C
C
C

```

```

Version Date:  October 17, 1984
Paul S. Weiss

```

```

Subroutine SSHCUR prints the current settings
on logical unit NU.

```

```

COMMON /CUR/ ANGLE, INTERV, NUMANG, MANGLE, IRNFLG
COMMON /SETS/ GATE(16), TIM(16), EXCFRC(2), CLOCK, INTACQ, NCHAN
COMMON /LASSET/ LASDWL, FRQLAS, LASSTP, FSRLAS, LASCHA
COMMON /LOPSET/ ANLPBE, ANLPFN, ANLPIN, LPNRFQ, ANLPCU, LPFLAG
COMMON /NRMSET/ ANGNRM, INTNRM, NRMRPT, NRMFLG
COMMON /POLSET/ ANGPOL, POLSTP, POSIT, IPOSIT, IPLFLG
COMMON /TSTSET/ TSTANG, NUMTST, TSTCUR, TSTFLG
COMMON /FNAME/ INAME(7), ISTORE

C
NUNIT = NU
100 WRITE(NUNIT,110) NCHAN, CLOCK, INTACQ, GATE(1), GATE(2), EXCFRC(1)
110 FORMAT(/, ' The Quad Scalers and Laser Gate Generator are in use.'
1,/, '1X,I1,' data channels are being used.'
2,/, ' The clock frequency is ',F3.1,' Hz.'
3,/, ' The countdown interval is ',I5,'.'
4,/, ' The gate widths are: A = ',F5.3,' msec, B = ',F5.3,' msec.'
5,/, ' The Excited State Fractions are: ',F6.4,' and ',F6.4,/)
WRITE(NUNIT,2100) (INAME(I),I=1,7), ISTORE
2100 FORMAT(' The file ',7A2,' has recorded ',I5,' TGS countdowns.')
WRITE(NUNIT,3100) ANGLE, INTERV, NUMANG
3100 FORMAT(' The detector angle is currently ',F5.1,' degrees'
1,/, ' The countdown interval is ',I5,'.'
2,/, '1X,I3,' detector angles have been measured.')
IF(LPFLAG.NE.0) WRITE(NUNIT,3200) 'in Loop Mode.'
IF(NRMFLG.GT.0) WRITE(NUNIT,3200) 'Normalizing.'
IF(IPLFLG.NE.0) WRITE(NUNIT,3200) 'rotating the '
1,'laser polarization.'
IF(TSTFLG.GT.0) WRITE(NUNIT,3200) 'in Test Mode.'
3200 FORMAT(' The acquisition is currently ',A13, ':',A19)
IF(IRNFLG.GT.0) WRITE(NUNIT,3300)
3300 FORMAT(' The TGS is counting down.')
C
C IF CONFIGURATION WAS WRITTEN TO DISK, WRITE IT TO THE PRINTER ALSO
C
IF(NUNIT.NE.9) GO TO 9000
NUNIT = 6
GO TO 100
9000 RETURN
END

SUBROUTINE SSHDEF(NU)
C File SSHDEF.FOR begins on the previous line.
C
C Version Date: October 17, 1984
C Paul S. Weiss
C
C

```


C Subroutine SSHDEF prints the array definitions to logical unit
C number NU.
C

COMMON /SETS/ GATE(16),TIM(16),EXCFRC(2),CLOCK,INTACQ,NCHAN
COMMON /CHAEF/ CHAEF(20,10)

C

NUNIT = NU

100

DO 2000 I=1,NCHAN

WRITE (NUNIT,1200) I,(CHAEF(J,I),J=1,20)

1200

FORMAT(' Channel #',I1,' is:',/,1X,20A4)

2000

CONTINUE

C

C

IF THIS IS TO BE WRITTEN TO DISK, PRINT ALSO

C

IF(NUNIT.NE.9) GO TO 9000

NUNIT = 6

GO TO 100

9000

RETURN

END

SUBROUTINE SSHDSP(NU)

File SSHDSP.FOR begins on the previous line.

C

C

Version Date: October 23, 1984

Paul S. Weiss

C

C

C

C

Subroutine SSHDSP shows the current display mode on logical
C unit NU.
C

C

COMMON /DISP/ IDSP(1064),MODSPT,MODSPB,DSPB,DSTEP,NDSP,INDEP

COMMON /DSPCHA/ MDSPT,NDSPT,MDSPB,NDSPB

DATA TOP1,TOP2,BOT1,BOT2 /'uppe','r','lowe','r'/

C

NUNIT = NU

100

MD = MODSPT

TB1 = TOP1

TB2 = TOP2

M = MDSPT

N = NDSPT

1050

GO TO (1100,1200,1300,1400,1500,1600),MD

1100

WRITE(NUNIT,1110) TB1,TB2,M,'Signa','l.'

1110

FORMAT(' The ',A4,A1,' display is Channel ',I1,1X,A5,A2,A6)

GO TO 2000

1200

WRITE(NUNIT,1210) TB1,TB2,M,N,'Difference.'

1210

FORMAT(' The ',A4,A1,' display is Channels ',I1,',',I1

1,1X,A11,A10,A3)

GO TO 2000

```

1300 WRITE(NUNIT,1210) TB1,TB2,M,N,'Excited Sta','te Signal.'
      GO TO 2000
1400 WRITE(NUNIT,1210) TB1,TB2,M,N,'Difference ','Signal/Noi','se.'
      GO TO 2000
1500 WRITE(NUNIT,1110) TB1,TB2,M,'Signa','l/','Noise.'
      GO TO 2000
1600 WRITE(NUNIT,1110) TB1,TB2,M,'Time.'
2000 IF(TB1.NE.TOP1) GO TO 8000
      MD = MODSPB
      TB1 = BOT1
      TB2 = BOT2
      M = MDSPB
      N = NDSPB
      GO TO 1050
8000 IF(INDEP.EQ.0) WRITE(NUNIT,8010) 'to the same scale. '
      IF(INDEP.NE.0) WRITE(NUNIT,8010) 'scaled independently.'
8010 FORMAT(' The upper and lower display channels are ',A21)
      WRITE(NUNIT,8110) DSPB,(DSPB + ((NDSP-1.)*DSTEP)),DSTEP
8110 FORMAT(' The display window is from ',F9.5,' to ',F9.5
1,' degrees, ',/,', in steps of ',F8.5,' degrees.')
C
C IF THIS IS TO BE WRITTEN TO DISK, PRINT ALSO
C
      IF(NUNIT.NE.9) GO TO 9000
      NUNIT = 6
      GO TO 100
9000 RETURN
      END

```

```

SUBROUTINE SSHLOP(NU)

```

```

File SSHLOP.FOR begins on the previous line.

```

```

Version Date: October 23, 1984
Paul S. Weiss

```

```

Subroutine SSHLOP prints the current Loop Mode parameters
on logical unit NU.

```

```

COMMON /LOPSET/ ANLPBE,ANLPFN,ANLPIN,LPNRFQ,ANLPCU,LPFLAG

```

```

NUNIT = NU
100 WRITE(NUNIT,110) ANLPBE,ANLPFN,ANLPIN,LPNRFQ,ANLPCU
110 FORMAT(/,' The Loop goes from ',F5.1,' to ',F5.1,' degrees in '
1,F5.2,' degree steps.'
2,/,', Normalization occurs every',I5,' angles.'
3,/,', The current angle in the Loop is ',F5.1,' degrees.')

```

```

IF THIS IS TO BE WRITTEN TO DISK, PRINT IT ALSO

```

```

IF(NUNIT.NE.9) GO TO 9000
NUNIT = 6
GO TO 100
9000 RETURN
END

```

SUBROUTINE SSHMD(NU)

File SSHMD.FOR begins on the previous line.

C
C
C
C
C
C
C
C
C
C

Version Date: October 17, 1984
Paul S. Weiss

Subroutine SSHMD writes out the detector settings to logical
unit NU.

```

COMMON /DET/ AGRD,AFIL,VEB,VIE,VEXT
1, VEN, QPST, QPR, MAS, VEX, VDK, VPMT
C

```

```

NUNIT = NU
100 WRITE(NUNIT,110) AGRD,AFIL,VEB,VIE,VEXT
1, VEN, QPST, QPR, MAS, VEX, VDK, VPMT
110 FORMAT(/, ' The detector settings are: '
1,/, ' Grid Current: ',F4.1,' mA'
2,/, ' Filament Current: ',F4.2,' A'
3,/, ' Electron Beam Energy: ',F5.0,' V'
4,/, ' Ion Energy: ',F7.2,' V'
5,/, ' Ion Extraction Voltage: ',F5.0,' V'
6,/, ' Entrance Lens Voltage: ',F5.0,' V'
7,/, ' Quadrupole Mass Setting = ',F5.2,' Resolution = ',F5.2
8, ' Mass =',I5
9,/, ' Exit Lens Voltage = ',F6.0,' V'
1,/, ' Doorknob Voltage = ',F5.1,' kV'
2,/, ' Photomultiplier Voltage = ',F6.0,' V')

```

C
C
C

IF WRITING TO DISK, PRINT ALSO

```

IF(NUNIT.NE.9) GO TO 9000
NUNIT = 6
GO TO 100
9000 RETURN
END

```

SUBROUTINE SSHMP(NU)

File SSHMP.FOR begins on the previous line.

C
C

```

C   Version Date:  October 23, 1984
C   Paul S. Weiss
C
C   Subroutine SSHMP outputs the Machine pressures and temperatures
C   to logical unit NU.
C

```

```

DIMENSION NONOFF(2)
COMMON /PRES/ PRM(8), IPRE(8), PFORE(8), IDG(8), IPEM(8)
1, PBACK(2), PION(3)
COMMON /TPRIM/ THMCPL(8)
COMMON /MACDEF/ TCDEF(8,4), NTC, PRDEF(8,6), NPR, BACK(4,2)
DATA NONOFF /'n ', 'ff'/

```

```

C
NUNIT = NU
100 WRITE(NUNIT,110) (PBACK(I), (BACK(J,I), J=1,4), I=1,2)
110 FORMAT(/, ' The source backing pressures are:'
1,/, ' Primary Source:      ', F8.1, ' torr with ', 4A4
2,/, ' Secondary Source:    ', F8.1, ' torr with ', 4A4)
WRITE(NUNIT,200) ((PRDEF(I,J), J=1,6), PRM(I), IPRE(I), PFORE(I)
1, NONOFF(IDG(I)), IPEM(I), I=1, NPR)
200 FORMAT(/, ' The Regional Pressures are:'
1,8(/, 1X, 6A4, 1X, F4.2, 'x10', I3, ' torr, foreline: ', F4.0
2, ' u, Degas 0', A2, ', ', I2, ' mA', :))
WRITE(NUNIT,300) (I, PION(I), I=1,3)
300 FORMAT(/, ' The ion pump currents are:', /
1,3(' Region ', I1, ': ', F6.1, ' uA '))
WRITE(NUNIT,400) ((TCDEF(I,J), J=1,4), THMCPL(I), I=1, NTC)
400 FORMAT(/, ' The measured Thermocouple voltages are:'
1,4(/, 2(1X, 4A4, 1X, F5.2, ' mV ', :)))

```

```

C
C   IF THIS IS TO BE WRITTEN TO DISK, PRINT ALSO
C

```

```

IF(NUNIT.NE.9) GO TO 9000
NUNIT = 6
GO TO 100
9000 RETURN
END

```

```

SUBROUTINE SSHNRM(NU)

```

File SSHNRM.FOR begins on the previous line.

```

C   Version Date:  October 23, 1984
C   Paul S. Weiss
C

```

```

C   Subroutine SCHNRM prints the current Normalization parameters
C   on logical unit NU.
C

```

```

COMMON /NRMSET/ ANGNRM, INTNRM, NRM RPT, NRMFLG

```

```

C
NUNIT = NU
100 WRITE(NUNIT,110) ANGNRM,INTNRM,NRMRPT
110 FORMAT(/,' Normalization occurs at ',F5.1,' degrees.'
1,/, ' The countdown interval is ',I5,', and is '
2,'repeated ',I3,' times.',/)

C
C IF THIS IS TO BE WRITTEN TO DISK, PRINT ALSO
C

IF(NUNIT.NE.9) GO TO 9000
NUNIT = 6
GO TO 100
9000 RETURN
END

SUBROUTINE SSHPOL(NU)
C File SSHPOL.FOR begins on the previous line.
C
C Version Date: October 23, 1984
C Paul S. Weiss
C
C Subroutine SSHPOL outputs the Polarization Rotation Mode
C parameters to logical unit NU.
C
C
COMMON /POLSET/ ANGPOL,POLSTP,POSIT,IPOSIT,IPLFLG
C
C
C
100 NUNIT = NU
WRITE(NUNIT,110) ANGPOL,POLSTP,INT((180./POLSTP)+0.5)
1, (POSIT*180./200.)
110 FORMAT(/,' The detector angle for the Polarization Rotation '
1,'Loop is ',F5.1,' degrees.'
2,/, ' The motor step size is ',F6.2,' degrees,'
3,/, ' which scans through 180 degrees in ',I3,' steps.'
4,/, ' The polarization position is ',F7.3,' degrees from'
4,' vertical.')
```

IF THIS IS TO BE WRITTEN TO DISK, PRINT ALSO

```

IF(NUNIT.NE.9) GO TO 9000
NUNIT = 6
GO TO 100
9000 RETURN
END

SUBROUTINE SSHTST(NU)
```

```

C                                     File SSHTST.FOR begins on the previous line.
C
C                                     Version Date:  October 23, 1984
C                                     Paul S. Weiss
C
C                                     Subroutine SSHTST prints the current Test mode parameters
C                                     on logical unit NU.
C
COMMON /TSTSET/ TSTANG,NUMTST,TSTCUR,TSTFLG
NUNIT = NU
100 WRITE(NUNIT,110) TSTANG,NUMTST,INT(1.E5*TSTCUR)
110 FORMAT(/,' The current Test mode angle is ',F5.1,' degrees.'
1,/,1X,I3,' countdowns can be taken at this angle.'
2,/, ' The current countdown will be #',I3,/)
C
C                                     IF THIS IS TO BE WRITTEN TO DISK PRINT IT ALSO
C
IF(NUNIT.NE.9) GO TO 9000
NUNIT = 6
GO TO 100
9000 RETURN
END

```

```

SUBROUTINE SSHVEL(NU)
C                                     File SSHVEL.FOR begins on the previous line.
C
C                                     Version Date:  October 23, 1984
C                                     Paul S. Weiss
C
C                                     Subroutine SSHVEL outputs the Velocity measurement parameters
C                                     and measurement on logical unit NU.
C
COMMON /LASSET/ LASDWL,FRQLAS,LASSTP,FSRLAS,LASCHA
COMMON /VELO/ DELF,HALFH,DELPIP,VELB,SPDRIO
NUNIT = NU
100 WRITE(NUNIT,110) FRQLAS,FSRLAS
110 FORMAT(/,' The Laser Frequency is ',F10.3,' cm-1.'
1,/, ' The Frequency Standard is ',F5.2,' GHz.')
IF(VELB.LE.0.) GO TO 8000
IF(SPDRIO.LE.0.) GO TO 7000
WRITE(NUNIT,2100) VELB,SPDRIO,DELF,HALFH,DELPIP
2100 FORMAT(' The beam velocity is ',F10.0,' cm/sec.'
1,/, ' The Speed Ratio is ',F5.2
2,/, ' The 45 to 90 degree separation was ',F10.4
3,/, ' The Half Height of the 45 degree peak was ',F10.4
4,/, ' The frequency standard separation was ',F10.4,/)

```

```

GO TO 8500
7000 TYPE 7010,VELB,DELF,DELPIP
7010 FORMAT(' The beam velocity is ',F10.3,' cm/sec.'
1,/, ' The Speed Ratio was not measured.'
2,/, ' The 45 to 90 degree separation was ',F10.4
4,/, ' The frequency standard separation was ',F10.4,/)
GO TO 8500
8000 TYPE *,'The velocity has not been measured.'
C
C IF WRITING TO DISK, ALSO PRINT
C
8500 IF(NUNIT.NE.9) GO TO 9000
NUNIT = 6
GO TO 100
9000 RETURN
END

```

SUBROUTINE SSTART(IOPT)

File SSTART.FOR begins on the previous line.

Version Date: September 3, 1984
Paul S. Weiss

Subroutine SSTART starts the TGS counting down using MACRO
subroutine SGO. It sets the display correctly for the
angle under study, so that the current point is brightened.

The argument of SSTART is:

IOPT=-1 Skip all queries.
IOPT=1 Query as to whether angle and settings are correct.

```

INTEGER*4 JDATA
COMMON /CUR/ ANGLE,INTERV,NUMANG,MANGLE,IRNFLG
COMMON /DATA/ DATA(256,20),WORK1(256),WORK2(256)
COMMON /SETS/ GATE(16),TIM(16),EXCFRC(2),CLOCK,INTACQ,NCHAN
COMMON /SDONE/ ISWFLG,JDATA(20)
COMMON /SCR/ SCR(20)

```

```

C
IF(IRNFLG.EQ.1) GO TO 8000
IF(IOPT.LE.0) GO TO 2000
TANG = ANGLE + 270.
IF(TANG.GE.360.) TANG = TANG - 360.
90 TYPE 100,TANG,INTERV
100 FORMAT(' The detector angle is ',F5.1,' degrees.'
1,/, ' The Countdown interval is ',I5,','
2,/, ' Are these correct and are you ready?')

```

```

ACCEPT 1000,ANS
1000  FORMAT(A1)
      IF(ANS.NE.'Y') GO TO 8500
2000  CALL SGO(ISWFLG,JDATA)
      TYPE 4100,7,0
4100  FORMAT(' TGS is running.',2A1)
      IRNFLG = 1
      ISWFLG = 0
      SCR(1) = ANGLE
      DO 5000 I=2,20
      SCR(I) = 0.
5000  CONTINUE
      RETURN
8000  TYPE 4100,7,7
8500  TYPE *,'Abort Requested Acquisition?'
      ACCEPT 1000,ANS
      IF(ANS.NE.'Y') GO TO 90
      RETURN
      END

```

SUBROUTINE STEST(IOPT)

File STEST.FOR begins on the previous line.

Version Date: September 27, 1984
Paul S. Weiss

Subroutine STEST starts or continues the Test Mode of TGS operation, running the TGS over continuously without interruption.

The argument IOPT determines whether Test Mode is to be continued or started over, as follows:

IOPT=0 Start Test Mode
IOPT=1 Continue Test Mode

WARNING: Subroutine STEST is the largest segment of overlay region 2. Enlarging it will directly increase the size of SANG.

```

INTEGER*4 JDATA
COMMON /CUR/ ANGLE,INTERV,NUMANG,MANGLE,IRNFLG
COMMON /SETS/ GATE(16),TIM(16),EXCFRC(2),CLOCK,INTACQ,NCHAN
COMMON /TSTSET/ TSTANG,NUMTST,TSTCUR,TSTFLG
COMMON /SDONE/ ISWFLG,JDATA(20)
COMMON /CHAEF/ CHAEF(20,10)

```

IF(IRNFLG.NE.0) GO TO 8800


```

TYPE 100
100  FORMAT(' Test Mode?  Are you sure?')
ACCEPT 1000,ANS
1000  FORMAT(A1)
      IF(ANS.NE.'Y') GO TO 8900
      TYPE *,'Change display window for test mode?'
      ACCEPT 1000,ANS
      IF(ANS.EQ.'Y') CALL SCHDWN(1)
      IF(IOPT.NE.0) GO TO 3000

C
C  IF STARTING TEST MODE, START FLAG COUNTER AT 0, AND QUERY AS TO
C  WHETHER OR NOT TO CLEAR OLD TEST MODE DATA, IF THERE IS ANY
C
      IF(TSTCUR.EQ.0.) GO TO 3000
      TYPE *,'Zero previous Test Mode Data?'
      ACCEPT 1000,ANS
      IF(ANS.EQ.'Y') CALL SZERO(3)
      TSTCUR = 0.

C
C  START HERE FOR BOTH STARTING AND CONTINUING TEST MODE
C
3000  TSTFLG = 1.
      TSTCUR = TSTCUR + .00001
      ANGLE = TSTANG + TSTCUR
      INTERV = INTACQ

C
C  QUERY AS TO DETECTOR POSITION, ETC. AND START TGS IN
C  SUBROUTINE SSTART
C
      CALL SSTART(1)
      GO TO 9000

C
C  IF TGS IS ALREADY RUNNING, SHOW THIS AND ABORT
C
8800  TYPE 8810
8810  FORMAT(' TGS is running')
C
C  IF TEST MODE IS CANCELLED AUTOMATICALLY OR BY USER, SHOW THIS
C
8900  TYPE 8910,7,7
8910  FORMAT(' Abort Test Mode',2A1)
9000  RETURN
      END

```

SUBROUTINE SVELO

File SVELO.FOR begins on the previous line.

Version Date: July 20, 1984

```

C      Paul S. Weiss
C
C      Subroutine SVELO determines the beam velocity from the
C      45 degree crossing of the laser.
C
C
COMMON /LASSET/ LASDWL,FRQLAS,LASSTP,FSRLAS,LASCHA
COMMON /VELO/ DELF,HALFH,DELPIP,VELB,SPDRIO
100  TYPE 110
110  FORMAT(' Enter the distance between the 45 and 90 '
1, 'degree peaks. ')
ACCEPT *,DELF
IF(DELF.LE.0.) GO TO 100
200  TYPE 210
210  FORMAT(' Enter the distance between frequency standard'
1, ' mark. ')
ACCEPT *,DELPIP
IF(DELPIP.LE.0.) GO TO 200
300  TYPE 310
310  FORMAT(' Enter the half width of the 45 degree peak. ')
ACCEPT *,HALFH
IF(HALFH.EQ.0.) GO TO 300
C
C      DETERMINE CONVERSION OF FREQUENCY TO VELOCITY
C
C       $FTOV = (3.00E+10 * 1.41421) / (FRQLAS * 30.)$ 
C
C      DETERMINE MEASURED DISTANCE TO VELOCITY
C
C       $DTOV = FTOV * FSRLAS / DELPIP$ 
C
C      DETERMINE VELOCITY
C
C       $VELB = DELF * DTOV$ 
2010 TYPE 2010,VELB
C      FORMAT(' The beam velocity is ',F10.0,' cm/sec. ')
C
C      DETERMINE SPEED RATIO
C
C       $SPDRIO = DELF / HALFH$ 
IF(SPDRIO.GT.0.) GO TO 5000
SPDRIO = 0.
TYPE *, 'The speed ratio was not measured.'
GO TO 9000
5000 TYPE 5010,SPDRIO
5010 FORMAT(' The speed ratio is ',F6.3)
9000 RETURN
END

```

SUBROUTINE SWRITE(IFLAG)

File SWRITE.FOR begins on the previous line.

Version Date: September 4, 1984
Paul S. Weiss

Subroutine SWRITE writes the raw data to logical unit 9, opened
in subroutine SFILE.

The argument of SWRITE is IFLAG, and it is a combination of all
of the flags as determined in SDONE.

```

LOGICAL*1 ITIME(8)
COMMON /FNAME/ INAME(7), ISTORE
COMMON /SETS/ GATE(16), TIM(16), EXCFRC(2), CLOCK, INTACQ, NCHAN
COMMON /SCR/ SCR(20)
CALL TIME(ITIME)
WRITE(9,100,ERR=9200) (ITIME(J), J=1,8), IFLAG
1, (SCR(I), I=1, ((2*NCHAN)+2))
100  FORMAT(1X,8A1,1X,I4,1X,F9.5,1X,F7.2,2(2(1X,F9.0),:),/
1,2(4(2(1X,F9.0),:),/))
ISTORE = ISTORE + 1
9000  RETURN
9200  TYPE 9210, (INAME(I), I=1,7), 7,7,7,7
9210  FORMAT(' Error writing to file ',7A2,4A1)
GO TO 9000
END

```

SUBROUTINE SZERO(IOPT)

File SZERO.FOR begins on the previous line.

Version Date: October 12, 1984
Paul S. Weiss

Subroutine SZERO zeroes some or all of the accumulated data
in array DATA, sets NUMANG and MANGLE accordingly.

The argument of SZERO specifies what angles to zero as follows:

```

IOPT=1  Zero all data.
IOPT=2  Zero data over a specified angular range.
IOPT=3  Zero all Test Mode data.

```

```

COMMON /CUR/ ANGLE,INTERV,NUMANG,MANGLE,IRNFLG
COMMON /TSTSET/ TSTANG,NUMTST,TSTCUR,TSTFLG
COMMON /DATA/ DATA(256,20),WORK1(256),WORK2(256)
NUMZER = 0

```

```

GO TO(1100,2100,3100),IOPT
C
C   ZERO ALL DATA
C
1100 TYPE *,'Zero Data Arrays? Are you sure?'
      ACCEPT 1000,ANS
1000  FORMAT(A1)
      IF(ANS.NE.'Y') GO TO 9000
      NUMZER = NUMANG
      GO TO 5000
C
C   ZERO DATA OVER A SEGMENT
C
2100  TYPE 2110,'first'
2110  FORMAT(/,' Enter ',A5,' angle of segment to zero')
      ACCEPT *,ANBE
      TYPE 2110,'last'
      ACCEPT *,ANFN
      TYPE 2210,ANBE,ANFN
2210  FORMAT(' Zero data from ',F9.5,' to ',F9.5
1,' degrees? Are you sure?')
      ACCEPT 1000,ANS
      IF(ANS.NE.'Y') GO TO 9000
C
      DO 2400 I=1,NUMANG
C
C   HAVE ALL THE ANGLES BEEN LOOKED AT?
C   IF SO, LEAVE LOOP
C
2230  IF(I+NUMZER.GT.NUMANG) GO TO 2500
C
C   IS DATA WITHIN SEGMENT?
C
      IF(DATA(I,1).LT.ANBE) GO TO 2400
      IF(DATA(I,1).GT.ANFN) GO TO 2500
      DO 2300 J=1,20
      DO 2250 IK=I,NUMANG-1
      DATA(IK,J) = DATA(IK+1,J)
2250  CONTINUE
2300  CONTINUE
      NUMZER = NUMZER + 1
C
C   SINCE DATA HAS BEEN SHIFTED, STAY AT THIS POSITION TO CHECK
C   NEXT POINT
C
      GO TO 2230
2400  CONTINUE
      GO TO 6000
C
C   SHIFT LATER DATA INTO PLACE

```

```

C
2500  IF(NUMZER.EQ.0) GO TO 8000
      DO 2550 IK=NUMANG-NUMZER,NUMANG-1
      DO 2540 J=1,20
      DATA(IK,J) = DATA(IK+1,J)
2540  CONTINUE
2550  CONTINUE
      GO TO 6000

C
C      ZERO DATA TAKEN IN TEST MODE
C
3100  TYPE 3110
3110  FORMAT(' Zero all Test Mode Data? Are you sure?')
      ACCEPT 1000,ANS
      IF(ANS.NE.'Y') GO TO 9000

C
      DO 3500 I=1,NUMANG

C
C      HAVE ALL THE POINTS BEEN CHECKED?
C      IF SO, LEAVE LOOP
C
3200  IF(I+NUMZER.GT.NUMANG) GO TO 5000
C
C      IS THIS DATA FROM TEST MODE?
C
      IF(INT(((20.*DATA(I,1))-FLOAT(INT(20.*DATA(I,1))))
1*1.E5).LT.1) GO TO 3500

C
C      SHIFT DATA INTO SPACE VACATED BY REMOVED TEST MODE ANGLE
C
      IF(I.GT.NUMANG-1) GO TO 3450
      DO 3400 IK=I,NUMANG-1
      DO 3300 J=1,20
      DATA(IK,J) = DATA(IK+1,J)
3300  CONTINUE
3400  CONTINUE
3450  NUMZER = NUMZER + 1
      GO TO 3200
3500  CONTINUE

C
C      ZERO TEST MODE ANGLE COUNTERS FOR OPTIONS 1 AND 3
C
5000  T= TSTFLG
      TSTFLG = 0.
      IF(T.GT.0.) TSTFLG = 1.
      TSTCUR = 0.

C
C      EXECUTE FOR EACH OPTION:
C      ZERO LAST SECTION OF DATA THAT IS NO LONGER USED
C

```

```
6000  IF(NUMZER.EQ.0) GO TO 8000
      DO 6500 IK=NUMANG-NUMZER+1,NUMANG
      DO 6400 J=1,20
      DATA(IK,J) = 0.
6400  CONTINUE
6500  CONTINUE
8000  TYPE 8010,NUMZER,7
8010  FORMAT(' Data at ',I3,' angles zeroed.',A1)
C
C      REDUCE THE NUMBER ANGLES TO THE NEW LOWER VALUE
C
      NUMANG = NUMANG - NUMZER
      MANGLE = MANGLE - NUMZER
9000  RETURN
      END
```

```

      .TITLE  ANGULAR SCAN ROUTINES
;                                     File SANGLE.MAC begins on the previous line.
      .IDENT  /103084/
;
;Version Date:  October 30, 1984
;Paul S. Weiss
;
;Angular Scan Routines to run the Timer-Gater Unit with program SANG.
;
;
;FORTRAN GLOBALS:
;
      .GLOBL  SCHDEF,SCOMM,SDISP,SDPOL,SINIT,SPRII,SSTART
;
;MACRO GLOBALS:
;
      .GLOBL  CLSHTR,DISPL
      .GLOBL  ENSPEC,EXSPEC,INIT
      .GLOBL  LCASE,MOT,OPSHTR,SCASUB
      .GLOBL  SCLEAR,SEXIT,SGO,STOPD,UCASE
      .MCALL  .INTEN,.PRINT
      .ENABL  LC
;
;
      .SBTTL  ADDRESSES
;
JSW=44
DATA0=166000
DATAHI=166002
SCAVEC=504
SCAPRI=506
LASVEC=510
LASPRI=512
MOTCSR=167000
SCAL0=167040
SCAL1=167042
SCAL2=167044
SCAL3=167046
SCALAM=167074
LASE0=167100
LASE1=167102
LASE2=167104
LASE3=167106
LASLAM=167134
STATU1=166010
STATU2=166012
TTRCSR=177560
LFCSR=167760
TGCSR=167770
TGOTBF=167772

```

```

TGINBF=167774
TGVECA=350
TGAPRI=352
TGVECB=354
TGBPRI=356
AIODAB=170406
DSPCSR=170440
DSPXYB=170442
DSPPCR=170444
DSPCAR=170446
DSPINV=340
DSPPRI=342

```

```

;
; .PAGE
; .SBTTL MACRO SUBROUTINES
;
;
; Subroutine INIT loads the interrupt vectors with the addresses
; of the interrupt service routines, and enables the Request B (Timer
; countdown completed) and Scaler (count overflow) interrupts.
;
INIT: RESET
      BIS      #100,0#TTRCSR      ; RESET TERMINAL INPUT ENABLE
      TST      (R5)+             ; SKIP ARGUMENT COUNTER
      MOV      (R5)+,0#SFLAG      ; LOAD END COUNTDOWN FLAG ADDRESS
      MOV      (R5),0#JDATAD      ; LOAD DATA ARRAY ADDRESS
      MOV      #TGINTA,0#TGVECA
      MOV      #0,0#TGAPRI        ; KEEP PRIORITY LOW TO ENABLE INPUT
      MOV      #TGINTB,0#TGVECB
      MOV      #200,0#TGBPRI
      MOV      #0,0#DSPCSR        ; CLEAR DISPLAY CSR
      MOV      #DSPINT,0#DSPINV   ; LOAD DISPLAY INTERRUPT VECTOR
      MOV      #0,0#DSPPRI       ; AND PRIORITY
      JSR      PC,SCLEAR         ; CLEAR SCALERS
      MOV      #0,0#STATU1
      MOV      #0,0#STATU2
      MOV      #SCAINT,0#SCAVEC   ; LOAD SCALER OVERFLOW INTERRUPT
                                      ; VECTOR
      MOV      #0,0#SCAPRI        ; KEEP SCALER PRIORITY LOW
      MOV      #SCAINT,0#LASVEC   ; LOAD LASER FLUORESCENCE SCALER
                                      ; INTERRUPT VECTOR
      MOV      #0,0#LASPRI        ; KEEP THIS PRIORITY LOW TOO
      BIC      #301,0#STATU1      ; DISABLE SCALER INTERRUPT
      MOVB     #24.,0#SCALAM
      MOVB     #24.,0#LASLAM
      MOV      #0,0#TGFLAG        ; CLEAR INTERRUPT FLAG WORD
      MOV      #0,0#TGCSR        ; CLEAR TIMER-GATER CSR
      BIS      #40,0#TGCSR        ; ENABLE B INTERRUPT
      TST      0#TGINBF          ; SEND DATA TRANSMITTED PULSE

```



```

MOV     #0,LFCSR                ;DISABLE LASER FLUORESCENCE
                                           ;PARALLEL LINE UNIT, AND CLOSE
                                           ;SHUTTER
RTS     PC

;
;Subroutine SEXIT disables all the interrupts in the system to allow
;termination of the program.
;
SEXIT:  MOV     #0,0#STATU1        ;TURN OFF QUAD SCALER
        MOV     #0,0#STATU2
        MOVB   #24.,0#SCALAM
        MOVB   #24.,0#LASLAM
        MOV     #0,0#TGCSR        ;TURN OFF TIMER-GATER
        MOV     #0,0#DSPCSR      ;TURN OFF DISPLAY
        RTS     PC

;
;Subroutine ENSPEC puts the monitor in special screen mode
;
ENSPEC: BIS     #10000,0#44        ;ENTER SPECIAL SCREEN MODE
        RTS     PC

;
;Subroutine EXSPEC takes the monitor out of special screen mode
;
EXSPEC: BIC     #10000,0#44        ;LEAVE SPECIAL SCREEN MODE
        RTS     PC

;
;Subroutine LCASE enables lower case input from terminal
;
LCASE:  BIS     #40000,0#44
        RTS     PC

;
;Subroutine UCASE disables lower case input from terminal
UCASE:  BIC     #40000,0#44
        RTS     PC

;
;Subroutine STOPD stops the display.
;
STOPD:  BIC     #103,0#DSPCSR      ;CLEAR DISPLAY INTERRUPTS
        RTS     PC

;
;Subrouine SGO starts the Timer-Gater Module counting down.
;

```

```

SGO:   TST      (R5)+           ;SKIP ARGUMENT COUNTER
        MOV      (R5)+,0#SFLAG ;LOAD END COUNTDOWN FLAG ADDRESS
        MOV      (R5),0#JDATAD ;LOAD DATA ARRAY ADDRESS
        JSR      PC,SCLEAR
        MOV      #40,0#TGCSR   ;ENABLE REQUEST B INTERRUPT
        MOV      #0,0#TGOTBF  ;SEND NEW DATA READY PULSE
        RTS      PC

```

;Subroutine MOT sends pulses from a CAMAC pulse generator
;to a stepping motor controller, which turns a polarization
;rotator.

;The argument of MOT is an integer, positive for clockwise
;rotation, and negative for counterclockwise rotation.

```

MOT:   MOVB     #1,0#MOTCSR    ;READ MOTOR STATUS WORD
        BIT     #1,0#DATALO   ;IS LAM SET?
        BEQ     MOT           ;NO, WAIT
        TST     (R5)+         ;SKIP ARGUMENT COUNT
        MOV     0(R5),R1      ;GET ARGUMENT, NUMBER OF STEPS
        TST     R1           ;IS R1 NEGATIVE?
        BGE     30$          ;NO
        NEG     R1           ;YES-MAKE POSITIVE
        BIS     #100000,R1    ;SIGN BIT = 1
30$:   BEQ     40$            ;DO NOT LOAD A ZERO
        MOV     R1,0#DATALO
        MOVB    #16.,0#MOTCSR ;LOAD COUNTER
40$:   RTS      PC

```

;Subroutine DISPL loads the display buffer for the DMA display unit.

;It must be called with two arguments:

;DSPAD: The address of a single precision integer array,
; prepared to be displayed as a point plot, with x and y
; coordinates stored alternately. All values range from
; 0 to 4095. The address of this array is stored
; in DSPAD.

;NUMDSP: The number of points to be displayed.

```

DISPL: BIC     #103,0#DSPCSR   ;DISABLE DISPLAY INTERRUPTS
        TST     (R5)+         ;SKIP ARGUMENT COUNT
        MOV     (R5)+,0#DSPAD ;STORE ADDRESS OF DISPLAY BUFFER
        MOV     0(R5),0#DSPPCR ;LOAD POINT COUNT REGISTER
        MOV     0(R5),0#DSPNPT ;LOAD NUMBER OF POINTS REGISTER
        ;FOR FUTURE REFERENCE

```

```

NEG      0#DSPPCR          ;TWO'S COMPLEMENT CODING OF PCR
MOV      0#DSPAD,0#DPCAR  ;INITIALIZE CURRENT ADDRESS REGISTER
BIS      #103,0#DPCSR    ;ENABLE DISPLAY INTERRUPT, AND START
RTS      PC

```

```

;
;
;
;Subroutine SCLEAR clears the eight Quad Scaler channels, and
;enables Scaler interrupts.
;

```

```

SCLEAR: BIC      #301,0#STATU1      ;DISABLE SCALER OVERFLOW INTERRUPTS
        MOV      #24.,0#SCALAM
        MOV      #24.,0#LASLAM
        MOV      #2,0#SCALO
        MOV      #2,0#SCAL1
        MOV      #2,0#SCAL2
        MOV      #2,0#SCAL3
        MOV      #2,0#LASE0
        MOV      #2,0#LASE1
        MOV      #2,0#LASE2
        MOV      #2,0#LASE3
        BIS      #301,0#STATU1      ;REENABLE SCALER INTERRUPTS
        MOV      #26.,0#SCALAM
        MOV      #26.,0#LASLAM
        RTS      PC
;
;
;

```

```

;Subroutine SCASUB reads the six Quad Scaler channels in use, then clears
;them. Their contents are returned in a double precision integer
;array: JDATA.
;

```

```

;SCASUB is called from TGINTB
;

```

```

SCASUB: MOV      R5,-(SP)          ;SAVE R5 ON STACK
        BIC      #301,0#STATU1
        MOV      #24.,0#SCALAM    ;DISABLE SCALER INTERRUPTS
        MOV      #24.,0#LASLAM
;

```

```

;LOAD THE ADDRESS OF JDATA INTO R5
        MOV      0#JDATAD,R5
;

```

```

;FIRST, EACH CHANNEL IS READ IN THROUGH DATA0
;AND DATAHI, AND THEN CLEARED, THE RESULT IS STORED IN
;THE ARRAY JDATA(1-4)

```

```

        MOV      #2,0#SCALO
        JSR      PC,VALUE
        MOV      #2,0#SCAL1
        JSR      PC,VALUE

```

```

MOV B    #2,0#SCAL2
JSR      PC,VALUE
MOV B    #2,0#SCAL3
JSR      PC,VALUE

```

```

;
;
;HERE THE VALUE OF THE LASER FLUORESCENCE SCALER CONTENTS ARE READ
;INTO DOUBLE PRECISION INTEGER ARRAY JDATA
;

```

```

MOV B    #2,0#LASE0
JSR      PC,VALUE
MOV B    #2,0#LASE1
JSR      PC,VALUE
MOV B    #2,0#LASE2
JSR      PC,VALUE
MOV B    #2,0#LASE3
JSR      PC,VALUE
MOV      (SP)+,R5      ;RESTORE R5 FROM STACK
RTS      PC           ;RETURN

```

```

;Subroutine VALUE stores the contents of one channel into one of
;the elements of a double precision integer array.
;

```

```

;VALUE is called from SCASUB
;

```

```

VALUE:  MOV    DATA0,(R5)+
        MOV    DATAHI,(R5)+
        RTS    PC

```

```

;Subroutine WAIT maintains control while the Timer-Gater is reset.
;WAIT waits for an interrupt from the Timer-Gater Module, then
;

```

```

WAIT:   TST    0#TGFLAG      ;HAS THERE BEEN AN INTERRUPT?
        BNE    REQ          ;IF SO, RETURN
        BR     WAIT         ;IF NOT, LOOP
REQ:    MOV    #0,0#TGFLAG   ;REMOVE REQUEST A FLAG
        RTS    PC          ;RETURN TO COMAND VIA REQIN & START

```

```

;Subroutine LASDAB sends a value to Digital to Analog converter
;channel B. This is used to scan the laser.
;

```

```

LASDAB: TST    (R5)+        ;SKIP ARGUMENT COUNT
        MOV    0(R5),0#AIODAB ;LOAD D/A VALUE
        RTS    PC

```

```

;
;Subroutine OPSHTR opens the shutter to the 45 degree laser crossing
;of the molecular beam by setting the CSRO bit of the secondary DRV11
;Parallel Line Unit.

```

```

OPSHTR: MOV    #1,0#LFCSR           ;OPEN SHUTTER
        RTS    PC

```

```

;Subroutine CLSHTR closes the shutter to the 45 degree laser crossing
;of the molecular beam by clearing the CSRO bit of the secondary DRV11
;Parallel Line Unit.

```

```

CLSHTR: MOV    #0,0#LFCSR           ;CLOSE SHUTTER
        RTS    PC

```

```

.PAGE
.SBTTL  INTERRUPT SERVICE ROUTINES

```

```

;Interrupt Service Routine DSPINT is for the DMA display unit.
;The point counter is reinitialized, as is the current address register,
;and then the unit is restarted.

```

```

DSPINT: BIC    #103,0#DSPCSR        ;DISABLE DISPLAY INTERRUPTS
        .INTEN 0,PIC                ;RUN REMAINING CODE AT PRIORITY 0
        MOV    0#DSPNPT,0#DSPPCR    ;LOAD POINT COUNTER
        NEG    0#DSPPCR
        MOV    0#DSPAD,0#DSPCAR     ;LOAD CURRENT ADDRESS REGISTER
        BIS    #103,0#DSPCSR        ;REENABLE DISPLAY INTERRUPTS
        RTS    PC                   ;AND START

```

```

;Interrupt Service Routine SCAINT is for Scaler count overflows.
;The Quad Scaler is cleared, and the end of the countdown occurs.

```

```

SCAINT: MOV    #0,0#TGCSR           ;DISABLE REQUEST B INTERRUPT
        BIS    #4,0#TGFLAG          ;SET OVERFLOW FLAG
        BIS    #40,0#TGCSR          ;REENABLE REQUEST B INTERRUPT
        .INTEN 0,PIC
        JSR    PC,SCLEAR            ;CLEAR SCALER INTERRUPTS
        BIC    #301,0#STATU1
        MOVB   #24.,0#SCALAM
        MOVB   #24.,0#LASLAM
        MOV    #0,0#TGFLAG          ;CLEAR FLAG FOR REQ A INTERRUPT
        TST    0#TGINBF             ;SEND A DATA TRANSMITTED PULSE

```

```

BIS      #100,0#TGCSR      ;ENABLE A REQUEST A INTERRUPT
JSR      PC,WAIT          ;WAIT FOR A REQUEST A INTERRUPT
                          ;I.E. TG HAS RESET
MOV      0#SFLAG,R5       ;SET ISWFLG FOR OVERFLOW CONDITION
MOV      #2,(R5)
RTS      PC
RTS      PC

```

```

;
;
;Interrupt Service Routine TGINTB is for the Request B line of
;the Timer-Gater Module Interface Board.

```

```

;It reads the Quad Scaler's contents using the MACRO subroutine
;SCASUB, then sets a flag and returns to WAIT

```

```

TGINTB: MOV      #0,0#TGCSR      ;DISABLE REQUEST B INTERRUPT
JSR      PC,SCASUB          ;READ AND CLEAR QUAD SCALER
        .INTEN  0,PIC
MOV      #0,0#TGFLAG        ;CLEAR FLAG FOR REQ A INTERRUPT
TST      0#TGINBF          ;SEND A DATA TRANSMITTED PULSE
BIS      #100,0#TGCSR       ;ENABLE A REQUEST A INTERRUPT
JSR      PC,WAIT          ;WAIT FOR A REQUEST A INTERRUPT
                          ;I.E. TG HAS RESET
MOV      0#SFLAG,R5       ;SET ISWFLG
MOV      #1,(R5)
RTS      PC

```

```

;
;
;Interrupt Service Routine TGINTA is for the Request A line
;of the Timer-Gater Interface Board. It sets a flag, and returns
;control to WAIT, which then returns to COMAND.

```

```

TGINTA: MOV      #0,0#TGCSR      ;DISABLE REQUEST A INTERRUPT
BIS      #1,0#TGFLAG        ;SET REQUEST A FLAG BIT
RTI

```

```

;
;
; .PAGE
; .SBTTL ARGUMENT BLOCKS, VARIABLES, ETC.

```

```

;
;
;JDATAD: .WORD
;SFLAG: .WORD
;TGFLAG: .WORD
;DSPNPT: .WORD
;DSPAD: .WORD
; .END

```

```
!File CNSANG.COM
!Compilation File for Angular Scan Program SANG
!
!Version Date:  October 30, 1984
!Paul S. Weiss
FORTRAN/NOLINENUMBERS SANG
!SANG contains the Main program SANG, and subroutine SCOMM
FORTRAN/NOLINENUMBERS SACCUM
FORTRAN/NOLINENUMBERS SCANG
FORTRAN/NOLINENUMBERS SCHDEF
FORTRAN/NOLINENUMBERS SCHDSP
FORTRAN/NOLINENUMBERS SCHDWN
FORTRAN/NOLINENUMBERS SCHLOP
FORTRAN/NOLINENUMBERS SCHMAD
FORTRAN/NOLINENUMBERS SCHMAP
FORTRAN/NOLINENUMBERS SCHNRM
FORTRAN/NOLINENUMBERS SCHPAR
FORTRAN/NOLINENUMBERS SCHPOL
FORTRAN/NOLINENUMBERS SCHKST
FORTRAN/NOLINENUMBERS SCHVEL
FORTRAN/NOLINENUMBERS SCMLST
FORTRAN/NOLINENUMBERS SCOMLC
FORTRAN/NOLINENUMBERS SCOMLD
FORTRAN/NOLINENUMBERS SCOMLG
FORTRAN/NOLINENUMBERS SCOMLL
FORTRAN/NOLINENUMBERS SCOMLM
FORTRAN/NOLINENUMBERS SCOMLN
FORTRAN/NOLINENUMBERS SCOMLP
FORTRAN/NOLINENUMBERS SCOMLR
FORTRAN/NOLINENUMBERS SCOMLS
FORTRAN/NOLINENUMBERS SCOMLT
FORTRAN/NOLINENUMBERS SCOMLV
FORTRAN/NOLINENUMBERS SCOMLW
FORTRAN/NOLINENUMBERS SCOMLZ
FORTRAN/NOLINENUMBERS SDISP
FORTRAN/NOLINENUMBERS SDLONO
FORTRAN/NOLINENUMBERS SDLOP
FORTRAN/NOLINENUMBERS SDNRM
FORTRAN/NOLINENUMBERS SDONE
FORTRAN/NOLINENUMBERS SDPOL
FORTRAN/NOLINENUMBERS SDSIN
FORTRAN/NOLINENUMBERS SDTST
FORTRAN/NOLINENUMBERS SFILE
FORTRAN/NOLINENUMBERS SGRAPH
FORTRAN/NOLINENUMBERS SGTSCR
FORTRAN/NOLINENUMBERS SINIT
FORTRAN/NOLINENUMBERS SLEAVE
FORTRAN/NOLINENUMBERS SLOOP
FORTRAN/NOLINENUMBERS SNUCH
FORTRAN/NOLINENUMBERS SNORM
```

FORTRAN/NOLINENUMBERS SOUT
FORTRAN/NOLINENUMBERS SOVER
FORTRAN/NOLINENUMBERS SPOLAR
FORTRAN/NOLINENUMBERS SPRII
FORTRAN/NOLINENUMBERS SSAVE
FORTRAN/NOLINENUMBERS SSHCUR
FORTRAN/NOLINENUMBERS SSHDEF
FORTRAN/NOLINENUMBERS SSHDSP
FORTRAN/NOLINENUMBERS SSHLOP
FORTRAN/NOLINENUMBERS SSHMD
FORTRAN/NOLINENUMBERS SSHMP
FORTRAN/NOLINENUMBERS SSHNRM
FORTRAN/NOLINENUMBERS SSHPOL
FORTRAN/NOLINENUMBERS SSHTST
FORTRAN/NOLINENUMBERS SSHVEL
FORTRAN/NOLINENUMBERS SSTART
FORTRAN/NOLINENUMBERS STEST
FORTRAN/NOLINENUMBERS SVELO
FORTRAN/NOLINENUMBERS SWRITE
FORTRAN/NOLINENUMBERS SZERO
MAC SANGLE

!File CPSANG.COM
!Copy command file for Angular Scan Program SANG
!
!Version Date: October 30, 1984
!Paul S. Weiss
!
COPY I:SANG.FOR O:SANG.FOR
COPY I:SACCUM.FOR O:SACCUM.FOR
COPY I:SCANG.FOR O:SCANG.FOR
COPY I:SCHDEF.FOR O:SCHDEF.FOR
COPY I:SCHDSP.FOR O:SCHDSP.FOR
COPY I:SCHDWN.FOR O:SCHDWN.FOR
COPY I:SCHLOP.FOR O:SCHLOP.FOR
COPY I:SCHMAD.FOR O:SCHMAD.FOR
COPY I:SCHMAP.FOR O:SCHMAP.FOR
COPY I:SCHNRM.FOR O:SCHNRM.FOR
COPY I:SCHPAR.FOR O:SCHPAR.FOR
COPY I:SCHPOL.FOR O:SCHPOL.FOR
COPY I:SCHTST.FOR O:SCHTST.FOR
COPY I:SCHVEL.FOR O:SCHVEL.FOR
COPY I:SCMLST.FOR O:SCMLST.FOR
COPY I:SCOMLC.FOR O:SCOMLC.FOR
COPY I:SCOMLD.FOR O:SCOMLD.FOR
COPY I:SCOMLG.FOR O:SCOMLG.FOR
COPY I:SCOMLL.FOR O:SCOMLL.FOR
COPY I:SCOMLM.FOR O:SCOMLM.FOR

COPY I:SCOMLN.FOR O:SCOMLN.FOR
COPY I:SCOMLP.FOR O:SCOMLP.FOR
COPY I:SCOMLR.FOR O:SCOMLR.FOR
COPY I:SCOMLS.FOR O:SCOMLS.FOR
COPY I:SCOMLT.FOR O:SCOMLT.FOR
COPY I:SCOMLV.FOR O:SCOMLV.FOR
COPY I:SCOMLW.FOR O:SCOMLW.FOR
COPY I:SCOMLZ.FOR O:SCOMLZ.FOR
COPY I:SDISP.FOR O:SDISP.FOR
COPY I:SDLONO.FOR O:SDLONO.FOR
COPY I:SDLOP.FOR O:SDLOP.FOR
COPY I:SDNRM.FOR O:SDNRM.FOR
COPY I:SDONE.FOR O:SDONE.FOR
COPY I:SDPOL.FOR O:SDPOL.FOR
COPY I:SDSIN.FOR O:SDSIN.FOR
COPY I:SDTST.FOR O:SDTST.FOR
COPY I:SFILE.FOR O:SFILE.FOR
COPY I:SGRAPH.FOR O:SGRAPH.FOR
COPY I:SGTSCR.FOR O:SGTSCR.FOR
COPY I:SINIT.FOR O:SINIT.FOR
COPY I:SLEAVE.FOR O:SLEAVE.FOR
COPY I:SLOOP.FOR O:SLOOP.FOR
COPY I:SNORM.FOR O:SNORM.FOR
COPY I:SNUCH.FOR O:SNUCH.FOR
COPY I:SOUT.FOR O:SOUT.FOR
COPY I:SOVER.FOR O:SOVER.FOR
COPY I:SPOLAR.FOR O:SPOLAR.FOR
COPY I:SPRII.FOR O:SPRII.FOR
COPY I:SSAVE.FOR O:SSAVE.FOR
COPY I:SSHCUR.FOR O:SSHCUR.FOR
COPY I:SSHDEF.FOR O:SSHDEF.FOR
COPY I:SSHDSP.FOR O:SSHDSP.FOR
COPY I:SSHLOP.FOR O:SSHLOP.FOR
COPY I:SSHMD.FOR O:SSHMD.FOR
COPY I:SSHMP.FOR O:SSHMP.FOR
COPY I:SSHNM.FOR O:SSHNM.FOR
COPY I:SSHPOL.FOR O:SSHPOL.FOR
COPY I:SSHTST.FOR O:SSHTST.FOR
COPY I:SSHVEL.FOR O:SSHVEL.FOR
COPY I:SSTART.FOR O:SSTART.FOR
COPY I:STEST.FOR O:STEST.FOR
COPY I:SVELO.FOR O:SVELO.FOR
COPY I:SWRITE.FOR O:SWRITE.FOR
COPY I:SZERO.FOR O:SZERO.FOR
COPY I:SANGLE.MAC O:SANGLE.MAC
COPY I:CNSANG.COM O:CNSANG.COM
COPY I:CPSANG.COM O:CPSANG.COM
COPY I:LSANG.COM O:LSANG.COM

```
!File LSANG.COM
!LINK command file for Angular Program
!Version Date: October 30, 1984
!Paul S. Weiss
R LINK
SANG, SANG.MAP, =SANG, SANGLE/I//
SACCUM/0:1
SCANG/0:1
SCHDEF/0:1
SCHDSP/0:1
SCHDWN/0:1
SCHLOP/0:1
SCHMAD/0:1
SCHMAP/0:1
SCHNRM/0:1
SCHPAR/0:1
SCHPOL/0:1
SCHTST/0:1
SCHVEL/0:1
SCMLST/0:1
SCOMLC/0:1
SCOMLD/0:1
SCOMLG/0:1
SCOMLL/0:1
SCOMLM/0:1
SCOMLN/0:1
SCOMLP/0:1
SCOMLR/0:1
SCOMLS/0:1
SCOMLT/0:1
SCOMLV/0:1
SCOMLW/0:1
SCOMLZ/0:1
SDISP/0:1
SDLONO/0:1
SDLOP/0:1
SDNRM/0:1
SDPOL/0:1
SDSIN/0:1
SDTST/0:1
SFILE/0:1
SGRAPH/0:1
SGTSCR/0:1
SINIT/0:1
SLEAVE/0:1
SOUT/0:1
SOVER/0:1
SPRII/0:1
SSAVE/0:1
SSHCUR/0:1
```

SSHDEF/0:1
SSHDSP/0:1
SSHLOP/0:1
SSHMD/0:1
SSHMP/0:1
SSHNRM/0:1
SSHPOL/0:1
SSHTST/0:1
SSHVEL/0:1
SSTART/0:1
SVELO/0:1
SWRITE/0:1
SZERO/0:1
SDONE/0:2
SLOOP/0:2
SNORM/0:2
SNUCH/0:2
SPOLAR/0:2
STEST/0:2
//
\$SHORT

^C

B. Data Acquisition for Time-of-Flight Measurements: The New Multichannel Scaler and Program TUF

1. The Purpose of the Multichannel Scaler

A multichannel scaler (MCS) is used for measuring the time-of-flight of scattered atoms or molecules from a point of modulation (e.g. reaction or collision center, or modulating wheel, chopper, or laser) to a point of detection (e.g. ionizer and subsequent ion optics). This time is typically on the order of microseconds, as is the spread in the distribution of typical time-of-flight (TOF) spectra.

A multichannel scaler used for measuring TOF spectra counts a series of pulses in consecutive channels, where each channel corresponds to a well defined time interval after an initial trigger pulse. For example, after a trigger pulse arrives at the MCS, the first channel records data pulses from 0 to 1 μsec , the second channel records data pulses from 1 to 2 μsec , and the n^{th} channel records data from $n-1$ to n μsec . When another trigger pulse arrives at the MCS, the sequence immediately begins again with the first channel adding the present data to that recorded after previous trigger pulses. The scan described above has a "dwell time" of 1 μsec , that is, after each trigger pulse arrives at the MCS the channels are addressed sequentially with each channel recording data for 1 μsec .

A 4096 channel scaler has been designed and built in collaboration with Jacques Millaud and Fred Vogelsberg of the LBL Department of Instrument Science and Engineering. The scaler is a double width CAMAC module, and can interface to any of the numerous computers which can be equipped with a CAMAC Dataway Interface (IEEE Standard 583-1975).² Only Digital Equipment Corporation LSI-11 series computers (namely 11, 11/2, 11/23, and 11/73)⁵ have been programmed to run the MCS thus far. The specifications for the scaler are given below.

This multichannel scaler was built to replace a 256 channel scaler built by Randall Sparks and Vince Randolph in 1978.¹¹ Because of the advance in IC design, it was clear that a new scaler could be built with substantially better capabilities. The new scaler has 16 times the memory, 16 times the counting ability, can count over 3 times as long, has 6 times the time resolution, is half the size, and uses approximately one third of the power of the old scaler.

At the time of its design (1984), the wait for some of the most advanced chips was over 1 year. Thus, the choice of IC logic often was not at the cutting edge, but was sufficient for our space and time constraints. Even now, it is possible to see significant improvements that could be made in reducing the dead time, and increasing the time resolution and the maximum counting rate.

Table I. The CAMAC commands for the MCS.

<u>Command</u>	<u>Function</u>
N.F0.A0	Read MCS Control Status Register.
N.F0.A1	Read the number of triggers remaining.
N.F0.A3	Read the memory data.
N.F8.A0	Test LAM. ⁵
N.F18.A0	Load MCS Control Status Register.
N.F18.A1	Load the number of triggers.
N.F18.A2	Load the dwell counts.
N.F18.A3	Load the memory address.

2. CAMAC Commands for the New Multichannel Scaler

Table I is a list of CAMAC commands which drive the multichannel scaler. In order to use these refer to the manual for the CAMAC crate controller in use. All CAMAC crate controllers have the ability to issue these commands, but each has its own protocol for doing so. All programs and examples below are written for an LSI-11 computer with a Kinetic Systems Model 3912-Z1G crate controller.¹⁰ All load (F18) commands load values from the data register (low 16 bit word: "DATA0" in CAMAC parlance) into the appropriate MCS register. All read (F0) commands load values from the MCS into the data register (DATA0). A description of the various commands follows.

Table II. Definitions of Control Status Register Bits. A "(1)" implies that the corresponding bit is set when the condition is true.

<u>Bit</u>	<u>Read/Write</u>	<u>Meaning</u>
0	R/W	LAM Enable (1).
1		Not used.
2	R/W	Read Data Enable (1).
3	R/W	Acquisition Enable (1).
(4	W	<u>CLEAR</u> , not implemented in hardware)
5	R	Overflow Flag (1)
5	W	Test mode. (1)
6	R	End Sweep (1).
7	R	LAM Flag (1).
8-15		Not Used.

Reading and Writing the Control Status Register:

The meaning of the bits of the Control Status Register (CSR) are shown in Table II. R refers to read only bits, W refers to write only bits, and R/W refers to bits which can be both read and written. If an attempt is made to write to a read only bit, the word being written is masked so that the bit is not written, and no error of any sort is generated. If a condition is true, the bit is set, as is shown by a "(1)" after the bit definition in table II, and below. If a bit is cleared a "(0)" is shown.

In order to start accumulating data for a TOF spectrum, bit 3 must be set, while bit 2 must be clear. This has the effect that data

acquisition is enabled, and the MCS memories cannot be read. In program TUF, bit 0 is always set at this point to enable interrupts. An alternative to this method of detecting an end sweep is to repeatedly poll CSR bit 6 for an end of sweep. Bit 5 is used for a self test of the MCS unit. The 20 MHz clock is shunted in as the input to the scalars, and a constant signal is observed if the triggers are supplied. This is enabled in the Test command of program TUF. If connected, CSR bit 4 would provide a means to check the MCS with no data input (when 0) by gating off the data input, as well as a clear function (when 0). Normal operation and data acquisition would occur if bit 4 was set high (1). The CSR bits are set by first writing the appropriate word to the data word (DATA0), and then loading these into the MCS with the N.F18.A0 command. This is shown in the MACRO subroutine BEGIN, in program TUF.

The interrupt-driven structure chosen leaves the program a freer hand to do more lengthy work between end sweeps without fear of significantly reducing the data acquisition rate. The disadvantage of the interrupt structure is that if the interrupts occur too often for the program to get through the necessary overhead, it will stop. This can be avoided by lengthening the time between interrupts, by increasing the number of triggers per sweep, and/or by reducing the trigger rate. This is particularly important in the case of cross-correlated data (discussed in chapter I), for which the preparation of the display involves a rather lengthy calculation (which can take several seconds).

The control status register can be queried to determine whether a sweep has been completed, an overflow has occurred, or the MCS is set so that its memories can be read (bits 6 and 7, bit 6, or bit 2, respectively). This is done by issuing the N.F0.A0 command and then checking the appropriate bits of the CAMAC data word (DATA0), or storing this value for future reference. This is done in the MACRO interrupt service routine MCSINT in program TUF.

Reading and Writing the Number of Triggers:

The number of triggers is loaded in the same way as the control status register, that is through the CAMAC data word (DATA0). The number of triggers must be converted to its two's complement before being loaded. The loading is done by the N.F18.A1 command as shown in MACRO subroutine LOADTR in program TUF. The maximum number of triggers is 65535, but the program TUF allows a maximum of only 32767 so that two byte integers can conveniently be used.

Without interfering with the data acquisition the number of triggers remaining in a sweep can be read out of the MCS with the N.F0.A1 command. Issuing the command moves the number of triggers remaining into the CAMAC data word. In program TUF, this is only done in the case of a scaler overflow, as shown in the MACRO interrupt service routine MCSINT.

Write the Dwell Count:

The dwell count determines the time interval for which pulses are counted in each channel. The count is the number of 50 nsec intervals for which data collection is to occur for each channel. Thus the dwell count is simply the dwell time divided by 50 nsec. The dwell count is first loaded into the CAMAC data word, and then written to the MCS register using the N.F18.A2 command, as shown in the MACRO subroutine LOADDW in program TUF. There is no facility to read back the dwell count. The minimum dwell count is 3, and the maximum dwell count is 4095, giving minimum and maximum dwell times of 150 nsec, and 204.75 μ sec, respectively. The maximum dwell time in program TUF is arbitrarily set at 200 μ sec.

.R

Load the Memory Address and Read the Memory Contents:

In order to read the memory contents, bit 2 of the control status register must be set as discussed above. Then, each memory address must be entered by loading the address of the channel to be read (0 to 4095, or 0 to 7777₈) into the CAMAC data word (DATA0), and then issuing the N.F18.A3 command. Next, the contents of the memory are read out to the CAMAC data word by issuing the N.F0.A3 command. The CAMAC data word is then added to the appropriate array element stored in the controlling computer's memory. This is shown in MACRO subroutine READMS in program TUF. Note that there is no reason that the memory must be read out sequentially.

Test LAM:

The interrupt (LAM -- for "look at me") flag can be tested by issuing the command N.F8.A0.¹² This causes the LAM to be asserted and if enabled causes an interrupt of the computer. This feature is not used in program TUF.

3. Multichannel Scaler Hardware Specifications

The above summary of CAMAC commands for use with the MCS has included many of its specifications, but a more complete list is given in table III. The scaler speed could be increased (by interchanging faster pin-compatible memories) and the dead time decreased¹³ in a straightforward manner if this were found to be necessary, but at present counting rates in excess of 1 MHz are rare, and the current set-up is sufficient.

The schematics, circuit board layout, and a tape for the automatic wire wrap of the circuit board were generated by a CAD system developed by the Instrument Engineering group at LBL. A 2 A fuse and a 1 V drop diode (to change CAMAC +6V power to +5V) are soldered between the +6V power line from the CAMAC crate and the board's power in circuit. Otherwise, wire wraps interconnect all pins of the 80 IC sockets.

Table III. Multichannel Scaler Hardware Specifications.

Size:	Double width CAMAC module ¹⁴ with one wire-wrapped socketed circuit board.
Power:	+6V, 2 A supplied by CAMAC crate.
Dwell:	Minimum: 100 nsec per channel. ¹⁵ Maximum: 204.75 μ sec per channel. ¹⁶ Increment: 50 nsec per channel.
Triggers per sweep:	Minimum: 1. Maximum: 65535. ¹⁷ Increment: 1.
Sweeps:	Under software control, no limit.
Dead Time:	Between channels: <10 nsec. Average: 25 nsec after previous data pulse. Maximum: 50 nsec after previous data pulse. ¹³
Maximum Counts per Channel:	Per Trigger: 32767. Per Sweep: 32767.
Scaler Speed:	20 MHz (120 MHz internal scalers).
Memory Speed:	90 nsec.
Maximum Trigger Rate:	Nominally 900 kHz -- the time between trigger pulses must be at least 500 nsec + 4 dwell periods.

Table IV. Front Panel Connections and Indicators.

Inputs:	Data:	TTL (+5V), 50 nsec.
	Trigger:	TTL (+5V), 500 nsec.
	Trigger Gate:	TTL (+5V), Constant when trigger is to be suppressed.
Output:	RCO:	TTL (+5V), 50 nsec, on the trailing edge of each dwell period.

LED Indicators:

Power on:	On when module is powered.
LAM:	On when LAM is set.
Trigger Bits:	On when associated trigger word bit is 0. Off when associated trigger word bit is 1.

Inputs and Outputs

The front panel connections and LED indicators are summarized in table IV. The triggers supplied to the MCS should be TTL (+5V), and at least 500 nsec long. No data acquisition is done in the first 500 nsec as this time is used to set up the address counters, memories, and store data from a previous trigger if necessary. Data pulses should be TTL (+5V), and as close to 50 nsec long as possible. This ensures that the pulse is counted exactly once, as it will then straddle the rising edge of one 20 MHz clock pulse to which it will be synced. The

triggers can be gated with a constant TTL voltage applied to the Trigger Gate input. The RCO output provides a 50 nsec TTL pulse out at the beginning of each dwell period.

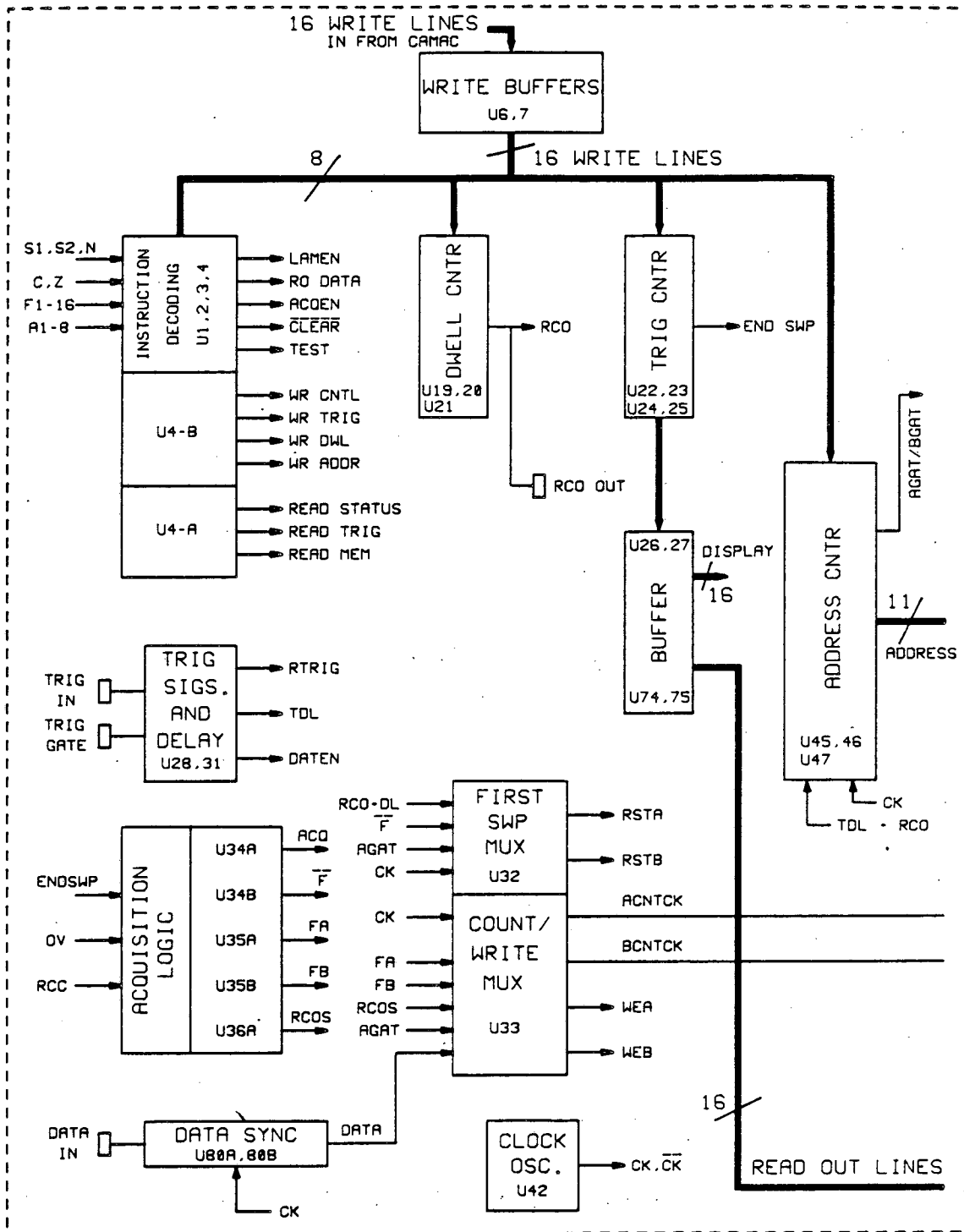
Front Panel Indicators

The "power on" LED is on at all times that the CAMAC crate is powered. The LAM light is set when a LAM is set, and is cleared on reset. As triggers are supplied to the MCS, the front panel LEDs show the scaler counting down triggers to their preset value. After the preset trigger countdown, all LEDs are lit. When there is some number remaining to be counted, the lights summing up to the number remaining are off.

4. Multichannel Scaler Circuit Logic and Signal Descriptions

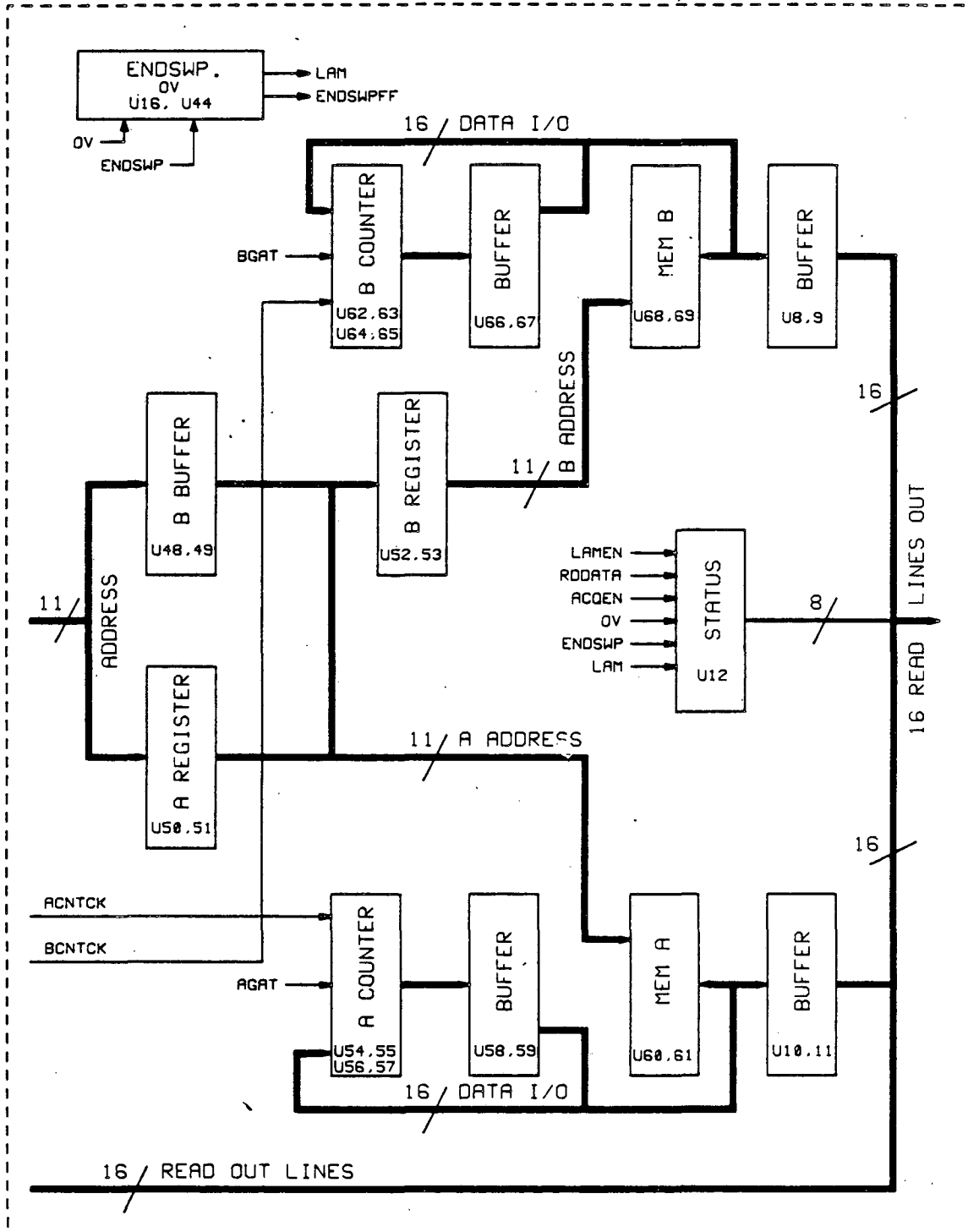
What follows is a description of the signals and IC chips on the circuit diagrams.¹⁸ It is not necessary to understand this in order to use the MCS, but it would be helpful in modifying or repairing the MCS. Figures 2a and 2b schematically show the functions of the various IC groups as well as the common read and write lines they share. The "U" numbers below and in figure 2 refer to the chips used in the MCS. The acronymic names refer to signals that can be found on the circuit diagram. Table V lists the various signal names and their functions and/or derivations.

Fig. 2. (a) and (b) Schematic of the new LBL multichannel scaler.
The "U" numbers refer to the IC numbers on the circuit
diagram and layout drawings.¹⁸



XBL 863-787

Fig. 2(a)



XBL 863-786

Fig. 2(b)

Table V. The signals used in the circuit diagram of the MCS¹⁸ and their definitions and/or derivations.

ACNTCK [BCNTCK]	Clocked data counts to Channel A [B] counters.
ACQEN	Enables the start of data acquisition.
ADDR	Address word (12 bit) for memory read out.
AGAT [BGAT]	Square wave signals to control switching between A and B count channels -- period is twice the dwell time ($\overline{AGAT} = BGAT$).
\overline{CLEAR}	When set data is allowed, when clear data is inhibited.
DATEN	Delayed trigger signal -- when set enables data counters.
DL	Delayed trigger signal which provides predata resets and configures an address latch.
DWELL	Dwell count word.
ENDSWP	End of sweep -- set when trigger counters have completed count up from preset level to overflow.
F	Set after the first scan is completed, allows counters to be preloaded with memory data before counting the current data.
FA, FB	Levels set after trigger delay to provide phase of channel A [B] counter resets and write sequences.
LAM	Interrupt signal to CAMAC bus -- identical to CSR bit 7.
LAMEN	LAM enable set by CAMAC -- identical to CSR bit 0.
OV	Overflow flag, set on counter overflow -- identical to CSR bit 5.
PCP, PTRIG, PTW	Signals at end of scan to ensure that only data from a complete dwell period are transferred to memory.
PEA [PEB]	Load Counter A [B] signal.
RCO	Dwell Counter Overflow, the falling edge of which ends one dwell period and starts another -- identical to front panel RCO out.

Table V, cont.

RD DATA	Set by CAMAC to allow data readout -- identical to CSR bit 2.
RSTA [RSTB]	Reset for channel A [B] during the first scan of each sweep.
RTRIG, TDL	Delayed trigger signals to configure counters and address for the following data scan.
TRIG	External pulse required to start a scan.
TRIGGER	Trigger word loaded through CAMAC, preset in trigger counters.
WEA [WEB]	Write enable to transfer Counter A [B] data to memory.

The clear function of the MCS is currently not implemented. A de facto clear is made when the previous data is not read from the memories into the counters on the first trigger of each sweep. Acquisition is started with the signals ACQ, F, FA, and FB. The flipflops U34, U35, and U36 control the conditions after the first trigger and for subsequent scans.

The dwell timing is managed by counters U19, U20, and U21. They generate the clock-synchronized RCO signal pulses which drive the address advance in the scalers and indirectly drive the load, latch, read, and output functions of the counters and memories.

The data acquisition is accomplished with minimal dead time by having two identical sets of counters and memories. The two sets are toggled back and forth, so that while data is accumulated on one channel, the other channel is storing its previously acquired data and

preparing for its next acquisition. The two channels are referred to as A and B. Note that all odd channels are in A and all even channels are in B. The addressing is simplified as the final bit of the address determines whether that address is in channel A or B. A special timing sequence has been worked out to allow the loading, latching, etc. of the data to the correct channel at all times.¹⁹ The address counters are U45, U46, and U57. The addressing is accomplished with an asymmetric set of channel latches, buffers, and registers. Each of these is associated primarily with one channel, but services both channels. These are: the A channel address latches U50 and U51, the B channel address buffers U48 and U49, and the B channel address registers U52 and U53. Signals AGAT and BGAT drive the switching between channels A and B.

Multiplexers U32 and U33 generate: RSTA and RSTB to carry out the required resets on the first trigger of each sweep, PEA and PEB to load the counters, ACNTCK and BCNTCK to provide clock pulses to count the incoming data, and WEA and WEB to enable memory writing. The multiplexers are gated by AGAT. These signals control: the channel A counters U54, U55, U56, and U57, the channel A latches U58 and U59, the channel A memories U60 and U61, the channel B counters U62, U63, U64, and U65, the channel B latches U66 and U67, and the channel B memories U68 and U69. The input data pulses are shifted and latched by U80, U39, and U73. This switching avoids either missing a data pulse or counting one pulse twice, since only one data pulse can occur per clock pulse. The memories are currently 6116 type with a read or write cycle

of 90 nsec. If the memories were exchanged for faster ones, the minimum dwell time could be lowered to 100 nsec per channel.¹⁵

Trigger counters U22, U23, U24, and U25 accept four bits each of the trigger word, count up to the maximum possible (64k), and drive the front panel LEDs. Their overflow signals the end of sweep. The ENDSWP and LAM signals are set by flipflops U16 and U44.

If a trigger pulse comes before the end of a scan through the channels, a new scan is begun after 500 nsec. U28 and U31 generate signals RTRIG, DL, TDL, and DATEN which permit address and data resets, and synchronize the start of the next scan, as well as PTRIG, PCP and PTW which ensure that only data from the final complete dwell period is written into memory.

Communication with the CAMAC crate is accomplished through the CAMAC read lines R1, R2, R4, R8, and R16, write lines W1, W2, W4, W8, and W16, function codes F1, F2, F4, F8, and F16, and address lines A1, and A2, which are decoded and carried into the MCS. The input buffers for writing are U6 and U7, for instructions are U1 and U2, and for the status word bits LAMEN, ACQEN, DATEN, and TEST is U5. The readouts buffers are: U74 and U75 for the trigger word, U8, U9, U10, and U11 for data, and U12 for the status word. The status word (control status register in software terms) signals LAMEN, RD DATA, ACQEN, OV (overflow), ENDSWP, and LAM are latched at U12. The selected function commands (e.g. write trigger word -- F18.A1) control the destination of the data words DWELL, TRIGGER, and ADDR through common write lines with U4. The selected function commands also control the readout of the

data words (stored) CSR, DATA, and TRIGGER. Data readout of all 4096 channels takes approximately 10-20 msec.

5. Introduction to Program TUF

The program TUF drives the CAMAC multichannel scaler described above. A listing follows in section 6. It has been designed to run on DEC LSI 11, 11/2, 11/23, and 11/73 computers⁵ equipped with the MCS in a CAMAC crate driven by a Kinetic Systems 3912-Z1G crate controller.¹⁰ A direct memory access display driver (Data Translation DT2771²⁰) is required on the Q-Bus of the LSI-11. This drives an oscilloscope or equivalent, and is referred to only as "display" below. The oscilloscope is not necessary for program execution, but is extremely useful at all times. If plotting is to be done, a Hewlett Packard 7470A or 7475A plotter²¹ is required. The operating system used is RT-11 and the version of TUF shown is in use with RT-11 version 5.0.

The command structure is very similar to that of program SANG described in Appendix A. Execution begins with the main routine TUF, but after initialization and setting defaults in subroutine TINIT, control is passed to subroutine TCOMM where it remains except for subsequent subroutine calls until program completion.

All commands from the keyboard are processed by TCOMM using DEC function subroutine ITTINR as in program SANG. Commands are one or two letters followed by a carriage return. The one exception to this is the use of arrows on VT52 and VT100 compatible terminals. The arrows

are used to adjust the display window, and no carriage return is required. It is possible to avoid the use of the arrows by using the normal structured commands.

The program is heavily commented throughout. At the beginning of each routine the file in which it is found, a version date, and a brief resume of its function are given. The meanings of all of the COMMON variables are listed in the first two pages of the main routine TUF. The commands are listed and explained throughout subroutine TCOMM, and on the help screens provided by TCMLST and all nine of the TCOML* subroutines. The use of the arrows for changing the display is explained in subroutines TCOMM and TCDISP, and on the help screen provided by subroutine TCOMLD.

All input to the program is from the console terminal. All output is in ASCII form and when written to a disk file can be easily manipulated with the normal DEC editors. In data files, a header section is terminated with a control-C, and followed by rows of 8 data points listed as real numbers. A program entitled PAN is currently used to process the data.

All hardware functions are carried out by MACRO subroutines located in the file XBL.MAC. These are all modular and are often called from more than one FORTRAN subroutine. This file also contains the hardware initialization routine INIT and the interrupt service routines MCSINT and DSPINT for the MCS and the display driver, respectively. All MACRO subroutines are declared Global to allow access from

the FORTRAN subroutines. Note that all calling subroutines must also be declared Global.

The program TUF is far too large for the LSI-11 to load all at once (as with program SANG) so that it is overlaid with a total of 32 segments using the LINKer command file LTUF.COM. Also, a number of concessions have been made to decrease the size of the program, such as separating all of the help screens into separate files TCMLST.FOR, and TCOML*.FOR, and overlaying them into different segments. The listing shown is within a few words of the limit of the system, and great care should be taken if any section of it is expanded. As with program SANG, all of the FORTRAN routines are compiled with the /NOLINENUMBERS option as shown in the compilation command file CNLTUF.COM, and the LINKed with the %SHORT error messages as shown in the LINKer command file LTUF.COM so as to save space. If a section absolutely must be enlarged and will affect the total program size, the command structure of TCOMM could be split up into overlaid subroutines to save some room. Alternatively, all processors running TUF could be converted to LSI-11/23 or LSI-11/73 CPUs with at least 128k bytes memory, and some of the data arrays could be declared VIRTUAL.

6. Listing of Program TUF

On the following pages program TUF is listed. The order of the files is exactly that done by the backup/update/printout command file COPTUF.COM, which is included as well.

PROGRAM TUF

File TUF.FOR begins on the previous line.

Version Date: November 10, 1985
Paul S. Weiss

This main routine just establishes all the COMMON areas, calls two initialization routines, starts the display, and transfers control over to subroutine TCOMM.

```

INTEGER*4 JTRIG
COMMON /DATA/ ACCUM(4096),XCORR(256),WORK(256),NEW(4096),NSWEEP
COMMON /DISP/ IDSP(512),INEW,ICORR,IBACK,NCORR,IADV,IRES,IQIK
COMMON /MCSMAX/ DWLMAX,DWLMIN,MAXSWP,MAXTRG
COMMON /SETS/ DWELL,ICHAN,ISWEEP,ITRIG,EDELAY,NCHAN,IOFSET,IEXT
COMMON /SWFLAG/ ISWFLG,JTRIG
COMMON /TERM/ ITERM
COMMON /TITANG/ TITLE(10),ANGLE

```

DEFINITIONS OF /COMMON/ VARIABLES AND ARRAYS

COMMON Block /DATA/ Contains the data and work arrays.

ACCUM(I) The accumulated data for channels I=1-4096.
 XCORR(I) The cross-correlated data for I=1-256.
 WORK(I) The work array for display I=1-256.
 NEW(I) The new data array for channels I=1-4096.
 NSWEEP Not used.

COMMON Block /DISP/ Contains the Display array and parameters.

IDSP(I) The array for display by the Direct Memory Access Display Driver (Data Translation DT2771 or equivalent).
 INEW The display new data flag. INEW=0 => Display accumulated data. INEW=1 => Display only data from most recent sweep.
 ICORR The cross-correlation display flag. ICORR=0 => Display uncorrelated data. ICORR=1 => Display cross-correlated data.
 IBACK The display background subtraction flag. IBACK=0 => Subtract background from displayed data. IBACK=1 => Display data with background included.
 NCORR The number of channels per cross-correlation channel.
 IADV The number of channels after ICHAN to begin displaying data.
 IRES The display resolution in channels.

C IQIK The quick display flag. If IQIK=0, the data is displayed
 C before restarting the MCS (this prevents the program from
 C getting hung up if the number of triggers is small). If
 C IQIK=1, the data is accumulated and displayed while the
 C MCS is counting down (for maximum efficiency, and minimal
 C overhead delay).
 C
 C COMMON Block /MCSMAX/ Contains the minima and maxima for various
 C MCS settings.
 C
 C DWLMAX The maximum dwell time.
 C DWLMIN The minimum dwell time.
 C MAXSWP The maximum number of sweeps.
 C MAXTRG The maximum number of triggers per sweep.
 C
 C COMMON Block /SETS/ Contains the MCS settings.
 C
 C DWELL The dwell time in usec.
 C ICHAN The initial channel (for display and output only, all channels
 C are recorded and kept in memory).
 C ISWEEP The number of sweeps requested (a sweep is of ITRIG triggers).
 C ITRIG The number of triggers per sweep.
 C EDELAY The external delay in usec.
 C NCHAN The number of channels (for output only, see ICHAN above).
 C IOFSET The cross-correlation offset, in channels.
 C IEXT The external dwell flag. Not currently used.
 C
 C COMMON Block /SWFLAG/ Contains the sweep counter, and the number of
 C triggers measured.
 C
 C ISWFLG The sweep counter. ISWFLG<0 for no new data to be
 C examined => remain in Command Mode. ISWFLG>0 =>
 C The number of sweeps remaining. ISWFLG=0 for the
 C acquisition has been completed.
 C JTRIG The triggers measured counter in INTEGER*4. If
 C JTRIG<0, an overflow has occurred.
 C
 C COMMON Block /TTERM/ Contains the terminal type specification.
 C
 C ITERM The terminal type: ITERM=0 for unknown, ITERM=52 for
 C VT52 compatible, and ITERM=100 for VT100 compatible
 C
 C COMMON Block /TITANG/ Contains the title and detector angle for output
 C purposes only.
 C

```

C      TITLE(I)  The title, for output up to 40 ASCII characters.
C      ANGLE     The detector angle.
C
C
C
C
C*****
C
C
C
C
C      .INIT SETS UP INTERRUPT VECTORS
C
C      MCS = INIT(ISWFLG,JTRIG)
C
C      TINIT SETS UP THE INITIAL VALUES OF ALL:
C              MCS PARAMETERS (STORED IN /SETS/)
C              TERMINAL TYPE (STORED IN /TERM/)
C              DISPLAY PARAMETERS (STORED IN /DISP/)
C              ALLOWED RANGE OF MCS PARAMETERS (STORED IN /MCSMAX/)
C
C      CALL TINIT
C
C      TINIT HAS JUST ASKED IF DEFAULT VALUES ARE SATISFACTORY
C      GET ANSWER
C
C      ACCEPT 1000,ANS
1000  FORMAT(A1)
      IF(ANS.EQ.'Y') GO TO 1100
      CALL TCHAN(0)
      CALL TDEF(0)
1100  CALL TTERM(0)
      CALL TDISP
C      TRANSFER CONTROL TO ROUTINE COMMAN FOR ACTUAL USE OF TOF
      CALL TCOMM
      END

C      SUBROUTINE TCOMM
C
C              Second routine of file TUF.FOR.
C
C      Version Date:  November 8, 1985
C      Paul S. Weiss
C
C      Subroutine TCOMM maintains control of operations for the program.
C
C      It accepts 1 or 2 character commands from the user, then calls the
C      appropriate subroutines.
C
C      The arrows of VT52 and VT100 compatible terminals are also used.

```

C These change the window data displayed at any time.

C

```

INTEGER COM1,COM2,COMT
INTEGER*4 JTRIG
COMMON /DATA/ ACCUM(4096),XCORR(256),WORK(256),NEW(4096),NSWEEP
COMMON /DISP/ IDSP(512),INEW,ICORR,IBACK,NCORR,IADV,IRES,IQIK
COMMON /MCSMAX/ DWLMAX,DWLMIN,MAXSWP,MAXTRG
COMMON /SETS/ DWELL,ICHAN,ISWEEP,ITRIG,EDELAY,NCHAN,IOFSET,IEXT
COMMON /SWFLAG/ ISWFLG,JTRIG
COMMON /TERM/ ITERM
COMMON /TITANG/ TITLE(10),ANGLE

```

C

C

C

THE FOLLOWING IS A TABLE OF THE ASCII CHARACTERS USED AS COMMANDS

```

DATA IA,IB,IC,ID,IE /65,66,67,68,69/
DATA IF,IG,IH,II,IL,IM,IN /70,71,72,73,76,77,78/
DATA IO,IP,IQ,IR,IS,IT /79,80,81,82,83,84/
DATA IU,IW,IZ /85,87,90/

```

TYPE 2100

ISWFLG = -1

TYPE 95

FORMAT(' Command?',/)

1

95

C

C

C

RECORD COMMAND ENTRY USING SPECIAL SCREEN MODE

CALL ENSPEC

200

IF(ISWFLG.GE.0) CALL TDONE

COM1 = ITTINR(1)

IF(COM1.LT.0) GO TO 200

C

IF AN ARROW WAS TYPED, DETERMINE WHICH

IF(COM1.EQ.27) GO TO 700

C

IGNORE CARRIAGE RETURNS AND LINE FEEDS

IF((COM1.EQ.13).OR.(COM1.EQ.10)) GO TO 200

COM2 = 32

C

C

C

ECHO CHARACTERS

250

TYPE 255,COM1,COM2

255

FORMAT('+',2A1,25X)

300

IF(ISWFLG.LT.0) GO TO 320

CALL TDONE

GO TO 250

320

COMT = ITTINR(1)

IF(COMT.LT.0) GO TO 300

IF(COMT.EQ.13) GO TO 500

380

COM2 = COMT

390

TYPE 255,COM1,COM2

400

IF(ISWFLG.LT.0) GO TO 420

CALL TDONE

GO TO 390

```

C
C   LOOK FOR CARRIAGE RETURN, OR ANOTHER CHARACTER
C
420  COMT = ITTINR(1)
      IF(COMT.LT.0) GO TO 400
      IF(COMT.EQ.13) GO TO 500
C
C   IF MORE THAN TWO CHARACTERS ARE TYPED IN, SHIFT COM2 TO COM1
C
      COM1 = COM2
      GO TO 380
C
C   READ SECOND HALF OF CARRIAGE RETURN (LINE FEED)
C
500  COMT = ITTINR(1)
      IF(COMT.LT.0) GO TO 500
      TYPE 510,COM1,COM2
510  FORMAT('+',2A1,25X,/)
      CALL EXSPEC
C
C   EXIT SPECIAL SCREEN MODE BEFORE CHECKING COMMAND LIST
C
      GO TO 1100
C
C   IF AN ARROW WAS TYPED IN, THIS SECTION DETERMINES WHICH
C   ARROW IT WAS AND THEN CALLS SUBROUTINE DISPR TO CHANGE
C   THE FORMAT OF THE DISPLAY
C
C
C   TO USE WITH A VT52 COMPATIBLE TERMINAL, THE SECOND CHARACTER
C   OF THE ARROW DETERMINES THE DIRECTION OF THE ARROW TYPED
C
      IF(ITERM.LT.100) GO TO 710
700  COMT = ITTINR(1)
      IF(COMT.LT.0) GO TO 700
C
C           THE ARROWS ARE DEFINED AS FOLLOWS:
C
C   DIRECTION  VT100  VT52          EFFECT
C
C   UP         $[A    $A           RAISE DISPLAY STEP SIZE
C   DOWN       $[B    $B           LOWER DISPLAY STEP SIZE
C   RIGHT      $[C    $C           INCREASE INITIAL DISPLAY CHANNEL BY STEP SIZE
C   LEFT       $[D    $D           DECREASE INITIAL DISPLAY CHANNEL BY STEP SIZE
C
710  COMT = ITTINR(1)
      IF(COMT.LT.0) GO TO 710
      IF(COMT.EQ.IA) CALL TCDISP(1)
      IF(COMT.EQ.IB) CALL TCDISP(2)
      IF(COMT.EQ.IC) CALL TCDISP(3)

```

```

IF(COMT.EQ.ID) CALL TCDISP(4)
GO TO 200

```

```

MATCH UP COMMANDS AND EXECUTE DESIRED FUNCTION
THE BASIC COMMANDS ARE:

```

```

A*   Analyze Commands
C*   Change Commands
D*   Display Commands
E    Exit
G*   Graph Commands
H    Help
L*   Load Commands
P*   Print Commands
R*   Read and Reset Commands
S*   Show and Start Commands
T    Test MCS
W*   Write Commands
Z    Zero Arrays

```

```

A*

```

```

The analyze commands are:

```

```

AC   Analyze Chopper for Gate Width
AD   Analyze Dip in TOF
AH   Analyze Help
AP   Analyze Peak in TOF

```

```

1100 IF(COM1.NE.IA) GO TO 1201
      IF(COM2.NE.IC) GO TO 1121
      CALL TANAL(1)
      GO TO 1
1121 IF(COM2.NE.ID) GO TO 1131
      CALL TANAL(2)
      GO TO 1
1131 IF(COM2.NE.IP) GO TO 1141
      CALL TANAL(3)
      GO TO 1
1141 IF(COM2.NE.IH) TYPE 9100
      CALL TCOMLA
      GO TO 1

```

```

C*

```

```

The change commands are:

```

```

CA   Change All Settings
CC   Change Correlation Method
CD   Change Dwell Time
CE   Change External Delay
CH   C Help

```

C	CI	Change Initial Channel
C	CN	Change Number of Channels
C	CO	Change Offset for Cross-Correlation
C	CP	Change Detector Position
C	CS	Change Sweep Counts
C	CT	Change Trigger Counts
C	CU	Change User Terminal
C	CW	Change Display Window
C		
1201	IF(COM1.NE.IC)	GO TO 1301
	IF(COM2.NE.IA)	GO TO 1211
	CALL TCHAN(0)	
	CALL TDEF(0)	
	GO TO 1	
1211	IF(COM2.NE.IC)	GO TO 1216
	CALL TCHCOR(0)	
	GO TO 1	
1216	IF(COM2.NE.ID)	GO TO 1221
	CALL TCHAN(1)	
	GO TO 1	
1221	IF(COM2.NE.IE)	GO TO 1236
	CALL TCHAN(5)	
	GO TO 1	
1236	IF(COM2.NE.II)	GO TO 1251
	CALL TCHAN(4)	
	GO TO 1	
1251	IF(COM2.NE.IN)	GO TO 1255
	CALL TCHAN(6)	
	GO TO 1	
1255	IF(COM2.NE.IO)	GO TO 1256
	CALL TCHCOR(1)	
	CALL TDSMOD	
	GO TO 1	
1256	IF(COM2.NE.IP)	GO TO 1266
	CALL TDEF(2)	
	GO TO 1	
1266	IF(COM2.NE.IS)	GO TO 1271
	CALL TCHAN(3)	
	GO TO 1	
1271	IF(COM2.NE.IT)	GO TO 1276
	CALL TCHAN(2)	
	GO TO 1	
1276	IF(COM2.NE.IU)	GO TO 1281
	CALL TTERM(1)	
	GO TO 1	
1281	IF(COM2.NE.IW)	GO TO 1299
	GO TO 1381	
1299	IF(COM2.NE.IH)	TYPE 9100
	CALL TCOMLC	
	GO TO 1	

```

C
C
C      D*
C      The define and display commands are:
C          DA      Display Accumulated Data
C          DB      Display Background
C          DC      Display Correlated Data
C          DH      D Help
C          DL      Display Low Trigger Count
C          DN      Display No Background
C          DQ      Display Quickly
C          DR      Display Refresh
C          DS      Display Single Sweeps
C          DT      Define Title
C          DU      Display Uncorrelated Data
C          DW      Display: Change Window
C
1301  IF(COM1.NE.ID) GO TO 1401
      IF(COM2.NE.IA) GO TO 1321
      INEW = 0
      GO TO 1389
1321  IF(COM2.NE.IB) GO TO 1331
      IBACK = 1
      GO TO 1389
1331  IF(COM2.NE.IC) GO TO 1336
      IF(ICORR.EQ.1) GO TO 1
      ICORR = 1
      GO TO 1388
1336  IF(COM2.NE.IL) GO TO 1341
      IQIK = 0
      GO TO 1389
1341  IF(COM2.NE.IN) GO TO 1346
      IBACK = 0
      GO TO 1389
1346  IF(COM2.NE.IQ) GO TO 1351
      IQIK = 1
      GO TO 1389
1351  IF(COM2.NE.IR) GO TO 1361
      CALL TDISP
      GO TO 1
1361  IF(COM2.NE.IS) GO TO 1366
      INEW = 1
      GO TO 1389
1366  IF(COM2.NE.IT) GO TO 1371
      CALL TDEF(1)
      GO TO 1
1371  IF(COM2.NE.IU) GO TO 1381
      IF(ICORR.EQ.0) GO TO 1
      ICORR = 0
      GO TO 1388
1381  IF(COM2.NE.IW) GO TO 1399

```



```

CALL TCDISP(5)
1388 CALL TDISP
1389 CALL TDSMOD
GO TO 1
1399 IF(COM2.NE.IH) TYPE 9100
CALL TCOMLD
GO TO 1

C
C E
C Exit
C
1401 IF(COM1.NE.IE) GO TO 1501
CALL TLEAVE
GO TO 1

C
C G*
C The graph commands are:
C GH G Help
C GL Graph Line Plot
C GP Graph Point Plot
C
1501 IF(COM1.NE.IG) GO TO 1555
IF(COM2.NE.IL) GO TO 1521
CALL TPLLOT(1)
GO TO 1
1521 IF(COM2.NE.IP) GO TO 1531
CALL TPLLOT(0)
GO TO 1
1531 IF(COM2.NE.IH) TYPE 9100
CALL TCOMLG
GO TO 1

C
C H
C Help -- Print out command list.
C
1555 IF(COM1.NE.IH) GO TO 1601
CALL TCMLST
GO TO 1

C
C L*
C The load commands are:
C LA Load All
C LD Load Dwell Time
C LH L Help
C LI Load Initial Channel
C LN Load Number of Channels
C LS Load Sweep Counts
C LT Load Trigger Counts
C
1601 IF(COM1.NE.IL) GO TO 1701

```

```

IF(COM2.NE.IA) GO TO 1621
CALL TLOAD(0)
GO TO 1
1621 IF(COM2.NE.ID) GO TO 1641
CALL TLOAD(1)
GO TO 1
1641 IF(COM2.NE.IN) GO TO 1651
CALL TLOAD(2)
GO TO 1
1651 IF(COM2.NE.II) GO TO 1661
CALL TLOAD(3)
GO TO 1
1661 IF(COM2.NE.IS) GO TO 1671
CALL TLOAD(4)
GO TO 1
1671 IF(COM2.NE.IT) GO TO 1681
CALL TLOAD(5)
GO TO 1
1681 IF(COM2.NE.IH) TYPE 9100
CALL TCOMLL
GO TO 1

```

C
C
C
C
C
C
C
C
C
C
C
C

P*

The available Print commands are:

PC	Print Configuration
PH	P Help
PI	Print Information on the Line Printer
PL	Print Data on the Line Printer
PP	Print Data on the Terminal with Pauses
PR	Print Current Scaler Contents on the Line Printer
PT	Print Data on the Terminal

```

1701 IF(COM1.NE.IP) GO TO 2801
IF(COM2.NE.IC) GO TO 1711
CALL TSHOCO(6)
GO TO 1
1711 IF(COM2.NE.II) GO TO 1721
CALL TPRII(6)
GO TO 1
1721 IF(COM2.NE.IL) GO TO 1731
CALL TPRDT(6)
GO TO 1
1731 IF(COM2.NE.IP) GO TO 1736
CALL TPRDT(-7)
GO TO 1
1736 IF(COM2.NE.IR) GO TO 1741
CALL READMS(NEW)
PRINT 1737, (NEW(II), II=ICHAN, (ICHAN+NCHAN-1))
1737 FORMAT(16(/,8(2X,I6,:)))
CALL RSTART

```

```

GO TO 1
1741 IF(COM2.NE.IT) GO TO 1751
      CALL TPRDT(7)
      GO TO 1
1751 IF(COM2.NE.IH) TYPE 9100
      CALL TCOMLP
      GO TO 1

C
C   R*
C   RA      Read Ascii Data File
C   RH      Read and Reset Help
C   RM      Reset MCS (Halt Acquisition)
C   RS      Reset System Hardware
C

2801 IF(COM1.NE.IR) GO TO 3001
      IF(COM2.NE.IA) GO TO 2846
      CALL TREDAS
      GO TO 1
2846 IF(COM2.NE.IM) GO TO 2866
      CALL STOPR
      GO TO 1
2866 IF(COM2.NE.IS) GO TO 2899
      CALL RINIT
      GO TO 1
2899 IF(COM2.NE.IH) TYPE 9100
      CALL TCOMLR
      GO TO 1

C
C   S*
C   The available show and start commands are:
C       SC      Show Configuration
C       SD      Show Display Mode
C       SE      Scan Extend
C       SH      S Help
C       ST      Start
C

3001 IF(COM1.NE.IS) GO TO 3501
      IF(COM2.NE.IC) GO TO 3011
      CALL TSHOC(7)
      GO TO 1
3011 IF(COM2.NE.ID) GO TO 3021
      CALL TDSMOD
      GO TO 1
3021 IF(COM2.NE.IE) GO TO 3031
      CALL TSTART(1)
      GO TO 1
3031 IF(COM2.NE.IT) GO TO 3041
      CALL TSTART(0)
      GO TO 1
3041 IF(COM2.NE.IH) TYPE 9100

```

```

CALL TCOMLS
GO TO 1

C
C   T
C   Test MCS
C
3501 IF(COM1.NE.IT) GO TO 4001
      CALL TSTMCS
      GO TO 1

C
C   W
C   Write Commands
C       WF      Write Data File with Full Header
C       WH      Write Help
C       WI      Write Data File with Informational Header
C       WN      Write Data File with no Header
C
4001 IF(COM1.NE.IW) GO TO 4101
      IF(COM2.NE.IF) GO TO 4036
      CALL TWRA(0)
      GO TO 1
4036 IF(COM2.NE.II) GO TO 4051
      CALL TWRA(1)
      GO TO 1
4051 IF(COM2.NE.IN) GO TO 4099
      CALL TWRA(-1)
      GO TO 1
4099 IF(COM2.NE.IH) TYPE 9100
      CALL TCOMLW
      GO TO 1

C
C   Z Command
C   Zero Data Arrays
C
4101 IF(COM1.NE.IZ) GO TO 4500
      TYPE *, 'Zero Arrays? Are you sure?'
      ACCEPT 1000,ANS
1000 FORMAT(A1)
      IF(ANS.EQ.'Y') CALL TZERO
      GO TO 1

C
C   TYPE OUT THE FOLLOWING IF AN UNRECOGNIZED COMMAND WAS ISSUED
C
4500 TYPE 9100
      TYPE 2100
2100 FORMAT(' For a list of commands, type H')
      GO TO 1
9100 FORMAT(/, ' This is not a command.')
      RETURN
      END

```

SUBROUTINE TANAL(IOPT)

File TANAL.FOR begins on the previous line.

Version Date: November 8, 1985
Paul S. Weiss

Subroutine TANAL does the analysis of the TOF scan to give peak or dip positions in a region of the TOF spectrum of choice. It also determines the proper gate width for a Timer-Gater module based upon the beam modulation done by a tuning fork chopper (option 1).

WARNING: TANAL is the limiting segment of overlay region 2.
Enlarging it will increase the total size of TUF.

Argument IOPT determines the manner in which the data is interpreted, as follows:

IOPT = 1	The data is assumed to be the TOF of beam chopped by a tuning fork, and the appropriate Gate Width is determined.
IOPT = 2	The data is assumed to be from hole burning, and the depth and width of the hole are determined.
IOPT = 3	The data is assumed to be a normal TOF, and the height and width of the peak are determined.

```

COMMON /DATA/ ACCUM(4096),XCORR(256),WORK(256),NEW(4096),NSWEEP
COMMON /MCSMAX/ DWLMAX,DWLMIN,MAXSWP,MAXTRG
COMMON /SETS/ DWELL,ICHAN,ISWEEP,ITRIG,EDELAY,NCHAN,IOFSET,IEXT
TYPE 2000,'alyze.','','
2000 FORMAT(/,' Enter beginning and ending channels of segment to a'
1,A7,A21)
ACCEPT *,IB,IE
IF(IOPT.NE.1) GO TO 3000
IBB = IB
IBE = IE
GO TO 3200
3000 TYPE 2000,'verage ','for background level.'
ACCEPT *,IBB,IBE
3200 BACK = 0.
LEN = IBE - IBB

C
C IF SEGMENT ENDS WERE ENTERED IN THE WRONG ORDER
IF(LEN.GE.0) GO TO 4000
I = IBE
IBB = IBB
IBB = I
LEN = - LEN

```

```

4000 DO 4100 I=IBB,IBE
      BACK = BACK + ACCUM(I)
4100 CONTINUE
      BACK = BACK / (LEN + 1)
      LEN = IE - IB
      IF(LEN.GE.0) GO TO 5000
      I = IE
      IE = IB
      IB = I
      LEN = - LEN

C
C IOP DETERMINES WHETHER TO LOOK FOR A PEAK OR A DIP
C
5000 IOP = 1
      IF(IOPT.EQ.2) IOP = -1

C
C INITIALIZE VALUE AND POSITION OF MAXIMUM (/MINIMUM)
C
5050 TOP = ACCUM(IB)
      ITOP = IB
      DO 5100 I=IB,IE

C
C CHECK FOR NEW MAXIMUM (/MINIMUM) VALUE
      IF(((ACCUM(I)-TOP)*IOP).LT.0.) GO TO 5100
      TOP = ACCUM(I)
      ITOP = I
5100 CONTINUE
      UPDN = 'maxi'
      IF(IOP.EQ.-1) UPDN = 'mini'
      TYPE 5200,UPDN,ITOP
5200 FORMAT(/,' The ',A4,'mum of this segment occurs in channel ',I4)
      HALFH = (TOP + BACK) / 2
      DO 6100 I=ITOP,IE
      IF(((ACCUM(I) - HALFH) * IOP).LT.0.) GO TO 6300
6100 CONTINUE
      IGS = 0
      TYPE 6200,UPDN,'slow'
6200 FORMAT(' No half ',A4,'mum point found on the ',A4,' side.')
      GO TO 7000
6300 IGS = I - ITOP
      TYPE 6400,UPDN,'slow',IGS,(IGS*DWELL)
6400 FORMAT(' Half ',A4,'mum point on the ',A4,' side is '
1,I4,' channels = ',F7.0,' usec.')
7000 LEN = ITOP - IB + 1
      DO 7100 I=1,LEN
      IF(((ACCUM(ITOP-I+1) - HALFH) * IOP).LT.0.) GO TO 7500
7100 CONTINUE
      IGF = 0
      TYPE 6200,UPDN,'fast'
      GO TO 8000

```

```

7500  IGF = I - 1
      TYPE 6400,UPDN,'fast',IGF,(DWELL * IGF)
C
C  IF ANALYZING A TUNING FORK CHOPPER PRODUCED TOF, EITHER GO BACK
C  AND FIND DIP NOW, OR IF THAT HAS BEEN DONE, FIND PROPER GATE WIDTH
C
8000  IF(IOPT.NE.1) GO TO 9000
      IF(IOP.NE.1) GO TO 8100
      GWON = (IGF + IGS) * DWELL
      IOP = -1
      GO TO 5050
8100  GWOFF = (IGF + IGS) * DWELL
      TYPE 8110,'on ',GWON,'off',GWOFF,AMIN1(GWON,GWOFF)
8110  FORMAT(/,2(/,' The beam is ',A3,' for ',F7.0,' usec.')
```

1,/, ' Set the gate width at ',F7.0,' usec.',/)

```

9000  RETURN
      END
      SUBROUTINE TCDISP(ICDISP)
C
C                                     File TCDISP.FOR begins on the previous line.
C
C  Version Date:  July 23, 1984
C  Paul S. Weiss
C
C  Subroutine TCDISP changes the display window either from the arrow
C  function keys or through the DW command.
C
C  ARROWS ARE DEFINED AS FOLLOWS:
C
C      UP          $[A    RAISE DISPLAY STEP SIZE
C      DOWN       $[B    LOWER DISPLAY STEP SIZE
C      RIGHT     $[C    INCREASE INITIAL DISPLAY CHANNEL BY STEP SIZE
C      LEFT      $[D    DECREASE INITIAL DISPLAY CHANNEL BY STEP SIZE
C
C
COMMON /DISP/ IDSP(512), INEW, ICORR, IBACK, Ncorr, IADV, IRES, IQIK
COMMON /SETS/ DWELL, ICHAN, ISWEEP, ITRIG, EDELAY, NCHAN, IOFSET, IEXT
GO TO (2100,2200,2300,2400,2500),ICDISP
2100  IF(IRES.LT.16) IRES = IRES + 1
      GO TO 8000
2200  IF(IRES.GT.1) IRES = IRES - 1
      GO TO 8000
2300  IF(IADV.LT.(4096 - IRES)) IADV = IADV + IRES
      GO TO 8000
2400  IF(IADV.GE.IRES) IADV = IADV - IRES
      GO TO 8000
2500  TYPE *, 'Enter initial channel to be displayed'
      ACCEPT *, J
      IADV = J - ICHAN
      IF(IADV.LT.0) IADV = 0
      IF(J.LE.4096) GO TO 2900
      TYPE *, 'Out of Range.'
```

```

      GO TO 2500
2900  TYPE *, 'Enter display step size in channels (1-16)'
      ACCEPT *, IRES
      IF((IRES.GT.16).OR.(IRES.LE.0)) GO TO 2900
8000  RETURN
      END

```

```

SUBROUTINE TCHAN(IDEVIC)

```

```

      File TCHAN.FOR begins on the previous line.

```

```

      Version Date:  October 15, 1984
      Paul S. Weiss

```

```

      Subroutine TCHAN accepts new values of the various settings
      of the multichannel scaler registers.  It then loads these new
      values into the proper registers of the computer and MCS unit.

```

```

      The argument IDEVIC determines which of these settings are to be
      entered by the user, as follows:

```

```

      IDEVIC = 0      Change all settings.
      IDEVIC = 1      Change the dwell time.
      IDEVIC = 2      Change the number of triggers per sweep.
      IDEVIC = 3      Change the number of sweeps.
      IDEVIC = 4      Change the initial channel.
      IDEVIC = 5      Change the external delay time.
      IDEVIC = 6      Change the number of channels.

```

```

      INTEGER*4 JTRIG

```

```

      COMMON /DATA/ ACCUM(4096),XCORR(256),WORK(256),NEW(4096),NSWEEP
      COMMON /MCSMAX/ DWLMAX,DWLMIN,MAXSWP,MAXTRG
      COMMON /SETS/ DWELL,ICHAN,ISWEEP,ITRIG,EDELAY,NCHAN,IOFSET,IEXT
      COMMON /SWFLAG/ ISWFLG,JTRIG

```

```

      IF(IDEVIC.EQ.0) GO TO 2100
      GO TO (2100,2200,2300,2400,2500,2600), IDEVIC
2100  TYPE 2101,DWELL
2101  FORMAT(' Enter the dwell time in microseconds (currently ',F7.2
      1,' usec).')
      ACCEPT *,DWELL
      IF((DWELL.GT.(DWLMIN-0.05)).AND.(DWELL.LE.(DWLMAX+.05)))
      1 GO TO 2150
      TYPE 2110,DWLMIN,DWLMAX
2110  FORMAT(/,' The dwell time must be between ',F5.2,' and '
      1,F7.2,' microseconds!')
      GO TO 2100
2150  CALL TLOAD(1)
      IF(IDEVIC.NE.0) RETURN
2200  TYPE 2201,ITRIG
2201  FORMAT(' Enter the number of triggers per sweep (currently ',I5

```



```

1,').')
ACCEPT *, ITRIG
IF((ITRIG.GT.0).AND.(ITRIG.LE.MAXTRG)) GO TO 2250
TYPE 2210,MAXTRG
2210  FORMAT(/,' The number of triggers must be between 1 and ',I5)
      GO TO 2200
2250  CALL TLOAD(5)
      IF(IDEVIC.NE.0) RETURN
2300  TYPE 2301,ISWEEP
2301  FORMAT(' Enter number of sweep counts (currently ',I5,').')
      ACCEPT *, ISWEEP
      IF((ISWEEP.GT.0).AND.(ISWEEP.LE.MAXSWP)) GO TO 2350
      TYPE 2310,MAXSWP
2310  FORMAT(/,' The number sweeps must be between 1 and ',I5)
      GO TO 2300
2350  CALL TLOAD(4)
      IF(IDEVIC.NE.0) RETURN
2400  TYPE 2401,ICHAN
2401  FORMAT(' Enter initial channel (currently ',I4,').')
      ACCEPT *, ICHAN
      IF((ICHAN.GT.0).AND.(ICHAN.LT.4096)) GO TO 2450
      TYPE 2420
2420  FORMAT(/,' The initial channel must be between '
1, ' 1 and 4096!')
      GO TO 2400
2450  CALL TLOAD(3)
      IF(IDEVIC.EQ.0) GO TO 2600
      RETURN
2500  TYPE 2501,EDELAY
2501  FORMAT(' Enter external delay in microseconds (currently '
1,F10.3,' usec).')
      ACCEPT *, EDELAY
      IF(IDEVIC.NE.0) RETURN
2600  TYPE 2601,NCHAN
2601  FORMAT(' Enter the number of channels (currently ',I4,').')
      ACCEPT *, NCHAN
      IF((NCHAN.GT.0).AND.(NCHAN.LE.4096)) GO TO 2650
      TYPE *, 'The number of channels must be between 1 and 4096'
      GO TO 2600
2650  CALL TLOAD(2)
9000  RETURN
      END

```

SUBROUTINE TCHCOR(IOPT)

File TCHCOR.FOR begins on the previous line.

C
C
C
C

Version Date: July 23, 1984
Paul S. Weiss

```

C
C   Subroutine TCHCOR changes the number of channels per TOF wheel
C   slot and the cross-correlation offset
C
COMMON /DISP/ IDSP(512), INEW, ICORR, IBACK, NCORR, IADV, IRES, IQIK
COMMON /SETS/ DWELL, ICHAN, ISWEEP, ITRIG, EDELAY, NCHAN, IOFSET, IEXT
IF (IOPT.GT.0) GO TO 5000
1   TYPE 100
100  FORMAT(/, ' How many MCS channels per TOF wheel slot?')
    ACCEPT *, NCORR
    IF ((NCORR.GT.0).AND.(NCORR.LE.16)) GO TO 9000
    TYPE 200, 1, 16
200  FORMAT(/, ' Value must be between ', I1, ' and ', I3, '.')
    GO TO 1
C
C   CHANGE OFFSET
C
5000 TYPE 5100
5100 FORMAT(/, ' Enter zero offset for cross-correlation')
    ACCEPT *, IOFSET
    IF ((IOFSET.GE.0).AND.(IOFSET.LE.255)) GO TO 9000
    TYPE 200, 0, 255
    GO TO 5000
9000 RETURN
    END

SUBROUTINE TCMLST
C
C   File TCMLST.FOR begins on the previous line.
C
C   Version Date:  October 15, 1984
C   Paul S. Weiss
C
C   Subroutine TCMLST lists the main commands for TPUF.  It serves as
C   the main help screen.
C
5100 TYPE 5100
    FORMAT(/, ' The available commands are as follows:')
    1, /, '  A*   Analyze Commands'
    2, /, '  C*   Change Commands'
    3, /, '  D*   Define and Display Commands'
    4, /, '  E    Exit'
    5, /, '  G*   Graph Commands'
    6, /, '  H    Help')
    TYPE 5200
5200 FORMAT('
L*      Load Commands'
2, /, '  P*   Print Commands'
3, /, '  R*   Read and Reset Commands'
4, /, '  S*   Show and Start Commands'
5, /, '  T    Test MCS'
6, /, '  W*   Write Data Commands'

```

```

7,/, ' Z      Zero Data Arrays')
TYPE 5300
5300  FORMAT(/, ' To get a listing of the various options of'
1,/, ' a starred command, ',/, ' enter an "H" in place of the "*" '
2,/, ' (i.e. "PH" for a list of the Print commands).')
RETURN
END

```

SUBROUTINE TCOMLA

File TCOMLA.FOR begins on the previous line.

C
C
C
C
C
C
C

```

Version Date:  July 23, 1984
Paul S. Weiss

```

Subroutine TCOMLA lists all the A* commands.

```

TYPE 100
100  FORMAT(/, ' The available Analyze options are as follows:'
1,/, ' AC      Analyze Chopper for Gate Width'
3,/, ' AD      Analyze Dip (for Hole Burning)'
5,/, ' AH      A Help'
2,/, ' AP      Analyze Peak',/)
RETURN
END

```

SUBROUTINE TCOMLC

File TCOMLC.FOR begins on the previous line.

C
C
C
C
C
C
C

```

Version Date:  October 12, 1984
Paul S. Weiss

```

Subroutine TCOMLC lists all the C* commands.

```

TYPE 100
100  FORMAT(/, ' The available Change options are as follows:'
1,/, ' CA      Change All Settings'
2,/, ' CC      Change Correlation Method'
3,/, ' CD      Change Dwell Time'
4,/, ' CE      Change External Delay'
5,/, ' CH      C Help'
6,/, ' CI      Change Initial Channel')
TYPE 200
200  FORMAT('
8,/, ' CN      Change Number of Channels'
8,/, ' CO      Change Offset for Cross-Correlation'
9,/, ' CP      Change Detector Position'
9,/, ' CS      Change Sweep Counts'
1,/, ' CT      Change Trigger Counts'
2,/, ' CU      Change User Terminal Type'

```

```

3,/,,' CW      Change Window for Display',/)
RETURN
END

```

SUBROUTINE TCOMLD

File TCOMLD.FOR begins on the previous line.

Version Date: October 12, 1984
Paul S. Weiss

Subroutine TCOMLD types out the available D* commands and explains the use of the arrows in changing the display.

TYPE 100

100 FORMAT(/,' The available define and display options '

1,' are as follows:'

1,/,,'	DA	Display Accumulated Data'
2,/,,'	DB	Display Background'
3,/,,'	DC	Display Correlated Data'
4,/,,'	DH	D Help'
5,/,,'	DL	Display Speed for Low Trigger Counts'
5,/,,'	DN	Display No Background'
6,/,,'	DQ	Display Quickly'
6,/,,'	DR	Display Refresh'
7,/,,'	DS	Display Single Sweeps'
8,/,,'	DT	Define Title'
8,/,,'	DU	Display Uncorrelated Data'
9,/,,'	DW	Display: Change Window',/)

TYPE 200

200 FORMAT(/,' The arrows on your terminal can be used'

1,' to change the',/,,' display window as follows:'

2,/,,' Up/Down Increase/Decrease the Display Step Size'

3,' by 1 channel'

4,/,,' Left/Right Change the Initial Channel to be displayed by'

5,/,,' -/+ the Display Step',/)

RETURN

END

SUBROUTINE TCOMLG

File TCOMLG.FOR begins on the previous line.

Version Date: July 23, 1984
Paul S. Weiss

Subroutine TCOMLG lists all of the G* commands.

TYPE 1535

1535 FORMAT(/,' The available Graph options are as follows:'

```

1,/, ' GH      G Help'
2,/, ' GL      Graph Line Plot'
3,/, ' GP      Graph Point Plot',/)
RETURN
END

```

SUBROUTINE TCOMLL

File TCOMLL.FOR begins on the previous line.

```

Version Date: July 23, 1984
Paul S. Weiss

```

Subroutine TCOMLL lists all the L* load commands.

TYPE 100

```

100 FORMAT(/, ' The available Load options are as follows'
1,/, ' LA      Load All'
2,/, ' LD      Load Dwell Time'
3,/, ' LH      L Help'
4,/, ' LI      Load Initial Channel'
5,/, ' LN      Load Number of Channels'
6,/, ' LS      Load Sweep Counts'
7,/, ' LT      Load Trigger Counts')
RETURN
END

```

SUBROUTINE TCOMLP

File TCOMLP.FOR begins on the previous line.

```

Version Date: July 23, 1984.
Paul S. Weiss

```

Subroutine TCOMLP type out the available P* print commands.

TYPE 100

```

100 FORMAT(/, ' The available print options are as follows:'
1,/, ' PC      Print Configuration'
2,/, ' PH      P Help'
3,/, ' PI      Print Information (from the User) on '
3, 'the Line Printer'
4,/, ' PL      Print Data on the Line Printer'
5,/, ' PP      Print Data on the Terminal Pausing for each'
6, 'Screen'
7,/, ' PR      Print Current Scaler Contents on the Line Printer'
8,/, ' PT      Print Data on the Terminal')
RETURN
END

```

SUBROUTINE TCOMLR

File TCOMLR.FOR begins on the previous line.

Version Date: October 11, 1984
 Paul S. Weiss

Subroutine TCOMLR lists all the R* commands.

TYPE 100

```
100 FORMAT(//, ' The Read and Reset Commands are: '
1,/, ' RA      Read Ascii Data File'
2,/, ' RH      Read and Reset Help'
3,/, ' RM      Reset MCS (Halt Acquisition)'
4,/, ' RS      Reset System Hardware',//)
RETURN
END
```

SUBROUTINE TCOMLS

File TCOMLS.FOR begins on the previous line.

Version Date: July 23, 1984
 Paul S. Weiss

Subroutine TCOMLS lists the available S* show and start commands.

TYPE 100

```
100 FORMAT(//, ' The Show and Start options are as follows: '
1,/, ' SC      Show Configuration'
2,/, ' SD      Show Display Mode'
3,/, ' SE      Scan Extend'
4,/, ' SH      S Help'
5,/, ' ST      Start')
RETURN
END
```

SUBROUTINE TCOMLW

File TCOMLW.FOR begins on the previous line.

Version Date: October 11, 1984
 Paul S. Weiss

Subroutine TCOMLW lists all the W* commands

TYPE 100

```
100 FORMAT(//, ' The Write Commands are: '
1,/, ' WF      Write Data File with a Full Header'
```

```

2,/, ' WH      Write Help'
3,/, ' WI      Write Data File with Entered Information in'
3, ' Header'
4,/, ' WN      Write Data File with No Header',//)
RETURN
END

```

```

SUBROUTINE TDEF(IOPT)

```

```

File TDEF.FOR begins on the previous line.

```

```

Version Date:  November 8, 1985
Paul S. Weiss

```

```

Subroutine TDEF changes the title and detector angle for TUF, both
these values are cosmetic and have no effect other than for output
to console, printer, or data file.

```

```

The argument IOPT is defined as follows:

```

```

IOPT=0  Change Title and Detector Angle.
IOPT=1  Change Title.
IOPT=2  Change Detector Angle.

```

```

COMMON /TITANG/ TITLE(10),ANGLE
IF(IOPT-1) 1100,1100,2100
1100 TYPE 1110,(TITLE(I),I=1,10)
1110 FORMAT(' The current title is:',/,1X,10A4,/, ' Change this?')
ACCEPT 1000,ANS
1000 FORMAT(A1)
IF(ANS.NE.'Y') GO TO 2000
TYPE *, 'Enter title.'

C
C  ENABLE LOWER CASE INPUT
C
CALL LCASE
ACCEPT 1310,(TITLE(I),I=1,10)
1310 FORMAT(10A4)
C
C  DISABLE LOWER CASE INPUT
C
CALL UCASE
2000 IF(IOPT.NE.0) GO TO 9000
2100 TYPE 2110,ANGLE
2110 FORMAT(' The current detector angle is ',F6.2,' degrees.'
1,/, ' Change this?')
ACCEPT 1000,ANS
IF(ANS.NE.'Y') GO TO 9000
TYPE *, 'Enter detector angle'
ACCEPT *,ANGLE

```

9000 RETURN
END

SUBROUTINE TDISP

File TDISP.FOR begins on the previous line.

Version Date: July 23, 1984
Paul S. Weiss

Subroutine TDISP sets up the array to be displayed IDSP. If the data is cross-correlated, subroutine TCORR is called. Note that the display is stopped before the array is altered and restarted after it has been recalculated.

WARNING: TDISP is in the root segment of TUF. Enlarging it will enlarge the already precariously large size of TUF.

INTEGER*4 JTRIG
COMMON /DATA/ ACCUM(4096),XCORR(256),WORK(256),NEW(4096),NSWEEP
COMMON /DISP/ IDSP(512),INEW,ICORR,IBACK,NCORR,IADV,IRES,IQIK
COMMON /MCSMAX/ DWLMAX,DWLMIN,MAXSWP,MAXTRG
COMMON /SETS/ DWELL,ICHAN,ISWEEP,ITRIG,EDELAY,NCHAN,I0FSET,IEXT
COMMON /SWFLAG/ ISWFLG,JTRIG

SET VALUES IF DATA IS TO BE CROSS-CORRELATED

IF(ICORR.NE.1) GO TO 1500
ND = 255
IBEG = 1
ISTEP = NCORR
GO TO 2000

SET FINAL DISPLAY CHANNEL ND
SO THAT IT IS NOT GREATER THAN THE LAST CHANNEL RECORDED

1500 IBEG = ICHAN + IADV
ISTEP = IRES
ND = 256
IF((IBEG + (256*ISTEP)).GT.4097)
1 ND = ((4097 - IBEG)/ISTEP)

SEE IF ONLY SINGLE SWEEP DATA IS TO BE DISPLAYED

2000 IF(INEW.EQ.1) GO TO 3000

PREPARE ACCUMULATED DATA

DO 2500 I=1,ND
KPLAT = IBEG + ((I-1) * ISTEP) - 1
WORK(I) = 0.


```

DO 2400 J=1,ISTEP
ISUB = KPLAT + J
WORK(I) = WORK(I) + ACCUM(ISUB)
2400 CONTINUE
2500 CONTINUE
GO TO 4000

C
C PREPARE SINGLE SWEEP DATA
C
3000 DO 3500 I=1,ND
KPLAT = IBEG + ((I-1) * ISTEP) - 1
WORK(I) = 0.
DO 3400 J=1,ISTEP
ISUB = KPLAT + J
3400 CONTINUE
WORK(I) = WORK(I) + FLOAT(NEW(ISUB))
3500 CONTINUE
C
C IF DISPLAY IS TO BE CROSS-CORRELATED DATA, CALL TCORR TO DO THIS
C
4000 IF(ICORR.NE.1) GO TO 4100
WORK(255) = (WORK(1) + WORK(254))/2.
CALL TCORR

C
C FIND MINIMUM AND MAXIMUM OF DISPLAY
C
4100 YMIN = WORK(1)
YMAX = YMIN
DO 5000 I=1,ND
IF(WORK(I).GT.YMAX) YMAX = WORK(I)
IF(WORK(I).LT.YMIN) YMIN = WORK(I)
5000 CONTINUE
C
C IF NO BACKGROUND SUBTRACTION IS TO BE DONE, SET YMIN TO 0
C
7000 IF((IBACK.EQ.1).AND.(YMIN.GT.0.)) YMIN = 0.
C
C SCALE DISPLAY ARRAY TO 12 BITS (0 TO 4095)
C
DIVR = YMAX - YMIN
IF(DIVR.EQ.0.) DIVR = 1.
DIVR = 4095./DIVR

C
C BEFORE ALTERING IDSP, STOP THE DISPLAY
C
CALL STOPD

C
C LOAD DISPLAY ARRAY IDSP
C
DO 7500 I=2,512,2

```



```

C      WHEN BIT IS FALSE (ISEQ = F), SUBTRACT VALUE OF WORK
C
      IF(ISEQ(KNTR)) GO TO 1800
      XCORR(I) = XCORR(I) - WORK(J)
      GO TO 2000
1800   XCORR(I) = XCORR(I) + WORK(J)
2000   CONTINUE
2500   CONTINUE
      DO 4000 I=1,255
      WORK(I) = XCORR(I)
4000   CONTINUE
      RETURN
      END

```

SUBROUTINE TDONE

File TDONE.FOR begins on the previous line.

```

C
C      Version Date: July 23, 1984
C      Paul S. Weiss
C
C      Subroutine TDONE collects the data from the MCS using the MACRO
C      subroutine READMS. It determines whether a counter overflow
C      has occurred by checking the flag/data word JTRIG set in interrupt
C      service routine MCSINT. If JTRIG is negative, an overflow has
C      occurred after -JTRIG triggers. If JTRIG is positive, a sweep
C      of JTRIG triggers has been completed successfully.
C      The new data is placed in integer array NEW by READMS, and is added
C      to the accumulated data array ACCUM.
C      If the display quickly mode has been chosen (i.e. if the DQ command
C      has been executed) the MCS is restarted if sweeps remain to be
C      accumulated, and then the display routine is called. This
C      eliminates the overhead involved in calculating the display array.
C      If the display speed for low trigger counts has been chosen
C      (default, or by command DL), the current data is displayed, and
C      then the MCS is restarted if sweeps remain.
C
C
C

```

```

      INTEGER*4 JTRIG
      COMMON /DISP/ IDSP(512), INEW, ICORR, IBACK, NCORR, IADV, IRES, IQIK
      COMMON /DATA/ ACCUM(4096), XCORR(256), WORK(256), NEW(4096), NSWEEP
      COMMON /SETS/ DWELL, ICHAN, ISWEEP, ITRIG, EDELAY, NCHAN, IOFSET, IEXT
      COMMON /SWFLAG/ ISWFLG, JTRIG

```

```

C
C      FIRST CALL READMS, THE MACRO ROUTINE TO READ THE SCALER
C

```

```

      TRIGS = AJFLT(JTRIG)
      IF(TRIGS.LT.0) GO TO 6000
      IF(ISWFLG.EQ.0) GO TO 3000
      TYPE 1200, ISWFLG, 7
1200   FORMAT('+', I5, ' sweeps remaining.', A1)

```

```

GO TO 4000
3000 TYPE 3100,TRIGS,7,7,7,7,7,7,7,7,7,7
3100 FORMAT('*****'
1,/, ' Scan has been completed'
2,/, ' with ',F9.0,' triggers.'
3,/, ' *****',10A1
4,/, ' Command?',/)
4000 CALL READMS(NEW)
C
C RESTART MCS USING THE MACRO RSTART IF SWEEPS REMAIN TO BE DONE
C AND IF IN "QUICK DISPLAY" MODE
C
IF((ISWFLG.GT.0).AND.(IQIK.GT.0)) CALL RSTART
DO 4200 I=1,4096
IF(NEW(I).GE.0) GO TO 4150
ACCUM(I) = ACCUM(I) + 65536.
4150 ACCUM(I) = ACCUM(I) + FLOAT(NEW(I))
4200 CONTINUE
GO TO 7000
6000 TYPE 6100,(-TRIGS),ISWFLG,7,7,7,7
6100 FORMAT(/, ' Count Overflow has occurred after ',F6.0,' triggers'
1, ' with ',I5,' sweeps remaining.',4A1
2,/, ' Lower trigger count before restarting.'
3,/, ' Command?',/)
GO TO 8900
7000 CALL TDISP
C
C RESTART MCS USING THE MACRO RSTART IF SWEEPS REMAIN TO BE DONE
C AND IF IN "LOW TRIGGER COUNT DISPLAY" MODE
C
IF((ISWFLG.GT.0).AND.(IQIK.EQ.0)) CALL RSTART
8900 ISWFLG = -1
RETURN
END

SUBROUTINE TDSMOD
C
C File TDSMOD.FOR begins on the previous line.
C
C Version Date: July 24, 1984
C Paul S. Weiss
C
C Subroutine TDSMOD types out the current display parameters.
C
COMMON /DISP/ IDSP(512), INEW, ICORR, IBACK, NCORR, IADV, IRES, IQIK
COMMON /SETS/ DWELL, ICHAN, ISWEEP, ITRIG, EDELAY, NCHAN, IOFSET, IEXT
IF(INEW.EQ.1) GO TO 2200
TYPE 2100, 'accumulated data, '
2100 FORMAT(/, ' The current display is of ',A18)

```

```

GO TO 2500
2200 TYPE 2100,'single sweep data,'
2500 IF(ICORR.EQ.1) GO TO 3000
      IB = ICHAN + IADV
      IE = IB + (256*IRES) - 1
      IF(IE.LE.4096) GO TO 2600
      ND = (4097 - IB)/IRES
      IE = IB + (ND*IRES) - 1
2600 TYPE 2650,IB,IE,IRES
2650 FORMAT(' channels ',I4,' to ',I4,', in steps of ',I2,' channels,')
      GO TO 4000
3000 TYPE 3100,I0FSET
3100 FORMAT(' cross-correlated with an offset of ',I4)
4000 IF(IBACK.EQ.0) GO TO 4500
      TYPE 4100,'included.',''
4100 FORMAT(' with the background level ',A9,A2)
      GO TO 5000
4500 TYPE 4100,'subtracte','d.'
5000 IF(IQIK.EQ.0) GO TO 5200
      TYPE 5110,'quickly.'
5110 FORMAT(' The display is refreshed ',A8,/)
      GO TO 9000
5200 TYPE 5110,'slowly.'
9000 RETURN
      END

```

SUBROUTINE TINIT

```

C                                     File TINIT.FOR begins on the previous line.
C
C   Version Date:  November 10, 1985
C   Paul S. Weiss
C
C   Subroutine TINIT initializes most of the common variables
C   for the multichannel scaler.
C
      INTEGER*4 JTRIG
      COMMON /DATA/ ACCUM(4096),XCORR(256),WORK(256),NEW(4096),NSWEEP
      COMMON /DISP/ IDSP(512),INew,ICORR,IBACK,NCORR,IADV,IRES,IQIK
      COMMON /MCSMAX/ DWLMAX,DWLMIN,MAXSWP,MAXTRG
      COMMON /SETS/ DWELL,ICHAN,ISWEEP,ITRIG,EDELAY,NCHAN,I0FSET,IEXT
      COMMON /SWFLAG/ ISWFLG,JTRIG
      COMMON /TERM/ ITERM
      COMMON /TITANG/ TITLE(10),ANGLE
C
      DATA TITLE /'Seco','ndar','y So','urce',' TOF',5*' '/
C
      TYPE 5
      FORMAT(//,' TOF Program'
1,/, ' Version Date:  November 10, 1985',///)
C

```

```
C      INITIALIZE ALLOWED VARIABLE RANGES
C
      DWLMIN = 0.15
      DWLMAX = 200.
      MAXSWP = 32767
      MAXTRG = 32767

C
C      INITIALIZE MCS SETTINGS
C
      DWELL = 100.
      ICHAN = 1
      NCHAN = 256
      ISWEEP = 10
      ITRIG = 100
      EDELAY = 0
      IOFSET = 0
      IEXT = 0
      ANGLE = 0.

C
C      INITIALIZE TERMINAL SETTING
C
      ITERM = 100

C
C      INITIALIZE DISPLAY SETTINGS
C
      IADV = 0
      IRES = 1
      INEW = 0
      ICORR = 0
      IBACK = 1
      IOFSET = 0
      NCORR = 1
      IQIK = 0
      CALL TZERO

C
C      SHOW CURRENT CONFIGURATION
C
      CALL TSHOCO(7)
      TYPE *, 'Are these default values satisfactory?'

C
C      ANSWER IS READ IN MAIN ROUTINE TPUF
C
      RETURN
      END
```

```
C      SUBROUTINE TLEAVE
```

```
C      File TLEAVE.FOR begins on the previous line.
```

```

C      Version Date: July 23, 1984
C      Paul S. Weiss
C
C      Subroutine TLEAVE is the termination routine.
C
C      TYPE *, 'Exit? Are you sure?'
C      ACCEPT 1000,ANS
1000   FORMAT(A1)
C      IF(ANS.NE.'Y') RETURN
C
C      STOP THE MCS
C
C      CALL STOPR
C
C      STOP THE DISPLAY
C
C      CALL STOPD
C      STOP
C      END

```

SUBROUTINE TLOAD(IDEVIC)

File TLOAD.FOR begins on the previous line.

```

C      Version Date: July 23, 1984
C      Paul S. Weiss
C
C      Subroutine TLOAD loads the already stored value of a specified
C      setting into the appropriate register of the computer or
C      multichannel scaler unit using the MACRO subroutines LOADDW,
C      LOADSW, and LOADSW.
C
C      The value of the argument IDEVIC determines which settings are
C      to be loaded into their registers, as follows:
C      IDEVIC = 0      Load all settings.
C      IDEVIC = 1      Load dwell counts.
C      IDEVIC = 2      Load number of channels.
C      IDEVIC = 3      Load initial channel.
C      IDEVIC = 4      Load sweep counter.
C      IDEVIC = 5      Load trigger counter.
C
C
C      COMMON /SETS/ DWELL, ICHAN, ISWEEP, ITRIG, EDELAY, NCHAN, IOFSET, IEXT
C      IF(IDEVIC.EQ.0) GO TO 2100
C      GO TO (2100,2200,2300,2400,2500), IDEVIC
2100   CALL LOADDW(INT(4096. - (DWELL*20.)))
C      IF(IDEVIC.NE.0) RETURN
2200   IF(IDEVIC.NE.0) RETURN
2300   IF(IDEVIC.NE.0) RETURN

```

```

2400 CALL LOADSW(ISWEEP)
      IF(IDEVIC.NE.0) RETURN
2500 CALL LOADTR(ITRIG)
      RETURN
      END

```

```

      INTEGER FUNCTION TLRDY(BNAME,LNAME)

```

```

      File TLRDY.FOR begins on the previous line.

```

```

      Version Date:  October 15, 1984
      Paul S. Weiss

```

```

      Function TLRDY checks to see if a file already exists with the
      name in the arguments INAME and BNAME, and its length in
      characters is argument LNAME.

```

```

      WARNING:  TLRDY is the limiting segment of overlay region 1.
      Enlarging it will expand the total size of TUF.

```

```

      The value of TLRDY returned is as follows:

```

```

      TLRDY=-1      Successfully opened file, therefore it
                   already exists.
      TLRDY=1      Unsuccessfully tried to open file, therefore
                   it does not already exist.

```

```

      LOGICAL*1 BNAME(10)

```

```

      ASSUME FAILURE TO OPEN FILE, MEANING IT IS OK TO USE THIS NAME

```

```

      TLRDY = 1

```

```

      CHECK AND SEE IF FILE ALREADY EXISTS

```

```

1700 OPEN(UNIT=9,ERR=9000,NAME=BNAME,TYPE='OLD')
      TLRDY = -1
9000 RETURN
      END

```

```

      SUBROUTINE TPLOTT(LINE)

```

```

      File TPLOTT.FOR begins on the previous line.

```

```

      Version Date:  November 8, 1985
      Paul S. Weiss

```

```

      Subroutine TPLOTT plots out the TOF scans on the HP 7470A or HP 7475A
      plotter.

```



```

COMMON /DATA/ ACCUM(4096),XCORR(256),WORK(256),NEW(4096),NSWEEP
COMMON /DISP/ IDSP(512),INEW,ICORR,IBACK,NCORR,IADV,IRES,IQIK
COMMON /SETS/ DWELL,ICHAN,ISWEEP,ITRIG,EDELAY,NCHAN,I0FSET,IEXT
DATA NESC/27/

```

C
C
C
C

```

SET UP THE HP 7470A OR HP 7475A PLOTTER

```

```

CALL ASSIGN(9,'PL:',3,'NEW')
WRITE(9,10) NESC,'.I11;;;17:',NESC,'.N;19:'
FORMAT('$',A1,A9,A1,A6)

```

10

C

```

C XON AND XOFF HAVE NOW BEEN ESTABLISHED, ESC I11;;;17 SETS THE XON
C THRESHOLD TO 11 REMAINING BYTES AND XON CHARACTER TO DC1, ESC .N;19:
C SETS THE XOF CHARACTER TO DC3.

```

C

C

```

INITIALIZE THE PLOTTER.

```

C

C

C

```

WRITE(9,*) 'IN;SP 1;SC 0,4095,0,4095;'

```

C

C

C

```

GIVE RANGE OF PLOT

```

C

```

WRITE(9,*) 'IP 500,600,9500,7000;'

```

C

C

C

C

```

PLOT THE FIRST POINT

```

```

WRITE(9,*) 'PA ',IDSP(1),',',',',IDSP(2),',';PD;'

```

```

DO 2000 I=2,256

```

```

IARG = (2*I)

```

```

IF(LINE.EQ.1) WRITE(9,*) 'PA ',IDSP(IARG-1),',',',IDSP(IARG),',';'

```

```

IF(LINE.EQ.0) WRITE(9,*) 'PU;PA ',IDSP(IARG-1)

```

```

1,',',IDSP(IARG),',';PD;'

```

2000

```

CONTINUE

```

C

C

C

```

PEN UP, RETURN PEN, AND MAKE PAPER EASY TO REMOVE

```

```

WRITE(9,*) 'PU;SP;PA 4000,4000;'

```

C

C

C

```

MAKE SURE PLOT IS COMPLETED BY CLEARING OUT BUFFER

```

```

REWIND 9

```

```

CLOSE(UNIT=9)

```

9000

```

RETURN

```

```

END

```

```

SUBROUTINE TPRDT(IDOUT)

```

C

C

File TPRDT.FOR begins on the previous line.

```

C      Version Date:  October 11, 1984
C      Paul S. Weiss
C
C      Subroutine TPRDT outputs the data on the line printer or the
C      terminal.
C
C      The argument IDOUT determines to which device to write data, and
C      if to the terminal, whether or not to pause every 128 channels.
C      The available values of IDOUT are:
C
C          IDOUT=-7      Write data to the terminal with pauses.
C          IDOUT=6      Write data to the line printer.
C          IDOUT=7      Write data to the terminal.
C
C
C      INTEGER*4 JTRIG
C      COMMON /DATA/ ACCUM(4096),XCORR(256),WORK(256),NEW(4096),NSWEEP
C      COMMON /MCSMAX/ DWLMAX,DWLMIN,MAXSWP,MAXTRG
C      COMMON /SETS/ DWELL,ICHAN,ISWEEP,ITRIG,EDELAY,NCHAN,IOfSET,IEXT
C      COMMON /SWFLAG/ ISWFLG,JTRIG
C
C      NUNIT IS THE LOGICAL UNIT NUMBER TO WHICH DATA WILL BE WRITTEN
C
C      NUNIT = IABS(IDOUT)
C      IST = ICHAN
C      900  IFIN = IST + 128
C          IF(IFIN.GT.(ICHAN + NCHAN)) IFIN = ICHAN + NCHAN
C          WRITE(NUNIT,1200) IST, (IFIN-1), (ACCUM(I),I=IST, (IFIN-1))
C      1200 FORMAT(' Channels ',I4,' to ',I4,16(/,8(1X,F9.0,:)))
C          IF(IFIN.EQ.(ICHAN + NCHAN)) GO TO 8000
C          IST = IFIN
C
C      IF PRINTOUT IS TO TERMINAL WITH PAUSES EVERY 128 CHANNELS, QUERY
C      AS TO WHETHER OR NOT TO CONTINUE, WHILE PAUSING
C
C      IF(IDOUT.GT.0) GO TO 900
C      TYPE *, 'Discontinue output?'
C      ACCEPT 1000,ANS
C      1000 FORMAT(A1)
C          IF(ANS.NE.'Y') GO TO 900
C
C      COMPLETE PRINTOUT IF TO LINE PRINTER
C
C      8000 IF(NUNIT.EQ.6) REWIND 6
C      9000 RETURN
C          END
C
C      SUBROUTINE TPRII(NU)
C
C      File TPRII.FOR begins on the previous line.
C

```

```

C      Version Date:  November 8, 1985
C      Paul S. Weiss
C
C      Subroutine TPRII prints information on the line printer or
C      into a disk file to be associated with a data file.
C
      LOGICAL*1 CHAR(72),ITIME(8)
      INTEGER JDATE(3)
      IF(NU.EQ.9) GO TO 500
      TYPE 310
310    FORMAT(/,' Include date and time?')
      ACCEPT 1000,ANS
1000   FORMAT(A1)
      IF(ANS.NE.'Y') GO TO 1100
500    CALL IDATE(JDATE(1),JDATE(2),JDATE(3))
      CALL TIME(ITIME)
      WRITE(NU,610) JDATE(1),JDATE(2),(JDATE(3)+1900),(ITIME(I),I=1,8)
610   FORMAT(/,' Date:  ',2(I2,'/'),I4,/, ' Time:  ',8A1,/)
C
C      IF INFORMATION IS TO BE WRITTEN TO DISK, ALSO PRINT IT
C
      IF(NU.EQ.9) WRITE(6,610) JDATE(1),JDATE(2)
      1,(JDATE(3)+1900),(ITIME(I),I=1,8)
1100   TYPE 1110
1110   FORMAT(/,' Type information in.  To stop, begin a line with'
      1,' a =',/)
C
C      ENABLE LOWER CASE INPUT
C
      CALL LCASE
1200   DO 1205 I=1,72
      CHAR(I) = 0
1205   CONTINUE
      ACCEPT 1210,(CHAR(I),I=1,72)
1210   FORMAT(72A1)
      IF(CHAR(1).EQ.61) GO TO 8500
      WRITE(NU,1310) (CHAR(I),I=1,72)
1310   FORMAT(1X,72A1)
C
C      IF INFORMATION IS TO BE WRITTEN TO DISK, ALSO PRINT IT
C
      IF(NU.EQ.9) WRITE(6,1310) (CHAR(I),I=1,72)
      GO TO 1200
C
C      DISABLE LOWER CASE INPUT
C
8500   CALL UCASE
9000   RETURN
      END

```

SUBROUTINE TREDAS

File TREDAS.FOR begins on the previous line.

C
C
C
C
C
C
CVersion Date: November 8, 1985
Paul S. Weiss

Subroutine TREDAS reads in a previously recorded data file.

```

INTEGER*4 JTRIG, JJTRIG
LOGICAL*1 CHAR(72)
COMMON /DATA/ ACCUM(4096), XCORR(256), WORK(256), NEW(4096), NSWEEP
COMMON /MCSMAX/ DWLMAX, DWLMIN, MAXSWP, MAXTRG
COMMON /SETS/ DWELL, ICHAN, ISWEEP, ITRIG, EDELAY, NCHAN, IOFSET, IEXT
COMMON /SWFLAG/ ISWFLG, JTRIG
TYPE *, 'Read Ascii data file into data array? Are you sure?'
ACCEPT 1000, ANS
1000  FORMAT(A1)
      IF(ANS.NE.'Y') GO TO 9000
      TYPE 1110
1110  FORMAT(/, ' Enter the full data file name', /)
      CALL ASSIGN(9, -10, 'OLD')

C
C  READ AND TYPE THROUGH THE CONTROL C THAT DESIGNATES
C  THE END OF THE HEADER
C
TYPE *, 'The header is as follows:'
1200  READ(9, 1210, END=2000) (CHAR(I), I=1, 72)
1210  FORMAT(72A1)
      IF(CHAR(1).EQ.3) GO TO 2000
      TYPE 1310, (CHAR(I), I=1, 72)
1310  FORMAT(1X, 72A1)
      GO TO 1200
2000  TYPE 2010, ICHAN
2010  FORMAT(/, ' What is the channel to which the first data point '
1, ' in the stored array'
2, /, ' should be added (the initial channel is now ', I4, ')?')
ACCEPT *, IC
      IF((IC.LE.0).OR.(IC.GE.4097)) GO TO 2000
2100  TYPE 2110, NCHAN
2110  FORMAT(/, ' How many points should be read from the stored array'
1, ' (the number of', /, ' channels is now ', I4, ').')
ACCEPT *, NC
      IF(NC.LE.0) GO TO 2100
      IF(MOD(NC, 8).NE.0) NC = NC + 8

C
TYPE 2210
2210  FORMAT(' How many triggers were recorded in this file (please'
1, ' include a decimal point)?')
ACCEPT *, TRIGN

```

C

```

C      CONVERT REAL TO INTEGER*4
C
C      I = JAFIX(TRIGN,JJTRIG)
C
C      ADD NUBER OF TRIGGERS TO THOSE RECORDED
C
C      I = JADD(JTRIG,JJTRIG,JTRIG)
C
C      READ AND ADD TO ACCUMULATED DATA
C      OFFSET INITIAL CHANNEL TO TAKE INTO ACCOUNT THE INITIAL
C      VALUES OF I AND J IN THE DO LOOPS
C
C      NOTE THAT IF THE NUMBER OF POINTS IN THE DATA FILE IS NOT DIVISIBLE
C      BY 8, THEN THE LAST FEW POINTS ARE LOST
C
C      IC = IC - 9
C      DO 4000 I=1,NC/8
C      READ(9,*,END=8000) (WORK(J),J=1,8)
C      DO 3900 J=1,8
C      ACCUM(IC + (8*I) + J) = ACCUM(IC + (8*I) + J) + WORK(J)
3900   CONTINUE
4000   CONTINUE
8000   CLOSE(UNIT=9)
9000   RETURN
      END

```

```

C      SUBROUTINE TSHOCO(NUNIT)
C                                     File TSHOCO.FOR begins on the previous line.
C
C      Version Date:  November 8, 1985
C      Paul S. Weiss
C
C      Subroutine TSHOCO shows the present hardware and software
C      configuration in the system.
C
C      The argument NUNIT is the logical unit to which the
C      configuration will be written.
C
C      INTEGER*4 JTRIG
C      COMMON /SWFLAG/ ISWFLG,JTRIG
C      COMMON /DISP/ IDSP(512),INEW,ICORR,IBACK,NCORR,IADV,IRES,IQIK
C      COMMON /SETS/ DWELL,ICHAN,ISWEEP,ITRIG,EDELAY,NCHAN,I0FSET,IEXT
C      COMMON /TITANG/ TITLE(10),ANGLE
C
C      WRITE(NUNIT,1510) (TITLE(I),I=1,10),ANGLE
1510   FORMAT(/,1X,10A4,/,,' The detector angle is ',F6.2,' degrees.')
```

```

C      WRITE(NUNIT,2010) DWELL,ITRIG,ISWEEP,ICHAN,(ICHAN+NCHAN-1),EDELAY

```

```

2010  FORMAT(//, ' The 4096 Channel Multichannel Scaler is in use.'
      1,/, ' The dwell time is ',F7.2,' microseconds per channel.'
      2,/, ' There are ',I5,' triggers per sweep, and ',I5,' sweeps.'
      4,/, ' Channels ',I4,' to ',I4,' are recorded.'
      5,/, ' The external delay time is ',F10.1,' microseconds.')
```

C

```

      IF(IEXT.GT.0) WRITE(NUNIT,2210)
2210  FORMAT(' An external dwell clock is in use.')
```

C

```

      TRIGS = ABS(AJFLT(JTRIG))
      WRITE(NUNIT,4110) TRIGS
4110  FORMAT(/,1X,F10.0,' triggers have been measured.',/)
      RETURN
      END
```

C

```

SUBROUTINE TSTART(ILK)
      File TSTART.FOR begins on the previous line.
```

C

```

      Version Date:  July 23, 1984
      Paul S. Weiss
```

C

```

      Subroutine START loads all the appropriate registers,
      then starts the TOF unit.
      This is all done by calling the appropriate macros.
```

C

```

      START will clear the data arrays if ILK = 0.
```

C

```

      INTEGER*4 JTRIG
      COMMON /DATA/ ACCUM(4096),XCORR(256),WORK(256),NEW(4096),NSWEEP
      COMMON /DISP/ IDSP(512),INEW,ICORR,IBACK,NCORR,IADV,IRES,IQIK
      COMMON /SETS/ DWELL,ICHAN,ISWEEP,ITRIG,EDELAY,NCHAN,IOfSET,IEXT
      COMMON /SWFLAG/ ISWFLG,JTRIG
      NSWEEP = 0
      IF(ILK.NE.0) GO TO 2000
      CALL TZERO
```

C

```

      IF MCS IS RUNNING, WAIT FOR COMPLETION
```

C

```

2000  ISWFLG = 1
      IF(IRUN(1).NE.1) GO TO 2500
```

C

```

      IF MCS IS RUNNING, SEND IT ONE LAST TRIGGER TO DO
```

C

```

      CALL LOADTR(1)
2100  IF(ISWFLG.GE.0) GO TO 2400
      GO TO 2100
```

C

```

      REMOVE THE EXTRA TRIGGERS COUNTED IN JTRIG, AS THE LAST SWEEP WAS
      NOT SAVED
```

C


```

CALL TLOAD(0)
3000 TYPE 3100
3100 FORMAT(/,' Test Mode? Are you sure?')
ACCEPT 1000,ANS
1000 FORMAT(A1)
IF(ANS.NE.'Y') GO TO 9000
C
C START MCS WITH TEST BIT SET HIGH IN CONTROL STATUS WORD
C
CALL BEGIN(32)
TYPE 5000
5000 FORMAT(' MCS running')
9000 RETURN
END

```

SUBROUTINE TTERM(N)

File TTERM.FOR begins on the previous line.

```

C
C
C Version Date: March 10, 1984
C Paul S. Weiss
C
C Subroutine TTERM changes the terminal setting.
C
COMMON /TERM/ ITERM
TYPE 100,ITERM
100 FORMAT(/,' The terminal you are using is currently '
1,'listed as a VT',I3,/)
IF(N.GT.0) GO TO 2000
TYPE 200
200 FORMAT(' To change the terminal listing, type CU',/)
RETURN
2000 TYPE 2100
2100 FORMAT(' Enter if your terminal is compatible with:'
3,/, ' 52 VT52'
4,/, ' 100 VT100'
5,/, ' 0 none of the above',/)
ACCEPT *,ITERM
TYPE 100,ITERM
RETURN
END

```

SUBROUTINE TWRA(IOPT)

File TWRA.FOR begins on the previous line.

```

C
C
C Version Date: October 16, 1984
C Paul S. Weiss

```


Subroutine TWRA writes an ASCII file to disk. It includes a header terminated with a ^C.

The argument IOPT determines whether or not to write a full header to the file, as follows:

IOPT=-1 Write no header.
 IOPT=0 Write a full header, including the title, detector angle, configuration, and any other important information.
 IOPT=1 Write only information entered by the user.

LOGICAL*1 BNAME(10),B,OTHER
 INTEGER INAME(6),TLRDY
 COMMON /DATA/ ACCUM(4096),XCORR(256),WORK(256),NEW(4096),NSWEEP
 COMMON /SETS/ DWELL,ICHAN,ISWEEP,ITRIG,EDELAY,NCHAN,I0FSET,IEXT
 EQUIVALENCE (INAME(1),BNAME(1))

GET NAME FOR FILE

100 TYPE 110
 110 FORMAT(/,' Enter the six letter data file name.',/)
 ACCEPT 210,(INAME(I),I=1,3)
 210 FORMAT(3A2)
 INAME(4) = '.T'
 INAME(5) = 'UF'
 INAME(6) = 0

IF THE FIRST LETTER IS A SPACE, OR ANY CHARACTER OTHER THAN A LETTER
 GO BACK AND GET THE CORRECT FILENAME

IF(BNAME(1).LT.64) GO TO 100

IF THERE ARE FEWER THAN SIX LETTERS, SHIFT THE EXTENSION DOWN

LNAME = 10
 DO 600 I=1,6
 B = BNAME(7-I)

IF THE CHARACTER IN QUESTION IS A LETTER OR NUMBER, SAVE IT
 OTHERWISE ELIMINATE

IF((B.GT.64).OR. ((B.GT.47).AND.(B.LT.58))) GO TO 700

KEEP TRACK OF NAME LENGTH

```

C
  LNAME = 10 - I
  DO 550 J=7-I,10-I
  BNAME(J) = BNAME(J+1)
550  CONTINUE
  BNAME(11-I) = 0
600  CONTINUE
C
C   SEE IF FILE ALREADY EXISTS, IF SO, SEE IF IT CAN BE WRITTEN OVER,
C   IF IT MUST BE PRESERVED, GET A NEW FILE NAME
C
700  I = TLRDY(INAME,BNAME,LNAME)
C
C   IF FILE DOES NOT EXIST, GO AHEAD AND OPEN IT
C
  IF(I.GT.0) GO TO 1100
C
C   IF IT DOES EXIST, CLOSE IT AND SEE IF IT IS TO BE WRITTEN OVER
C
  CLOSE(UNIT=9,DISPOSE='SAVE')
C
C   IF FILE IS NOT TO BE WRITTEN OVER, GET A NEW NAME
C
  TYPE 810, (BNAME(I), I=1, LNAME), 7, 7, 7, 7, 7
810  FORMAT(1X, 10A1, ' already exists! '
  1, 'Would you like to write over it?', 5A1)
  ACCEPT 1000, ANS
1000 FORMAT(A1)
C
C   IF THE FILE ALREADY EXISTS, AND IS NOT TO BE WRITTEN OVER,
C   RETURN A VALUE OF 0, SO THAT A NEW FILE NAME CAN BE ENTERED
C
  IF(ANS.NE.'Y') GO TO 100
C
C   OTHERWISE, OPEN FILE
C
1100 CALL ASSIGN(9, INAME, LNAME, 'NEW', 'CC')
2200 TYPE 2210, (BNAME(I), I=1, LNAME), 7, 7, 7, 7, 7, 7, 7, 7
2210 FORMAT(' The file: ', 10A1
  1, ' has been opened successfully!', 8A1)
C
C   GO TO THE TOP OF THE PRINTER PAGE, AND PRINT FILE NAME
C
  PRINT 3010, 12, (BNAME(I), I=1, LNAME)
3010 FORMAT(1X, 11A1)
C
C   DECIDE WHAT TYPE OF HEADER TO WRITE
C
  IF(IOPT) 3300, 3100, 3200
C

```

```

C      WRITE CONFIGURATION TO FILE AND PRINTER
C
3100   CALL TSHOCO(9)
      CALL TSHOCO(6)
3200   TYPE *, 'Write any additional information to file?'
      ACCEPT 1000,ANS
C
C      CALL SUBROUTINE TPRII TO WRITE A HEADER TO THE DATA FILE
C
      IF(ANS.EQ.'Y') CALL TPRII(9)
C
C      WRITE A CONTROL C TO DESIGNATE THE END OF THE HEADER
C
3300   WRITE(9,3301) 3
3301   FORMAT(1X,A1)
C
C      WRITE THE DATA TO THE DATA FILE FROM THE INITIAL CHANNEL,
C      THROUGH THE NUMBER OF CHANNELS REQUESTED
C
      NC = NCHAN/8
      IF(MOD(NCHAN,8).NE.0) NC = NC + 1
      DO 4500 I=1,NC
      IBASE = ICHAN + (8 * (I-1)) - 1
      WRITE(9,4010) (ACCUM(IBASE + J), J=1,8)
4010   FORMAT(8(1X,F9.0))
4500   CONTINUE
C
C      CLOSE FILE
C
      CLOSE(UNIT=9,DISPOSE='SAVE')
C
C      ALSO, PRINT DATA
C
      CALL TPRDT(6)
      RETURN
      END

      SUBROUTINE TZERO
C
C      File TZERO.FOR begins on the previous line.
C
C      Version Date: February 22, 1984
C      Paul S. Weiss
C
C      Subroutine ZERO zeroes the arrays used to store data.
C
      INTEGER*4 JTRIG
      COMMON /DATA/ ACCUM(4096),XCORR(256),WORK(256),NEW(4096),NSWEEP
      COMMON /MCSMAX/ DWLMAX,DWLMIN,MAXSWP,MAXTRG

```

```
COMMON /SETS/ DWELL, ICHAN, ISWEEP, ITRIG, EDELAY, NCHAN, IOFSET, IEXT  
COMMON /SWFLAG/ ISWFLG, JTRIG  
DO 500 I=1,256  
XCORR(I) = 0.  
WORK(I) = 0.  
500 CONTINUE  
DO 600 I=1,4096  
NEW(I) = 0  
ACCUM(I) = 0.  
600 CONTINUE  
END
```

```
.TITLE NEW LBL TOF MACROS
```

```
File XBL.MAC begins on the previous line.
```

```
Macros for using the new LBL multichannel scaler
```

```
Version Date: November 5, 1985
```

```
Paul S. Weiss
```

```
.SBTTL GLOBALS
.GLOBL TLEAVE, TANAL, TCHAN, TLOAD, TDSMOD, TSTMCS
.GLOBL TPLOT, TPRDT, TSHOCO, TSTART, TWRA, TCOMM
.GLOBL TDISP, TDONE, TCORR, TCHCOR, TZERO, MCSINT, DSPINT
.GLOBL TPRII, TDEF
.GLOBL INIT, RINIT, LOADDW, LOADSW, LOADTR
.GLOBL BEGIN, CLEAR, DISPL, ENSPEC, EXSPEC, STOPR, READMS
.GLOBL RSTART, STOPD, IRUN, LCASE, UCASE
.MCALL .INTEN, .PRINT
```

```
.PAGE
```

```
.SBTTL ADDRESSES
```

```
DSPVEC=340
DSPPRI=342
MCSVEC=410
MCSPRI=412
DATA0=166000
DATAHI=166002
LAML0=166004
LAMHI=166006
STATU1=166010
STATU2=166012
MCSA0=166100
MCSA1=166102
MCSA2=166104
MCSA3=166106
DSPCSR=170440
DSPXYB=170442
DSPPCR=170444
DSPCAR=170446
TTRCSR=177560
TTTCSR=177564
TTTBUF=177566
```

```
.PAGE
```

```
.SBTTL MACRO SUBROUTINES
```

```
;Subroutine INIT initializes the system
;and then loads all of the interrupt vectors and
;priorities. INIT is called from the main routine of the TOF
;program.
```

```

;
INIT:  TST      (R5)+          ;SKIP ARGUMENT COUNT
        MOV      (R5)+,0#FLAGAD ;LOAD SWEEP FLAG ADDRESS
        MOV      (R5)+,0#TRGAD  ;LOAD TRIGGER COUNTER ADDRESS
        MOV      #0,0#DATALO    ;CLEAR TRIGGERS
        MOVVB   #18.,0#MCSA1
        MOV      #0,0#DATALO
        MOVVB   #18.,0#MCSA0    ;CLEAR MCS CSR
        MOV      #6,0#STATU1   ;CLEAR CAMAC STATUS REGISTERS
        MOV      #0,0#STATU2
        MOV      #MCSINT,0#MCSVEC ;LOAD MCS INTERRUPT VECTOR
        MOV      #340,0#MCSPRI  ;SET MAXIMUM PRIORITY FOR MCS
                                   ;INTERRUPT
        BIC      #103,0#DSPCSR  ;CLEAR DISPLAY
        MOV      #DSPINT,0#DSPVEC ;LOAD DISPLAY INTERRUPT VECTOR
        MOV      #340,0#DSPPRI  ;LOAD DISPLAY PRIORITY
        RTS      PC
;
;
;

```

;Subroutine RINIT initializes all the hardware on the system.

```

RINIT:  RESET          ;ISSUE HARDWARE RESET (B INITL)
        BIS      #100,0#TTRCSR ;RESET TERMINAL INPUT ENABLE
;
;
;

```

;Subroutine LOADDW loads the dwell counts into the proper register of the MCS unit.

```

LOADDW: TST      (R5)+          ;SKIP ARGUMENT COUNT
        MOV      0(R5),0#DATALO ;GET DWELL COUNTS
        MOVVB   #18.,0#MCSA2    ;LOAD DWELL COUNTS
        RTS      PC
;
;
;

```

;Subroutine LOADSW loads the number of sweeps into a word accesible to the MACRO routines, SWEEPS.

```

LOADSW: TST      (R5)+          ;SKIP ARGUMENT COUNT
        MOV      0(R5),0#SWEEPS ;GET SWEEP COUNTS
        RTS      PC
;
;
;

```

;Subroutine LOADTR loads the number of triggers into the trigger counter.

```

LOADTR: TST      (R5)+          ;SKIP ARGUMENT COUNT
        MOV      0(R5),R1       ;GET TRIGGER COUNTS
        MOV      R1,0#TRIGS    ;SAVE NUMBER OF TRIGGERS
;
;
;

```

```

MOV     #0,RO
SUB     R1,RO           ;GET TWO'S COMPLEMENT OF TRIGGER
MOV     RO,0#DATALO    ;COUNTS
MOV     RO,0#TRIGLD    ;STORE VALUE TO BE LOADED FOR TRIGGERS
MOVB    #18.,0#MCSA1   ;LOAD TRIGGER COUNTS
RTS     PC

```

```

;Subroutine CLEAR clears the trigger counter

```

```

CLEAR:  MOV     0#TRGAD,R5           ;CLEAR NUMBER OF TRIGGERS
        MOV     #0,(R5)+
        MOV     #0,(R5)
        RTS     PC

```

```

;Subroutine BEGIN starts the TOF

```

```

;BEGIN is called with one argument, the argument contains the bits that need
;to be set in the control status register to enable the test frequency
;(these are 40, 100, and 200 octal) or external clock (this is 2)
;It is not necessary to send the Acquisition and LAM enable bits.

```

```

;If BEGIN is called as an integer function, the value loaded into the CSR
;is returned.

```

```

BEGIN:  BIC     #300,0#STATU1        ;DISABLE CAMAC LAM
        BIS     #1,0#STATU1         ;SET DII BIT, SEE CAMAC CRATE
                                           ;CONTROLLER MANUAL
        MOV     #0,0#DATALO         ;DISABLE MCS LAM AND DATA ACQUISITION
        MOVB    #18.,0#MCSAO
        TST     (R5)+
        MOV     #11,RO
                                           ;SKIP ARGUMENT COUNT
                                           ;SET BITS FOR DATA ACQUISITION AND
                                           ;LAM ENABLE
        BIS     0(R5),RO            ;EXTERNAL DWELL OR TEST FREQUENCY?
1$:     MOV     RO,0#CSRLD          ;STORE PROPER VALUE OF CSR FOR MCSINT
        MOV     RO,0#DATALO        ;LOAD DATALO
        MOVB    #18.,0#MCSAO       ;LOAD CSR INTO MCS
        BIS     #301,0#STATU1      ;ENABLE CAMAC LAMS
        RTS     PC

```

```

;Subroutine RSTART restarts the MCS

```

```

RSTART: BIC     #300,0#STATU1
        MOV     0#TRIGLD,0#DATALO ;RELOAD TRIGGERS

```

```

MOV B #18,0#MCSA1
MOV #0,0#CSRLD,0#DATALO
MOV B #18,0#MCSAO ;START MCS AND ENABLE LAM
BIS #300,0#STATU1 ;ENABLE CAMAC LAM'S
RTS PC

```

```

;Function subroutine IRUN returns a 1 as its value if the MCS acquisition
;enable bit is on.

```

```

IRUN: MOV #0,RO ;RETURN 0 IF MCS NOT RUNNING
MOV B #0,0#MCSAO ;READ MCS CSR
BIT #1,0#DATALO
BEQ 1$
MOV #1,RO ;RETURN 1 IF MCS IS RUNNING
1$: RTS PC

```

```

;Subroutine DISPL loads the display buffer for the DMA display unit.

```

```

;It must be called with two arguments:

```

```

;DSPAD: The address of a single precision integer array,
; prepared to be displayed as a point plot, with x and y
; coordinates stored alternately. All values range from
; 0 to 4095. The address of this array is stored
; in DSPAD.

```

```

;NUMDSP: The number of points to be displayed.

```

```

DISPL: BIC #103,0#DSPCSR ;DISABLE DISPLAY INTERRUPTS
TST (R5)+ ;SKIP ARGUMENT COUNT
MOV (R5)+,0#DSPAD ;STORE ADDRESS OF DISPLAY BUFFER
MOV #0(R5),0#DSPPCR ;LOAD POINT COUNT REGISTER
MOV #0(R5),0#DSPNPT ;LOAD NUMBER OF POINTS REGISTER
;FOR FUTURE REFERENCE
NEG #0#DSPPCR ;TWO'S COMPLEMENT CODING OF PCR
MOV #0#DSPAD,0#DSPCAR ;INITIALIZE CURRENT ADDRESS REGISTER
BIS #103,0#DSPCSR ;ENABLE DISPLAY INTERRUPT, AND START
RTS PC

```

```

;Subroutine ENSPEC puts the monitor in special screen mode

```

```

ENSPEC: BIS #10000,0#44 ;ENTER SPECIAL SCREEN MODE
RTS PC

```

```

;Subroutine EXSPEC takes the monitor out of special screen mode

```



```
EXSPEC: BIC    #10000,0#44      ;LEAVE SPECIAL SCREEN MODE
        RTS    PC
```

```
;Subroutine LCASE enables lower case input from terminal
```

```
LCASE:  BIS    #40000,0#44
        RTS    PC
```

```
;Subroutine UCASE disables lower case input from terminal
```

```
UCASE:  BIC    #40000,0#44
        RTS    PC
```

```
;Subroutine STOPR turns off interrupts
```

```
STOPR:  MOV    #0,0#DATALD      ;CLEAR MCS CSR
        MOVB  #18.,0#MCSAO
        RTS    PC
```

```
;Subroutine STOPD stops the display
```

```
STOPD:  CLR    0#DSPCSR         ;CLEAR DISPLAY INTERRUPTS
        RTS    PC
```

```
;Subroutine READMS reads the 4096 multichannel scaler channels into
;the array specified in NEW
```

```
;Subroutine READMS must be called with one argument,
;NEW is the array the new data is to be entered into.
```

```
READMS: TST    (R5)+
        MOV    (R5),R4          ;GET NEW DATA ADDRESS
        MOV    #4,0#DATALD     ;ENABLE READ MEMORY AND
        MOVB  #18.,0#MCSAO     ;DISABLE DATA ACQUISITION AND LAM
        MOV    #4096.,R5      ;READ ALL 4096 POINTS INTO NEW
        MOV    #0,R3           ;REGISTER 3 CONTAINS MEMORY ADDRESS
2$:     MOV    R3,0#DATALD
        MOVB  #18.,0#MCSA3     ;LOAD MEMORY ADDRESS
        MOVB  #0.,0#MCSA3     ;READ MEMORY
        MOV    0#DATALD,R2
```

```

MOV      R3,0#DATAL0
MOV      #18.,0#MCSA3      ;LOAD MEMORY ADDRESS
MOV      #0.,0#MCSA3      ;READ MEMORY
CMP      0#DATAL0,R2      ;WAS VALUE THE SAME TWO TIMES?
BNE      2$                ;IF NOT, READ IT TWO MORE TIMES
MOV      0#DATAL0,(R4)+   ;IF SO, MOVE IT TO ARRAY NEW(I)
INC      R3
SOB      R5,2$
MOV      #0,0#DATAL0      ;RESET CSR
MOV      #0,0#MCSAO
RTS      PC

```

```

;
;
.PAGE
.SBTTL  INTERRUPT SERVICE ROUTINES
;
;

```

```

;Interrupt service routine MCSINT services the Multichannel Scaler.
;It checks to see whether an overflow or an end sweep has caused
;the interrupt. Then, it adds the number of triggers taken in
;that sweep, decrements the sweep counter, and in so doing, sets
;a flag for the FORTRAN routine COMMAN to see.
;

```

```

MCSINT: MOV      #0,0#MCSAO      ;READ CSR OF MCS
MOV      0#DATAL0,0#OVRFLG
MOV      #0,0#DATAL0      ;DISABLE DATA ACQUISITION AND LAM
MOV      #18.,0#MCSAO
BIC      #300,0#STATU1      ;DISABLE CAMAC LAM'S
.INTEN  0,PIC              ;DROP PRIORITY
MOV      0#TRGAD,R5        ;GET ADDRESS OF TRIGGER COUNTER
ADD      0#TRIGS,(R5)+     ;ADD THE NUMBER OF TRIGGERS IN THE
ADC      (R5)              ;LATEST SWEEP
BIT      #100,0#OVRFLG     ;CHECK FOR END SWEEP
BNE      1$                ;IF SWEEP END DETECTED CONTINUE WITH
;NORMAL INTERRUPT SERVICE
;OTHERWISE SERVICE OVERFLOW
;READ NUMBER OF TRIGGERS REMAINING

MOV      #0,0#MCSA1      ;READ NUMBER OF TRIGGERS REMAINING
MOV      0#TRGAD,R5
SUB      0#DATAL0,(R5)     ;SUBTRACT THE NUMBER OF
SBC      2(R5)             ;TRIGGERS REMAINING ON MCS
COM      (R5)+            ;MAKE INTEGER*4 NEGATIVE
COM      (R5)
MOV      0#FLAGAD,R5      ;LOAD NUMBER OF SWEEPS REMAINING
MOV      0#SWEEPS,(R5)
RTS      PC

1$: DEC      0#SWEEPS      ;DECREMENT SWEEP COUNT
MOV      0#FLAGAD,R5      ;LOAD NUMBER OF SWEEPS REMAINING
MOV      0#SWEEPS,(R5)
RTS      PC
;

```

```

;
;Interrupt Service Routine DSPINT is for the DMA display unit.
;The point counter is reinitialized, as is the current address register,
;and then the unit is restarted.
;
;

```

```

DSPINT: MOV     DSPNPT,0#DSPPCR           ;LOAD POINT COUNTER
        NEG     0#DSPPCR
        MOV     DSPAD,0#DSPCAR           ;LOAD CURRENT ADDRESS REGISTER
        MOV     #103,0#DSPCSR           ;REENABLE DISPLAY INTERRUPTS
        RTI                                     ;AND START
;
;

```

```

        .PAGE
        .SBTTL  WORDS, ARGUMENT BLOCKS, DATA BLOCKS, ETC.
;
;

```

```

FLAGAD: .WORD
TRGAD:  .WORD
CSRLD:  .WORD
SWEEPS: .WORD
TRIGS:  .WORD
TRIGLD: .WORD
DSPNPT: .WORD
DSPAD:  .WORD
OVRFLG: .WORD
SAVR:   .BLKW 4
OUTARG: .BLKW 4
        .END INIT

```

```
!File CNLTUF.COM
!Compile command file for Time of Flight Programs
!
!Version Date: November 13, 1984
!Paul S. Weiss
FORT/NOLINENUMBERS TUF.FOR
FORT/NOLINENUMBERS TANAL.FOR
FORT/NOLINENUMBERS TCDISP.FOR
FORT/NOLINENUMBERS TCHAN.FOR
FORT/NOLINENUMBERS TCHCOR.FOR
FORT/NOLINENUMBERS TCMLST.FOR
FORT/NOLINENUMBERS TCOMLC.FOR
FORT/NOLINENUMBERS TCOMLA.FOR
FORT/NOLINENUMBERS TCOMLD.FOR
FORT/NOLINENUMBERS TCOMLG.FOR
FORT/NOLINENUMBERS TCOMLL.FOR
FORT/NOLINENUMBERS TCOMLP.FOR
FORT/NOLINENUMBERS TCOMLR.FOR
FORT/NOLINENUMBERS TCOMLS.FOR
FORT/NOLINENUMBERS TCOMLW.FOR
FORT/NOLINENUMBERS TDEF.FOR
FORT/NOLINENUMBERS TDISP.FOR
FORT/NOLINENUMBERS TDONE.FOR
FORT/NOLINENUMBERS TDSMOD.FOR
FORT/NOLINENUMBERS TINIT.FOR
FORT/NOLINENUMBERS TLEAVE.FOR
FORT/NOLINENUMBERS TLOAD.FOR
FORT/NOLINENUMBERS TLRDY.FOR
FORT/NOLINENUMBERS TPLOT.FOR
FORT/NOLINENUMBERS TPRDT.FOR
FORT/NOLINENUMBERS TPRII.FOR
FORT/NOLINENUMBERS TREDAS.FOR
FORT/NOLINENUMBERS TSHOCO.FOR
FORT/NOLINENUMBERS TSTART.FOR
FORT/NOLINENUMBERS TSTMCS.FOR
FORT/NOLINENUMBERS TTERM.FOR
FORT/NOLINENUMBERS TWRA.FOR
FORT/NOLINENUMBERS TZERO.FOR
MAC XBL.MAC
QLTUF
```

```
!File COPTUF.COM
!Copy command file for Time of Flight Programs
!
!Version Date:  October 15, 1984
!Paul S. Weiss
!
COPY I:TUF.FOR O:TUF.FOR
COPY I:TANAL.FOR O:TANAL.FOR
COPY I:TCDISP.FOR O:TCDISP.FOR
COPY I:TCHAN.FOR O:TCHAN.FOR
COPY I:TCHCOR.FOR O:TCHCOR.FOR
COPY I:TCMLST.FOR O:TCMLST.FOR
COPY I:TCOMLA.FOR O:TCOMLA.FOR
COPY I:TCOMLC.FOR O:TCOMLC.FOR
COPY I:TCOMLD.FOR O:TCOMLD.FOR
COPY I:TCOMLG.FOR O:TCOMLG.FOR
COPY I:TCOMLL.FOR O:TCOMLL.FOR
COPY I:TCOMLP.FOR O:TCOMLP.FOR
COPY I:TCOMLR.FOR O:TCOMLR.FOR
COPY I:TCOMLS.FOR O:TCOMLS.FOR
COPY I:TCOMLW.FOR O:TCOMLW.FOR
COPY I:TDEF.FOR O:TDEF.FOR
COPY I:TDISP.FOR O:TDISP.FOR
COPY I:TDONE.FOR O:TDONE.FOR
COPY I:TDSMOD.FOR O:TDSMOD.FOR
COPY I:TINIT.FOR O:TINIT.FOR
COPY I:TLEAVE.FOR O:TLEAVE.FOR
COPY I:TLOAD.FOR O:TLOAD.FOR
COPY I:TLRDY.FOR O:TLRDY.FOR
COPY I:TPLOT.FOR O:TPLOT.FOR
COPY I:TPRDT.FOR O:TPRDT.FOR
COPY I:TPRII.FOR O:TPRII.FOR
COPY I:TREDAS.FOR O:TREDAS.FOR
COPY I:TSHOCO.FOR O:TSHOCO.FOR
COPY I:TSTART.FOR O:TSTART.FOR
COPY I:TSTMCS.FOR O:TSTMCS.FOR
COPY I:TTERM.FOR O:TTERM.FOR
COPY I:TWRA.FOR O:TWRA.FOR
COPY I:TZERO.FOR O:TZERO.FOR
COPY I:XBL.MAC O:XBL.MAC
COPY I:CNLTUF.COM O:CNLTUF.COM
COPY I:COPTUF.COM O:COPTUF.COM
COPY I:LTUF.COM O:LTUF.COM
```

```
!File LTUF.COM
!LINK command file for Time of Flight Program
!Version Date: October 15, 1984
R LINK
TUF,TUF.MAP,=TUF,TDISP,XBL/I//
!TUF contains the main routine TUF, and the subroutine COMMAN.
!TDISP contains the display subrroutines: TDISP, and CORR
!XBL contains the MACROs: INIT, LOADDW, LOADSW, LOADTR, CLEAR,
!     BEGIN, RSTART, IRUN, DISPL, ENSPEC, EXSPEC, STOPR, STOPD,
!     READMS, and the interrupt service routines: MCSINT, and
!     DSPINT
TCDISP/0:1
TCHCOR/0:1
TCMLST/0:1
TCOMLA/0:1
TCOMLC/0:1
TCOMLD/0:1
TCOMLG/0:1
TCOMLL/0:1
TCOMLP/0:1
TCOMLR/0:1
TCOMLS/0:1
TCOMLW/0:1
TDEF/0:1
TDSMOD/0:1
TLEAVE/0:1
TLOAD/0:1
TLRDY/0:1
TPLOT/0:1
TPRDT/0:1
TPRII/0:1
TSHOCO/0:1
TZERO/0:1
TANAL/0:2
TCHAN/0:2
TDONE/0:2
TINIT/0:2
TREDAS/0:2
TSTART/0:2
TSTMCS/0:2
TTERM/0:2
TWRA/0:2
//
$SHORT
```

^C

C. References

1. NIM is a standard modular instrumentation bin which supplies power only on a bus at ± 12 V, ± 24 V, and sometimes ± 6 V.
2. IEEE Standard Modular Instrumentation and Digital Interface System (CAMAC), (Institute of Electrical and Electronic Engineers, New York, 1975).
3. Q-Bus refers to a DEC standard bus for the LSI-11 series computers.⁵
4. RCA Electronic Components, Harrison, New Jersey.
5. Digital Equipment Corporation, Maynard, Massachusetts. For a description of the various processors used, see the Processor Handbook, Digital Equipment Corporation, Maynard, Massachusetts (1984).
6. Joerger Enterprises, Inc., East Northport, New York.
7. see the RT-11 Programmer's Reference Manual, Digital Equipment Co., Maynard, Massachusetts (1983).
8. Superior Electric Co., Bristol, Connecticut.
9. Spectra-Physics, Mountain View, California.
10. Kinetic Systems, Evansport, Illinois.
11. R. K. Sparks, Ph.D. Thesis, University of California, Berkeley, California (1979).
12. Any F command in which the 8 bit (bit 3) is set (i.e. 8-15, 24-31) and any subaddress is used will test the LAM function.

13. The data pulses are tied to the next 20 MHz clock pulse, and no other pulses can be recorded until this clock pulse. Thus the maximum dead time is the time between clock pulses -- 50 nsec, and the average dead time is half this -- 25 nsec. By changing to a 100 MHz clock (divided down for its other timing purposes), it would be a relatively simple matter to reduce the maximum dead time to 10 nsec, and the average dead time to 5 nsec.
14. A prototype unit exists that is a triple width CAMAC module, but the front and back are offset from the standard positions, so that 4 CAMAC slots are required.
15. The MCS has not been adequately tested with a 100 nsec dwell time as yet, so that TUF uses 150 nsec as the minimum dwell time.
16. The program TUF arbitrarily sets the maximum dwell time at 200 μ sec.
17. The program TUF sets the maximum number of triggers at 32767 for convenience, as described in the text.
18. LBL Electronics Drawings: A22952 and A22953, Lawrence Berkeley Laboratory, Berkeley, California (1985).
19. See the timing diagrams for the MCS, not included here due to space limitations, LBL Electronics Drawings: A153T-1, Lawrence Berkeley Laboratory, Berkeley, California (1985).
20. Data Translation, Inc., Natick, Massachusetts.
21. Hewlett Packard, Palo Alto, California.

This report was done with support from the Department of Energy. Any conclusions or opinions expressed in this report represent solely those of the author(s) and not necessarily those of The Regents of the University of California, the Lawrence Berkeley Laboratory or the Department of Energy.

Reference to a company or product name does not imply approval or recommendation of the product by the University of California or the U.S. Department of Energy to the exclusion of others that may be suitable.

*LAWRENCE BERKELEY LABORATORY
TECHNICAL INFORMATION DEPARTMENT
UNIVERSITY OF CALIFORNIA
BERKELEY, CALIFORNIA 94720*